ISTITUTO SUPERIORE DI SANITÀ

ISS/NIH Collaborative Programme
2006 Progress Report Meeting

Istituto Superiore di Sanità
Rome, July 4-6, 2006

Proceedings edited by
Enrico Garaci (a), Cristina D'Addazio (b) and Fabiola Giuliano (b)

(a) President of the Istituto Superiore di Sanità
(b) Office of the President

ISSN 1123-3117
Rapporti ISTISAN
06/50

Istituto Superiore di Sanità
ISS/NIH Collaborative Programme. 2006 Progress Report Meeting. Istituto Superiore di Sanità. Rome, July 4-6, 2006.
Proceedings edited by Enrico Garaci, Cristina D'Addazio and Fabiola Giuliano
2006, ix, 305 p. Rapporti ISTISAN 06/50

In July 2003, the National Institutes of Health (NIH) of the United States of America and the Istituto Superiore di Sanità (ISS) of Italy signed an agreement aimed at strengthening the ongoing research cooperation between USA and Italy. Over the years, the programme was able to create new partnerships and to foster the establishment of innovative synergies, the exchange of young researchers, and the merging of the best available skills, talents and know-how in different fields of biomedical sciences. This book of proceedings, which contains the presentations of the first progress report meeting held in Rome on 4-6 July 2006, is a proof of the outstanding scientific level of this collaborative research programme. It is divided into four sections according to the meeting programme: Cancer, Neurosciences, Cardiovascular, and Infectious diseases.

Key words: Cancer, Neurosciences, Cardiovascular, Infectious Diseases, Collaborative Programme, ISS-NIH

Istituto Superiore di Sanità
ISS/NIH Programma di Collaborazione. 2006 Progress Report Meeting. Istituto Superiore di Sanità. Roma, 4-6 luglio 2006.
Atti a cura di Enrico Garaci, Cristina D'Addazio e Fabiola Giuliano
2006, ix, 305 p. Rapporti ISTISAN 06/50 (in inglese)

Nel luglio 2003, i *National Institutes of Health* (NIH) americani e l'Istituto Superiore di Sanità (ISS) hanno firmato un accordo mirato a rafforzare la cooperazione scientifica tra Italia e USA. Nel corso degli anni il programma ha permesso di ampliare le collaborazioni e di promuovere nuove sinergie attraverso lo scambio di giovani ricercatori e la condivisione delle migliori competenze, conoscenze e capacità in diversi campi delle scienze biomediche. Questo volume contiene le presentazioni del primo convegno, tenuto a Roma il 4-6 luglio 2006, sullo stato di avanzamento dei lavori e testimonia il notevole livello scientifico del programma di collaborazione. Il rapporto è diviso in quattro sessioni: Cancro, Neuroscienze, Malattie Cardiovascolari, e Malattie infettive.

Parole chiave: Cancro, Neuroscienze, Malattie cardiovascolari, Malattie infettive, Programma di collaborazione, ISS-NIH

Per informazioni su questo documento scrivere a: presidenza@iss.it.

Il rapporto è accessibile online dal sito di questo Istituto: www.iss.it.

Presidente dell'Istituto Superiore di Sanità e Direttore responsabile: *Enrico Garaci*
Registro della Stampa - Tribunale di Roma n. 131/88 del 1° marzo 1988

Redazione*: Paola De Castro, Sara Modigliani* e *Sandra Salinetti*
La responsabilità dei dati scientifici e tecnici è dei singoli autori.

INDICE

C. Cancer cell biology

Poster

SESSION 2
NEUROSCIENCES

A. Behavioural neuroscience: from basics to psychiatry

B. Neurodegenerative disorders

Poster

SESSION 3
CARDIOVASCULAR

Plenary lecture

A. Immunity and infectious diseases

B. Vaccines

C. Immunity and metabolic diseases

Poster

PREFACE

In July 2003, the National Institutes of Health (NIH) of the United States of America and the Istituto Superiore di Sanità (ISS) of Italy signed an agreement aimed at strenghtening the ongoing research cooperation betweeen USA and Italy. Over the years, the program was able to create new partnerships and to foster the establishment of innovative synergies, the exchange of young researchers, and the merging of the best available skills, talents and know-hows in different fields of biomedical sciences.

This book of proceedings, which contains the presentations of the first progress report meeting held in Rome on 4-6 July 2006, is a proof of the outstanding scientific level of this collaborative research program. The agreement included the bilateral financing and the joint implementation of innovative projects in different areas, such as cancer, cardiovascular and pulmonary diseases, neurosciences, rehabilitation, communicable disease (including HIV/AIDS) and drug addiction, with the understanding that new research fields could be identified in the future. In addition to the disease specific research programs, five overarching methodological aspects deserve to be highlighted: pathogenesis and translational research, early diagnosis of disease and biomarkers, innovative approaches to therapy, public health aspects, prevention medicine and vaccines.

Pathogenetic aspects with translational perspective are investigated in: cancer (base excision repair mechanisms; endogenous reverse transcription; cyclin D-dependent kinase; mitochondrial remodeling; oxydative DNA damage; gene expression profiling; viral oncogenesis); neurosciences (relationship between gene alteration, environment and cognitive impairment; role of autoantibodies; gender difference in seizure sensitivity; immunopathogenesis of multiple sclerosis); cardiovascular and respiratory diseases (interaction between macrophages and atherogenic lipoproteins; effects of components of the Mediterranean diet; influence of redox changes in respiratory diseases); and infectious diseases (immune evasion mechanisms; immune control mechanisms).

Early diagnosis is the focus of research projects on cancer (serum proteomics) and cardiovascular diseases (molecular imaging of atherosclerotic plaques), while innovative therapeutic approaches are studied for cancer (dendritic cell-mediated immune therapy; adjuvant therapy; microRNA interference; molecular prediction of treatment response), chronic pain (new pharmacological targets), multiple sclerosis, HIV (integrase inhibitors).

Public health research is present in cancer projects (establishment of patient information services; evaluation of cancer prevention programs), communicable diseases (blood screening for Creutzfeldt-Jacob; inactivation of transmissible spongiform encephalopathy), cardiovascular (evaluation of rehabilitation and of calorie restriction programs) and alcohol abuse projects.

Finally, vaccine and preventive research is present in almost all areas covered by the agreement, and specifically in cancer and HIV/AIDS programs.

While building a common vision of research horizons, the agreement put aside resources for the creation of partner interventions in resource limited countries, aiming at reducing inequalities in health access at the global level.

The cooperation between ISS and NIH proved to be extremely fruitful and offered the opportunity to achieve very encouraging outcomes, as it appears in this publication. Therefore we strongly hope to continue in this direction to obtain, as already envisaged, further successful results.

We are very proud to present to the scientific community this interim report. Besides the merits of the Institutions who made this agreement possible, a special acknowledgement should go to the dedicated scientists who believed in the added value of this collaborative international research program.

Enrico Garaci
President of the Istituto Superiore di Sanità

Letter of Intent
Between
The National Institutes of Health
of the United States of America
and the
Istituto Superiore di Sanitá
of the Italian Republic

The National Institutes of Health of the United States of America (NIH) and the Istituto Superiore di Sanitá (ISS) of the Italian Republic, desiring to strengthen the existing links reaffirmed in the Memorandum of Understanding signed April 17, 2003 between the U.S. Department of Health and Human Services and Italy's Ministry of Health, intend to work to increase cooperation in the fields of biomedical and behavioral sciences, and related training.

Among the areas of initial mutual interest are cancer; cardiovascular disease; pulmonary disease; women's health; neuroscience, including neurodegenerative disease research; medical rehabilitation research; communicable diseases, including HIV/AIDS; and tobacco control. Other areas of research may be identified in the future by mutual consent.

In addition, both sides intend to work in partnership and within the missions of their respective agencies to advance efforts that reduce global health disparities.

Mechanisms to support collaboration may include:

- Organization and conduct of joint workshops;
- Identification of joint training opportunities for researchers, including those from developing countries and economies in transition;
- Exchange of scientists;
- Exchange of information;
- Exchange of materials;
- Joint research projects, including translational and clinical research;
- Joint research in third countries, including developing countries and economies in transition; and
- Other forms of cooperation, including support for scientists from developing countries and economies in transition in joint U.S.-Italy efforts.

Activities under this Letter of Intent are to be conducted subject to the laws, policies, and regulations and the availability of appropriated funds and other resources of the host and sponsoring countries. Each side should cover the international airfare and subsistence costs of its participants. With respect to joint projects, the two sides should work together to identify project costs as collaborative projects are developed.

On the Italian side, this Letter of Intent should cover cooperative activities undertaken or implemented by the ISS and is intended to also include participation of other Italian scientific and research organizations engaged in related research activities, as appropriate. NIH and ISS may convene meetings of Principals, in the form of a Policy Forum, as deemed appropriate, in order to review progress in the implementation of activities under this Letter of Intent.

This Letter of Intent becomes effective upon signature by the government representatives below.

Signed at Rome, in duplicate, this 28 day of July, 2003.

FOR THE NATIONAL INSTITUTES OF HEALTH OF THE UNITED STATES OF AMERICA:

FOR THE ISTITUTO SUPERIORE DI SANITA' OF ITALY:

Session 1
CANCER

Session 1. Plenary lecture

SELECTIVE ISOLATION, ENRICHMENT, AND MS SEQUENCING OF CANDIDATE BIOMARKERS IN BLOOD: CARRIER PROTEIN BOUND LOW MOLECULAR WEIGHT PROTEINS AND PEPTIDES

Maria Letizia Polci (a,b), Serena Camerini (a,b), Weidong Zhou (a), Emanuel F Petricoin (a), Lance A Liotta (a)
(a) Center for Applied Proteomics and Molecular Medicine, George Mason University, Manassas, Virginia, USA
(b) Istituto Superiore di Sanità, Rome, Italy

Introduction

The circulatory proteome is considered the pre-eminent source of clinically relevant biomarkers and the principal source of information about the overall physiological state (1). Recently, it has been proposed that the low molecular weight (LMW) component of the proteome may hold an especially rich and previously unexplored source of diagnostic information because it contains an active record of its ongoing physiological state as reflected by the proteomic and metabolic products it sheds to the blood (1-3). Moreover, investigators have found that most of this LMW information that is found *in vivo*, is bound to circulating high abundance carrier proteins such as albumin (2,4-7). This binding appears able to impede the facile and rapid excretion of the peptides and small molecules by kidney filtration, thereby mass action kinetics provides a means to amplify low abundant information to a concentration detectable by proteomic approaches such as mass spectrometry (2,8-10). The circulatory proteome is a very complex matrix in which protein concentration can range more than 10 orders of magnitude, and 90% of the total protein composition is constituted by a very restricted number of high molecular weight proteins (11). Consequently most biomarker discovery strategies begin with a series of fractionation methods that employ native depletion and removal methods, such as affinity chromatography, or size filtration, to remove the high abundance proteins such as albumin and immunoglobulin (12-17). Unfortunately, given the proclivity of LMW molecules to bind to these same proteins, biomarker discovery that is underpinned by LMW analysis and which utilizes such depletion methods, will throw out the same molecular information that is sought after originally. Nevertheless, it is absolutely necessary to exclude the high abundance proteins, such as albumin, from downstream analysis since these proteins make it nearly impossible to characterize any biomarker candidate that could be a million to billion fold less abundant. Thus it is critically important to develop a method that can efficiently isolate and enrich for the LMW archive while concomitantly eliminating high abundance resident proteins (10). To be able to detect these LMW molecules it would be necessary to detach them from the carrier proteins using denaturing conditions that are often not compatible with commonly used downstream immunodepletion strategies for albumin and other high molecular weight proteins (14). Here we describe a methodology for the facile isolation of LMW and low abundance proteins purification based on a continuous elution denaturing electrophoresis. In the past this device has been used for isolating individual components from crude or partially

purified samples (18-21). It represents an effective means of fractionating complex protein mixtures according to their molecular weight under denaturing conditions. The major disadvantage offered by this tool is the requirement for SDS that consequently doesn't make the output directly usable for mass spectrometric sequencing because of the SDS (22). Thus an important goal of the new method described here was to remove the SDS without diluting or diminishing the yield of the fractionated molecules obtained after electrophoresis. The strategy described in this report allows for the nearly complete elimination of high molecular weight proteins while collecting the LMW proteins and peptides that are simultaneously fractionated and enriched. This methodology can then serve to be implemented as an upfront step for downstream proteomic analysis using labelled (e.g. ITRAQ) or unlabelled approaches.

Materials and methods

Blood collection and serum preparation

Blood samples were drawn from healthy individuals under full Institutional Review Board approval and patient consent. Specimens were collected in red-top Vacutainer Tubes and allowed to clot for 1 hr on ice, followed by centrifugation at 4°C for 10 min at 2000g. The serum supernatant was divided in aliquots and stored in -80°C until needed. 10 serum samples were mixed together in a single aliquot that was used for all experiments.

LMW protein harvesting by continuous elution electrophoresis

100 µl of serum was mixed with 2xSDS-PAGE Laemmli Buffer (containing 200mM DTT), boiled for 10 min, and loaded on Prep Cell (Model 491 Prep Cell, Bio-Rad Laboratories, CA) in which 5 cm length 10% acrylamide gel was polymerized. Electrophoresis was performed under a constant voltage of 250V. Immediately after the bromophenol blue indicator dye was eluted from the system, LMW peptides and proteins migrated out of the gel and were trapped in a dialysis membrane (elution chamber). These molecules were then eluted at a flow rate of 400µl/min by a buffer with the same composition of the Tris-Glycine running buffer and collected at different times.

SDS removal from the Prep Cell fractions

Elimination of SDS from the collected fractions was performed by three main procedures:

- *Concentration by membrane filtration*
  Samples were applied on to Centricon tubes with a molecular weight cut-off of 5kDa (Amicon Ultra, Millipore) and spun at 3000g for 15 min. Two washes were performed with a Tris-Glycine buffer without SDS to further reduce the SDS concentration of the fractions. At the end of the process the fractions were concentrated up to approximately 300µl.
- *TCA precipitation*
  The Centricon-concentrated LMW fraction obtained by the Prep Cell was made up to a final volume of 300µl, and then an acid precipitation was carried out by incubating the fractions with 10% TCA (v/v), on ice for 1h. After that the mixture was spun at 15000g for 30 min, at 4°C, and the resultant precipitant pellet was washed by cold acetone and then dissolved in 8M urea in an ultrasound bath for 1h.

– *Ion-exchange chromatography*
LMW fractions obtained by the Prep Cell were processed using a commercially available ion-exchange matrix (Proteo Spin Detergent Clean-Up Micro Kit, Norgen Biotek Corporation, Canada) following protocols outlined by the manufacturer for both acidic and basic proteins, resulting in a final volume of 55 μl.

Nanoflow reversed-phase liquid chromatography-tandem MS (nanoRPLC-MS/MS)

To evaluate the integrity of the isolated SDS-free LMW archive and its potential for downstream MS/MS analysis and characterization, the samples from each of the three procedures were analyzed by traditional bottom-up MS approaches.

Bioinformatic analysis

Tandem mass spectra were matched against Swiss-Prot human protein database through SEQUEST algorithm (23) incorporated in Bioworks software (version 3.2, Thermo Electron) using tryptic cleavage constraints and static cysteine alkylation by iodoacetamide. For a peptide to be considered legitimately identified, it had to achieve cross correlation scores of 1.5 for $[M+H]^{1+}$, 2.0 for $[M+2H]^{2+}$, 2.5 for $[M+3H]^{3+}$, and a probability cut-off for randomized identification of $p<0.01$.

Results and discussion

Herein we describe and prove the utility of the development of stepwise process that begins with the effective stripping and fractionation of the LMW archive from the carrier proteins, using a continuous flow electrophoresis system. After a purification step the outcome is a series of SDS-Free fractions of LMW molecules. The isolated fractions are then analyzed by enzymatic digestion followed by LC-MS/MS analysis. In Figure 1 the proposed method is schematized.

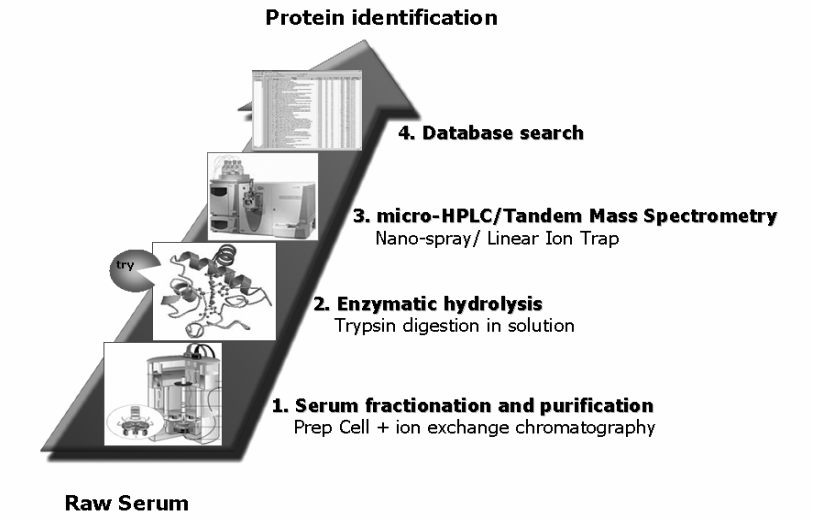

Figure1. Overall description of the method for the selective isolation, enrichment and identification of carrier protein bound Low Molecular Weight proteins and peptides in the blood

Elimination of SDS for downstream proteomic analysis

After visualization of the LMW molecules present in each Prep Cell fraction in a SDS-PAGE, we choose the fractions containing proteins and peptides whose molecular weight was lower than Immunoglobin G (IgG) light chain. Half of this fraction was concentrated by Centricon membrane and TCA precipitated and the other half was cleaned and concentrated using a commercial kit registered as "Proteo Spin" (Norgen Biotek Corporation, Canada), that claimed efficient SDS removal, by analyzing both the acidic and basic protocols as outlined by the manufacturer.

The results obtained with these two methods were compared by loading the purified and concentrated fractions on a SDS-PAGE. As shown in Figure 2 the yield from both acidic (lane 2) and basic (lane 3) protocol of the Proteo Spin is much higher than TCA precipitation (lane 4).

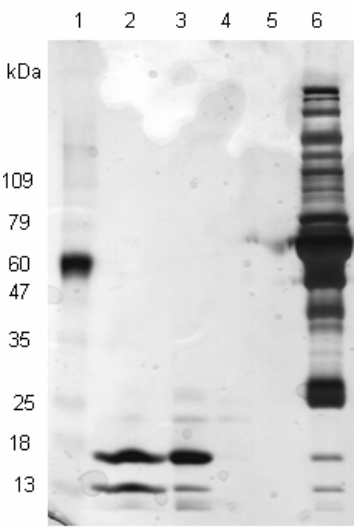

Figure 2. Silver stained SDS PAGE (4-20%) of the LMW fractions after SDS elimination by Proteo Spin.

Lane 1: Molecular weight marker; Lane 2,3: 10 min Prep Cell fraction, equivalent to 0.2µl of raw serum, treated by Proteo Spin respectively with the acidic and the basic protocol; Lane 4: TCA-precipitated 10 min Prep Cell fraction equivalent to 0.2µl of raw serum; Lane 6: Raw serum (0.2µl); Lane 5: Empty well.

Further, the subsequent quality of the elution profile from Proteo Spin treated Prep Cell fraction is satisfactory, indicating that SDS has been efficiently eliminated.

Evaluation of the method efficiency by LC-MS/MS analysis

In order to validate the method in the SDS removal and in the low abundance proteins enrichment, an aliquot of both acidic and basic Proteo Spin kit eluates coming from a LMW Prep Cell fraction was independently analyzed by LC-MS/MS. The data obtained from these two LC-MS/MS analyses were combined and afterwards compared with the LC-MS/MS results derived from the combination of two injections of tryptic mixtures obtained from direct digestion of raw serum. In the unfractionated serum it was possible to identify 70 unique proteins while in the purified fractions 140 unique proteins were detected in total. Among these

sequenced proteins 44 were present in both of the sets while 26 were recognized only in unfractionated serum and 96 only in the fractions obtained by combining the Prep Cell fractionation with Proteo Spin treatment.

The analysis of the distribution of protein abundance (11) seen in raw serum compared to the LMW enrichment method indicates that a higher number of low abundance proteins (represented by the 1% of the total serum protein content) can be identified by using the described purification strategy (Figure 3).

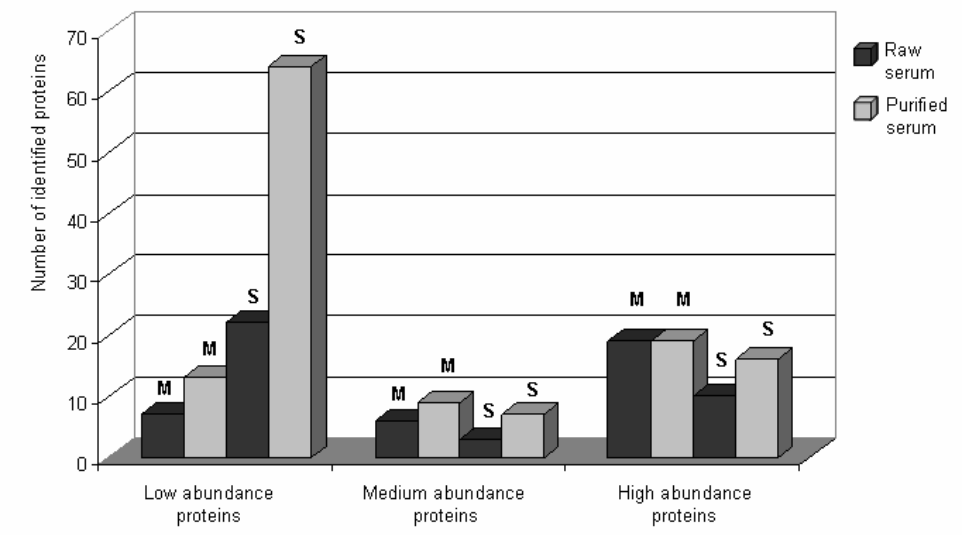

Figure 3. Abundance distribution of the serum proteins detected in raw and purified serum samples

Low, medium and high abundance serum proteins [11] identified with multi peptide (M) and single peptide hits (S) in LMW enriched and purified samples (light bars) and in raw serum (dark bars) are compared.

In particular, we observed a 50% increase in both the single peptide and multi peptide hits of the low abundance serum proteins identified by using the proposed strategy (S and M light bars in Figure 3) compared to direct sequencing of unfractionated serum (S and M dark bars). The number of identified proteins is expected to increase somewhat with repeated iterations (25): we attempted to verify this hypothesis and to understand the number of iterations that provides a large coverage of uniquely found molecules.

With this aim in mind, the fractions coming from the acidic and the basic SDS removal procedure were trypsinized and subjected to MS/MS analysis 4 times each to reach a total of 8 independent repetitions. This process then yielded 172 and 190 proteins that were respectively identified after the acidic and the basic procedure. A total of 255 unique proteins were identified: among these proteins 107 (42%) were seen in both sets and 148 (58%) were identified only in one of the two sets. These results indicate that the total number of identified proteins seems to reach a maximum number after 8 iterations, as reported in Figure 4.

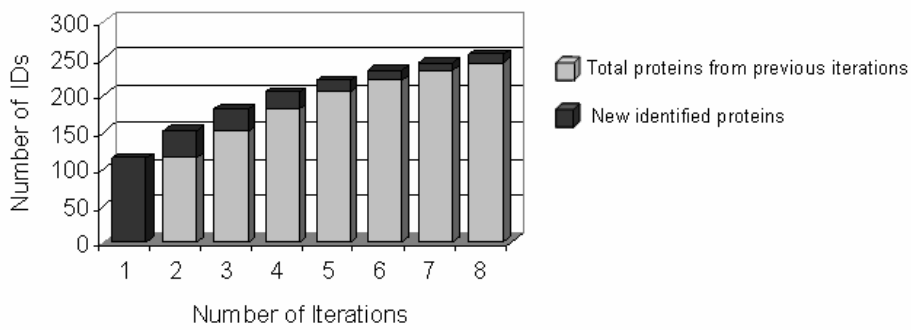

Figure 4. Trend of total protein identifications (IDs) versus number of iterations. The total number of identified proteins is reported for each iteration of the LC-MS analysis of the purified serum samples. Light bars indicate proteins identified in the previous repeats while dark bars represent the new identifications

In particular, the ability to identify new proteins with multiple peptide hits did not increase appreciably after the third iteration, while new identifications performed with single peptide hits trends to a plateau after 8 iterations (Table 1).

Table 1. Representation of peptide hits and protein identifications acquired after subsequent iterations of LC-MS analysis of purified serum samples. (IDs: identifications)

Number of iterations	Number of unique protein IDs	Number of multi peptide protein IDs	Number of single peptide protein IDs
8	255	46	209
7	243	46	197
6	233	46	187
5	219	46	173
4	204	46	158
3	181	46	135
2	152	44	108
1	114	42	72

Thus, using the linear ion trap employed here, the identification of the lowest abundant molecules, likely those with only single peptide hits found only once, appears to reach saturation around 8 independent iterations. Representative MS/MS spectra of two tryptic peptides coming from low abundance serum proteins (25-27) identified solely using our LMW fractionation method, found after 8 independent LC-MS repeats, are reported (Figure 5) to exhibit the identification of a peptide that appeared iteratively with a large number of peptide hits and a protein that was found multiple independent times but with only one peptide hit found multiple times. Panel A shows the MS^2 spectrum of the peptide (102-122) of Tetranectin (M.W.: 22.567kDa) that has been identified 8 times with 3 peptides while panel B shows the MS^2 spectrum of the peptide (81-103) of Serum Amyloid A4 (M.W.: 14.807kDa) identified 7 times with one peptide. Both of these examples illustrate the utility of our method to analyze and identify low abundance and low molecular weight molecules.

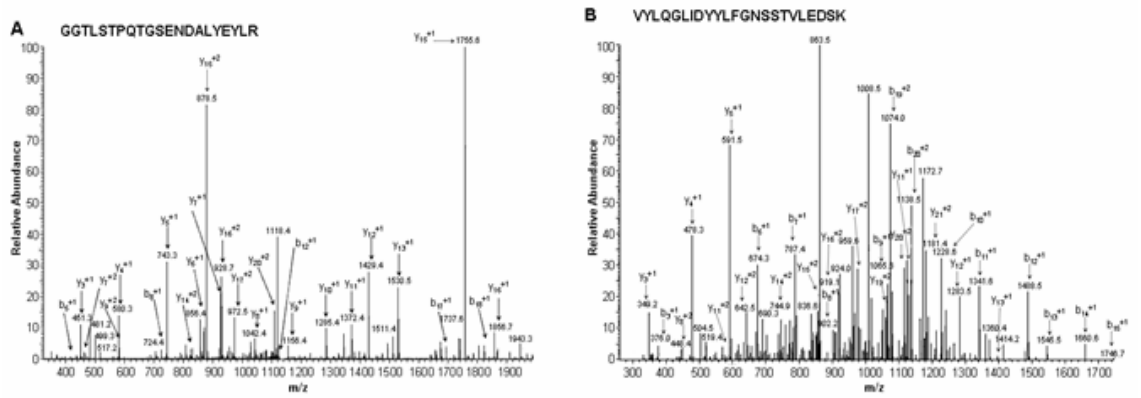

Figure 5. Representative MS/MS spectra of Tetranectin and Serum Amyloid A4 identified in the purified serum after 8 LC-MS repeats. Tetranectin has been identified 8 times with 3 peptides: the MS/MS spectrum of the peptide (102-122) is shown in panel A. Serum Amyloid A4 has been identified 7 times with one peptide (81-103) and its MS/MS spectrum is reported in panel B

Acknowledgements

This work was partly supported by the Italian Istituto Superiore di Sanità in the framework Italy/USA cooperation agreement between the US Department of Health and Human Services and the Italian Ministry of Public Health. We would like to express our gratitude to Prof. Enrico Garaci for making this collaborative research program possible. We would like to thank Prof. Cesare Peschle, Dr. Francesco Facchiano and Dr. Marco Crescenzi for their support and advices in the achievements of this work.

References

1. Liotta LA, Ferrari M, Petricoin EF. Clinical proteomics: written in blood. *Nature* 2003;425(6961):905.
2. Lowenthal MS, Mehta AI, Frogale K, Bandle RW, *et al*. Analysis of albumin-associated peptides and proteins from ovarian cancer patients. *Clin Chem* 2005;51:1-13.
3. Petricoin EF, Ardekani AM, Hitt BA, Levine PJ, *et al*. Use of proteomic patterns in serum to identify ovarian cancer. *The Lancet* 2002;359(9306):572-7.
4. Lopez MF, Mikulskis A, Kuzdzal S, Bennett DA, Kelly J, *et al.* High-resolution serum proteomic profiling of Alzheimer disease samples reveals disease-specific, carrier-protein-bound mass signatures. *Clin Chem* 2005;51(10):1946-54.
5. Burtis CA, Ashwood ER, *Tietz, fundamentals of clinical chemistry.* 5th ed. Philadelphia, PA: W.B. Saunders Company; 2001.
6. Mehta AI, Ross S, Lowenthal MS, Fusaro V, Fishman DA, *et al.* Biomarker amplification by serum carrier protein binding. *Dis Markers* 2003-2004;19(1):1-10.
7. Sjobring U, Falkenberg C, Nielsen E, Akerstrom B, Bjorck L. Isolation and characterization of a 14-kDa albumin-binding fragment of streptococcal protein G. *J Immunol* 1988;140(5):1595-9.
8. Dennis MS, Zhang M, Meng YG, Kadkhodayan M, *et al*. Albumin binding as a general strategy for improving the pharmacokinetics of proteins. *J Biol Chem* 2002;277(38):35035-43.

9. Lee VHL. *Peptide and protein drug delivery*. New York: Marcel Dekker; 1991.

10. Tirumalai RS, Chan CK, Prieto DaRue A, Issaq HJ, *et al.* Characterization of the low molecular weight human serum proteome. *Mol Cell Proteomics* 2003;2(10):1096-103.

11. Anderson NL, Anderson NG. The human plasma proteome: history, character, and diagnostic prospects. *Mol Cell Proteomics* 2002;1(11):845-867.

12. Sato AK, Sexton DJ, Morganelli LA, Cohen EH, *et al.* Development of mammalian serum albumin affinity purification media by peptide phage display. *Biotechnol Prog* 2002;18(2):182-92.

13. Adkins JN, Varnum SM, Auberry KJ, Moore RJ, *et al*. Toward a human blood serum proteome: analysis by multidimensional separation coupled with mass spectrometry. *Mol Cell Proteomics* 2002;1(12):947-55.

14. Zolotarjova N, Martosella J, Nicol G, Bailey J, *et al.* Differences among techniques for high-abundant protein depletion. *Proteomics* 2005;5(13):3304-13.

15. Wang YY, Cheng P, Chan DW. A simple affinity spin tube filter method for removing high-abundant common proteins or enriching low-abundant biomarkers for serum proteomic analysis. *Proteomics* 2003;3(3):243-8.

16. Merrel K, Southwick K, Graves SW, Esplin MS, *et al*. Analysis of low-abundance, low-molecular-weight serum proteins using mass spectrometry. *J Biomol Tech* 2004;15(4):238-48.

17. Rothemund DL, Locke VL, Liew A, Thomas TM, *et al*. Depletion of the highly abundant protein albumin from human plasma using the Gradiflow. *Proteomics* 2003;3(3):279-87.

18. Davidsson P, Westman A, Puchades M, Nilsson CL, Blennow K. Characterization of proteins from human cerebrospinal fluid by a combination of preparative two-dimensional liquid-phase electrophoresis and matrix-assisted laser desorption/ionization time-of-flight mass spectrometry. *Anal Chem* 1999;71(3):642-7.

19. Nilsson CL, Puchades M, Westman A, Blennow K, Davidsson P. Identification of proteins in a human pleural exudate using two-dimensional preparative liquid-phase electrophoresis and matrix-assisted laser desorption/ionization mass spectrometry. *Electrophoresis* 1999;20(4-5):860-5.

20. Meng F, Du Y, Miller LM, Patrie SM, *et al.* Molecular-level description of proteins from saccharomyces cerevisiae using quadrupole FT hybrid mass spectrometry for top down proteomics. *Anal Chem* 2004;76(10):2852-8.

21. Meng F, Cargile BJ, Patrie SM, Johnson JR, *et al*. Processing complex mixtures of intact proteins for direct analysis by mass spectrometry. *Anal Chem* 2002;74(13):2923-9.

22. Zhang N, Li L. Effects of common surfactants on protein digestion and matrix-assisted laser desorption/ionization mass spectrometric analysis of the digested peptides using two-layer sample preparation. *Rapid Commun Mass Spectrom* 2004;18(8):889-896.

23. Yates JR, Eng JK, McCormack AL, Schieltz D. Method to correlate tandem mass spectra of modified peptides to amino acid sequences in the protein database. *Anal Chem* 1995;67(8):1426-36.

24. Liu H, Sadygov RG, Yates JR. A model for random sampling and estimation of relative protein abundance in shotgun proteomics. *Anal Chem* 2004;76(14):4193-201.

25. Hogdall CK. Human tetranectin: methodological and clinical studies. *APMIS Suppl* 1998;86:1-31.

26. Hogdall CK, Christensen L, Clemmensen I. The prognostic value of tetranectin immunoreactivity and plasma tetranectin in patients with ovarian cancer. *Cancer* 1993;72(8):2415-22.

27. Yamada T, Miyake N, Itoh K, Igari, J. Further characterization of serum amyloid A4 as a minor acute phase reactant and a possible nutritional marker. *Clin Chem Lab Med* 2001;39(1):7-10.

28. Linke T, Ross, AC, Harrison EH. Profiling of rat plasma by surface-enhanced laser desorption/ionization time-of-flight mass spectrometry, a novel tool for biomarker discovery in nutrition research. *J Chromatogr A* 2004;1043(1):65-71.

Session 1. Plenary lecture

LMW PROTEIN FRAGMENTS MAY DETECT EARLY STAGE BREAST CANCER

Gordon Whiteley (a), Sally Rucker (a), Chenwei Liu (a), Simona Colantonio (a), Andrea Sacconi (a), Enzo Mammano (b), Giorgia Marconato (b), Cosimo Di Maggio (b), Donato Nitti (b), Mario Lise (b,c), Claudio Belluco (c)
(a) Clinical Proteomics Reference Lab, NCI-Frederick, Gaithersburg, MD, USA
(b) Department of Oncological and Surgical Sciences, University of Padova, Padova, Italy
(c) CRO- IRCCS, National Cancer Institute, Aviano, Italy

Introduction

Breast cancer is the leading cause of cancer mortality in women worldwide. While screening by mammography has been shown to reduce breast cancer mortality, this test is not as useful in early stages of disease where the lesions are smaller or in cases where the breast tissue is denser (1). Detection at early stages also results in a more favorable outcome, especially in women with pT1a tumors. The search for early biomarkers using conventional techniques has been largely unsuccessful. Recently, serum proteomic profiling has emerged as a technology with great potential for early detection of disease with reports of patterns for a variety of cancers and other disease conditions. (2-4). The advances in mass spectrometry, computer bioinformatics, robotics and more powerful computers have made these discoveries possible (5).

The goals of the Clinical Proteomics Reference Lab are to develop and validate proteomics pattern recognition methods to the standards of the FDA. In doing so, we utilize serum sample sets that are well characterized and have valid clinical data for comparison. The serum sets that were obtained first from the University of Padova and then from several additional sites in Italy provided us with such a set that could not only be used for the development of new methods but also help validate some of our earlier findings.

Sample processing and mass spectrometry

There were a total of 369 samples analyzed in this study. The first group were 324 consisting of 154 normal samples and 170 early stage cancer samples. The second group consisted of 15 normal samples and 30 early stage cancer samples received approximately one year after the first study. Samples were thawed and 10 µl aliquots were obtained. These were used immediately for high resolution surface enhanced laser desorption ionization (SELDI) using an IMAC surface which is known to have a high affinity for albumin. Albumin was targeted because of the association of low molecular weight peptides and proteins with carrier proteins and the fact that these may be the source of diagnostic information (6). All steps were carried out on a Tecan Genesis 200 robotic processor to ensure reproducibility. A 5 µl aliquot was applied to the surface and incubated for 30 minutes. After washing with PBS and water, CHCA was applied as the matrix and was dried. The arrays were then read in an ABI Q-Star XL equipped with a Ciphergen P1000 interface. The spectra were extracted into an SQL database for processing. All spectra were examined for quality and spectra showing low total ion current

were eliminated. Spectra were then normalized to total ion current and randomly split into a training set (70% of samples each from the normal and cancer groups) and a testing set (30% of samples).

Pattern bioinformatics

The bioinformatics developed at the CPRL utilize two basic paths as outlined in Figure 1. For the first method, each data point is examined in the groups of training samples and a Wilcoxon test is used to determine if there is any discriminating potential. The top 250 peaks showing the greatest power are selected and they are then used to build three classifiers as outlined below.

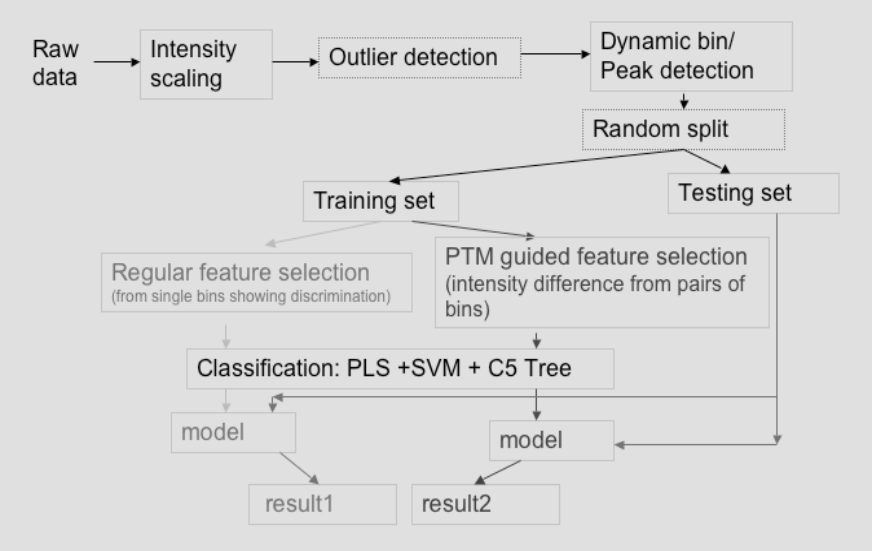

Figure 1. CPRL Classification methods

The second method of peak selection involves the possibility of classification based on post translational modifications (PTM's). This method looks at peak ratios at given distances that would correlate with a PTM: 1 (deamidation), 2 (disulfide bond formation) and 80 (phosphorylation). These three have been shown to be associated with cancer (7-9). The ratios of each peak pair in the normal samples are compared with the peak pair ratios in the cancer group. Those pairs showing a significant difference are then selected to be fed into the bioinformatics classification tools outlined below.

The classifiers consist of three very different methods: C 5.0 decision tree (Clementine), partial least squares (SAS) and the support vector machine (libsys SMV). Each of these classifiers is independently trained on a training set of samples and the best model for each algorithm is selected to classify samples held in an evaluation set of samples. These samples have not been part of the training and are used simply to evaluate sensitivity and specificity. When the samples are classified, each method "votes" on the classification of the unknown samples. Where there is agreement, the samples are classified as cancer or normal; where there is no agreement, the samples are called "unknown".

Results of studies and discussion

The demographics of the breast cancer samples used are outlined in Table 1. The training, testing and masked validation sets all showed similar age ranges with the average age ranging from 55 to 60 years. However, the masked validation set had a larger number of stage T1a samples than the earlier training and testing sets.

Table 1. Demographics of study samples

Group	Number	Average age (range)	Stage of disease (number)
Training set			
Normal	109	55.0 (36-80)	
Cancer	126	59.1 (38-88)	1a (8) 1b (39) 1c (79)
Masked Testing Set			
Normal	45	60.8 (37-75)	
Cancer	44	59.8 (39-79)	1a (3) 1b (13) 1c (28)
Masked Validation Set (14 months later)			
Normal	15	60.5 (47-75)	
Cancer	30	58.6 (36-77)	1a (16) 1b (11) 1c (3)

The predicted performance was calculated for each model based on a 10% cross validation within the training set of samples and the results for each individual method are outlined in Table 2.

Table 2. Predicted performance of each model

Model	Sensitivity	Specificity
C5.0 decision tree	83.61%	91.80%
SVM	78.69%	86.89%
Partial Least Square	83.61%	90.16%
C5.0+SVM +PLS	90.32%	90.32%

The performance was then validated using the 30% of samples that were held and not used as part of training. This showed performance of 83.3% sensitivity and 96.8% specificity based on 61 samples. A blinded set of samples was collected over the next year and was then used to evaluate the algorithm to demonstrate the stability of the system. Although the sample numbers were low (15 normal and 30 cancer), the age distribution was similar to the previously used samples and the sensitivity of 97% and specificity of 80% were very similar to that observed one year earlier (Table 3).

Table 3. Performance of algorithm over 14 months

C5nn+pls+svm	0-normal	1-cancer
Original Results*		
Normal	30	1
Cancer	5	25
Results on new samples 14 months later**		
Normal	12	3
Cancer	1	29

*Sensitivity: 83.3%, specificity: 96.8%.
**Sensitivity:97%, specificity: 80%.

The top peaks used by the C5.0 decision tree are shown in Figure 2. Although there are differences seen between the normal and cancer groups, the differences are not sufficient for any single peak to be used. Only a combination of these peaks could give sensitivity and specificity confirming that a single biomarker for breast cancer probably does not exist.

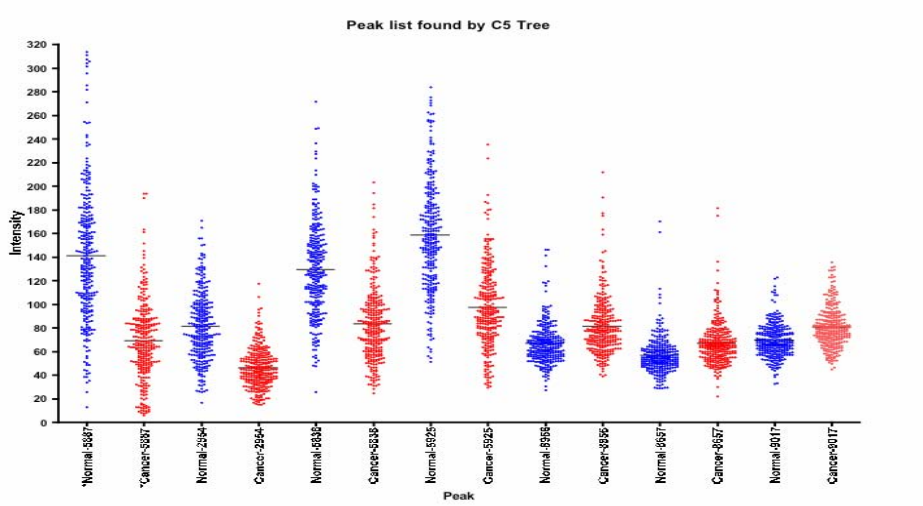

Figure 2. Top peaks used in the C5.0 Decision Tree

The performance of this test was compared with mammography using BI-RADS score demonstrating that many samples that would be missed by mammography were detected by this method (Table 4). This suggests that a blood test would be a valuable adjunct to imaging tests like mammography especially for early stages of the disease where treatment is more successful.

Table 4. Classification of serum cancer samples from masked testing set by proteomic pattern according to BI-RADS mammogram

	Cancer	Normal
BI-RADS 3	3/3	0/3
BI-RADS 4	16/17	1/17
BI-RADS 5	13/14	1/14

Identification of some of the peptides and proteins that are carried on albumin and may be associated with disease was carried out. Albumin was separated from serum samples using cibachrome blue capture, washing and then elution by acetonitrile. The resulting solution was dried, reconstituted, trypsin digested and analyzed by LC MS/MS using nanospray as previously described (10). This revealed many peptide fragments that have not been found in serum before and could be associated with cancer. A list of these is found in Table 5. Since the time of this study, further protein fragments have been identified and it would appear that the patterns seen would be useful as tools to guide identification of those proteins that are associated with disease and could be early markers.

Table 5. Protein fragments found only in early stage breast cancer pool

Parental Protein	Accession ID
Alpha-amylase 2B precursor	P19961
Alpha-amylase, salivary precursor	P04745
Alpha-mannosidase IIx	P49641
Cellular repressor of E1A-stimulated genes	O75629
Cystatin A	P01040
Cystatin SN precursor	P01037
Glucosamine-6-phosphate isomerase	P46926
Kallistatin precursor	P29622
Olfactory receptor 9Q1	Q8NGQ5
Prolactin-inducible protein precursor	P12273
Protein Plunc precursor	Q9NP55
Short palate, lung and nasal epithelium carcinoma associated protein 2 precursor	Q96SN8
Calcium binding protein 1 (calbrain)	Q8N6H5
Solute carrier family 13, member 3	Q8WWT9
Von Ebner's gland protein precursor	P31025
CDK5 regulatory subunit associated protein 2	Q96SN8
Myeloid/lymphoid or mixed-lineage leukemia protein 4	Q9UMN6
Phosphatidylinositol 3-kinase regulatory beta subunit	O00459
Tumor protein p73	O15350

In order to refine this guidance, we utilized a more sophisticated mass spectrometer system than our original profiling study. This system is outlined in Figure 3 and involves the specific targeting of fragments that are associated with albumin.

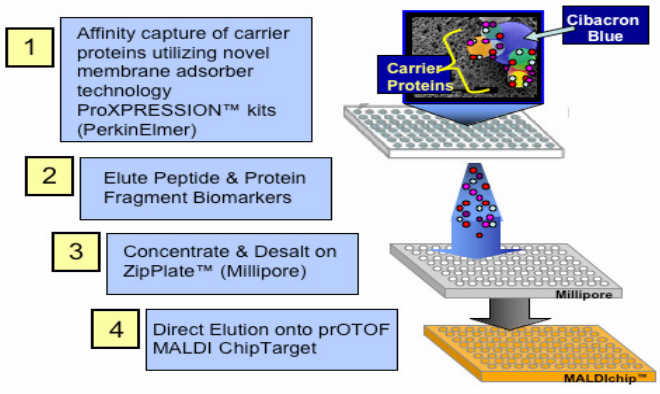

Figure 3. ProXpression™ Methodology

The albumin is first captures on cibachrome blue plates, washed and the load is eluted into solution. The peptides and protein fragments are then recovered and concentrated on a ZipPlate with a C18 base. This is then eluted and directly spotted on a target using a solution of CHCA matrix in acetonitrile and using a 3µl volume. The target is then analyzed in a PerkinELmer prOTOF mass spectrometer. This instrument has an orthoganol design that yields high resolution data that is very tolerant of rough target surfaces. The collisional cooling keeps fragments in tact, something that we utilized in our data analysis (2). Our assumption was that post-translational modifications would also be intact and could be detected by the instrument. We therefore specifically looked for these modifications and looked for peak pair ratios rather than differences between normal and cancer sera that were shown by individual peaks. In looking for peak pair ratios corresponding to phosphorylation, deamidation and disulfide bond formation, we had demonstrated that a low number of peak pairs could be identified that differentiated ovarian cancer and cutaneous t-cell lymphoma samples from normal samples. We therefore analyzed the breast cancer samples to see if this was also the case. Our findings showed that a sensitivity of 93.5% and a specificity of 91.69% could be attained using 24 peak pairs (48 peaks total). This information can now be used to specifically target these peak pairs for identification from the long list of potential peptides and protein fragments that have been randomly identified in these samples as well as the long list of peaks that were used in our first analysis.

Conclusions

The use of profiling in early diagnosis is still a long way from being practical in the routine clinical lab setting. It requires specialized equipment, laboratories and a highly trained and diverse staff to be successful. However, we have demonstrated that it is feasible both on the basis of long-term algorithm stability and the use of algorithms that are simple and utilize knowledge of the disease mechanism. The results of the PTM study target very specific proteins and peptides for identification and hopefully panels of tests can be developed that will have routine clinical lab application and practicality.

Acknowledgements

The entire CPRL staff is a dedicated and focused group that have worked on developing and validating profiling technology. Without their work, these studies would not have been possible or completed. The invaluable collaboration with our colleagues in Italy have provided the crucial materials – the patient samples and information that are the foundation of this work.

References

1. Elmore JG, Armstrong K, Lehman CD, Fletcher SW. Screening for breast cancer. *JAMA* 2005;293:1245-56.
2. Lopez MF, Mikulskis A, Kuzdzal S, Bennett DA, Kelly J, Golenko E, DiCesare J, Denoyer E, Patton WF, Ediger R, Sapp L, Ziegert T, Lynch C, Kramer S, Whiteley GR, Wall MR, Mannion DP, Della Cioppa G, Rakitan JS, Wolfe GM. High-resolution serum proteomic profiling of Alzheimer disease samples reveals disease-specific, carrier-protein-bound mass signatures. *Clin Chem* 2005;51:1946-54.

3. Petricoin EF, Ardekani AM, Hitt BA, Levine PJ, Fusaro VA, Steinberg SM, Mills GB, Simone C, Fishman DA, Kohn EC, Liotta LA. Use of proteomic patterns in serum to identify ovarian cancer. *Lancet* 2002;359:572-7.
4. Li J, Orlandi R, White CN, Rosenzweig J, Zhao J, Seregni E, Morelli D, Yu Y, Meng XY, Zhang Z, Davidson NE, Fung ET, Chan DW. Independent validation of candidate breast cancer serum biomarkers identified by mass spectrometry. *Clin Chem* 2005;51:2229-35.
5. Whiteley GR. Proteomic patterns for cancer diagnosis-promise and challenges. *Mol Biosyst* 2006;2:358-63.
6. Mehta AI, Ross S, Lowenthal MS, Fusaro V, Fishman DA, Petricoin EF 3rd, Liotta LA. Biomarker amplification by serum carrier protein binding. *Dis Markers* 2003;19:1-10.
7. Mann M, Jensen ON. Proteomic analysis of post-translational modifications. *Nat Biotechnol* 2003;21:255-61.
8. Li C, Thompson CB. Cancer. DNA damage, deamidation, and death. *Science* 2002;298:1346-7.
9. Bae SC, Lee YH. Phosphorylation, acetylation and ubiquitination: the molecular basis of RUNX regulation. *Gene* 2006;366:58-66.
10. Lowenthal MS, Mehta AI, Frogale K, Bandle RW, Araujo RP, Hood BL, Veenstra TD, Conrads TP, Goldsmith P, Fishman D, Petricoin EF 3rd, Liotta LA. Analysis of albumin-associated peptides and proteins from ovarian cancer patients. *Clin Chem* 2005;51:1933-45.

Session 1. Plenary lecture

THE IMMUNOLOGICAL CONSTANT OF REJECTION

Franco Marincola
Department of Transfusion Medicine, Clinical Centre, NIH, Bethesda, MD, USA

The recent progress in tumor immunology exemplifies the successful application of modern biotechnology for the understanding of the complex natural or therapy-induced phenomenon of immune-mediated rejection of cancer. Tumor antigens recognized by T cells were identified and successfully utilized in active immunization trials for the induction of tumor-antigen specific T cells (1,2).

However, this achievement has left the clinicians and researchers perplexed by the paradoxical observation of the immunization-induced T cells, which can recognize tumor cells in standard assays but most often cannot induce tumor regression.

We believe that successful immunization is one of several steps required for tumor clearance, but more work needs to be done to understand how T cells can localize and be effective at the receiving end within a tumor microenvironment in most cases not conducive to the execution of their effector function (3-5).

Therefore, we suggest that the key to the understanding of this complex phenomenon relies on the real-time study of tumor/host interactions in the tumor microenvironment (6). Conventional immunology has extensively studied specific interactions between immune and cancer cells.

Additional investigations have identified cofactors that may enhance the effectiveness of such interactions. As the molecular understanding of individual interactions increases, it is becoming apparent that no single mechanism can in itself explain the phenomenon of tumor rejection.

Most likely, the contribution of several components of the innate and adaptive immune response is required for successful tumor rejection. These components may be variably recruited and activated within the tumor microenvironment by the production of molecules with immune modulatory properties by tumor and bystander cells. Such complexity can only be appreciated and solved by high throughput tools capable of providing a global view of biological processes as they occur (6).

We have previously suggested that a promising strategy for the understanding of melanoma immune responsiveness could consist of the study of tumor/host interactions *ex vivo* through genetic profiling of serial fine needle aspirate biopsies that allow direct correlation between experimental results and clinical outcome (7-9) (Figure 1, adapted from Ref. 7).

By prospectively studying the transcriptional profile of melanoma metastases during immunotherapy, we observed that immune responsiveness is predetermined by an immune reactive microenvironment. Interestingly, the addition of systemic interleukin-2 therapy to active specific immunization seems to increase the frequency of immune rejections of cancer. Functional profiling of the effect of interleukin-2 in tumors suggested that this cytokine induces or enhances the effector function of immunization-induced T cells by causing an acute inflammatory process at the tumor site that can in turn recruit and activate T cells (7-9).

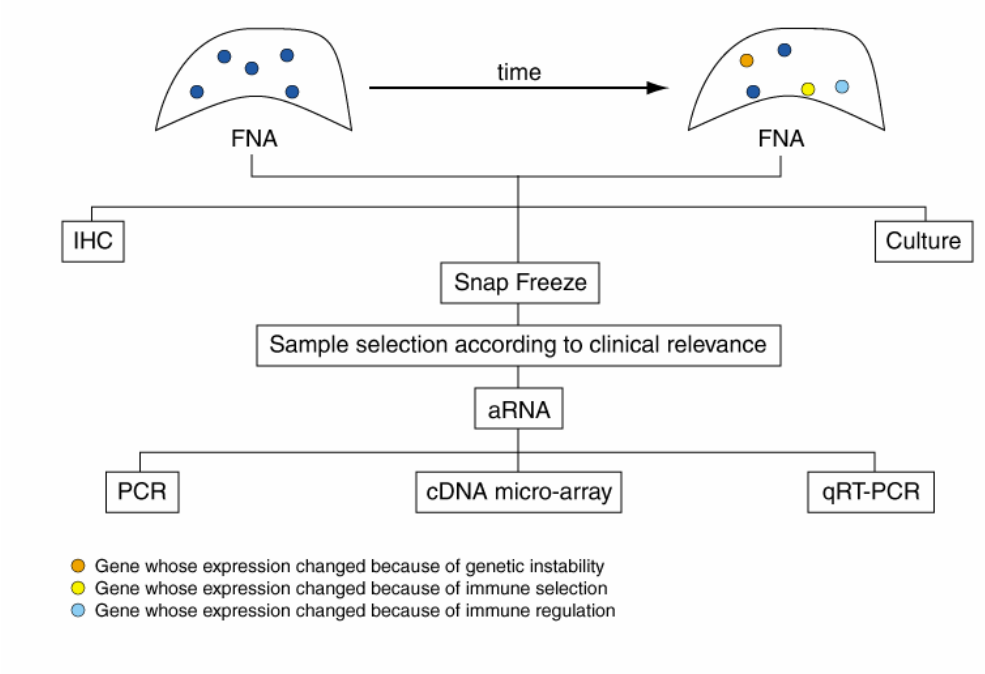

Figure 1. Suggested strategy for the collection of large libraries of relevant clinical samples with minimum cost and effort

The FNA sample is analyzed by IHC to ensure that adequate material is obtained. Cells from the aspirate are cultured in the presence or absence of IL-2 to develop TIL/tumor-cell pairs, and the majority of the specimen is simply frozen. Because of the relatively low incidence of clinical responses, it is expected that a large number of samples need to be collected to identify the few clearly responding lesions. These few clinically relevant samples and appropriate controls can then be processed further in gene expression analysis studies. Abbreviations: aRNA, anti-sense RNA; FNA, fine-needle aspirate; IHC, immunohistochemistry; IL-2, interleukin 2; qRT-PCR, quantitative real-time polymerase chain reaction; TIL, tumor-infiltrating lymphocyte

The basic understanding of the molecular basis of the immune response of the host against melanoma very much points to a tissue-specific event quite similar to the specialized rejection of allograft in transplantation, or the exquisite tissue-specificity of auto-immune responses such as in the case of thyroiditis, early onset insulin-dependent diabetes, systemic lupus erythematosus etc. As in allograft rejection and autoimmunity, the presence of antigen-specific immune responses seems to be a requisite of immune rejection, but it is not sufficient in itself and other triggering events are necessary to induce tumor rejection through a switch from a chronic to an acute inflammatory process (7), similarly to acute allograft rejection or the development of flares of autoimmunity (10-12). Interestingly, the identity of this secondary stimulus required for the completion of the immune rejection is becoming clearer in the last decade through the study of other rejection models encompassing experimental diabetes (10) or the immune-mediated rejection of basal cell carcinoma by toll receptor agonists (13) and kidney allograft rejection (12). Although the biology underlying rejection of cancer or allograft, determining autoimmunity or inducing tissues damage during pathogen infections is complex and multifaceted, common patterns are starting to emerge that lead to a common final outcome in which tissue destruction occurs that in some cases is associated with resolution of the pathogenic process (cancer, acute pathogen infection) in other unwanted side effects, tissue damage and organ failure.

Gene profiling analysis has recently pointed out similarities in various rejection models. Clinical observations based on global transcript analysis converge into common signatures; a first one, always presents in response to immune stimulation but not sufficient alone to induce rejection, is represented by the activation of genes associated with the function of type I or type II interferons (ISGs) (9,15). A second signature, more directly associated with immune rejection, appears to include activation of cellular effector mechanisms involving direct target killing (5,9,12). The cytokines responsible for such activation remain elusive, although recent work from our laboratory suggests that such cytokines may belong to the classic pathway of mononuclear phagocyte activation (15). While ISGs appear to be necessary but not sufficient alone to induce immunologically mediated tissue destruction, IEF signatures represent a recurrent theme in distinct pathological conditions and a valuable biomarker of terminal immune differentiation toward the elimination of unwanted tissues. This observation may reconcile the ambiguous role attributed to inflammation in cancer progression. It is clear that chronic inflammation promotes tumor growth, while acute inflammatory reactions are required for therapeutic effects against cancer.

References

1. van der Bruggen P, Traversari C, Chomez P, *et al*. A gene encoding an antigen recognized by cytolytic T lymphocytes on a human melanoma. *Science* 1991;254:1643-7.
2. Rosenberg SA. Cancer vaccines based on the identification of genes encoding cancer regression antigens. *Immunol Today* 1997;18:175-82.
3. Marincola FM, Wang E, Herlyn M, Seliger B, Ferrone S. Tumors as elusive targets of T cell-based active immunotherapy. *Trends Immunol* 2003;24:335-42.
4. Monsurrò V, Wang E, Panelli MC, Nagorsen D, Jin P, Katia Z, Smith K, Ngalame Y, Even J, Marincola FM. Active-specific immunization against cancer: is the problem at the receiving end? *Semin Cancer Biol* 2003;13:473-80.
5. Monsurrò V, Wang E, Yamano Y, Migueles SA, Panelli MC, Smith K, Nagorsen D, Connors M, Jacobson S, Marincola FM. Quiescent phenotype of tumor-specific CD8+ T cells following immunization. *Blood* 2004;104:1970-8.
6. Wang E, Panelli MC, Monsurro V, Marincola FM. A global approach to tumor immunology. *Cell Mol Immunol* 2004;1:256-65.
7. Wang E, Marincola FM. A natural history of melanoma: serial gene expression analysis. *Immunol Today* 2000;21:619-23.
8. Wang E, Miller LD, Ohnmacht GA, Mocellin S, Perez-Diez A, Petersen D, Zhao Y, Simon R, Powell JI, Asaki E, Alexander HR, Duray PH, Herlyn M, Restifo NP, Liu ET, Rosenberg SA, Marincola FM. Prospective molecular profiling of subcutaneous melanoma metastases suggests classifiers of immune responsiveness. *Cancer Res* 2002;62:3581-6.
9. Panelli MC, Wang E, Phan G, Puhlmann M, Miller L, Ohnmacht GA, Klein HG, Marincola FM. Gene-expression profiling of the response of peripharal blood mononuclear cells and melanoma metastases to systemic IL-2 administration. *Genome Biol* 2002;3:RESEARCH0035.
10. Lang KS, Recher M, Junt T, Navarini AA, Harris NL, Freigang S, Odermatt B, Conrad C, Ittner LM, Bauer S, Luther SA, Uematsu S, Akira S, Hengartner H, Zinkernagel RM. Toll-like receptor engagement converts T-cell autoreactivity into overt autoimmune disease. *Nat Med* 2005;11:138-45.
11. Ochsenbein AF, Klenerman P, Karrer U, Ludewig B, Pericin M, Hengartner H, Zinkernagel RM. Immune surveillance against a solid tumor fails because of immunological ignorance. *Proc Natl Acad Sci U S A* 1999;96:2233-8.

12. Sarwal M, Chua MS, Kambham N, Hsieh SC, Satterwhite T, Masek M, Salvatierra O Jr. Molecular heterogeneity in acute renal allograft rejection identified by DNA microarray profiling. *N Engl J Med* 2003;349:125-38.

13. Urosevic M, Maier T, Benninghoff B, Slade H, Burg G, Dummer R. Mechanisms underlying imiquimod-induced regression of basal cell carcinoma in vivo. *Arch Dermatol* 2003;139:1325-32.

14. Stroncek DF, Basil C, Nagorsen D, Deola S, Arico E, Smith K, Wang E, Marincola FM, Panelli MC. Delayed polarization of mononuclear phagocyte transcriptional program by type I interferon isoforms. *J Transl Med* 2005;3:24.

15. Nagorsen D, Deola S, Smith K, Wang E, Monsurro V, Zanovello P, Marincola FM, Panelli MC. Polarized monocyte response to cytokine stimulation. *Genome Biol* 2005;6:R15.

Session 1A. New therapeutic strategies

MICRORNAS IN HEMATOPOIESIS AND CANCER

Cesare Peschle
Department of Haematology, Oncology and Molecular Medicine, Istituto Superiore di Sanità, Rome, Italy

MicroRNAs (miRs) are a novel regulatory class of non-coding, single-stranded RNAs of ~22 nucleotides, identified in plants and animals. MiRs repress protein expression at post-transcriptional level, mostly through base pairing to the 3' untranslated region (UTR) of the target mRNA, thus leading to its degradation and/or reduced translation. MiRs have been shown to control basic biological functions, such as cell proliferation and differentiation. Furthermore, in diverse types of cancer miRs may function as "oncomirs". Despite these advances, only few targets for the ~300 known mammalian miRs have been validated so far.

Our group identified and characterized several miRs involved in the regulation of normal and neoplastic hematopoiesis and a miR that controls cardiac hypertrophy, as outlined below.

Dissecting microRNA expression in human hematopoiesis: lineage- and stage-specific profiles and functional significance

We have assayed the level of miRs in serum-free unilineage culture of cord blood (CB) CD34+ cells through the erythroid (E), megakaryocytic (Mk), granulocytic (G) and monocytic (Mo) series at discrete stages of differentiation up to terminal maturation. The assay included control CB T cells. The analysis was performed by microarray and confirmed by Northern blot. Altogether, 49 miRs are expressed at significant levels in hematopoiesis. Cluster analysis indicates lineage-specific expression patterns. Furthermore, miR levels are mostly downmodulated through the sequential stages of differentiation/maturation. A group of 12 single or clustered miRs is sharply modulated (> 10-fold) in hematopoiesis according to specific patterns, thus suggesting their key functional role.

This group includes: (a) miR-223, downmodulated in the E series, but upmodulated in the other lineages; (b) miR-221/222, miR-146 and miR-155 declining more sharply in E than other lineages; (c) miR-17/20/106 and miR-25, miR-32, declining prevailingly in the G and Mo series; (d) a miR group showing little downmodulation in the Mk or Mo lineages (miR-123, -130a or miR-181a, b, respectively); (e) miR-99b, -100 downmodulated in all lineages; (f) miR-210 upmodulated in all lineages. Bioinformatic analysis suggests that these miRs have important targets, which have been in part verified by the luciferase target assay.

Relevant examples include miR-221/222 and -130a targeting kit receptor, miR-146 targeting SDFR/CXCR4, miR 181a, b, 99b and 100, 210 targeting diverse HOX genes (respectively, HOXB5, A1 and A3).

Altogether, these studies pave the way to indepth studies on the regulatory role played by a large set of miRs in normal hematopoiesis.

MicroRNAs 221 and 222 inhibit normal erythropoiesis and erythroleukemic cell growth via Kit receptor downmodulation

In E culture of CB CD34+ progenitor cells, the level of miR 221 and 222 is gradually and sharply downmodulated. Hypothetically, this decline could promote erythropoiesis by unblocking expression of key functional proteins. Indeed, (a) bioinformatic analysis suggested that miR 221 and 222 target the 3'UTR of kit mRNA; (b) the luciferase assay confirmed that both miRs directly interact with the Kit mRNA target site; (c) in E culture undergoing exponential cell growth, miR downmodulation is inversely related to increasing Kit protein expression, whereas Kit mRNA level is relatively stable.

Functional studies show that treatment of CD34+ progenitors with miR 221 and 222, via oligonucleotide transfection or lentiviral vector infection, causes impaired proliferation and accelerated differentiation of E cells, coupled with downmodulation of Kit protein: this phenomenon, observed in E culture releasing endogenous Kit ligand (KL), is magnified in E culture supplemented with KL. Furthermore, transplantation experiments in NOD-SCID mice reveal that miR 221 and 222 treatment of CD34+ cells impairs their engraftment capacity and stem cell activity. Finally, miR 221 and 222 gene transfer impairs proliferation of the kit+ TF1 erythroleukemic cell line.

Altogether, our studies indicate that the decline of miR 221 and 222 during exponential E growth unblocks Kit protein production at mRNA level, thus leading to expansion of early erythroblasts. Furthermore, the results on Kit+ erythroleukemic cells suggest a potential role of these microRNAs in cancer therapy.

MicroRNAs 155, 221 and 222 control megakaryopoiesis at progenitor and precursor level through Ets-1 multitargeting

MiR expression profiling in unilineage MK culture of human CB CD34+ hematopoietic progenitor cells (HPCs) indicated that miR-155, -221 and -222 are abundant in HPCs, but then sharply decline starting from initial MK differentiation. Hypothetically, this decline may promote megakaryopoiesis by favouring expression of a key functional target. Bioinformatic analysis predicted that miR-155, -221 and -222 target Ets-1, a transcription factor up-regulated in megakaryopoiesis, which transactivates relevant Mk genes. Luciferase assay indicated a direct interaction of each of these miRs with the 3'UTR of Ets-1.

Functional studies showed that enhanced expression of the three miRs impairs proliferation, differentiation and maturation of MK cells. This inhibition is largely mediated via enhanced degradation of Ets1 mRNA and down-modulation of Ets-1 protein: in fact, similar inhibitory results were obtained by RNA interference against Ets-1. Finally, HPCs transfected with miR-155, -221, and -222 showed a significant reduction of their MK clonogenic capacity, suggesting that down-modulation of these miRs favours MK progenitor recruitment and commitment.

Altogether, our results indicate that miR-155/221/222 control the Mk lineage at both progenitor and precursor level through Ets-1 mRNA multitargeting.

MicroRNAs 17-5p/20a/106a function as a master gene complex controlling monocytopoiesis through AML1 targeting

We investigated the role of miR 17-5p, 20a and 106a in Mo differentiation-maturation. In unilineage Mo culture generated by CB hematopoietic progenitor cells these miRs are downmodulated, whereas the transcription factor AML1 is upmodulated at protein but not mRNA level. Since miR-17/20/106 bind the AML1 mRNA 3'UTR, their decline may unblock AML1 translation. Accordingly, miR-17/20/106 transfection suppresses AML1 protein expression, leading to M-CSF receptor (M-CSFR) downmodulation, stimulates blast proliferation and inhibits Mo differentiation-maturation. Treatment with anti-miR-17/20/106 oligonucleotides causes opposite effects. Knockdown of AML1 by siRNA mimics the action of miR-17/20/106 on monocytopoiesis, indicating that AML1 is the major target of miR-17/20/106. In addition, AML1 binds the miR-17 cluster promoter and transcriptionally inhibits miR-17/20 expression.

These studies indicate that monocytopoiesis is controlled by a regulatory circuitry involving miR-17/20/106, AML1 and M-CSFR, whereby miR-17/20/106 function as a master gene complex interlinked with AML1 in a mutual negative feedback loop.

MicroRNA-133 controls cardiac myocyte hypertrophy

We report that the cardiac-specific miR-133 is critical in determining cardiac myocyte cell (CMC) hypertrophy. Endogenous expression of miR-133 is markedly downmodulated in cardiac hypertrophy. Both *in vitro* and *in vivo* functional studies indicate that: (a) miR-133 enforced expression suppresses hypertrophy, as indicated by increased CMC size and protein synthesis, cytoskeletal structural reorganization and re-expression of fetal genes. Conversely, (b) suppression of miR-133 by decoy sequences induces a dramatic CMC hypertrophy, even in the absence of any hypertrophic stimuli. We also identify targets of miR-133, including the nuclear factor NELF-A, involved in heart genesis, and the signal transduction kinase CDC42, implicated in hypertrophy; expression of both targets is inversely related to miR-133 expression at protein level, whereas mRNA expression is unmodified.

Altogether, our data indicate that miR-133 is a master gene controlling cardiac hypertrophy.

References

1. Felli N, *et al*. Dissecting microRNA expression profiles in human hematopoiesis: lineage- and stage-specific patterns and potential functional significance. *Proc Natl Acad Sci* (*in preparation*).
2. Felli N, Fontana L, Pelosi E, Botta R, Bonci D, Facchiano F, Liuzzi F, Lulli V, Morsilli O, Santoro S, Valtieri M, Calin GA, Liu Chang-Gong, Sorrentino A, Croce CM, Peschle C. MicroRNAs 221 and 222 inhibit normal erythropoiesis and erythroleukemic cell growth via kit receptor downmodulation. *Proc Natl Acad Sci* 2005;102:18081-6.
3. Marziali G, Pelosi E, Lulli V, Biffoni M, Felli N, Romania P, Liuzzi F, Croce CM, Fontana L, Coppola S, Peschle C. MicroRNAs 155, 221 and 222 control megakaryopoiesis at progenitor and precursor level through Ets-1 multitargeting. *J Exp Med* (*submitted*).

4. Fontana L, Pelosi E, Greco P, Testa U, Liuzzi F, Croce CM, Brunetti E, Peschle C. The microRNAs 17-5p/-20a/106a function as a master gene complex controlling monocytopoiesis through AML1 targeting. *Nat Cell Biol* (*Article, submitted*).
5. Carè A, Catalucci D, Felicetti F, Bonci D, Ruiz-Lozano P, Gallo P, Segnalini P, Bang ML, Croce CM, Peschle C, Condorelli GL. MicroRNA 133 controls cardiac myocyte hypertrophy. *Nat Med* (*Article, under revision*).

Session 1A. New therapeutic strategies

CLINICAL TRIALS USING IFN-α AS A VACCINE ADJUVANT: NEW STRATEGIES FOR THE MOLECULAR MONITORING OF THE IMMUNE RESPONSE

Filippo Belardelli (a), Eleonora Aricò (a), Franco Marincola (b), Ena Wang (b)
(a) Department of Cell Biology and Neurosciences, Istituto Superiore di Sanità, Rome, Italy
(b) Department of Transfusion Medicine, Clinical Centre, NIH, Bethesda, USA

Background and major objectives

Dr. Belardelli's group at the ISS has been working for many years on the mechanisms of antitumor action of IFN-α. The results of recent studies performed by the ISS group have provided evidence on novel activities exerted by IFN on cells of the immune system, including promoting effects on the differentiation/activation of dendritic cells (DCs). These results have represented the background for suggesting a novel use of IFN-α as vaccine adjuvant in humans. Recently, the ISS group has coordinated a pilot trial aimed at determining the effects of IFN-α, administered as adjuvant of Melan-A/MART1 and gp100 peptides, on immune responses in stage IV melanoma patients. A marked enhancement of $CD8^+$ T cells recognizing melanoma peptides was observed, along with increase in the percentage of monocyte/dendritic cell precursors expressing co-stimulatory molecules (1). Other two clinical studies aimed at evaluating the vaccine adjuvant activity of IFN-α in anti-HBV vaccination strategies on both in healthy subjects and in immunocompromised patients have been promoted by the ISS group. These trials have been funded by the EC and are still in course. In addition to the antibody response, other immunological end-points, including the T cell response to HBV antigens and the phenotype/function of monocytes/DC precursors, are included in these studies. While the immunological end-points of these studies are expected to provide important information on the *in vivo* effects of IFN-α as immune adjuvant, there is the important need to define new strategies for the molecular tracking of the immune response. In this regard, Dr. F. Marincola (NIH) has recently developed new methods for the monitoring of the antitumor immune response based on the use of microarrays technology providing a first "proof of evidence" on the potential importance of these novel methodologies. Thus, the main general objective of this project was to develop a strategic interaction between these two laboratories aimed at defining new methods and novel platforms for a molecular tracking of the immune response suitable for monitoring and possibly predicting the response to IFN-α used as a vaccine adjuvant in clinical trials. To foster the interaction between the 2 groups, a researcher from the ISS (Dr. E. Aricò) has spent 2 years in Dr. Marincola's laboratory at the NIH, with the specific aim to develop new microarrays technologies particularly suitable for a molecular tracking of the response to IFN using peripheral blood mononuclear cells (PBMC) from cytokine-treated patients.

Another objective of this project was to develop a new platform for the analysis of the single nucleotide polymorphisms in several cytokine and cytokine receptors, with particular interest in the role of the SNP present in the genes encoding for IFN-α and IFN-α receptor in the response to the cytokine. This part of the project has been initiated by Dr. Aricò in Dr. Marincola's

laboratory but is still ongoing, and will be continued in Dr. Belardelli's laboratory after Dr. Aricò has moved back to Rome.

Main results

Studies on gene expression profiles in PBMCs from melanoma patients treated with IFN- α and melanoma peptides

In the context of the clinical study mentioned above (1), we used microarray technology to profile gene expression in PBMC from melanoma patients treated with tumor antigen peptides in combination with IFN-α. PBMC were isolated before and 24 hours following IFN-α administration. Collections coincided with the 1st and 4th vaccinations (times T0 and T42 days, respectively). Total RNA isolated from PBMC underwent two rounds of amplifications to obtain antisense RNA. Test samples and reference sample were labeled with Cy5-dUTP and Cy3-dUTP respectively. Test-reference sample pairs were mixed and co-hybridized to custom made17K cDNA microarrays. Data were analyzed via mAdb Gateway Analysis tool, and further analyzed using Cluster and TreeView software. Unsupervised hierarchical clustering (class discovery) of the complete data set did not segregate PBMC collected before from those collected after IFN-α treatment. However, an IFN-α signature was clearly detectable when supervised clustering (class comparison) was performed. In particular, 35 genes were specifically induced by the IFN-α treatment, during the first and the second round of treatment. Comparison of gene-expression patterns between the samples collected before and after the first IFN-α treatment identified 134 genes differentially expressed at a <0.005 significance level. Interestingly, unsupervised hierarchical clustering based on these genes distinguished the samples collected before and after the second IFN-α administration (class prediction) confirming that this signature is consistently induced by IFN-α treatment. In a separate study, we have also used microarrays to characterize the molecular gene expression profiles of DCs generated *in vitro* from monocytes after IFN-α treatment as compared to reference cells. Of note, there was a common signature of IFN-induced genes, which included genes involved in immunological pathways, such as antigen processing and presentation, cytokine and chemokine activity. In conclusion, our study provides a global description of the *in vivo* effects of IFN-α and its molecular signature, thus opening perspectives into the comprehension of the mechanisms of action and, possibly, into the identification of molecular markers of the clinical response to IFN.

Studies on PBMC from healthy subjects vaccinated with HBV vaccine and IFN-α used as an adjuvant

PBMCs from healthy subjects vaccinated with the HBV vaccine were use for gene profile analyses. Cells were collected on four different time points: before (T0) and 24 hours after (T0+24) the first vaccine administration, before (T1m) and 24 hours after (T1m+24) the second vaccine administration (1 month). Gene profiling analysis was first performed on samples collected from 5 donors from groups vaccinated with HBV vaccine plus placebo or with 1MU or 3MU of IFN-α. PBMC RNA was labeled by *in vitro* retrotranscription in the presence of Cy5-dUTP. At the same time, a reference RNA, consisting of a pool of RNAs isolated from untreated healthy donors, was labeled by *in vitro* retrotranscription in the presence of Cy3-dUTP. Test and reference samples were mixed in equal proportion and co-hybridized to the

array slides. After the detection of the fluorescent signal, data were analyzed using Eisen cluster and Treeview software, and by application of statistical analysis. We first analyzed samples collected from donors receiving placebo together with the vaccine, by performing a Class Comparison between PBMCs collected before and after both cycles of vaccination. From an ensemble of analyses, we concluded that no significant effect on PBMC gene expression profile could be ascribed to the administration of vaccine administered with placebo. We then moved to analyze the effects of the simultaneous administration of vaccine and IFN-α on gene expression profile. We first focused on the group of donors receiving 1 MU of IFN-α, by performing a class comparison between PBMC collected on T0 and T0+24. The results showed that 301 genes were differentially expressed between these time points. The same kind of analysis was carried out on PBMCs collected before and after the second cycle of vaccination, and revealed that 171 genes were differentially expressed between samples collected on T1m and 24 hours after the treatment. Interestingly, when we used the genes found to be differentially expressed between T0 and T0+24 to cluster all samples collected during the study, we obtained the segregation of all PBMCs collected before from PBMCs collected after the vaccine+IFN administration, regardless of the time they were collected. This observation indicated that the effects of the treatment of vaccine+IFN on PBMC gene expression profile were consistently induced after each repeated administration of the treatment; thus, according to the modulation observed after the first vaccination cycle, it was possible to predict what was going to happen after the second one. The comparison of the lists of genes modulated after the first or the second vaccination cycle confirmed the consistency of the transcripts whose expression was affected by the first or second vaccine+IFN administration. The functional annotation of these transcripts revealed that most of the genes downregulated by the treatment were involved in cellular metabolism and other cellular processes, while genes upregulated by vaccine+IFN administration belonged to the defense response, intracellular signaling cascade, regulation of cell proliferation and protein metabolism functional categories. Of note, the list of genes whose expression was augmented after vaccine+IFN administration, did not include only genes known to be induced by the cytokine, like the ones encoding oligo 2',5'-oligoadenylate synthetase, MxA and B (interferon-induced cellular resistance mediator protein), and many other interferon-inducible proteins. Many genes involved in other relevant immunological functions were also induced by the vaccine+IFN administration (Table 1). Among them, we found genes encoding for proteasome subunits and ubiquitin-related protein degradation, IL-15 and its receptor, chemokines, TLR-6 and genes involved in T cell mediated response. A more extensive analysis of the lists of genes modulated by 1 MU of IFN-α is currently under way, together with the examination of PBMCs collected from donors receiving 3 MU of IFN-α together with the vaccine.

Although a direct comparison of the results obtained in the two different studies was not possible, due to the different conditions in which the blood samples had been collected, we tried to verify whether the same gene lists were modulated by the IFN treatment in the two cohorts of patients. To this aim, we selected the list of genes found to be upregulated 24 hours after the IFN treatment in melanoma patients, and used this list to cluster samples collected from healthy donors in the HBV study. Interestingly, according to the gene expression of this gene list, we could segregate samples collected from healthy donors before the treatment from samples collected after IFN administration, showing that the modulation of these genes exerted by IFN was similar in the two cases. The same segregation was obtained when we selected genes upregulated in healthy donors after IFN treatment and used them to cluster samples collected in the melanoma study. Also in this case, samples segregated according to the treatment. These results showed that, in spite of the differences found in the lists of genes significantly up or downregulated after the IFN treatment, the modulation of the all set of genes was similar in the two studies (Figure 1).

Table 1. Genes up-regulated 24 hrs after the IFN treatment annotated in the Immune Response gene group

Gene	Description
ADAR	adenosine deaminas
APOL3	apolipoprotein L, 3
BST2	bone marrow stromal cell antigen 2
C2	complement component 2
C3AR1	C3a receptor
CCR1	C-C chemokine receptor 1
CXCL10	chemokine (C-X-C motif) ligand 10
FCGR1A	immunogobulin gamma FC receptor
FCGR3A	CD16=Fcgamma receptor IIIa
FCN2	ficolin
G1P2	Interferon-induced 17 KD protein
G1P3	interferon, alpha-inducible protein (clone IFI-6-16)
GBP1	guanylate binding protein 1
HLA-A	major histocompatibility complex, class I, A
HLA-DOA	MHC Class II=DN alpha
HLA-F	major histocompatibility complex, class I, F
IFI16	IFI16=interferon-gamma-inducible
IFIT1	Interferon-induced 56-KDa protein
IFIT2	Interferon-induced 54 KD protein
IFITM2	interferon induced transmembrane protein 2 (1-8D)
IFITM3	Interferon-inducible protein 1-8U
IL1RN	IL-1 receptor antagonist
IRF7	IRF-7=interferon regulatory factor-7
ITGAL	CD11A=Integrin, alpha
LGALS3BP	Mac-2 binding protein
MX1	interferon-induced cellular resistance mediator protein
MX2	interferon-induced cellular resistance mediator protein
NMI	IL-2 and IFN-gamma inducible potentiator of STAT
OAS1	2',5'-oligoadenylate synthetase 1
OAS2	2'-5'-oligoadenylate synthetase 2
PLA2G4B	phospholipase A2
PSME2	proteasome activator subunit 2 (PA28 beta)
SERPING1	serine (or cysteine) proteinase inhibitor
SN	sialoadhesin
TLR6	toll-like receptor 6
TNFSF10	TRAIL=Apo-2 ligand
TNFSF13B	BAFF
TRIM22	tripartite motif-containing 22
TYROBP	TYRO protein tyrosine kinase binding protein

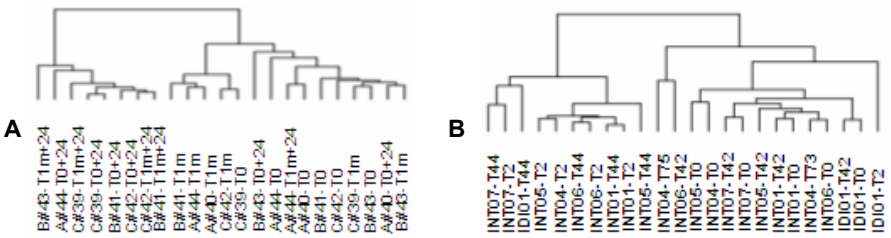

Figure 1. Comparison of the expression of the genes upregulated by the IFN-α in the 2 clinical trials reported.

***A**: The clustering analysis of the samples collected in the HBV study was limited to the genes found upregulated after the IFN treatment in melanoma patients. Based on the expression of these genes, samples collected before and after the treatment clustered separately, showing that a similar modulation of the transcription profile was obtained in the two cohorts of subjects. **B**: the same analysis was performed by using the genes upregulated after the IFN treatment in healthy donors to cluster samples collected during the melanoma trial, which segregated according to the treatment.*

Development and validation of a SNP platform for cytokine and cytokine-related genes.

The two laboratories are also cooperating for the development of a new microarray platform for measuring single nucleotide polymorphisms (SNP) for the IFN receptor with the final aim of establishing a novel and validated strategy for predicting the response to IFN using DNA samples from patients.

The platform has been designed and obtained in Dr. Marincola's laboratory, and it will be fully validated at the ISS by Dr. Aricò in collaboration with other ISS researchers involved in microarray-based studies. In particular, the *in vitro* model of peripheral blood isolated monocytes shortly exposed to IFN was developed, and the response to the cytokine in terms of transcriptional profiling and release of soluble factors in the supernatants was analyzed. These features will be evaluated together with the presence of SNP in IFN and IFN receptor genes in donors' DNA, in order to find possible correlations between the response to the cytokine and the presence of SNP in IFN and IFN receptor genes. The discovery of functional SNP involved in the response to IFN-α will be eventually exploited to the SNP analysis on the DNA collected in the clinical trials mentioned above, and the possible correlation between the presence of SNP and different patterns of gene expression profiles observed in different individuals after the administration of the IFN-α will be also evaluated.

References

1. Di Pucchio T, Pilla L, Capone I, Ferrantini M, Montefiore E, Urbani F, Patuzzo R, Pennacchioli E, Santinami M, Cova A, Sovena G, Arienti F, Lombardo C, Lombardi A, Caporaso P, D'Atri S, Marchetti P, Bonmassar E, Parmiani G, Belardelli F, Rivoltini L. Immunization of stage IV melanoma patients with Melan-A/MART-1 and gp100 peptides plus IFN-α results in the activation of specific CD8+ T cells and monocyte/dendritic cell precursors. *Cancer Res* 2006;66:4943-51.
2. Aricò E, Wang E, Tornesello ML, Tagliamonte M, Lewis GK, Marincola FM, Buonaguro FM, Buonaguro L. Immature monocyte derived dendritic cells gene expression profile in response to Virus-Like Particles stimulation. *J Transl Med* 2005;3:45.
3. Stroncek DF, Basil C, Nagorsen D, Deola S, Aricò E, Smith K, Wang E, Marincola FM, Panelli MC. Delayed polarization of mononuclear phagocyte transcriptional program by type I interferon isoforms. *J Transl Med* 2005;3:24.
4. Gabriele L, Moretti F, Pierotti MA, Marincola FM, Foà R, Belardelli F. The use of microarray technologies in clinical oncology. *J Transl Med* 2006;4:8.

Session 1A. New therapeutic strategies

IDENTIFICATION OF NEW TUMOR-ASSOCIATED ANTIGENS AND THEIR USAGE FOR NEW THERAPEUTIC STRATEGIES BASED ON THE COMBINATION OF CHEMOTHERAPY AND IMMUNOTHERAPY FOR COLORECTAL CANCER PATIENTS

Enrico Proietti (a), Cristina Maccalli (a), Steven A Rosenberg (b), Paul F Robbins (b)
(a) Department of Cell Biology and Neurosciences, Istituto Superiore di Sanità, Rome, Italy
(b) Surgery Branch, NCI, NIH, Bethesda, MD, USA

Scientific background

Colorectal cancer (CRC) is one of the more frequent cancers in Western Countries and the prognosis is fatal for patients with advanced disease. The lack of spontaneous regression (Francis et al., *Br J Surg* 84,1997), the described low frequency of the *in vitro* generation of tumor specific T cells from tumor infiltrating lymphocytes (TIL) (Balch et al., *Arch Surg*, 125, 1990) and the failure (Rosenberg et al., *J Clin Oncol*, 10, 1992; Hawkins et al., J. *Immunother*, 15, 1994; Greco et al., *J Clin Oncol*, 14, 1996) in clinical response by the first generation of immunotherapy protocols for CRC led to consider this tumor poorly immunogenic and refractory to immunotherapy. However, the progress in the knowledge of tumor immunobiology, in the methods for molecular identification of TAA recognized by T cells and for the *in vivo* enhancement of the immune response through myelodepletion, contributed to open new perspectives in the immunotherapy of CRC. Indeed, the presence of intra-epithelial CD8+ T cells in CRC lesions has been shown as a strong predictor of better survival independently on Duke's stage (Naito et al., *Cancer Res*, 58, 1996; Guidoboni et al. *Am J Pathol*, 159, 2001), indicating the compatibility with the antitumor immunity theory in which CD8+ T cells play a central role as effectors of antitumor activity. Pre-clinical studies have produced a consistent amount of data regarding the need to overcome suppressive regulatory and tolerogenic control of T cell subsets in tumor-bearing hosts (Antony et al., *J Immunother*, 25, 2002; Overwijk et al., *J Exp Med*, 198, 2003) and the positive influence of chemotherapy treatment on the activation/expansion of adoptively transferred tumor-specific T cells (North et. al., *J Exp Med*, 4, 1982; Proietti et al. *J Clin Invest* 2, 1998). In particular, a non-myeloablative dose of cyclophosphamide (CTX) or a gamma ray sub-lethal irradiation administered 5 hrs prior to immune cell adoptive transfer (given as a whole splenocyte population), completely cured mice bearing highly metastatic tumor implants, whereas single treatments failed. Furthermore, adoptive cell transfer following non-myeloablative chemotherapy provides the opportunity to overcome tolerogenic mechanisms; indeed, results from clinical trials demonstrated the engraftment and persistence in the peripheral blood of transferred cells in correlation with significant clinical response for neoplastic patients (Dudley et al., *Science*, 25, 2002; Dudley et al., *Nat Rev Cancer*, 9, 2003).

Progress report

The principal objectives of this study are: 1. to extend the molecular and functional characterization of new TAA for CRC and verify whether these molecules can represent molecular targets for the prognosis and the therapy of this disease; 2. the transfer of the obtained results from point 1 to design new clinical trials based on the combination of chemotherapy and immunotherapy (active immunization or adoptive cell transfer) for CRC patients.

Characterization of new TAAs in CRC

Objectives of the first part of this project are: i) to validate the relevance of the new tumor associated antigen COA-1 in eliciting an immune response in CRC patients and to determine whether the immune response against this TAA can correlate with the progression of the disease; ii) to determine new HLA class I or class II-restricted epitopes isolated from COA-1 that can elicit an antitumor immune response; iii) to identify new TAAs for CRC.

i) A study recently carried out at NCI (Surgery Branch, Chief. Dr. Rosenberg, NCI, NIH, Bethesda, MD, USA) aimed to the immunological characterization of CRC led to the identification of a novel TAA, denominated COA-1 (Maccalli et al., *Cancer Res* 63, 2003). The COA-1-derived immunogenic epitope was identified and shown to be recognized by $CD4^+$ T lymphocytes in association with HLA DRβ1*0402 or *1301 molecules. With the aim to validate the immunological role of this TAA for CRC, pre-clinical studies have been set-up to verify the immunogenic potency of the new TAA COA (Maccalli et al., 2003); *in vitro* stimulation of PBMCs from DRβ1*0402^+ or *1301^+ CRC patients with the COA-1 derived HLA class II-restricted epitope have been carried out. We could isolate anti-COA-1 and tumor specific $CD4^+$ T cells from all the evaluated patients (n.7) with progressive disease (Duke's stage C and D); on the contrary, a failure in generating COA-1 specific T cells was observed in CRC patient (n.4) with early stage tumor (Dukes' A and B). These results indicate that COA-1 can be a relevant antigen for the antitumor immune response in CRC patients correlating with the progression of the disease (manuscript in preparation). Furthermore, dendritic cells generated by 3-day culture with IFN-α and GM-CSF (IFN-DCs) from monocytes of one CRC patient have been used in an autologous setting, after loading with CRC cell lysate, for *in vitro* stimulation of PBMCs leading to the isolation of either anti-COA-1 and tumor reactive $CD4^+$ lymphocytes, see Figure 1. These evidences suggest that COA-1 can represent an immunodominant antigen mediating an antitumor immune response in CRC patients (manuscript in preparation). The laser scanning co-focal microscopy analysis, carried out on a panel of normal and tumor cell lines by using a specific polyclonal antibody directed to COA-1, showed a differential pattern of cellular distribution and of association with members of the cytoskeleton between normal and tumour cells. Furthermore, different mechanisms of cellular processing and trafficking of this TAA have been demonstrated in normal or tumour cell lines (manuscript in preparation). Moreover, we are currently investigating the antibody response directed to COA-1 in CRC patients: preliminary results showed that specific antibodies could be found only in the cases with detectable tumor mass. We have been collecting serum from CRC patients at different stage of the disease with the aim to confirm these results and to correlate them with the follow-up of the patients. Moreover, the possible presence of soluble protein, as native or modified form, in the serum of these patients will be investigated. The conclusive data will allow identifying whether this antigen can represent a marker for the prognosis of the disease.

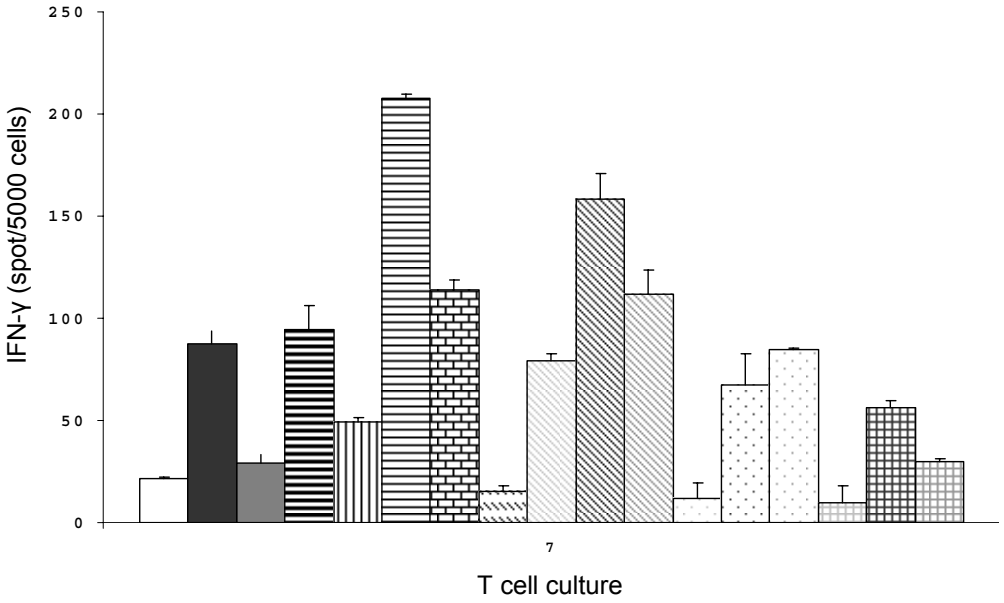

PBMCs isolated from one DRβ1*0402$^+$ and 1301$^+$ CRC patient were *in vitro* stimulated with autologous IFN-DCs pulsed with the autologous tumor cell lysate. Seven independent T cell cultures were set-up and weekly re-stimulated with autologous IFN-DCs loaded with tumor lysate; after 3 weeks of culture the reactivity of these T lymphocytes was evaluated by detection of IFN-γ release (ELISPOT) after incubation with the following target cells: the autologous DRβ1*0402$^+$ and *1301$^+$ 1869 col. tumor cell line (black bar); the 1869 col. cells pre-incubated with anti-HLA-DR mAb L.2.4.3 (grey bar); the autologous DRβ1*0402$^+$ and *1301$^+$ 1869 col. tumor cell line transduced with a retroviral vector encoding for CIITA (1869-CIITA) (bar with dark horizontal lines); the 1869-CIITA col. cells pre-incubated with anti-HLA-DR mAb L.2.4.3 (bar with vertical lines); the allogeneic DRβ1*0402$^+$ 1847 col. cells (bar with grey horizontal lines); the 1847 col. tumor cells pre-incubated with anti-HLA-DR mAb L.2.4.3 (walled bar); the autologous B cells *in vitro* culture with CD40L (CD40L-B, bar with diagonal dotted lines); the autologous 1869 EBV-B cell lines (bar with clear grey diagonal lines); the 1869 EBV-B cells pulsed with COA-1 epitope (bar with black diagonal lines); the 1869 EBV-B cells pulsed with COA-1 epitope and incubated with anti-HLA-DR mAb L.2.4.3 (bar with dark grey vertical lines); the 293 cells expressing DRβ1*0402 or DRβ1*1301) and transiently transfected with the pcDNA3.1 vector encoding for GFP (clear dotted bar or bar with clear small squares, respectively) or for COA-1 (black dotted bar or bar with black small squares, respectively) black dotted or horizontal wall bar) or for carrying the 3' end of the COA-1 gene (1D8, grey dotted bar or bar with grey small squares, respectively). The data in the Figure are representative of one T cell culture (n.7). The data shown represent averages of triplicates with SD≤ 15 %; statistical analysis of differences between means of IFN-γ released by T cells has been performed by two-tailed t-test.

Figure 1. IFN-γ released by PBMCs from one CRC patients *in vitro* stimulated with IFN-DCs loaded with the autologous tumor cell lysate

ii) We have identified, using specific software, a list of COA-1-derived peptides binding to HLA-A2 molecules. The application of the iTopia technology by Beckman Coulter (Bachinsky et al., 2005) led to the determination, by *in vitro* functional analysis, of the effective efficiency and stability of the peptides/MHC complexes, allowing us to select a limited number (n.6) of functionally characterized peptides to be used for *in vitro* stimulation of PBMCs isolated from HLA-A2$^+$ CRC patients. We have carried out preliminary experiments for one CRC patient leading to the identification of three HLA class I-restricted immunogenic epitope that could elicit anti-COA-1 and tumor specific CD8$^+$ T lymphocytes. Though these experiments need to be extended to all the selected HLA-A2$^+$ CRC patients, the available results indicate that MHC class I-restricted epitope can be isolated from the TAA COA-1, and that this antigen can represent a useful tool to characterize the immune response to CRC and to design new immunotherapy clinical trials.

iii) The possibility to isolate new TAAs for CRC will be investigated. IFN-DCs loaded with tumor lysates or tumor derived apoptotic bodies will be used, in an autologous setting, for eliciting T cell-mediated antitumor response from PBMCs of CRC patients. These T cell populations will represent valuable and necessary probes for the identification of new TAAs. The molecular isolation of TAAs recognized by these T cells will be achieved by strategies previously used to identify most of melanoma-associated antigens and the COA-1 antigen (Maccalli et al, 2003). The realization of this experimental part is dependent on the availability of *in vitro* established CRC cell lines or purified tumor cells from surgical specimens and autologous PBMCs collected at different time point to obtain enough cells to generate either DCs or effectors T lymphocytes. We have been collected reagents from CRC patients and we have successfully *in vitro* established tumor cell lines from two CRC patients. These reagents will allow setting up the described experiment. Once new TAAs will be isolated from CRC, *in vitro* pre-clinical studies will be carried out to allow their validation as useful reagents to induce a specific immune response in CRC patients.
Taken together the results obtained from this part of the study will not only allow us to validate the usage of COA-1 antigen for active immunization of cancer patients, but will also enable us to verify a possible special efficacy of IFN-DCs in inducing anti-CRC immune responses.

The transfer of the obtained results from point 1 to design new clinical trials based on the combination of chemotherapy and immunotherapy (active immunization or adoptive cell transfer) for CRC patients

This part of the project was focused on the definition of the parameters crucial for an autologous antitumor lymphocyte transfer in CRC patients following a non-myeloablative conditioning regimen.

To this purpose, preclinical studies in murine models were performed showing the importance of chemotherapy treatment before lymphocyte administration in activating tumor-specific cytotoxic T cell expansion and migration into the tumor tissue and in inducing a subsequent tumor rejection. As one of the mechanisms involved in chemotherapy-induced T cell activation/expansion is the over production of cytokines controlling the lympho-hemopoiesis (cytokine storm), we performed an extensive real time PCR analyses to characterize the cytokines induced by cyclophosphamide administration in the spleen, lymphnodes and bone marrow cells from tumor-bearing transferred mice

The results obtained (Table 1) showed, for the first time, that CTX administration actively induces the expression of common gamma chain cytokines as well as hemopoietic factors regulating homeostatic expansion. In fact, two days after CTX treatment IL-7, IL-2 and IL-21 were strongly over-expressed in the bone marrows of treated mice. Of note, the expression of IL-7 and IL-15 mRNA was also increased in the spleen. It is generally assumed that homeostatic proliferation is mainly driven by cytokines sharing a common gamma chain in their receptors (IL-2, IL-7, IL-15 and IL-21). Among these cytokines, IL-7 is known to play a pivotal role, as it was shown to be indispensable for homeostatic expansion of naive $CD8^+$ and $CD4^+$ T cells in lymphopenic hosts and for $CD8^+$ T cell survival in normal hosts. IL-15 is involved in the control of memory $CD8^+$ T cell survival and division and can enhance the *in vivo* antitumor activity of adoptively transferred, tumor-reactive $CD8^+$ T cell. In addition, IL-21 can synergize with either IL-7 or IL-15 in driving the proliferation of $CD8^+$ T cells, in inducing the differentiation of B cells into plasma cells and in enhancing the activity of NK cells. On the contrary, homeostatic cytokines do not induce proliferation of regulatory T cells and, in addition, IL-7 and IL-15 can abrogate their suppressive activity.

Table 1. Evaluation of cytokine gene expression after CTX treatment

mRNA (day 2)	Fold increase (mean)	
	bone marrow	spleen
GM-CSF	9.82	2.43
IL-1	2.81	0.67
IL-7	17.76	2.92
IL-15	1.53	2.34
IL-2	3.95	1.02
IL-21	5.52	0.71
IFN-γ	6.08	1.06
IL-4	0.86	0.94
IL-10	8.12	0.82
TNF-α	1.41	1.79
IL-6	0.68	0.65
IL-13	7.94	1.88

C57BL/6 mice were injected s.c. with RBL-5 tumor cells. Eleven days later, mice were treated i.p. with CTX or left untreated as control. Two days after CTX injection, bone marrows (BM) and spleens (Spl) were collected and GM-CSF, IL-1β, IL-7, IL-15, IL-2, IL-21, IFN-γ, IL-4, IL-10, TNF-α, IL-6 and IL-13 gene expression was analyzed by real-time PCR. Relative mRNA levels were calculated by the comparative cycle threshold (CT) method and were normalized by β-actin expression. Each value represents the mean fold change of mRNA level of five individual mice with respect to the mean level of the corresponding untreated controls (only changes higher than 2-fold are considered statistically significant).

Finally, we analyzed the expression of cytokines involved in the polarization towards a Th1 or a Th2 type of immune response. Real-time PCR experiments showed that the Th1 cytokines IL-2 and IFN-γ were over-expressed two days after CTX administration, while IL-4 (Th2 cytokine) and IL-6 were down-regulated. The finding that IL-10 and IL-13 mRNAs were also increased upon CTX treatment suggests that CTX can initially induce a Th0 phenotype, which is followed by a polarization toward a Th1 type of immune response, as suggested by the increase of IFN- γ and the decrease of IL-10 plasma levels in mice treated with CTX and immune cell adoptive transfer. Of note, IL-13 has been shown to affect the activation and maturation of dendritic cells and to prevent the blockade of their differentiation induced by tumor cells and may therefore counteract escape mechanisms exploited by tumors at this level.

Altogether these results suggest a new mechanism by which CTX, through the induction of homeostatic cytokines, may redirect the immune system from a state of tolerance to an effective antitumor immunity.

On the basis of these preclinical results, a clinical trial was set up to demonstrate the ability of a chemotherapeutic drug to enhance a tumor-specific immune response in patients treated with a tumor vaccine. This study, performed in melanoma patients, as a first model for a well antigenically characterized tumor, combined a standard dacarbazine (DTIC, a cyclophosphamide analogue) treatment with the vaccination with melanoma peptides (Melan-A/Mart-1 and Gp 100) in association with Montanide and interferon alpha. The results obtained in 10 patients (5 patients treated with vaccine alone and 5 patients treated with vaccine + DTIC) showed that DTIC strongly increased the number and the cytolytic activity of tumor-specific T lymphocytes, thus demonstrating, for the first time, the need of combining chemotherapy with a tumor vaccine to increase antitumor immune responses. Further clinical studies have been planned to combine chemotherapy and antitumor COA-1 vaccination in CRC patients in view of obtaining high CRC-specific T lymphocyte numbers to be used for the ultimate lymphocyte transfer after a non myeloablative conditioning regimen in the same CRC patients.

Session 1A. New therapeutic strategies

EVALUATION OF THE POTENTIAL ROLE OF THE NEW CANCER-TESTIS ANTIGEN BORIS FOR THE DEVELOPMENT OF NOVEL STRATEGIES OF IMMUNOTHERAPY OF CANCER

Giulia Romagnoli (a), Paola Borghi (a), Dmitri Lokinov (b), Victor Lobanenkov (b),
Michael Agadjanyan (c), Herbert C Morse III (b), Filippo Belardelli (a), Lucia Gabriele (a)
(a) Department of Cell Biology and Neurosciences, Istituto Superiore di Sanità, Rome, Italy
(b) National Institute of Allergy and Infectious Diseases, National Institutes of Health, Bethesda, MD, USA
(c) Institute for Molecular Medicine, Huntington Beach, CA, USA

Cancer-testis (CT) antigens are characterized by restricted expression in different tumors but not in normal tissues other than testis, a site of immunologic privilege (1). CT antigens are also called shared tumor-specific antigens as they are expressed in a broad spectrum of various types of human neoplasms (2,3). Interestingly, T-cell tolerance to peptides derived from CT proteins appears to be incomplete because functional T-cell responses have been found to be generated as a consequence of CT protein expression in tumor cells (4). In fact, $CD8^+$ T cells specific for CT antigens are found in many patients with a variety of neoplasms of different origin (5,6). In addition, clinical trials have demonstrated that CT epitope-specific CTL can be induced in cancer patients and their induction correlates, in many instances, with partial or complete tumor responses (7). Based on this, CT antigens represent ideal targets have for inducing specific immune responses in tumor-bearing host. Thus, the identification of immunogenic epitopes of CT antigens expressed by different human tumors remains a major issue in the development of efficient vaccination strategies.

BORIS (Brother of the Regulator of Imprinted Sites) is a recently described CT antigen, paralogue of the ubiquitously expressed tumor suppressor gene CTCF (8). BORIS and CTCF share the same central 11Zn fingers (11ZF) that mediate specific interactions with varying about 50-bp target sites. BORIS and CTCF are normally expressed in mutually exclusive patterns in tight association with epigenetic reprogramming events in male germ cell development. In fact, BORIS is never expressed in any tissues besides testis, while CTCF is expressed in all somatic cells. Recent studies indicate that BORIS expression is activated abnormally in many different cancer cell lines and primary tumors, including but not limited to breast, lung, prostate, colon, and multiple mieloma (9-11).

Very recently it has been reported that the aberrant activation of BORIS contributes to derepression of NY-ESO-1 during pulmonary carcinogenesis (11). Moreover the conditional expression of BORIS in normal fibroblasts results in demethylation and derepression of MAGE-A1 and reactivation of other CT genes (10). These results suggest that BORIS is likely tethering epigenetic machinery to a novel class of CTCF/BORIS 11ZF target sequences that mediate induction of CT antigens. Importantly, murine BORIS antigen when tested as a component of anti-cancer vaccine using the very aggressive, highly metastatic and poorly immunogenic 4T1 mammary carcinoma-based mouse model of breast cancer, significantly prolonged the survival of mice, delayed the appearance of tumours and inhibited tumour growth (12). Overall, these data indicate that BORIS is expressed very early in malignancy, mediates the induction of other

CT genes and may augment the immunogenicity of certain cancers. Thus, BORIS represents an attractive new target for immunotherapy of many tumors.

The research aim of this proposal was to combine the characterization of selected antigens of BORIS and the setting of an efficient strategy for delivering these antigens to the immune system in an attempt to optimize vaccination in patients with BORIS-positive tumors. To this end, the first experimental part of this study has been focused on identifying BORIS antigenic peptides recognized by $CD8^+$ T cells.

First, we focused on finding class I-restricted peptides by screening the BORIS protein sequence, in particular the amino- and carboxy-termini which diverge completely from the paralogue CTCF, for the presence of peptides bearing consensus residues for HLA-A2.1 and HLA-B7, which together are expressed by about 60% of the Caucasian population, using the BIMAS program (available from: http://bimas.dcrt.nih.gov/molbio/hla-bind/indix.htlm).

We selected six peptides with high affinity for HLA-A*0201 and two for HLA-B*0702 (Table 1).

Table 1. Affinity of BORIS-derived Peptides for HLA-A*0201 and HLA-B*0702 molecules

HLA specificity	Start	Sequence	Score [a]
A*0201	8	VLSEQFTKI	138162
	21	VLTVSNSN	118238
	16	KLAVSLAET	59989
	41	ILQKHGEN	57937
	59	SVLEEEVE	20000
	10	QQQEGVQ	27264
B*0702	283	KPHLCHLCL	80000
	59	SVLEEEVEL	20000

[a] Estimate of half time of dissociation of a molecule containing this sequence
BORIS-derived synthetic peptides bearing consensus sequences for HLA-A*0201 and HLA-B*0702 and their predicted affinities for these molecules, expressed by a score number. These peptides were tested in the HLA-A*0201- and HLA-B*0702-transgenic mouse models.

Accordingly, we assayed the capacity of the identified class I-restricted BORIS peptides to induce *in vivo* tumor-specific CTL in humanized HLA-A*0201- and HLA-B*0702-transgenic mice. These mice have been already used by other groups to characterize the immunogenicity of cancer- and virus-derived CTL epitopes, and have permitted the identification of new epitopes of tumor antigens and evaluation of their potential use in vaccine formulations (13).

Briefly diverse group of transgenic mice were injected s.c. with each peptide. After 11 days, spleen cells were restimulated *in vitro* for further 6 days with the same peptide and tested for CTL capacity on peptide-pulsed target cells.

As indicated in Figure 1, we found that one HLA-A*0201-restricted peptide, namely peptide 8, was able to stimulate antigen-specific CD8+ T cells in transgenic mice as revealed by considerable production of IFN-γ detected using an ELISPOT assay. Moreover, $CD8^+$ T cells induced by peptide 8 were also endowed with cytotoxic potential given their significant CTL activity assayed by Cr51 release. A second peptide of BORIS protein, presented by HLA-B*0702, resulted immunogenic in transgenic mice (data not shown).

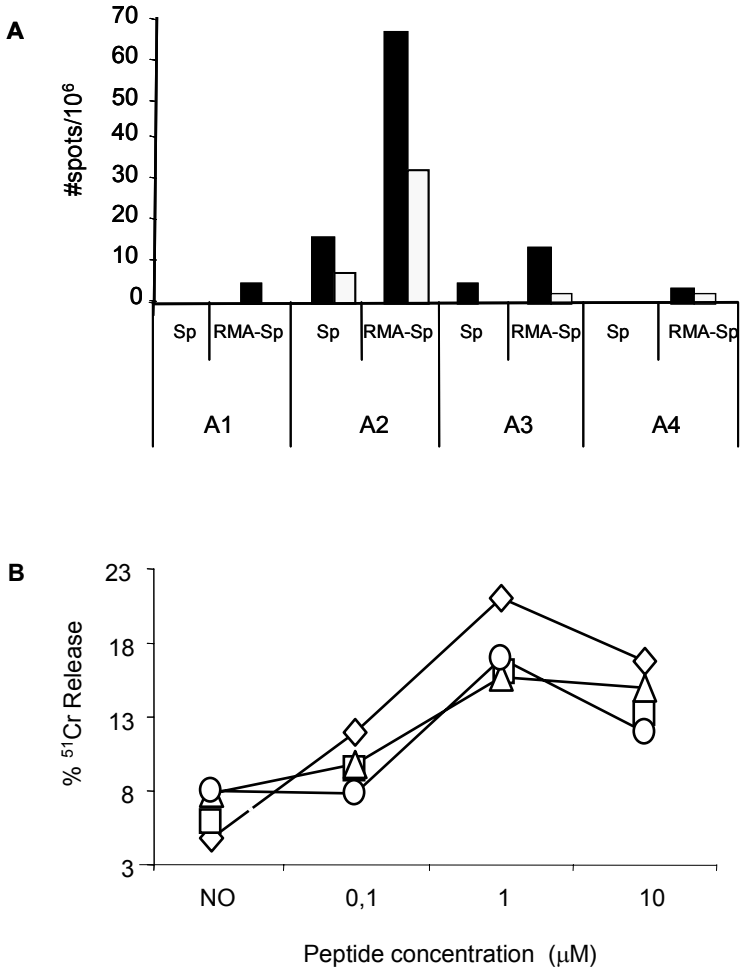

Figure 1. (A) IFN-γ Elispot assay on spleens of HLA*A0201- transgenic mice immunized with the HLA*A0201 peptide 8. IFN-γ secretion was stimulated in the presence of mouse antigen presenting cells transfected with HLA*A0201 cells (RMA) or only with spleen cells (Sp), loaded (black bars) or not (white bars) with the peptide 8. A1, A2, A3 and A4 represent individual mice. Data represent two out of six experiments and are presented as triplicate mean number of spots per 10^6 spleen cells. (B) CTL responses of HLA*A0201- transgenic mice mediated by the HLA-A*0201 specific peptide 8. Cytotoxic activity was determined in a standard ^{51}Cr release assay, using as targets RMA cells pulsed or not with different concentrations of peptide 8. A1, A2, A3 and A4 represent individual mice. Specific lysis was determined according to the following formula: % specific lysis=cpm (sample-spontaneous)/cpm (total-spontaneous)X100

Importantly these results demonstrate for the first time the immunogenicity of two BORIS-derived peptides. To further confirm these data we evaluate whether the immunogenic BORIS peptide 8 identified in transgenic mice was recognized by human T cells. To this end, PBMC from HLA-A*0201 healthy donors were repeatedly stimulated with autologous DCs pulsed with the HLA-A*0201-restricted peptide 8. We found that peptide 8-specific $CD8^+$ T cells were generated as revealed by high production of IFN-γ after stimulation with peptide-pulsed T2 target cells using an ELISPOT assay (Figure 2).

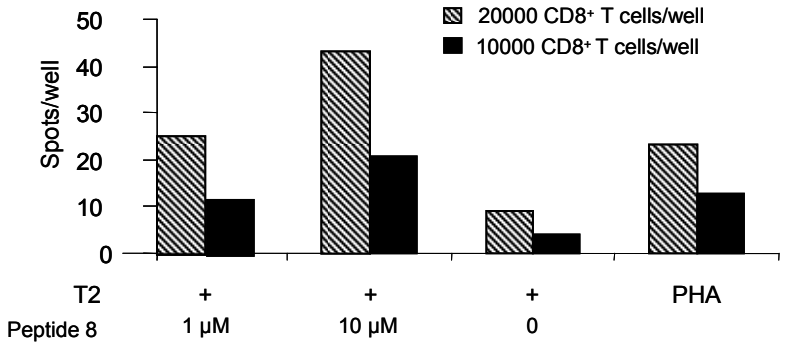

Figure 2. IFN-γ Elispot assay on peptide 8-stimulated $CD8^+$ T cells of a HLA-A0201 Healthy Donor. 1x104 or $2x10^4$ sorted-$CD8^+$ cells were incubated with T2 target cells previously loaded with peptide 8 at the indicated concentration or unloaded as negative control. As positive control the same number of $CD8^+$ T cells was plated with 1µg/ml PHA

Significantly, IFN-γ production by antigen-specific $CD8^+$ T cells was highly induced by T2 target cells loaded with peptide 8, in a dose dependent manner, as compared to $CD8^+$ T cells stimulated with PHA. The experiments aimed at evaluating the immunogenicity in humans of the HLA-B*0702-resticted peptide identified in mice are in progress. Currently, we are carrying out experiments aimed at assessing whether BORIS-peptide specific CD8+ T cells are capable to recognize endogenously processed BORIS antigens in target cells after transfection with the BORIS protein.

Overall our data strongly argue for the potential use of BORIS in antitumor immunotherapy applications in patients with breast, lung, prostate and other neoplasms.

References

1. Zendman AJ, Ruiter DJ, Van Muijen GN. Cancer/testis-associated genes: identification, expression profile, and putative function. *J Cell Physiol* 2003;194(3):272-88. Review.
2. Scanlan MJ, Gure AO, Jungbluth AA, Old LJ, Chen YT. Cancer/testis antigens: an expanding family of targets for cancer immunotherapy. *Immunol Rev* 2002;188:22-32. Review.
3. Scanlan MJ, Simpson AJG, Lloyd J Old. The cancer/testis genes: Review, standardization, and commentary. *Cancer Immunity* 2004;4:1.
4. Neumann F, Wagner C, Preuss KD, Kubuschok B, Schormann C, Stevanovic S, Pfreundschuh M. Identification of an epitope derived from the cancer testis antigen HOM-TES-14/SCP1 and presented by dendritic cells to circulating CD4+ T cells. *Blood* 2005;106(9):3105-13. Epub 2005 Jul 19.
5. Goodyear O, Piper K, Khan N, Starczynski J, Mahendra P, Pratt G, Moss P. CD8+ T cells specific for cancer germline gene antigens are found in many patients with multiple myeloma, and their frequency correlates with disease burden. *Blood* 2005;106(13):4217-24. Epub 2005 Sep 6.
6. Bricard G, Bouzourene H, Martinet O, Rimoldi D, Halkic N, Gillet M, Chaubert P, Macdonald HR, Romero P, Cerottini JC, Speiser DE. Naturally acquired MAGE-A10- and SSX-2-specific CD8+ T cell responses in patients with hepatocellular carcinoma. *J Immunol* 2005;174(3):1709-16.
7. Baumgaertner P, Rufer N, Devevre E, Derre L, Rimoldi D, Geldhof C, Voelter V, Lienard D, Romero P, Speiser DE. Ex vivo detectable human CD8 T-cell responses to cancer-testis antigens. *Cancer Res* 2006;66(4):1912-6.

8. Loukinov D, Pugacheva E, Vatolin S, Pack SD, Moon H, Chernukhin I, Mannan P, Larsson E, Kanduri C, Vostrov AA, Cui H, Niemitz EL, Rasko JE, Docquier FM, Kistler M, Breen JJ, Zhuang Z, Quitschke WW, Renkawitz R, Klenova EM, Feinberg AP, Ohlsson R, Morse HC 3rd, Lobanenkov VV. BORIS, a novel male germ-line-specific protein associated with epigenetic reprogramming events, shares the same 11-zinc-finger domain with CTCF, the insulator protein involved in reading imprinting marks in the soma. *Proc Natl Acad Sci USA* 2002;99(10):6806-11.
9. Klenova EM, Morse HC 3rd, Ohlsson R, Lobanenkov VV. The novel BORIS + CTCF gene family is uniquely involved in the epigenetics of normal biology and cancer. *Semin Cancer Biol* 2002;12(5):399-414. Review.
10. Vatolin S, Abdullaev Z, Pack SD, Flanagan PT, Custer M, Loukinov DI, Pugacheva E, Hong JA, Morse H 3rd, Schrump DS, Risinger JI, Barrett JC, Lobanenkov VV. Conditional expression of the CTCF-paralogous transcriptional factor BORIS in normal cells results in demethylation and derepression of MAGE-A1 and reactivation of other cancer-testis genes. *Cancer Res* 2005;65(17):7751-62.
11. Hong JA, Kang Y, Abdullaev Z, Flanagan PT, Pack SD, Fischette MR, Adnani MT, Loukinov DI, Vatolin S, Risinger JI, Custer M, Chen GA, Zhao M, Nguyen DM, Barrett JC, Lobanenkov VV, Schrump DS. Reciprocal binding of CTCF and BORIS to the NY-ESO-1 promoter coincides with derepression of this cancer-testis gene in lung cancer cells. *Cancer Res* 2005;65(17):7763-74.
12. Loukinov D,Ghochikyan A, Mkrtichyan M, Ichim TE, Lobanenkov VV, Cribbs DH, Agadjanyan MG. Antitumor efficacy of DNA vaccination to the epigenetically acting tumor promoting transcription factor BORIS and CD80 molecular adjuvant. *J Cell Biochem* 2006;98(5):1037-43.
13. Firat H, Garcia-Pons F, Tourdot S, Pascolo S, Scardino A, Garcia Z, Michel M-L, Jack RW, Jung G, Kosmatopoulos K, Mateo L, Suhrbier A, Lemonnier FA, Langlade-Demoyen P. H-2 class I knockout, HLA-A2.1-transgenic mice: a versatile animal model for preclinical evaluation of antitumor immunotherapeutic strategies. *Eur J Immunol* 1999;29:3112-21.

Session 1A. New therapeutic strategies

EFFECTS OF TYROSINE KINASE INHIBITOR IMATINIB (GLIVEC) ON WILD TYPE AND DRUG RESISTANT KAPOSI'S SARCOMA CELLS

Elisabetta Straface (a), Rosa Vona (a), Sabrina Basciani (b), Roya Khosravi-Far (c)
(a) Department of Therapeutic Research and Medicines Evaluation, Istituto Superiore di Sanità, Rome, Italy
(b) La Sapienza University, Rome, Italy
(c) Department of Pathology, Harvard Medical School, Beth Israel Deaconess Medical Center, Boston, USA

Introduction

Receptor with tyrosine kinase activity plays a key role in the pathogenesis of tumours and provide a rational target for cancer therapies (1,2). Glivec (Imatinib) is a small molecule tyrosine kinase inhibitor that has significant efficiency in the treatment of chronic myelogenous leukaemia and of some solid tumours (3). Considering that: i) an overexpression of platelet-derived growth factor receptor (PDGF-R) has been described in many solid tumours and that ii) PDGF signaling has a role in Kaposi sarcoma (KS) (4), the most common tumour associated with HIV infection, we investigated the response of KS cells to Glivec and we characterized the pathways involved in this response. In addition, considering that multidrug resistance represents the main cause of cancer therapy failure, we also investigated the effects of Glivec in a Kaposi's cell line resistant to Indinavir, a protease inhibitor used in HIV therapy.

Materials and methods

Cells culture and treatments

The wild type Kaposi's sarcoma cell line (wtSLK) was kindly provided by Prof. Roberto Cauda (Department of Infectious Diseases, Catholic University, Rome, Italy). The cells were grown in RPMI-1640 supplemented with 10% FCS, 2 mM glutamine and antibiotics. Indinavir resistant SLK subclone (SLKIDV) was selected from the original *wt*SLK cell line by exposure to 50 μM of the drug. Drug resistance was maintained by adding relevant concentrations of the drug every 4 weeks. Cells were cultured in drug-free medium for at least ten days before experimental procedures. Degrees of resistance were assessed in terms of MTT assay (5) and the P-gp and/or MRP function (6). Cells were treated with Glivec (Novartis) at different concentrations (15, 25 and 35 μM) in the growth medium at 37°C in a 5%CO2 atmosphere for 48 h.

Cell growth

Cell proliferation was analyzed by performing growth curves both in *wt*SLK and SLKIDV cells. Cell number was determined by counting cells daily using the trypan blue (GIBCO) exclusion test.

Analytical cytology

For static and flow cytometry analyses, *wt*SLK and SLKIDV cells were fixed with 4% paraformaldehyde in phosphate-buffered saline (PBS) for 30 min at room temperature. After washing in the same buffer, cells were permeabilized with 0.5 Triton X-100 (Sigma) in PBS for 5 min. For PDGF-β receptor (phosphorylated and non phosphorylated), (α and β) tubulin and vimentin (Santa Cruz Biotechnology) monoclonal antibodies directed against these antigens were used. After 30 min at 37°C, cells were washed and then incubated with an anti-mouse fluorescein-linked whole antibody (Sigma) or an anti-mouse rhodamine-linked whole antibody (Sigma). For actin detection cells were stained with fluorescein-phalloidin (Sigma) at 37°C for 30 min. For phosphorylated Akt (P-AKT, Santa Cruz Biotechnology) and survivin (Chemicon) polyclonal antibodies direct against these antigens were used. After 30 min at 37°C, cells were washed and then incubated with an anti-rabbit fluorescein-linked whole antibody (Sigma).

For apoptosis detection the nuclei were stained with Hoechst 33258 (Sigma) at 37°C for 15 min. For a qualitative analysis all samples were mounted on glass cover-slips with glycerol-PBS (2:1) and analyzed by intensified video microscopy (IVM) with a Nikon Microphot fluorescence microscope equipped with a Zeiss Ccd camera. Regarding flow cytometry analyses, all the samples were recorded with a FACScan flow cytometer (Becton Dickinson, Mountain View, CA) equipped with a 488 nm argon laser. A least 20,000 events have been acquired. The median values of fluorescence intensity histograms were used to provide a semi-quantitative analysis.

Morphometric analyses

Quantitative evaluation of apoptotic cells was performed counting at least 300 cells at high magnification (500x) at the fluorescence microscope.

Caspases activity

Activation state of the caspase 8, 9 and 3 was evaluated by using the CaspGLOW fluorescein active caspase staining Kit (MBL, Woburn, MA, USA). This kit provides a sensitive means for detecting activated caspases in living cells. The assay utilizes specific caspases inhibitors (IETD-FMK for caspase 8, LEHD-FMK for caspase 9 and DEVD-FMK for caspase 3) conjugated to FITC as the fluorescent marker. These inhibitors are cell permeant, nontoxic and irreversibly bind to caspase active form. The FITC label allows detection of activated caspases in apoptotic cells directly by flow cytometry. Control and treated Hep-2 cells were incubated with FITC-IETD-FMK, FITC-LEHD-FMK or FITC-DEVD-FMK for 1 hour at 37 °C following manifacturer instruction. After this time samples were washed three times and immediately analyzed on a cytometer by using FL-1 channel. Two additional experimental controls were also considered: i) samples prepared by pre-treating cells with specific inhibitors of caspase 8, 9 or 3 and ii) unlabelled cells (negative control).

Western Blotting

To study the effect on the phosphorylation of PDGF-α and PDGF-β receptors, subconfluent cells shifted to 0.1% FBS overnight, were cultured with and without 15 μmol/l Glivec for 4 hours followed by an additional 10 min of incubation in the absence or in the presence of 10 ng/ml human recombinant PDGF-BB (Roche). At the end of incubation, cells were washed with

PBS, harvested and cells pellet was lysed in the ice-cold radioimmunoprecipitation assay (RIPA) buffer (20 mM tris-HCl, ph 7.5, 150 mM NaCl, 1 mM EDTA, 1 mM EGTA, 2.5 mM sodium pyrophosphate, 200 mM PMSF, 1 mg/ml leupeptin, 1 mg/ml aprotinin plus 1% Triton X-100), followed by centrifugation at 14000 rpm at 4°C for 20 min. Protein concentration was determined using the Bradford protein assay method. Equal amounts (80 μg) of sample protein were loaded onto 7% SDS-polyacrylamide gels and then electrotransferred onto nitrocellulose membranes which were incubated with 1:300 dilution of the following primary antibodies: affinity-purified polyclonal rabbit anti-phospho-PDGFR-α (anti-p-PDGFR-α Sigma), anti-phospho-PDGFR-β. (anti-p-PDGFR-β, Sigma) and monoclonal mouse anti-actin (Santa Cruz, Biotechnology). Membranes were then incubated with the horseradish peroxidase-conjugated secondary antybodies (1:10000 dilution; Santa Cruz Biotechnology). Detection was performed using enhanced chemiluminescence (ECL, Amersham Life Science, Arlington Heights, IL). Secondary antibodies alone served as negative controls. Protein bands were quantified by densitometric analysisn using a densitometry computer software (Kodak Digital Science, Rochester).

Results

For the first, we characterized both *wt* and resistant SLK cell lines. In particular, the expression of phosphorylated and non phosphorylated PDGF receptor and cell growth were detected by flow cytometry. As depicted in the Figure 1, with respect to wt cells, SLK resistent to indinavir, showed an increased expression of phosphorylated PDGF recptor (A) and a decreased cell growth (B).

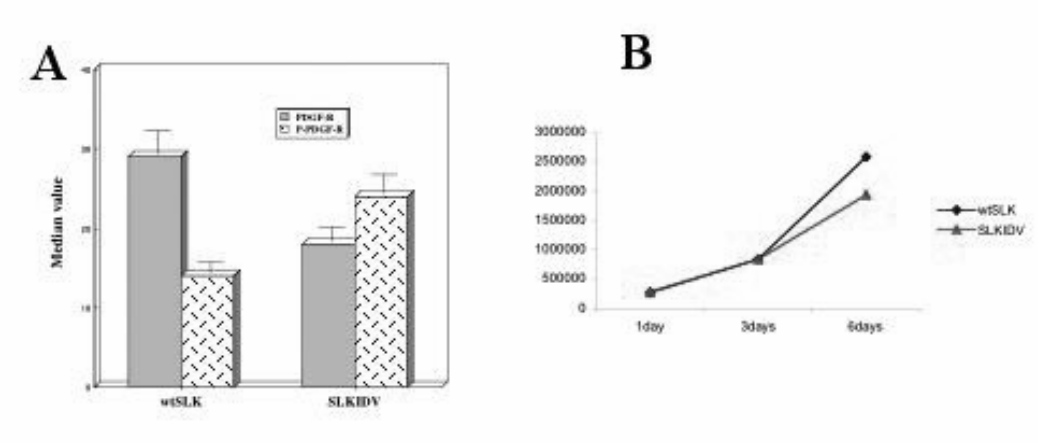

Figure 1. Expression of PDGF-receptor (A) and cell growth (B) in both *wt* and IDV SLK cells

Moreover, in both cell lines, analysis of cytoskeletal elements was detected by static and flow cytometry. In particular, distribution and expression of actin, tubulin and vimentin were analysed. As depicted in Figure 2 a redistribution of these proteins and an increased expression of actin and vimentin were detected in SLKIDV with respect to *wt* cells.

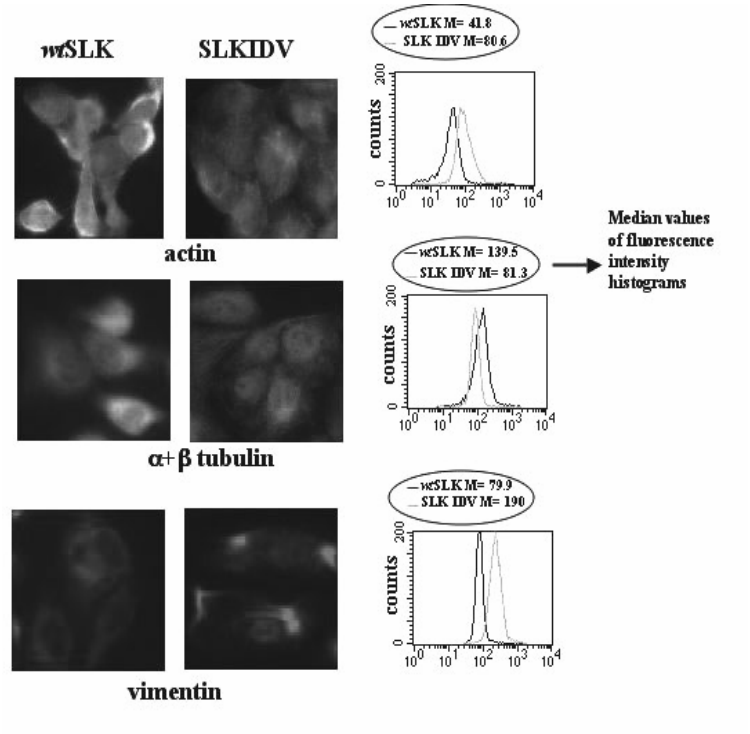

Figure 2. Cytoskeleton analysis

In consideration of the importance of same molecules in the response to apoptotic stimuli, we analysed the distribution and the expression of: i) survivin, an inhibitor of apoptosis protein (IAP) that interacts with and inhibits caspase 3 (7) and ii) phosphorylated Akt, a protein kinase that promotes cell survival by phosphorylating and inhibiting proteins involved in apoptosis (8). As depicted in Figure 3, a redistribution and an increased expression of these molecules were detected in resistance SLK with respect to *wt* cells.

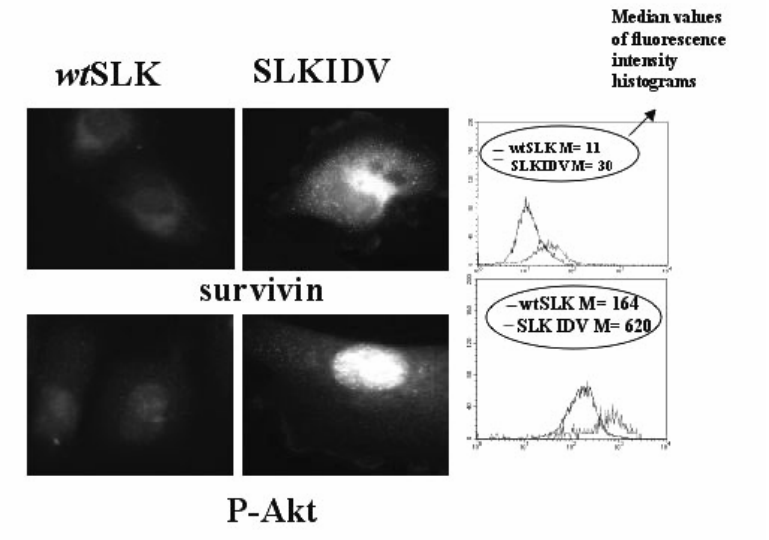

Figure 3. Proteins involved in cell survival

After cell characterization, we exposed both cell lines to different concentrations of Glivec (15, 25 and 35 μM) for 48h. As depicted in Figure 4 Glivec was able to induce apoptosis in a dose dependent manner in both cell lines.

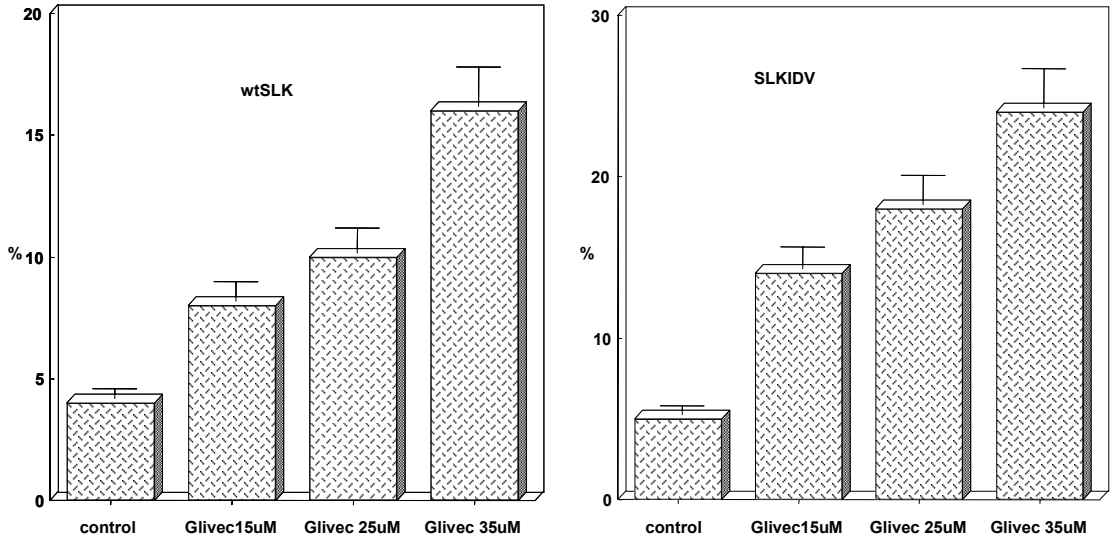

Figure 4. Percentage of apoptotic cells 48h after Glivec exposure

Apoptosis, or programmed cell death, is a mechanism by which cells die if DNA damage is not repaired (9) and occurs through two main pathways. The first, referred to as the extrinsic or cytoplasmic patway, is triggered through the death receptors. The second is the intrinsec or mytochondrial pathway that when stimulated leads to the release of cytocrome-c from the mitochondria and activation of the death signal. Both pathway involving the activation of a cascade of proteases called caspase that cleave regulatory and structural molecules, culminating in the death of the cell. Considering that intrinsic and extrinsic pathways converge to caspase 3 by caspase 8 (in the extrinsic pathway) and caspase 9 (in the intrinsic pathway) we evaluated the activate state of these caspases in both wt and resistant SLK cells. Data shown in Figure 5 indicate that Glivec is able to induce apotosis by activating caspase 9 and 3. No differences in the activation state was detected for caspase 8 (data not shown).

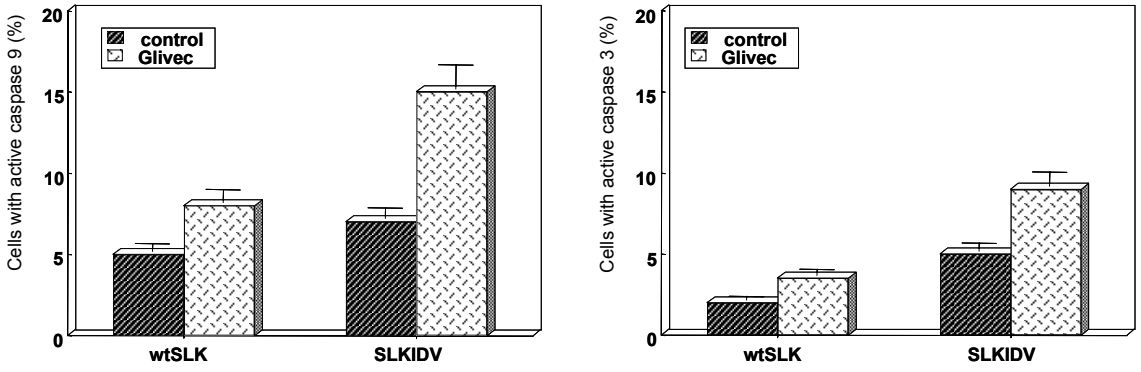

Figure 5. Percentage of cells with active caspase 3 48h after exposure to 15 μM Glivec

In order to verify if Glivec induces apoptosis inhibiting phosphorylation of PDGF-R, western blotting analysis was carried out. As depicted in Figure 6 the Glivec inhibits both α and β PDGF receptor phosphorilation either in the presence or absence of inhibitor (PDGF-BB).

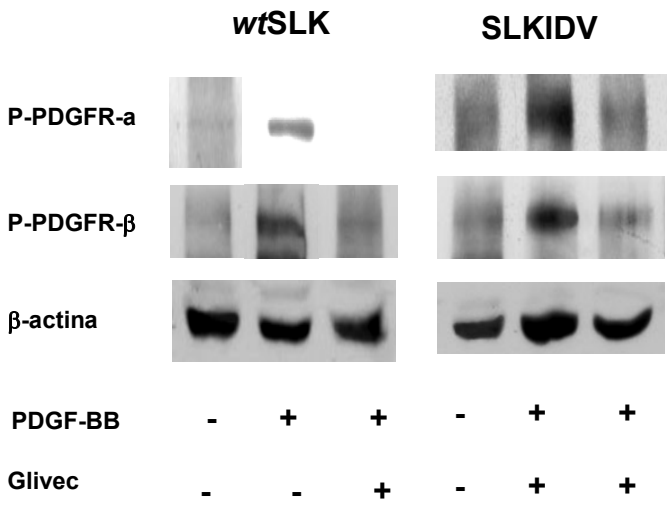

Figure 6. Analysis of phosphorylated form of α and β PDGF receptors by western blotting

Conclusions

These preliminary results clearly indicate that Glivec: i) is able to induce apoptosis not only in *wt* but, more importantly, also in IDV resistant Kaposi sarcoma cells via ii) inhibition of PDGF receptor phosphorylation and iii) activation of mitochondria apoptotic pathway. Moreover, our data suggest that Glivec, reducing the drug resistance phenomenon that frequently occurs during HIV therapy, could be an important drug in the clinical managements of AIDS-associated Kaposi sarcoma in combination with conventional chemotherapy.

References

1. Blume-Jensen, Hunter T. Oncogenic kinase signalling. *Nature* 2001;411:355-65.
2. Sawyers C. Targeted cancer therapy. *Nature* 2004;432:294-7.
3. Koon HB, Bubley GJ, Pantanowitz L, Masiello D, Smith B, Crosby K, Proper J, Weeden W, Miller TE, Chatis P, Egorin MJ, Tahan SR, Dezube BJ. Imatinib-induced regression of AIDS-related Kaposi's sarcoma. *Journal of Clinical Oncology* 2005;23:982-9.
4. Fiorentini G, Rossi S, Lanzanova G, Biancalani M, Palomba A, Bernardeschi P, Dentico P, De Giorgi U. Tyrosine kinase inhibitor imatinib mesylate as anticancer agent for advanced ocular melanoma expressing immunoistochemical C-kit (CD 117): preliminary results of a compassionate use clinical trial. *Journal of Experimental Clinical Cancer Research* 2003;22:17-20.

5. Laroche-Clary A, Larrue A, Robert J. Down-regulation of bcr-abl and bcl-x(L) expression in a leukemia cell line and its doxorubicin-resistant variant by topoisomerase II inhibitors. *Biochemical Pharmacol*ogy 2000;60:1823-8.

6. Lucia MB, Savarino A, Straface E, Golotta C, Rastrelli E, Matarrese P, Rutella S, Malorni W, Cauda R. Role of lymphocyte multidrug resistance protein 1 in HIV infection: expression, function, and consequences of inhibition. *Journal of Acquired Immune Deficiency Syndrome* 2005;40:257-66.

7. Tamm I, Wang Y, Sausville E, Scudiero DA, Vigna N, Oltersdorf T, Reed JC. IAP-family protein survivin inhibits caspase activity and apoptosis induced by Fas (CD95), Bax, caspases, and anticancer drugs. *Cancer Research* 1998;58:5315-20.

8. Brunet A, Bonni A, Zigmondi MJ, Lin MZ, Juo P, Hu LS, Anderson MJ, Arden KC, Blenis J, Greenberg ME. AKT promotes cell survival by phosphorylating and inhibiting a Forkhead transcription factor. *Cell* 1999;96:857-68.

9. Lowe SW, Lin AW. Apoptosis in cancer. *Carcinogenesis* 21:485-95.

Session 1B. Mechanisms of cancer onset

PROTEOMIC INVESTIGATION OF THE MECHANISMS CONTROLLING THE CYCLIN D-DEPENDENT KINASE

Deborah Pajalunga, Alessia Mazzola, Anna Maria Salzano, Gabriele De Luca, Marco Crescenzi
Department of Environment and Primary Prevention, Istituto Superiore di Sanità, Roma, Italy

The project has been carried out strictly adhering to the original proposal. It has yielded results that carry high significance for basic science and that are likely applicable in therapeutic settings.

Previous work from this group has shown the critical importance of cyclin D-dependent kinase activity (DK) in the regulation of the postmitotic state of terminally differentiated (TD) cells (1). The first goal of the project was to identify the molecular mechanisms that repress such activity in TD cells. By exploiting complementary proteomics and biochemistry techniques, it has been possible to answer this question satisfactorily.

TD skeletal muscle cells (myotubes) have been infected with recombinant adenoviruses carrying cyclin D1 or cdk4, the main catalytic partner of cyclin D1 in the biological systems examined. Cdk4-containing complexes have been immunoprecipitated and electrophoretically resolved. The coprecipitated proteins have been identified using complementary mass spectrometry techniques: mass fingerprint with a MALDI-TOF mass spectrometer and tandem mass spectrometry with an electrospray ion-trap instrument. Among the identified proteins, particularly interesting was the cyclin-dependent kinase inhibitor, p21.

On the basis of the information obtained in the preceding experiments, p21 expression has been suppressed through RNA interference (RNAi). Surprisingly, the sole suppression of p21 triggered mitotic reactivation in 65% of the myotubes. The percentage of reactivated myotubes rose above 80% if, in addition to p21, another member of the Kip family of inhibitors, p27, was also suppressed by RNAi. To understand the mechanisms through which suppression of cell cycle inhibitors induces cell cycle reactivation, a new series of immunoprecipitation-mass spectrometry studies were performed. These experiments further dissected the cdk4-containing complexes, showing that their main constituents are cyclin D3, p21, and PCNA. When cyclin D3 RNAi or expression of a dominant-negative mutant of cdk4 (dncdk4) were performed along with p21 RNAi, cell cycle reentry was completely abrogated, indicating that proliferative reactivation depends critically on cyclin D3/cdk4 complexes. A thorough biochemical characterization of reactivated myotubes yielded results in full agreement with this model. Particularly intriguing was the observation that p21 RNAi-mediated myotube reactivation did not require exogenous growth factors, in apparent contradiction with the well-established notion that serum growth factors are required for cyclin D synthesis and cyclin D/cdk4 complex assembly. However, we were able to show that complexes containing at least cdk4, cyclin D3, and p21 are abundantly present in non-manipulated myotubes. These preformed complexes, though normally held inactive by p21, require growth factors for neither synthesis nor assembly, hence being serum independent.

We then asked whether other non-proliferative states are actively maintained by cell cycle inhibitors. To address this question, primary human fibroblasts rendered quiescent by serum starvation and contact inhibition were subjected to RNAi for various cell cycle inhibitors, including p21, p27, and p18. Quiescent fibroblasts were also reactivated by with high efficiency by RNAi for one or more inhibitors. Finally, senescent primary human embryo kidney (HEK)

cells were reactivated as well (80%) by interference with p21 alone. This result is particularly important as senescent cells, similar to postmitotic ones, are traditionally regarded as irreversibly non-proliferating.

Altogether, the experiments described thus far constitute an exemplary instance of successful application of modern proteomics techniques to an important biological problem. The results have gone much beyond expectations, allowing us to conclude that, at variance with the prevailing opinion, the physiological non-proliferative states are actively maintained and are not the result of the mere absence of proliferation-promoting regulation.

The ability to trigger or promote proliferation of a wide variety of cell types through the simple, temporary, reversible suppression of cell cycle inhibitors affords a means to culture cell types endowed with poor replicative potential, among which most human stem cells. These results have a great potential for applications in the fields of wound healing, bioengineering, tissue repair, and regeneration, whenever cell proliferation is limiting. Experiments to explore these avenues are in progress.

During the studies described above, we highlighted a significant cell-cycle regulatory mechanism, of likely relevance to neoplastic transformation. In short, it is a positive feed-back loop between the E2F family of transcription factors and cyclin E. We demonstrated that E2F overexpression, common in human tumors, increases the half-life of the cyclin E protein, thus increasing its cellular levels and deregulating the cell cycle. These results have been described in Ref. 2.

This project has been carried out in collaboration with Dr. Ettore Appella (Chief, Chemistry Section, Laboratory of Cell Biology, NCI) and Dr. Donald P. Bottaro (Urologic Oncology Branch, Center for Cancer Research, NCI).

References

1. Latella L, Sacco A, Pajalunga D, Tiainen M, Macera D, D'Angelo M, Felici A, Sacchi A, Crescenzi M. Reconstitution of cyclin D1-associated kinase activity drives terminally differentiated cells into the cell cycle. *Mol Cell Biol* 2001;21(16):5631-43.
2. Pajalunga D, Crescenzi M. Regulation of cyclin E protein levels through E2F-mediated inhibition of degradation. *Cell Cycle* 2004;3(12):1572-8.

Session 1B. Mechanisms of cancer onset

ROLE OF THE OXIDATIVE DNA DAMAGE IN GENOME INSTABILITY AND CANCER

Flavia Barone, Filomena Mazzei, Gabriele De Luca, Maria Teresa Russo, Margherita Bignami
Department of Environment and Primary Prevention, Istituto Superiore di Sanità, Roma, Italy

Inactivation of mismatch repair (MMR) is associated with a dramatic genomic instability that is observed experimentally as a mutator phenotype and microsatellite instability (MSI). It has been implicit that the massive genetic instability in MMR defective cells simply reflects the accumulation of spontaneous DNA polymerase errors during DNA replication. We recently identified oxidation damage, a common threat to DNA integrity to which purines are very susceptible, as an important cofactor in this genetic instability. Since these findings have important mechanistic and clinical implications, we extended our studies using biochemical and biophysical assays as well as *in vivo* animal models.

In vitro assays

We previously identified the dNTP pool as a likely source of mutagenic DNA 8-oxoG and demonstrated that DNA MMR prevented oxidation-related frameshifts in mononucleotide repeats. We have shown that both Klenow fragment and DNA polymerase α can utilize 8-oxodGTP and incorporate the oxidized purine into model frameshift targets. The human MutS α mismatch repair factor recognized DNA 8-oxoG efficiently in some contexts that resembled frameshift intermediates in the same C or A repeats. DNA 8-oxoG in other slipped/mispaired structures in the same repeats adopted configurations that prevented recognition by MutS α and by the OGG1 DNA glycosylase thereby rendering it invisible to DNA repair. These findings are consistent with a contribution of oxidative DNA damage to frameshifts. They also suggest how MMR might reduce the burden of DNA 8-oxoG and prevent frameshift formation (1).

Using oligonucleotides based on the frameshift hotspot of the HPRT gene, we also investigated how a single 8-oxoG modified the structural and dynamic properties of the G6 tract. A 30 ns molecular dynamics (MD) simulation indicated compression of the minor groove in the immediate vicinity of the lesion. Fluorescence polarization anisotropy (FPA) and MD demonstrated that 8-oxoG increases DNA torsional rigidity and also constrains the movement of the single-stranded region at the single/double stranded DNA junction of model DNA replication template/primer. These constraints influenced the efficiency of primer extension by Klenow (exo-) DNA polymerase (2).

Our previous work implicated oxidized adenine bases in oxidation-related mutations. 2-hydroxyadenine (2-OH-A), a product of DNA oxidation, is a potential source of mutations. We thus investigated the effects of template 2-OH-A within A repeats using DNA polymerases with different fidelities. We tested DNA polymerases from three different families: A, B and Y in primer extension experiments. Our results showed that a 2-OH-A in the template strand is a strong block for Klenow fragment, DNA polymerase α and DNA polymerase η, whereas the Dpo4 polymerase efficiently replicated 2-OH-A. The 2-OH-A bypass by each of these enzymes induced base substitutions while Dpo4 also introduced single base deletions. The human MutS α

mismatch recognition factor recognized oligonucleotides containing 2-OH-A base pairs, including the preferred 2-OH-A:T, as well as 2-OH-A located in a repeat mimicking a frameshift intermediate. Mismatch repair might therefore help counteract the effects of 2-OH-A incorporated from the oxidized dNTP pool (manuscript submitted). These experiments are done in collaboration with T. Kunkel (NIHS).

In vivo models

Oxidative DNA damage is one of the most common threats to genome stability and multiple DNA repair enzymes provide protection from the effects of oxidized DNA bases. We used *in vivo* models to evaluate the role of different repair pathways in the control of oxidative DNA lesions. In mammalian cells, base excision repair (BER) (3) mediated by the OGG1 and MYH DNA glycosylases prevents the accumulation of 8-oxoguanine (8-oxoG) in DNA. When steady-state levels of DNA 8-oxoG were measured in *myh*$^{-/-}$ and *myh*$^{-/-}$/*ogg1*$^{-/-}$ mice, an age-dependent accumulation of the oxidized purine was found in lung and small intestine of *myh*$^{-/-}$/*ogg1*$^{-/-}$ mice. Since there is an increased incidence of lung and small intestinal cancer in *myh*$^{-/-}$/*ogg1*$^{-/-}$mice, these findings are consistent with a causal role for unrepaired oxidized DNA bases in cancer development (4).

We previously presented *in vitro* evidence that MMR participates in the repair of oxidative DNA damage and *msh2*$^{-/-}$ mouse embryo fibroblasts also have increased steady state levels of DNA 8-oxoG. To investigate whether DNA 8-oxoG also accumulates *in vivo*, basal levels were measured in several organs of 4 month-old *msh2*$^{-/-}$ mice and their wild-type counterparts. *Msh2*$^{-/-}$ mice had significantly increased levels of DNA 8-oxoG in spleen, heart, liver, lung, kidney and possibly small intestine but not in bone marrow, thymus or brain. The tissue-specificity of DNA 8-oxoG accumulation in *msh2*$^{-/-}$ and other DNA repair defective mice suggests that DNA protection of different organs is mediated by different combinations of repair pathways (5).

Incorporation of 8-oxoG into DNA is normally minimized by MTH1, a hydrolase which degrades 8-oxodGTP to 8-oxodGMP. In order to evaluate the contribution of the oxidized dNTP pool to the overall burden of DNA 8-oxoG and to tumorigenesis, we constructed a new transgenic mice in which the human hMTH1 is overexpressed. In comparison to wild-type animals, a high level of hMTH1 expression reduced both steady-state and Paraquat-induced levels of DNA 8-oxoG in several organs. Surprisingly, increased hMTH1 expression provided a strong protection against neurodegeneration induced by 3-nitropropionic acid, a neurotoxin which induces striatal lesions in a model for Huntington disease (unpublished results).

References

1. Macpherson P, Barone F, Maga G, Mazzei F, Karran P, Bignami M. 8-oxoguanine incorporation into DNA repeats in vitro and mismatch recognition by MutSalpha. *Nucleic Acids Res* 2005;33(16):5094-105.
2. Barone F, Lankas F, Spackova N, Sponer J, Karran P, Bignami M, Mazzei F. Structural and dynamic effects of single 7-hydro-8-oxoguanine bases located in a frameshift target DNA sequence. *Biophys Chem* 2005;118(1):31-41.
3. Pascucci B, Russo MT, Crescenzi M, Bignami M, Dogliotti E. The accumulation of MMS-induced single strand breaks in G1 phase is recombinogenic in DNA polymerase beta defective mammalian cells. *Nucleic Acids Res* 2005;33(1):280-8.

4. Russo MT, De Luca G, Degan P, Parlanti E, Dogliotti E, Barnes DE, Lindahl T, Yang H, Miller JH, Bignami M. Accumulation of the oxidative base lesion 8-hydroxyguanine in DNA of tumor-prone mice defective in both the Myh and Ogg1 DNA glycosylases. *Cancer Res* 2004;64(13):4411-14.
5. Russo MT, De Luca G, Degan P, Bignami M. Different DNA repair strategies to combat the threat from 8-oxoguanine, *Mutat Res* (E-publication ahead of print).

Session 1C. Cancer cell biology

IMMUNOTHERAPY OF DRUG UNRESPONSIVENESS TUMORS. SELECTION AND CHARACTERIZATION OF HUMAN SINGLE CHAIN FRAGMENT VARIABLE (SCFV) MONOCLONAL ANTIBODIES AGAINST CEA

Maurizio Cianfriglia, Michela Flego, Alessandro Ascione, Silvia Zamboni, Valentina Imperiale, Mara Gellini, Maria Luisa Dupuis
Department of Therapeutic Research and Medicines Evaluation, Istituto Superiore di Sanità, Rome, Italy

ISS-NIH research project: objectives and future development

Every year, more than 200.000 new cases of cancer are diagnosed in Italy. In proportion with the magnitude of the population similar number of cancers are diagnosed in other west countries. Regrettably, despite recent developments, effectiveness of chemotherapy is still rather limited for most types of cancer, including tumors of the skin (melanoma), colon, lung, kidney, pancreas, and liver. In addition, cancers may become resistant through cellular mechanisms, the prime example of which is the elevated expression of an ATP-dependent drug-efflux pump, termed P-glycoprotein (P-gp) (1). While treatment of malignant solid tumors with conventional approaches is largely unsuccessful, recent years have seen the emergence of several therapeutic strategies involving monoclonal antibodies (mAb) or related antibody fragments for the treatment of malignancy (2). mAbs can be developed with high specificity for antigens expressed on tumor cells and can exact a variety of antitumor responses, thus, the use of mAbs as an alternative or augmentation to therapy offers significant advantages over traditional forms of cancer treatment (3).

In collaboration with Suresh V. Ambudkar (ISS/NIH research project: Somatic and recombinant monoclonal antibodies for the diagnosis and therapy of drug unresponsiveness tumors showing an intrinsic and/or an acquired, Mdr1-P-glycoprotein, mediated phenotype) we are exploring the suitability of an antibody based therapy for the treatment of cancers no more susceptible to conventional chemotherapy. The main objectives of these studies include: 1) human monoclonal antibodies in single chain fragment (scFv) format directed against cell surface determinants selectively expressed in drug unresponsiveness tumors, 2) human scFvs and murine monoclonal antibodies in f(ab)' format directed against MDR1-P-glicoprotein for structure/function study of the multidrug resistance phenomenon.

In the present article the results we have obtained concerning the isolation of human scFv antibodies directed against carcinoembryonic antigen (CEA) for selectively target and disclose sites of CEA-expressing cancers in patients will be presented and discussed.

CEA in cancer research

CEA is an attractive target for immunotherapeutic purposes because of its expression profile in solid tumors, its role in tumor progression, and its immunogenicity (4). In particular, one of

the member of the CEA family of proteins, CEACAM1, has received considerable interest as a cancer antigen target (5). Preclinical studies in melanomas show that expression of the cell adhesion molecule, CEACAM1, is an independent factor of the metastasis risk, with a predictive value superior to that of tumor thickness (6). Moreover, specific CEACAM1 gene mutation inhibits the invasive growth of melanomas, and treatment with anti-CEACAM monoclonal antibodies blocks CEACAM1-enhanced cell invasion and cell migration in a dose-dependent manner (7). In fact, clinical studies in a 10-year follow-up indicate that expression of the cell adhesion molecule CEACAM1 in primary tumors in melanoma patients is associated with the subsequent development of metastatic disease (6). CEACAM1 also appears to be a promising endothelial target for bladder cancer therapy; this molecule is involved in the switch from non invasive and non vascularized to invasive and vascularized bladder cancer (8). Furthermore, CEACAM1, which is not expressed in the lung, has been identified in 2/3 of primary adenocarcinomas from this tissue and is considered a significant independent prognostic factor for survival (9). The selection and characterization of human anti-CEA single-chain antibody fragments (scFv) is a first step toward the construction of new anticancer monoclonal antibodies designed for optimal blood clearance and tumor penetration. The construction of libraries of recombinant antibody fragments that are displayed on the surface of filamentous phage, and the selection of phage antibodies against target antigens, have become an important technological tool in generating new monoclonal antibodies for research and clinical applications (2). Human antibodies obtained by this method do not induce harmful immune response in patients, in comparison with murine monoclonal antibodies produced by the classic hybridoma techniques. Moreover, the affinity of selected antibodies can be improved through construction of mutant antibody libraries giving clones with greater affinity. Thus, naïve or semi-synthetic human antibody libraries can be used in the search for specific antibodies without immunization with respective antigens. We describe in this paper the selection of a new anti-CEA single-chain antibody fragment, MA39, from an ETH-2 synthetic antibody library (10). This antibody recognizes human CEA protein in ELISA, Western blot and flow cytometry. The single-chain antibody was affinity-maturated by mutagenesis *in vitro*. The dissociation constant of the new maturated anti-CEA E8 antibody (1.39×10^{-8}) was decreased more than 10-fold compared to the original MA39 (1.71×10^{-7}). The specificity of E8 scFv was assessed by flow cytometry on a broad panel of human cells and BOSC23 cells, ectopically expressing members of the CEACAM protein family, and by immunohistochemical staining of tumor and normal human tissues.

Selection and specificity of human scFv anti CEA

In order to isolate phage-displayed specific antibodies, an aliquot of the human synthetic ETH-2 library containing approximately 1×10^{12} TU was panned on biotinylated CEA (10). After three rounds of selection, characterized by a progressive growth of output phage titer, several CEA-specific scFvs were isolated, since no cross-reactivity with streptavidin-coated plates was observed (data not shown). MA39, a phage antibody clone, one of the most reactive in ELISA, was cultured and quantities of purified scFv were produced for further investigation. Biochemical and immunohistochemical studies indicate that scFv MA39 recognizes a genuine CEA epitope in its extracellular domain. In immunohistochemical and biochemical studies MA39 binds to human colon carcinoma LoVo cells, recognizes a 200 kDa molecule of purified CEA antigen and it also stains human adenocarcinoma xenograft in mouse (Figure 1).

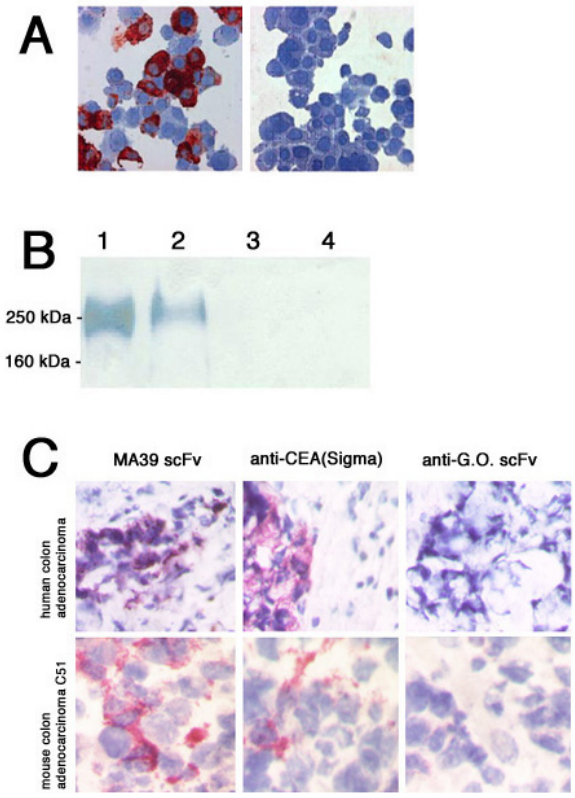

Figure 1. Recognition of CEA by MA39 antibody. A. Immunodetection of CEA in LoVo cells by MA39 scFv (left slide). The same slide preparation incubated with irrelevant anti-glucose oxidase (a protein not present in mammals) scFv antibody (anti-G.O., right slide). B. Biochemical patterns of the MA39 on purified CEA (lane 1) and LoVo cellular extract (lane 2). Lanes 3 and 4 show the reactivity of identical proteins with irrelevant anti-G.O. scFv. C. Staining of cryosections from human colon carcinoma xenograft in mouse. Commercially available anti-CEA antibody and irrelevant anti-G.O. antibodies were used as positive and negative controls, respectively

Maturation of anti-CEA scFv antibody

The first maturation library was constructed by introducing random mutations into CDR3 regions of heavy or light chains with low frequency, or by inclusion of 2-3 NNS random triplets at the 5' and 3' ends of heavy chain CDR3 of the MA39 scFv gene as previously described (10). The library was affinity-selected three times against CEA protein.

A second maturation library was selected twice against CEA protein, then single-stranded DNA was purified from phage pool and subjected to repeated error-prone mutagenesis; it was subsequently panned against target protein. A number of random clones (E1-E16) from last phage pool were isolated, tested for CEA recognition and sequenced. Equal quantities of soluble antibodies were tested by ELISA for their capacity to bind CEA protein (Figure 2). The E8 scFv, having higher reactivity, was prepared together with MA39 in large amounts for measurement of their affinity and investigation of specificity.

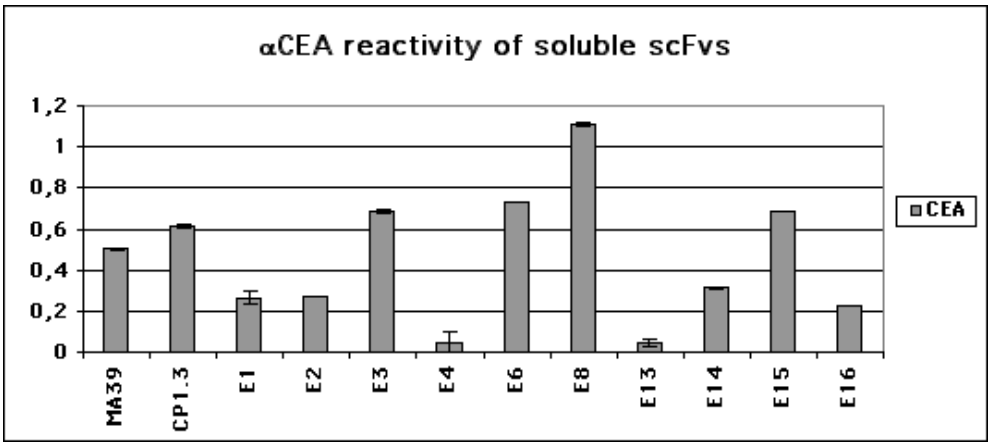

Figure 2. ELISA reactivity of original and mutated anti-CEA antibodies. Equal quantity of the soluble scFv antibodies were assayed on CEA-coated plates. Bound scFvs were developed by using anti-FLAG secondary antibody. Results are expressed as A = A405-A620. Data reported are the average values of two independent assays

Comparison of original and affinity-maturated scFv antibodies

Plasmon resonance studies with BiacoreX provided quantitative measures of scFv-antigen binding and dissociation kinetics. The KD was calculated on the basis of the measured ka and kd rate constants by using a 1:1 Langmuir model for simple bimolecular interactions (Table 1) reports the kinetic values of the parental and affinity-matured scFvs, determined on the CEA-coated chip. The original MA39 antibody has over 10 times lower affinity with the antigen, compared to E8, due to a slower association rate. The maturation process did not affect the dissociation rate.

Table 1. Kinetic values of parental and affinity matured single chains

ScFv	kon (+/- SE)	koff (+/- SE)	KD
MA39	2.08E+04 (4.39E+02)	3.57E-03 (8.64E-05)	1.71E-07
E8	1.98E+05 (3.36E+03)	2.74E-03 (5.32E-05)	1.39E-08

Recognition of CEACAM proteins, human cells and human tumors by E8 scFv

The affinity-maturated scFv E8 was tested for binding on eight different transiently transfected cell lines, each expressing a different member of the CEACAM protein family. According to this study the scFv antibody is reactive with CEACAM1 (BGP, CD66a),

CEACAM3 (CGM1, CD66d) and CEACAM5 (CEA, CD66e). This CEACAM recognition pattern of scFv E8 was also verified on a large panel of human cells which included 18 tumor cell lines, adult primary fibroblasts, PBMC subpopulations CD4 and CD14 and neutrophils. As shown in Table 2 and in Figure 3, the scFv E8 strongly reacts with melanoma metastatic cells, and to a lesser extent, with colon carcinomas HT29 and LoVo, breast carcinoma MCF7, small cell lung carcinoma H69 and primary melanomas. In contrast, we see no binding with cervical carcinoma, several human leukemias, CD4 and CD14 subpopulations nor with human neutrophils.

Table 2. Flow-cytometry determination of the binding level of the scFv clone M39 and its affinity-matured variant E8 on living/intact human cells

Cell type	Tissues	MA39	E8	Notes
HT29	Colon adenocarcinoma	+	++	a
LoVo	Colon adenorcacinoma	+	++	
KB3.1	Squamous cell carcinom	-	-	
MCF7	Breast carcinoma	+/-	+	
U937	Monocytic lymphoma	-	-	
Mel.1	Primary melanoma	+/-	+	b
Mel.2	Primary melanoma	+/-	+	
Mel.3	Metastatic melanoma	++	+++	
Mel.4	Metastatic melanoma	++	+++	
CEM	Acute T-cell leukemia	-	-	
H69	Small-cell lung carcinoma	-	-	
Jurkat	Acute T cell leukemia	-	-	
GLC4	Small-cell lung carcinoma	-	-	
K562	Chronic myelogenous leukemia	-	-	
RPMI-8226	B-cell myeloma	-	-	
Mv4-11	Acute monocytic leukemia	-	-	
THP1	Acute myeloid leukemia	-	-	
HF	Adult primary fibroblasts	-	-	
HL60	Acute promyelocytic leukemia	-	-	
PBMC	Total	-	-	c
CD4+		-	-	
CD14+		-	-	
Granulocytes		-	-	
Neutrophiles		-	-	

a:Stained cells: -, (0-5 %); +/-, (6-25 %); +, (26-50 %); ++, 51-75 %); +++, (76-100 %)
b: melanoma cells derived from characterized specimen of tumour patient.
c: PBMC and specific cell subpopulations derived from blood from health donors. No differences were observed in MA39 or E8 reactivity using cells from different donors.

Immunodetection of CEA by the human scFv E8 antibody on samples from drug unresponsiveness tumors

We examined E8 scFv specificity by immunohistochemical staining on a large panel of samples obtained through cryostatic sectioning of various normal human tissues, human melanomas and lung cancers. E8 scFv specifically binds only tumor tissue. No unspecific staining was observed on a broad panel of human organs (Table 3, Figure 3). Weak background

labeling of lung tissue was registered in one case out of nine tested. Negative control anti-G.O. antibody showed no staining (data not shown).

Table 3. **Immunohistochemical staining on cryostatic tissue sections.**

Tissue sample	Positivly stained/Total tested samples
Melanoma	7/34
Normal skin	0/9
Lung cancer	15/35 (8 strong)
Normal lung	1/9 (few cells)
Normal tissues/organs	Negative on 29 different organs

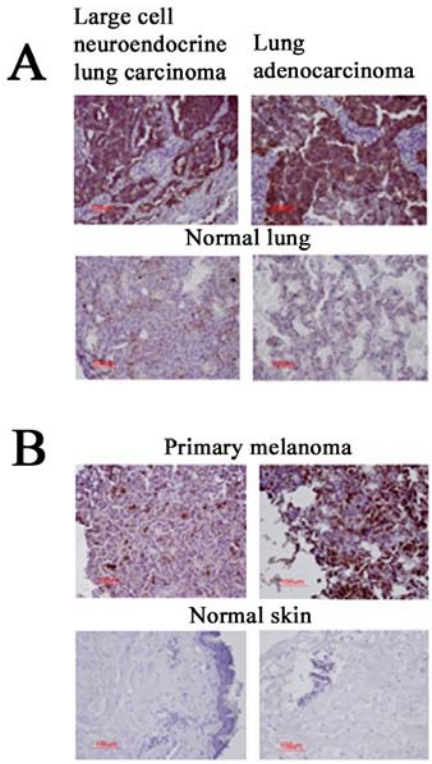

Figure 3. Staining of cryosections from normal lung and lung carcinomas (A), normal skin and primary melanomas (B). Tumor tissues show strong staining with E8 scFv antibody

Conclusion

The data reported and discussed in this paper indicate that this new immunoreagent meets several criteria for a potential anticancer compound: it is human, hence poorly or not immunogenic; it binds selectively and with good affinity to a CEA epitope expressed on human

tumors, including melanoma, metastatic melanoma, lung, breast and colon carcinomas. It is particularly interesting that there is no reactivity in various normal human cells, including distinct classes of lymphocyte subpopulations and neutrophils, as well as a broad panel of human organs. While these findings propose scFv E8 for target therapy and diagnosis of solid tumors, further anticancer utilization of such a specific antibody, including direct inhibition of tumor cell proliferation and metastasization, needs to be carefully investigated.

References

1. Szakacs G, Paterson JK, Ludwig JA, Booth-Genthe C, Gottesman MM. Targeting multidrug resistance in cancer. *Nat Rev Drug Discov* 2006;5(3):219-34.
2. Hoogenboom HR. Selecting and screening recombinant antibody libraries. *Nat Biotechnol* 2005;23(9):1105-16.
3. Sharkley RM, Goldenberg DM. Targeted therapy of cancer: new prospects for antibodies and immunoconjugates. *CA Cancer J Clin* 2006;56(4):226-43.
4. Thompson JA, Grunert F, Zimmermann W. Carcinoembryonic antigen gene family: molecular biology and clinical perspectives. *J Clin Lab Anal* 1991;5(5):344-66.
5. Hammarstrom S. The carcinoembryonic antigen (CEA) family: structures, suggested functions and expression in normal and malignant tissues. *Semin Cancer Biol* 1999;9(2):67-81.
6. Thies A, Moll I, Berger J, Wagener C, Brummer J, Schulze HJ, Brunner G, Schumacher U. CEACAM1 expression in cutaneous malignant melanoma predicts the development of metastatic disease. *J Clin Oncol* 2002;20(10):2530-6.
7. Ebrahimnejad A, Streichert T, Nollau P, Horst AK, Wagener C, Bamberger AM, Brummer J. CEACAM1 enhances invasion and migration of melanocytic and melanoma cells. *Am J Pathol* 2004;165(5):1781-7.
8. Oliveira-Ferrer L, Tilki D, Ziegeler G, Hauschild J, Loges S, Irmak S, Kilic E, Huland H, Friedrich M, Ergun S. Dual role of carcinoembryonic antigen-related cell adhesion molecule 1 in angiogenesis and invasion of human urinary bladder cancer. *Cancer Res* 2004;64(24):8932-8.
9. Laack E, Nikbakht H, Peters A, Kugler C, Jasiewicz Y, Edler L, Brummer J, Schumacher U, Hossfeld DK. Expression of CEACAM1 in adenocarcinoma of the lung: a factor of independent prognostic significance. *J Clin Oncol* 2002;20(21):4279-84.
10. Viti F, Nilsson F, Demartis S, Huber A, Neri D. Design and use of phage display libraries for the selection of antibodies and enzymes. *Methods Enzymol* 2000;326:480-505.

Session 1C. Cancer cell biology

MITOCHONDRIAL REMODELING MODULATES CELL FATE

Paola Matarrese (a), Anna Maria Giammarioli (a), Zara Zakeri (b), Walter Malorni(a)
(a) Department of Therapeutic Research and Medicines Evaluation, Istituto Superiore di Sanità, Rome, Italy
(b) MARC U-Star Program Director, Queens College of City University of New York, New York

Introduction

Mitochondria are essential organelles for life and death of the cell, as they provide most ATP and regulate several cellular pathways, from Ca^{2+} signalling to apoptosis. During apoptosis, they integrate intrinsic and extrinsic signals by releasing protein cofactors from their intermembrane space to the cytosol, where these are required for activation of effector caspases (1). The alteration of mitochondrial function is commonly detected in both apoptotic process and autophagy (2). In particular, in apoptotic cell death the loss of MMP is considered as a latest executioner event associated with the release of apoptogenic factors. In the same vein, in autophagic cell death the mitochondrial membrane undergoes depolarization but it is followed, later, by the capture of these organelles inside the autophagosomes (3). Functional versatility of mitochondria is matched by a complex morphology. Mitochondria display a complex ultrastructure, and in the cytosol of certain cell types they appear interconnected and networked. The shape of the mitochondrial network and of the individual mitochondria results from the balance of fusion and fission processes, regulated by a growing family of "mitochondria-shaping" proteins. In mammalian cells, known regulators of mitochondrial fission include cytosolic DRP-1 and its mitochondrial receptor hFis1.(4). This fusion-fission equilibrium is tightly controlled: during cytokinesis mitochondria fragment to be equally distributed into daughter cells; during cell death DRP-1 is recruited to the mitochondria to induce fission and mitochondrial cristae fuse and their narrow tubular junction widens to increase the availability of cytochrome *c* to be released (the so called "cristae remodelling" pathway). The importance of these processes is further substantiated, as mutations in mitochondria-shaping proteins can cause some neurodegenerative diseases. In fact, gene defects provoking an impairment of mitochondrial function can lead to increased oxidative stress and consequent cytotoxicity. On the other hand, a decreased apoptotic rate is associated as well with disturbances of mitochondrial fission. In particular, in cancer cells, intrinsically resistant to cell death induction, an impairment of mitochondrial fission events has been detected. With this in mind, our initial efforts have been focused at the analyses of the mechanism underlying the fission/fusion processes of mitochondria in different cell types: lymphoblastoid cells, lymphocytes, melanoma cells and neuronal cells.

Materials and methods

Characterization of the apoptotic response to different stimuli

Cells are treated with stimuli belonging to three categories: i) "classic" BH3-only BCL-2 family members such as BID, which require mitochondria to recruit the apoptotic cascade; ii)

intrinsic stimuli, such as staurosporine, etoposide, brefeldin A, which have proven to require mitochondria and adequate Ca^{2+} concentration in the endoplasmic reticulum to induce death; iii) mitochondria utilizing, Ca^{2+}-dependent stimuli, which induce death by recruiting the mitochondrial pathway only if adequate filling of intracellular Ca^{2+} stores and hence adequate mitochondrial Ca^{2+} uptake is granted. Apoptosis is measured citofluorimetrically by following the exposure of phosphatidyl serine on the outer leaflet of the plasma membrane. Mitochondria are isolated from our cellular models and are treated with apoptotic stimuli including recombinant tBID. We determined the amount of cytochrome c released after apoptotic stimuli using a quantitative ELISA assay. We also monitored MMP during apoptosis induced by the outlined stimuli using epifluorescence and confocal microscopy of our cellular models loaded with the potentiometric dye TMRM. These assays have been related to measurements of mitochondrial remodeling performed by electron microscopy.

Analysis of cell death pathway: apoptosis or autophagy

We investigate the role of mitochondrial abnormalities in apoptosis and autophagy specific inhibitors of cell death have been used. Cells were treated as follows: i) with staurosporine (STS, 1 μM) for 18 h or ii) withdrawal of growth factors (starvation, SRV) for 72 h. Both treatments were also performed in cells pre-incubated for 2 h with pan caspase inhibitor zVAD-FMK (50 μM) or 3-metil-adenine (3-MA, 10mM), an autophagy-hindering drug. Cells treated with zVAD-FMK or 3-MA alone were considered as controls. Quantitative evaluation of cell death was performed by flow (annexin V positivity) and static (Hoechst) cytometric methods as stated elsewhere (4).

Analysis of mitochondria remodelling during cell death

MMP changes will be analyzed after cell starvation procedure (SRV) and STS treatment. Treatments with pan-caspase inhibitor zVAD or autophagy inhibitor 3-MA before cell death induction via STS or SRV were also conducted in order to study the possible modulating effects of these two compounds cell death-associated mitochondrial changes. TEM analyses to point to the distribution and coalescence of mitochondria have also been used. Autophagic cell death is investigated by analysis of autophagic vacuoles by labeling with the autofluorescent drug monodansylcadaverine (MDC). Acidic compartments will be labeled by incubating the cells with LysoTracker. Cells were analyzed by Intensified Video Microscopy (IVM). To evaluate the volume and acidity of lysosomal compartment LysoTracker and LysoSensor, respectively are used.

Fusion ability of mitochondria

The Huntington's lymphoblasts isolated from patients with different length of CAG repeats will be tested for their ability of fusing the four mitochondrial membranes using a polyethylene glycol (PEG) fusion assay. The fusion assay will allow us to quantify a relationship between CAG repeats of different length and changes in the efficiency of the fusion machinery.

Analysis of mitochondrial function

Mitochondria are isolated by standard differential centrifugation procedures. The isolated mitochondria will be checked for respiratory control. Then we will investigate the underlying

mechanism by measuring mitochondrial membrane potential (MMP) following tetraphenyl phosphonium (TPP) or rhodamine 123 equilibrium distribution and by mapping the site of the deficiency at the individual respiratory chain complexes.

Analysis of the cristae topology

Cell mitochondria and isolated mitochondria will be analyzed by transmission electron microscopy. 3D tomographic reconstruction of mitochondria in thick sections will allow specific measurements of cristae junction opening.

Cells

In vitro cell cultures (both primary and stable) transfected and ingegnerized, including cybrid systems and rho0 models are considered. Static cytometry analysis for qualitative analyses of cell growth features and cytoskeletal components as well as of organelle ultrastructures. These include immunocytochemistry, fluorescence microscopy of GFP-transfected cells, immunohistochemistry and scanning and transmission electron microscopy.

Results

We report here the results obtained on T cells and neuroepithelial cells. We also report the alterations of the fission process as detected in cells under induction of senescence and proapoptotic stimulation (Figure 1). The possible implications of mitochondrial changes in terms of MMP in regulating apoptotic susceptibility and the role of mitochondrial membrane potential in regulating cell fate will also be described (Figure 2). In particular, we found that induction of apoptosis by using drugs able to activate mitochondrial-mediated cell death lead to a well evident increase of mitochondrial fission process (Figure 1, left). Conversely, the induction of the so-called premature senescence as previously described (Ref.) lead to the formation of a sort of mitochondrial network in neuroepithelial cells. Interestingly, these cells were resistant to apoptosis induction (Figure 1, right).

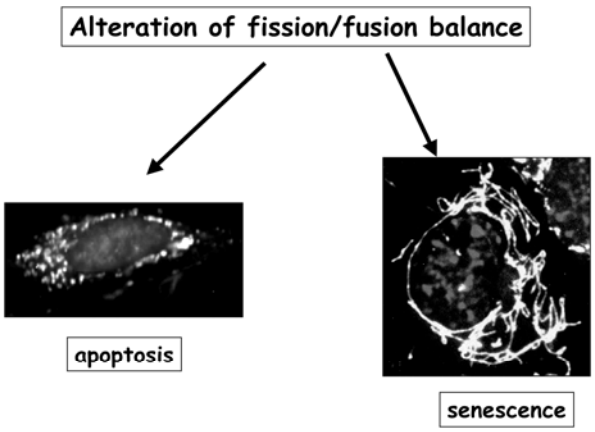

Figure 1. Alteration of fission and/or fusion balance

A second point investigated regards the implication of an increased mitochondrial membrane potential in modulating cell susceptibility to apoptosis. In fact, treatments with agents able to induce mitochondria hyperpolarization, e.g. interferon cytokine, induced a significant increase of cells with increased MMP. This increase was followed as late event to typical changes occurring in apoptosis execution, i.e. the loss of MMP. This means that one can modulate the apoptotic susceptibility of cells by using mitochondriotropic drugs able to sensitize cells to the following drug treatment associated with apoptosis (Figure 2).

In particular, when the percentage of cells with increased MMP increased (boxed areas), the following apoptotic induction was more valuable at late time points with respect to cells directly administered with pro-apoptotic drug. Conversely, using agents or drugs that impair MMP increase, i.e. mitochondria hyperpolarization, we also detected an impairment of the apoptotic cell death process (not shown).

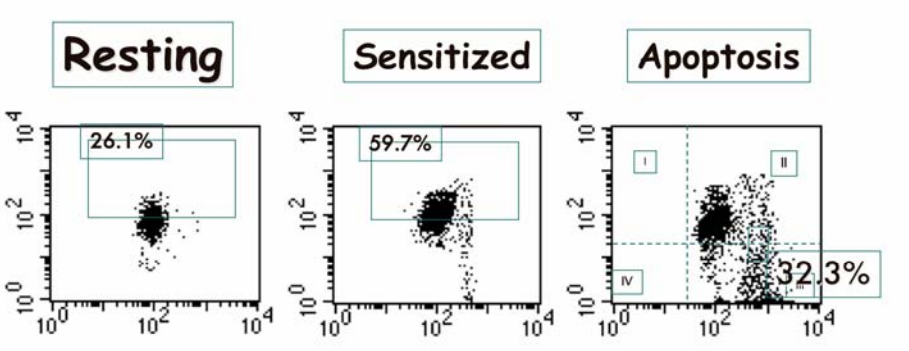

Figure 2. Increased mitochondrial membrane potential (MMP) and cell susceptibility to apoptosis

We further investigated the possible structural and functional modifications occurring in mitochondria in T cells. These results are summarized in Figure 3.

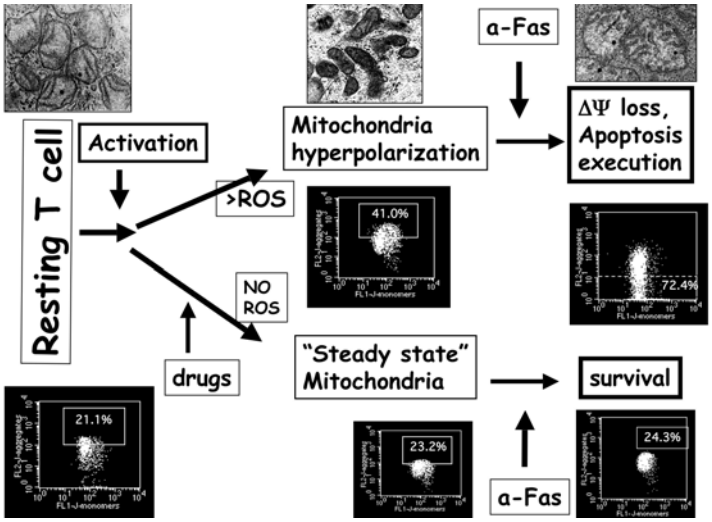

Figure 3. Structural and functional modifications occurring in mitochondria in T cells

Briefly, we found that static and flow cytometric analyses allow to point out a series of mitochondrial alterations and/or remodeling that is associated with cell fate. In particular, morphological and functional features of mitochondria can be modified by using mitochondriotropic agents that can interfere with MMP. Agents that increase MMP without inducing apoptosis per se, are also able to bolster pro-apoptotic activity of drugs, e.g. of anticancer drugs, whilst agents that impair mitochondria hyperpolarization, e.g. HIV protease inhibitors, also block apoptotic cell death.

Conclusions

The possibility to modulate cell fate, including apoptosis, via drugs that specifically interfere with cell homeostasis without inducing injury *per se* but simply bolstering or hindering cell damage is an important challenge of the last years. The interest on this matter is due to the impressive role detected for apoptosis in human pathology. It is in fact well known that a number of diseases are associated (or determined) by an increased apoptotic rate whilst other are associated (or determined) by a decreased apoptotic rate. A short representative summarizing some of these pathologies is included herein (Table 1). In fact, the importance of these results resides on the role of apoptosis regulation and manipulation in the clinical practice, i.e. in the possibility to determine cell fate.

Table1. Disease associated with apoptosis

Through inhibition of apoptosis	Through excess of apoptosis
Cancer	**Neurodegenerative diseases**
Colorectal	Alzheimer's disease
Glioma	Amyotrophic Lateral Sclerosis
Hepatic	Parkinson's disease
Neuroblastoma	Huntington's disease
Leukaemia and lymphoma	Epilepsy
Prostate	**Haematologic disease**
Autoimmune diseases	Aplastic anaemia
Systemic Lupus Erythematosus	Myelodysplastic Syndrome
Autoimmune Lymphoproliferative Syndrome	T $CD4^+$ lymphocytopenia
Thyroid diseases	G6PD deficiency
Inflammatory diseases	**Tissue damage**
Bronchial Asthma	Myocardial infarction
Inflammatory intestinal disease	Cerebrovascular accident
Pulmonary inflammation	Ischaemic renal damage
Viral Infections	Polycystic kidney
Adenovirus	**Viral Infections**
Baculovirus	AIDS

References

1. Green DR, Kroemer G. The pathophysiology of mitochondrial cell death. *Science* 2004;305(5684):626-9.
2. Boya P, Gonzalez-Polo RA, Casares N, Perfettini JL, Dessen P, Larochette N, Metivier D, Meley D, Souquere S, Yoshimori T, Pierron G, Codogno P, Kroemer G. Inhibition of macroautophagy triggers apoptosis. *Mol Cell Biol* 2005;25(3):1025-40.

3. Mormone E, Matarrese P, Tinari A, Cannella M, Maglione V, Farrace MG, Piacentini M, Frati L, Malorni W, Squitieri F. Genotype-dependent priming to self- and xeno-cannibalism in heterozygous and homozygous lymphoblasts from patients with Huntington's disease. *J Neurochem* 2006;98(4):1090-9.
4. Matarrese P, Tinari A, Mormone E, Bianco GA, Toscano MA, Ascione B, Rabinovich GA, Malorni W. Galectin-1 sensitizes resting human T lymphocytes to Fas (CD95)-mediated cell death via mitochondrial hyperpolarization, budding, and fission. *J Biol Chem* 2005;280(8):6969-85.

Session 1C. Cancer cell biology

THE ROLE OF TRANSCRIPTION FACTORS OF THE IRF FAMILY, IRF-1 AND IRF-8, IN THE GENERATION OF DENDRITIC CELL-MEDIATED TUMOR IMMUNITY: NOVEL APPROACHES TO CANCER THERAPY

Alessandra Fragale, Anna Lisa Remoli, Angela Battistini
Department of Infectious, Parasitic and Immuno-Mediated Diseases, Istituto Superiore di Sanità, Rome, Italy

Introduction

IRFs constitute a family of transcription factors whose first member, IRF-1, was originally identified as a regulator of the virus-inducible enhancer-like elements on the human IFN-β gene. Following the initial identification of the first two, structurally related, members Irf-1 and -2, seven additional cellular members have now been reported. Members of this family share a homologous DNA-binding domain characterized by some strictly conserved amino acids, particularly the five triptophan repeats, and a less conserved C-terminus, which acts as a regulatory domain. Thus, some of them function as activators and other as repressors or activators, depending on the target gene. Except for IRF-4 and IRF-8, which are expressed exclusively in cells of the immune system, other IRFs are expressed in most cell types where they exert a broad range of activities including regulation of cell growth and differentiation, haematopoiesis, oncogenesis, inflammation and immune responses. The distinct and not overlapping role of each family member are thought to be the result of slightly different DNA binding specificity, patterns of expression and/or association with other regulators (1).

The antitumor activities of, in particular, IRF-1 and IRF-8 have been well documented. Ectopic expression of IRF-1, in fact, strongly inhibits cell proliferation in several cell types and conversely overexpression of IRF-2 leads to the oncogenic transformation of NIH3T3 cells and tumor formation in nude mice reversed by the concomitant overexpression of IRF-1. The antioncogenic or tumor-suppressor function of IRF-1 is further demonstrated by the reversion of the tumorigenic phenotype exerted by the c-Myc and the c-fos oncogenes and by the studies in embryo fibroblasts from IRF-1 deficient mice. Clinical studies further indicate that IRF-1 may function as a tumor suppressor, preventing the development of some forms of human leukaemia (2). These effects are also mediated by the regulation of adaptive immune responses mediated by IRF-1. Mice deficient in IRF-1 gene are, in fact, 90% deficient in mature $CD4^{-}CD8^{+}$ T cells in the thymus. A defective Th1 responses along with exclusive Th2 differentiation, impaired macrophage production of interleukin-12, impaired natural killer (NK) cell development and NK cell-mediated cytotoxicity *in vivo* are all, also, observed in IRF-$1^{-/-}$ mice (1).

Similarly, IRF-8 has been implicated in antitumor activities. IRF-$8^{-/-}$ mice develop a syndrome similar to human chronic myelogenous leukaemia (CML) and 30% of IRF-$8^{-/-}$ mice undergo acute blasts crisis characterized by the clonal expansion of leukemic cells. IRF-8 is down regulated in Bcr-Abl-induced murine chronic myelogenous leukaemia-like disease and in the human system a down modulation of IRF-8 mRNA expression is observed in several human CML and acute leukaemia cases. IRF-8 is, similarly to IRF-1, involved in antigen-specific

immunity with the stimulation of an efficient CTL and Th1 response. This effect is mediated by the induction of Il-12 and IFN-γ and of a cascade of other secondary and tertiary proinflammatory cytokines acting at different levels on tumor cells (1).

Both IRF-1 and IRF-8 has been also implicated in myeloid progenitor cells differentiation where they exert a specific role in lineage commitment of granulocytes and monocytes, respectively, acting in opposite fashion in promoting selected lineage programs and suppressing unrelated ones (3,4). More recently, the essential role of IRF-8 in the development and maturation of two subsets of DC i.e. $CD8\alpha^+$ and plasmacytoid DC has also been reported (5).

Dendritic cells (DC) are crucial components of the immune system owing to their essential role in the induction and control of T cell immunity and in the modulation of responses by NK and B cells. These cells have the capacity to capture, internalize and process antigen for presentation in the context of MHC molecules to any T cell with a receptor that is specific for the foreign-peptide-MHC complexes on the DC surface. DC can also regulate the response made, dictating the cytokines expressed by responding T cells, but also can down-regulate T-cell activation playing a role in the induction of tolerance (6,7). All these functions are elicited by distinct DC subpopulations with different phenotypic and functional profiles. Functional diversity can be related to their differentiation state as well as their specific location, depending on differential interactions with antigen and immune system effectors cells (8). Recently, DC are becoming promising alternative tools for vaccination and immunotherapy of several diseases including immunotherapy of cancer, chronic viral infections, autoimmunity and allergy (9,10). In this context isolated DC loaded with tumor antigens *ex-vivo* and administered as vaccine, have been found to induce protective and antitumor immunity in experimental models (11). Pilot clinical trials of DC vaccination for a variety of human cancers are underway and new methods for targeting tumor antigens to DCs *in vivo* as well as for increasing the capacity of antigen presentation to target cells in order to enhance vaccine protection are actively investigated. *Ex-vivo* gene transfer with viral and non-viral vectors is frequently used to obtain the expression of the tumor antigens and the efficacy of this approach is greatly enhanced if DC are transfected with a number of genes which encode immunostimulating factors, including cytokines and co-stimulatory molecules (12).

In this context, the joint project ISS-NIH whose American partner is Dr. Keiko Ozato at the National Institute of Child Health and Human Development, NIH, deals with the use of IRF-1 and IRF-8 transcription factors alone or in combination as tools for the generation of DC more active in the immunotherapy of cancer. We expected that IRFs-engineered DC display superior antigen-presentation and/or evocation of a long lasting antitumor T and B cell response.

Results and discussion

In the first phase of the project at ISS, we determined which subset of DC is stimulated after IRF-1 and/or IRF-8 expression and evaluated the extent of DCs activation and functionality dependent on IRFs expression

The results obtained indicated that IRF-1 is involved in the generation and activation of CD8α+ DCs and in immune homeostasis through the control of plasmacytoid and tolerogenic DC generation. Indeed, IRF-1 deficient mice exhibit a predominance of plasmacytoid DC and a selective reduction of conventional DC, especially the CD8α+ subset (Table 1 and Figure 1).

Table 1. Reduced percentage of CD11c ^{high} and increased percentage of CD11c^{low} DCs in lymphoid organs of IRF-1$^{-/-}$ mice

		Spleen	s-dLN	mLN	Thymus
WT	CD11c $^{+}$	39.6	40.7	24.8	6.2
	CD11c ^{high}	31.3	15.1	15.1	-
	CD11c ^{low}	8.5	23.4	10.9	-
IRF-1$^{-/-}$	CD11c $^{+}$	28.6	40.7	21.5	9.5
	CD11c^{high}	14.3	10.7	7.27	-
	CD11c^{low}	13.9	28.9	14.43	-

The indicated lymphoid organs from IRF-1$^{-/-}$ or WT mice were pooled and enriched for DC by Nycodenz density-gradient centrifugation, the low-density cell fraction was stained for CD11c and analysis was performed according to the expression of this marker and by forward side scatter properties. Two regions were drawn on DC populations expressing CD11c at low and high levels and the percentage of gated-cells was determined. Numbers are representative of at least five independent experiments.

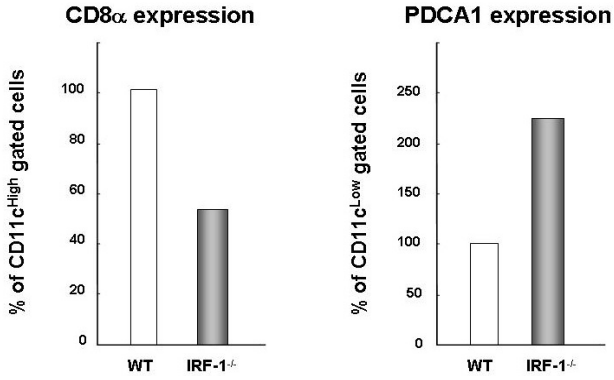

Figure 1. Decreased expression of CD8α and increased expression of PDCA1 in CD11c^{High} and CD11c^{Low} DC in IRF-1$^{-/-}$ mice

Moreover, DC from IRF-1-/- mice were less efficient in stimulating the proliferation of allogeneic T cells and instead induced suppressive activity in allogeneic CD4+CD25+ regulatory T cells (Figure 2) (13).

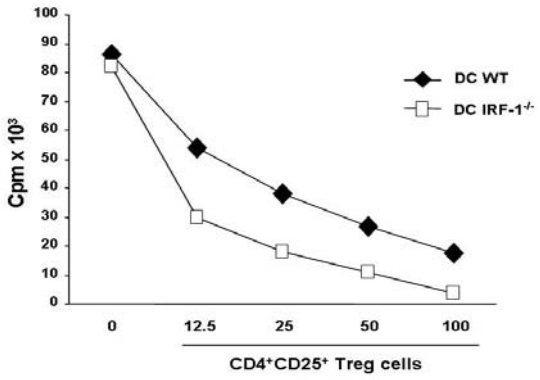

Figure 2. DC from IRF-1$^{-/-}$ mice induce suppression activity in allogeneic CD4$^+$CD25$^+$ Treg cells

Indeed, there is growing evidence that immature or partially matured DC can induce tolerance. Accordingly, we found that the tolerogenic characteristics of IRF-$1^{-/-}$ DC may also contribute to constitutive suppressor mechanisms including the maintenance of an immature/anergic DC phenotype and the induction of activated $CD4^+CD25^+$ Treg. IRF-1 deficient mice exhibit, in fact, a tolerogenic-polarized immune system characterized by a selective and marked increase in $CD4^+CD25^+$ Treg cells, with a highly differentiated and activated tolerogenic phenotype. A specific binding and transcriptional regulation by IRF-1 of the master gene regulator of Treg was also demonstrated (Table 2 and Ref. 16).

Table 2. Increased Percentage of $CD4^+CD25^+$ T reg cells in Lymphoid Organs of IRF-$1^{-/-}$ Mice

	Spleen	Skin-draining LN	Mesenteric LN	Thymus
WT	2.3	3.9	3.1	11.4
IRF-1 $^{-/-}$	6.8	9.1	7.2	18.3

On the other hand, IRF-8 is involved in the development and activity of $CD8\alpha^+$ subset but not in that of $CD8\alpha^-$ subset. Conversely, an opposite effect as compared to IRF-1 is exerted on the differentiation of plasmacytoid DC which are completely absent in IRF-8-/- mice (14,15 and Figure 3). These findings may be particularly relevant in the field of tumor vaccination where the use of plasmacytoid DC, as inducers of tolerogenic T cells, must be avoided and the maturation stage of DC used for antigen loading must be carefully tested.

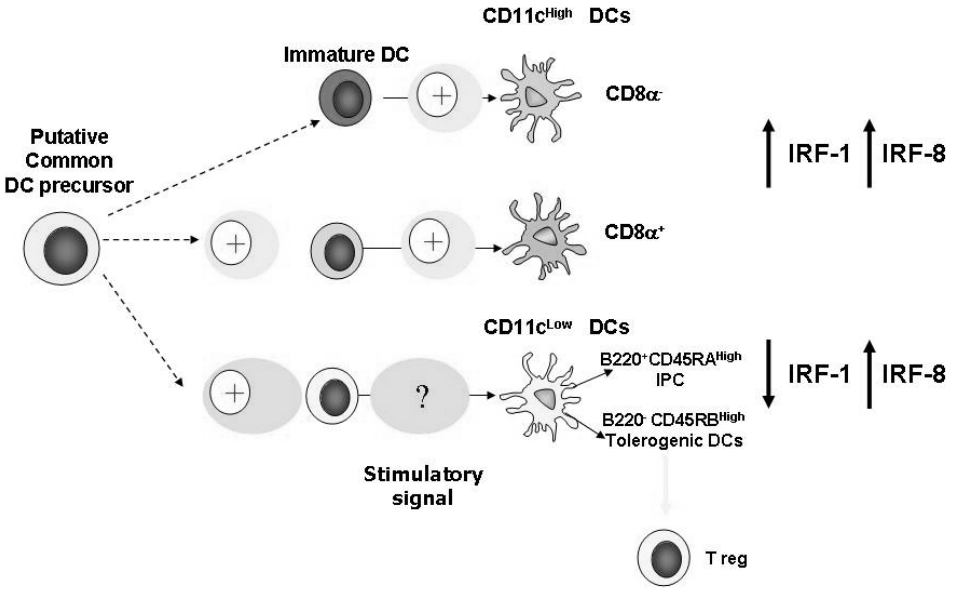

Figure 3. IRF-1/IRF-8 cross-talk in the control of DC development and activation

From the results so far obtained and summarized in Figure 4 we can thus conclude that IRF-1 and IRF-8 can be considered useful tools for the manipulation of DC and T cells in new therapeutic strategies for shaping immune responses. We therefore planned to go on in the

setting and preparation of vector suitable for DC infection and in the evaluation of the ability of IRF-engineered DC to stimulate specific and superior immune responses.

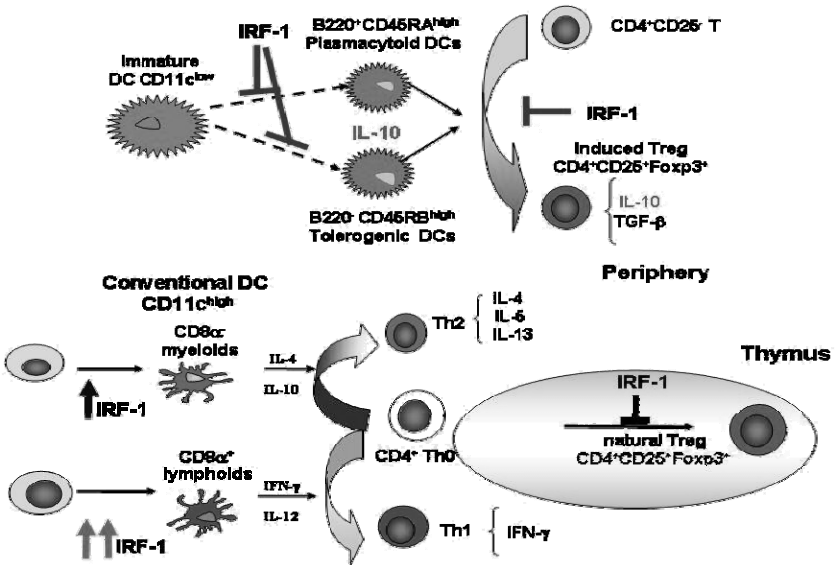

Figure 4. Role of IRF-1 in DC and Treg cells development

Finally, in the context of the joint project, Dr. Remoli spent a period in the Laboratory of Keiko Ozato at the NIH, extending the study of the IRF-8 transcriptional activity in monocytes and looking at the physical and functional interactions with the chromatin remodeling factor BRG1. By classical, as well as innovative, techniques such as FRAP (Fluorescence recovery after Photobleaching) which allows to measure in intact cells the interaction of proteins with chromatin, and BiFc (Bifluorescence Complementation) which visualizes physical protein-protein interactions in living cells, she demonstrated that both IRF-1 and Irf-8 interact with BRG1 as well as with other proteins of the BAF complex. These interactions determine the accessibility of the specific transcription factors to the promoter of their target genes. Beside them the IL-12 p40 is of particular interest in the setting of an efficient adaptive immune response.

These results have been the object of a PhD thesis and of joint manuscript in preparation.

References

1. Taniguchi T, Ogasawara K, Takaoka A, Tanaka N. IRF family of transcription factors as regulators of host defence. *Annu Rev Immunol* 2001;19:623-55.
2. Taniguchi T, Lamphier MS, Tanaka N. IRF-1: the transcription factor linking the interferon response and oncogenesis. *Biochim Biophys Acta* 1997;1333:M9-M17.
3. Coccia EM, Stellacci E, Valtieri M, Masella B, Feccia T, Marziali G, Hiscott J, Testa U, Peschle C, Battistini A. Ectopic expression of Interferon regulatory factor-1 potentiates granulocytic differentiation. *Biochem J* 2001;360:285-94.

4. Tamura T, Nagamura-Inoue T, Shmeltzer Z, Kuwata T, Ozato K. ICSBP direct bipotential Myeloid progenitor cells to differentiate into mature macrophages *Immunity* 2000;13:155-65.
5. Zenke, M., Hieronymus, T. Towards an understanding of the transcription factor network of dendritic cell development. *Trends Immunol* 2006;27:140-5.
6. Banchereau J, Briere F, Caux C, Davoust J, Lebecque S, Liu YJ, Pulendran B, Palucka K. Immunobiology of Dendritic cells. *Annu Rev Immunol* 2000;18:767-811.
7. Ardavin C. Origin, precursors and differentiation of mouse dendritic cells. *Nature Rev* 2003;3:1-9.
8. Shortman K, Liu Y-J. Mouse and human dendritic cell subtypes. *Nature Rev* 2002;2:151-61.
9. Fong L, Engleman EG. Dendritic cells in cancer immunotherapy. *Ann Rev Immunol* 2000;18:245-73.
10. Jonuleit H, Schmitt E, Steinbrink K, Enk AH. Dendritic cells as a tool to induce anergic and regulatory T cells. *Trends Immunol* 2001;22:394-400.
11. Timmerman JM, Levy R. Dendritic cell vaccines for cancer immunotherapy. *Annu Rev Med* 1999;50:507-29.
12. Tirapu I, Rodriguez-Calvillo M, Qian C, Duarte M, Smerdou C, Palencia B, Mazzolini G, Prieto J, Melero I. Cytokine gene transfer into dendritic cells for cancer treatment. *Curr Gene Ther* 2002;2:79-89.
13. Gabriele L, Fragale A, Borghi P, Sestili P, Stellacci E, Venditti M, Schiavoni G, Sanchez M, Belardelli F, Battistini A. IRF-1 deficiency skews the differentiation of dendritic cells towards plasmacytoid and tolerogenic features. *J Leuk Biol* 2006 in press.
14. Tsujimura H, Tamura T, Gongora C, Aliberti J, Reis e Sousa C, Sher A, Ozato K. ICSBP/IRF-8 retrovirus transduction rescue dendritic cell development in vitro. *Blood* 2003;101:961-9,
15. Schiavoni G, Mattei F, Sestili P, Borghi P, Venditti M, Morse HC 3rd, Belardelli F, Gabriele L. ICSBP is essential for the development of mouse Type I interferon-producing cells and for the generation and activation of CD8α+ Dendritic cels. *J Exp Med* 2002;11:1415-25.
16. Fragale A, Gabriele L, Borghi P, Stellacci E, Ilari R, Lanciotti A, Venditti M, Belardelli F, Battistini A. Selective regulatory function of IRF-1 in the development of $CD4^{+}CD25^{+}$ T Regulatory T Cells (submitted).

Session 1C. Cancer cell biology

PROTEIN ELECTRONICS

Alessandra Luchini (a,b), Emanuel Petricoin (b), Lance A. Liotta (b), David H. Geho (b)
(a) CRO-IRCCS National Cancer Institute, Aviano, Italy.
(b) Center for Applied Proteomics and Molecular Medicine, George Mason University, Manassas, VA

Introduction

Varied technologies are being applied in clinical research with the hope of identifying disease-related molecular changes. Examples of these include genomic arrays, protein microarrays, and mass spectrometry. Particular interest is currently aimed at the expressed protein content of diseased tissues. There exists currently no intrinsic amplification system for proteomic studies, as is found with DNA and the polymerase chain reaction. In order to identify how proteins are modified in disease states, highly sensitive detection and analysis technologies must be developed and utilized.

Currently, a variety of proteomic tools exist, including gel electrophoresis, Western blots, mass spectrometry, UV spectroscopy, and chromatography. A key element of the electrophoretic tools is the differential behavior of proteins within an applied electrical field. For example, the migration of a protein within a polyacrylamide gel under the application of an electrical field is commonly used to evaluate the molecular size of proteins in everyday biomedical research.

The transport of charges within a protein is an underutilized property that could potentially be used to characterize proteins. Protein electronics utilizes the latest in nanofabricated test bed structures and techniques to study the charge transport in proteins. It is hoped that test systems generated out of this area of research may someday have applicability in biomedical research and in clinical settings.

Origins of molecular electronics

Miniaturization of integrated circuits has revolutionized science and technology. In the 1960's, Moore foresaw the enormous number of transistors that could be fit onto a single silicon wafer (1). Anticipating a time when the maximal number of transistors that could be engineered out of silicon-based materials was achieved, scientists soon thereafter began exploring alternative means of enabling charge transport other than using materials such as silicon. In the mid 1970s the idea of enclosing a few or even a single molecule between electrodes was proposed. The goal of this work was to create molecular electronics platforms that could perform the basic functions of digital electronics such as rectification, amplification, and storage (2).

Since these early efforts, much research has been directed towards the development of electronic devices incorporating single or small assemblies of organic molecules (3). Using a wide range of chemical functionalities, varied electronic structures can be created via molecular self-assembly. Because these functionalities are operative at the angstrom to nanometer scale, it is possible to generate exceedingly small test architectures and structures. Further, based on

chemical functionalities, they can be elaborated using basic synthetic chemistry approaches in order to fashion diverse electrical structures. Such chemical malleability is an attractive feature of molecular electronics, as it enables rational "tuning" of electrical properties as well as the possibility of creating complex electronic structures.

Previous experimental research has demonstrated that different molecular structures mediate varying degrees of charge transport. For example, Long et al demonstrated differential charge transport between undecanethiol (C11), oligo(phenylene ethynylene) (OPE), and oligo(phenylene vinylene) (OPV) (4). In order to make such measurements, refined test bed structures have been constructed. Beyond the assembly of organized molecular monolayers, one of the most important issues in molecular based electronics is the development of a fabrication process that is characterized by high yield in parallel assembly of devices and does not damage the activity of molecular wires.

One platform based on magnetically directed assembly that has both of these requirements has been recently reported (4,5). With this system, silica particles are coated with metal, which enables magnetically directed self assembly of the particles in such a manner that a micron-sized gap is bridged. The test bed electrode is coated with elemental gold. Test molecules are immobilized onto the gold using standard bioconjugate techniques. It is this system that provided insight into the charge transport properties of undecanethiol (C11), oligo(phenylene ethynylene) (OPE), and oligo(phenylene vinylene) (OPV) (6).

Protein electronics

Like carbon, silicon can stably form four covalent bonds with other atoms. By itself, pure silicon is a poor conductor of electrical current. When doped with an impurity such as a phosphorous containing compound, silicon may become more conductive and function as a semiconductor. Saturated hydrocarbon structures are poor conductors of electrical current. As described above, other carbon-based structures, however, can be more effective in charge transport.

Using a limited set of amino acid building blocks, a vast array of polymeric structures, or proteins, can be fashioned. Amino acids are linked via a repetitive motif, namely the peptide bond that forms between the carboxy terminus of one amino acid and the amino terminus of the following amino acid. The distinct chemical attributes of the naturally occurring amino acids resides within the side chains of the amino acids. Proteins are ordered structures that fold based on intrinsic primary amino acid sequence as well as with the assistance of other proteins that facilitate folding, such as chaperonins. From a molecular electronics perspective, the uniformity of the peptide bond coupled with the diversity of amino acid side chains creates a remarkably diverse palette from which one can create charge transport media. An attractive feature of proteins is their ability to self assemble into macromolecular structures that mediate complex physiological tasks. Affinity properties of proteins, in large part contributed by the surface topology and biochemical characteristics of a protein, enable this self assembly. For this reason, electrical structures built out of proteins would have the added properties of controlled alteration by the addition of affinity binding partners. In comparison, silicon, unless modified with bio-reactive functionalities, is relatively inert.

The electrical properties of both limited protein structural elements, like alpha helices, and mature proteins, like casein, have been previously studied (7). Of particular interest is the effect on charge transport that covalent coupling of a small ligand, methylglyoxal, to casein was found to have (8). The addition of small molecules to polypeptides therefore represents an approach for the modulation of electron transport within a protein electronics device. The working

hypothesis is that the binding of a guest species to single host molecules can be studied electrically by wiring the host molecules to two electrodes. Peptides are very desirable candidates as host molecules because there is vast choice of different sequences that can be optimized to obtain high binding strength and specificity to a targeted host molecule (9).

Examining how posttranslational modifications alter charge transport in polypeptides

Given recent advances in nanofabrication, which have led to the development of highly parallel testing arrays, we are now exploring the applicability of this technology for testing biomedically relevant polypeptides. These nanofabricated structures can be coated with elemental gold, which provides a convenient linkage site for polypeptides. More specifically, the elemental gold forms a covalent bond with the sulfhydryl group present in cysteines. This type of polypeptide immobilization strategy has been previously utilized to immobilize alpha helical peptides onto gold coated test surfaces (10). The orientation of the helices axis was proved to be dependent on the solvent used for the deposition, the length and the chemical composition of the chain (11).

We are currently utilizing a similar test bed to study the effects of polypeptide structure on charge transport. More specifically, synthetic polypeptides containing a cysteine moiety are immobilized onto the gold electrodes of the test structure. As described above, the cysteine residue provides a site for covalent coupling with the gold surface. The gap in the electronics device is bridged using the metallized silica spheres described previously. Once assembled, this test system allows us to measure charge transport across the peptides. Our preliminary experimental data indicates that this system is effective for studying the charge transport in synthetic polypeptides.

One of the important goals for our program is to understand how controlled structural change in a peptide effects charge transport in a protein semiconductor. By developing reliable structure/charge transport correlates, we hope to contribute an important set of knowledge for molecular electronics research. Long term, the field of protein electronics may yield new classes of biomedical sensors and computing devices. It is also possible that label-free evaluation of proteins may be enabled by this research.

Acknowledgments

This work was partly supported by the Italian Istituto Superiore di Sanità in the framework Italy/USA cooperation agreement between the US Department of Health and Human Services and the Italian Ministry of Public Health. The authors appreciate the generous support of Dr. Vikas Chandhoke and the Department of Life Sciences at George Mason University. We would like to acknowledge stimulating discussions with Dr. David Long, Dr. Iosif Vaisman, Dr. Ranganathan Shashidhar, Dr. Enrico Garaci, Dr. Alfonso Colombatti, and Dr. Claudio Belluco, Dr. Barney Bishop, and Dr. Victor Morozov.

References

1. Moore GE, Cramming more components onto integrated circuits. *Electronics* 1965;38(8):114-7.
2. Aviram A, Ratner M. Molecular rectifiers. *Chem Phys Lett* 1974;29:277-83.

3. Joachim C, Gimzewski JK, Aviram A. Electronics using hybrid-molecular and mono-molecular devices. *Nature* 2000;408:541-8.
4. Long DP, Patterson CH, Moore MH, Seferos DS, Bazan GC, Kushmerick JG. Magnetic directed assembly of molecular junctions. *Applied Physics Letters* 2005;86:153105.
5. Kushmerick JG, Blum AS, Long DP. Metrology for molecular electronics. *Analytica Chimica Acta* 2006;(568):20-7.
6. Szent-Gyorgyi A. Towards a new biochemistry? *Science* 1941;93:609-11.
7. Pethig R, Szent-Gyorgyi A. Electronic properties of the casein-methylglyoxal complex. *Proc Natl Acad Sci U S A* 1977;74:226-8.
8. Xiao X, Xu B, Tao N. Changes in the conductance of single peptide molecules upon metal-ion binding. *Angew Chem Int Ed* 2004;43:6148-52.
9. Sek S, Swiatek K, Misicka A. Electrical behavior of molecular junctions incorporating α-helical peptide. *J Phys Chem B* 2005;109(49):23121-4.
10. Miura Y, Kimura, S. Formation of oriented helical peptide layers on a gold surface due to the self-assembling properties of peptides. *Langmuir* 1998;14:6935-40.

Session 1C. Cancer cell biology

PHOSPHOPROTEOMIC ANALYSIS OF PRIMARY AND METASTATIC COLORECTAL CANCER: NEW INSIGHTS FOR CANCER THERAPY

Claudio Belluco (a), Enzo Mammano (b), Mariaelena Pierobon (b), Valerie Calvert (c), Mario Lise (a,b), Emanuel Petricoin (c), Lance Liotta (c)
(a) Division of Surgical Oncology, CRO – IRCCS, National Cancer Institute, Aviano, Italy
(b) Department of Oncological and Surgical Science, Surgery Branch, University of Padova, Padova, Italy
(c) Center for Applied Proteomics and Molecular Medicine, George Mason University, VA, USA

Introduction

Colorectal cancer (CRC) is the second leading cause of cancer-related death in western countries and the liver represents the most common site of metastatic disease and the major determinant of survival in patients with this type of neoplasm (1). About 70% of patients with CRC liver metastases have unresectable disease and, in these patients, chemotherapy achieves median survival of only 15 months (2). New and more effective agents are therefore needed for the treatment of these patients. Extracellular stimuli, such as hormones, growth factors and cytokines, regulate biological cell functions by altering the levels of protein phosphorylation, which represent the initial and crucial event for most signaling pathways inside the cell. Protein kinases, by phosphorylating substrate proteins, direct the activity, localization and overall function of proteins involved in complex functions such as cell growth and differentiation, cell cycle control and apoptosis, which are often disregulated in cancer development and progression (3,4). Protein kinases are, therefore, considered important targets for molecular therapeutics (5). Reverse phase protein microarray is a new technique, which has been recently developed to map the state of key signal transduction pathways from human biopsy specimens by looking at dozens of kinase substrates at once through multiplexed phospho-specific antibody analysis (6). In this study, we investigated by reverse phase protein microarray the phosphoproteomic satus of different protein kinases in primary CRC and in liver metastasis.

Materials and methods

Frozen tissue samples from five primary CRCs without distant metastasis, three patient-matched primary CRCs and synchronous liver metastasis and five CRC metachronous liver metastasis were used for this study. Tissue samples were collected directly in the operating room and immediately snap frozen and stored in liquid nitrogen until used. Eight-micron sections were obtained and approximately 20,000 cells from each tissue sample were microdissected by Laser Capture System (Arcturus Engineering, Mountain View, CA, USA). Cells were lysed for 30 min at 75 °C using a 1:1 mixture TPER Reagent (Pierce, Rockford, IL, USA) and 2× Tris–Glycine SDS Sample Buffer (Novex/Invitrogen). After cell lysis, cells were boiled for 10 min and stored at 4 °C for arraying. Three nanoliters of lysate were arrayed by a pin and ring GMSE 417 Arrayer (Affymetrix, Santa Clara, CA, USA) onto nitrocellulose slides.

Arrayed slides were prepared for staining by reacting with Reblot (Chemicon, Temencula, CA, USA) followed by two washes with PBS washing buffer. Slides were then treated overnight with I-Block (Applied Biosystem, Bedford, MA, USA). To estimate the total protein amount, selected arrays were stained with Sypro Ruby Protein Blot Stain (Molecula Probes, Eugene, OR, USA) and visualized on a Fluorchem™ imagin system (Alpha Innotech, San Leandro, CA, USA). Slides were stained on an automated slide stainer (Dako, Carpinteria, CA, USA) using a biotin-linked peroxidase catalyzed signal amplification. Finally, the primary antibodies at concentrations ranging from 1:50 to 1:1000 were applied for 30 min followed by the secondary link antibody for 30 min (concentration 1:10 for antimouse antibodies and 1:5000 for antirabbit antibodies). Twenty nine commercially available primary antibodies were used: Cleaved Caspase 3 (D175) 1:50 (Cell Signaling Technology, Beverly, MA, USA), Phospho-CREB (S133) 1:200 (Cell Signaling Technology), Phospho-ERK 1/2 (T202/Y204) 1:500 (Cell Signaling Technology), Phospho-IRS1 (S616) 1:500 (Biosource, Camarillo, CA, USA), Phospho-IKBα (S32) 1:100 (Cell Signaling Technology), EGFR 1:50 (Cell Signaling Technology), pGSK-3 alpha/beta (Ser21/9) 1:1000 (Biosource), Phospho-cKit (Y719) 1:100 (Cell Signaling Technology), Phospho-EGFR (Y1148) 1:100 (Biosource), Phospho-STAT1 (Y701) 1:200 (Cell Signaling Technology), ErbB2 1:50 (Neomarkers, Lab Vision Corporation, Fremont, CA, USA), Phospho-PDGFRb (Y716) 1:100 (Upstate, Waltham, MA, USA), Phospho-PKCá (S657) 1:1000 (Upstate), Cox2 1:200 (Upstate), Phospho-mTOR (S2448) 1:100 (Cell Signaling Technology), Phospho-MARCKS (S152/156) 1:50 (Cell Signaling Technology), Phospho-P38 (T180/Y182) 1:50 (Cell Signaling Technology), Phospho-PTEN (S380) 1:200 (Cell Signaling Technology), Phospho-STAT3 (S727) 1:50 (Biosource), Phospho-Aurora A/AIK (T288) 1:100 (Cell Signaling Technology), Phospho-Zap 70 (Y493) 1:200 (Cell Signaling Technology), pJNK/SAPK (Thr183/Tyr185) 1:50 (Cell Signaling Technology), pNF-kB p65 (Ser536) 1:50 (Upstate), Cleaved Caspase 9 (D315) 1:50 (Cell Signaling Technology), Phospho-BAD (S112) 1:100 (Cell Signaling Technology), Phospho-c-Abl (T735) 1:50 (Cell Signaling Technology), Phospho-STAT1 (S727) 1:1000 (Upstate), Phospho-AKT (S473) 1:50 (Cell Signaling Technology), Phospho-ErbB2/Her2 (Y1248) 1:1000 (Upstate). The specificity of each antibody was previously tested by Western blotting. Stained slides were scanned individually on a UMAX PowerLook III scanner (UMAX, Dallas TX, USA) at 600 dpi and saved as TIF files. The TIf images for antiboby-stained and Sypro-stained slides images were analyzed with ImageQuant 5.2 (Molecular Dynamics, Sunyvale, CA, USA). For each antibody, the average pixel intensity value for the first point in each dilution curve was divided by the corresponding value of the Sypro-stained total protein slide. Unsupervised hierarchical two-way clustering analysis was used for comparing the signalling profiles of the different samples.

Results

Unsupervised hierarchical two-way clustering analysis of the signaling pathway using 29 different endpoints demonstrated that the phosphoproteomic profile of the liver metastases was entirely different from that of the primary tumors. This difference was also observed in the three patient-matched primary CRCs and liver metastases. Overall, most of the protein kinases appeared to be overexpressed in the liver metastases compared to the primary tumors compared to the primary tumors.

Discussion

While gene microarrays can provide important information about somatic genetic taxonomy, they are unable to provide a full picture of the fluctuating signaling events that occur at the proteomic level. In fact, cellular signaling events are driven by protein–protein interactions, post-translational protein modifications and enzymatic activities that cannot be accurately predicted or described by transcriptional profiling methods alone (4,7). Recently, antibodies have been developed to specifically recognize the phosphorylated isoform of kinase substrates. In theory, it could be possible to evaluate the state of entire portions of a signaling pathway or cascade, even though the cell is lysed, by looking at dozens of kinase substrates at once through multiplexed phospho-specific antibody analysis. Protein microarrays offer the promise to dramatically multiplex, quantify, accelerate and miniaturize this type of analysis over any existing format (8,9). Our study demonstrates that reverse phase protein microarray analysis of human primary CRC and liver metastases is feasible and requires only approximately 20,000 cancer cells to perform multiplexed phosphoproteomic fingerprinting of a large number of signaling endpoints simultaneously. This analysis can be performed using new software tools that employ well-founded statistical methods to compare relative levels of phospho-specific endpoints across different tissues from several different patients. Unsupervised hierarchical clustering analysis of the signaling pathway portraits identified new signaling circuitry that was associated with a metastatic specific molecular network and a primary tumor specific circuit. Clustering analysis revealed that the signaling networks in use within primary CRC dramatically change upon metastasis. This finding, which might be explained by a direct influence of the organ microenvironment on the neoplastic cells, re-emphasizes the need to perform molecular network analysis of the metastatic process itself when therapeutic targeting is considered. Moreover, analysis and identification of important metastatic signaling networks could yield new insights into target selection for targeted therapeutics. In the future, this new technique may be used to map the state of key pathways of patient's tissue samples before starting chemotherapeutic treatment to choose an individualized and optimized combination therapy. Since our findings are of potential clinical relevance, further studies using larger study sets will need to confirm our data and to evaluate if the same type of tumor has different phosphorylated phenotypes in different metastatic organs.

References

1. Jemal A, Tiwari RC, Murray T, Ghafoor A, Samuels A, Ward E, *et al*. American Cancer Society Cancer Statistics, 2004. *CA Cancer J Clin* 2004;54(1):8-29.
2. Liu LX, Zhang WH, Jiang HC. Current treatment for liver metastases from colorectal cancer. *World J Gastroenterol* 2003;9(2):193-200.
3. Manning G, Whyte DB, Martinez R, Hunter T, Sudarsanam S. The protein kinase complement of the human genome. *Science* 2002;298(5600):1912-34.
4. Blume-Jensen P, Hunter T. Oncogenic kinase signalling. *Nature* 2001;411(6835):355-65.
5. Petricoin EF, Liotta LA. Molecular profiling of human cancer. *Nat Rev Genet* 2000;1:48-56.
6. Paweletz CP, Charboneau L, Bichsel VE, Simone NL, Chen T, Gillespie JW, *et al*. Reverse phase protein microarrays which capture disease progression show activation of pro-survival pathways at the cancer invasion front. *Oncogene* 2001;20(16):1981-9.
7. Ge H, Walhout AJ, Vidal M. Integrating domicT information: a bridge between genomics and systems biology. *Trends Genet* 2003;19:551-60.

8. Nielsen UB, Cardone MH, Sinskey AJ, MacBeath G, Sorger PK. Profiling receptor tyrosine kinase activation by using Ab microarrays. *Proc Natl Acad Sci U S A* 2003;100:9330-5.
9. Liotta LA, Espina V, Mehta AI, Calvert V, Rosenblatt K, Geho D, *et al*. Protein microarrays: meeting analytical challenges for clinical applications. *Cancer Cell* 2003;3(4):317-25.

Session 1. Poster

CANCER INFORMATION PROGRAM FOR PATIENTS

Stefano Vella (a), Edward L. Trimble (b), Mary Anne Bright (c), Chris Thomsen (d)
(a) Department of Therapeutic Research and Medicines Evaluation, Istituto Superiore di Sanità, Rome, Italy
(b) National Cancer Institute, National Institutes of Health, Bethesda, MD, USA
(c) Cancer Information Service – NCI, National Institutes of Health, Bethesda, MD, USA
(d) National Center for Complementary and Alternative Medicine – NCI, National Institutes of Health, Bethesda, MD, USA

Introduction

In the last few years the interest in health-related information has remarkably increased, and the National Institutions try to give careful data to all patients who need. Cancer patients in particular, with their friends and families, need accurate and timely answers about risk factors, prevention, treatment, research, clinical trials and availability of new drugs.

In the USA, the National Cancer Institute's Cancer Information Service provides the latest and most accurate cancer information to patients, their families, the public, and health professionals. In Italy, one of the missions of the Italian Institute of Health is to improve public health through qualified information.

In 2005, the NIH and the ISS, with the essential help of patient associations, joined together to develop a program on information for cancer patients. We believe that this collaboration will expanded our ability to partner to reduce cancer health disparities. In addition, international cancer control and cancer research programs improve our ability to understand, prevent, and treat cancer and our ability to assist and support cancer patients.

Activities

Patient-oriented information booklet

The project on "cancer information" started on 2005 and the first step has been the publication [in collaboration with AIMaC (Associazione Italiana Malati di Cancro, parenti e amici / Association of cancer patients)] of a patient-oriented information booklet. This booklet offers effective information to patients about cancer and non conventional treatments called CAM (Complementary and Alternative Medicine).

In fact, CAM represents an important and current argument of discussion. The booklet tries to give clear answers to questions like: what are CAM, when and why patients use CAM, where to find specialists and what to ask them. Counseling, psychotherapy, self-help groups, yoga are examples of methods based on the psychological approach that cancer patients can use during their standard cure. Other CAM treatments include manipulations, biological methods as phytotherapy, Bach flowers, homeopathy. A very important aspect in using CAM was stressed in the booklet: the risk of side effects of some natural products ("Natural doesn't mean safe"), and the risk to abandon conventional therapies.

Conference on non-conventional treatments for cancer patients

The booklet, which was the result of the joint cooperation among the Italian Institute of Health, AIMaC, the National Cancer Institute and the National Center for Complementary and Alternative Medicine, was presented at a congress on 16th December, 2005 on: "Non-Conventional Treatments for Cancer Patients. How to provide reliable information".

This event represents an integral part of the ISS-NIH joint project and the meeting gathered together oncologists, scientists, experts of CAM, communication experts, psychologists and cancer patient associations. The booklet and the meeting proceedings are available at AIMaC web-site (www.aimac.it)

Patients and cancer clinical trials

Another ongoing project of the ISS-NIH collaboration is the provision of timely and accurate information to cancer patients about clinical trials. This is a delicate topic because changes are occurring in cancer treatment and patients are in need of a respected and independent guidance.

Public institutions also have the responsibility to ensure that information regarding experimental treatments is timely delivered. Cancer patients are eager to participate to studies of new treatments. However, it is important that information on clinical trials is given with caution and possibility of accessing clinical trials of new treatments are delivered, so that the patient itself can weight risks and potential benefits of its participation. Benefit could indeed arise from an early access to new therapies, while there is the risk of unknown side effects and lack of efficacy.

In conclusion, the ISS-NIH ongoing collaboration for cancer patient information has the objective to provide high quality cancer information services and resources on all aspects of cancer, for those concerned or affected by cancer.

The collaboration will therefore: promote the collaboration between Cancer Information Services; share information and tools for management, evaluation, training, and quality; act as a forum for exchange and discussion; develop and update service minimum standards; increase awareness of Cancer Information Services; support the development of new services throughout the country.

Session 1. Poster

BASE EXCISION REPAIR: MECHANISM AND RELEVANCE TO CANCER SUSCEPTIBILITY

Valeria Simonelli, Mariarosaria D'Errico, Eugenia Dogliotti
Department of Environment and Primary Prevention, Istituto Superiore di Sanità, Rome, Italy

Introduction

The relevance of DNA repair for human health was originally demonstrated with the discovery of defects in the nucleotide excision repair in the cancer-prone genetic disease xeroderma pigmentosum and subsequently in the relationship of mismatch repair to colon cancer. Recent studies suggest that less dramatic reductions in DNA repair capacity are observed at a polymorphic frequency in the general population, potentially leading to an increased susceptibility to several types of cancer.

Different lesions are repaired by different and sometimes overlapping mechanisms. BER is the main enzymatic pathway for the repair of structurally non-distorting and non-bulky lesions, such as oxidised, alkylated, deaminated bases and apurinic/apyrimidinic (AP) sites (1). BER is a multienzymatic and highly coordinated process which can proceed through two different subpathways (short patch- and long patch-BER), which differ for the size of the repair patch and for the enzymatic complexes that catalyze the repair cascade (2). For many years no direct relationship between BER defects and disease has been reported. Recently, several studies have demonstrated a correlation between mutations of BER genes and different types of cancer (1). Moreover, evidence is emerging that an imbalance in BER proteins, by altering the tight coordination of the BER pathway, might expose the cells to the cytotoxic and/or mutagenic effects of unattended BER intermediates. This would potentially result in increasing the spontaneous mutation frequency and thus cancer risk. This hypothesis is supported by the recent finding of a correlation between increased expression of BER enzymes and microsatellite instability (MSI) in tissues of patients affected by ulcerative colitis, a chronic inflammatory disease associated with colon cancer risk (3).

To understand the involvement of BER in genome stability maintenance and in particular in the response to oxidative stress, the expression profile of BER genes and their functionality was tested in a tissue potentially characterised by inflammatory process: the gastric mucosa. This project was carried out in collaboration with the laboratory of Dr. S.H. Wilson, Laboratory of Structural Biology, NIEHS-NIH, North Carolina, USA.

Despite a dramatic reduction in incidence and mortality rates, gastric cancer (GC) still represents the fourth most common cancer in the world and the second leading cause of cancer death (4). Among European countries, Italy has one of the highest death rates for stomach neoplasms, with marked internal variability. In particular, gastric cancer incidence and mortality are highest in the central-northern regions and lowest in southern Italy (5). Risk is elevated in those with a GC family history, but several lines of evidence suggest that environmental factors are involved too. A major risk factor of GC is the infection by *Helicobacter pylori*, which causes oxidative damage (6,7). *H. pylori* induces infiltration of the gastric mucosa by neutrophils, macrophages, T and B lymphocytes which produce large amounts of reactive oxygen species (ROS) in host defence reactions. However, this inflammatory response is unable

to clear the infection and leaves the host prone to complications resulting from chronic inflammation. BER is the main mechanism of protection from oxidative DNA damage. Thus, the functionality of BER might be crucial for avoidance of genotoxicity by ROS in gastric epithelial cells.

Pol β expression level and genome stability

DNA polymerase β (Pol β) is the key enzyme that, in short patch BER, catalyses the resynthesis of a single nucleotide at the site of the lesion and the removal of the 5'-deoxyribose 5-phosphate (5'dRp) termini that originates from incision of the abasic site, after damaged base removal. The 5'dRp elimination is the rate limiting step and it is necessary to allow completion of the repair process (8,9). In mammalian cells, functional alterations of the dRP lyase domain of Pol β lead to hypersensitivity to the cytotoxic effects of alkylating agents (10).

Several lines of evidence indicate that Pol β expression level is crucial for genetic stability. Pol β gene is characterized by a low expression level throughout the cell cycle and it is inducible under stress (11). Pol β overexpression might lead to dramatic consequences such as increased gene mutation, microsatellite instability, chromosome instability and tumorigenesis (Figure 1).

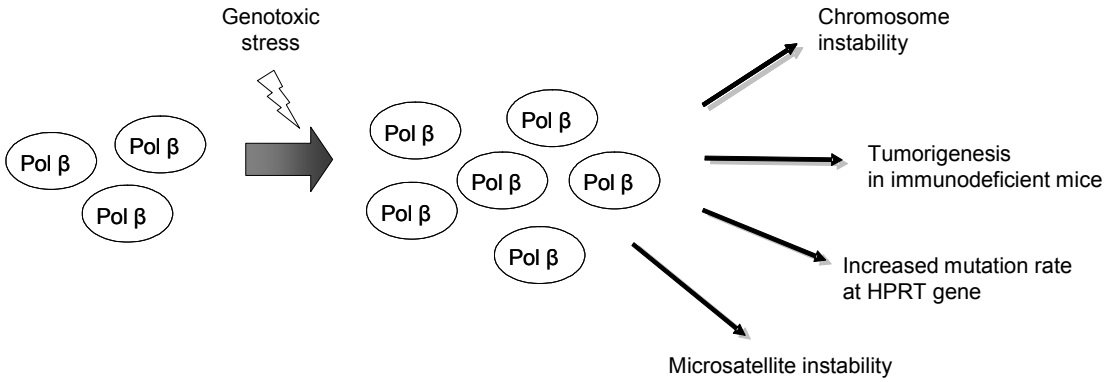

Figure 1. Consequences of Pol β overexpression in mammals

Moreover, overexpression of Pol β in cancer cells can enhance resistance to chemotherapeutic agents. The mechanism by which overexpressed Pol β increases mutation frequency is still unclear and contrasting data have been presented. Many tumour tissues, belonging to different tissues types (uterus, breast, ovary, stomach and skin tumours) are characterised by high frequency of Pol β overexpression by 2-fold or more (12). Thus, it has been proposed that overexpression of Pol β and also of other specialized polymerases in tumours could correlate with an increased mutation frequency and contribute to generate a "mutator phenotype".

A smaller percentage of tumours is characterised by Pol β downregulation. A previous study has shown that Pol β haploinsufficiency results in genomic instability (13). In particular, half the gene dosage does not contribute to tumorigenesis in young mice but it leads to an increase in the mutagenic response to carcinogen exposure (Figure 2).

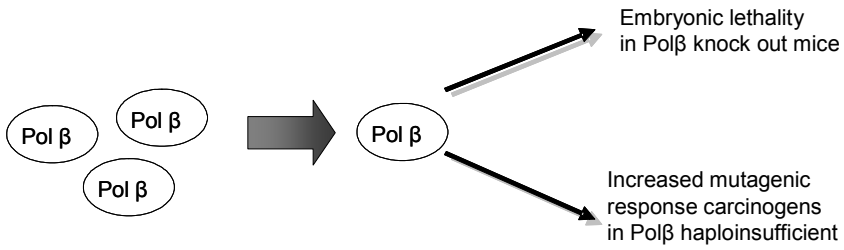

Figure 2. Consequences of Pol β downregulation in mammals

It is well established that Pol β mouse defective cells are hypersensitive to methylating agents and less efficient in the rejoining of induced single-strand breakes, compared to wild type mouse fibroblasts (9). Moreover, they show increased induced sister chromatid exchange and mutation frequency (14-16). The inability to tolerate carcinogen exposure has important human health implications. Polymorphisms that alter Pol β function on one chromosome could impact the cell through haploinsufficiency.

Not only imbalanced Pol β expression but also deletions of chomosome 8p characterize many types of cancer. Losses in this area are associated with more aggressive cancer forms.

The role of Pol β splicing variants in gastric cancer

It is becoming increasingly clear that, besides gene mutations and alterations of gene expression, also splice variants are associated with human pathologies suggesting that they are not only the products of a legitimate alternative splicing process (17). Multiple Pol β splice variants have been identified in many cell types, including cancer cells. To analyze the status of Pol β in GC tissues, genomic DNA and RNA from normal and tumour tissues of GC patients were screened for mutations in the coding region of Pol β and identification of Pol β variants, respectively. Sequence analysis of eight DNA samples did not reveal any mutation, neither in exon sequences nor in splicing junctions. However, RNA analysis of samples from twenty patients and three gastric cancer cell lines showed the presence of numerous splicing variants, in both normal and tumour tissues. Splicing variants were also found in gastric mucosa and blood samples from healthy patients. Among the most frequent exon loss (2, 5, 6, 9, alfa), exon 2 skipping was the predominant event (Figure 3).

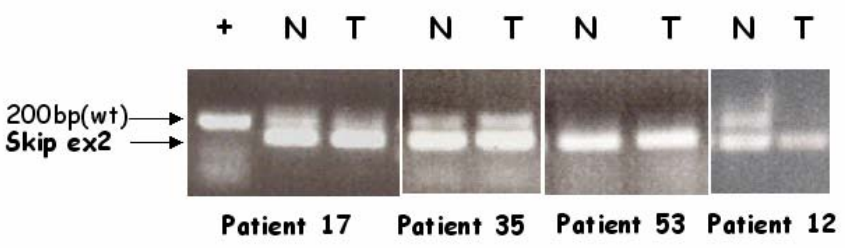

Figure 3. Example of exon 2 skipping in normal (N) and tumour (T) tissues of GC patients. The expected PCR fragment size for exon 2-skipped Pol β cDNA is 142bp, compared to a 200bp fragment amplified from non-skipped Pol β cDNA (wild type, wt).

Quantitative PCR analysis of normal and tumour tissues of seven GC patients and four blood samples of healthy patients revealed that about 50% of Pol β mRNA was represented by the exon 2-deleted mRNA.

Exon 2 skipping is predicted to produce a 26-aminoacids protein, likely avoided of any catalytic activity. Since splicing variants are not tumour-specific, we hypothesized that Pol β splicing variants could be involved in the regulation of Pol β expression levels. To support this hypothesis a dominant negative activity of the exon 11-deleted Pol β splice variant has been described in the cells (18) and *in vitro* experiments indicated a competitive inhibition between truncated domains of Pol β and wild type protein (19). To characterize the exon 2-deleted variant we constructed a mammalian expression vector containing the exon 2-deleted Pol β c-DNA and transfected it into Pol β-defective and proficient murine fibroblasts. The exon 2-deleted variant is transcribed in the recipient cells but it was not detectable by western blot using antibodies directed against different domains of Pol β. To analyse the functional activity of the exon 2-deleted variant, BER capacity and cell survival in response to methylating agents were measured in Pol β null mouse fibroblasts expressing the splice variant. The results clearly indicated that the exon 2-deleted variant, if translated, was deprived of any DNA repair activity. Moreover, since the expression of the exon 2-deleted variant in Pol β mouse proficient cells did not affect neither the DNA repair capacity nor the alkylation damage sensitivity of the host cells we can exclude a dominant negative activity of this variant.

Preliminary data of induction of Pol β after DNA damage suggest that a comparable increase in exon 2-deleted variant and wild type Pol β mRNA occurs in damaged cells.

An open question is whether the exon 2-deleted mRNA might play a regulatory role. It is increasingly evident that RNA itself presents a wide repertoire of biological functions and that it is widely employed in gene regulation, especially in higher eukaryotes (20). The human genome expresses a great variety of non-coding RNAs (ncRNAs) that are mainly involved in regulatory networks. We know that our Pol β splice variant transcripts are polyadenilated. Experiments are in progress to compare the Pol β exon 2-deleted and wild-type mRNA stability.

Little is known about the function of Pol β splice variants and the mechanism by which they are produced (regulated or aberrant splicing?). Their presence even in normal tissues suggest that they are not futile products of splicing but they play a role in the cell. Future research should address this question.

DNA repair gene expression profile in GC

Since Pol β overexpression and, more in general, an imbalance in BER genes could lead to genome instability, microsatellite instability (MSI) and expression of a large set of DNA repair genes was analysed in 100 primary GC. We first classified 19 cancers as MSI positive. These cancers were matched by age, sex and grade with MSI-negative (MSS) cancers characterized by lack of instability. Gene expression array analysis was performed on 19 MSS and 12 MSI paired tumor and normal RNAs and 7 additional MSI tumor samples that did not have the normal counterpart. Distinct changes in the gene expression profiles were identified between MSS and MSI tumors that might explain the better prognosis associated with MSI GC (D'Errico et al., manuscript in preparation). The data obtained by further analysis of DNA repair genes by quantitative PCR were examined using unsupervised principal component analysis (PCA). This analysis allows the complex character of the studied phenomenology to be maintained by avoiding any a priori filtering of the initial information. The resulting data will separate samples on the basis of groups of genes which are co-regulated. PCA analysis revealed distinctively separated groups for MSI and MSS tumor samples. The genes that differentiated MSI from

MSS tumors were MLH1 that belongs to MMR pathway and Pol β. The involvement of MLH1 confirms the role played by MMR in acquiring MSI. The novel finding is the deregulation of Pol β in association with this phenotype (D'Errico et al., manuscript in preparation). To gain insights into the mechanisms behind this phenomenon the AGS gastric cancer cell line was transfected with a vector expressing Pol β to obtain Pol β overexpressing clones. Cells were assessed for MSI at approximately 45 population doublings. No evidence of MSI was obtained giving rise to the hypothesis that both a defect in MMR (down-regulation of MLH1) and an imbalance (Pol β overexpression) in BER are necessary to induce MSI. Experiments are in progress to verify whether overexpression of Pol β lead to MSI in a MMR defective background.

Concluding remarks

The study of DNA repair genes and the identification of new genes by the expression profile analysis may have a pivotal role for a better comprehension of the molecular mechanisms involved in GC development.

References

1. Fortini P, Pascucci B, Parlanti E, D'Errico M, Simonelli V, Dogliotti E. The base excision repair: mechanisms and its relevance for cancer susceptibility. *Biochemie* 2003;85:1053-71.
2. Frosina G, Fortini P, Rossit O, Raspaglion G, Cox LS, Lane DP, Abbondandolo A, Dogliotti E. Two pathways for base excision repair in mammalian cells. *J Biol Chem* 1996;271:9573-8.
3. Hofseth LJ, Khan MA, Ambrose M, Nikolayeva O, Xu-Welliver M, Kartalou M, Hussain SP, Roth RB, Zhou X, Mechanic LE, Zurer I, Rotter V, Samson LD, Hurris CC. The adaptive imbalance in base excision-repair enzymes generates microsatellite instability in chronic inflammation. *J Clin Invest* 2003;112:1887-94.
4. Parkin DM, Bray FI, Devesa SS. Cancer burden in the year 2000. The global picture. *Eur J Cancer* 2001;37(Suppl. 8):S4-S66.
5. Parkin DM, Whelan SL, Ferlay J, *et al*. Cancer incidence in five continents. *Volume VIII Lyon: IARC Scientific Publications* 2002;155:362.
6. Palli D, Saieva C, Gemma S, Gomez-Miguel MJ, Luzzi I, D'Errico M, Masala G, Matullo G, Ozzola G, Sera F, Zanna I, Dogliotti E, Testai E. GSTT1 and GSTM1 Gene Polymorphisms and Gastric Cancer In A High-Risk Italian Population. *Int J Cancer* 2005;115:284-9.
7. Palli D, Saieva C, Luzzi I, Masala G, Topa S, Sera F, Gemma S, Zanna I, D'Errico M, Zini E, Guidotti S, Valeri A, Fabbrucci P, Moretti R, Testai E, del Giudice G, Ottini L, Matullo G, Dogliotti E, Gomez-Miguel MJ. Interleukin-1 gene polymorphisms and gastric cancer risk in a high-risk Italian population. *Am J Gastroenterol* 2005;100:1941-8.
8. Matsumoto Y, Kim K. Excision of deoxyribose phosphate residues by DNA polymerase β during DNA repair. *Science* 1995;269:699-702.
9. Sobol RW, Horton JK, Kuhn R, Gu H, Singhal RK, Prasad R, Rajewsky K, Wilson SH. Requirement of mammalian DNA polymerase-beta in base excision repair. *Nature* 1996;379:183-6.
10. Sobol RW, Prasad R, Evenski A, Baker A, Yang X, Horton JK, Wilson SH. The lyase activity of the DNA repair protein β-polymerase protects from DNA-damage-induced cytotoxicity. *Nature* 2000;405:807-10.
11. Cabelof DC, Raffoul JJ, Yanamadala S, Guo Z, Heydari AR. Induction of DNA polymerase beta-dependent base excision repair in response to oxidative stress in vivo. *Carcinogenesis* 2002;23:1419-25.
12. Albertella MR, Lau A, O'Connor MJ. The overexpression of specialized DNA polymerases in cancer. *DNA Repair* 2005;4:583-93.

13. Cabelof DC, Guo Z, Raffoul JJ, Sobol RW, Wilson SH, Richardson A, Heydari AR. Base excision repair deficiency caused by polymerase β haploinsufficiency: accelerated DNA damage and increased mutational response to carcinogens. *Cancer Res* 2003;63:5799-807.
14. Ochs K, Sobol RW, Wilson SH, Kaina B. Cells deficient in DNA polymerase β are hypersensitive to alkylating agent-induced apoptosis and chromosomal breakage. *Cancer Res* 1999;59:1544-51.
15. Sobol RW, Wilson SH. Mammalian DNA beta-polymerase in base excision repair of alkylation damage. *Prog Nucleic Acid Res Mol Biol* 2001;68:57-74.
16. Sobol RW, Watson DE, Nakamura J, Yakes FM, Hou E, Horton JK, Ladapo J, Van Houten B, Swenberg JA, Tindall KR, Samson LD, Wilson SH. Mutations associated with base excision repair deficiency and methylation-induced genotoxic stress. *Proc Natl Acad Sci USA* 2002;99:6860-6.
17. Faustino NA, Cooper TA. Pre-mRNA splicing and human disease. *Genes Dev* 2003;17:419-37.
18. Bhattacharyya N, Banerjee S. A novel role of XRCC1 in the functions of a DNA polymerase beta variant. *Biochemistry* 2001;40:9005-13.
19. Casas-Finet JR, Kumar A, Karpel RL, Wilson SH. Mammalian DNA polymerase β: characterization of a 16 kDa transdomain fragment containing the nucleic acid-binding activities of the native enzyme. *Biochemistry* 1992;31:10272-80.
20. Mattick JS, Makunin IV. Non-coding RNA. *Hum Mol Genet* 2006;15(Spec No 1):R17-29.

Session 1. Poster

EFFICACY OF CANCER CONTROL: A PUBLIC HEALTH PERSPECTIVE

Arduino Verdecchia (a), Eric Feuer (b)
(a) National Centre for Epidemiology, Surveillance and Health Promotion, Istituto Superiore di Sanità
(b) Cancer Control and Population Studies, NCI, National Insitutes of Health, Bethesda, Md, USA

The project involves two main actions to improve comparability of cancer statistics between Europe and US.

Update of the European population-based cancer registry data base

Cancer incidence and survival data are available up to the year 2002 in US-SEER areas. In Europe, incidence data are published only up to 1997, while patients' survival figures are not systematically available after the year of diagnosis 1994. In order to reduce this temporal gap, we promoted a coordinate update of the EUROCARE data bases with incidence and survival data referred to the most recent period available from European cancer registries. Ninety-seven registries from 22 European countries have sent their most recent data, when possible up to the years of diagnosis 2002 and with completed follow-up for vital status until the end of 2003. All the files received were checked for errors and inconsistencies between the different data items, according to a common set of rules. Historical data since 1978 were re-classified by using the last international classification for oncology, ICDO-3, to assure comparability with recent data and US data. Also the amount of information was expanded by including systematically information on stage and treatments. Some preliminary statistics on the new database are reported in Table 1.

The database includes today data on almost 11 millions of cancer cases diagnosed in Europe between 1978 and 2002. About 80% of cases were microscopically verified, and more than 30% of cases regard cancers diagnosed at age 75 or more. Survival analysis will be carried out in two steps. Classical cohort analysis will be performed on the data from 3,358,000 cases diagnosed in the period 1995-1999 and followed up at least four years, until December, 2003. The most up-to-date survival estimates will be derived from period-based analysis for the years of follow-up 2000-2002.

Cancer statistics in US and Europe are now aligned and comparable for the first time and ready for the most innovative survival analysis, the period survival analysis. Very update comparative survival analysis in US and Europe is in progress.

Table 1. General characteristics of the EUROCARE-4 database: number of cancer patients by period of diagnosis, percent of cases microscopically verified, and percent of patients aged 75 or more years, by country (in bold countries with national cancer registration)

Country	Cases total	Cases 1978-1994	Cases 1995-1999	Cases 2000-2002	% microscopically confirmed	% > 74
Austria	736,223	416,952	201,329	117,942	81	33.7
Belgium	144,713	-	81,920	62,793	90	28.0
Czech Republic	56,659	24,325	19,868	12,466	86	23.0
Denmark	544,783	407,145	137,638	-	93	31.0
Finland	456,796	280,880	107,133	68,783	93	31.2
France	215,123	129,963	84,631	529	89	26.4
Germany	144,776	90,609	33,040	21,127	88	28.7
Iceland	22,294	13,443	5,349	3,502	96	32.2
Ireland	114,086	17,979	96,107	-	86	33.7
Italy	1,117,580	441,946	462,657	212,977	85	32.7
Malta	8,482	2,464	6,018	-	88	26.1
Netherland	305,254	121,695	120,131	63,428	95	29.0
Norway	461,051	290,021	104,208	66,822	92	35.5
Poland	179,947	71,055	65,104	43,788	74	21.5
Portugal	32,917	-	32,917	-	94	24.2
Slovenia	144,605	87,972	34,430	22,203	88	21.5
Spain	230,790	113,500	107,933	9,357	86	28.1
Sweden	981,328	633,711	211,358	136,259	98	35.7
Switzerland	133,632	73,441	44,749	15,442	97	32.5
UK_England	3,826,914	2,418,269	1,124,130	284,515	69	35.4
UK_N.Ireland	59,886	16,741	43,145	-	81	34.9
UK_Scotland	705,020	441,308	163,868	99,844	81	33.3
UK_Wales	319,570	205,975	70,422	43,173	32	34.4
Europe	10,942,429	6,299,394	3,358,085	1,284,950	81	33.2

Quantitative models development and extensive application

Within the collaboration with NCI, our study contributed to develop statistical methods for computing cancer prevalence. The PREVAL method is aimed at estimating limited duration prevalence from cancer registry incidence and survival data. A specific software has been implemented to make the method easily available to user dealing with cancer registries data. The software is now part of the package SEER*Stat, a statistical software for the analysis of cancer registries data developed and systematically maintained by NCI, and distributed free of charge all over the world.

The COMPREV method is aimed at estimating the unobserved part of the prevalence, arising from cancer diagnosed before the start of registration. The method is now implemented by a specific software distributed by NCI (http://srab.cancer.gov/comprev/). Figure 1 shows for example the completeness index estimates provided by the COMPREV software for colorectal cancer prevalence for a registry with a 10 year duration of registration. The completeness index is the proportion of observed prevalent cases over the complete prevalence. The completeness index estimates are presented on the left and are plotted on the right by age class.

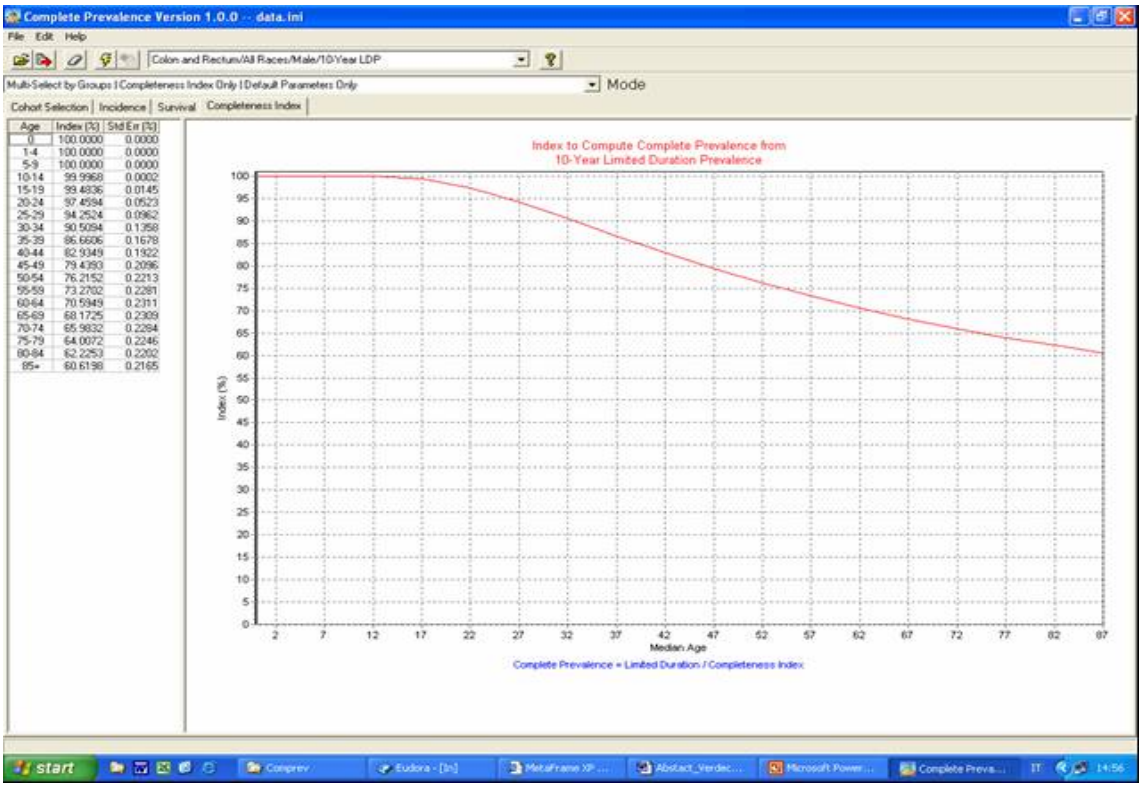

Figure 1. Completeness index for limited prevalence at 10 years by age class, from COMPREV software

Finally, the DEVCAN method estimates the lifetime cancer risk in a population. Also for DEVCAN, a specific software has been implemented (http://srab.cancer.gov/devcan/).

An extensive application of MIAMOD/PIAMOD method and software was attempted within this project to estimate and project the cancer burden in US by Federal State. All cancer combined and breast cancer were analysed. Incidence, prevalence, survival and mortality were estimated and projected to 2010, by State in US. With this study we developed a rather unexplored field in the US cancer statistics, i.e. the geographical variation of levels and trends.

The estimation method strictly relies on State-specific observed cancer mortality data and on survival estimates by State. The latter is obtained by applying ecological models to the US SEER survival data, incorporating the most relevant demographic, socio-economic and health-related variables affecting cancer survivorship. Table 2 shows, as an example, the prevalence estimates in 2010 for breast cancer by State.

The results we obtained, in particular cancer prevalence by State, are going to be made available in the NCI web site : http://statecancerprofiles.cancer.gov/.

Table 2. Breast cancer prevalence projections in US 2010 by single State: total number of prevalent cases and prevalence proportion per 100,000

State	#Prevalent cases	Prevalent proportion
Alabama	33621	1458
Alaska	3861	1158
Arizona	47728	1660
Arkansas	17742	1280
California	270935	1482
Colorado	36639	1570
Connecticut	33646	1904
Delaware	7561	1797
District of Columbia	3689	1264
Florida	177494	2091
Georgia	54947	1210
Hawaii	11674	1841
Idaho	10692	1523
Illinois	106036	1631
Indiana	49987	1583
Iowa	30500	2079
Kansas	23581	1715
Kentucky	27254	1303
Lousiana	30188	1291
Maine	13791	2119
Maryland	51368	1790
Massachusetts	63614	1944
Michigan	91284	1785
Minnesota	52639	2045
Mississippi	16547	1105
Missouri	46467	1598
Montana	8549	1880
Nebraska	16122	1824
Nevada	16288	1438
New Hampshire	13355	2059
New Jersey	77210	1742
New Mexico	14752	1512
New York	163755	1654
North Carolina	64079	1483
North Dakota	7000	2258
Ohio	94290	1624
Oklahoma	25771	1448
Oregon	35107	1968
Pennsylvania	112622	1828
Rhode Island	9667	1785
South Carolina	29896	1403
South Dakota	7493	1954
Tennessee	38759	1299
Texas	145939	1256
Utah	14960	1179
Vermont	5687	1847
Virginia	59870	1581
Washington	57103	1487
West Virginia	13168	1470
Wisconsin	51808	1184
Wyoming	5609	2236

References

1. Capocaccia R, De Angelis R. Estimating the completeness of prevalence based on cancer registry data. *Stat Med* 1997;16:425-40.
2. Merrill RM, Feuer EJ, Cappacaccia R, Mariotto A. Cancer prevalence estimates based on tumor registry data in the SEER Program. *Int J Epidemiol* 2000;29:197-207.
3. Clegg L, Gail M, Feuer EJ. Estimating the variance of disease prevalence estimates from population-based registries. *Biometrics* 2002;58(3):684-8.
4. De Angelis GD, De Angelis R, Frova L, Verdecchia A. MIAMOD: a computer program to estimate chronic disease morbidity using mortality and survival data. *Computer Methods and Programs in Biomedicine* 1994;44:99-107.
5. Verdecchia A, De Angelis G, Capocaccia R. Estimation and projections of cancer prevalence from cancer registry data. *Stat Med* 2002;21(22):3511-26.
6. Mariotto A, Warren JL, Knopf KB, Feuer EJ. The prevalence of colorectal cancer patients under care in the US. *Cancer* 2003;98:1253-61.
7. Fay MP. Estimating age conditional probability of developing disease from surveillance data. *Popul Health Metr* 2004;2(1):6.
8. Mariotto A, Simonetti A, *et al*. Improvement in risk estimates of developing cancer when estimates of the cancer-free population are available. *In preparation*.
9. Simonetti A, Mariotto A, *et al*. Method to Estimate Complete prevalence of Cancers diagnosed at childhood age. *In preparation*.
10. Verdecchia A, Tavilla A, *et al*. Variation of breast cancer incidence and prevalence in US states. *In preparation*.

Session 1. Poster

ENDOGENOUS REVERSE TRANSCRIPTASE ACTIVITY AND CHROMATIN REMODELING IN TRANSFORMED CELLS

Ilaria Sciamanna (a), Tom Misteli (b), Corrado Spadafora (a)
(a) Service for Biotechnology and Animal Welfare, Istituto Superiore di Sanità, Rome, Italy
(b) Cell Biology and Genomes Group, National Cancer Institute, NIH, Bethesda, USA

Introduction

Reverse transcriptase (RT) was first described as an enzyme required for replication of infective retroviruses. In higher eukaryotes, including humans, non-telomeric endogenous RT is encoded by two major families of repeated elements: the retroposons LINE-1 and endogenous retroviruses ERVs. Together these families of retroelements account for nearly 45% of the genome. The endogenous RT is differentially expressed in a variety of pathological and physiological cellular processes: basal levels of expression are detected in normal somatic cells and differentiated tissues, while high levels of expression are detected in transformed cells, pre-implantation embryos, placenta, the mammalian genital tract, germ cells and gametes.

Work carried out in our laboratory has shown that pharmacological inhibition of endogenous RT with nevirapine and efavirenz – two RT inhibitors widely used in AIDS therapy – reduces drastically cell proliferation, promotes differentiation of transformed cells, induces a reprogramming of gene expression (1-3). Moreover, RT inhibitors antagonize tumor progression in nude mice inoculated with human tumorigenic cell lines (A-375 melanoma, HT29 colon carcinoma, H69 small cell lung carcinoma and PC3 prostate carcinoma) (3, 4). Discontinuation of RT inhibitors treatment resumes both the original high proliferation rate *in vitro* and tumor progression in *in vivo* essays and re-establishes the same gene expression profile of non-treated cells, thus suggesting that endogenous RT activity is involved in an epigenetic control of cellular functions (1, 3). Consistently, we have obtained similar results by down-regulating the expression of the RT-encoding LINE-1 retroelement family by RNA interference (RNAi) (3,5) in tumorigenic cell lines. In the framework of the cooperation Program between ISS and NIH, in collaboration with Dr. Tom Misteli, Cell Biology and Genomes Group, National Cancer Institute, NIH, Bethesda, USA, we have undertaken a research program aiming at the clarification of the role, if any, of endogenous RT activity in chromatin remodeling and in the control of gene expression in transformed cells.

Results

Gene expression profiles

In order to investigate the molecular mechanism underlying RT-mediated control of cell proliferation and differentiation, we compared the gene expression profiles in A375 human melanoma cells exposed and non-exposed to the RT inhibitor Nevirapine.

Total RNA was isolated from A375 human melanoma cell lines continuously exposed for 12 days to 350 µM Nevirapine or to DMSO (control) and analyzed by microarray technology, using Affymetrix Human Genome U133A 2.0 chip array, containing 14500 known human genes. For each condition, we analyzed RNA extracted from two independent experiments.

Following this procedure, we identified a total of 170 nevirapine-modulated genes whose expression level was modulated (down- or up-regulated) by at least 1.5-fold relative to control cells.

Figure 1 shows a gene ontology classification of the modulated genes according to their biological functions performed with the "FatiGO" software (http://fatigo.bioinfo.cnio.es). It is clear that some gene categories are over-represented in nevirapine-treated samples as compared to the total population of expressed genes in untreated control. Among those, the most over-represented are:

– "morphogenesis", from 7,8% in control to 27.27% in nevirapine-treated sample
– "organ development", from 5,78% in control to 18,18% in nevirapine-treated sample
– "growth", from 1,48% in control to 8,08% in nevirapine-treated sample

Figure 1. Gene ontology classification

These results confirm the conclusion that endogenous RT has a key role in the overall regulation of gene expression profiles and that groups of genes involved in the process of growth and development are preferential targets.

Chromatin organization

Gene localization

The broad reprogramming of gene expression caused by RT inhibition suggests that the endogenous RT is part of a molecular mechanism implicated in control of chromatin function. In an attempt to clarify this mechanism we addressed the question whether RT inhibition causes a remodelling of chromatin architecture. To this end, we investigated if key genes, following nevirapine treatment, were relocated to a nuclear compartment with novel functional features, thereby influencing their expression level.

The nuclear position of genes cannot be rigorously assessed in A-375 cells, due their high level of aneuploidy and therefore experiments were performed on murine teratocarcinoma F9 cell line, which was also found to be very responsive to nevirapine treatment (1). Genes positions were localized on interphase chromatin of F9 cells exposed and non-exposed to nevirapine by FISH (Fluorescent In Situ Hybridization) assays using specific probes for:

- cyclin D1 (*CcnD1*), whose expression is heavily down-regulated in nevirapine-treated F9 cells (Figure 2, panel A)
- the centromere of murine chromosome 7 (*chr 7-cen*), where the CcnD1 gene is located.

The CcnD1 gene was localized in interphase nuclei by measuring its relative distance from the centromere of chromosome 7, as exemplified in Figure 2, panel B. We also measured the relative distance between the homologous centromeres of the two chromosomes 7.

The results summarized in Figure 2, panel C indicate that nevirapine exposure (grey histograms, also see nev in Table 1) increases the distance between CcnD1/FITC and chr7-cen/Cy3 (see also panel B). In the latter, the distance between CcnD1 gene and chr7-cen peaks at 11.1-16.6 μm, while in untreated cells (black histograms and ctr in Table 1) the peak is between 5.6-11 μM: thus, the average increase in the modal distance is about 5.5 μm.

To assess whether the increased distance between the CcnD1 gene and its centromere in nevirapine-exposed nuclei reflects a global nuclear reorganization, we also measured the distance between the two homologous chr. 7 centromeres (Figure 2 Panel D). We found that the modal distance between homologous centromeres increases by 5.5 μm in nevirapine-exposed (grey histograms) compared to non-exposed nuclei (black histograms).

Thus, centromeres of homologous chromosomes move apart upon RT inhibition, and the extent of their distance is comparable to that occurring between the CcnD1 gene and the centromere on the same chromosome.

We next asked if chromatin reorganization is maintained or lost upon drug removal from the medium. Figure 2, panel E shows the recorded distance between FISH signals for CcnD1/FITC and Chr7-cen/Cy3 in nuclei of control DMSO-treated (ctr) or nevirapine-treated cells after drug removal (nev-released) from the medium: the results clearly show that the difference between untreated (black histograms) and nev-released cells (dot histograms) is lost within a few days after drug removal, and that the size distribution in the two cell populations now largely overlaps. This finding correlates well with our previous observations that removal of RT inhibitors resumes high CcnD1 expression levels and cell proliferation rates.

Table 1. Distance between CcnD1 allele and chr.7 centromere in the nucleus

	Distance (μm) between CcnD1 locus and chr-7 centromere							Recorded signals
	0-5,5	5,5-11	11,1-16,6	16,7-22,2	22,3-27,7	27,8-33,3	33,4-50	
CTR	38	53	28	14	2	2	0	137
NEV	31	35	15	6	2	4	0	137

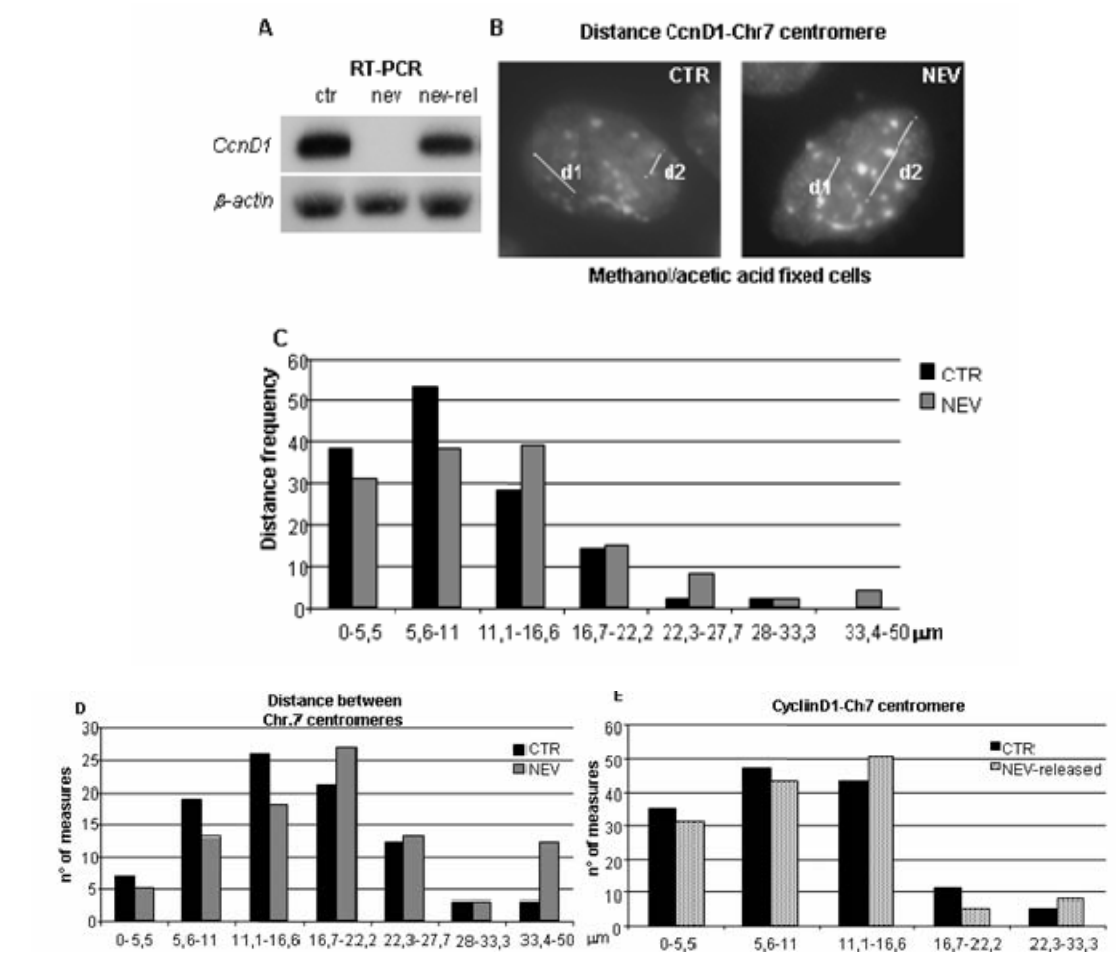

Figure 2. Gene localization

Heterochromatin

The relocalization of cyclin D1 gene and, more significantly, of chr.7 centromeres suggested that a general reorganization of the chromatin architecture takes place following RT inhibition. To assess if other nuclear compartments were also affected, we investigated the structure of the heterochromatin in F9 cells and in cells exposed to nevirapine.

As shown in Figure 3, panel A, F9 cells untreated (CTR) or nevirapine-treated (NEV) were fixed with paraformaldehyde (PFA), then stained with DAPI. DAPI-bright dots (i.e pericentromeric heterocromatin) were counted under a confocal microscope in 100 nuclei in two independent experiments. Heterochromatic dots were defined as "small" or "large foci" when they extended over an area smaller than, and larger than 4μm, respectively (Figure 3, panel B). The results in panel C show that "large" foci remain substantially unchanged in the two populations; instead, small foci in nevirapine-treated cells doubled in number (average: 26 small dots/nucleus) compared to control cells (average: 15 small dots/nucleus). This indicates that novel foci of heterochromatinization assemble in RT-inhibited cells.

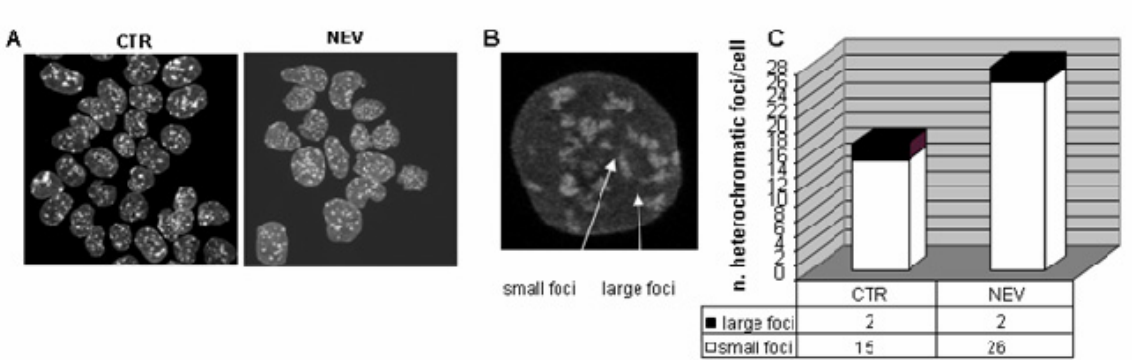

Figure 3. Heterochromatin

The rearrangement of constitutive heterochromatic domains following RT inhibition was further supported by immunofluorescence (IF) experiments using an antibody against trimethyl-K9 H3 histone, a heterochromatin specific marker.

Figure 4, panel A shows that histone H3 is overmethylated at Lys9 in nevirapined-treated (NEV) compared to untreated (CTR) nuclei. Differences in histone methylation levels between the two populations are reflected in the increased intensity of H3-trimetK9 immunofluorescence signals in NEV cells compared to controls, acquired at the same laser intensity (bright dots). Global increasing of H3 trimethyl-K9 was also confirmed by Western blot analysis performed on nuclear protein extracts from NEV-treated (NEV) and untreated (DMSO) F9 cells; equivalent protein loading is shown by red ponceau staining. Furthermore, an increased number of H3-trimetK9–labeled heterochromatic foci are clearly visible in nevirapine-treated nuclei (Figure 4 panel C), in further support of the DAPI staining results.

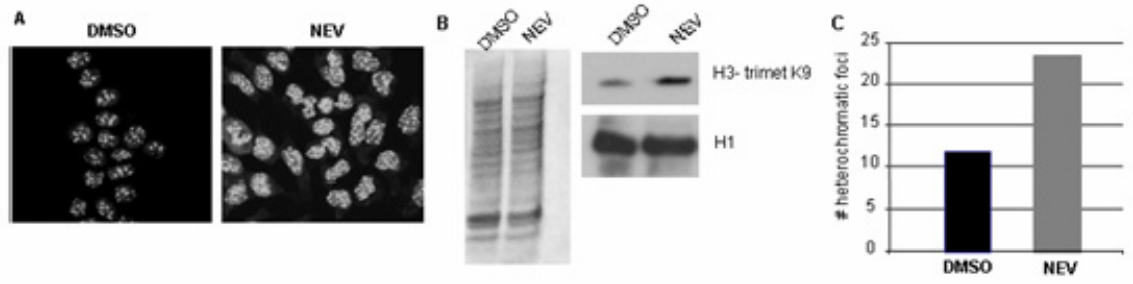

Figure 4. Nevirapined-treated (NEV) and untreated (CTR) nuclei

Thus, Nevirapine treatment induces not only the relocalization of key genes in nuclei, but also global changes in the overall chromatin architecture.

Conclusions

The results here obtained thus far implicate the endogenous RT in control of several aspects of chromatin function and architecture:

- RT inhibition causes a wide modulation of gene expression by microarray analysis;
- RT inhibition by nevirapine causes the nuclear relocalization of protein-coding genes (cyclin D1) and, more generally, a global reorganization of nuclei, as suggested by the relocalization of the Chr.7 centromeres in nevirapine-exposed nuclei;
- Heterochromatic domains are heavily affected by RT inhibition, and their number is doubled in nevirapine-treated compared to untreated cells;
- RT inhibition increases the level of trimethylation of Lys9 in histone H3, which is a typical hetherochromatic marker.

Together, these data provide novel insight into the ability of RT to modulate gene expression at the epigenetic level. The mechanistic link between RT inhibition and nuclear reorganization remains a challenging question to be further investigated in future studies.

References

1. Mangiacasale R, Pittoggi C, Sciamanna I, Careddu A, Mattei E, Lorenzini R, Travaglini L, Landriscina M, Barone C, Nervi C, Lavia P, Spadafora C. Exposure of normal and transformed cells to nevirapine, a Reverse Transcriptase inhibitor, reduces cell growth and promotes differentiation. *Oncogene* 2003;22:2750-61.
2. Landriscina M, Fabiano A, Altamura S, Bagala C, Piscazzi A, Cassano A, Spadafora C, Giorgino F, Barone C, Cignarelli M. Reverse Transcriptase inhibitors down-regulate cell proliferation in vitro and in vivo and restore TSH signaling and iodine uptake in human thyroid anaplastic carcinoma. *J. Clin Endocrinol Metab* 2005;90:5663-71.
3. Sciamanna I, Landriscina M, Pittoggi C, Quirino M, Marelli C, Beraldi R, Mattei E, Serafino A, Cassano A, Sinbaldi-Vallebona P, Garaci E, Barone C, Spadafora C. Inhibition of endogenous reverse transcriptase antagonizes human tumor growth. *Oncogene* 2005;24:3923-31.
4. Sinibaldi-Vallebona P, Lavia P, Garaci E, Spadafora C. A role for endogenous reverse transcriptase in tumorigenesis and as a target in differentiating cancer therapy. *Genes Chrom. Cancer* 2006;45:1-10.
5. Oricchio E, Beraldi R, Sciamanna I, Tolstonog GV, Schumann GG, Spadafora C. Distinct roles for LINE-1 and Herv-K retroelements in cell proliferation, differentiation and tumor progression. 2006 (submitted).

Session 2
NEUROSCIENCES

Session 2A. Behavioural neuroscience: from basics to psychiatry

EARLY RISK FACTORS FOR NEUROPSYCHIATRIC DISEASES: COMPARATIVE APPROACHES TO INVESTIGATE INTERACTIONS BETWEEN GENES AND ENVIRONMENT

Francesca Cirulli (a), Nadia Francia (a), Igor Branchi (a), Luigi Aloe (b), Stephen J Suomi (c), Enrico Alleva (a)

(a) Department of Cell Biology and Neurosciences, Istituto Superiore di Sanità, Rome, Italy

(b) Institute of Neurobiology and Molecular Medicine, CNR, European Brain Research Institute (EBRI), Rome, Italy

(c) Laboratory of Comparative Ethology, National Institute of Child Health and Human Development (NICHD), National Institutes of Health, Bethesda, MD, USA

Quality of family life influences the development of individual differences in vulnerability to psychopathology throughout life (1). Severe conditions such as physical or sexual abuse, in addition to persistent emotional neglect or family conflict, can compromise growth, intellectual development and lead to increase risk for adult obesity, depression and anxiety disorders (1,2).

Both genetic and experiential factors can contribute to the development of psychopathology (3,4). This novel approach envisioning gene-environment interactions goes beyond the old and simple assumption of a linear relationship between genes and behaviour, supporting the view that genes influence the susceptibility to environmental "pathogens" (5).

In one of the first studies involving gene-environment interactions, Caspi and co-workers (6) have shown that a functional polymorphism in the promoter region of the serotonin transporter (*5-HTT*) gene would moderate the influence of stressful life events on vulnerability to depression. Individuals with one or two copies of the *5-HTT* 'short' allele exhibited more depressive symptoms, diagnosable depression and suicidality following stressful life events than individuals with two copies of the 'long' allele (6). Additional gene-environment findings are emerging.

In two studies of attention-deficit hyperactivity disorder, polymorphisms in the dopamine system interacted with antenatal risk factors (such as low birth weight and maternal use of alcohol) to predict key symptoms associated with the disorder (for a review see 5).

The study of gene-environment interactions has been the province of epidemiology, in which genotypes, environmental pathogens exposures and disorder outcomes are studied as they naturally occur in the human population (5).

However, research in the neuroscience field needs to complement psychiatric genetic epidemiology by specifying the more proximal role of nervous system reactivity in the gene-environment interaction. As an example, the quality and quantity of experience that can predispose an individual towards psychopathology and the specific neural substrates affected are still open questions. Appropriate animal models in which genotype and environmental factors can be manipulated under controlled conditions are needed to answer these questions, as well as to identify the basic mechanisms leading from gene x environment interactions to susceptibility to psychopathology (7,8).

Epigenetic factors transducing the effects of early experiences and shaping adult social behaviour: role of neurotrophins

Epigenetic factors, such as early trauma, abuse or neglect might lead to a dysregulation of the normal developmental brain program, ultimately resulting in a greater susceptibility for mental disorders or neurodegeneration. However, there is a lack of detailed information about the neuroadaptive mechanisms linking specific features of the early rearing environment to adult susceptibility to psychopathology.

Neurotrophins such as Nerve growth factor (NGF) and Brain-derived neurotrophic factor (BDNF; 9,10) might represent early markers of such dysregulation. Neurotrophic factors are good candidates for mediating long-term effects of experience on brain function since they are involved in synaptic and morphological plasticity with maximal levels at times of neuronal growth, differentiation and synaptogenesis (9). Neurotrophins have been shown to be involved in the response to psychosocial stress in animal models and in psychiatric disorders in humans (11,12).

As for NGF, a number of studies conducted by our group, in collaboration with the Institute of Neurobiology and Molecular Medicine (CNR-EBRI, Rome), have suggested an involvement of this neurotrophin in emotionally arousing situations, being released during intraspecific fighting in mice (11,13). In addition, increased circulating levels of NGF have been found in soldiers undergoing their first jump with a parachute (14). High circulating levels of NGF have also been found in spouses caring for Alzheimer's patients (15), suggesting that highly stressful situations, often combined with depressed mood, might be characterized by higher levels of circulating NGF. Interestingly, administration of haloperidol can reduce levels of NGF in psychotic patients, suggesting a possible role for this neurotrophin in psychiatric disorders (16). As for BDNF, this molecule playing a role in neuroplasticity has been associated with depressive disorders. Indeed, the gene for this neurotrophin is a risk locus for depression (17,18). Recent studies have also suggested a direct link between the efficacy of antidepressants and increased levels of a neurotrophin such as BDNF (19).

It is possible to hypothesize that changes in the levels of neurotrophic factors during critical periods of brain development might affect vulnerability to stress and psychopathology at adulthood (7). Indeed studies performed in rodents have shown that neurotrophins are sensitive to manipulations of the mother-infant relationship and, more in general, of the rearing environment (20-23). In particular, we have shown that NGF levels increase in an age- and time-dependent fashion following maternal separation in rodents (21,22), while a prolonged maternal deprivation can lead to a long-term reduction in BDNF levels in the prefrontal cortical areas of rats (23).

In addition, recent studies have indicated long-term changes in NGF and BDNF regulations and in social behaviour following early social enrichment in mice (20). Changes in the expression of neurotrophins as a result of early adverse experiences, such as maternal separation, could exert both short- and long-term effects on neurobehavioural plasticity, resulting in important changes in social competences or response to stressful stimulations at adulthood (7,12,20).

A non-human primate model for studying gene by environment interactions in behavioural research

The non-human primate model is particularly useful for studying the role of gene-environment interactions in the development of psychopathology (24). Indeed, most psychopathology revolves around social functioning and, compared to rodents, non-human primates are endowed by complex social behaviours and social structures that more closely approximate those characterizing humans. Moreover, the rearing environment of non-human primates can be tightly controlled. In fact, similarly to rodents, macaques with histories of early life stress have been shown to exhibit impulsive aggression, incompetent social behaviour and increased behavioural and endocrine responsivity to stress (8).

Over the past 15 years, the Laboratory of Comparative Ethology (LCE) in Poolsville (MD, USA) has developed and refined a compelling rhesus monkey model for studying the origins, developmental course, and long-term consequences of individual differences in physiological reactivity. Dramatic individual differences have been described in rhesus monkey infants exposed to environmental novelty and social challenge (25). The physiological patterns that characterize high reactivity (such as increased adrenocortical output, increased monoamine turnover) and impulsive aggressiveness (impaired serotonergic function) in rhesus monkeys mirror those seen in highly reactive and aggressive children, respectively (25,26). Such differences among rhesus monkeys seem to be: i) highly heritable, appear early in life and remain relatively stable throughout development when environments do not change dramatically; ii) affected by early rearing experiences; and iii) associated with differential risk for developing anxiety- and depressive- like disorders (in the case of high reactive monkey infants) and extreme aggressiveness (for unusually impulsive young monkeys) later in life.

Recent studies have revealed a significant interaction between histories of early-life stress and the genetic background in this primate model (24). More in detail, variations in the serotonin transporter gene-linked polymorphic region have been shown to increase the likelihood of developing a vulnerable phenotype (27,28). These effects are highly dependent upon the early life history of the monkeys: infant rhesus macaques exposed to early stress (reared in the presence of peers, rather than by the mother) show exaggerated adrenocortical responses to stress at adulthood if they carry a copy of the short allele of the serotonin transporter gene (*l/s rh5-HTTLPR*), compared to subjects carrying two long alleles (*l/l rh5-HTTLPR*; 24).

The serotonin transporter is a protein critical to regulating serotonin function in the brain. Serotonin plays a pivotal role in many forms of psychopathology, with the specific serotonin reuptake inhibitors and other serotonin agents being some of the most widely prescribed psychotropic medications. Although much research up to date has been concentrating on this neurotransmitter, new approaches and new molecular targets are needed to develop effective therapeutic drugs for the treatment of depression and mood disorders. The main hypothesis underlying these studies is that, because of their involvement in brain development and function, neurotrophins might be important factors involved in early gene x environment regulations and in mediating the effects of early stressful or traumatic experiences on behavioural dysfunctions and psychopathology.

Changes in the levels of neurotrophins in differentially-reared rhesus macaques: a preliminary study

Aim of this ISS-NIH collaborative study was to establish a methodological protocol to measure levels of neurotrophins (NGF and BDNF) in rhesus macaques, as a function of age and rearing condition. The levels of NGF and BDNF have been measured both in the cerebrospinal fluid and in plasma in order to establish possible correlations between central and peripheral markers of neuroplasticity and behavioural dysfunction.

Preliminary results obtained in this study indicate that, independently from rearing condition, plasma concentrations of NGF increase significantly with age in rhesus macaques ($F(2, 9) = 8.64$; $p = 0.0081$; see Figure 1). An opposite trend has been observed for plasmatic levels of BDNF, 1 month-old monkeys showing higher plasma BDNF concentrations than 1-year or 7-years-old subjects ($F(2, 9) = 3.62$; $p = 0.0701$; Figure 1). While to date, no clear findings have been reported on changes in NGF levels in human serum as a function of age, levels of BDNF are in line with findings in humans showing reduced concentrations in older individuals (29).

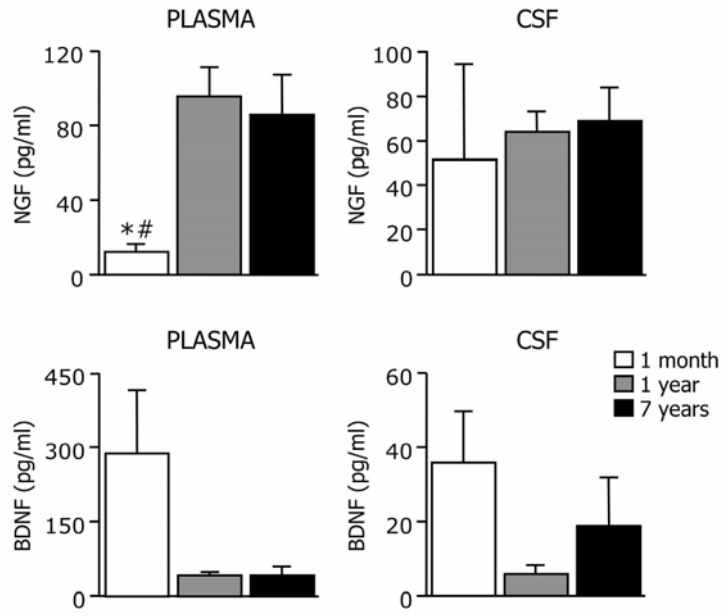

Figure 1. Plasma and CSF levels of NGF and BDNF in 1month-, 1 year-, and 7 years-old Rhesus macaques. *Post-hoc*: 1 month vs *1 year, or #7 years, p< 0.05. Data are mean values ± SE

No age differences emerged for NGF and BDNF concentrations measured in the cerebrospinal fluid (CSF), nor a correlation between CSF and plasma levels for these neurotrophins. However, CSF BDNF levels were found to decrease with age similarly to plasma concentrations. There is evidence that BDNF serum levels are closely related to BDNF concentrations in the central nervous system (30). Large amounts of BDNF are stored in human platelets, as reflected by high serum levels of BDNF (29). Notably, BDNF is not produced by platelets but it is acquired from external sources. Platelet BDNF could originate from the central nervous system, since this neurotrophin readily crosses the blood–brain barrier (31). Thus,

serum BDNF might reflect the amount of brain-derived BDNF taken up by circulating platelets, which might represent a unique BDNF transportation system in the human body (32).

In a further analysis, NGF and BDNF plasma levels of 5-months-old subjects reared in the absence of the mother and with the continuous (Peer-reared, PR) or intermittent (Surrogate-peer-reared, SPR) presence of social companions were compared with normally reared infants (Mother-reared, MR). CSF samples from these subjects were also assayed for concentrations of the serotonin metabolite, 5-hydroxyindoleacetic acid (5-HIAA), the noradrenalin metabolite, 3-methoxy-4-hydroxyphenylglycol (MHPG), and the dopamine metabolite, homovanillic acid (HVA). Results indicate that early stress affected plasma levels of neurotrophins in 5-month-old infant rhesus monkeys. NGF levels did not differ among the experimental groups, however a trend towards an increase in NGF levels in the two groups reared without their mother was found (SPR>PR>MR). By contrast, MR subjects showed higher levels of plasmatic BDNF ($F(2, 16) = 4.42$; $p = 0.0296$), especially when compared with SPR monkeys (Table 1).

Table 1. Plasma levels (pg/ml) of NGF and BDNF in 5 months-old Mother- (MR), Peer-only- (PR) and Surrogate-peer-reared (SPR) monkeys. Data are mean values ± SE

	NGF	BDNF
		*
MR	11.7±3.0	230.1±85.0
PR	38.5±18.0	173.1±54.0
SPR	55.0±42.0	38.1±9.0

Post-hoc: *MR vs SPR; $p<0.05$

The MR group showed also higher CSF levels of MHPG than both the PR and SPR groups ($F(2, 22) = 13.37$; $p = 0.0002$; Table 2). Moreover, CSF levels of 5-HIAA measured in MR monkeys were higher than PR ones ($F(2, 22) = 3.26$; $p = 0.0576$; Table 2). Finally, CSF concentrations of HVA were higher in SPR monkeys when compared to PR ones ($F(2, 229 = 5.68$; $p = 0.0102$; see Table 2), while no differences were found between SPR and MR groups or between PR and MR groups.

Table 2. CSF levels (pmol/ml) of 5-HIAA, HVA and MHPG in 5 months-old Mother- (MR), Peer-only- (PR) and Surrogate-peer-reared (SPR) monkeys. Data are mean values ± SE

	5-HIAA	HVA	MHPG
	#	§	# *
MR	412.9±26.0	1568.3±72.0	159.9±5.0
PR	327.3±21.0	1241.3±122.0	112.5±7.0
SPR	381.2±12.0	1722.7±77.0	120.7±6.0

Post-hoc: #MR vs PR; *MR vs SPR; §PR vs SPR; $p<0.05$

The increased levels of NGF in the SPR group could be due to more complex and frequent social interactions with peers resulting from the lack of contact-comfort by the mother. Indeed, compared to MR, PR and SPR show higher levels of play behaviour and social interactions with peers. These playful/aggressive interactions could then result in higher NGF plasma concentrations, in line with findings in the literature indicating an involvement of this neurotrophin both in social interactions and in emotional/stressful situations (14,15). Thus, higher levels of NGF might reflect greater perceived stress in monkeys reared in the absence of

the mother. These same groups showed also reduced BDNF levels. This finding, as previously suggested in the rodent literature, could be interpreted as indicating reduced neuroplasticity as a result of exposure to early chronic stress (7,23). The data on CSF 5-HIAA concentrations indicating reduced serotonin function in peer-reared monkeys, are in line with the BDNF findings and confirm previous results obtained in this primate model (26). Thus this preliminary study indicates that a reduction in both BDNF and serotonin metabolites characterizes subjects exposed to early stressful conditions, confirming the important relationship between serotonin function and BDNF (33).

Conclusions and perspectives

The comparative approach used in these studies has revealed important changes in the levels of NGF and BDNF both as a function of age and as a consequence of the quality of the rearing environment.

The preliminary findings obtained in this study suggest that changes in plasma levels of neurotrophins might function as peripheral markers of early adversity, being differentially affected by changes in the rearing environment. Increased levels of NGF in monkeys reared without adults might reflect stressful social interactions with their peers, in the absence of the mother. As for BDNF, reduced peripheral levels characterize subjects exposed to early stress. BDNF levels in human serum have been shown to correlate with the severity of depression and low serum BDNF concentrations are currently discussed as a risk factor for the development of mood disorders and as a potential biological marker for depression (34,35). The finding that monkeys experiencing maternal separation show overall reduced BDNF levels suggest a major impact of the disruption of the mother-infant relationship on this marker of brain plasticity and suggest that this procedure might result in long-term effects on behaviour.

Further studies are currently in progress to validate the use of NGF and BDNF as peripheral markers of brain plasticity in this primate model. The availability of easy-to-collect and easy-to-screen neurobiological indices could be important tools to predict meaningful gene x environment interactions underlying increased susceptibility to psychopathology. Indeed, BDNF polymorphisms impact on the incidence of anxiety-related personality traits and mood disorders in humans (36,37) and a possible role in this model still needs to be investigated.

Overall, these studies could be relevant to identify effective behavioural strategies as well as suggesting possible pharmacological targets for the prevention and cure of mood disorders, also according to the individual life histories and individual differences in the genotype.

Acknowledgments

Work was supported by the Collaborative Programme ISS-NIH (Project “Early risk factors for neuropsychiatric diseases. Comparative approaches to investigate interactions between genes and environment”; Rif. 0F14) to EA and FC. Authors thank Francesca Capone for technical support and Igor Branchi for critical reading.

References

1. Heim C, Nemeroff CB. The role of childhood trauma in the neurobiology of mood and anxiety disorders: preclinical and clinical studies. *Biol Psychiatry* 2001;49:1023-39.

2. Cicchetti D, Toth SL. A developmental psychopathology perspective on child abuse and neglect. *J Am Acad Child Adolesc Psychiatry* 1995;34:541-65.
3. Heim C, Nemeroff CB. The impact of early adverse experiences on brain systems involved in the pathophysiology of anxiety and affective disorders. *Biol Psychiatry* 1999;46:1509-22.
4. Yehuda R, Schmeidler J, Siever LJ, Binder-Brynes K, Elkin A. Individual differences in posttraumatic stress disorder symptom profiles in Holocaust survivors in concentration camps or in hiding. *J Trauma Stress* 1997;10:453-63.
5. Caspi A, Moffitt TE. Gene-environment interactions in psychiatry: joining forces with neuroscience. *Nat Rev Neurosci* 2006;7:583-90.
6. Caspi A, Sugden K, Moffitt TE, Taylor A, Craig IW, Harrington H, *et al*. Influence of life stress on depression: moderation by a polymorphism in the 5-HTT gene. *Science* 2003;301:386-9.
7. Cirulli F, Berry A, Alleva E. Early disruption of the mother-infant relationship: effects on brain plasticity and implications for psychopathology. *Neurosci Biobehav Rev* 2003;27:73-82.
8. Suomi SJ. Early stress and adult emotional reactivity in rhesus monkeys. *Ciba Found Symp* 1991;156:171-88.
9. Thoenen H. Neurotrophins and neuronal plasticity. *Science* 1995;270:593-8.
10. Levi-Montalcini R. The nerve growth factor 35 years later. *Science* 1987;237:1154-62.
11. Alleva E, Petruzzi S, Cirulli F, Aloe L. NGF regulatory role in stress and coping of rodents and humans. *Pharmacol Biochem Behav* 1996;54:65-72.
12. Branchi I, Francia N, Alleva E. Epigenetic control of neurobehavioural plasticity: the role of neurotrophins. *Behav Pharmacol* 2004;15:353-62.
13. Aloe L, Alleva E, Bohm A, Levi-Montalcini R. Aggressive behavior induces release of nerve growth factor from mouse salivary gland into the bloodstream. *Proc Natl Acad Sci U S A* 1986;83:6184-7.
14. Aloe L, Bracci-Laudiero L, Alleva E, Lambiase A, Micera A, Tirassa P. Emotional stress induced by parachute jumping enhances blood nerve growth factor levels and the distribution of nerve growth factor receptors in lymphocytes. *Proc Natl Acad Sci U S A* 1994;91:10440-4.
15. Hadjiconstantinou M, McGuire L, Duchemin AM, Laskowski B, Kiecolt-Glaser J, Glaser R. Changes in plasma nerve growth factor levels in older adults associated with chronic stress. *J Neuroimmunol* 2001;116:102-6.
16. Aloe L, Iannitelli A, Bersani G, Alleva E, Angelucci F, Maselli P, *et al*. Haloperidol administration in humans lowers plasma nerve growth factor level: evidence that sedation induces opposite effects to arousal. *Neuropsychobiology* 1997;36:65-8.
17. Neves-Pereira M, Mundo E, Muglia P, King N, Macciardi F, Kennedy JL. The brain-derived neurotrophic factor gene confers susceptibility to bipolar disorder: evidence from a family-based association study. *Am J Hum Genet* 2002;71:651-5.
18. Sklar P, Gabriel SB, McInnis MG, Bennett P, Lim YM, Tsan G, *et al*. Family-based association study of 76 candidate genes in bipolar disorder: BDNF is a potential risk locus. Brain-derived neutrophic factor. *Mol Psychiatry* 2002;7:579-93.
19. Vaidya VA, Duman RS. Depression--emerging insights from neurobiology. *Br Med Bull* 2001;57:61-79.
20. Branchi I, D'Andrea I, Sietzema J, Fiore M, Di Fausto V, Aloe L, *et al*. Early social enrichment augments adult hippocampal BDNF levels and survival of BrdU-positive cells while increasing anxiety- and "depression"-like behavior. *J Neurosci Res* 2006;83:965-73.
21. Cirulli F, Alleva E, Antonelli A, Aloe L. NGF expression in the developing rat brain: effects of maternal separation. *Dev Brain Res* 2000;123:129-34.
22. Cirulli F, Micera A, Alleva E, Aloe L. Early maternal separation increases NGF expression in the developing rat hippocampus. *Pharmacol Biochem Behav* 1998;59:853-8.
23. Roceri M, Cirulli F, Pessina C, Peretto P, Racagni G, Riva MA. Postnatal repeated maternal deprivation produces age-dependent changes of brain-derived neurotrophic factor expression in selected rat brain regions. *Biol Psychiatry* 2004;55:708-14.
24. Barr CS, Newman TK, Becker ML, Parker CC, Champoux M, Lesch KP, *et al*. The utility of the non-human primate; model for studying gene by environment interactions in behavioral research. *Genes Brain Behav* 2003;2:336-40.

25. Higley JD, Suomi SJ. Reactivity and social competence affect individual differences in reaction to severe stress in children: investigations using nonhuman primates. In: Pfeffer CR (Ed.). *Intense stress and mental disturbance in children*. New York: American Psychiatric Press, inc.; 1996. p. 3-58.
26. Higley JD, King ST Jr, Hasert MF, Champoux M, Suomi SJ, Linnoila M. Stability of interindividual differences in serotonin function and its relationship to severe aggression and competent social behavior in rhesus macaque females. *Neuropsychopharmacology* 1996;14:67-76.
27. Champoux M, Bennett A, Shannon C, Higley JD, Lesch KP, Suomi SJ. Serotonin transporter gene polymorphism, differential early rearing, and behavior in rhesus monkey neonates. *Mol Psychiatry* 2002;7:1058-63.
28. Bennett AJ, Lesch KP, Heils A, Long JC, Lorenz JG, Shoaf SE, *et al*. Early experience and serotonin transporter gene variation interact to influence primate CNS function. *Mol Psychiatry* 2002;7:118-22.
29. Lommatzsch M, Zingler D, Schuhbaeck K, Schloetcke K, Zingler C, Schuff-Werner P, *et al*. The impact of age, weight and gender on BDNF levels in human platelets and plasma. *Neurobiol Aging* 2005;26:115-23.
30. Karege F, Bondolfi G, Gervasoni N, Schwald M, Aubry JM, Bertschy G. Low brain-derived neurotrophic factor (BDNF) levels in serum of depressed patients probably results from lowered platelet BDNF release unrelated to platelet reactivity. *Biol Psychiatry* 2005;57:1068-72.
31. Pan W, Banks WA, Fasold MB, Bluth J, Kastin AJ. Transport of brain-derived neurotrophic factor across the blood-brain barrier. *Neuropharmacology* 1998;37:1553-61.
32. Fujimura H, Altar CA, Chen R, Nakamura T, Nakahashi T, Kambayashi J, *et al*. Brain-derived neurotrophic factor is stored in human platelets and released by agonist stimulation. *Thromb Haemost* 2002;87:728-34.
33. Mattson MP, Maudsley S, Martin B. BDNF and 5-HT: a dynamic duo in age-related neuronal plasticity and neurodegenerative disorders. *Trends Neurosci* 2004;27:589-94.
34. Karege F, Perret G, Bondolfi G, Schwald M, Bertschy G, Aubry JM. Decreased serum brain-derived neurotrophic factor levels in major depressed patients. *Psychiatry Res* 2002;109:143-8.
35. Shimizu E, Hashimoto K, Okamura N, Koike K, Komatsu N, Kumakiri C, *et al*. Alterations of serum levels of brain-derived neurotrophic factor (BDNF) in depressed patients with or without antidepressants. *Biol Psychiatry* 2003;54:70-5.
36. Schumacher J, Jamra RA, Becker T, Ohlraun S, Klopp N, Binder EB, *et al*. Evidence for a relationship between genetic variants at the brain-derived neurotrophic factor (BDNF) locus and major depression. *Biol Psychiatry* 2005;58:307-14.
37. Sen S, Nesse RM, Stoltenberg SF, Li S, Gleiberman L, Chakravarti A, *et al*. A BDNF coding variant is associated with the NEO personality inventory domain neuroticism, a risk factor for depression. *Neuropsychopharmacology* 2003;28:397-401.

Session 2A. Behavioural neuroscience: from basics to psychiatry

IMPLICATION OF AUTOANTIBODIES TO NEURO-RECEPTOR FRAGMENTS IN ETIOLOGY OF COMPULSIVE BEHAVIOUR AND DRUG ADDICTION

Giovanni Laviola (a), Francesca Capone (a), Walter Adriani (a), Oleg Granstrem (b), Ronald I Herning (c)

(a) Department of Cell Biology and Neurosciences, Istituto Superiore di Sanità, Rome, Italy

(b) Department of Neurology & Neurosurgery, Pavlov's State Medical University, St. Petersburg, Russia

(c) Molecular Neuropsychiatry Branch,National Institute of Drug Abuse, National Institutes of Health, Bethesda, MD, USA

Substance abuse, dependence and addiction are serious personal problems and a public health concern. Despite considerable experimental effort, our knowledge concerning the etiopathology of compulsive and uncontrolled drug use is still rather limited. Specifically, crucial steps under investigation are: 1) risk factors that make some individuals more vulnerable than others and 2) physiological correlates and/or determinants of the transition from misuse into overt addiction.

Recent evidence indicates that increased levels of autoantibodies (aAb), directed to several central nervous system (CNS) antigens, are detected in the blood of patients with neuropsychiatric disorders as well as in experimental animal models (1,2). With respect to drug abuse, the presence of elevated levels of antibodies to mu-opioid receptors has been demonstrated in chronic opiate addicts (3). In this line, with a recent study in mice (4), we have shown a drastic elevation of autoantibodies to mu-delta opioid (MDOR) and AMPA (but not NMDA) glutamate receptor subunits, following repeated morphine administration. In contrast, neither a psychostimulant drug such as d-amphetamine, nor a commonly abused substance such as nicotine, had any effects on the levels of these autoantibodies following a similar regimen of administration (4). Thus, it is possible to hypothesize that antigenic receptor peptide fragments may be released by chronically morphine-exposed brains, and may produce an auto-immune response and all the consequences thereof. In particular, we hypothesized that circulating aAbs to MDOR and AMPA subunits may influence drug-related psychoactive effects and behaviour.

Based on this background, the present project aimed to investigate the hypothesis that changes in levels of aAbs, induced by immunization with selected peptide fragments (MDOR, or GluR1 subunit of AMPA glutamate receptors), would affect the behavioural profile in animal models. The objective was to assess variations in spontaneous behaviour and in animals' response to acute and chronic morphine. As a whole, the immunization of mice with either GluR1 or MDOR peptide fragments determined as expected an increment in the serum levels of aAbs to both peptides. Levels of aAbs to NR-2 subunit of NMDA receptors, measured as negative control, remained stable after immunization. These immunized mice were then followed for a number of behavioural and psychopharmacological parameters:

- *Circadian cycle of spontaneous home-cage activity*
  Mice exhibited the expected circadian rhythm in activity patterns, with a reduced basal activity during the light phase and a robust increment in proximity of the light switch off/on. Interestingly, these activity profiles differed in the three experimental groups, depending on the peptide fragment used for immunization. Basal activity in GluR1

immunized group was significantly more marked, in that GluR1 immunized mice exhibited significant hyperactivity, compared to MDOR-immunized and Vehicle mice.

– *Rewarding properties of morphine*
By means of the conditioned place preference test, MDOR immunization was demonstrated to alter behavioural response of mice to morphine's rewarding effects (see Figure 1). In this classical test, mice are repeatedly exposed to one "paired" chamber following drug administration, and to a different "unpaired" chamber following saline injection. Morphine is expected to produce a significant preference for the drug-paired chamber, compared to the controls injected with saline in both chambers. For both the Vehicle and GluR1-immunized groups, repeated pairing between the chamber and morphine was sub-threshold and did not produce a conditioned preference. Conversely, within the MDOR-immunized group, a clear-cut conditioned place preference appeared. Such data clearly indicate a marked potentiation of morphine's incentive effects in MDOR immunized mice.

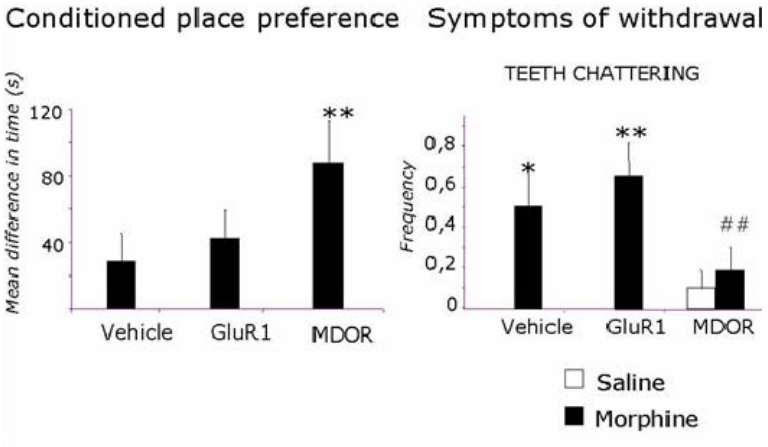

Figure 1. Left panel: conditioned place preference testing in drug-free state. Mice had free access for 10 min to the entire apparatus, consisting of one drug-associated "paired" chamber and one saline-associated "unpaired" chamber. Data present mean (+ S.E.M.) time (s) spent in drug-free state inside the drug paired minus the unpaired compartment (n=6). * P < 0.05 compared with saline-pairing controls of the same immunization group.
Right panel: physical signs of dependence, as measured during the naloxone-precipitated withdrawal syndrome in mice. Opiate dependence was induced by repeated i.p. injections of morphine, control mice were injected with saline (n=6). Withdrawal was precipitated by injection of naloxone (1 mg/kg, s.c.). Values are means (+ S.E.M.). * P < 0.05; ** P< 0.001 compared with the saline-exposed group; # P < 0.05; ## P< 0.001 compared with the other immunization groups exposed to the same drug treatment

– *Behavioural response to morphine*
Mice were made opiate dependent by administering escalating dosages of morphine, twice/day for 6 days. Upon the last drug dose, mice were scored for behavioural response in an open-field. Locomotor activity following exposure to a novel testing environment is indeed a parameter that is classically considered an index of vulnerability to addictive drugs (5). Both MDOR and GluR1 immunization markedly affected the behavioural

response to novelty after repeated morphine administration. For time spent in *Locomotor Activity*, indeed, morphine administration was sub-threshold for the Vehicle control group. Conversely, a marked drug-induced hyperactivity was shown by both MDOR and GluR1 immunized groups. Such data clearly indicate a marked potentiation of morphine-induced arousing effects in MDOR (and also GluR1) immunized mice.
For the frequency of *Rearing*, morphine treatment was again sub-threshold within the Vehicle group. Conversely, within the MDOR and GluR1 immunized groups, the drug reduced levels of *Rearing behaviour*. Interestingly, a change in baseline behaviour was observed for saline-injected mice of the GluR1 immunization group: an increment of basal *Rearing* was observed. A change in baseline behaviour was also found for *Self Grooming*. Indeed, compared to the Vehicle and MDOR-immunized controls, GluR1-immunized mice exhibited a marked increment in the frequency of this *auto-directed* behaviour.

– *Physical signs of dependence: naloxone-induced withdrawal*
The purpose of making opiate dependent mice was then to precipitate withdrawal with an acute injection of the antagonist naloxone. This procedure allows to evaluate aversive states induced by drug abstinence (6). Signs of morphine dependence consisted in *Tremors* and *Teeth Chattering* behaviours. No evidence of these behaviours was obviously found in saline-history control mice that never received morphine. In contrast, this stereotyped behaviour was elicited by naloxone in morphine-history mice from all immunization groups. As for the frequency of *Teeth Chattering*, however, this compulsive behaviour was elicited particularly in GluR1 and Vehicle groups, whereas significantly low levels were found for the MDOR immunization group (see Figure 1). Such a finding indicates a marked reduction of the opiate abstinence syndrome following MDOR immunization.
Similarly, morphine-history mice exhibited significantly higher levels of time spent in compulsive *Sniffing* behaviour, compared to saline-history controls. This was true for both GluR1 and Vehicle groups, but not for the MDOR-immunization group. Moreover, time spent in *Sniffing* behaviour was significantly higher in GluR1-immunization mice than the corresponding Vehicle and MDOR groups. This finding was consistent with data from circadian activity, in that GluR1-immunized mice exhibited a marked increment of *environment-directed* behaviours.

– *Neurochemical assessment in brain areas*
Mu-opioid receptors density was measured in the cortex and in the striatum brain areas at sacrifice. Repeated morphine treatment induced a feedback decrease in the density of mu-receptors for both Vehicle and GluR1 immunized mice. Conversely, this adaptive down-regulation response was completely absent in the MDOR immunized group.
This study investigated the potential role of altered serum levels of aAbs directed to opioid and AMPA receptors in the modulation of spontaneous behaviour as well as in the response to the prototypical addictive drug, morphine. Interestingly, the two immunization groups induced specific changes in mice behavioural phenotype. A peculiar profile, consisting of increased sensitivity to morphine-induced arousal and rewarding effects but reduced naloxone-precipitated withdrawal, was found in MDOR-immunized mice, compared to other groups. Conversely, GluR1 immunization was associated with increased levels of spontaneous home-cage activity, enhanced novelty-induced self-grooming and elevated abstinence-induced sniffing. These findings are relevant for modeling immune–related factors contributing to individual vulnerability to drug addiction.

In a previous study, Dambinova and Izykenova (7) used a recombinant m-d-opioid-receptor (MDOR) fragment as antigen, to demonstrate the presence of aAbs to MDOR in the blood of rats trained to self-administer heroin as well as in human drug abusers. The same fragment was used as an immunogen in the present study. In summary, our results indicate that an elevation in levels of circulating autoantibodies against MDOR is associated with: 1) an increased response to positive rewarding effects of morphine; 2) less physical signs of abstinence and naloxone-precipitated withdrawal; 3) an impaired adaptation to repeated morphine treatment, revealed by the lack of feedback regulation on brain mu-receptors expression. These multiple consequences may be subserved by autoantibody action on separate brain circuits that also mediate distinct opiate effects. This study indicates for the first time that fundamental parameters for the modulation of addictive processes, in terms of drug incentive effects and/or physical signs of dependence from morphine, can be modulated in some way by central opioid neuroreceptors auto-immunity. Similarly, autoantibodies directed against the m-opioid receptor reduce the morphine's rewarding effect, in parallel with reduced dependence and/or withdrawal (8).

Mice immunized with the GluR1 peptide fragment were characterized by increased spontaneous (home-cage) and morphine-induced locomotor activity. Moreover, the very high levels of auto-directed *Grooming* behaviour, exhibited by GluR1-immunized mice when exposed to a novel cage, suggests a peculiar coping response possibly served by a marked activation of central dopaminergic system. In fact, the novelty-induced *Grooming* behaviour is considered a reliable indirect index of stress, and interestingly elevated levels of novelty-induced stress have been also proposed as an index of vulnerability to abused drugs (5). Finally, our results show that naloxone-precipitated withdrawal symptoms in GluR1 mice consisted of elevated levels of compulsive cage Sniffing, an environment-directed stereotypy. Such data suggest that severity of precipitated abstinence from morphine, rather than merely increased, is redirected towards compulsive exploration of the surrounding environment. As a whole, this picture is suggesting that GluR1-immunized mice display a reduced capacity to cope with environmental challenges, which in turn has been implicated as a factor allowing the emergence of behavioural disorders. Compared to MDOR group, GluR1 mice exhibited in response to experimental challenges a quite opposite profile, consisting of elevated basal- and drug-induced motor activity and more severe physical signs of withdrawal.

– *Clinical evidence*

The present project has allowed to strengthen the collaboration between ISS and NIH. Indeed, a population of human subjects, who are abusers of different drugs, were characterized according to psychometric scales at the NIDA Center in Baltimore (USA). This group looks at risk factors for substance abuse, such as family history of psychiatric problems, psychiatric consequences, poor school performance/ADHD, cognitive deficits. These factors are interrelated with outcomes of substance abuse such as medical consequences, conduct disorder/antisocial behaviour (ASPD), aggressive and violent behaviour. Subjects were followed over one month of monitored drug abstinence with the following: laboratory tests (EKG, blood tests etc.), neurological EEG, full neurological exam, TCD, structured psychiatric evaluation (DSM-IIIR or DSM-IV), neuropsychological evaluation.

Preliminary investigation was started on blood samples from these human subjects. This study aimed to look for a correlation between levels of brain-directed autoantibodies and

type of drug abused, duration of drug exposure, and behavioural traits, including degree of drug dependence. These preliminary data are reported in Figure 2.

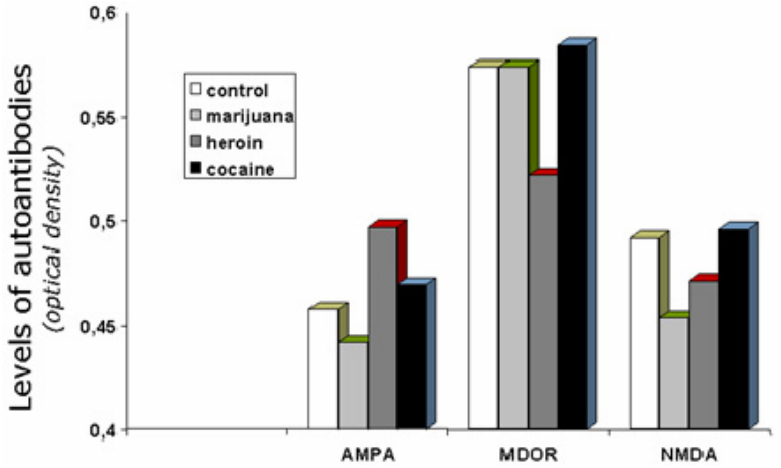

Figure 2. Preliminary data on drug users. Autoantibodies to AMPA-GluR1, MDOR, and NMDA-NR2 peptide fragments in the serum of healthy volunteers and human subjects after one month of controlled abstinence from marijuana, heroin, cocaine. Data represent mean optical density in the ELISAs

– *Preclinical evidence*
We described specific variations of basal and drug altered neurobehavioural phenotype in mice whose sera present an important elevation of circulating aAbs directed to MDOR and GluR1 neuro-receptor fragments. Even though the exact mechanisms of such an effect needs to be further elucidated, the present findings implicate a possible pathophysiological role for changes in serum titers of brain-directed autoantibodies (9). In particular, based on what observed in immunized mice, aAbs to MDOR and GluR1 in human addicts may be proposed to exert major consequences on drug-related behaviour. Individual levels of circulating MDOR and/or GluR1 aAbs could lead to significant inter-individual differences in the rewarding efficacy and withdrawal symptoms, as a function of opiate doses. In particular, the rewarding power of morphine, and the aversive states associated to morphine abstinence, may be significantly altered by MDOR-directed auto-immunity. On the contrary, increased levels of aAbs to GluR1 may increase liability to express basal hyperactivity and restlessness, together with an altered coping with external stressors and environmental challenges. These features may affect levels of motivation to seek for and consume opiate drugs. Based on these considerations, it could be speculated that auto-immune responses may provide a contribution during the development of drug addiction in human subjects.

Acknowledgments

This study was supported by the NIH-ISS Collaborative Project (grant to GL). We wish to thank the CIS Biotech Inc. (USA) for providing the peptide sequences for this study.

References

1. Whitney KD, McNamara JO. Autoimmunity and neurological disease: Antibody modulation of synaptic transmission. *Annu Rev Neurosci* 1999;22:175-95.
2. Lang B, Dale RC, Vincent A. New antibody mediated disorders of the central nervous system. *Curr Opin Neurol* 2003;16:351-7.
3. Izykenova GA, Sirenko VV, Dambinova SA. Immunodiagnostics of drug addiction. *J Problems Drug Abuse* 1995;1:45-9.
4. Granstrem OK, Adriani W, Izykenova GA, Dambinova SA, Laviola G. Specific changes in levels of autoantibodies to glutamate and opiate receptors induced by morphine administration in rats. *Neurosci Lett* 2006;403:1-5.
5. Piazza PV, Deminiere JM, Le Moal M, Simon H. Factors that predict individual vulnerability to amphetamine self-administration. *Science* 1989;245:1511-3.
6. Maldonado R, Saiardi A, Valverde O, Samad TA, Roques BP, Borrelli E. Absence of opiate rewarding effects in mice lacking dopamine D2 receptors. *Nature* 1997;388:586-9.
7. Dambinova SA, Izykenova GA. Recombinant mu-delta receptor as a marker of opiate abuse. *Ann N Y Acad Sci* 2002;965:497-514.
8. Sanchez-Blazquez P, Rodriguez MD, Garzon J. Antibodies directed against the mu-opioid receptor alleviated multiple signs of morphine withdrawal in mice. *Life Sci* 1996;59:PL87-92.
9. Margutti P, Delunardo F, Ortona E. Autoantibodies associated with psychiatric disorders. *Curr Neurovasc Res* 2006;3:149-57.

Session 2A. Behavioural neuroscience: from basics to psychiatry

GENDER DIFFERENCE IN SEIZURE SENSITIVITY: ROLE OF STEROIDS AND NEUROACTIVE STEROIDS

Alberto Loizzo (a), Andrea Fortuna (a), Gabriella Galietta (a), Irene Guarino (a,b), Stefano Loizzo (a), Giovanni Biggio (c), Alessandro Concas (c), Mariangela Serra (c), Flavia Franconi (b)
(a) Department of Therapeutic Research and Medicines Evaluation, Istituto Superiore di Sanità, Rome, Italy
(b) Centre of Excellence for Biotechnology, University of Sassari, Italy, and GIO.I.A Foundation onlus
(c) Centre of Excellence for Neurobiology of Addiction, University of Cagliari, Italy

Introduction

During the past 20 years, it has become increasingly evident that the treatment of epilepsy must be tailored to specific patient populations. One area of research has focused on the medical treatment of women with epilepsy. It is now clear that hormonal variations within the normal menstrual cycle can cause what are known as catamenial seizures. Conversely, epilepsy can disrupt the normal hormonal cycle, leading to reproductive and endocrine dysfunction. In addition, antiepileptic drugs (AEDs) can have unique side effects in women (Isojarvi, 1993; 1998; 2001); they may cause changes in endocrine function and reproductive health (Foldvary et al, 2001); reduce the effectiveness of oral contraceptives (Foldvary et al, 2001), produce birth defects in developing fetuses, and cause sexual dysfunction (Kalayjian and Morrell, 2000; Lambert, 2001). As new therapies for epilepsy are added to the armamentarium, these effects must be weighed during selection of appropriate treatment for women with epilepsy. In view of the previous of suggestions it has been published in "Expert Consensus Guideline Series: Treatment of Epilepsy" a section specifically dedicated to women (Karceski et al, 2001).

Although gender differences in mortality, growth and susceptibility to diseases have been evidenced since foetal and neonatal life, they are generally believed to start at puberty. Indeed, gender differences really seem to initiate in uterus: as an example, Y chromosome is known to accelerate the growth and increase glucose metabolism. At birth, growth curve and heart rate are different in males and females, while sexual dimorphism in fat patterning starts at 5-7 years of age. This is not surprising because the genetic sex in turn controls the development of gonadal sex. The question is whether sex chromosome genes, which are present in different quantities in the genomes of males and females, might be expressed differently and cause sex-specific patterns of development and/or function. Male mammals possess genes on the non-recombining region of the Y chromosome (NRY), that encode 27 distinct proteins, which might act to cause masculine patterns. Alternatively, genes on the non-pseudoautosomal portion of the X chromosome (NPX), which are present in two doses in females but only a single dose in males, could cause sex-specific differences. These differences are balanced by X silencing. Nevertheless, at least in humans a significant percentage of NPX genes escape inactivation. Therefore, cells containing genes, which escape to silencing, could express higher gene products and this could have important implications. It implicates the possible different responses of embryos, foetuses and infants to maternal pharmacological treatments (either in pregnancy and in lactation) and their relevant consequences, for example in developmental toxicology.

Therefore, it was set up a stress model in lactation dedicated to study the effect of neonatal stress on adultood. The application of experimental paradigm produce behavioural alterations

relative to the forced-swim test which also appears to have two types of potential responses - a more passive response of floating and the more active escape responses of swimming, climbing the walls of the swim tank, and diving. The behavioural alterations are accomplished by important increase in plasma corticosterone and ACTH and alterations in glucose metabolism. The alterations linked to the glucose metabolism are prevented by an inhibitory amino acid such as taurine administered during lactation.

Our project starts basically from the studies of endocrine/metabolic/neurophysiological changes in mice, in basal conditions, and following those pathophysiological changes in adult life which were triggered by a mild stress model chronically applied to the newborn animal: the model consists of brief (10 min) isolation from mother plus sham injection starting at birth, and applied daily during lactation period up to weaning (21 days of life). This model is followed by a number of central and peripheral residual effects perduring up to the adult life (cf Loizzo et al, 2002). Therefore, we performed a series of experiments aimed at studying the effects induced by this model on male and female mice of the outbred strain CD1; then we applied this model to a well-known genetic model of seizures (inbred DBA/2 mice), and finally we studied the relationship between a model of seizures induced by kindling in the rat, i.e., in the rat treated with repeated doses of pentamethylenetetrazol (PTZ), and the cerebral level of neurosteroids in males and females.

Experimental procedures

Investigations were performed using several procedures. All experiments were carried out in accordance with the guidelines of the Council of European Communities 86/609/EEC and the protocols were approved by the Bioethical Committee of the Istituto Superiore di Sanità (Rome, Italy).

- Animals were handled as previously described in Loizzo et al. (2003); Franconi et al. (2004) and Loizzo et al. (2006). Briefly, different series of multiparous pregnant mice of the CD-1 outbred strain and the DBA/2 inbred strain were received, and about 12 h after birth male pups of similar weight were selected and six pups per litter were randomly put together and cross-fostered, and randomly assigned to one of the groups: 1) non neonatal-handled mice (Controls): the pups were left undisturbed with their mothers, except for cage cleaning twice a week; 2) vehicle-treated handled mice (Handled): for 21 days, the pups were removed daily (10 min) from the home cage and grouped in a container with fresh bedding material and injected s.c. with sterile saline (1 ml/kg body weight). After weaning, the animals were re-housed three per cage, and left undisturbed until being sacrificed, with the exception of body weighing and cage cleaning. In other experiments, the same procedures were adopted for litters of female mice, bred in parallel with litters of male mice.
- At 30 days of age, mice underwent pain sensitivity tests (tail-flick and hot-plate test, according previously described methods- see Pieretti et al, 1991).
- At 80 days of age, male and female DBA/2 mice were implanted with chronic epidural stainless steel electrodes, and after 8-10 days they underwent electroencephalographic (EEG) and visual-flash evoked responses (VER), according to previously published methods (Lopez et al, 2002). Then, EEG was examined and sleep-weekfulness cycle and epileptiform patterns were sistematically identified; EEG also underwent time- and frequency-domain elaboration. Also VERs were studied, and after digital band-pass 60-300 Hz filtering rapid oscillatory potentials (PO) were extracted and measured.
- A model of epilepsy in male and female rats (kindling) was studied. Repeated systemic administration of a subconvulsive dose of PTZ, a blocker of the γ- aminobutyric acid type

A ($GABA_A$) receptor, induces the progressive development of seizures. In this phase of the project, PTZ (25 mg/kg) was administered intraperitoneally to male rats three times a week for 8-12 weeks. This treatment regimen induces in most of rats a "fully-kindled" condition. However, the same treatment in a group of animals do not develop seizures (non kindled). Neuroactive steroids (allopregnanolone and THDOC) have been extracted by brain tissue with ethyl acetate, purified and separated by high pressure liquid chromatography (HPLC) on lichrosorb-diol column developed with a discontinuous2-propanol in n-exane gradient. Quantification of each steroid has been performed by radioimmunoassay with specific antibodies. The method was applied in male rats, and in female rats in different times of the hormonal cycle.

Main results

Gender and pain threshold studies. At 30 days of age, control male CD1 mice showed a threshold soil to thermal pain (hot-plate response) of the same levels as control females. However, male mice which had undergone stressful procedures at this age showed a threshold soil consistently higher than controls, whereas stressed female did not show any differences versus controls (Table 1).

Table 1. Effect of handling and gender on nociceptive responses measured in male and female mice at 30 days of age. Values are in s, means ±SEM. * is for p<0.001, handled males (HM) *vs* non-handled males (NHM), *vs* handled females (HF), and *vs* non-handled females (NHF)

Groups	NHM	HM	NHF	HF
Response(s)	38±2	50±3*	35±1	37±2

Gender and body weight studies. Adult male CD1 stressed mice at 90 and 120 days of age weighed consistently more than controls, and this confirms previous data. In the present experiments we found that CD1 females were overweight as well, versus control females (Table 2).

Table 2. Effect of handling and gender on weight increment in adult mice at the age of 90 days. Values are in g, means ±SEM. * is for p<0.001, handled males (HM) *vs* non-handled males (NHM), and ° is for p<0.001 for handled females (HF) *vs* non-handled females (NHF)

Groups	NHM	HM	NHF	HF
Body weight (90 d)	42.7±0.5	45.0±0.7 *	33.3±0.6	35.3±0.7

Gender and Basic Neurophysiological Studies. Basic neurophysiological studies performed up to date showed some interesting differences between genders, and between control and neo-natally stressed mice. *Visual evoked responses* (VER). In male DBA/2 mice the wave N1 was recorded at a mean latency of 32.9 ±0.4 ms, in female mice at a latency of 35.5 ±0.4 ms ($P<0.01$). The cholinomymetic drug physostigmine (0.05mg/kg i.p.) further decreased the latency only in male mice. VER amplitude of N1 in males and females was 37.4 ±2.5 μV and 38.4 ±2.7 μV, respectively, the difference was not significant. Administration of physostigmine induced significant decrease of amplitude in female mice, 25 min after drug (26,3 ±4 μV; $P<0.05$), and not in males (31.8 ±2.6 μV). In another experiment, a partial analysis of results (in

progress) indicates that in male control mice N1 VER latency is 31 ± 0.8 ms versus 27.1 ± 1.0 in stressed ones. Power-spectral analysis indicated that the spectral content of OP, performed up to 300 Hz, does not vary between genders, thus suggesting that although the VER message transmitted through visual pathways is more rapid in male mice, the content of OP message is apparently the same. However, the spectral pattern analyzed according to both the frequency - and the time-domain, evidenced an interesting difference in the high frequencies spectral time-related evolution between basal EEG recorded in adult controls and in neonatally stressed DBA/2 mice in both genders. Figure 1 shows a sample of the results.

Gender and epileptiform EEG pattern. Neonatal handled mice, as adults, had consistent less polispike - and-waves complexes per recording hour versus controls (mean 8.5 ± 3.1 versus 27.6 ± 6.5, $p < 0.05$). However, no consistent difference has been yet observed in the incidence, or in latency, or in mortality following audiogenic seizures performed at 22 days of age, in males versus females, or in controls versus stressed.

Long-term effects induced by neonatal stress on brain and plasma steroids. At the end of the repeated stressful procedures, pituitary adrenocorticotropin (ACTH) and both plasmatic ACTH and corticosterone of CD1 male mice were consistently increased over controls. These effects were observed at least up to the 120th day of age. However, hypothalamic levels of corticotropin releasing hormone were strongly depressed in adults versus controls, thus suggesting that some forms of feedback regulation system in the hypothalamus-pituitary (Table 3).

Table 3. Effects of handling on hypothalamus-pituitary-adrenal hormones in the adult male mouse. Plasma corticosterone (ng/ml plasma) and ACTH (pg/ml plasma) are consistently increased in HM *vs* NHM, whereas hypothalamic corticotrophin releasing hormone (CRH, pg/µg protein) is consistently depressed in HM. This indicates a disruption in the negative feed-back mechanisms of hormone regulation. * indicates significant difference from NHM (p<0.001)

Groups	NHM	HM
Plasma corticosterone	23.7±1.6	49.7±4.0 *
Plasma ACTH	75.0±5.2	306.0±13.0 *
Hypothalamic CRH	21.3±1.5	5.5±0.7 *

Long-term effects induced by early taurine treatment in mice. It is known that taurine is agonist of glycine receptors and there are some suggestions that during the development it is the favourite agonist for glycinergic receptors. Therefore we analyzed the effect of neonatal taurine administration. The neonatal handling model adopted induces gender-related metabolic alterations. For example, males are overweight and have elevated fasting glucose and plasma lipid alterations, while female do not present such alterations. In males, neonatal taurine administration consistently prevents the increase in fasting plasma glucose induced by neonatal handling, and additionally taurine seems to increase insulin secretion induced by glucose, without altering insulin sensitivity. In the very same experimental model, taurine does not modify plasma lipids and MDA, an index of oxidative stress. At 140 days of age, mice which were handled during the neonatal period show consistent decrease in immobility time in forced swimming test, and taurine did not influence this parameter. Electrophysiological experiments in brain slices obtained from adult mice show that input–output curves in hippocampal CA1 were increased by taurine administration during the lactation period. Hence, neonatal administration of taurine might permanently modify the functioning of hippocampus, at least in males. Research are in progress to evaluate the effect of taurine in females.

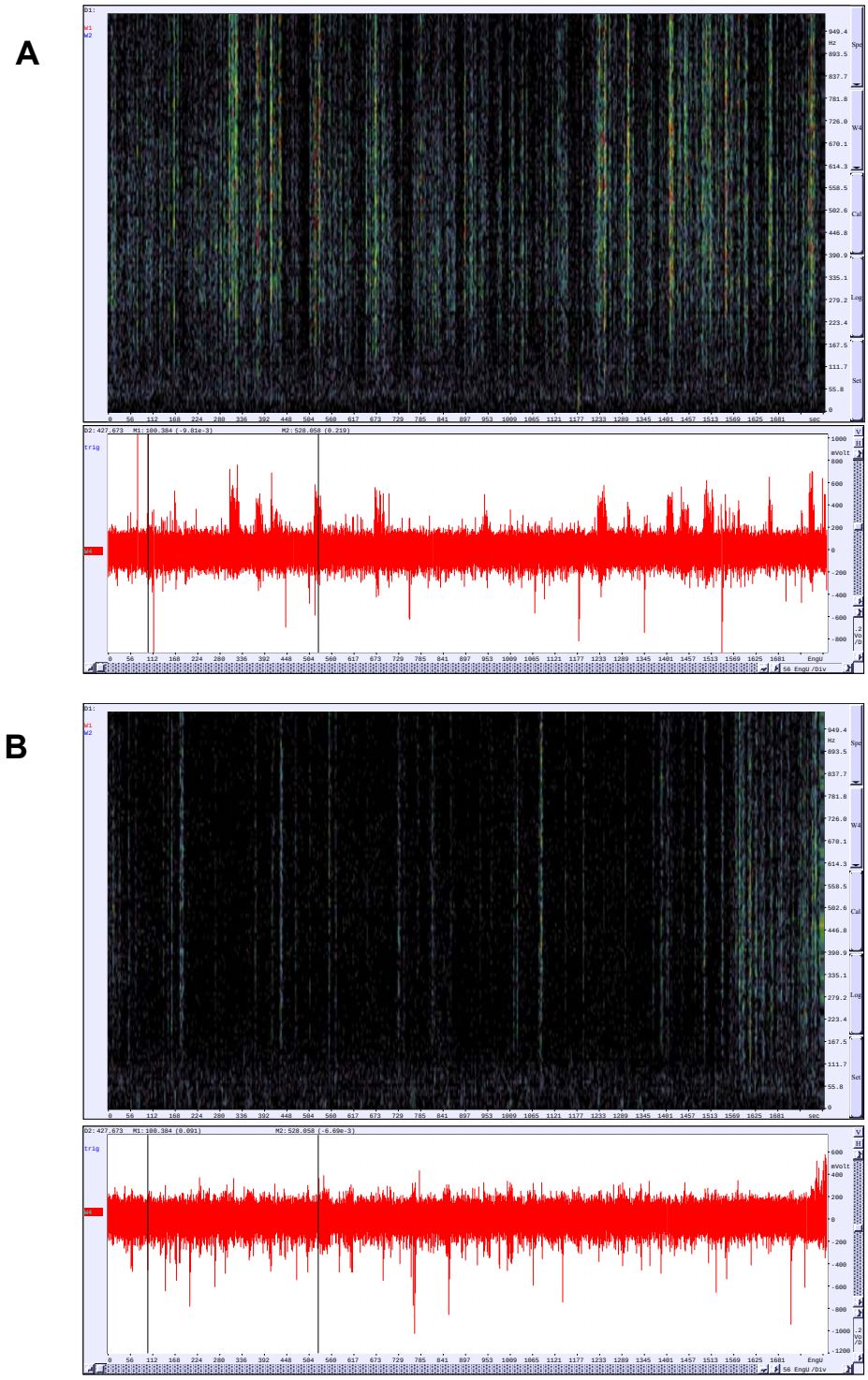

Figure 1. Spectrograms elaborated from a 30 min EEG recorded in a control DBA/2 male mouse (NHM) (A), and EEG recorded in a DBA/2 HM (B).
Abscissa, time in seconds. Ordinate. Upper part of the figures, power spectra , from 50 Hz (baseline) up to 500 Hz (top of the figure) whose intensity is characterized through colors (from green = low intensity, up to red = high intensity). Ordinate. Lower part of the figure: compressed EEG; amplitude is in μV

Kindling, gender and neurosteroids in rats. The results of these experiments demonstrate that the cerebrocortical and plasma concentrations of allopregnanolone and THDOC are not modified in the "fully kindled" rats with respect to control animals. On the contrary, "non kindled" rats showed a concentration of allopregnanolone and THDOC both in the cerebral cortex and plasma significantly higher than neurosteroids in the brain and plasma of "fully kindled" and control rats. More interesting, allopregnanolone basal cortical levels were consistently higher in all phases of the estrous cycle in female rats versus level found in males (6-12 ng/g of tissue in female rats versus 0.8±0.01 in males).

Conclusions

Preliminary results indicate that female animals do behave differently from males in several parameters connected with neurophysiology and cerebral excitability, and that neonatal stress strongly influences metabolic, endocrine and neurophysiological parameters. Studies on endocrine and receptoral mechanisms (in progress) may contribute to clarify etiopathogenesis and perhaps to help therapy of catamenial epilepsies.

Acknowledgement

This paper was supported in part by NIH-ISS Collaborative Project "Gender difference in seizure sensitivity: role of steroids and neuroactive steroids", and in part by ISS Project "Developmental Pharmacology". Thanks are due to Dr M Rogawski for suggestions and criticism. We thank also Mr Stefano Fidanza and Mr Adriano Urcioli for care of animals.

References

1. Carta S, Bennardini F, Loizzo A, Galietta G, Seghieri G, Guarino I, Franconi F. Neonatal taurine administration modifies glucose metabolism in adult life. *32° Congresso Nazionale della Società Italiana di Farmacologia Abstracts.* Torino: Edizione Minerva Medica SPA; 2005; p 158.
2. Dazzi L, Serra M, Porceddu ML, Sanna A, Chessa MF, Biggio G. Enhancement of basal and pentylenetetrazol (PTZ)-stimulated dopamine release in the brain of freely moving rats by PTZ-induced kindling. *Synapse* 1997;26(4):351-8.
3. Foldvary N. Treatment issues for women with epilepsy. *Neurol Clin North Am* 2001;19(2):409-25.
4. Franconi *et al*. Taurine administration during lactation modifies hippocampal CA1 neurotransmission and behavioural programming in adult male mice. *Brain Res Bull* 2004;63(6):491-7.
5. Galietta G *et al*. Administration of antisense oligonucleotide against pro-opiomelanocortin prevents enduring hormonal alterations induced by neonatal handling in male mice. *Eur J Pharmacol*, Accepted for publication
6. Guarino *et al*. A chronic implant to record electroretinogram, visual evoked potentials and oscillatory potentials in awake, freely moving rats for pharmacological studies. *Neural Plast* 2004;11(3-4):241-50.
7. Isojarvi JIT, Rattya J, Myllyla VV, *et al*. Valproate, lamotrigine, and insulinmediated risks in women with epilepsy. *Ann Neurol* 1998;43:446-51.
8. Isojarvi JIT, Tauboll E, Pakarinen AJ, *et al*. Altered ovarian function and cardiovascular risk factors in valproate-treated women. *Am J Med* 2001;111:290-6.

9. Isojarvi JIT, Laatikainen TJ, Pakarinen AJ, *et al*. Polycystic ovaries and hyperandrogenism in women taking valproate for epilepsy. *N Engl J Med* 1993;329:1383-8.
10. Kalayjian L, Morrell MJ. Female sexuality and neurological disease. *J Sex Ed Ther* 2000;25(1):89-95.
11. Lambert M. Seizures, hormones, and sexuality. *Seizure* 2001;10:319-40.
12. Karceski SC, Morrell MJ, Carpenter D. The Expert Consensus Guideline Series: Treatment of epilepsy. *Epilepsy & Behavior* 2001;2(6):A1-A50.
13. Loizzo A, *et al*. Vas deferens response to selective opioid receptor agonists in adult mice is impaired following postnatal repeated mild stress. *Eur J Pharmacol* 2003;458:201-5.
14. Loizzo A *et al*. Naloxone prevents cell-mediated immune alterations in adult mice following repeated mild stress in the neonatal period. *Br J Pharmacol* 2002;135(5):1219-26.
15. Loizzo *et al*. Overweight and metabolic and hormonal parameter disruption are induced in adult male mice by manipulations during lactation period. *Pediatr Res* 2006;59:111-5.
16. Loizzo *et al*. Neonatal handling induces increased body weight increment curve in adult mice of both sexes, and impaired fasting glucose pattern in adult males but not in females. Manuscript in preparation.
17. Pieretti S, d'Amore A, Loizzo A. Long-term changes induced by developmental handling on pain threshold: effects of morphine and naloxone. *Behavioral Neuroscience* 1991;105:215-8.
18. Pierobon P, Minei R, Porcu P, Sogliano C, Tino A, Marino G, Biggio G, Concas A. Putative glycine receptors in Hydra: a biochemical and behavioural study. *Eur J Neurosci* 2001;14(10):1659-66.

Session 2B. Neurodegenerative disorders

HIGH PRESSURE/TEMPERATURE INACTIVATION OF TRANSMISSIBLE SPONGIFORM ENCEPHALOPATHY AGENTS IN BIOLOGICAL PRODUCTS

Franco Cardone (b), Hanin Abdel-Haq (b), Angela De Pascalis (b), Vito Berardi (b), Marco Sbriccoli (b), Silvia Graziano (b), Angelina Valanzano (b), Paul Brown (a), Maurizio Pocchiari (b)
(a) National Institutes of Health, Bethesda, MD, USA
(b) Department of Cell Biology and Neurosciences, Istituto Superiore di Sanità, Rome, Italy

Introduction

Since 1995, over 190 patients with variant Creutzfeldt-Jakob disease (vCJD) have died as a result of having consumed processed meat products contaminated by the agent of bovine spongiform encephalopathy (BSE). Almost all cases have occurred in the United Kingdom, yet a growing number of European and non-European countries have had indigenous cases and future cases may appear in any country in which BSE in cattle have occurred or BSE-infected meat products have been imported from exposed countries (1). Governments in Europe, as elsewhere, have taken steps to minimize the risk of exposure to BSE. However, implementation of these precautions has not been uniform, and continuous inspections are required to assure compliance with regulatory strategies. The recent identification of BSE in indigenous cattle in Canada and Japan, the appearance of a new strain of TSE in cattle (e.g., the amyloidotic BSE or BASE), and the finding of a few cases of BSE in small ruminants have raised worries over the safety of food (2-3). A complementary strategy based on the inactivation of infectivity in processed meat would therefore be an attractive further safeguard to human health, but neither of the two proven inactivating methods – autoclaving or exposure to strong alkali or bleach – are applicable to foodstuffs (4). In 1991, Knorr and Heinz demonstrated that a single five-minute pulse of 1400 MPa at 140°C was effective in destroying prion protein from scrapie-infected hamster brain. Ten years later, in a review article, Masson and co-workers (5) reported unpublished data showing that the pathological prion protein (PrPres, a biochemical marker of TSE infectivity) associated with an experimental hamster strain of spongiform encephalopathy was partially inactivated by pressures higher than 500 MPa but no details were reported, i.e., condition of the sample, time and temperature of treatment. Shortly after, we and other authors reported that a range of high pressure-temperature combinations could be used for TSE removal (6-9). In our study, we exposed hot dogs spiked with an experimental strain of TSE (the hamster-adapted scrapie strain 263K) to three or ten one-minute pulses of 690, 1000, or 1200 MPa at 135°C, and observed up to 5 log reductions of prion protein, and up 6 log reductions of infectivity (6). The degree of prion protein reduction (measured by Western blot) was a reliable indicator of the degree of infectivity reduction (measured by bioassay), making it possible to gauge the effectiveness of pressure when bioassay is impractical, e.g., when testing strains of bovine spongiform encephalopathy. These results revealed only some of the potential applications of high pressure/temperature technology. A full application of the methodology to foods, biological materials and medical devices requires a careful evaluation of the inactivation

efficiency since this might vary when applied to various substrates (i.e., hot dogs versus hamburger) or to distinct prion strains.

The objective of our project is to explore a larger range of pressure/temperature/pulse combinations, and to verify the efficiency of inactivation for additional prion strains (e.g., natural and experimentally adapted BSE, experimentally adapted vCJD) in a variety of biological products and materials.

Materials and methods

Infectious samples were taken from brain of cow with BSE, mice with experimental BSE or vCJD, and hamsters with 263K scrapie. Samples were mechanically homogenized and reduced to a homogenous paste.

Substrate tissues were hot dog, pet food, corned beef, baby food, beef *paté*, and hamburgers. These were mechanically homogenized and reduced to a homogenous paste.
Samples for each study were prepared as following:

1. *Pressure/temperature dose-response inactivation curve*

Sample:	One part of 263K brain plus 9 parts of hot dog homogenate
Test conditions:	a. 600, 800, 1000, 1200 MPa for 5-min at 132°C b. 1200 MPa for 5-min at 115, 118, 125, 130, 134°C c. 600 and 1200 MPa for 1, 2, 3, 4, or 5 min at 125°C
Sample analysis:	Western blot for PrPres.

2. *Inactivation of high titres of prions by means of long-term (2 hours) treatments*

Sample:	One part of 263K brain plus 9 parts of hot dog homogenate
Test conditions:	400, 600, 890 MPa for 120-min at 60°C
Sample analysis:	Western blot for PrPres.

3. *Inactivation of high and low concentration of prions in hot-dog paste*

Samples:	One part of 263K brain plus 9 parts of hot dog homogenate (high infectivity, ~ 10^8 LD_{50}/g); 263K brain paste diluted 10^{-5} in hot dog homogenate (low infectivity, ~ 10^5 LD_{50}/g).
Test conditions:	690 MPa for 5-min at 132°C
Sample analysis:	Western blot for PrPres and bioassay for infectivity.

4. *Inactivation of prions mixed with various processed meat products*

Sample:	One part of 263K brain plus 9 parts of meat product homogenate
Test conditions:	600 MPa for 5-min at 130°C
Sample analysis:	Western blot for PrPres

5. *Inactivation of different prion strains*

Samples:	200 mg samples of brains (263K, cattle BSE, mouse BSE, mouse vCJD)
Test conditions:	600 MPa for 5-min at 130°C
Sample analysis:	Bioassay for infectivity.

Pressure treatments were performed on aliquots of TSE brain pastes, which were spiked into meat products. Each sample was heat sealed in double bags, immersed in a vessel filled with pressure transfer medium and then placed into the chamber of the high-pressure apparatus. The chamber was completely filled with hot pressure transfer medium and then subjected to pressurization. Chamber temperatures and pressures were continuously recorded during each test run.

Western blot and bioassay analyses on samples were performed as described (6).

Results

To evaluate the relative contribution of pressure, temperature and time during high pressure processing we prepared aliquots of ground hot dogs mixed with brain material (spike) from 263K scrapie-infected Syrian hamsters. The samples were subjected to a panel of treatments where two parameters were fixed and one was subjected to incremental variations. The results showed that the reduction of PrPres titre was mainly regulated by depended upon pressure (Table 1) and temperature (Table 2).

Table 1. PrPres reduction in 263K-spiked hot dogs treated for five minutes at constant temperature and variable pressure

Treatment			Amount of barain loaded in the gel (µg)								
Pressure (MPa)	**Temp. (°C)**	**Time (min)**	**1000**	**330**	**100**	**33**	**10**	**3.3**	**1**	**0.3**	**0.1**
Ambient	Ambient	-					+	+	+	+	-
600	132	5			+	+	-				
800	132	5		+	±	-					
1000	132	5	+	±	-						
1200	134	5	-								

Table 2. PrPres reduction in 263K-spiked hot dogs treated for five minutes at constant pressure and variable temperature

Treatment			Amount of barain loaded in the gel (µg)								
Pressure (MPa)	**Temp. (°C)**	**Time (min)**	**1000**	**330**	**100**	**33**	**10**	**3.3**	**1**	**0.3**	**0.1**
Ambient	Ambient	-					+	+	+	+	-
1200	115	5	+	+	+	-					
1200	118	5	+	+	+	-					
1200	125	5	+	+	-						
1200	130	5	+	±	-						
1200	134	5	-								

No reduction was observed beyond the exposure time of more than 3-5 minutes (Table 3).

Table 3. PrPres reduction in 263K-spiked hot dogs treated at constant pressure and temperature for 1-5 minutes

Treatment			Amount of brain loaded in the gel (µg)						
Pressure (MPa)	**Temperature (°C)**	**Time (min)**	**100**	**33**	**10**	**3.3**	**1**	**0.3**	**0.1**
ambient	ambient	-	+	ND	+	+	+	+	-
600	125	1	+	+	+	+	-		
600	127	2	+	+	+	+	-		
600	127	3	+	+	±	-			
600	126	4	+	+	±	-			
600	127	5	+	+	±	-			

It is to note that the influence of each factor is not equivalent. At the mildest conditions of treatment (600 MPa at 125-127°C for 1 minute) only a minimal reduction of PrPres was obtained (1 logarithm). When the duration of treatment was progressively increased by 1-min increments, only a further half-log PrPres reduction was achieved after three minutes. This level remained unchanged even when the time of treatment was prolonged to 4 or 5 minutes. Higher reduction was obtained only by increasing the temperature, the pressure, or both.

Interestingly, a similar level of PrPres reduction was obtained by using different combinations of pressure and temperature, which can be properly selected to obtain the desired effect. Our data show that pressure is the parameter that allows the finest tuning of inactivation.

The length of treatment seems to be more relevant when pasteurization temperatures are applied. It was recently reported that 120 min at 800 MPa/60°C remove about 6.4 log of 263K scrapie infectivity and reduce PrPres under the level of detection by Western blotting (7-9). To date, we have been unable to duplicate these Western blot results: PrPres was still detectable in 0.3 µg of 263K-brain treated at 890 MPa/60°C for 120 min, similarly to untreated samples (Table 4) (10). The measurement of infectivity in these samples by end-point bioassay is in course.

Table 4. PrPres reduction in 263K-spiked hot dogs treated at pasteurization temperature for 120 min

Treatment			Amount of brain loaded in the gel (µg)			
Pressure (MPa)	**Temperature (°C)**	**Time (min)**	**3.3**	**1**	**0.33**	**0.1**
ambient	60	120	+	+	±	-
			+	+	±	-
			+	+	±	-
			+	+	±	-
400	60	120	+	+	±	-
			+	+	±	-
			+	+	±	-
			+	+	±	-
600	60	120	+	+	-	
			+	+	-	
			+	+	-	
			+	+	-	
890	60	120	+	+	±	-
			+	+	±	-
			+	+	±	-
			+	+	±	-

After this first set of experiments, we used treatment conditions (600-700 MPa at 125-130°C for 5 minutes) that are accessible by large industrial machines. As the capacity to yield standard results is an essential requisite for an industrial process, the first goal was to evaluate the repeatability of the inactivation effect on hot dog paste spiked with high or low amounts of 263K scrapie. Measurement of PrPres in highly infectious samples subjected to the same treatment in separate runs showed 2-logarithms reduction in each sample with an excellent reliability within and between samples (Table 5). Animal bioassays of HPT-treated low-infectivity samples (5.4 log LD_{50}/g) showed no traces of infectivity in 5 repeats, traces of infectivity in two, and more than 2 logs reduction in one sample (Table 6).

Table 5. PrPres reduction in HPT-treated replicate aliquots of 263K-spiked hot dogs

Treatment			Amount of brain loaded in the gel (µg)						
Pressure (MPa)	**Temperature (°C)**	**Time (min)**	**100**	**33**	**10**	**3.3**	**1**	**0.33**	**0.1**
ambient	100	5				+	+	±	-
						+	+	±	-
690	128	5	+	+	-				
			+	+	-				
690	128	5	+	+	-				
				+	-				
690	128	5	+	+	-				
			+	+	-				
690	127	5	+	+	-				
			+	+	-				
690	126	5	+	+	-				
			+	+	-				
690	123	5	+	+	-				
			+	+	-				
690	127	5	+	+	-				
			+	+	-				
690	127	5		+	-				
			+	+	-				

Table 6. Infectivity bioassay of HPT-treated replicate aliquots of 263K-spiked hot dog

Treatment			Infectivity bioassay		
Pressure (MPa)	**Temperature (°C)**	**Time (min)**	**Infected/inoculated**	**Incubation periods (mean ± SD)**	**Estimate titre (log LD_{50}/g)**
ambient	100	5	6/6	103.2 ± 6.0	5.0°
690	128	5	6/7	112, 138, 138, 169, 221, 341	2.3-3.3
690	128	5	1/9	247	< 2.3
690	128	5	0/5	-	< 1.3
690	127	5	0/5	-	< 1.3
690	126	5	0/7	-	< 1.3
690	123	5	0/9	-	< 1.3
690	127	5	0/8	-	< 1.3
690	127	5	2/10	156, 217	< 2.3

° Infectivity in this sample was calculated on the basis of a published dose-incubation period curve (Pocchiari M, Casaccia P, Ladogana A. J Infect Dis 1989;160:795-802). In treated samples the infectious titre was estimated on the basis of the percentage of infected animals following a worst case assumption: < 0 LD50/ 5 mg of inoculum if no animal is infected; < 1 LD50/ 5 mg of inoculum if < 50% of the animals are infected; 1-10 LD50/ 5 mg of inoculum if the percentage of animals infected is >50% and <100%.

The decontamination efficiency of the HPT treatment was also poorly influenced by the substrate meat products, which are highly heterogeneous for texture, water content, and composition. PrPres removal of at least 4 logarithms was observed in all six distinct meat products (Table 7).

Table 7. PrPres reduction in spiked meat substrates treated at 600 MPa/130°C for 5 minutes

Sample	PrPres reduction (log LD_{50})
Cat food	4.0
Corned beef	4.0
Baby food	3.5
Beef pate	3.5
Hamburger	4.0
Hot dog	4.0

When brains from animals with natural and experimental TSEs were pressurized, we found that all samples were sensitive to the inactivation process, with some variability among different TSEs in the removal of PrPres (from 0.6 to 1.5 logs) (Table 8).

Table 8. PrPres reduction in brain pastes from different TSE strains treated at 600 MPa/132°C for 5 min

Sample	PrPres reduction (log LD_{50})
Cow BSE	0.6
Mouse BSE (6PB1)	1.0
Mouse vCJD	1.5
GSH 263K scrapie	1.5

Conclusions

The results of our study demonstrate that industrially feasible conditions of high pressure/temperature treatment significantly reduce the TSE infectious load of meat products. These treatments do not cause any loss in the organoleptic features of the products, but rather increase the tenderness and the palatability of the product (Meyer, Brown, Cardone, Pocchiari, unpublished data) with only a limited reduction of nutritional properties (5).

Commercially available high-pressure machines, capable of operating at 600-700 MPa, can process million tons annually at a cost of a few Euro cents per kilogram of final product. The commercial application of this procedure would further reduce the risk of animal to human transmission by meat products potentially contaminated with BSE or other emerging TSE agents. The identification of BSE in small ruminants where infectivity is not restricted to CNS tissues, the appearance of a novel prion strain of cattle (i.e., BASE) with unknown properties in terms of tissue distribution and pathogenicity for humans, and the presence of PrPres/infectivity in muscles of various species of TSE-infected hosts, suggest that food safety still needs attention (11-12).

Finally, HPT-treatment may also be easily adaptable to other potentially infectious biological products and by-products, such as ‘specified risk materials’, which are currently destroyed with great loss of resources for the community.

Acknowledgements

We are grateful to Maurizio Bonanno, and Nicola Bellizzi for clinical evaluation of animals in the bioassay. This work has been partially supported by the ISS-NIH collaborative program (0F14), the Ministero della Salute, Italy, PF 1% 2002/3ABF, the Neuroprion Network of Excellence, and the National Cattlemen's Beef Association, USA.

References

1. Available from www.cjd.ed.ac.l/vcjdworld.htm, last visited 18/09/2006
2. Eloit M, Adjou K, Coulpier M, Fontaine JJ, Hamel R, Lilin T, Messiaen S, Andreoletti O, Baron T, Bencsik A, Biacabe AG, Beringue V, Laude H, Le Dur A, Vilotte JL, Comoy E, Deslys JP, Grassi J, Simon S, Lantier F, Sarradin P. BSE agent signatures in a goat. *Vet Rec* 2005;156:523-4.
3. Casalone C, Zanusso C, Acutis P, Ferrari S, Capucci L, Tagliavini F, Monaco S, Caramelli M. Identification of a second bovine amyloidotic spongiform encephalopathy: molecular similarities with sporadic Creutzfeldt-Jakob disease. *Proc Natl Acad Sci USA* 2004;101:3065-70.
4. Taylor DM. Inactivation of transmissible degenerative encephalopathy agents: A review. *Vet J* 2000;159:10-7.
5. Masson P, Tonello C, Balny C. High-pressure biotechnology in medicine and pharmaceutical science. *J Biomed Biotechnol* 2001;1:85-8.
6. Brown P, Meyer R, Cardone F, Pocchiari M. Ultra-high pressure inactivation of prion infectivity in processed meat: a practical method to prevent human infection. *Proc Natl Acad Sci USA* 2003;100:6093-7.
7. Fernández García A, Heindl P, Voigt H, Buttner M, Wienhold D, Butz P, Starke J, Tauscher B, Pfaff E. Reduced proteinase K resistance and infectivity of prions after pressure treatment at 60°C. *J Gen Virol* 2004;85:261-4.
8. Fernández García A, Heindl P, Voigt H, Buttner M, Butz P, Tauber N, Tauscher B, Pfaff E. Dual Nature of the Infectious Prion Protein Revealed by High Pressure. *Biochemistry* 2005;280:9842-7.
9. Heindl P, Fernández García A, Buttner M, Voigt H, Butz P, Tauscher B, Pfaff E. Some physico-chemical parameters that influence proteinase K resistance and the infectivity of PrPSc after high pressure treatment. *Braz J Med Biol Res* 2005;38:1223-31.
10. Cardone F, Brown P, Meyer R, Pocchiari M. Inactivation of transmissible spongiform encephalopathy agents in food products by ultra high pressure-temperature treatment. *Biochim Biophys Acta* 2006;1764:558-562.
11. Andreoletti O, Simon S, Lacroux C, Morel N, Tabouret G, Chabert A, Lugan S, Corbiere F, Ferre P, Foucras G, Laude H, Eychenne F, Grassi J, Schelcher F. PrPSc accumulation in myocytes from sheep incubating natural scrapie. *Nat Med* 2004;10:591-3.
12. Thomzig A, Cardone F, Kruger D, Pocchiari M, Brown P, Beekes M. Pathological prion protein in muscles of hamsters and mice infected with rodent-adapted BSE or vCJD. *J Gen Virol* 2006;87:251-4.

Session 2B. Neurodegenerative disorders

IMMUNOPATHOGENESIS AND THERAPY OF MULTIPLE SCLEROSIS

Francesca Aloisi, Barbara Serafini, Sandra Columba-Cabezas
Department of Cell Biology and Neurosciences, Istituto Superiore di Sanità, Rome, Italy

Multiple sclerosis (MS) is the most common chronic inflammatory disease of the central nervous system (CNS) affecting young adults. Although the etiology of MS is still unknown, several clinical and experimental evidences indicate that migration of presumably autoreactive T and B lymphocytes in the CNS represents an important event in MS pathogenesis and in the development of demyelination and neurodegeneration. The fate and antigenic specificity of lymphocytes homing to the inflamed CNS remain however unknown. Recent work has disclosed the possibility that the chronic inflammatory process triggers or is driven by a cascade of local events that are responsible for the intracerebral survival, expansion and activation of pathogenic immune cells (Serafini *et al.*, 2004; Babbe *et al.*, 2000; Skulina *et al.*, 2004). This CNS compartmentalized immune response manifests with a persistent intrathecal production of immunoglobulins and with the enrichment in MS lesions and cerebrospinal fluid of MS patients of clonally related CD8+ cytotoxic T cells and B cells, whose expansion is presumably driven by a sustained antigenic stimulation in the target tissue. The identification of autoreactive T and B cell clones and of the mechanisms that promote lymphocyte growth and activation in the MS brain represents a common goal of the research activities that have been carried out in our laboratory and by Dr Paolo Muraro and Dr. Roland Martin in the Cellular Immunology Section, Neuroimmunology Branch, at the National Institute of Neurological Diseases and Stroke (NINDS), NIH. The latter group has used spectratyping of the T-cell receptor (TCR) 'complementarity-determining region 3' (CDR3) to analyze the clonotypes of T lymphocytes isolated from the cerebrospinal fluid of MS patients (Muraro *et al.*, 2006). This technique consists in the amplification by polymerase chain reaction (PCR) and electrophoretic resolution of the spectrum of different CDR3 lenghts of clonal TCR rearrangements and has been successfully utilized to identify the expanded clonotypes in the cerebral compartment. Recent work of the NIH group has demonstrated a lower clonal diversity of the T-cell repertoire during disease exacerbation (relapse) in a patient with relapsing remitting MS with a more restricted number of dominant peaks present in the majority of families of TCR beta chain variable gene fragments, as compared to the remission phase. The reduced complexity of the CDR3 repertoire during disease exacerbation is indicative of antigen specific clonal expansion and demonstrates that the composition of T-cell clones in the CSF can vary significantly in different phases of the disease. Further studies using combinatorial peptide libraries have allowed to establish that CD4+ T-cell clones, which appear expanded in the CSF during a clinical exacerbation, recognize a poly-arginine motif characteristic of the ubiquitary virus Torque Teno (TT) Virus and cross react with multiple peptide ligands of proteins derived from commensal and pathogenic microorganisms (Sospedra *et al.*, 2005). Furthermore, the same CSF-derived CD4+ T-cell clones whose frequency is expanded during active clinical disease recognize stimulatory ligands derived from microbial and human proteins in the context of several HLA-DR e DQ molecules (Sospedra *et al*., 2006). The identification of expanded T-cell clones in the CSF of MS patients has therefore allowed the characterization of immune cells infiltrating the injured CNS which show cross reactivity with self and non-self proteic fragments, whose antigenic

presentation may occur in a promiscuous manner in association with different HLA class II molecules.

Since it is conceivable that the clones which expand in the CNS during active clinical disease represent the effector T cells involved in the inflammatory process, it is important to verify whether the process of clonal expansion might be sustained at the local level in the context of lymphoid-like microenvironments. The studies described below represent a first attempt to analyze in detail the cellular interactions that may promote immune responses in the cerebral compartment during MS.

Our studies focussed initially on the characterization of antigen presenting cells (APC) which are essential for the initiation of immune responses, namely dendritic cells, and on their interactions with T and B lymphocytes within MS demyelinated lesions and in the inflamed meninges. To this purpose, a careful immunohistochemical analysis using appropriate cell markers was performed on autopsy cerebral tissue from MS cases with different disease courses (relapsing-remitting, primary progressive and secondary progressive). Fixed brain tissue blocks (frozen or embedded in paraffin) were provided by the UK MS Tissue Bank at Imperial College London (Director Prof. Richard Reynolds), with which our group has established a fruitful collaboration since three years. The study was approved by the ISS Ethical Committee. To visualize the different cell types and examine their localization and interactions, we used immunohistochemical and double immunofluoresecence techniques with a panel of antibodies that recognize dendritic cells of the myeloid lineage (DC-SIGN, CD1a, DC-LAMP, fascin, CD83, CD86), plasmacytoid dendritic cells (BDCA-2), follicular dendritic cells of mesenchymal origin (CD35, CXCL13), T lymphocytes (CD3), B lymphocytes (CD20), plasma cells (CD138), and markers of cell proliferation (Ki67) and apoptosis (activated caspase-3). The following results were obtained:

Dendritic cells (DC) of the myeloid lineage with an immature and mature phenotype were detected in the majority of active, chronic active and chronic inactive MS lesions and in the meninges of about 30% of the MS cases examined. DC accumulated mainly in perivascular position, in close contact with CNS-infiltrating leukocytes. Notably, DC-T cell interactions were also observed in scarcely inflamed blood vessels, where DC processes directly contacted the few extravasating lymphocytes. Within the perivascular cuffs, numerous DC-SIGN+ DC were found that express CD86, a costimulatory molecule with a key role in T- cell activation, and contain degradation products of myelin lipids as well as myelin basic protein (MBP). Most importantly, in the lesions of a subset of patients with secondary progressive MS we could show that DC establish direct contacts with small round cells expressing the nuclear antigen Ki67 and that most of the proliferating cells are CD8+ cytotoxic T cells. These data represent the first direct evidence that the interaction between DC loaded with myelin antigens and T cells may represent a key event in T-cell expansion and presumably activation within MS lesions. The data obtained also provide the first morphological evidence in MS that an adaptive cell-mediated immune response can be sustained (rather than inhibited, as suggested in several previous studies) behind the blood-brain barrier and define the perivascular space as the preferential niche for this process (Serafini *et al.*, 2006).

Follicular dendritic cells (FDC) of mesenchymal origin are essential in the processes of expansion, selection and maturation of B lymphocytes due to their ability to present antigens on their membrane in the form of immunocomplexes and to produce chemokines that regulate B-cell homing to follicles and cytokines that promote B-cell proliferation and survival. In a previous study (Serafini *et al.*, 2004) we identified cells expressing FDC markers (such as CD35 and the lymphoid chemokine CXCL13) in the inflamed meninges of a subset of cases with secondary progressive MS and demonstrated development of fully organized ectopic B-cell follicles containing not only B cells and FDC, but also plasma cells and T cells. The formation

of functional ectopic germinal centers was confirmed more recently by the demonstration of proliferating, intrafollicular B cells and of cells expressing activated caspase-3 and producing immunoglobulins, which indicates that clonal expansion, cell selection mediated by an apoptotic mechanism and B-cell differentiation into Ig-producing cells are all processes that take place within these abnormal structures (Serafini *et al.*, unpublished data). DC of the myeloid lineage were detected at the periphery but not inside meningeal ectopic follicles. Interestingly, we found that plasmacytoid dendritic cells also accumulate within and outside the meningeal follicles (Serafini *et al.*, unpublished data). Since plasmacytoid dendritic cells have a key role in the process of B-cell maturation through the secretion of type-I interferon and interleukin-6 it can be envisaged that accumulation of these cells in the MS meninges might play a role in follicle formation and/or maintenance. Because B cells could have a pathogenic role in autoimmune diseases not only due to autoantibody production, but also to their ability to act as APC for T-cell stimulation and to produce pro-inflammatory mediators, it is likely that the formation of ectopic follicles in a subset of patients with secondary progressive MS also represents an important mechanism for the maintenance of intracerebral T-cell responses.

All together, the above findings support our initial hypothesis that the inflammatory process associated with MS is sustained at the local level by the formation of lymphoid-like microenvironments, therefore allowing the continuous generation of activated T and B cells and the availability of immune molecules that can be harmful to CNS cells (Aloisi and Pujol-Borrell, 2006).

As a further step toward the identification of novel targets for MS immunotherapy, we performed a parallel study in an experimental model of MS, experimental autoimmune encephalomyelitis (EAE), in which we atttempted to counteract CNS inflammation and ectopic lymphoid tissue formation. Lymphotoxin (LT) $\alpha_1\beta_2$, a membrane heterotrimer belonging to the tumor necrosis factor (TNF) family, binds to the LTβ receptor (LTβR) and plays a key role in the development and maintenance of the lymphoid microenvironment (Fu *et al.*, 1995; Gonzales *et al.*, 1998; Ngo *et al.*, 1999). Because lymphotoxin (LT) $\alpha_1\beta_2$ is essential for lymphoid tissue organization, in preliminary experiments we used real-time PCR to demonstrate that LTβ and LTβ receptor (LTβR) gene expression is upregulated in the CNS of SJL mice immunized with PLP 139-151 peptide both at disease onset and during subsequent relapses. Next, we used the decoy receptor LTβR-immunoglobulin fusion protein (provided by Dr. Jeff Browning, Biogen Idec, Boston, MA) to block the interaction of lymphotoxin (LT) $\alpha_1\beta_2$ with the LTβ receptor (LTβR) in mice with established EAE and evaluate the effect of systemic and local treatments with the fusion protein on disease progression and formation of meningeal B-cell follicles (Columba-Cabezas *et al*., 2006). We found that systemic and local blockade of the LT pathway with LTβR-Ig results in protracted and transient inhibition of EAE clinical signs, respectively. LTβR-Ig treatment also reduced the number and size of meningeal B-cell aggregates, prevented the formation of organized ectopic follicles and inhibited CXCL13 gene expression in the EAE-affected CNS. These results indicate that targeting of molecules involved in lymphoid organogenesis could represent a valid strategy to inhibit the formation of ectopic follicles, which likely contribute to the maintenance of abnormal, intrathecal humoral immune responses in CNS autoimmune diseases.

In conclusion, we expect that the studies reported above might contribute to a better comprehension of the immunopathogenetic mechanisms involved in MS and to define new therapeutic strategies aimed at interfering with immune processes that become compartmentalized in the CNS during chronic inflammation.

Our work was supported by the ISS-NIH Collaboration Programme and in part by FP6 Integrated Project of the European Community NeuroproMiSe LSHM-CT-2005-018637 (to FA).

References

1. Aloisi F, Pujol-Borrell R. Lymphoid neogenesis in chronic inflammatory diseases. *Nature Rev Immunol* 2006;6:205-17.
2. Babbe H, Roers A, Waisman A, Lassmann H, Goebels N, Hohlfeld R, Friese M, Schroder R, Deckert M, Schmidt S, Ravid R, Rajewsky K. Clonal expansions of CD8(+) T cells dominate the T cell infiltrate in active multiple sclerosis lesions as shown by micromanipulation and single cell polymerase chain reaction. *J Exp Med* 2000;192:393-404.
3. Columba-Cabezas S, Griguoli M, Rosicarelli B, Magliozzi R, Ria F, Serafini B, Aloisi F. Suppression of established experimental autoimmune encephalomyelitis and formation of meningeal lymphoid follicles by lymphotoxin βreceptor-Ig fusion protein. *J Neuroimmunol* 2006;epub ahead of print.
4. Muraro PA, Cassiani Ingoni R, Chung K, Packer A, Sospedra M, Martin R. Clonotypic analysis of cerebrospinal fluid T cells during disease exacerbation and remission in a patient with multiple sclerosis. *J Neuroimmunol* 2006;171(1-2):177-83.
5. Serafini B, Rosicarelli B, Magliozzi R, Stigliano E, Capello E, Mancardi GL, Aloisi F. Dendritic cells in multiple sclerosis lesions: maturation stage, myelin uptake and interaction with proliferating T cells. *J Neuropathol Exp Neurol* 2006;65:1-18.
6. Serafini B, Rosicarelli B, Magliozzi R, Stigliano E, Aloisi F. Detection of ectopic B-cell follicles with germinal centers in the meninges of patients with secondary progressive multiple sclerosis. *Brain Pathol* 2004;14:164-74.
7. Skulina C, Schmidt S, Dornmair K, Babbe H, Roers A, Rajewsky K, Wekerle H, Hohlfeld R, Goebels N. Multiple sclerosis: brain-infiltrating CD8+ T cells persist as clonal expansions in the cerebrospinal fluid and blood. *Proc Natl Acad Sci U S A* 2004;101(8):2428-33.
8. Sospedra M, Muraro PA, Stefanová I, Zhao Y, Chung K, Li Y, Giulianotti M, Simon R, Mariuzza R, Pinilla C, Martin R. Redundancy in Antigen Presenting Function of the HLA-DR and -DQ Molecules in the Multiple Sclerosis-Associated HLA-DR15 Haplotype. *J Immunol* 2006;176:1951-61.
9. Sospedra M, Zhao Y, zur Hausen H, Muraro PA, Hamashin C, de Villiers E-M, Pinilla C, Martin R. Recognition of conserved amino acid motifs of common virus and its role in autoimmunity. *PLoS Pathogens* 2005;1(4):e41. Epub 2005 Dec 16.

Session 2B. Neurodegenerative disorders

GLIAL-MEDIATED MODULATION OF STRIATAL DOPAMINERGIC NEUROTRANSMISSION: ROLE OF ADENOSINE AND METABOTROPIC GLUTAMATE RECEPTORS

Patrizia Popoli (a), Sergi Ferré (b)
(a) Department of Therapeutic Research and Medicines Evaluation, Istituto Superiore di Sanità, Rome, Italy
(b) NIDA, Department of Health and Human Services, National Institutes of Health, Bethesda, MD, USA

Introduction

Although most of the symptoms occurring in diseases such as Parkinson's disease, Huntington chorea and schizophrenia have been classically ascribed to hypo- or hyper-activity of the dopaminergic system, in the last few years increasing importance has been attributed to the modulatory role of other neurotransmitter systems on the dopaminergic transmission. The glutamatergic and the adenosinergic systems, in particular, are now being regarded as interesting targets for treating "dopaminergic" diseases. Among the receptors activated by adenosine and glutamate, adenosine A_{2A} receptors and subtype 5 of the metabotropic glutamate receptors are the most abundantly expressed in the striatum, where they contribute to the regulation of motor activity, synaptic plasticity and excitotoxic processes. Stimulation of striatal A_{2A} receptors induces dopamine release, although the mechanisms responsible for such an effect remains to be determined. The lack of A_{2A} receptors in the dopaminergic terminals, but their presence in glutamatergic terminals and glia, suggests that A_{2A}-induced dopamine release could be secondary to the increase in glutamate levels, since endogenous glutamate release increase extracellular striatal dopamine. This hypothesis is supported by *in vivo* microdialysis experiments, which showed that intrastriatal perfusion of CGS21680 (an adenosine A_{2A} receptor agonist), stimulates glutamate outflow. Glial cells play an important role in the regulation of extracellular glutamate levels, since re-uptake by neurons and glial cells is the only mechanism by which the activity of released glutamate is terminated. Interestingly, both A_{2A} and mGlu5 receptors are expressed by glial cells and could thus be involved in the above mechanism. Moreover, activation of striatal mGlu5 receptors induced an increase in glutamate outflow very similar to that induced by A_{2A} receptor agonists. Finally, striatal A_{2A} and mGlu5 receptors have been found to functionally interact and to form heteromeric complexes in the striatum. Thus, striatal dopaminergic neurotransmission could be modulated by mean of an adenosine-glutamate interaction, and glial-related mechanisms could be involved.

Aim

The aim of this project was to verify the hypothesis that striatal dopaminergic neurotransmission could be modulated by means of interacting adenosine and glutamate

receptors (mostly of the A_{2A} and mGlu5 subtypes, respectively), and that glial cells could be involved in such an interaction.

Materials and method

Animals. Adult male Wistar or Sprague Dawley rats (280-320 g) were used. The animals were kept under standardised temperature, humidity and lighting conditions, with free access to water and food. Animal care and use followed the directives of the Council of the European Communities (86/609/EEC).

Microdialysis experiments. Under Equithesin (3 ml/kg) anesthesia, rats were placed in a Kopf stereotaxic apparatus and implanted with a concentric dialysis probe (mod CMA/12, 4 mm length, Carnegie Medicine, Sweden) into the striatum (stereotaxic coordinates in mm from bregma, sagittal suture and dura, respectively: A=+2.0, L=+2.5; V=-6.8). Twenty-four hours after surgery the probe was perfused at a rate of 2 μl/min with a Ringer's solution for at least 2 hours, and the dialysates were then collected every 5 min in a refrigerated fraction collector and then frozen until assay. The glutamate or dopamine content was measured by reverse-phase high performance liquid chromatography coupled to a fluorometric or electrochemical detector, respectively.

Slice electrophysiology. Rats were decapitated, the brain removed and corticostriatal slices (300 μm thick) including the neocortex and the neostriatum cut with a vibratome. Extracellular field potentials (FPs) were recorded in the mediodorsal striatum with a glass microelectrode and evoked at the frequency of 0.05 Hz by stimulation of the white matter between the cortex and the striatum with a bipolar twisted NiCr-insulated electrode (50 μm o.d.) the mean basal FP amplitude was calculated, and the effects of the drugs expressed as percentage variation with respect to basal values.

Six-hydroxydopamine lesion. Under Equithesin (3 ml/kg) anaesthesia, animals were placed in a Kopf stereotaxic apparatus. Unilateral injections of 6-hydroxydopamine (6-OH-DA, 8μg / 4μl of 0.2% ascorbic acid saline solution) were performed in the left nigrostriatal pathway (coordinates with respect to bregma: A= -2.4; L= + 1.2; V= -7.8 mm) by means of an Hamilton syringe (mod. 701). Starting 3 weeks after the lesion, the animals' ability to rotate in response to apomorphine (0.05 mg/kg subcutaneously) was tested. Contralateral rotations induced by apomorphine were measured 3-4 times at weekly intervals. Only animals showing at least 50 turns/ 5 min in the last test were included in the study. Thirty minutes prior to starting the experiments, the animals were placed in rotation bowls in a soundproof experimental room.

Summary of the main results

Objective 1: to verify whether A_{2A} and/or mGlu5 receptor antagonists are able to counteract the increase in striatal glutamate induced by blockade of glial glutamate uptake

Active uptake by neurons and glial cells is the main mechanism for maintaining extracellular glutamate at low, non toxic concentrations. Activation of adenosine A_{2A} receptors increases

extracellular glutamate levels, while A_{2A} receptor antagonists reduce stimulated glutamate outflow. We examined the ability of adenosine A_{2A} receptor antagonists to prevent the increase in glutamate levels induced by blockade of the glutamate uptake. In rats implanted with a microdialysis probe in the dorsal striatum, perfusion with 4 mM L-trans-pyrrolidine-2,4-dicarboxylic acid (PDC, a transportable competitive inhibitor of glutamate uptake), or 10 mM dihydrokainic acid (DHK, a non transportable competitive inhibitor that mainly blocks the glial glutamate transporter GLT-1), significantly increased extracellular glutamate levels. The effects of PDC and DHK were completely prevented by the adenosine A_{2A} receptor antagonists SCH 58261 (0.01 mg/kg i.p.) and/or ZM 241385 (5 nM *via* probe). Since an impairment in glutamate transporter function is thought to play a major role in neurodegenerative disorders, the regulation of glutamate uptake may be one of the mechanisms of the neuroprotective effects of A_{2A} receptor antagonists (1).

Objective 2: to study the influence of mGlu5 receptors on glial glutamate release

In the frame of a study on the potential neuroprotective effects of the metabotropic glutamate receptor 5 (mGlu5R) antagonist 2-Methyl-6-(phenylethynyl)-pyridine (MPEP), in microdialysis experiments we found that this compound significantly reduced (in the same way as the A_{2A} antagonists did) (2) the increase in glutamate levels induced by 5 mM quinolinic acid (QA) (3). The ability of MPEP to inhibit QA-induced glutamate outflow indicates that mGlu5 receptors do modulate glial uptake, since it is known that the effects of QA involve an impairment of glial glutamate transporter. These results are in line with a previous study from our group, showing that the mGlu5 receptor agonist CHPG increases extracellular glutamate levels in the striatum, and that such an effect is modulated by adenosine A_{2A} receptors.

Objective 3: to establish whether A_{2A} receptor agonists are able to stimulate dopamine release in the ventral striatum and whether the effects of A_{2A} receptor stimulation are influenced by drugs acting on mGlu5Rs

By using *in vivo* microdialysis techniques, we found that local perfusion of the selective A_{2A} receptor agonists CGS 21680 elicited significant increases in extracellular levels of dopamine and glutamate in the shell of the nucleus accumbens (NAc). Co-perfusion with the selective A_{2A} receptor antagonist MSX-3 counteracted dopamine and glutamate release induced by CGS 21680. These results indicate that modulation of dopamine release in the shell of the NAc by A_{2A} receptors is mostly secondary to their opposite modulatory role on glutamatergic neurotransmission (4). In another microdialysis study (5), we found that acute systemic administration of motor-activating doses of the A_{2A} receptor antagonist MSX-3 significantly decreased extracellular levels of dopamine and glutamate in the shell of the rat nucleus accumbens (NAc). Finally, in a recent paper it was established that striatal glutamatergic neurotransmission is under the presynaptic control of adenosine A_1-A_{2A} receptor heteromers (6).

Objective 4: to verify whether the functional interaction existing between A_{2A} and mGlu5 receptors is influenced by dopaminergic denervation

The mGlu5 receptors and the adenosine A_{2A} receptors are highly expressed in the striatum where they are colocalized on striopallidal neurons. In electrophysiological experiments (7) we found that adenosine A_{2A} receptors may exert both a permissive and a facilitatory role on mGlu5R-induced effects in the striatum. Moreover, in previous studies we had demonstrated the occurrence of functional interactions among mGlu5, adenosine A_{2A} and dopamine D_2 receptors in the regulation of striatal functioning, and hypothesized that such an interaction may play a main role in the pathogenesis of striatal disorders. In the frame of the present ISS-NIH project, we wanted to verify whether dopaminergic denervation could influence the above mentioned A_{2A}/mGlu5 interaction. The finding that, in the striatum of 6-hydroxydopamine-lesioned rats (an experimental rodent model of Parkinson's disease), the ability of A_{2A} receptor ligands to modulate mGlu5-dependent effects is preserved, confirms that the A_{2A}/mGlu5 interaction may represent an additional target for the development of therapeutic strategies towards Parkinson's disease (8).

References

1. Pintor A, Galluzzo M, Grieco R, Pèzzola A, Reggio R, Popoli P. Adenosine A_{2A} receptor antagonists prevent the increase in striatal glutamate levels induced by glutamate uptake inhibitors. *J Neurochem* 2004;89:152-6.
2. Tebano MT, Pintor A, Frank C, Domenici MR, Martire A, Pepponi R, Potenza RL, Grieco R, Popoli P. Adenosine A_{2A} receptor blockade differentially influences excitotoxic mechanisms at pre- and postsynaptic sites in the rat striatum. *J Neurosci Res* 2004;77:100-7.
3. Popoli P, Pintor A, Tebano MT, Frank C, Pepponi R, Nazzicone V, Grieco R, Pèzzola A, Reggio R, Minghetti L, De Berardinis MA, Martire A, Potenza RL, Domenici MR. Neuroprotective effects of the mGlu5R antagonist MPEP towards quinolinic acid-induced striatal toxicity: involvement of pre- and post-synaptic mechanisms and lack of direct NMDA blocking activity. *J Neurochem* 2004;89:1479-89.
4. Quarta D, Ferre S, Solinas M, You ZB, Hockemeyer J, Popoli P, Goldberg SR. Opposite modulatory roles for adenosine A_1 and A_{2A} receptors on glutamate and dopamine release in the shell of the nucleus accumbens. Effects of chronic caffeine exposure. *J Neurochem* 2004;88:1151-8.
5. Quarta D, Borycz J, Solinas M, Patkar K, Hockemeyer J, Ciruela F, Lluis C, Franco R, Woods AS, Goldberg SR, Ferré S. Adenosine receptor-mediated modulation of dopamine release in the nucleus accumbens depends on glutamate neurotransmission and N-methyl-D-aspartate receptor stimulation. *J Neurochem* 2004;91:873-80.
6. Ciruela F, Casado V, Rodriguez RJ, Lujan R, Burgueno J, Canals M, Borycz J, Rebola N, Goldberg SR, Mallol J, Cortes A, Canela EI, Lopez-Gimenez JF, Milligan G, Lluis C, Cunha RA, Ferré S, Franco R Presynaptic control of striatal glutamatergic neurotransmission by adenosine A_1-A_{2A} receptor heteromers. *J Neurosci* 2006;26:2080-7.
7. Domenici MR, Pepponi R, Martire A, Tebano MT, Potenza RL, Popoli P. Permissive role of adenosine A_{2A} receptors on metabotropic glutamate receptor 5 (mGluR5)-mediated effects in the striatum. *J Neurochem* 2004;90:1276-1279.
8. Domenici MR, Potenza RL, Martire A, Coccurello R, Pèzzola A, Reggio R, Tebano MT, Popoli P. Chronic treatment with the mGlu5R antagonist MPEP reduces the functional effects of the mGlu5R agonist CHPG in the striatum of 6-hydroxydopamine-lesioned rats: Possible relevance to the effects of mGlu5R blockade in Parkinson's disease. *J Neurosci Res* 2005;80:646-54.

Session 2. Poster

NEUROBEHAVIOURAL PHENOTYPING OF GENETICALLY-MODIFIED MOUSE MODELS OF MENTAL RETARDATION: FROM GENE ALTERATION TO COGNITIVE AND SOCIAL IMPAIRMENT

Laura Ricceri (a), Maria Luisa Scattoni (a,b), Jacqueline Crawley (b)
(a) Department of Cell Biology and Neurosciences, Istituto Superiore di Sanità, Rome, Italy
(b) Laboratory of Behavioural Neurosciences, National Institute of Mental Health, National Institutes of Health, Bethesda, MD, USA

The need of studying behaviour during ontogeny in mouse models of neuro-developmental disorders

Analysis of behaviour during the developmental period (within the first weeks of life) can be extremely informative when applied to genetically modified mice modeling human neurodevelopmental disorders. During early postnatal development in the mouse, several important processes that will shape brain structure and function are proceeding. Neurogenesis in the hippocampus, a structure associated with higher cognitive functions such as learning and memory, occurs during the early postnatal period. Additionally, neuronal differentiation, maturation and synaptogenesis continue in this critical window of early postnatal development. Aberrant brain development has long been considered a neural substrate for many forms of mental retardation. It stands to reason that a detailed analysis of specific sensory-motor and behavioural responses during ontogeny may help to detect the onset of pathogenetic events or identify a specific functional alteration before compensatory effects in adulthood mask it (1). Early behavioural testing also provides a behavioural phenotype on which potential therapeutic strategies could be tested, starting from the early phases of development, when recovery could be more likely.

Neurobehavioural characterization of genetically modified mice during ontogeny is, however, still sporadic. Most of the studies on animal models of neurodevelopmental disorders, including X-linked forms of mental retardation, Rett syndrome, or autistic spectrum disorders are focused on adulthood, without considering neonatal or adolescent behavioural phenotypes.

The lack of behavioural characterization during the developmental period is surprising because these animal models are supposed to mimic neurological and cognitive symptoms in humans that emerge already during infancy. Moreover, complete methods for studying mouse neurobehavioural development are now available (1). Behavioural competencies of rodent pups have been described extensively in the last decades; these studies have used several behavioural endpoints, appropriate for each maturational stage, and standardized the methodological procedures to assess the ontogeny of sensory-motor, cognitive and social repertoires (1). One of the main aims of our collaborative ISS-NIH project has been to perform detailed analyses of neonatal behavioural responses in selected mouse models of neurodevelopmental disorders, with special emphasis on the social *repertoire* (2).

Early alterations in the neonatal behavioural phenotype of a mouse model of Rett syndrome

Rett syndrome is a severe neurodevelopmental disorder and is the second genetic cause of mental retardation affecting 1 on 20.000 individuals. Classically, only girls are affected as the syndrome is usually lethal in male embryos. Affected girls generally appear healthy until between 6 and 18 months of age, when development appears to *plateau* and then motor and cognitive skills regress (3). Stereotypical hand movements, absent or very limited language, severe autistic-like features, as well as potentially life-threatening seizures, respiratory dysfunction and severe kyphoscoliosis ensue. Although symptoms are not usually identified until late infancy, it has been very recently reported that subtle deficits actually appear in younger infants. These features include mild hypotonia, poor suck, and weak cry as well as abnormal movements of face, hand, and body (4,5).

The discovery (6) that mutation in the gene encoding methyl-CpG-binding protein 2 (MECP2) – a transcriptional silencer through DNA methylation – causes up to 96% of Rett cases has eventually provided insights into the genetic basis of the disorder (7). The MECP2 gene encodes a protein that binds specifically to methylated CpG pairs of DNA sequences and, in association with the co-repressor Sin3a and histone deacetylases, condenses chromatin structure making DNA inaccessible to transcriptional machinery. While MECP2 mRNA is ubiquitous, the protein has been found at high levels in the brain where it is preferentially expressed in neuronal nuclei (8). Importantly, developmental Mecp2 expression in mouse and human correlates with brain maturation and with establishment of synapses. Indeed, considering the pattern of Mecp2 developmental expression, Johnston and colleagues have hypothesised that developing synapses are the primary target of the pathology (8).

The potential benefit of animal models that reproduce Rett symptoms is enormous, and has led to the generation of three different mouse models characterised by manipulations of MECP2 gene (9-11). Biochemical, pathological and behavioural features of these three mouse lines have been analysed and compared to the human condition. What is still missing - in all Rett animal models so far available - is a detailed behavioural phenotyping during development. Such developmental approach could provide early behavioural hallmarks (e.g. subtle abnormal motor responses) in line with the recent data on Rett patients (4,5) well before the onset of the behavioural manifestations identified so far only at adulthood in the mouse models of Rett.

In collaboration with Joanne Berger-Sweeney at the Department of Biology at Wellesley College, we examined somatic growth, somatosensory reflexes and ultrasonic calls from postnatal day (pnd) 3 through 18 in $Mecp2^{1lox}$ mutant mice, one of the mouse model of Rett Syndrome (11). Somatic development increases steadily and appears similar to wildtype controls in both Mecp2 null male and Mecp2 heterozygous female mice.

The data from the somatosensory reflex battery indicate a mutation-induced transient delay in the development in motor coordination of hind limbs and in cliff aversion responses. This *deficit* is consistent with the motor coordination *deficits* noted in Mecp2 males at adulthood, as well as with very early motor deficits detected in Rett patients (5,7).

Interestingly, both Mecp2 null males and heterozygous females exhibited dramatic increases in ultrasonic vocalizations (USVs) in response to social isolation; these differences were evident as early postnatal day (pnd) 5 (see Table 1). This is the earliest and most prominent sign detected in Mecp2 mutant mice: it might indicate either an altered response to social isolation or alteration of respiratory function (12). Further testing will be necessary to clarify whether hyperreactivity to neonatal isolation or respiratory *deficits* are responsible for the altered

behavioural response. Interestingly, USVs are increased in infancy after cholinergic blockade (13) and cholinergic *deficits* have been documented in Rett individuals (14).

In conclusion, the current study suggests that we can detect changes that result from altered Mecp2 expression in the neonatal period in mice. These data indicate USVs as an neonatal behavioural response to be used during experiments testing early therapeutic interventions.

Table 1. Altered neurobehavioural development in MECP2 mouse pups

Test	Male	Female
Somatic growth		
Body Length	---	---
Body Weight	---	---
Tail Length	---	---
Somato-motor reflexes		
Cliff Aversion	▼*	---
Forelimb Grasping	---	---
Forelimb Placing	---	---
Hindlimb Grasping	▼*	---
Hindlimb Placing	▼*	▼*
Level Screen Test	---	---
Vertical Screen Test	---	---
Slow Righting	---	---
Slow Righting Time	---	---
Geotaxis Response	---	---
Ultrasound vocalizations		
Number of calls (3 min)	▲** (pnd 5)	▲* (pnd 7)

p<0.05; ** p<0.01; ▼ significant delay in acquisition of an adult-like response; ▲ significant increase in number of calls; data from (15).

Early alterations in a putative mouse model of autistic *spectrum* disorders

Deficits in reciprocal social interactions and social communication are two of the three diagnostic symptoms of autism. Discovering or developing a genetic strain of mice that models these features could therefore be beneficial to autism research. Previous research has shown that adult BTBR T+ tf/J mice are less social that adult C57BL/6J mice (16). To address the social communication domain, the current experiments measured USVs of infant C57BL/6J and BTBR T+ tf/J mice. USVs by infant mice elicit pup retrieval and maternal behaviours (2,12,17), suggesting that these calls may play an important role as a means of social communication between mother and infant.

Diminished or abnormal ultrasonic vocalizations could model an important feature of autism (18), in that this behaviour may be indicative of altered responsiveness to neonatal social isolation or to maternal stimuli (2).

BTBR T+ tf/J mice emitted significantly more calls, and those calls were of significantly longer duration than the C57BL/6J mice (see Figure 1). While the predicted *deficit* in calling was not found, the converse result of higher calls may indicate that the BTBR T^{+}tf/J mice respond to separation from the home cage and dam differently from the C57BL/6J mice (20,21).

These results suggest that the BTBR T^+ tf/J mice may serve as a good model for social and emotional abnormalities observed in autism and that the role of maternal stimuli in modulating the vocalization responses should be further investigated.

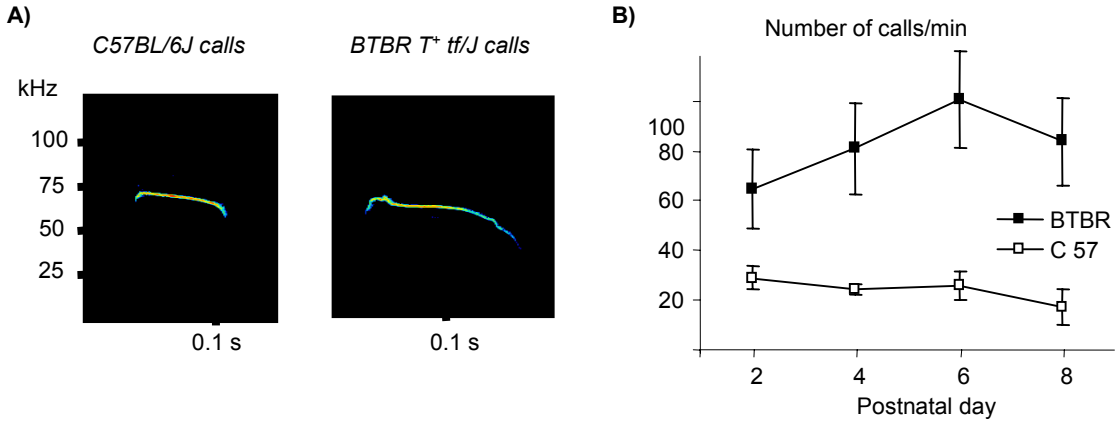

Figure 1. A) Representative ultrasonic calls of C57BL6/J and BTBR T+/tf/J mice (note the longer duration of the BTBR T+tf/J call). B) BTBR T+tf/J mice made significantly more calls per minute than C57BL/6J mice, at all ages tested, p< 0.0001. Data from (19)

The results so far obtained in MECP2 and BTBR T^+ tf/J mice indicate that early behavioural responses can be measured during mouse development, thus making researchers dealing with animal models of neurodevelopmental disorders aware of the possibilities to quantify abnormal behavioural patterns in young mice.

Some final considerations can be drawn. A first one is that in the case of neurodevelopmental disorders, behavioural phenotyping should start from the beginning, that is from the early phases of postnatal development. If social behaviour is of interest, the mother-pup interaction cannot be left aside. USVs emitted in neonatal isolation, the effect of "maternal potentiation", and homing responses are valuable tests for an early behavioural phenotyping battery (2).

A second point is that the early behavioural phenotyping not only may provide early markers for timed therapeutic intervention, but it will also allow in mouse experimental models of neurodevelopmental disorders to draw developmental trajectories (correlating alterations in early and later phases of behavioural development within the same experimental subjects).

Finally special attention should be devoted to USVs, both in developing and adult stages. Thanks to the recent advances in sound spectrographic analysis, quantitative/qualitative UV parameters could indeed become a milestone for mouse social behaviour phenotyping (2).

Acknowledgements

Supported by ISS-NIH 0F14 "Neurobehavioral phenotyping of genetically-modified mouse models of mental retardation: from gene alteration to cognitive impairment"

References

1. Branchi I, Ricceri L. Transgenic and knock-out mouse pups: the growing need for behavioral analysis. *Genes Brain Behav* 2002;1(3):135-41.
2. Ricceri L, Moles A, Crawley JN. Behavioural phenotyping of mouse models of neurodevelopmental disorders: relevant social behaviour patterns across the life span. *Behav Brain Res* 2006;in press.
3. Percy AK, Lane JB. Rett syndrome: model of neurodevelopmental disorders. *J Child Neurol* 2005;20(9):718-21.
4. Trevarthen C, Daniel S. Disorganized rhythm and synchrony: early signs of autism and Rett syndrome. *Brain Dev* 2005;27(Suppl 1):S25-S34.
5. Einspieler C, Kerr AM, Prechtl HF. Is the early development of girls with Rett disorder really normal? *Pediatr Res* 2005;57(5 Pt 1):696-700.
6. Amir RE, Van den Veyver IB, Wan M, Tran CQ, Francke U, Zoghbi HY. Rett syndrome is caused by mutations in X-linked MECP2, encoding methyl-CpG-binding protein 2. *Nat Genet* 1999;23(2):185-8.
7. Zoghbi HY. MeCP2 dysfunction in humans and mice. *J Child Neurol* 2005;20(9):736-40.
8. Johnston MV, Blue ME, Naidu S. Rett syndrome and neuronal development. *J Child Neurol* 2005;20(9):759-63.
9. Shahbazian M, Young J, Yuva-Paylor L, Spencer C, Antalffy B, Noebels J, *et al.* Mice with truncated MeCP2 recapitulate many Rett syndrome features and display hyperacetylation of histone H3. *Neuron* 2002;35(2):243-54.
10. Guy J, Hendrich B, Holmes M, Martin JE, Bird A. A mouse Mecp2-null mutation causes neurological symptoms that mimic Rett syndrome. *Nat Genet* 2001;27(3):322-6.
11. Chen RZ, Akbarian S, Tudor M, Jaenisch R. Deficiency of methyl-CpG binding protein-2 in CNS neurons results in a Rett-like phenotype in mice. *Nat Genet* 2001;27(3):327-31.
12. Hofer MA. Unexplained infant crying: an evolutionary perspective. *Acta Paediatrica* 2002;91:491-6.
13. Branchi I, Campolongo P, Alleva E. Scopolamine effects on ultrasonic vocalization emission and behavior in the neonatal mouse. *Behav Brain Res* 2004;151(1-2):9-16.
14. Wenk GL, Hauss-Wegrzyniak B. Altered cholinergic function in the basal forebrain of girls with Rett syndrome. *Neuropediatrics* 1999;30(3):125-9.
15. Picker JD, Yang R, Ricceri L, Berger-Sweeney J. An altered neonatal behavioral phenotype in Mecp2 mutant mice. *Neuroreport* 2006;17(5):541-4.
16. Moy SS, Nadler JJ, Young NB, Perez A, Holloway LP, Barbaro RP, *et al.* Mouse behavioral tasks relevant to autism: Phenotypes of 10 inbred strains. *Behav Brain Res* 2006; in press.
17. Branchi I, Santucci D, Alleva E. Ultrasonic vocalisation emitted by infant rodents: a tool for assessment of neurobehavioural development. *Behav Brain Res* 2001;125(1-2):49-56.
18. Crawley JN. Designing mouse behavioral tasks relevant to autistic-like behaviors. *Ment Retard Dev Disabil Res Rev* 2004;10(4):248-58.
19. McFarlane HG, Scattoni ML, Crawley JN. Juvenile social interactions and pup ultrasonic vocalizations in BTBR T+ tf/J versus C57BL/6 mice. In: *Society for Neuroscience*; Atlanta; 2006.
20. Dichter GS, Brunelli SA, Hofer MA. Elevated plus-maze behavior in adult offspring of selectively bred rats. *Physiol Behav* 1996;60(1):299-304.
21. Winslow JT, Hearn EF, Ferguson J, Young LJ, Matzuk MM, Insel TR. Infant vocalization, adult aggression, and fear behavior of an oxytocin null mutant mouse. *Horm Behav* 2000;37(2):145-55.

Session 2. Poster

ROLE OF ORFANIN FQ/OP4 RECEPTOR SYSTEM IN THE CONTROL OF OPIOID TOLERANCE

Amalia Di Giannuario (a), Stefano Pieretti (a), Toni Shippenberg (b)
(a) Department of Therapeutic Research and Medicines Evaluation, Istituto Superiore di Sanità, Rome, Italy
(b) Neuroscience Section, Behavioural Neuroscience Laboratory, National Institutes of Drug Abuse, National Institutes of Health, Bethesda, MD, USA

Introduction

Although morphine is widely used for treatment of moderate to severe pain in cancer and non cancer patients, the development of side effects such as hyperalgesia, convulsions, dependence and analgesic tolerance hampers its clinical use (1). Since the advent of opiates in the treatment of acute or chronic pain, the separation of the therapeutic from the undesired effects has been an elusive goal. In simple terms tolerance can be described as the need for increasing drug dosage to achieve the same effect. The identification of the anti-opioid activity of orphanin FQ/OP4 receptor (OFQ/OP4r) system seems to suggest new approaches in the control of opioid tolerance (2). Aim of this study was to explore whether the OP4r agonist orphanin or the antagonist [Nphe1,Arg14,Lys15] nociceptin-NH2 named UFP-101 (3): i) administered chronically for 5 days together with morphine affected the development of tolerance to the antinociceptive effect of the opioid; ii) or injected in a single dose on the day 5 of chronic administration of morphine restored the antinociceptive effect in mice rendered tolerant to the opioid.

Materials and methods

Animals

Male CD1 mice (27-32 g Charles River Italy), were housed in a climatically controlled room (temperature 21-22 ± 1°C; 12:12 h light/dark cycle) with food and water available *at libitum*. Animals used in this study were cared for and used in accordance with European Community and national regulations (CEE Council 86/609; DL.vo 116/92).

Drug administration

Drugs were dissolved in sterile 0.9 % NaCl solution (vehicle, Ve) and injected intraperitoneally (i.p.), or intracerebroventricularly (i.c.v., by a cannula 26 gauge surgically implanted under Equitesin anaesthesia 5 ml/kg/i.p., in the right lateral ventricle 2 mm lateral, 2 mm caudal to bregma at a depth of 3 mm) as previously described (4). To induce opioid tolerance morphine was administered once a day for five consecutive days (M, 7 mg/kg/5 days i.p., Salars Italy). Then, we studied the effects of orphanin and UFP-101 on the development and established opioid tolerance. To this end vehicle (3 µl i.c.v.), orphanin (1 nmol/3 µl; Tocris UK) and UFP-101 (2 nmol/3µl i.c.v. Tocris UK) were injected: i) once a day for five days, 5 min after the daily

injection of morphine (7 mg/kg/5 days i.p.) or vehicle (5 ml/kg/5 days i.p.); ii) on the day 5, 10 min after the last administration of morphine (7 mg/kg/5 days i.p.) or vehicle (5 ml/kg/5 days i.p.).

Nociceptive assay

For tolerance studies, nociceptive responses were measured in each mouse on alternate days 1, 3 and 5, immediately before and at the peak effect of the opioid (i.e., 30 min after morphine administration) by using the hot plate test. The hot plate test consisted of placing the animal onto a plate (48.5 ± 1°C) surrounded by a cylindrical Plexiglass jar, and recording the latency of the first avoidance response (paw licking, or jumping). A cut-off time of 60 sec was adopted in order to prevent tissue damage.

Statistical analysis

Data were latencies of response expressed as mean ± s.e. of responses in sec. Statistical comparisons between means were performed by two-way analyses of variance (ANOVA), followed by Newman-Keuls *post-hoc* test. $P<0.05$ was considered to be significant.

Results

Single or repeated i.c.v. administration of Vehicle (Ve, 3 µl/5 days i.c.v.) or UFP-101 (UFP, 2 nmol/5 days i.c.v.) did not modify the nociceptive responses, while a clear pronociceptive effect was observed on the day 1 in the hot plate test after a single injection of orphanin (OFQ, 1 nmol/5 days i.c.v.). Tolerance to this hyperalgesic effect occurred after chronic administration of orphanin. On the first day of treatment morphine induced a clear antinociceptive effect, which progressively decreased from day 3 up to day 5, reflecting the development of antinociceptive tolerance (Table 1). Orphanin but not UFP-101 administered on day 1 together with morphine reduced the analgesic effect of the opioid showing anti-analgesic activity. Tolerance to this anti-analgesic effect appeared on the day 3, when orphanin was able to prevent the development of tolerance to the antinociceptive effect of morphine. Also UFP-101 administered chronically together with the opioid prevented the development of tolerance to the antinociceptive effect of morphine (Table 1).

Table1. Effects of chronic administration of orphanin and UFP-101 on the development of tolerance to the antinociceptive effect of morphine (Hot plate test)

Drugs	Pre-drug	Day 1	Day 3	Day 5
Ve	19.7±0.8	21.0±1.0	20.0±0.8	18.0±0.9
OFQ	18.5±0.7	10.0±1.0*	19.0±0.6	21.0±1.0
UFP	19.0±0.9	21.0±1.2	18.5±0.7	21.0±0.7
M	17.6±5.0	55.0±3.0 *	43.0±3.2 *	32.0±3.5*
OFQ+M	18.0±1.0	40.0±2.9 *°	53.0±2.5 *°	52.0±3.0 *°
UFP+M	18.6±0.5	56.0±1.5 *	55.0±1.4 *°	54.0±2.0 *°

Morphine (M, 7 mg/kg/5 days i.p.) induced antinociceptive effects which progressively decreased from the day 1 up to day 5 (tolerance). Orphanin (OFQ, 1 nmol/5 days i.c.v.) reduced the antinociceptive effect of M on day 1. This anti-analgesic activity disappeared on day 3 when OFQ prevented the appearance of morphine tolerance. Also UFP-101(UFP, 2 nmol/5 days i.c.v.) prevented the development of tolerance to the antinociceptive effect of morphine. Data were mean ± s.e. of responses in sec. Statistical analysis was performed by using ANOVA and *post hoc* Newman-Keuls test. * P<.01 vs Ve and ° P<.01 vs M.

Results obtained in animals rendered tolerant to morphine showed that the single administration of orphanin on the day 5 did not modify opioid tolerance. On the contrary UFP-101 injected on the day 5 inhibited the expression of tolerance then restoring the antinociceptive effect in mice made tolerant to morphine (Table 2).

Table 2. Effects of QFQ and UFP-101 administered in a single dose on the day 5 of chronic morphine administration (M, 7 mg/kg/5 days i.p.) (Hot plate test)

Drugs	Pre-drug	Day 1	Day 3	Day 5
Ve	18.0±1.8	20.0±1.0	18.8±1.0	19.0±2.0
OFQ	20.0±0.5	19.0±1.0	19.5±1.3	16.0±0.7
UFP	18.6±0.7	20.5±1.2	19.0±0.9	18.2±0.7
M	18.5±0.7	56.0±1.5 *	42.0±2.8 *	31.0±2.7 *
M+OFQ	17.0±0.7	55.0±1.4 *	38.6±2.7 *	26.4±2.0
M+UFP	17.9±0.6	52.0±2.0 *	38.0±3.1 *	49.5±1.5 *°

UFP-101 (2 nmol i.c.v.) but not OFQ (1 nmol i.c.v.) inhibited the expression of tolerance restoring the antinociceptive effect of the opioid in morphine tolerant mice.
Data were mean ± s.e. of responses in sec. Statistical analysis was performed by using ANOVA and *post hoc* Newman-Keuls test. * P<.01 vs Ve and ° P<.01 vs M.

Discussion

Chronic morphine administration over five days enhanced spinal OP4r (5) and the synthesis of orphanin in intracerebroventricular perfusate, periaqueductal gray, and amygdala of morphine tolerant animals (6), suggesting that opiate tolerance resulted by an enhanced anti-opioid activity of the OP4r/OFQ system. We have now reported that orphanin induced pronociceptive effect that disappeared after chronic administration suggesting a desensitization of OP4r. According with previous studies, the peptide reduced the antinociceptive effect of morphine on the day 1 exhibiting anti-analgesic properties. Furthermore, the loss of tolerance of its anti-analgesic activity observed on the day 3 appeared to be responsible of the inhibitory effect of orphanin on opioid tolerance. Like orphanin, chronic administration of the antagonist UFP-101 prevented the development of morphine tolerance. Instead UFP-101 but not orphanin injected in a single dose restored the antinociceptive effect of the opioid in mice rendered tolerant to morphine. Thus, if opioid tolerance depends on the activation of orphanin/OP4r system, the desensitization of OP4r induced by orphanin as well as the inhibition exerted by UFP-101 of the anti-opioid activity might explain the fact that the agonist and the antagonist both prevented opioid tolerance.

Aknowledgements

We thank Stefano Fidanza, Adriano Urciuoli and Alessio Gugliotta for technical assistance. This work was supported by funds of collaborative projects between the National Institutes of Health of the United States of America and the Istituto Superiore di Sanità of Italy (0F16).

References

1. Jage J. Opioid tolerance and dependence - do they matter? *Eur J Pain* 2005;9:157-62.

2. Harrison LM, Kastin AJ, Zadina JE. Opiate tolerance and dependence: receptors; G-proteins and antiopiates. *Peptides* 1998;19(9):1603-30.
3. Calò G, Rizzi A, Rizzi D, Bigoni R, Guerrini R, Marzola G, Marti M, McDonald J, Morari M, Lambert DG, Salvadori S, Regoli D. [Nphe1, Arg 14, Lys 15]nociceptin-NH2, a novel and selective antagonist of the nociceptin/orphanin FQ receptor. *Br J Pharmacol* 2002;136:303-11.
4. Di Giannuario A, Rizzi A, Pieretti S, Guerrini G, Bertorelli R, Salvadori S, Regoli D, Calò G. Studies on the antinociceptive effect of [Nphe1]nociceptin(1-13)NH2 in mice. *Neurosci Lett* 2001;316:25-8.
5. Ueda H, Inoue M, Takeshima H, Iwasawa Y. Enhanced spinal nociceptin receptor expression develops morphine tolerance and dependence. *J Neurosci* 2000;20:7640-7.
6. Yuan L, Han Z, Chang JK, Han JS. Accelerated release and production of orphanin in brain of chronic morphine tolerant rats. *Brain Res* 1999;826:330-4.

Session 2. Poster

NEW PHARMACOLOGICAL TARGET IN CHRONIC PAIN AND INFLAMMATION: THE F-MLF RECEPTOR FAMILY

Stefano Pieretti (a), Amalia Di Giannuario (a), Mariantonella Colucci (a), Francesco Maione (a), Philip M Murphy (b)
(a) Department of Therapeutic Research and Medicines Evaluation, Istituto Superiore di Sanità, Rome, Italy
(b) Chief, Laboratory of Molecular Immunology, Head, Molecular Signaling Section, National Institute of Allergy and Infectious Diseases, National Institutes of Health, Bethesda, MD, USA

Introduction

The receptors for formylated peptides (FPRs) belong to the G protein-coupled receptors family, three members of which have been cloned so far in human tissues and cells. Recently eight genes have been identified in mice, at least three of which translated into protein, (1). fMLF is one of the first identified FPRs ligand which binds two FPRs, the high-affinity FPR and its low-affinity variant FPR-like1 (FPRL1) in human cells. In the last years several novel peptide agonists have been identified, including peptide domain derived from the envelope proteins of human immunodeficiency virus type 1 (HIV-1) and at least three amyloidogenic polypeptides, the human acute phase protein serum amyloid A, the 42 amino acid form of β amyloid peptide and a 21 amino acid fragment of human prion (1). Until recently, it has been thought that FPRs are specifically expressed in neutrophils and monocytes where they potently modulate chemotaxis. However, the presence of FPRs has been demonstrated in different nonhematopoietic cells, such as hepatocytes, dendritic cells, and microglial cells suggesting that FPR agonists may influence cellular mechanisms other than the inflammatory response (1). It has long been known that blood-borne leukocytes are implicated in the development of inflammatory pain and there is a growing body of evidence suggesting a functional link between blood borne neutrophils and the development of pain behaviour. The first evidence comes from data obtained with the Europhile chemo attractant leukotriene B_4 that was found to induce a thermal hyperalgesia not observed in the rat hind paw when animals were depleted of circulating neutrophils (2).

New inside into the involvement of FPRs in inflammatory and pain states can arise from mice lacking of FPRs. $FPR^{-/-}$ mice developed normally, but showed enhanced susceptibility to bacterial infection due to a increased bacterial load in spleen and liver, suggesting a defect in innate immunity. Indeed in these mice neutrophils were not able to respond to chemoattractant as the FPRs agonist formyl-methionyl-leucyl-phenylalanine (fMLF) (3).

These studies may give new impulse to the knowledge and treatment of chronic pain and inflammation-based diseases. From the above data the purpose of our study was to investigate using agonist and antagonist to FRPs and mice lacking of FRPs: the peripheral and central FRS role in the nociceptive threshold lowering associated with chronic inflammatory states and whether FRS are involved in the development of chronic inflammation states.

Materials and methods

Animals

CD-1 (Charles River, Italy), C57BL/6 (WT) and FPR -/- mice (Gao et al., 1999) weighing 25-30 g were used for all experiments. Animal care and use conformed to the Italian Law Decree of 27/01/92, No. 116.

Nociception assays

Formalin test. In the formalin test, 20 µl of a 1% solution of formalin in saline was injected subcutaneously (s.c.) into the dorsal surface of the right or left hind paw of the mouse, using a microsyringe with a 27-gauge needle. The total amount of time (s) that the animal spent licking or biting the paw after the formalin injection, at intervals of 5 min was recorded for a period of 40 min (4). *Hot plate test.* A metal plate 25 x 25 cm (Socrel Mod. DS-37, Ugo Basile, Italy) heated to a constant temperature of 48 ± 0.1°C on which a plastic cylinder 20 cm diameter, 18 cm high was used. The time of latency (s) was recorded from the moment the animal was inserted inside the cylinder up to when it first licked its paws or jerked them off the hot plate. The measurement was terminated if the following occurred: the latency exceeded the cut-off time of 60 s or if the mouse jumped off the hot plate. (4). *Tail flick test.* Tail flick latency was obtained using a tail flick unit (Socrel Mod DS-20, Ugo Basile, Italy), consisting of an infrared radiant light source (100 W bulb, 15 V). The light source was focused onto a photocell utilizing an aluminum parabolic mirror. The mice were gently hand-restrained with a glove during the trials. Radiant heat was focused 1–2 cm from the tip of the tail, and the latency time (s) the mouse took to flick its tail was recorded. The measurement was terminated if the latency exceeded the cut off time 15 s at 15 V (4).

Edema induction

Mice received a subcutaneous administration of 50 µl of zymosan 1% w/v in saline in the dorsal surface of the right or left hind paw. Paw volume was measured using a hydroplethismometer specially modified for small volumes (Ugo Basile, Italy), 1 h before the injection and at 1, 2, 3, 4 and 24 h thereafter. The increase in paw volume was evaluated as difference in percentage between the paw volume at each time-point and the basal paw volume (5).

Mouse air pouch model

Air pouches were developed by s.c. injection of 10 ml sterile air into the back of mice. Three days later 5 ml of sterile air was re-injected in the same cavity. After another three days (six days after the first air injection), 1 ml of zymosan 1% w/v or vehicle (saline) was injected into the air pouch. After 4h from zymosan injection, mice were sacrificed with CO2 and exudates in the pouch was collected with 1 ml of saline and placed in graduated tubes and centrifuged at 125 x g for 10 minutes. The pellet was suspended in 500 µl of saline and total leukocyte count was evaluated by optical microscopy in the cell suspension diluted with Turk's solution. The compounds tested or vehicle, were administrated intra-pouch 30 minutes before zymosan injection at three different doses (1, 3 and 10 µg/pouch) (6).

Drugs. FPR agonists and antagonists were chosen from a library and synthesized as previously reported (7-8). The FPR agonist formyl-MLF (fMLF) and the FPR antagonist N-t-butoxycarbonyl-MLF (Boc_1) and Boc-F-$_D$L-F-$_D$L-F-OH (Boc_2) were purchased from Bachem AG (Bubendorf, Switzerland). All the other materials were obtained from Sigma-Aldrich S.r.L. (Milan, Italy). In the first series of experiments, peptides or vehicle were administered s.c. into the dorsal surface of the right or left hind paw of the mouse in a volume of 20 µl, 30 min before formalin. In the second series of experiments, peptides or vehicle were administered into the left cerebral ventricles (i.c.v.) 30 min before formalin. For i.c.v. administration, compounds were injected directly into the lateral cerebral ventricle in mice as previously reported (9).

Data analysis and statistics

Data were analyzed using analysis of variance (ANOVA) or Student's t-test procedure for verifying the significance between two selected means. Statistical significance was always assumed for $P<0.05$.

Results and discussion

A general summary of our experiments is showed in Table 1. We found the FPR agonists, as the prototype fMLF able to reduce the nociception induced by formalin both after peripheral and central administration (Table 1). On the contrary, the FPR agonists did not change the response to thermal stimuli (hot plate and tail flick test). The administration of the classical FPR antagonist Boc_1 did not affect the nociceptive threshold of mice whereas Boc_2, administered at relatively high doses, reduced the nociceptive effects of formalin (Table 1). In the same way, the tested FPR antagonists showed an antinociceptive profile as Boc_2. Data from zymosan assay, demonstrated that the above peptides did not change oedema development (Table 1) whereas FPRs agonists positively or negatively modulate chemotaxis in the air pouch models depending upon the doses tested (Table 1). FPR antagonists reduced the number of cells in pouch exudates.

Table 1. Summary of the effects induced by FPRs agonists (Ag) or the FPRs antagonist (Ant) in the formalin test (FT), hot plate test (HP), tail flick test (TF), paw oedema (PE) and in the air pouch model (APM)

	FT[1]	HP[1]	TF[1]	PE[2]	APM[3]
$fMLF_p$	+	none	none	none	LW: + HD: -
$fMLF_c$	+	none	none	n.d.	n.d.
Ag_p	+	none	none	none	LW: + HD: -
Ag_c	+	none	none	n.d.	n.d.
$Boc_{1P\ or\ C}$	none	none	none	n.d.	n.d.
Boc_{2P}	LW: none HD: +	none	none	n.d.	-
Boc_{2c}	LW: none HD: +	none	none	n.d.	n.d.
Ant_P	+	none	none	none	-
Ant_C	+	none	none	n.d.	n.d.
[4]FPRs-/-mice	-	none	-	n.d.	n.d.

$_P$ and $_C$ indicate peripheral and central administration respectively. LW is for low doses and HD is for high doses
1: Plus, anti-nociceptive effects; minus, pro-nociceptive effects; **2**: Minus, reduction in paw oedema; plus, increase in paw oedema; **3**: Minus, reduction in cell number; plus, increase in cell number; **4**: Minus = reduction of the nociceptive threshold; plus = increase of the nociceptive threshold.

Thus chemotaxis data can explain why agonist and antagonist behave the same in nociceptive tests. FPR -/- mice appeared to have the same neurological and behavioural profile as wild type mice with the exception in the response to nociceptive stimuli. As reported in Table 1, nociceptive threshold in FPR -/- mice is lowered in formalin test and in the tail flick test. From the above data appear that peripheral FPRs have a role in inflammatory nociception. Besides an effect on neutrophil migration or on the neutrophil component of formalin-induced nociception, other hypotheses can be put forward for the antinociceptive effect displayed by FPR agonist and antagonist. Recent data showed local treatment with antisera to IL-1β or TNF-α significantly reduced the flinching behaviour during the late, but not early, phase of the formalin test (10). These results suggest that the two cytokines IL-1β and TNF-α are involved in the nociceptive behaviour induced by formalin. Thus, inhibition of cytokine release could also contribute to the anti-nociceptive property of FPR. For instance, the FPR agonist $Anxa1_{2\text{-}26}$ inhibits the hyperalgesic effects induced by TNF-α and PGE_2 administration as well as the release of these two mediators by a murine macrophage-like cell-line stimulated with LPS (11). Thus, the inhibitory effects that FPR agonist exerts on cytokine release can reduce the formalin-induced nociceptive behaviour observed in the late phase of the test. Another potential tissue target, as suggested from the results obtained after central administration, is the microglia. Recently, the presence of the FPR receptor in murine microglial cells was reported (12) and microglial activation has important effects on pain processing (13). Since microglial activation appears to occur only after inflammatory or persistent pain (14), the lack of efficacy of FPRs agonist or antagonist in acute nociception models (hot plate test and tail flick test) is not surprising. In conclusion, this investigation confirms the role of FRS in nociception. Indeed, the FPRs agonists were able to reduce the nociception evoked by long duration stimuli and mice lacking of FPRs are more sensible to nociceptive stimuli than wild type mice. However, depending on the dose used FPRs agonist can have pro- or anti-inflammatory effects. Pro-inflammatory effects did not occur after FPRs antagonist treatment, thus FPRs antagonist appeared more suitable than FPRs agonist for further development as anti-inflammatory drug.

Aknowledgements

We thank Stefano Fidanza and Adriano Urciuoli for technical assistance. This work was supported by funds of collaborative projects between the National Institutes of Health of the United States of America and the Istituto Superiore di Sanità of Italy.

References

1. Le Y, Murphy PM, Wang JM. Formyl-peptide receptors revisited. *Trends Immunol* 2002;23:541-8.
2. Levine JD, Gooding J, Donatoni P. The role of the polymorphonuclear leukocyte in hyperalgesia. *J Neurosci* 1985;3025-9.
3. Gao JL, Lee EJ, Murphy PM. Impaired antibacterial host defense in mice lacking the N-formylpeptide receptor. *J Exp Med* 1999;189:657-62.
4. Pieretti S, Di Giannuario A, De Felice M, Perretti M, Cirino G. Stimulus-dependent specificity for annexin 1 inhibition of the inflammatory nociceptive response: the involvement of the receptor for formylated peptides. *Pain* 2004;109(1-2):52-63.

5. Pieretti S, Dominici L, Di Giannuario A, Cesari N, Dal Piaz V. Local anti-inflammatory effect and behavioral studies on new PDE4 inhibitors. *Life Sci* 2006;79:791-800.
6. Bucci M, Roviezzo F, Cicala C, Sessa WC, Cirino G. Geldanamycin, an inhibitor of heat shock protein 90 (Hsp90) mediated signal transduction has anti-inflammatory effects and interacts with glucocorticoid receptor in vivo. *Br J Pharmacol* 2000;131(1):13-6.
7. Dalpiaz A, Ferretti ME, Pecoraro R, Fabbri E, Traniello S, Scatturin A, Spisani S. Phe-D-Leu-Phe-D-Leu-Phe derivatives as formylpeptide receptor antagonists in human neutrophils: cellular and conformational aspects. *Biochim Biophys Acta* 1999;1432:27-39.
8. Dalpiaz A, Ferretti ME, Vertuani G, Traniello, Scatturin A, Spisani S. C- and N-terminal residue effect on peptide derivatives' antagonism toward the formyl-peptide receptor *Eur J Pharmacol* 2002;436:187-96.
9. Porreca F, Mosberg HI, Hurst R, Hruby VJ, Burks TF. Roles of p, 6 or IC opioid receptors in spinal and supraspinal mediation of gastrointestinal transit effects and hot-plate analgesia in the mouse. *J Pharmacol Exp Ther* 1984;230:341-8.
10. Granados-Soto V, Alonso-Lopez R, Asomoza-Espinosa R, Rufino MO, Gomes-Lopes LD, Ferreira SH. Participation of COX, IL-1 beta and TNF alpha in formalin-induced inflammatory pain. *Proc West Pharmacol Soc* 2001;44:15-7.
11. Ferreira SH, Cunha FQ, Lorenzetti BB, Michelin MA, Perretti M, Flower RJ, Poole S. Role of lipocortin-1 in the anti-hyperalgesic actions of dexamethasone. *Br J Pharmacol* 1997;121:883-8.
12. Cui Y, Le Y, Yazawa H, Gong W, Wang JM. Potential role of the formyl peptide receptor-like 1 (FPRL1) in inflammatory aspects of Alzheimer's disease. *J Leukoc Biol* 2002;72:628-35.
13. Watkins LR, Milligan ED, Maier SF Glial activation: a driving force for pathological pain. *Trends Neurosci* 2001;24:450-5.
14. DeLeo JA, Yezierski RP. The role of neuroinflammation and neuroimmune activation in persistent pain. *Pain* 2001;90:1-6.

Session 2. Poster

WOMAN, HEALTH, ALCOHOL: RISKS AND DAMAGES FROM ALCOHOL IN DIFFERENT WOMAN AGES. THE ROLE OF ABUSE MARKERS

Rosanna Mancinelli
Department of Environment and Primary Prevention, Istituto Superiore di Sanità, Rome, Italy

This research is a multidisciplinary, experimental study, aimed to monitor and evaluate the adverse effect of alcohol on health related to the complexity of alcohol action and its ability to interfere with biochemical, hormonal, immunological patterns. Clinical and biochemical studies are performed by researchers of the ISS, of the Centro Riferimento Alcologico Regione Lazio (CRARL) - University "La Sapienza" and of the National Institute on Alcohol Abuse and Alcoholism (NIAAA-NIH). The collaboration between these scientific structures in the field of alcohol biomedical research started from the 90's.

The present study is gender-focused to give a significant contribution to the knowledge of female alcohol problems. Up to today, the increasing female drinking, the lowering of their first-use age and the risks of severe damage for children exposed to alcohol in utero, are becoming an emerging alert for the health of woman and child. The best strategy is the improvement of scientific information to treat alcohol problems and, above all, to early identify risky behaviour to avoid or minimize alcohol related problems. In Italy, the scientific approach to the health and social alcohol problems is quite new. The regulations about the control of subjects driving under influence of alcohol are from the end of the 80's, much later than other European countries. The scientific and technical tools for their elaboration and application were defined on the basis of the experimental studies performed by ISS researchers. Italian law for alcohol and alcohol-related problems is dated 30/03/2001.

The present collaborative project includes biochemical, genetic, immunological, toxicological and neurobehavioural studies performed by five Operative Units. Laboratory research and analytical activities are performed in ISS laboratories. Clinical and psychological handling of the patients, data collection and patients selection on the basis of the individual peculiarities and the targets of the study, are performed by the medical staff of the University "La Sapienza". All the researchers meet frequently to discuss the results and exchange information. Up to now, NIH researchers have been involved in meeting, seminars, collaboration to scientific papers, planning of new projects.

The activities of all the Operative Units are in progress. The results have been presented in international meeting and congress, and scientific papers are in press. Biochemical, immunological, genetic and toxicological studies by analytical determinations on blood samples from alcoholic patients are performing to evaluate possible susceptibility factors to alcohol and possible synergic effects of the exposure to alcohol and environmental toxics. A study of feasibility has been realized for the neurobehavioural research about the effects on offspring of prenatal alcohol-exposure. One of the most significant results of the project is the increasing synergy between the involved researchers and, consequently, the creation of the "Italian Group for Alcoholism Research" (IGAR). IGAR, that includes researchers from ISS and University "La Sapienza", aims to promote biomedical research on effects of alcohol misuse and to widely spread scientific information on alcohol-related problems. On the basis of obtained results, new

scientific contacts have been arising and international network about "Woman and alcohol" is improving.

Some gender problems related to alcohol misuse resulted as particularly need to be studied:

- the mechanisms underlying the role of alcohol in the development of breast cancer,
- the female vulnerability to alcohol effects at different age in relation to hormonal status (e.g. early osteoporosis),
- the modifications of nutritional factors as vitamins and oligoelements,
- the mechanisms underlying the prenatal damage, above all in relation to vulnerability factors, to understand why alcohol prenatal damage is not dose-related.

The progress of the project will be devoted to improve knowledge about them.

Project activities

NIH Collaboration

Seminar 05/07/2005 *"Advances in Fetal Alcohol Spectrum Disorders"*. Prof. Eugene Hoyme, MD, Chief Dept. of Genetics Pediatry, Stanford University (USA).

Conference 09/11/2005 "Defining The Cognitive Behavioural Phenotype In Children With Fetal Alcohol Spectrum Disorders (FASD)". Prof. P. Kodituwakku, Neuropsychologist, University of New Mexico (USA).

References

1. Mancinelli R, Binetti R, Attilia ML, Spagnolo P, Romeo M, Rotondo C, Ceccanti M. Fattori nutrizionali, abuso alcolico e differenze: la vitamina B1 e suoi esteri. In: Cometa MF, Di Consiglio E, Gemma S, Laura Parisi L, Volpe MT (Ed.). *XIV Congresso Nazionale della Società Italiana di Tossicologia. Istituto Superiore di Sanità. Roma, 6-9 febbraio 2006. Riassunti*. Roma: Istituto Superiore di Sanità; 2006. (ISTISAN Congressi 06/C1). p. 120.
2. Mancinelli R, Riganò R, Buttari B, Margutti P, Ortona E, Profumo E, Colasanti T, Delunardo F, Mazzoli C, Ceccanti M. Abuso alcolico e sistema immunitario. In: Cometa MF, Di Consiglio E, Gemma S, Laura Parisi L, Volpe MT (Ed.). *XIV Congresso Nazionale della Società Italiana di Tossicologia. Istituto Superiore di Sanità. Roma, 6-9 febbraio 2006. Riassunti*. Roma: Istituto Superiore di Sanità; 2006. (ISTISAN Congressi 06/C1). p. 121.
3. Ticchi C, Attilia ML, Prastaro A, Toppo L, Rotondi C, Mancinelli R, Bertazzoni G, Nocente R, Ceccanti M. Consumo di alcol e malattie cardiovascolari: fattori di suscettibilità. In: Cometa MF, Di Consiglio E, Gemma S, Laura Parisi L, Volpe MT (Ed.). *XIV Congresso Nazionale della Società Italiana di Tossicologia. Istituto Superiore di Sanità. Roma, 6-9 febbraio 2006. Riassunti*. Roma: Istituto Superiore di Sanità; 2006. (ISTISAN Congressi 06/C1). p. 282.
4. Ceccanti M, Mancinelli R, Sasso GF, Allen JP, Binetti R, Mellini A, Attilia F, Toppo L, Attilia ML. Erythrocyte thiamine (Th) esters: a major factor of the alcohol withdrawal syndrome or a candidate marker for alcoholism itself? *Alcohol and alcoholism* 2005;40(4):283-90.
5. Buttari B, Profumo E, Mancinelli R, Ceccanti M, Riganò R. Inhibition of antigen-presenting cell functions by ethanol [abstract]. *Minerva medica* 2005;96(3 Suppl 1):65.
6. Mancinelli R, Attilia ML, Spagnolo P, Romeo M, Rotondo C, Ceccanti M. Female alcoholism and biomarkers: gender differences in vitamin B1 (Thiamine) levels [abstract]. *Alcohol and alcoholism* 2005;40(Suppl 1):i45-i46.

7. Buttari B, Profumo E, Mancinelli R, Attilia ML, Ceccanti M, Riganò R. Ethanol and its metabolites impair the maturation and function of monocyte-derived dendritic cells obtained from alcoholics and healthy subjects [abstract]. *Alcohol and alcoholism* 2005;40(Suppl 1):i35.
8. Margutti P, Delunardo F, Mancinelli R, Colasanti T, Riganò R, Salvati B, Attilia ML, Ceccanti M, Ortona E. Screening of an endothelial cDNA library identifies several potential autoantigens in chronic alchoolists with atherosclerotic plaque [abstract]. *Alcohol and alcoholism* 2005;40(Suppl 1):i37.
9. Ticchi C, Attilia ML, Prastaro A, Toppo L, Rotondo C, Mancinelli R, Nocente R, Ceccanti M. Homocysteine in alcoholics [abstract]. *Alcohol and alcoholism* 2005;40(Suppl 1):i31.
10. Ticchi C, Attilia ML, Prastaro A, Toppo L, Rotondo C, Mancinelli R, Stabene M, Nocente R, Ceccanti M. Apo-E in chronic alcoholics: a risk factor for cardiovascular diseases [abstract]. *Alcohol and alcoholism* 2005;40(Suppl 1):i36-i37.
11. Mancinelli R, Ceccanti M. (Ed.). Special Issue "Teratogenic effects of alcohol: from the defence of woman health to the prevention of prenatal damage." *Annali ISS* 2006;42(1):1-66.
12. Mancinelli R, Ceccanti M, Binetti R. Female drinking, environment and biological markers. *Annali ISS* 2006;42(1):31-39.
13. Fiorentino D, Coriale G, Spagnolo PA, Prattaro A, Attilia ML, Mancinelli R, Ceccanti M. Fetal Alcohol Syndrome Disorders: experience on the field. The Lazio study preliminary report. *Annali ISS* 2006;42(1):53-58.
14. Calhoun F, Attilia ML, Spagnolo PA, Rotondo C, Mancinelli R, Ceccanti M. National Institute on Alcohol Abuse and Alcoholism and the study of Fetal Alcohol Spectrum Disorders: The International Consortium. *Annali ISS* 2006;42(1):4-8.
15. Mancinelli R, Ceccanti M, Laviola G (Ed.). Special Issue "Fetal Alcohol Spectrum Disorders (FASD): from Experimental Biology to the Search for Treatment". *Neurosci Biobehav Rev* 2006 (in press).
16. Mancinelli R, Ceccanti M, Binetti R. Woman, alcohol and environment. Emerging risks and biolological markers. *Neurosci Biobehav Rev* 2006 (in press).
17. Ceccanti M, Spagnolo PA, Attilia ML, Chessa L, Mancinelli R, Stegagno M, Sasso GF, Romeo M. Prenatal exposure to alcohol and its outcome in a rural area in Italy. *Neurosci Biobehav Rev* 2006 (in press).
18. Mancinelli R. Biological markers of alcohol misuse. In: *New Research on Alcohol Abuse and Alcoholism* New York: Ed. Novaeditorial; 2006 (in press).

Session 2. Poster

THE CONTROL OF THE INITIATION AND THE INHIBITION OF VOLUNTARY MOVEMENTS: EXPERIMENTAL ANALYSIS AND THEORETICAL MODELLING OF THE NEURAL CORRELATES AT THE POPULATION LEVEL

Giovanni Mirabella (b), Pierpaolo Pani (b), Maurizio Mattia (a), Robert H Wurtz (c), Stefano Ferraina (b), Paolo Del Giudice (a)
(a) Department of Technology and Health, Istituto Superiore di Sanità, Rome, Italy
(b) Dipartimento di Fisiologia Umana e Farmacologia, Università di Roma "La Sapienza"
(c) Visuomotor Integration Section, Laboratory of Sensorimotor Research National Eye Institute, National Institutes of Health, Bethesda, MD, USA

Context and purpose

The project aims at characterizing the neural correlate of motor decision processes in non-human primates, by identifying signals and decoding procedures suited for providing information on the areas involved at the neural population level, to shed light on the cooperative dynamics of the underlying distributed network.

A distinctive aspect of our approach is the parallel extraction of the single unit activity (SUA), with standard spike-sorting procedures, and the raw signal recorded by the electrode, which we analyze in the Fourier frequency domain. While the so-called MUA (Multi Unit Activity) and LFP (Local Field Potential) frequency bands are frequently investigated, we extend our analysis to much higher frequencies (kHz and beyond), and argue with theoretical grounding that relevant information on the neuronal collective dynamics can be extracted by comparing the spectral time-dependent properties in the different frequency bands.

The combined analysis of single-unit activity and local field potentials recorded from multiple areas presents technical and conceptual challanges, and is presently an active area of research. Theoretical predictions on model networks, which have been and are developed in the project, add another dimension to the data analysis, promising in the long run to provide heuristic tools for guessing the pattern of functional connectivity underlying the observed task-related behaviour. A first example will be mentioned below.

As a long-term perspective of the project, understanding the neural underpinning of motor decision processes is a prerequisite for a principled approach to the design of Brain-Computer Interfaces (BCI, devices and procedures that decode the neural activity related to planning and executing motor acts, e.g. for driving artificial limbs, and/or selectively stimulate selected brain areas, to restore impaired functions). Conceptual and signal-analysis tools we are developing, aimed at the description at the neural population level, promise to be helpful in this respect.

Research summary for the first year

The mechanisms subserving the inhibitory control of movement are in several respects representative of the motor decision processes. We adopted the "countermanding paradigm" introduced by Logan in the '80, in which the subject is asked to execute a (reaching or saccadic) movement when a GO signal is turned on, but to inhibit (abort) such movement if a STOP signal intervenes during the reaction time (Figure 1).

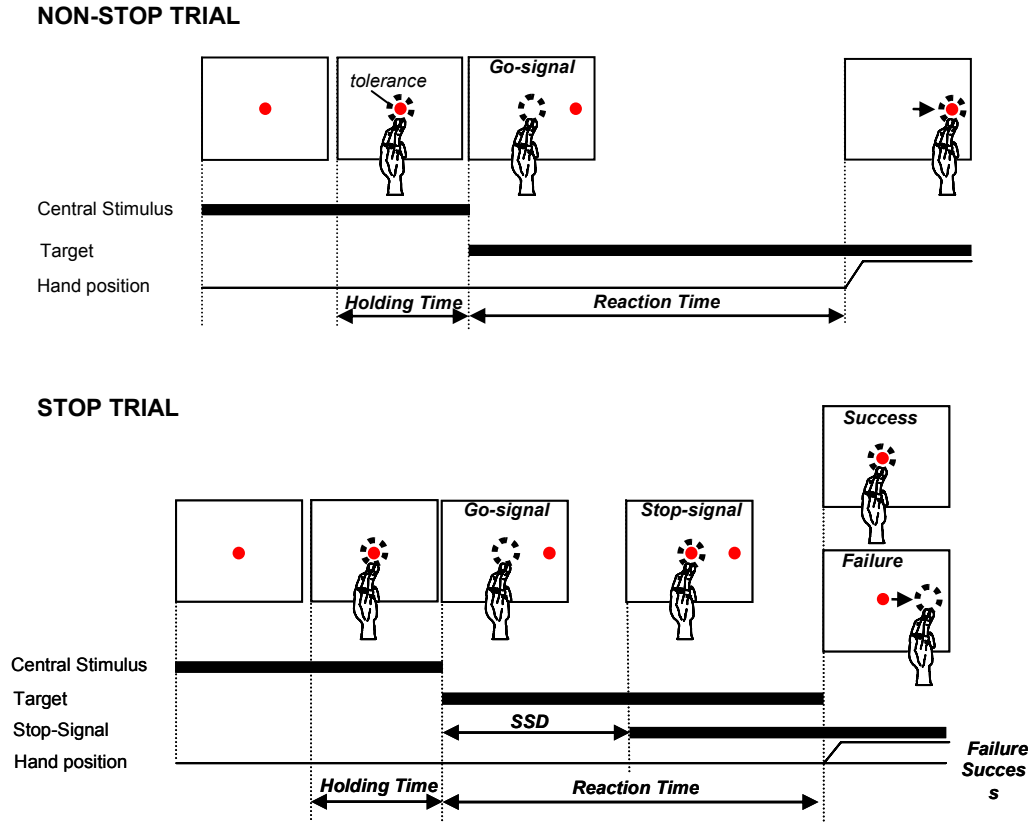

Figure 1. The Countermanding paradigm.
STOP trials and NON STOP trials are randomly intermixed. In NON STOP trials after a go signal the subject has to react as quickly as possible to reach a peripheral target. In STOP trials the subject is requested to withhold the movement whenever a stop signal follows the go signal with one of four possible delays (*stop signal delay*, *SSD*)

The countermanding protocol allows to estimate the 'Stop Signal Reaction Time' (SSRT), which is clearly not directly observable. While the case of saccadic movement inhibition has been thoroughly studied in recent years, little is known on the neural correlates of the motor inhibition for the reaching countermanding.

A monkey (*Macaca mulatta*) was trained to perform a reaching countermanding task. The monkey is sitting in front of a touch-screen, and instructed to reach visual targets, which appear in different positions on the screen. In 25% trials (STOP trials), randomly intermixed with 75%

NON-STOP trials, a stop signal was presented, with a variable delay (SSD, Stop Signal Delay) from the GO signal.

Variable SSD are introduced both for making the task less predictable for the monkey, and for spanning a significant range of monkey's performances, in order to measure the 'inhibition function', which is needed to infer the SSRT (short SSD are easy, long SSD are hard).

Neural activity was recorded from seven movable electrodes in a region covering the Dorsal Premotor areas in the frontal lobe, as well as more prefrontal areas. In parallel with the single unit activity, using standard filtering and sorting, the raw signal was also recorded with a 24 kHz sampling rate, and analysed off-line.

Figure 2 reports the main result derived from the analysis of SUA. For all the SSD the SUA for STOP and NON-STOP trials diverge before the end of the SSRT, which suggests that the recorded activity can be causally related to the reaching movement inhibition.

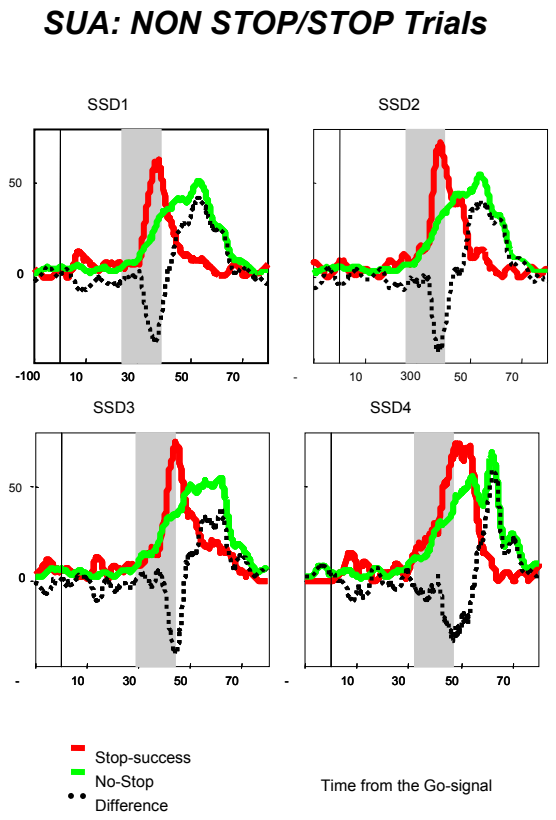

Figure 2. Results on the task-related single-unit activity.
Green solid lines are the PSTH (per-stimulus time histogram) for the NON_STOP trials;
red solid lines are the PSTH for the STOP trials, and the dotted black line is their difference.
All the PSTH are aligned to the GO signal. The four panels correspond to different SSD.
The grey shaded region represent the duration of the SSRT

The analysis of the unsorted raw signal is illustrated in Figure 3.

Panels A and B show two preliminary results meant to illustrate the potential of the approach.

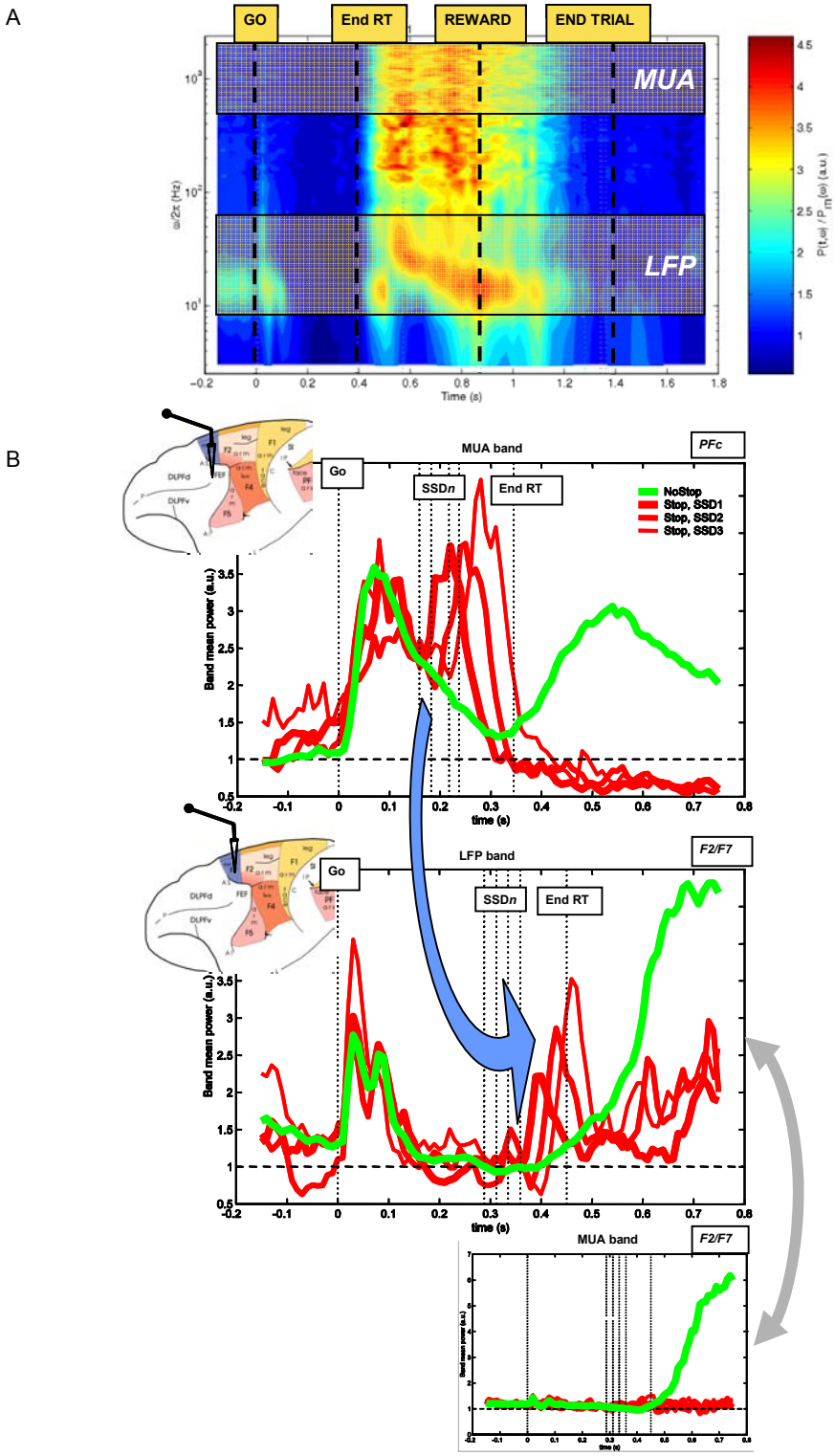

Figure 3. Task-related power modulation at the population level can suggest patterns of functional connectivity. A: Spectrogram of the raw electrode signal aligned to the GO signal relative to Inter-Trial Intervals. The MUA and LFP band are defined. B: Power spectral density, averaged in selected frequency bands, *vs* time, for STOP (red), NON-STOP (green) trials, for the two recording sites shown on the left. Red solid lines with different thickness correspond to different SSDs

The spectrogram in panel A shows a movement-related structure in NON-STOP trials: a marked power decrement just before the movement for all frequencies, followed by a power excess, for high frequencies (greater than 100 Hz), during the movement. A prominent power peak appears around 30 Hz and, as the movement proceeds, drifts towards lower frequencies, down to about 15 Hz when the reward signal occurs. As a working hypothesis, suggested also by our theoretical predictions on the relation between spectral power resonances and characteristic times of spike transmission, we propose that the movement-related power modulation is due to activity of neural populations in the vicinity of the electrode, while other time-dependent features at lower frequencies would be related to more distributed neural signals, as perhaps those due to reward expectation. This would account for the downward frequency shift in power for the no-stop trials.

Panel B shows an evocative relationship observed between the activity recorded from two different sites.

The most noteworthy feature is the hierarchy of power peaks related to the SSD values, expressed in the MUA band for the first site (prefrontal site, top plot), and the analogous sequence of power peaks occurring in the LFP band for the F2-F7 recording site, which appear as a shifted version of the former MUA peaks. No relevant MUA power structure is visible in the F2-F7 recordings, as illustrated by the small bottom plot.

According to the standard interpretation, the mean power in the MUA band is related to the local spiking activity, while the mean power in the LFP band is related to local or distributed synaptically transmitted reverberant activity. Therefore the combined analysis of LFP and MUA could provide information about the local or distributed nature of the synaptic communication between the neural populations involved.

The suggested scenario includes a STOP-related reverberant activity originating from PFc, which would be synaptically propagated to the (anatomically connected) area F2-F7, without significantly affecting the spiking activity of the latter, as witnessed by the absence of relevant MUA power modulation in F2-F7.

Short-term perspectives and outlook

A second monkey is now being trained and the experiments are scheduled for late fall 2006.

The US partner Dr. R.H. Wurtz came to visit the ISS-Roma1 group in the summer 2005; during the visit we could discuss and compare our preliminary results on the reaching countermanding, to the studies on the neural correlates of decision processes for eye movements, explored in a series of works by dr. Wurtz group.

In view of the potential for application to a BCI, less invasive recording devices have of course an appeal. We recently started recording from standard sub-dural grids of electrodes in epileptic patients performing motor or visual tasks; building on that experience, the context for cooperation with the NIH group got strengthened by the decision to add suitably engineered subdural grids to the standard depth electrodes for recording on monkeys, to check if the sole signal from the grid would provide the essential information which, when collected by the depth electrodes, is able to drive a BCI.

References

1. Mirabella G, Pani P, Mattia M, Del Giudice P, Ferraina S. *Countermanding neurons of dorsal premotor cortex in rhesus monkeys.* Vienna: FENS; 2006.

2. Mattia M, Mirabella G, Pani P, Ferraina S, Del Giudice P. *Neural Correlates of Motor Decision from Field Potentials.* Vienna: FENS; 2006.
3. Pani P, Mirabella G, Mattia M, Del Giudice P, Ferraina S. *Neural bases of context dependent reaction times in the dorsal premotor cortex of monkey* Edinburgh: CNS; 2006.
4. Mattia M, Mirabella G, Pani P, Ferraina S, Del Giudice P. *Neural correlates of motor decision from field potentials.* Atlanta: Society For Neuroscience meeting; 2006.
5. Mirabella G, Pani P, Del Giudice P, Mattia M, Ferraina S. *Neural basis of inhibitory control of reaching movements in the dorsal premotor cortex of rhesus monkeys.* Altanta: Society For Neuroscience meeting; 2006.
6. Martì D, Deco G, Del Giudice P, Mattia M. Reward-biased probabilistic decision-marking: Mean-field predictions and spiking simulations. *Neurocomputing* 2006;69:1175-8.
7. Szabo M, Deco G, Fusi S, Del Giudice P, Mattia M, Stetter M. Learning to attend: Modelling the shaping of selectivity in infero-temporal cortex in a categorization task *Biological Cybernetics* 2006;94:351.
8. Mirabella G, Pani P, Pare' M, Ferraina S. Inhibitory Control of reaching movements in humans. *Experimental Brain Research*, in press.
9. Brunamonti E, Ferraina S, Pare' M. Controlled movement processing: Evidence for a common inhibitory control of finger, wrist, and arm movements. *Journal of Neuroscience*, submitted.

Session 3
CARDIOVASCULAR

Session 3. Plenary lecture

COLLABORATION IN MEDICAL REHABILITATION: PAST ACCOMPLISHMENTS AND FUTURE OPPORTUNITIES

Steven J Stanhope (a), Michael Weinrich (b), Mary E Stuart (c), Richard Macko (d), Velio Macellari (e), Francesco Benvenuti (f), Simona Giampaoli (g), Gianfranco Spalletta (h), Aurelio Cappozzo (i)
(a) Physical Disabilities Branch, National Institutes of Health, Bethesda, MD, USA
(b) National Center for Medical Rehabilitation Research, National Institute of Child Health and Human Development, National Institutes of Health, Bethesda, MD, USA
(c) Department of Sociology and Anthropology, University of Maryland, Baltimore, USA
(d) Department of Neurology, University of Maryland, School of Medicine, Baltimore, USA
(e) Department of Technology and Health, Istituto Superiore di Sanità, Rome, Italy
(f) ASL11, Regione Toscana, Empoli-San Miniato, Italy
(g) National Centre for Epidemiology, Surveillance and Health Promotion, Istituto Superiore di Sanità, Rome, Italy
(h) Fondazione S. Lucia (IRCCS), Rome, Italy
(i) Istituto Universitario Scienze Motorie, Rome, Italy

Introduction

This contribution is strictly related to the ISS contribution to the ISS-NIH project "Obtaining Optimal Functional Recovery and Efficient Managed Care for the Chronic Stroke population". Briefly, the main objective of the project is to identify the best "managed care" strategies for stroke survivors. Such strategies should aim at maintaining patients' locomotor and main daily life functions, at preventing the onset of further disabilities and diseases, at improving the patients' quality of life. At the same time, they should optimise the use of economic resources. The best Italian answer to this question was identified as Adapted Physical Activity (APA), basically a community-based exercise program for clinically stable patients affected by chronic stroke, to be implemented at ASL 10 and 11 of Tuscany Region. The intervention consists of a 6 month program of exercise classes, offered 3 times per week at a community gym. In addition, patients are encouraged to exercise at home.

An important part of the project is the observation of the APA program implementation by some USA experts. From 9th to 18th of January 2006, two USA researchers - M. Stuart and M. Weinrich – conducted an independent audit in order to objectively assess APA procedures and protocols implemented in the project. A second independent audit started on March 17th 2006 and lasted for 15 days. This second audit was conducted by the USA researchers Michelle Pharr and Shawnisha Hester. A third audit took place in June 2006 conducted by R. Macko, C. Hafer-Macko, S. Roettgers and F. Ivey.

In the following part of this contribution, the first detailed report of the USA partners of the project is attached, which is referred to their first audit – January 2006.

APA CHRONIC STROKE TRIAL - ASL 11 - ITALY
FIRST REPORT - INDEPENDENT OBSERVERS
January 20, 2006
Team: Mary Stuart Sc.D. and Michael Weinrich, M.D.

Dates of observation: January 9, 2006 - January 18, 2006

Scope of observation: Observed sessions of APA program in three gyms (Empoli, Bassa, and S.M. Basso); patient assessments in ASL 11 and Florence; met with Drs Benvenuti, Taviani (Empoli), Segenni (Pisa), Federico Meyer (FL), physical therapists (Sarah and Theresa), Donato Papini, Enrico Roccato, Velio Macellari

Description of intervention and methods: This is a non-randomized clinical trial to assess the effectiveness of a community-based exercise program for patients with chronic stroke (defined as clinically stable and 9 or more months post stroke). Delayed entry comparison data will be obtained from nearby Pisa and Florence, where chronic stroke patients are being assessed in similar fashion but APA stroke programs are not yet operational.

The intervention consists of a 6 month program of exercise classes, offered 3 times per week at a community gym. In addition, patients are encouraged to exercise at home. The APA program at the community gym has 2 separate walking sessions per 1 hour long APA training session. Initially the walking sessions should be 6 minutes in length, but are gradually increased to 15 minutes each.

This should result in 30 total minutes of "aerobic walking training" - approximately the minimum formula that would be expected to improve metabolic fitness based on studies conducted at the Baltimore Center of Excellence. After an initial 8 week start-up phase for a group, patients will be encouraged to walk as fast as possible for the first and last 15 minutes of the hour. Thus all patients who complete the 6 month program will have had at least 4 months of aerobic walking training. During the remaining half hour of the APA stroke program, patients are engaged in a variety of exercises including stretching, balance training, and sit-to-stand. Participants must pay for the course themselves (the price is considered nominal - 24 Euros/month plus 10 Euros/year for insurance) and provide their own transportation.

A pilot APA stroke study found that 2 months of aerobic walking training produced significant improvement in impairment (Motricity Index), function (Berg Scale, SPPB, 6MTW), disability (Barthel Index), and QOL (SIS, GDS) measures. The pilot stroke APA had two courses in a hospital setting (e.g. a physiotherapy gymnasium with hospital safety measures). The participation rate was 100% for one course and 75% for the other. This trail differs from the pilot in scale and setting (45 people vs 20 people; 5 gymnasiums in the community vs 1 in the hospital), duration (6 months vs 2) and in that transportation is not provided by the Health Authority (it was provided in the pilot study). A major difference is that the pilot was essentially group physical therapy (taught by health professionals in a hospital setting, with health transportation), where the current program is a recreational program, in community gyms, taught by physical trainers, with transportation the responsibility of the individual rather than the health authority.

This study was designed to evaluate patients with chronic stroke. The main goal is to evaluate the size of the effect of the APA program on functional limitations (using as measures 6MTW and Berg scale). Secondary end points are to evaluate the size of the effect of the program on impairment (motricity index), disability (barthel) and QOL using the stroke impact scale. Another secondary goal is to identify demographic and social characteristics, health status and emotional status characteristics which influence participation in APA, The third is to determine the safety of APA programs at home and in the gyms (patients are contacted after every 3rd day that they do not participate). The fourth is to determine the size of the effect on the glucose tolerance test, measuring glucose and insulin.

This trail will test the hypotheses that a) similar results re cardiovascular effects, other clinical measures, and safety can be obtained in a large-scale community program as were obtained in the pilot; and b) that the majority of participants will continue to attend enough

sessions to obtain significant cardiovascular improvement despite the absence of transportation and the longer duration of the program.

Potential participants receive an initial comprehensive evaluation before being enrolled in the study and again at 6 months. A mini-evaluation is conducted at 3 months. A preparatory course is provided for those who will be enrolled in the APA stroke program. Transportation is provided by ASL 11 just for the evaluations and preparatory course.

Evaluations in ASL 11 are conducted at intake, 3 months and 6 months by a physician and two physical therapists. Staff conducting the evaluations are not blinded to participation in the APA program. To maximize standardization (inter-rater reliability) of the assessments, all of the physical therapists have been trained by the same physician and physical therapist using the same course, with the same procedure manual and protocols. In addition, inter-rater reliability will be assessed by having all evaluators conduct their evaluations on the same subset of patients and compare results. Additionally, members from the U.S. team will observe a sample of evaluations being conducted in ASL 11, Florence and Pisa. In addition, a sample of 10 evaluations using the Motricity and Berg Indexes will be filmed at baseline, 3 months and 6 months and sent for review by trained professionals in the U.S.

Findings

At this time, APA stroke courses are running in 3 gymnasiums (Bassa, Empoli and San Miniato Basso) and scheduled to begin in two others. Approximately 60 patients have been evaluated with 30 identified as meeting the protocols for APA stroke. It is anticipated that the remaining 15 participants will be identified and enrolled by the end of January. This will allow all participants to complete at least 6 months of APA and obtain the 6 month re-evaluation before the program shuts down for the August holidays. In the event that this is not possible, participants will have a "recovery period" in September prior to the last evaluation.

Additional patients will be added to the program as time and participants permit in order to increase the numbers of participants beyond the 45 minimum up to 60 (this is desirable to assure adequate power, allowing for drop-outs). ASL 11 has approximately 700 stroke survivors and anticipates that approximately 30% would be appropriate for the APA program. The controls are also expected to number 60 and will come from Florence and Pisa.

All current APA stroke programs have been operating less than 2 months in duration. Actual walking time ranged from 9 minutes total (4 + 5), 17 minutes total (7 + 10), 20 minutes total (15 + 5). Number of participants per session ranged from 1 to 11. Two courses were observed with one participant, both at the gym in San Miniato Basso. In this gym, a non-profit religious sponsored program, there are only 3 people enrolled in one class and 5 in the other. The instructor reported that transportation is a problem contributing to irregular attendance.

During the start-up period instructors have been allowed to use the last 10 minutes of the class as they think important. The result is that in one gym (Bassa) the last 10 minutes are given to stepping through hoops, around cones, and over poles of about 3-4" height or strings on the floor. This was the only exercise where people were observed to stumble - it was not uncommon for someone to trip over the raised poles or the hoops on the floor. Program staff believe these exercises may improve balance. However, they definitely slow the rate of speed since everyone lines up behind the slowest walker. In a large class this results in significant delays. Combined with late arrivals, helping participants take off and put on coats at the beginning and end of class, and a little socializing by participants, this significantly decreased the amount of brisk walking time. By contrast, the second gym had a well established protocol where faster patients walked around the outside and slower patients walked around the inside. Even with a large

group, this resulted in the appearance of patients effectively maximizing their walking speed without being delayed by other patients. In general, patients seemed to be walking with their usual assistive devices (a variety of canes were observed).

The ASL 11 APA team has expressed some concerns that the pilot program might have been boring because of the duration of walking exercise and might be more interesting and allow more socializing if there were less walking and more balance training. We note that the completion rate for the pilot APA stroke was very high, and that we did not observe more socializing during the balance training exercises when compared to walking.

Heart rate monitors have not yet been used in the gyms, however this phase is anticipated and a form has been made. Please note that base-line resting HR and HR after the 6 minute walk are obtained in the screening evaluation. HR following exercise, combined with patient age and resting heart-rate, will enable calculation of interim measures of aerobic effects.

At the time of our visit, Florence was evaluating their first patients. Pisa, with a continuing sincere interest, has had delays due to budget. They have now hired a physical therapist and expect to soon commence evaluations.

ASL 11 now has considerable experience with evaluations. The initial evaluation takes approximately 1 ½ - 1 ¾ hours to complete and includes: 1) the consent form; 2) obtaining demographic data, including distance from home to gym and architectural barriers in the home; 3) conducting a medical examination and recording type and characteristics of the stroke (including pyramidal and extra-pyramidal signs, cerebellar signs, and major clinical syndromes); 4) assessing co-morbidity as measured by the Cumulative Illness Rating Scale (CIRS); 5) cognitive state as measured by the Mini-Mental State Examiniation; 6) scale of communication disabilities; 7) six minute walking test and Borg scale; 8) falls in the previous 3 months; 9) upper and lower limb function as measured by the Motricity Index; 10) Berg Scale; 11) short physical performance battery; 12) disability as measured by the Barthel Index; 13) depression and quality of life as measured by the Hamilton Depression Scale; 14) caregiver burden (primary caregiver) as measured by the Caregiver Strain Index; 15) Stroke Impact Scale (SIS); and 16) laboratory exam for lipid profile and oral glucose tolerance test.

The six minute walk is a particularly important measure, since improvement is one of the primary outcome measures for the trial. Two issues are noted. The length of the walk way at ASL 11 is shorter than standard for the 6MTW - 7 meters compared to a recommended minimum of 30 meters. This is the only viable assessment location for ASL 11 and the length for the 6MTW in Florence and Pisa will also be 7 meters. Because of the additional turning time, the range of participants times can be expected to be slower than if patients were evaluated using the standard 30 meter length. Modest variation was also noted in the frequency and type of encouragement used by the 2 PTs in Empoli during the 6MTW, which has the potential to affect walking speed (more encouragement has been observed to increase walking speed).

A procedures manual has been developed that details protocols for the evaluation measures outlined above, as well as procedures for informing the general practitioner of the results of the evaluation, describing the program for APA exercises at the gymnasium and at home, and instructing participants to complete a diary of participation in the program. A form outlining in detail the home exercise program for the first 8 weeks is given to each person.

The SIS takes approximately 20 minutes to conduct. Program staff are concerned that this amount of time may not be warranted and would like to know if a short version of the SIS can be used in future studies. Filming the BERG and Motricity also take considerable time and it was agreed that this would be limited to 10 patients per site at baseline, 3 mo, and 6 mo (subject to approval by Dr.Macko).

The gymnasium keeps an attendance record on each participant, indicating days that the APA course is offered and days the individual attended. Attendance records are given monthly

to the research team. Inevitably, there are variations in the different gymnasiums. One is very bright and new but requires additional travel time. Another is older and darker, but conveniently located for many people.

Physical therapists who are members of the research team in ASL 11 observe classes at each gym once a week to ensure that the study protocols are being followed. There are two therapists and each goes regularly to the same gym.

Patients are referred to the APA stroke program by their general practitioners or other medical personnel in the health authority. In the future, staff hope to receive referrals of 100% of patients who are discharged from the hospital post stroke and need rehabilitation.

The status of non qualifying patients is worth noting. The major reason that a patient does not qualify is that he or she is too slow on the 6MTW. Parameters for participation for the 6MTW were set at $0.20 < APA < 0.60$. This relatively narrow range was selected to reduce variability in the analysis, rather than based on the predicted efficacy. There was also concern with safety of the program for patients with less than 0.20. Many of the patients who do not meet study parameters are eager to participate in APA stroke program. Consequently, some have been allowed to do this (although not enrolled in the study). There has been no evidence of safety problems in this practice. All patients will be reassessed on the same schedule with the same instruments regardless of whether they met study protocols except for the blood samples.

Conclusions and recommendations

ASL 11 is moving rapidly and staying on schedule with the implementation of the trial. This is important since all programs will close for the month of August. Evaluation of the comparison group from Florence and Pisa are slower but this is not a significant concern since they are not expected to change much in the absence of an intervention.

The research staff in ASL 11 appear well trained and enthusiastic – not a small accomplishment, since the research positions are temporary and the PT originally hired for the project was promoted when a permanent position opened up. The scope of the evaluation measures being implemented is daunting, but staff appear well trained, systematic and confident that they can do what is required of them.

The most serious concern is the variability in walking time and speed observed in the gyms. This is to be expected during the first two month start-up.

Main observations and suggestions are summarized here below:

- It is vital that the intervention be standardized, consistent with the pilot intervention protocol by the end of the first two months of each program.
- If instructors are to have flexibility, it should be with the balance training portion of the program, not the walking portion.
- It is recommended that the two physical therapists rotate among the gym classes to assure consistency of the intervention.
- In order to interpret the results, it will be important to record when the aerobic walking exercise reaches 30 minutes in a given gym class. Then, with the attendance data, it will be possible to calculate how many sessions each individual received with 30 minutes walking time.
- It was agreed that 10 filmed assessments at each phase of the evaluation for ASL 11, Florence and Pisa, would be adequate, assuming that when there are multiple assessors at one site, at least 5 films of each assessor should be made. This plan is to be reviewed by Dr. Macko.

– It was agreed that it would be helpful for the project to have assistance from the US universities (UMBC and UMB) in data analysis, including linking the clinical assessment data to administrative data regarding hospitalization, DME and pharmaceuticals. A time series analysis involving administrative data from Empoli, Florence and Pisa would be useful as part of the evaluation. The value of having one person do the analysis of administrative data from Florence, Pisa and Empoli was underscored by problems that have been identified with the pilot analysis of data from Empoli and Florence. It was agreed that it would be beneficial in moving this collaboration forward for Dr. Donato Papini to make a visit to the U.S. to meet with faculty at UMBC and UMB. Drs. Benvenuti, Stuart, and Papini should discuss tasks and timeframe in further detail and develop a plan. Consideration should be given to whether the US team (specifically UMBC and UMB students and faculty) can augment the Italian research team when HR monitoring is required at the gyms in June and July. UMBC students could be available to help with this task with sufficient advance planning.

Session 3. Plenary lecture

MOLECULAR IMAGING OF CARDIOVASCULAR DISEASES

Carina Mari Aparici (a), H.William Strauss(b)
(a) Nuclear Medicine, Center for Molecular and Functional Imaging China Basin SFVA Medical Center University of California San Francisco (UCSF), CA, USA.
(b) Nuclear Medicine Sloan Kettering Cancer Center, NY, USA

Introduction

More than 13 million persons suffer from coronary artery disease in the U.S, and of these 450,000 individuals will experience sudden death as their first manifestation of this atherosclerotic process. The need for practicing preventive cardiology and the importance of adequate screening of asymptomatic, subclinical atherosclerosis for the identification and treatment of the vulnerable patient has been very enphasized. Nevertheless, since <10% of the population who will test positive for atherosclerosis will experience a near-term event, additional risk stratification based on reliable markers of disease activity is needed to help further focus the search for the 'high risk' vulnerable patient in the future. The rupture of an active vulnerable atherosclerotic plaque is the last step before the development of a acute vascular event, thefore the specific identification of these culprit plaques at risk of rupture willl allow the specific identification of vulnerable patients at their highest risk.

Detection of active vulnerable plaques. Radiotracer approaches

The detection of atherosclerotic plaques has always been a goal for Nuclear Medicine. Many different tracers have been studied with this purpose. An ideal diagnostic technique for "high risk" patients would be that one that could specifically identify lesions at "high risk" of rupture. The development of molecular imaging techniques has allowed the identification and therefore targeting of specific molecular/cellular processes of the vulnerable plaque in living intact subjects. In animals with experimental atheroma with histological lesions class IV and V of the AHAC (American Heart Association Classification), which correspond to vulnerable plaques, striking localization of several probes has been seen. These lesions concentrate low density lipoprotein (1) FDG (2), diadenosine tetraphosphate (3), Z2D3 (an antibody which recognizes an epitope expressed on proliferating arterial smooth muscle cells) (4), depreotide, and the apoptosis marker annexin V (5) among others. A direct comparison of 8 tracers (using one as a control) was performed in rabbits fed a high fat /high cholesterol diet that had balloon injury to the aorta/iliac artery to determine their ability to localize in the arterial lesions. All the agents showed some localization in the lesions, although the best results were seen with annexin V and FDG.

To verify tracer localization in an animal model without physical injury to the vessel, another study was performed in apoE -/- transgenic mice deficient in LDL receptors, which are

genetically predisposed to marked hyperlipidemia that causes atheroma in the aorta. Studies with FDG and annexin demonstrated localization of both agents in the aortic lesions, which was slightly greater with annexin than FDG (6). The confirmation of FDG and annexin localization in both models suggests the localization of these tracers in human lesions. Both FDG and annexin provide high contrast between lesion and normal vessel, annexin has a higher contrast. In rabbits with experimental atheroma and in apoE deficient mice the striking localization of radiolabeled annexin V and FDG appeared to increase as plaques become more complex, suggesting that radiolabeled annexin V and FDG may be useful to both identify and characterize the vulnerability of a lesion.

Instrumentation

Identifying the radiotracers that localize in plaques addresses only part of the challenge of imaging atherosclerosis. In large superficial vessels, such as the carotid arteries, the feasibility of detecting lipid laden plaques using radiolabeled low density lipoprotein and external planar gamma camera imaging was first demonstrated in 1984 (7) and has been confirmed in several subsequent publications. In smaller vessels like the coronary arteries, the task is more daunting. The combination of small lumen size, constant motion, and small lesion size require higher resolution imaging. Complex cardiac motion is difficult to correct by gating, because the small changes in cardiac position due to respiration will blur the lesions. The detection problem is compounded by localization of even a small amount of the radiopharmaceutical in non-lesion tissue, since non-lesion tissue is several orders of magnitude more abundant than lesion tissue.

Many of these problems can be overcome by employing an intravascular detector. Lesion detection will require a system with high resolution and an ability to eliminate background activity in tissues outside the artery. Making the detector highly sensitive to beta radiation, with minimal sensitivity to gammas, eliminates the majority of the non-vascular background. This can be readily detected with an intravascular radionuclide detector (8). To make a device that may be useful for human use *in vivo* requires that the instrument be flexible, smaller than 3mm external diameter, and very sensitive. A recent study by Mari et al (9) analyzed the sensitivity of a flexible 1.5 mm beta-sensitive intravascular catheter with a built-in 0.5 mm scintillating thin-flexible fiber, in the detection of small active atherosclerotic plaques in apoE -/- mice placed on a high fat/high cholesterol diet using FDG-F^{18} for vulnerable plaque identification. Several other prototypes have already been developed some of them combining anatomical capabilities.

Summary

The combination of a radiopharmaceutical that identifies key molecular/cellular components characteristic of the active vulnerable plaque and a position sensitive catheter based radiation detector for the evaluation of small vessels is a promising team in the specific identification of high risk vulnerable patients.

References

1. Roberts AB, Lees AM, Lees RS, Strauss HW, Fallon JT, Taveras J, Kopiwoda S. Selective accumulation of low density lipoproteins in damaged arterial wall. *J Lipid Res* 1983;24:1160-7.

2. Vallabhajosula S, Fuster V. Atherosclerosis: imaging techniques and the evolving role of nuclear medicine. *J Nucl Med* 1997;38(11):1788-96.

3. Elmaleh DR, Narula J, Babich JW, Petrov A, Fischman AJ, Khaw BA, Rapaport E, Zamecnik PC. Rapid noninvasive detection of experimental atherosclerotic lesions with novel 99mTc-labeled diadenosine tetraphosphates. *Proc Natl Acad Sci U S A* 1998;95(2):691-5.

4. Carrio I, Pieri PL, Narula J, Prat L, Riva P, Pedrini L, Pretolani E, Caruso G, Sarti G, Estorch M, Berna L, Riambau V, Matias-Guiu X, Pak C, Ditlow C, Chen F, Khaw BA. Noninvasive localization of human atherosclerotic lesions with indium 111-labeled monoclonal Z2D3 antibody specific for proliferating smooth muscle cells. *J Nucl Cardiol* 1998;5(6):551-7.

5. Mari C, Nedelman M, Blankenberg F, Ghazarossian V, Strauss HW. Detection of active atheromas in a rabbit model: evaluation of 8 radiotracers. *JNM* 2001;42(5 suppl):45P.

6. Mari C, Blankenberg F, Narula Z, Narula J, Ghazarossian V, Tait J, Strauss HW. Tc-99m annexin V versus F-18-FDG in the identification of atherosclerotic plaques in apo e -/- mice. *J Nucl Med* 2002;43(suppl):1P.

7. Lees RS, Lees AM, Strauss HW. External imaging of human atherosclerosis. *J Nucl Med* 1983;24:154-6.

8. Strauss HW, Blankenberg FG. Small is beautiful: specialty imaging devices and the growth of nuclear cardiology. *J Nucl Cardiol* 2000;7(2):175-9.

9. Mari C, Yamaguchi Y, Ghazarossian V, Patt B, Blankenberg F, Strauss HW. Utility of a thin-flexible β-sensitive intravascular catheter to detect increased metabolic activity in atherosclerotic plaques. *Eur J Nucl Med Molec Imag* 2003.

Session 3. Plenary lecture

APPLICATION OF SPECT/CT IN MOLECULAR IMAGING OF ATHEROSCLEROTIC PLAQUES IN MICE

Benjamin MW Tsui (a), Yuchuan Wang (a), Greta SP Mok (a), Kathleen Gabrielson (a),
Alisa Walz-Flannigan (a), Martin G. Pomper (a), Franco Garibaldi (b), Stanislav Majewski (c)
(a) Division of Medical Imaging Physics, Department of Radiology Johns Hopkins University, Baltimore, MD, USA
(b) Department of Technology and Health, Istituto Superiore di Sanità, Rome, Italy
(c) Detector Group, Thomas Jefferson National Accelerator Facility, Newport News, VA, USA

Introduction

Cardiovascular diseases have been the leading cause of mortality in developed countries and have been increasing in an alarming rate in many developing countries in recent years largely due to change in diet. In many cardiovascular diseases, formation of atherosclerotic plaques is found in coronary arteries of the heart leading to myocardial perfusion abnormalities. Also, many neurological diseases are caused by formation of atherosclerotic plaques in the carotid arteries and other arteries in the neurological system. Most of the atherosclerotic plaques consist of a lipid core and a thick fibrous cap. They are 'stable' when left alone and do not normally cause mortality.

For reasons still under investigations, some atherosclerotic plaques go through a series of biochemical processes and become destabilized. During these processes, the fibrous cap reduces its thickness and eventually breaks off into the blood stream. The blockage of smaller arteries downstream is believed to be the cause of acute incidences such as sudden death and strokes. The understanding of the formation, development and destabilization of atherosclerotic plaques is highly significant in the understanding of cardiovascular and neurological diseases.

Various imaging techniques including x-ray angiography, intravascular ultrasound (IVUS), magnetic resonance imaging (MRI), and more recently, high resolution multi-detector computed tomography (MDCT) have been used to image the structure and composition of atherosclerotic plaques including the fibrous cap, lipid core and calcium deposit. With the development of new imaging agents and advances in high-resolution PET and SPECT instrumentation and imaging techniques, attempts have been made to image the biochemical and functional processes, including metabolism, angiogenesis and apoptosis, that are involved in the development, formation and destabilization of atherosclerotic plaques.

In this paper, we present a research study that investigates the application of high-resolution SPECT/CT instrumentation and techniques to image apoptosis that is involved in the development of atherosclerotic plaques in the ApoE-/- knockout mouse model. Technetium-99m labeled Annexin-V that targets apoptotic cells was used to image increased apoptosis that is hypothesized to be involved in the development and destabilization of atherosclerotic plaques. We report encouraging preliminary results using current SPECT/CT imaging technologies. Also, we present recent advances in high performance quantitative single and multi-pinhole SPECT imaging techniques and modular camera technologies that will improve the molecular SPECT/CT imaging techniques for biomedical imaging research.

Methods

Transgenic mouse model

The ApoE-/- knockout mouse model was created with a disrupted *Apoe* gene. It lacks *apoE*, a glycoprotein in the blood serum. Since apoE is involved in cholesterol transport to the liver and prevent the accumulation of cholesterol rich remnants in the plasma, an ApoE-/- mouse exhibits five times the normal amount of cholesterol in the serum plasma and spontaneous atherosclerotic lesions. We purchased ~5-week old ApoE-/- mice from the Jackson Laboratory for our experimental studies. The formation of atherosclerotic lesions was accelerated by feeding the animals with a high fat diet. Normal mice of the same age were also acquired and were fed with normal diet and were used as control.

SPECT/CT Instrumentation

A Gamma Medica-Idea X-SPECT system with a microSPECT and a microCT subunits was used in the preliminary imaging of the ApoE-/- mice. The microSPECT unit consists of two detector modules each consisted of a 6 mm thick and 12.5 cm x 12.5 cm pixellated NaI(Tl) crystal with 1.56 mm pitch and 200 micron gaps. Each detector module was fitted with a single pinhole collimator with a pinhole to detector distance of 9 cm and an aperture size of 1 mm. The single pinhole collimator-detector system provides a resolution of ~1.25 mm at 2.5 cm. The microCT unit consists of a low power 50 keV, 600 microAmp x-ray tube and a 12 cm x 12 cm CMOS detector with 50 micron pitch and a maximum acquired image matrix size of 2,048 x 2,048.

SPECT/CT image acquisition

Each pair of the age matched ApoE-/- and control mice was imaged in ~6-week intervals to track the development of the atherosclerotic plaques and to evaluate the SPECT/CT instrumentation and imaging techniques. The animals were injected through the tail vein with ~4-5 mCi of ^{99m}Tc labeled HYNIC Annexin-V obtained from the formerly Theseus Corporation. The SPECT projection data were acquired ~1 hour post-injection with a radius-of-rotation of ~3 cm. The single pinhole projection data were acquired into 128x128 matrices in 128 angular intervals over 360 degree at 20 sec/projection. In addition, a set of 3 point sources was used in a SPECT system calibration procedure to determine the geometric system misalignment parameters. The parameters were used in the 3D pinhole image reconstruction algorithm to achieve high-resolution and artifact-free SPECT images. For the best signal-to-noise ratio, the CT images were acquired in 512 x 512 projection matrices with 200 micron pixel size.

SPECT/CT image reconstruction and registration

In order to achieve high-resolution and artifact-free pinhole SPECT images, it is important to determine the SPECT system geometric misalignment parameters that include the center-of-rotation error, the tilt angles between the axis-of-rotation and the detector plane in the 3D space. The measured geometric parameters were then used in an 3D iterative OS-EM pinhole SPECT image reconstruction algorithm to achieve the best image quality. The 512 x 512 microCT projection data were reconstructed using an analytical cone-beam image reconstruction methods

into a 512x512x512 reconstructed image. It was then condensed and registered with the pinhole SPECT image.

Pinhole SPECT/CT imaging of the development of atherosclerotic plaques in ApoE-/- mice

To investigate the uptake of Annexin-V in the developmental stages of atherosclerotic plaques in the ApoE-/- mice, we imaged each pair of ApoE-/- and control mice at regular time intervals using the Gamma Medica-Idea X-SPECT SPECT/CT small animal system as described above. The pinhole SPECT, CT and registered SPECT/CT images were studied carefully to identify focal uptake of ^{99m}Tc labeled Annexin-V that may indicate location of possible atherosclerotic plaques.

Autoradiography and histology studies

To validate that the focal ^{99m}Tc labeled Annexin-V did indeed localized in the atherosclerotic plaques that likely occurred in the aorta, we sacrificed one of the ~35 week old ApoE-/- mouse that showed a high focal uptake and excised the aorta immediately after the imaging experiment. The excised aorta was slit, opened and placed on the phosphor detector of an autoradiography system. It was left overnight to obtain a high-resolution autoradiography image of the distribution of ^{99m}Tc labeled Annexin-V in the excised aorta. We then identified and sliced a thin section of the aorta that included regions with high and low focal ^{99m}Tc uptakes. The thin section was subjected to histological analysis.

New technologies for improved imaging of atherosclerotic plaques in mice

In order to study the development of atherosclerotic plaques in the ApoE-/- mice in more detail, that is, the detection of smaller lesions and ability to provide more accurate quantitation, we are engaged in the development of three pinhole SPECT imaging technologies as described below.

Quantitative 3D pinhole image reconstruction methods

To improve the quantitative accuracy of pinhole SPECT images, we have incorporated the physics of the imaging process, including photon attenuation and scatter within the object and the response function of pinhole collimator-detector, in the iterative OS-EM algorithm. The result is much improved image quality in terms of higher reconstructed image resolution and lower noise level in the reconstructed images and more accurate quantitation in terms of accuracy in the estimation of the amount of radioactivity *in vivo* from the reconstruction images.

New multi-pinhole imaging technology for improved detection efficiency

As the spatial resolution improves with the use of increasing smaller pinhole aperture size, there is a concurrent decrease in photon detection efficiency resulting in higher noise level in the single pinhole SPECT reconstructed images. The decrease in photon detection efficiency is proportional to the square of the decrease in spatial resolution. To increase the detection efficiency, we investigate the use of multi-pinhole data acquisition geometry and image reconstruction methods with the goal of lowering the image noise level while preserving

reconstructed images quality, i.e., without significant degradation in spatial resolution and increase in artifacts in the reconstructed images.

New detector technology for improved spatial resolution

The current detector technology is limited by relatively poor intrinsic resolution and the limited number of resolvable pixels. We are investigating new detector technology to improve the intrinsic resolution of pixellated scintillation detectors by increasing the number of resolvable pixels for improved overall pinhole SPECT resolution and the use of increased number of pinholes in multi-pinhole SPECT without significant loss of image resolution. Achievement of the goal will allow pinhole SPECT imaging of atherosclerotic plaques of smaller sizes than is possible using current detectors.

Results

SPECT/CT images of the development of atherosclerotic plaques in ApoE-/- mice

Figure 1 shows a series of SPECT/CT images from a longitudinal imaging study of a ApoE-/- mouse. The SPECT images show a high focal uptake of ^{99m}Tc Annexin V indicative of the development of an atherosclerotic plaque in the aorta region. Figure 2 show profiles of the focal Tc-99m uptake demonstrating an increased uptake of Annexin V from 20 to 27 weeks followed by a decrease to 37 week and undetectrable at 40 week. The results demonstrate the high-resolution imaging capability of the pinhole SPECT system and the feasibility of imaging atherosclerotic plaques of focal uptake of Tc-99m labeled Annexin V in the transgenic mouse.

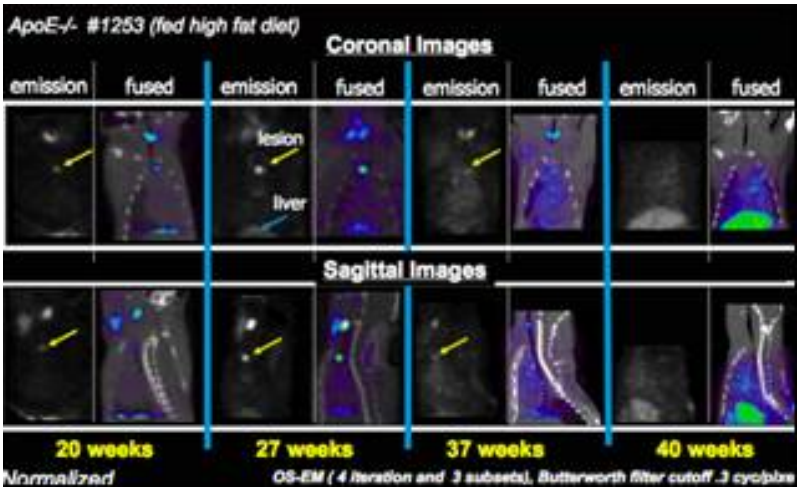

Figure 1. Pinhole SPECT and fused SPECT/CT coronal images of an ApoE-/- mouse injected with ~4 mCi of 99mTc labeled Annex V and imaged at 20, 27, 37 and 40 weeks. The images show a focal increased uptake of 99mTc at the same location above the heart and possibly in the aorta region. The focal uptake appears to increase over time and disappear at 40 week

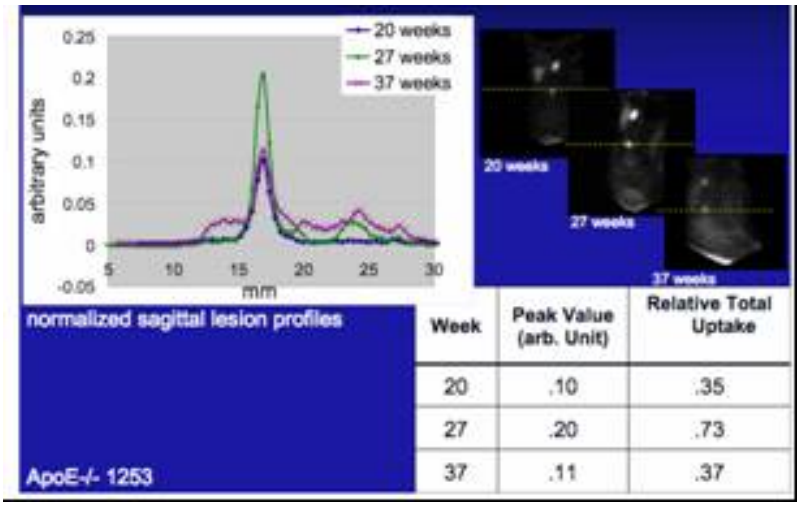

Week	Peak Value (arb. Unit)	Relative Total Uptake
20	.10	.35
27	.20	.73
37	.11	.37

Figure 2. Horizontal profiles across the same focal uptake in the aorta region in the coronal SPECT images obtained at 20, 27 and 37 week as shown in Figure 1. The profiles are normalized to the same unit injected dose of 99mTc. They indicate an increase of 99mTc from 20 to 27 weeks followed by a decrease to 37 week and undetectable at 40 week

To validate the Tc-99m labeled Annexin V uptake in atherosclerotic plaques, we sacrificed a ~37 week old ApoE-/- mouse right after the SPECT/CT imaging. The entire aorta and a section of the main artery were extracted and the aorta was cut open before placing flat on the simulated phosphor of an autoradiograph system. As shown in Figure 3, an autoradiography image show focal ^{99m}Tc laleled Annexin V uptakes in areas that correspond to atherosclerotic plaques in the aorta region and along the large artery. To further validate the uptake of Annexin V in atherosclerotic plaques, we cut a thin section through the aorta region for histology. Figure 4 shows the histological image through the section indicating low Annexin V uptake corresponds to normal arterial wall and high Annexin V uptake corresponds to arterial wall characteristics that are consistent with atherosclerotic plaques.

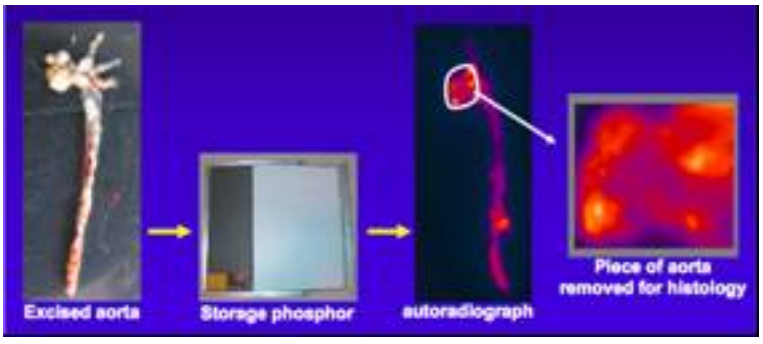

Figure 3. From left to right, photo of a excised aorta from a ~37 week old ApoE-/- mouse that shows multiple atherosclerotic plaques, the storage phosphor of the autoradiography system, an autoradiography image of the excised aorta, and an enlarged portion of the aorta removed for histology

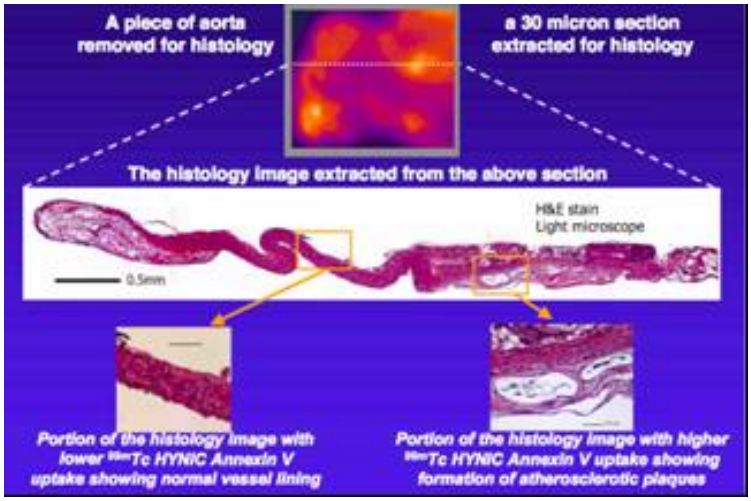

Figure 4. Histology of a thin section of the aorta shown in Figure 3, showing the areas with lower and higher 99mTc uptake corresponding to normal and abnormal membrane indication of atherosclerotic plaque formation.

New technologies for improved imaging of atherosclerotic plaques in mice

We have developed quantitative 3D pinhole image reconstruction methods to improve the quality and quantitative accuracy of 3D single pinhole images that can be achieved with the standard pinhole image reconstruction method. The method is based on the 3D OS-EM image reconstruction algorithm and models of the 3D pinhole imaging process as shown in the upper left diagram in Figure 5.

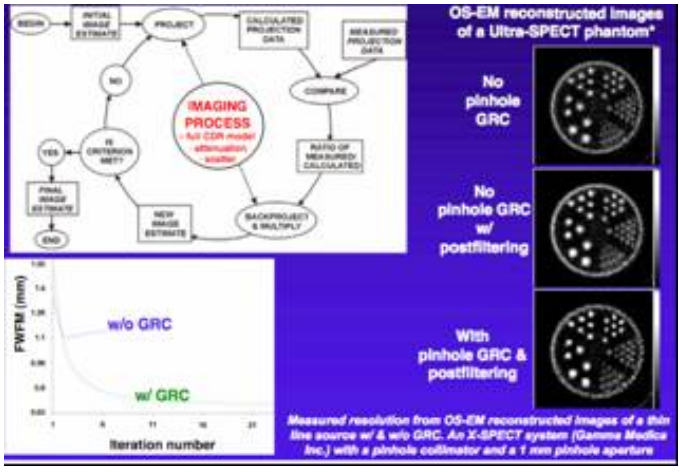

Figure 5. The quantitative 3D pinhole image reconstruction methods consists of (Upper Left) the 3D OS-EM image reconstruction algorithm and model of the image process. (Right Column) 3D OS-EM reconstructed images of a Data Spectrum Ultra-high resolution SPECT phantom with no geometric response correction (GRC), with GRC and with GRC & postfiltering. (Lower Left) The FWHM through the profiles of the reconstructed images of a point source with and without GRC

Figure 6 shows the geometric response function (GRF) of a general pinhole aperture with a keel edge can be considered as the overlap of the projections of the front and back aperture functions. The reconstructed images shown in the right column of Figure 5 show the reconstructed images of a Data Spectrum Ultra-high resolution SPECT phantom using the quantitative 3D image reconstructed method, where the geometric response function of the pinhole collimator is modeled in the projector and backprojector of the 3D OS-EM image reconstruction algorithm. The reconstruction images of the phantom with geometric response correction (GRC) show improved image resolution as well as lower image noise.

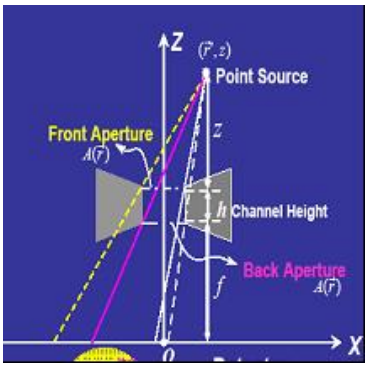

Figure 6. Geometric response function of a general pinhole aperture with a keel edge can be considered as the overlap of the projections of the front and back aperture functions

To improve the detection efficiency of pinhole SPECT, we have developed multi-pinhole SPECT imaging techniques. Figure 7 shows the comparison between reconstructed images of a Defrise phantom and a Data Spectrum Ultra-high resolution SPECT phantom obtained using a single pinhole collimator and a 4-pinhole collimator.

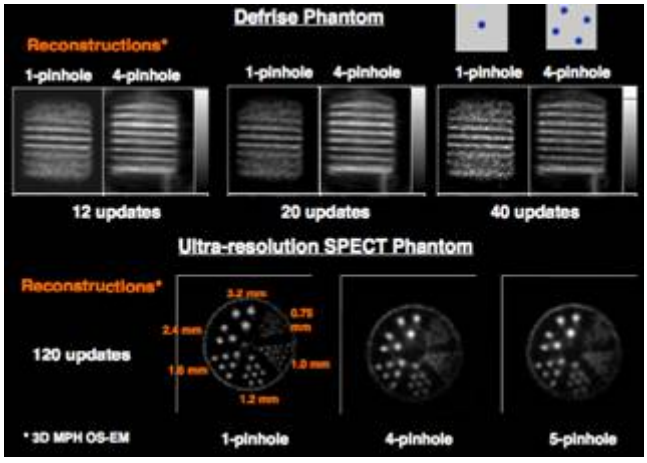

Figure 7. Comparison of 3D reconstructed images of a Defrise phantom and a Data Spectrum Ultra-high resolution SPECT phantom obtained using a single and a 4-pinhole collimator with the pinhole patterns shown in the upper right. The 4-pinhole images show decreased image noise level resulting from increased detected counts, reduced image artifacts in regions further away from the central plane and with minimum resolution degradation as compared to corresponding single pinhole images

The reconstructed images from the 4-pinhole collimator show decreased image noise level resulting from increased detected counts, reduced image artifacts in regions further away from the central plane and with minimum resolution degradation as compared to corresponding single pinhole images. Figure 8 shows results from imaging of a normal mouse injected with ^{99m}Tc MDP for bone imaging obtained using single, 4-pinhole and 5-pinhole collimators. Similar conclusions can be drawn from the small animal images as from the phantom images.

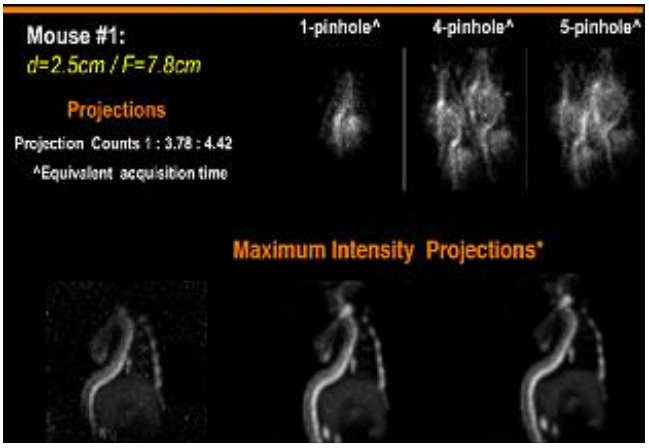

Figure 8. Comparison of the projection and 3D reconstructed images of a normal mouse injected with 99mTc MDP for bone imaging obtained using single, 4-pinhole and 5-pinhole collimators. The multi-pinhole images show decreased image noise level resulting from increased detected counts, reduced image artifacts in regions further away from the central plane and with minimum resolution degradation as compared to corresponding single pinhole images

Further improvement in image resolution of pinhole SPECT can be achieved through advances in the imaging detector. Our research groups at Johns Hopkins University (JHU), Baltimore, Maryland, USA, Thomas Jefferson National Accelerator Facility (TJNAF), Newport News, VA, USA and Italian Institute of Health are collaborating in this effort. The JHU and TJNAF collaborative effort is currently funded by a research grant from the National Institutes of Health (NIH), USA.

Figure 9 shows the typical state-of-the-art modular camera technology used in small animal pinhole SPECT systems. The camera module consists of a 10 cm x 10 cm pixellated scintillator array which is viewed by an 2 x 2 array of position sensitive multiple anode photomultiplier tubes (MAPMT). To improve the intrinsic resolution of the modular camera, the JHU and TJNAF are collaborating in investigating the use of new MAPMT technologies to resolve scintillation crystal arrays with increasingly smaller pixel size. Figure 10 shows results from a recent study by the collaboration, i.e., the ability to resolve a pixellated CsI(Tl) array with 1.0 mm pitch, 0.09 mm gap and 3 mm thickness using an array of the latest Hamamatsu H9500-256 MAPMT's. The achievement allows the development of a modular camera with 100 x 100 resolvable pixels to achieve pinhole SPECT imaging of a mouse with overall resolution of less than 1 mm. In Figure 11, we show a comparison of SPECT images of a normal mouse injected with ^{99m}Tc MDP for bone imaging obtained using a 10 cm x 20 cm modular camera with a pixellated NaI(Tl) crystal array with 1.2 mm pitch and a parallel-hole collimator and a pinhole collimator at different magnifications. The modular detectors is capable of resolving all ~18,500 pixel elements. By magnifying the object using the pinhole geometry, we are able to utilize an increasing number of pixel elements to resolve finer details in the SPECT images. The results demonstrate the importance of large number of resolvable pixels to achieve high overall image resolution in pinhole SPECT.

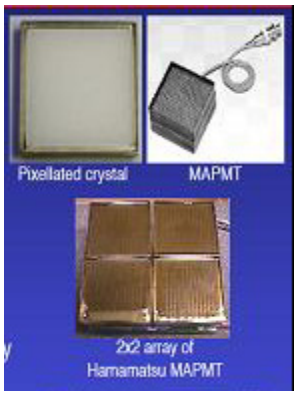

Figure 9. Typical state-of-the-art modular camera technology used in small animal pinhole SPECT systems. The camera module consists of a pixellated scintillator array which is viewed by an array of position sensitive multiple anode photomultiplier tubes (MAPMT)

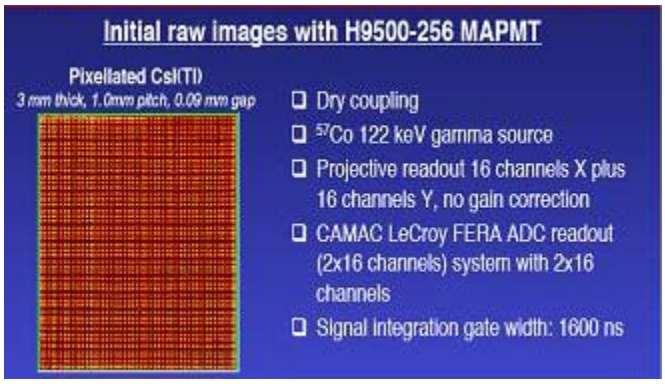

Figure 10. Recent advance achieved by a NIH funded collaborative project between the JHU and TJNAF groups. It demonstrates the ability to resolve a 10 cm x 10 cm pixellated CsI(Tl) array with 1.0 mm pitch, 0.09 mm gap and 3 mm thickness using an 2 x 2 array of the latest Hamamatsu H9500-256 MAPMT

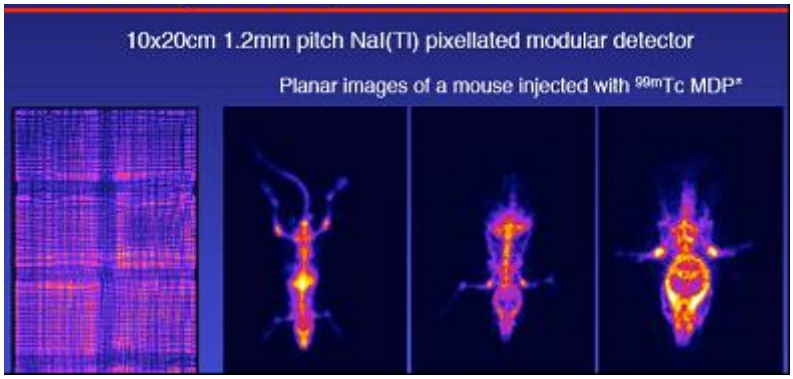

Figure 11. Comparison of SPECT images of a normal mouse injected with 99mTc MDP for bone imaging obtained using a 10 cm x 20 cm modular camera with a pixellated NaI(Tl) crystal array with 1.2 mm pitch and a parallel-hole collimator and a pinhole collimator at different magnifications. The modular detectors is capable of resolving all ~18,500 pixel elements. By magnifying the object using the pinhole geometry, we demonstrate the importance of large number of resolvable pixels to achieve high overall image resolution in pinhole SPECT

Conclusions

We have demonstrated the feasibility of investigating the development of atherosclerotic plaques in the ApoE-/- mouse model by tracking their uptake of ^{99m}Tc labeled Annexin V using high-resolution pinhole SPECT imaging techniques. Our preliminary results indicate an increased uptake of Annexin V in the developmental phase and possible decreased uptake in stable phase of atherosclerotic plaques. However, current pinhole SPECT technologies using state-of-the-art modular cameras based on pixellated crystal arrays and single pinhole aperture, and 3D pinhole image reconstruction methods are limited in resolving atherosclerotic plaques with sizes that are less than 1 mm.

We have described our work in developing quantitative 3D pinhole image reconstruction methods to provide improved image quality and quantitative accuracy as compared to the conventional methods, and multi-pinhole SPECT techniques to reduce reconstructed image artifacts and to increase the detection efficiency for lowering image noise as compared to single pinhole SPECT. Also, we are working to advance the technologies of modular camera by investigating the use of a new generation of position-sensitive multiple anode photomultiplier tubes (MAPMT) to resolve pixellated crystals with smaller pixel elements. These advances hold great promise to provide significant improvements in high-resolution pinhole SPECT for use in biomedical research such as the understanding of the development of atherosclerotic plaques which has significant impact on the diagnosis and treatment of cardiovascular and neurological diseases.

Acknowledgements

The work by the Johns Hopkins University (JHU) group and the collaboration between the JHU and the Thomas Jefferson National Accelerator Facility (TJNAF) group described in this report is supported by the NIH research grant R01 EB1558.

Session 3. Plenary lecture

STUDY OF HIGH RESOLUTION SPECT INSTRUMENTATION AND TECHNIQUES FOR MOLECULAR IMAGING OF SMALL ANIMALS

Franco Garibaldi (a), Michele Ballerini (a), Evaristo Cisbani (a), Stefano Colilli (a), Francesco Cusanno (a), Rolando Fratoni (a), Fausto Giuliani (a), Massimo Gricia (a), Maurizio Lucentini (a), Maria Lucia Magliozzi (a), Fabio Santavenere (a), Sergio Torrioli (a), Stan Majewski (b), Yuchuan Wang (c), Greta SP Mok (c), Benjamin MW Tsui (c)
(a) Department of Technology and Health, Istituto Superiore di Sanità, Rome, Italy
(b) Jefferson Lab, Newport News, VA, USA
(c) Johns Hopkins University, Baltimore, MD, USA

Introduction

The recent progress in biology is opening the way to a new approach to diseases. Moreover, the genome analysis of the individual patient and of his/her own pathology will point out prognostic factors that may guide therapies. Strong integration is needed between preclinical and clinical studies, therefore animal model studies play a key role.

An important component of molecular medicine is molecular imaging, where the molecular identification of cellular components, receptors and ligands may allow the detection of early or hidden lesions or other abnormalities. Recent availability of genetically modified mice has generated a rapid growth of interest in nuclear imaging of small animals, because it enables a wide range of human diseases to be studied in animal models. A key role is played by these techniques that allow imaging *in vivo* of biological processes with high (picomolar) sensitivity if a suitable gamma imaging system is available.

The design of imaging systems for small animals is very challenging due to the concurrent requirements of high spatial resolution and sensitivity.

Positron Emission Tomography (PET) detectors are very attractive for high sensitivity that can be attained, but they are intrinsically limited in spatial resolution that can be a critical parameter in some applications. On the other hand SPECT can offer in principle a comparable sensitivity, but at a much worse intrinsic spatial resolution. At the same time, a large spectrum of radiotracers is available for SPECT. High sensitivity SPECT systems are especially important in many radiotracer kinetic studies in small animals.

Our proposal to focus on the development of the next generation of high-resolution compact gamma imaging systems for SPECT using multipinhole an/or coded aperture collimation techniques will provide devices with both high resolution and high sensitivity that can not be achieved with the current technology. Indeed, the requirements for the detector in terms of spatial resolution and detection sensitivity are quite demanding.

In this paper we describe the design and construction of such high resolution high sensitivity SPECT system. The initial focus is on the detection of vulnerable atherosclerotic plaques and monitoring of stem cells for infarct repair in mice. The results of laboratory tests and preliminary measurements on ApoE-/- mice are also presented.

The bio-medical case

We embarked on a design of an imaging gamma detector for two specific applications: detection of vulnerable atherosclerotic plaques and homing of stem cells in the infarct repair model. Here we focus on atherosclerotic plaques. A detector for stem cell homing study would have similar characteristics (1,2).

Atherosclerosis is a systemic disease that affects most major arteries of the body and is the most common cause of premature death in the western world. It develops slowly and often asymptomatically, so that for many patients its first manifestation is sudden cardiac death, stroke, or myocardial infarction. The clinical challenge is not just in identifying the patient with atheroma but in recognizing specific lesions likely to cause clinical events. Until recently imaging technology for atherosclerosis has focused almost entirely on defining anatomic obstructions to flow. However, advances in our understanding of the cell biology that leads to clinical events in atherosclerosis have highlighted a clear need for imaging techniques that can provide information about plaque composition. Because plaques are common and patients can survive for many years with flow limiting lesions (when the underlying atheroma is stable, such as in chronic stable angina), only a small subset of all atheromas requires immediate treatment. These are the lesions most likely to cause a clinical event. X-ray, the current gold standard imaging tool, as well as MRI are able to provide information on plaque composition in some vascular beds but are unlikely to be able to provide metabolic data on plaque inflammatory cell activity, the major determinant of plaque stability. Better imaging approaches are needed (3-6).

Nuclear imaging has the potential to provide invaluable information on the cellular, metabolic, and molecular composition of the plaque. However, both scanning technology and the radiolabeled tracer molecules need to be improved to produce images of sufficient resolution and quality to allow detection and functional assessment of atherosclerotic lesions in medium-to-small arteries, such as those found in the coronary circulation. To fulfill this role, the imaging agent must have a high concentration only in these critical lesions, with a minimal concentration in other atheromas.

Study on the vulnerable plaque characterization with molecular imaging devices have been proposed and are under preliminary evaluation (3-6): biological hypothesis is formulated on a peculiarity of the vulnerable plaque (such as abnormal presence of apoptosis); an adequate radiotracer is developed (e.g. ^{99m}Tc combined to Annexin V that binds to apoptotic cells) tracer is imaged in a small animal model. High spatial resolution (the plaque in a mouse aorta is of the order of $0.5\times1\times4$ mm^3) and high sensitivity (above 0.3 cps/kBq) are required.

The detector

The needs of the atherosclerotic plaques study translate into the following SPECT system requirements (7): spatial resolution of 500 μm (which derives from the minimum plaque size), system sensitivity of 0.3 cps/kBq, active area (single module) of about 100×100 mm^2, in order to image a full mouse (4÷5 cm long) with a magnification factor of about 3 (if a pinhole collimator is used). A gamma detector matching such requirements has been designed and prototyped.

It is based on tungsten collimators (parallel hole, pinhole and coded aperture), a scintillator crystal (pixellated as well as continuous options have been considered) and Position Sensitive PhotoMultiplier Tubes (PSPMTs), with individual channel readout electronics.

The single detector module (collimator+scintillator+PSPMTs+electronics) shall be compact in order to be used in a multi-head configuration (4 to 8 modules around the animal) to increase the overall sensitivity.

Simulation

Extensive simulations have been done using the GEANT4 code (8) to optimize the detector performance. Arrays of pixellated as well as continuous scintillators have been considered coupled to PSPMTs having different anode pad size. In order to obtain high spatial resolution, the ratio between FWHM of the light cone emitted from the scintillator and the dimension of the "anode pixel" of PSPMTs has to be optimized (7,9,10). In fact good pixel identification is critical to obtain good high contrast images.

Previous studies by our team showed (7,9,10) that Signal to Noise Ratio (SNR) improves with smaller scintillator pixel size, provided small anode size is used. The size of the anode has to be small enough to be able to sample the light distribution with sufficient spatial frequency. Small anode size (3×3 mm^2) is needed for sampling scintillation light coming from 1.0×1.0 mm^2 pixels, while 6×6 mm^2 anode size are barely sufficient for 1.3×1.3 mm^2, and even smaller anode pad sizes (1.6×1.6 mm^2) are needed for sub-millimeter scintillator pixels. This substantially complicates the readout design because of the large number of required electronic channels.

Figure 1 shows light distribution in the "live" and "dead" detector areas, the number of photons, the spatial and energy resolution for CsI(Na) 100×100×3 mm^3, 0.8 mm pitch, and 0.5 mm pitch, as well as for 100×100 mm^2 $LaBr_3$(Ce) continuous, 3 mm thick.

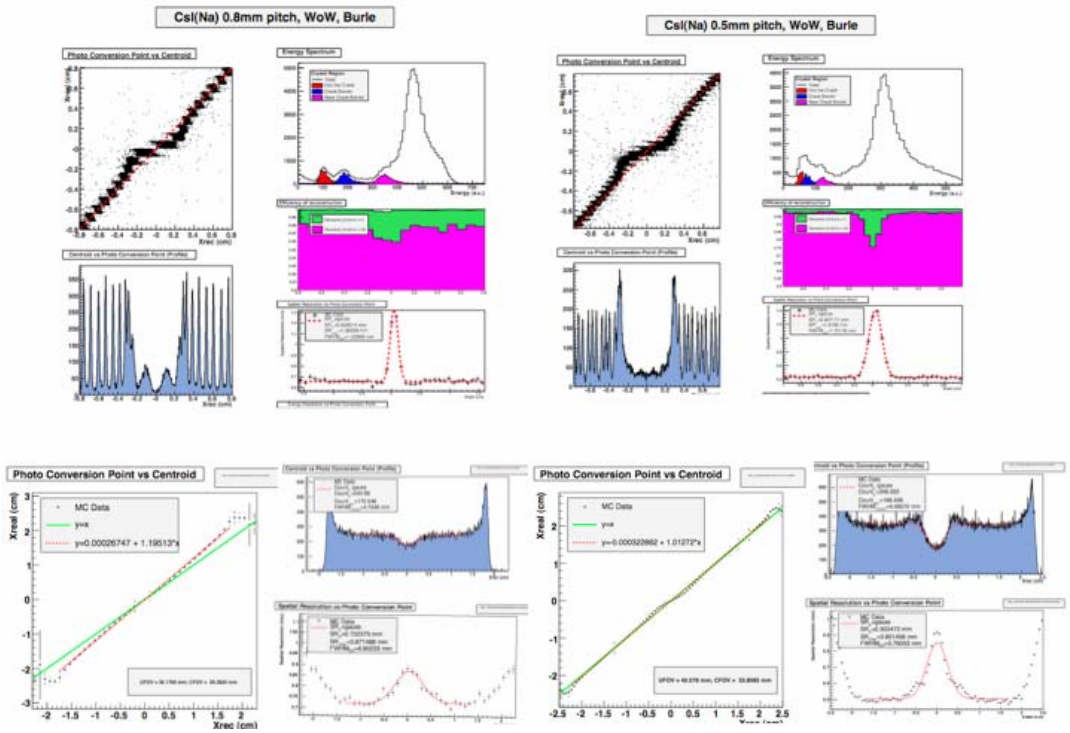

Figure 1. CsI(Na) 100x100 mm2 and 50x50 mm2, LaBr3(Ce) 100x100 mm2 (see text)

The scintillator with smallest studied pixel size is CsI(Tl) with 0.5 mm pixel pitch. Good pixel identification and very good spatial resolution is obtained. Nevertheless it should be noted that some problems arise in the "dead area" of PMTs. The light sampling is rather poor in this area, so spatial resolution and energy resolution decreases.

Detectors with scintillator as large as 100×100 mm^2 with larger pixel size have to be used; from our simulation 0.8 mm is the optimal choice because it allows better sampling of the light in the dead area, so better pixel identification and spatial resolution (still lower then in the "live" area). However, in practical implementations issues such as SNR in electronics and non-correctable non-uniformities in PMTs (especially at the edges) and in scintillators may limit the small size limit of the scintillator pixel to 1 mm.

Another potential scintillator solution is continuous $LaBr_3$(Ce) which has better spatial resolution but suffers from spatial non uniformities that are more difficult to be corrected in the dead PMTs regions. Moreover it has a reduced Field Of View (FOV) due to more pronounced edge effects, and it is still more expensive and difficult to grow in large dimensions (but 100×100 mm^2 sizes are available now). Two different surface treatments have been considered for the entrance window, diffusive (standard in the literature) and absorbing. With the diffusive treatment the number of photoelectrons is higher (producing better energy resolution) but the FOV is reduced (35%-40%) and shows quite significant response non-uniformity.

The absorptive option improves FOV, uniformity and spatial resolution because light distribution is narrower (the diffused photons would enlarge it).

We have to consider that the key performance parameter is SNR. In fact very small structures have to be imaged. Table 1 shows a comparison between three options. Pixellated scintillators offer the best SNR. This result is still under discussion.

Table 1. SNR from three different crystal configuration

Scintillator	Sensitivity (counts/μCi/s)	SNR
CsI(Tl) pixellated (0.8 mm)	0.81	1.92
LaBr3(Ce) (entrance w. absorptive)	0.77	1.41
LaBr3(Ce) (entrance w. diffusive)	0.80	1.37

All three considered scintillator solutions match the required performances, provided they are coupled to the right photodetectors (with small enough anode pixel size). Of course, these simulations have to be still validated by measurements before taking decision about the final detector layout.

Collimation techniques

Pinhole collimator with appropriate hole dimension and magnification factor was the first choice. It was clear that the efficiency would have been insufficient. For this reason multi-pinhole (at Johns Hopkins) and coded aperture collimation (at ISS) have been studied. Promising results have been already obtained by both groups. Significant increase of the efficiency (factor 8 to 30) can be obtained. Results are reported elsewhere (11,12).

Choice of the detector

The simulation results will drive the final choice of the detector layout taking into account also practical aspects (compactness) and cost. The results of simulation show that further study has to be made for the final choice of the detector layout. In fact two layouts are possible for the pixellated scintillator option: 100×100×3 mm^3 CsI(Na) 0.8-1.0 mm pitch or individual ~ 5cm modules with 0.5 mm pitch.

The $LaBr^3$(Ce) option will be more studied. However, it is more expensive and suffers from smaller FOV and more difficult to correct response non-uniformities.

"Scaling down option"

As mentioned above another option seems to be interesting. Simple calculation of FOV, spatial resolution and sensitivity shows that the single detector module can be chosen as small as 50×50 mm^2 with ~ 0.5mm scintillator pixel sizes. The performance would be similar to CsI(Tl) arrays with 0.8-1.0 mm pitch and 100×100 mm^2 area. The advantages in terms of cost, compactness, and complexity would be substantial.

Electronics and data processing

The PMT anode pad channels are read-out independently by a track-and-hold multiplexed system (based on the VATA IDE AS system). While more complicated, this solution optimizes the quality of imaging (in particular in terms of peak-to-valley and spatial distortions of the centroid maps). Multiplexing permits to reduce complexity and cost of electronics, resulting in the present solution in a 2 kHz event rate limit for this 1024 channel system, due to the write access speed of the mass storage sub-system. Higher rates can be obtained with more recent, still cost-effective, solutions (that are under evaluation) where a sparse readout logic is introduced at the track-and-hold stage or after the multiplexed ADCs. Higher flexibility of the independent channel readout (with respect to the conventional resistive chain) is exploited at different levels during the processing of the data: the collected charge centroid is computed on normalized gain channels after a proper spatial windowing (one of the advantages of the independent channel readout) that reduces distortion effects of the background and noisy channels. The centroid map of a flood calibration run defines the crystal (pixel) centers and therefore a local mapping of the PMT channels on the regular crystal grid; border and residual spatial distortions are then compensated by a projection of the centroid image from the PMT channel to the crystal grid defined by the above mapping.

Initial results

In parallel with simulation studies, we started building a prototype using available to us scintillator arrays and photodetectors. A prototype detector has been designed and built using pinhole tungsten collimator + CsI(Tl) scintillator array (100×100×3 mm^3, 1.0 mm pitch) + array of 4 PSPMTs (H9500 Hamamatsu, 3×3 mm^2 anode size).

Measurements have been made with a tungsten pinhole collimator (0.33 mm hole diameter). Figure 2 shows that a spatial resolution as good as 0.55 mm can be obtained.

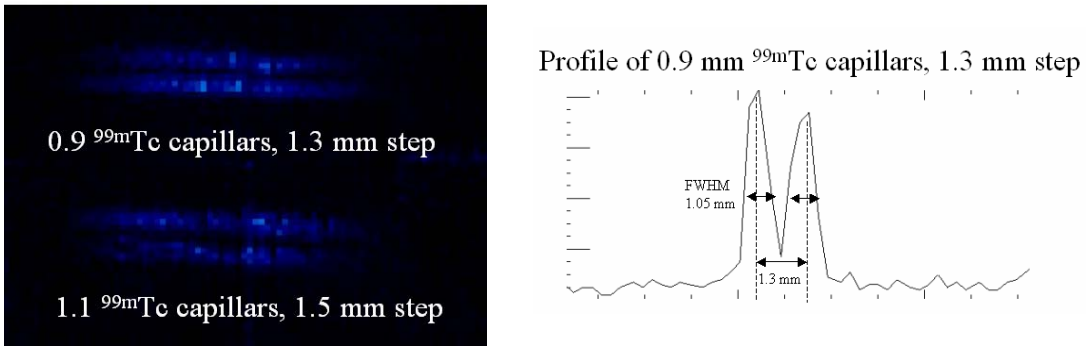

Figure 2. Measured spatial resolution (550 µm). CsI(Tl) 1 mm pitch; pinhole 0.33 mm

Preliminary measurements have been also made with animals. Figure 3 shows a maximum intensity retrojection image of a APOE-/- mouse injected with Annexin V labeled ^{99m}Tc in a mouse. The animal was too young to develop any detectable atherosclerotic plaque by the pinhole SPECT system. However, the image cleary shows the detailed activity distribution in the kidney demonstrating the high resolution imaging characteristics of the new detector used in the pinhole SPECT system and its potential of detecting small atherosclerotic plaques if they occur in the animal. These preliminary results show that a system able to detect vulnerable plaques in mice can be built.

The spatial resolution seems to be already sufficient. The sensitivity will be increased by using multi-pinhole and/or coded aperture techniques. Further simulation and measurements have to be done to optimize the final layout.

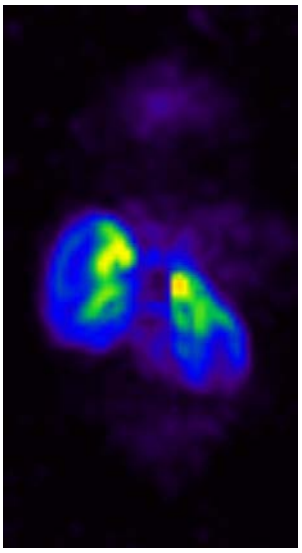

Figure 3. Maximum intensity reprojection Image of the kidney of APOE -/- mouse injected with Annexin V labeled with 99mTc. The detailed acitvity distribution in the kidney demonstrates the high resolution imaging characteristics of the new detector

Outlook

Advanced detectors for imaging with radionuclides are a vital tool in biomedical imaging research. This was the motivation behind our collaborative effort to develop high resolution and high sensitivity single photon imaging systems for molecular imaging of small animals that cannot be achieved with the currently implemented technology. Initial simulation and laboratory studies have been performed to design a system focused on a main goal of detecting vulnerable plaque in genetic modified mice. The same detector could be used for monitoring stem cell in the infarct repair in a mouse model.

Simulations and preliminary measurements have shown that indeed it is possible to build high resolution and high sensitivity detection systems to detect vulnerable plaque in mice using available imaging system components: position sensitive photomultipliers coupled to pixellated or continuous scintillators. Several prototypes of these systems are under construction and evaluation.

References

1. Gao J, *et al*. The dynamic in vivo distribution of bone marrow-derived mesenchymal stem cells after infusion. *Cells Tissues Organs* 2001;169:12-20.
2. Kraitchman DL, *et al*. Dynamic Imaging of Allogeneic Mesenchymal Stem Cells Trafficking to Myocardial Infarction. *Circulation* 2005;112:1454-64.
3. Strauss HW, *et al*. Imaging the Vulnerable Plaque: A Scintillating Light at the End of the Tunnel? *J Nucl Med* 2004;45(7):1106-7.
4. Davies JR, *et al*. Molecular and Metabolic Imaging of Atherosclerosis. *J Nucl Med* 2004;45(11):1898-907.
5. Tsui BMW, Wang Y. High-Resolution Molecular Imaging Techniques for Cardiovascular Research. *J Nucl Cardiol* 2005;12:262-7.
6. Tsui BMW, *et al*. Feasibility of microSPECT/CT imaging of plaques in a transgenic mouse model. In: Kupinski MA, Barrett HH (Ed.). *Small Animal SPECT Imaging.* Springer; 2005. p. 215-24.
7. Cisbani E, *et al*. Molecular Imaging with radionuclides: a powerful mean for studying biological processes in vivo. *Nucl Instr Meth A*, in press.
8. Agostinelli S, *et al*. GEANT4: a simulation toolkit. *Nucl Instr Meth Phys Res* 2003;A506:250-303.
9. Cusanno F, *et al*. Preliminary Evaluation of Compact Detectors for Hand-Held Gamma Cameras. *Phys Med* 2004;XX(2):65-7.
10. Magliozzi ML, *et al.* (Ed.). High resolution, high sensitivity detectors for molecular imaging of sall animals and tumor detection. *Proceeding of the 9th International Conference of Advanced detectors.* Como (Italy), October 17-21, 2005.
11. Garibaldi F, *et al*. Small animal imaging by single photon emission using pinhole and coded aperture collimation. *IEEE Trans on Nucl Sci* 2005;52(3 Pt 1):573-9.
12. Cusanno F, *et al*. High resolution, high sensitivity detectors for molecular imaging with radionuclides: the coded aperture option. *Nucl Instr Meth A*, in press (Elsevier reference NIMA 45669).

Session 3. Plenary lecture

OBTAINING OPTIMAL FUNCTIONAL RECOVERY AND EFFICIENT MANAGED CARE FOR THE CHRONIC STROKE POPULATION

Velio Macellari (a), Claudia Giacomozzi (a), Antonello Fadda (a), Francesco Benvenuti (b), Simona Giampaoli (c), Gianfranco Spalletta (d), Aurelio Cappozzo (e), Steven J Stanhope (f), Michael Weinrich (g), Mary E Stuart (h), Richard Macko (i)

(a) Department of Technology and Health, Istituto Superiore di Sanità, Rome, Italy
(b) USL11, Regione Toscana, Empoli-San Miniato, Italy
(c) National Centre for Epidemiology, Surveillance and Health Promotion, Istituto Superiore di Sanità, Rome, Italy
(d) Fondazione S. Lucia (IRCCS), Rome, Italy
(e) Dip. Di Scienze del Movimento Umano e dello Sport, Istituto Universitario Scienze Motorie, Rome, Italy
(f) Physical Disabilities Branch, National Institutes of Health, Bethesda, MD, USA
(g) National Center for Medical rehabilitation Research, National Institute of child Health and Human Development, National Institutes of Health, Bethesda, MD, USA
(h) Department of Sociology and Anthropology, University of Maryland, Baltimore, USA
(i) Department of Neurology, University of Maryland, School of Medicine, Baltimore, USA

Introduction

The American National Institute for Health considers stroke the leading cause of significant disabilities, with extremely high costs associated with it.

Thus, the main objective of this Project is to identify the best "managed care" strategies for stroke survivors. Such strategies should aim at maintaining patients' locomotor and main daily life functions, at preventing the onset of further disabilities and diseases, and at improving the patients' quality of life. At the same time, they should optimise the use of economic resources.

In the very preliminary phase of the Project, the need to gain useful knowledge with respect to issues like incidence of stroke events in Italy, stroke survival, and chronic stroke management was highlighted. To this purpose, an overall data revision was conducted on stroke databases which were available at the Local Health Agencies (ASL) 10 and 11 of the Tuscany Region (Italy). The focus of the revision was on the management of chronic stroke outcome and on the analysis of data – collected in the register for cerebro-vascular accidents – related to a set of patients in the area of Florence (Italy).

A detailed research plan was defined in the first part of the Project, which identified three, strongly connected, research lines: 1) supply and assessment of the effectiveness of Adapted Physical Activity (APA); 2) treatment of depression and assessment of how and to what extent depression affects the expected result of rehabilitation; 3) feasibility studies, design and application of the main methodologies of rehabilitation engineering.

Besides the above activities, a further one will be implemented within the Project which will mainly aim at educating, disseminating and promoting consent.

The following paragraphs give a detailed description of the activities conducted in the first 18 months of the Project.

Management of chronic stroke outcome in Italy

The generalised discussion on global health disparities led to the decision of carefully analysing data related to chronic stroke outcome. Factors like system organization and context where a disease is managed may have a critical role on the outcome. For this reason, a reliable analysis of efficacy and effectiveness of the implemented interventions must take into account for the above factors, which strongly depend on different organization conditions and which are characterised by different duration and magnitude of the selected rehabilitative paths. Tuscany ASL 10 and 11 are fairly close one to the other, however they have completely different characteristics in terms of both territory and structure. For this reason it was important: to compare the available health structures and resources; to compare their use of health services in the time frame of one year after the stroke event; to evaluate which indicators and data should be considered as mandatory to assess efficacy and effectiveness of the health services embedded in different contexts.

The methodology to assess health services as described above was based on two types of tools: qualitative tools – mainly consisting of interviews and on-the-field evaluations – and quantitative tools – basically analysis of administrative and health databases. Core of the study was the set of patients who experienced their first ischemic stroke in 2002. *Ad hoc* criteria were defined and applied to extract the above patients from the hospital database for patients discharge. Selected patients were then assessed along one year after the hospital discharge. Among the most relevant results, a significant lack of homogeneity was observed with respect to the management of patients' rehabilitation. ASL 10, in fact, mainly based rehabilitation on hospital structures, while ASL 11 mainly delivers it over the territory. Further interesting results are summarised below:

- average cost for drugs is slightly higher at ASL 10;
- the number of specialized medical examinations is comparable;
- when used as an outcome indicator, mortality is 4.6% higher at ASL11.

At the end of the phase Project which is currently under execution, the impact of critical changes at ASL 11 will be examined which might have significantly affected the above results. The changes - which mainly involve the service organization at ASL 11 - started in 2002.

Follow-up of a set of chronic stroke patients in the area of Florence

Based on the information collected in the national register for coronary and cerebro-vascular accidents, the Florence operative unit started a follow-up of a sample of definite cerebro-vascular events collected in the period 1998-1999. Such events, which had been previously validated by applying the MONICA methodology, formed the set of events which was used to construct the positive predictive values of the codes the hospital discharge diagnosis was based on (ICD-9 430-438) (1). The follow-up consisted in the analysis of survival at 28 days, at 1 year and at 5 years after the event (Table 1).

The main results of the study are briefly summarised here below:

- 331 out of 907 hospitalizations reported in the national register were validated and considered as definite cerebro-vascular events. The definite events corresponded to 331 patients; only 318 of them could be succesfully followed-up – the remaining 13 patients were classified as "lost", or showed incomplete datasets . For the 318 patients the survival was evaluated at 28 days, 1 year and 5 years after the event;

- averaged 5-years survival was 63%, slightly higher for women than for men (64% *vs* 62%); events due to thrombosis or embolism (71-72%) were more frequent than unclassified events or events due to hemorrhage (56%);
- multivariate analysis confirmed that the prognosis of those events which were due to hemorrhage is significantly worse than the prognosis of the remaining events (HR: 2.02; 95% CI: 1.26-3.32); the analysis also revealed that the sensible worsening of the prognosis is strictly related with the patient's age.

Table 1. National Register of Coronary and Cerebro-vascular Events: 5-year follow-up of definite cerebro-vascular events

Survived	Men	Women	Total
28 days	171	98	269
28 days (%)	*86.4*	*81.7*	*84.6*
1 years	151	92	243
1 year (%)	*76.3*	*76.7*	*76.4*
2 years	142	86	228
2 years (%)	*71.7*	*71.7*	*71.7*
3 years	134	82	216
3 years (%)	*67.7*	*68.3*	*67.9*
4 years	129	78	207
4 years (%)	*65.2*	*65.0*	*65.1*
5 years	123	77	200
5 years (%)	*62.1*	*64.2*	*62.9*

Research plan - details

Effectiveness of a community-based Adapted Physical Activity (APA) for chronic stroke

In September 2005 a meeting was held in Florence between the Italian partners of the Project and some of the consultants from USA (namely Richard Macko, Donald Steinwachs, Mary Stuart, Michael Weinrich). Main goals of the meeting were the definition of the global protocol design and of the main investigation tools.

On November 10th, 2005 the proposed investigation protocol was approved by the ASL 11 Local Ethical Committee. Part of the Project funding to ASL 11 was used to enrol 1 physiotherapist – 30 hours per week –, who was asked to locally coordinate the Project.

In November 2005 a dedicated course was implemented and delivered to clinicians and physiotherapists involved in the Project. They came from ASL11 (Empoli), ASL 5 (Pisa), and from Casa di Cura Ulivella-Glicini in Florence. The course focused on the use of the APA manual of tools.

Patients' recruitment started in December 2005 and lasted until the end of March 2006. 51 patients were recruited at ASL11 and included in the intervention group. Further 61 patients – 36 in Florence, 25 in Pisa – were recruited and included in the control group. In order to deliver APA to the intervention group, APA courses were set up in 5 small centers of the ASL 11 territory.

The following data on patients' treatment are referred to the period December 2005 – March 2006. Data referred to later periods, in fact, are still under process.

At the end of June 2006, 30 patients within each group – intervention and control group – had completed the 3-months follow-up. Briefly, APA seems to improve functional mobility, basic activity of daily living, and may provide cardiovascular conditioning. No relevant adverse clinical events were pointed out with regards to the intervention group – the patients who performed APA. However, 6 out of the 51 patients of the intervention group abandoned the study due to transportation problems – 4 out of 6 had family problems – 1 out of 6 had personal problems.

From 9th to 18th January 2006, two USA researchers - M. Stuart and M. Weinrich – conducted an independent audit in order to objectively assess APA procedures and protocols implemented in the Project. The final report of their audit is reported in the USA report on the state of the art of the present Project (see contribution by S. Stanhope et al). A second independent audit started on March 17th, 2006 and lasted for 15 days. This second audit was conducted by the USA researchers Michelle Pharr and Shawnisha Hester. A third brief audit took place in June 2006. In order to save money and promote visits by the USA researchers involved in the Project, guest-rooms were purposely delivered by ASL 11 in San Miniato (Pisa).

Assessment of how and to what extent depression affects the expected result of rehabilitation

In order to quantify the severity of depression in patients affected by chronic stroke, the Hamilton scale for depression was used, which included 17 items. As a first step of the study, a small group of neurologists was trained to supply the test requested by the Hamilton scale. Basically, they participated to a sequence of meetings and to an assessment trial performed by an expert psychiatrist. As a second step, a few chronic stroke patients were interviewed in order to assess the reliability of the proposed tool. The inter-operator differences in using the Hamilton scale were observed, and test-retest analysis was performed. The purpose of using the Hamilton scale within the Project is twice: i) to reliably quantify the depression level of the patients involved in the Project; ii) to assess the eventual effect of depression on the success of the rehabilitation process.

The Hamilton scale is currently delivered to the patients, but complete reports have not been produced yet.

Rehabilitation engineering

A wearable system to support gait rehabilitation was purposely designed and constructed on the basis of a patented measuring device previously developed at ISS Biomedical Engineering Laboratory (2). The main feature of the system is the on-line acoustic feedback of the quality, intensity and time of contact between foot and floor. Briefly, an electric signal is obtained by wearable sensorized insoles – easily adaptable to almost every kind of shoes.The signal is processed on-line through a novel combining algorithm and immediately transduced into an acoustic signal. The coding of this last signal was purposely studied to allow the patient to easily perceive any gait abnormality.

The whole system is easily wearable, wireless and with a little encumbrance. Data related to the patient's motor response are telemetrically transmitted on-line to a control unit. Thus the therapist can easily monitor the patient's performance. The off-line storage and analysis of data render the system a powerful tool for monitoring the rehabilitation progress of the patient,

besides being itself a useful rehabilitation tool. Preliminary measurements have been performed with a laboratory prototype of the system (Figures 1 and 2). Their results were encouraging. The realization phase of a certain number of its items is going to finish in a short time. After a short, preliminary use in the clinics, under controlled conditions and under the supervision of the therapists, each rehabilitation unit will be supplied to the patients to allow its use at home.

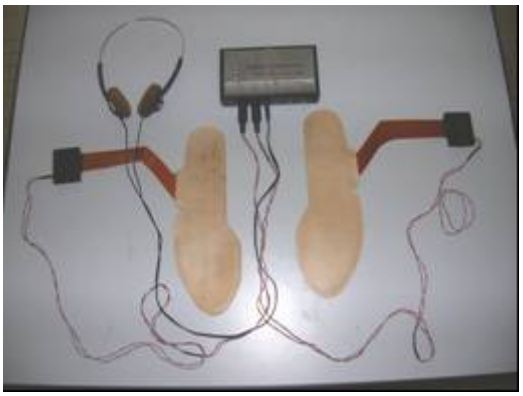

Figure 1. Main components of the wearable device: the sensorized ISS insoles (Italian patent n. RM96A000834), the wearable transmitting unit and the earphones for the acoustic feedback. The system also includes a receiver to send the data to the PC

Figure 2. An ISS researcher equipped with the feedback wearable device. The insoles have been inserted into common shoes

The device hereby described should be intended as a first rehabilitation tool to be validated in-the-field. Other sensorized rehabilitation tools, already described in the dedicated literature, might be re-designed, improved and specialized according to the specific indications delivered

by this preliminary study. As an example, it is reasonable to hypothesize a remote supervision of a set of devices for both rehabilitation and monitoring, thought as a part of a more exhaustive telerehabilitation service. Each telerehabilitation service might be highly specialized and patient-oriented. The starting point for such a kind of highly specialized services might be a general purpose telerehabilitation service developed under the Italian Project ITACA (M.I.U.R, Firb Project, art. 8, prot. RBNE01ENLN). ISS Department of Technology and Health was the coordinator of the Project. A prototype of the service is in the last phase of implementation at the above Department.

Education, dissemination, consent promotion

The University Institute for Motor Science of Rome has produced a course on Human Movement Analysis aimed at training health operators to the use of quantitative methodologies in the functional evaluation of patients. Relevant multimedia material is available on a CD. A reduced version of the course will be delivered as a pre-congress tutorial in October prior to the annual meeting of the Italian Society for Clinical Movement Analysis (SIAMOC).

A different educational approach is simultaneously under study at ISS. Based on ISS wide experience in the field, and on the specific experience the above ISS Department gained during the European Telerehabilitation Project HELLODOC (3), a feasibility study is in progress to evaluate the implementation of distance educational programmes within the Project. A reliable e-learning platform is in fact available at ISS Office for External Relationships (URE), and its potentialities might be effectively exploited to supply operator and patient-oriented teaching modules, and to test the setup of remote units for Project data collection and processing.

As for the dissemination aspect of the Project, the following meetings were scheduled (and partially held) up to now:

- Attività motoria preventiva e adattata: modelli organizzativi sul territorio. Place: ISS (Rome), June 8th, 2006.
- Rehabilitation research in chronic stroke: state of the art and perspectives of the ISS-NIH project "Obtaining Optimal Functional Recovery and Efficient Managed Care for the Chronic Stroke population". Place: ISS (Rome), October 16-17th, 2006.

Publications

The research conducted within the Project will mainly deliver long-term results, thus only one manuscript could be prepared up to now, which is currently in the publication process. The manuscript, which deals with the main results of the database analysis at ASL 10 and 11, was approved by the Project Responsibles in Baltimore (USA), in April 2006.

A paper will be hopefully published in a short time dealing with the follow-up of a set of chronic stroke patients in the area of Florence.

References

1. Documenti Agenzia Regionale Sanità, numero del 24.06.2006. Osservatorio di Epidemiologia. "L'assistenza ospedaliera e riabilitativa agli anziani in Toscana: ictus e Frattura di Femore"

2. Fadda A, Giacomozzi C, Macellari V. Comparative measurements to validate a new telemetric pressure insole system. In: *Procs. IMEKO, IEEE, SICE, 2nd International Symposium on Measurement Analysis and Modelling of Human Functions, 1st Mediterranean Conference on Measurement*, Genova, June 14-16 2004. (ISBN 88-901344-0-2) p.425-7.
3. Giacomozzi C, Cordella D, Rogante M, Scattareggia S, Magni R, Zampolini M, Bernabeu Guitart M, Ilsbroukx S, Huijgen B. A European e-learning experience in upper limb telerehabilitation. In: *IASTED International Conference on Telehealth*, Banff, Canada, July 3-5 2006.

Session 3. Plenary lecture

DIETARY LIPID AND FOAM CELL FORMATION: STUDY ON THE MECHANISMS INVOLVED IN CHYLOMICRON REMNANT UPTAKE BY MACROPHAGES AND MODULATION BY DIETARY LIPOPHILIC COMPOUNDS OF INTERACTION BETWEEN MACROPHAGE AND ATHEROGENIC LIPOPROTEINS

Elena Bravo (a), Mariarosaria Napolitano (a), Rani Rao (b), Howard Kruth (b)
(a) Department of Haematology, Oncology and Molecular Medicine, Istituto Superiore di Sanità, Rome, Italy
(b) NHLBI, National Institutes of Health; Bethesda, MD, USA

Introduction

Arteriosclerosis is the major cause of most heart attacks and strokes. A possible target in the struggle against development of arteriosclerosis and related diseases is the macrophage foam cell. Foam cells are monocyte-macrophages which have invaded the arterial tissue and scavenged atherogenic lipoproteins in an unregulated manner, becoming engorged with lipid (1). Atherogenic lipoproteins include both low-density lipoproteins (LDL) and chylomicron remnants (2,3).

Thus, different types of cholesterol-containing particles may enter macrophages. The fate of cholesterol that enters macrophages determines whether macrophages help or hinder cholesterol removal from the vessel wall. Thus, macrophage functions determine if cholesterol is removed from the lesions or accumulates in the vessel wall (4).

Both Dr. Kruth's (NIH, Bethesda) and Dr. Bravo's (ISS, Rome) research groups have carried out extensive work on foam cell formation. Their present joint project aims to understand better macrophage mechanisms for uptake of atherogenic lipoproteins and how these uptake mechanisms are modulated. These studies will be useful for directing macrophage function in atherosclerotic lesions towards beneficial rather than harmful effects (4-6).

Dietary lipids absorbed during digestion are packaged into large lipid particles called chylomicrons. Because of the large size of chylomicrons, it was assumed that they cannot enter the vessel wall nor interact with artery wall macrophages. On the contrary, it has been shown that the smaller chylomicron remnant particles may be taken up by several types of macrophages and cause extensive triacylglycerol (TG) and cholesterol (CH) accumulation in macrophages inducing foam cell formation (6,7,8).

The most accepted pathway for macrophage uptake of chylomicron remnants is via the LDL receptor mediated by the apolipoprotein E (apoE) component of chylomicron remnants functioning as the LDL receptor ligand (9,10). However, from studies in cells devoid of LDL receptor activity there is evidence that chylomicron remnant uptake pathways in macrophages may be independent of the LDL receptor and mediated also by other mechanisms (11,12). Currently, both receptor-dependent and independent processes are considered to play a role in the uptake of chylomicron remnants by macrophages (6,7) However, though it is now clear that

chylomicron remnants are pro-atherogenic lipoproteins, events leading to their incorporation by macrophages are poorly understood.

The aim of this study is to investigate the mechanisms that lead dietary lipids to induce lipid accumulation in macrophages. In particular, in the first part of the joint project, we investigated whether and how non-apoE-mediated receptor pathways are involved in the uptake of chylomicrons remnants by macrophages.

Evaluation of lipid accumulation

Human monocyte-derived macrophages (HMDM) are the major cellular progenitor of foam cells in the intima where atherosclerotic plaques form. This has raised substantial interest in factors that regulate lipid metabolism and receptors for lipoproteins in these cells (1). HMDM are of common use in both laboratories involved in this project (5,13) and, for this study, monocytes were isolated from human buffy coats with the methodologies routinely used in the two laboratories (5,13).

Since contamination by other lipoproteins is a problem in obtaining chylomicron remnants from human blood, for this study, we used chylomicron remnant-like particles (CRLP) a model widely used to study chylomicron remnants metabolism. Both CRLP containing (CRLP+) and lacking (CRLP-) human apoE were used in the study. Human apoE was added to the particles by incubation with human plasma (13).

To evaluate the induction of macrophage lipid accumulation by chylomicron remnants, HMDM were incubated for 24 h in the absence or the presence of different concentrations of cholesterol carried by CRLP. After the incubations, lipids were extracted from cells by Folch's method and macrophage TG and CH content were evaluated by fluorometric assay of lipid extracts (14,15).

Results

In this first phase of the ISS-NIH collaboration, the integration between the two research groups was accelerated by the work-stay of Dr. Mariarosaria Napolitano, from ISS to NIH.

The work carried by this researcher for this project has satisfied both groups and most of the experiments described in this section have been performed by Napolitano in the Dr Kruth's laboratory.

First, we investigated the role of apoE in the induction of macrophage lipid accumulation by chylomicron remnants. To this aim, we measured macrophage TG and CH content of macrophages incubated with either CRLP+ or CRLP- in comparison with cells not incubated with the particles (w/o CRLP). As shown in Figure 1, in comparison with CRLP+, the lack of apoE on CRLP particles reduced by about 50% the strong accumulation of TG induced by these particles, while the smaller increase of CH was not affected.

These results indicated that the macrophage lipid accumulation induced by chylomicron remnants is only partially due to apoE-receptor dependent uptake and that apoE-receptor independent mechanisms contribute to the process of foam cell formation.

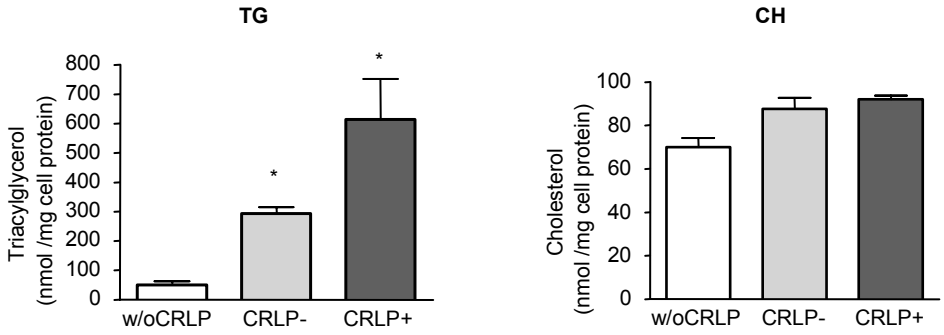

HMDM were incubated in serum-free IMDM alone (w/o CRLP) or with 80 mg cholesterol/ml carried by either CRLP+ (apoE-containing) or CRLP- (apoE-free). Cellular triacylglycerol and cholesterol content were then determined.* p<0.05 versus w/o CRLP

Figure1. Role of Apolipoprotein E in macrophage lipid accumulation induced by chylomicron remnants-like particles (CRLP)

Macropinocytosis, which is responsible for uptake of particles in the fluid-phase, has been shown to be responsible for induction of foam cells by LDL (5). Macropinocytosis is a function well expressed in activated macrophages and can be induced in cultured macrophage by treatment with phorbol esters (PMA). With the objective of investigating whether macropinocytosis is a pathway contributing to the uptake of apoE-free CRLP, HMDM were incubated with up to 80 ug CH/ml of apoE-free CRLP in the absence or in the presence of PMA (1µg/ml). Our results demonstrated that the induction of macropinocytosis does not enhance macrophage lipid accumulation over the concentration range of CRLP tested in this study (Figure 2).

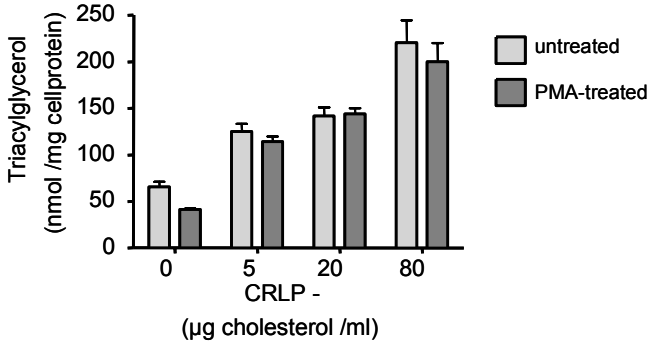

HMDM were incubated in serum-free IMDM with 0,5,20 or 80 mg cholesterol/ml carried by CRLP-. Cellular triacylglycerol and cholesterol content were determined.

Figure 2. Role of macropinocytosis on lipid accumulation by apoE-free chylomicron remnants-like particles (CRLP-).

It could be hypothesized that apoE, secreted in large amounts into the medium by human macrophages (16), is acquired by CRLP- during the incubations and mediate the receptor uptake of the apoE-free CRLP. To test the role of macrophage-secreted apoE, we measured the effects of the presence of apoE antibodies on macrophages lipid accumulation. To this aim HMDM were incubated for 24h with 80 μg cholesterol/ml in the presence of apoE antibodies. Control incubations were similarly carried out in the presence of anti-IgG antibodies. The results of this series of experiments are summarized in Figure 3 and showed no differences between TG and CH content accumulated in the cells in the 2 conditions, suggesting that the apoE secreted by macrophage is not involved in the uptake of the apoE-free CRLP.

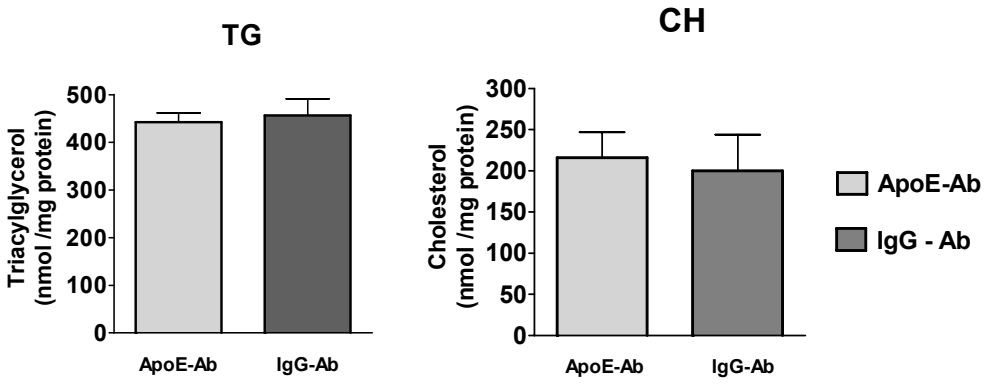

HMDM were incubated in serum-free IMDM with 80 μg cholesterol/ml CRLP- in the presence of apoE antibodies (ApoE-Ab) or anti-IgG antibodies (IgG-Ab). Cellular triacylglycerol and cholesterol content were determined.

Figure 3. Role of macrophage-secreted ApoE on lipid accumulation by apoE-free chylomicron remnants-like particles (CRLP-)

Discussion

The lipid in foam cells is often in the form of cholesteryl ester but, in some circumstances, TG may accumulate (17). This is relevant, because it is now clear that there is a relationship between abnormalities in the clearance from plasma of chylomicron remnants and accelerated progression of atherosclerosis. Elevated plasma TG and persistent increased levels of dietary remnants are considered emerging risk factors for cardiovascular disease and evidence exists that chylomicron remnants and a delay in their removal from serum are independent risk factors in the pathogenesis of atherosclerosis (18,19).

For lipoproteins of dietary origin, the chylomicron remnants, many different receptor and non-receptor mechanisms of uptake have been hypothesized, but the physiologic role of each of them is still debated.

The present collaborative ISS-NIH project first demonstrated that beside the apoE-mediated endocytic uptake of whole particles, also apoE receptor-independent mechanisms are involved on the induction of foam cells by chylomicron remnants. Then, the study has focused on the evaluation of mechanisms which can contribute to the receptor-independent uptake of

chylomicron remnants. We found that neither macropinocytosis nor macrophage apoE secretion play a determinant role on lipid accumulation induced by chylomicron remnants. On the contrary, we have some preliminary results (data not shown) indicating that, at least partially, the extracellular apoE-independent lipoprotein lipase (LPL) hydrolysis of TG carried by CRLP-, precedes the uptake of released fatty acids, contributing to the TG accumulation by the macrophages, as it has been reported for other TG-rich lipoproteins (13,20).

Outcome

The Authors of this work have been invited to present these results at the International Focused Meeting of the Biochemical Society "Diet and cardiovascular health: chylomicron remnants and their emerging role in vascular dysfunction in atherogenesis" that will be held in London 18-19 December 2006. The abstract "Apolipoprotein-E independent mechanisms in the macrophage uptake of chylomicron remnants-like particles" will be published in Biochemical Society Transaction (21).

References

1. Gerrity R. The role of the monocytes in atherogenesis: I. Transition of blood-borne monocytes into foam cells in fatty lesions. *Am J Pathol* 1981;103:181-90.
2. Steinberg D. Low density lipoprotein oxidation and its pathobiological significance. *J Biol Chem* 1997;272:20963-6.
3. Rapp JH, Lespine A, Hamilton RL, Colyvas N, Chaumeton AH, Tweedie-Harman J, Kotite L, Kunitake ST, Havel RJ, Kane JP. Triglyceride-rich lipoproteins isolated by selective affinity anti-apolipoprotein B immunosorption from human atherosclerotic plaque. *Arterioscler Thromb* 1994;14:1767-74.
4. Kruth HS. Macrophage foam cells and atherosclerosis. *Front Biosci* 2001;6:D429-55.
5. Kruth HS, Jones NL, Huang W, Zhao B, Ishii I, Chang J, Combs CA, Malide D, Zhang WY. Macropinocytosis is the endocytic pathway that mediates macrophage foam cell formation with native low density lipoprotein. *J Biol Chem* 2005;280:2352-60.
6. Napolitano M, Rivabene R, Avella M, Botham KM, Bravo E. The internal redox balance of the cells influences the metabolism of lipids of dietary origin by J774 macrophages: implication for foam cell formation. *J Vasc Res* 2001;38:350-60.
7. Mamo JC, Elsegood CL, Gennat HC, Yu K. Degradation of chylomicron remnants by macrophages occurs via phagocytosis. *Biochemistry* 1996;35:10210-4.
8. Van Lenten BJ, Fogelman AM, Jackson RL, Shapiro S, Haberland ME, Edwards PA. Receptor - mediated uptake of remnant lipoproteins by cholesterol-loaded human monocyte macrophages. *J Biol Chem* 1985;260:8783-8.
9. Koo C, Wernette-Hammond ME, Garcia Z, Malloy MJ, Uauy R, East C, *et al*. Uptake of cholesterol-rich remnant lipoproteins by human monocyte-derived macrophages is mediated by low density lipoprotein receptors. *J Clin Invest* 1988;81:1332-40.
10. Linton MF, Hasty AH, Babaev VR, Fazio S. Hepatic apoE expression is required for remnant lipoprotein clearance in the absence of the low density lipoprotein receptor. *J Clin Invest* 1998;101:1726-36.

11. Elsegood CL, Pal S, Roach PD, Mamo JC. Binding and uptake of chylomicron remnants by primary and THP-1 human monocyte-derived macrophages: determination of binding proteins. *Clin Sci* 2001;101:111-9.

12. Fujioka Y, Cooper AD, Fong LG. Multiple processes are involved in the uptake of chylomicron remnants by mouse peritoneal macrophages. *J Lipid Res* 1998;39:2339-49.

13. Napolitano M, Bravo E. Evidence of dual pathways for lipid uptake during chylomicron remnant like-particles processing by human macrophages. *J Vasc Res* 2006;43:355-66.

14. Mendez AJ, Cabeza C, Hsia SL. A fluorometric method for the determination of triglycerides in nanomolar quantities. *Anal Biochem* 1986;156:386-9.

15. Gamble W, Vaughan M, Kruth HS, Avigan J. Procedure for determination of free and total cholesterol in micro- or nanogram amounts suitable for studies with cultured cells. *J Lipid Res* 1978;19:1068-70.

16. Rosenfeld ME, Butler S, Ord VA, Lipton BA, Dyer CA, Curtiss LK, Palinski W, Witztum JL. Abundant expression of apoprotein E by macrophages in human and rabbit atherosclerotic lesions. *Arterioscler Thromb* 1993;13:1382-9.

17. Namatame I, Tomoda H, Arai H, Inoue K, Omura S. Complete inhibition of mouse macrophage-derived foam cell formation by triacsin. *J Biochem* 1999;125:319-27.

18. Fruchart JC, Brewer HB Jr, Leitersdorf E. Consensus for the use of fibrates in the treatment of dyslipoproteinemia and coronary heart disease. Fibrate Consensus Group. *Am J Cardiol* 1988;81:912-7.

19. Devaraj S, Vega G, Lange R, Grundy SM, Jialal I. Remnant-like particle cholesterol levels in patients with dysbetalipoproteinemia or coronary artery disease. *Am J Med* 1998;104:445-50.

20. Skarlatos SI, Dichek HL, Fojo SS, Brewer HB, Kruth HS. Absence of triglyceride accumulation in lipoprotein lipase-deficient human monocyte-macrophages incubated with human very low density lipoprotein. *J Clin Endocrinol Metab* 1993;76:793-6.

21. Napolitano M, Bravo E, Rani R, Kruth H. Apolipoprotein-E independent mechanisms in the macrophage uptake of chylomcron remnants-like particles. *Biochem Soc Trans* (accepted for publication).

Session 3. Plenary lecture

CALORIE RESTRICTION AND AGING IN HUMANS

Luigi Fontana (a,b)
(a) Department of Food Safety and Veterinary Public Health, Istituto Superiore di Sanità, Rome, Italy
(b) Division of Geriatrics and Nutritional Sciences and Center for Human Nutrition, Washington University School of Medicine, St. Louis, Missouri, USA

Overeating and a sedentary lifestyle have led to an epidemic of obesity and type 2 diabetes (1). The detrimental effects of obesity, particularly abdominal obesity, include insulin resistance, dyslipidemia, high blood pressure, chronic inflammation, increased oxidative stress, and changes in levels of growth factors and hormones (2). These and other pathophysiological effects of excess calorie intake/abdominal obesity result in acceleration of aging and a marked increase in aging associated diseases including cardiovascular diseases, cancer, type 2 diabetes and hypertension (3-7).

In contrast to these harmful effects of overeating, restriction of calorie intake has a wide range of benefits. Diet-induced weight loss in obese subjects decreases body fat, increases insulin sensitivity, decreases blood pressure, improves lipid profile, reduces bioavailable sex hormones and growth factors, decreases inflammation, protein glycation, and oxidative stress (8-11). In contrast, removal of large amounts of body fat by liposuction does not improve insulin sensitivity, increase serum adiponectin concentration, decrease metabolic risk factors for CHD, or decrease markers of inflammation (12). Therefore, negative energy balance which decreases size of fat cells, decreases free fatty acid release, improves the adipokine profile, and reduces or eliminates ectopic fat is critical for the beneficial metabolic effects in subjects affected by abdominal obesity (13-14).

Studies on laboratory animals and preliminary studies on humans have shown that more severe caloric restriction (without malnutrition) has additional benefits. Calorie restriction (CR) is the most extensively studied and effective intervention for slowing aging, and preventing carcinogenesis in laboratory animals (15,16). In mice and rats calorie restriction has been shown to prevent/delay many chronic diseases and to extend maximal lifespan up to 50% (15,16). If long-term CR with adequate nutrition promotes longevity in healthy human beings is not known. However, there are mounting evidences suggesting that this is an achievable goal also in humans. In a Scandinavian study of twins it has been calculated that the heritability of average life expectancy to be 20% to 30%; environmental differences accounted for at least 70% of the variations in age at death for the sets of twins studied (17). Secondly, observational studies of the inhabitants of the Okinawa island, that were eating approximately 30% less calories than the average Japanese, had 3 times more centenarians and a clear reduction in mortality rates related to cardiovascular disease and cancer than the average Japanese individuals (18). Finally, several recent epidemiological and experimental studies suggest that many of the metabolic, hormonal and structural changes that take place in CR rodents and monkeys occur also in healthy lean and overweight human beings practicing CR. These studies demonstrate that CR has a powerful protective effect against the major causes of secondary aging in humans, including atherosclerosis, obesity, type 2 diabetes, inflammation and hypertension (19-24). These effects of CR on secondary aging are mediated by beneficial effects on a number of major cardiovascular risk factors, which usually increase with advancing age. These include marked reductions in abdominal fat, blood pressure, serum glucose, serum insulin, total cholesterol,

LDL cholesterol, triglyceride and C-reactive protein levels (19-24). Some markers of longevity, and some metabolic and hormonal factors related to longevity in CR rodents are also positively altered by CR in humans. CR reduces body temperature, resting metabolic rate, and markers of oxidative stress in overweight subjects (25,26). CR improves diastolic function, a marker of primary aging (27). CR reduces growth factors, pro-fibrotic molecules and cytokines, including serum concentration of PDGF, TGF-beta and TNF-α (21,27). Long-term CR with adequate nutrition in healthy lean and weight-stable subjects is also associated with sustained low serum T3 concentration, similar to that found in CR rodents and monkeys (28). This effect is likely due to CR itself, rather than a decrease in body fat mass, and could be involved in slowing the rate of aging in humans as well.

In conclusion, whether or not CR increases maximal lifespan in humans remains, and probably will remain, an unanswered question. However, preliminary evidence suggests that humans develop some of the same adaptations to CR that occur in rats and mice. They include decreases in metabolic rate, oxidative stress, chronic inflammation and growth factors. These are among the adaptations that have been hypothesized to mediate the slowing of aging and protection against neoplasia by CR in rodents. CR in humans also has powerful protective effects against disease processes responsible for secondary aging, including atherosclerosis, type 2 diabetes and hypertension. It is anticipated that these studies will stimulate additional investigation of the effects of CR in humans. Measuring tissue specific effects of CR using genomic, proteomic and metabolomic techniques will foster the development of an understanding of the complex biological processes involved in the anti-aging effects of CR. Further elucidating the mechanisms that control longevity will be a major step in understanding the age-dependency of a range of chronic human diseases, and will help to improve the quality of life in old age.

References

1. Adams KF, Schatzkin A, Harris TB, Kipnis V, Mouw T, Ballard-Barbash R, Hollenbeck A, Leitzmann MF. Overweight, obesity, and mortality in a large prospective cohort of persons 50 to 71 years old. *N Engl J Med* 2006;355(8):763-78.
2. Montague CT, O'Rahilly S. The perils of portliness: causes and consequences of visceral adiposity. *Diabetes* 2000;49(6):883-8.
3. Kloting N, Bluher M. Extended longevity and insulin signaling in adipose tissue. *Exp Gerontol* 2005;40(11):878-83.
4. Lau DC, Dhillon B, Yan H, Szmitko PE, Verma S. Adipokines: molecular links between obesity and atherosclerosis. *Am J Physiol Heart Circ Physiol* 2005;288(5):H2031-41.
5. Calle EE, Kaaks R. Overweight, obesity and cancer: epidemiological evidence and proposed mechanisms. *Nat Rev Cancer* 2004;4(8):579-91.
6. Busby MJ, Bellantoni MF, Tobin JD, Muller DC, Kafonek SD, Blackman MR, Andres R. Glucose tolerance in women: the effects of age, body composition, and sex hormones. *J Am Geriatr Soc* 1992;40(5):497-502.
7. Rahmouni K, Correia ML, Haynes WG, Mark AL. Obesity-associated hypertension: new insights into mechanisms. *Hypertension* 2005;45(1):9-14.
8. Sjostrom CD, Peltonen M, Wedel H, Sjostrom L. Differentiated long-term effects of intentional weight loss on diabetes and hypertension. *Hypertension* 2000;36:20-5.
9. Dattilo AM, Kris-Etherton PM. Effects of weight reduction on blood lipids and lipoproteins: a meta-analysis. *Am J Clin Nutr* 1992;56:320-8.

10. Ziccardi P, Nappo F, Giugliano G, Esposito K, Marfella R, Cioffi M, D'Andrea F, Molinari AM, Giugliano D. Reduction of inflammatory cytokine concentrations and improvement of endothelial functions in obese women after weight loss over one year. *Circulation* 2002;105:804-9.

11. Davi G, Guagnano MT, Ciabattoni G, Basili S, Falco A, Marinopiccoli M, Nutini M, Sensi S, Patrono C. Platelet activation in obese women: role of inflammation and oxidant stress. *JAMA* 2002;288(16):2008-14.

12. Klein S, Fontana L, Young VL, Coggan AR, Kilo C, Patterson BW, Mohammed BS. Absence of an effect of liposuction on insulin action and risk factors for coronary heart disease. *N Engl J Med* 2004;350(25):2549-57.

13. Unger RH. Lipotoxic diseases. *Annu Rev Med* 2002;53:319-36.

14. Poirier P, Giles TD, Bray GA, Hong Y, Stern JS, Pi-Sunyer FX, Eckel RH, American Heart Association, Obesity Committee of the Council on Nutrition, Physical Activity, and Metabolism. Obesity and cardiovascular disease: pathophysiology, evaluation, and effect of weight loss: an update of the 1997 American Heart Association Scientific Statement on Obesity and Heart Disease from the Obesity Committee of the Council on Nutrition, Physical Activity, and Metabolism. *Circulation* 2006;113(6):898-918.

15. Weindruch R, Sohal RS. Caloric intake and aging. *N Engl J Med* 1997;337:986-94.

16. Masoro EJ. Overview of caloric restriction and ageing. *Mech Ageing Dev* 2005;126:913-22.

17. Ljungquist B, Berg S, Lanke J, McClearn GE, Pedersen NL. The effect of genetic factors for longevity: a comparison of identical and fraternal twins in the Swedish Twin Registry. *J Gerontol A Biol Sci Med Sci* 1998;53:M441-6.

18. Kagawa Y. Impact of Westernization on the nutrition of Japanese: changes in physique, cancer, longevity and centenarians. *Prev Med* 1978;7:205-17.

19. Walford RL, Harris SB, Gunion MW. The calorically restricted low-fat nutrient dense diet in Biosphere 2 significantly lowers blood glucose, total leukocyte count, cholesterol and blood pressure in humans. *Proc Natl Acad Sci USA* 1992;89:11533-7.

20. Verdery RB, Walford RL. Changes in plasma lipids and lipoproteins in humans during a 2-year period of dietary restriction in Biosphere 2. *Arch Intern Med* 1998;158:900-6.

21. Fontana L, Meyer TE, Klein S, Holloszy JO. Long-term calorie restriction is highly effective in reducing the risk for atherosclerosis in humans. *Proc Natl Acad Sci USA* 2004;101:6659-63.

22. Larson-Meyer DE, Heilbronn LK, Redman LM, Newcomer BR, Frisard MI, Anton S, Smith SR, Alfonso A, Ravussin E. Effect of calorie restriction with or without exercise on insulin sensitivity, beta-cell function, fat cell size, and ectopic lipid in overweight subjects. *Diabetes Care* 2006;29(6):1337-44.

23. Racette SB, Weiss EP, Villareal DT, Arif H, Steger-May K, Schechtman KB, Fontana L, Klein S, Holloszy JO. One year of caloric restriction in humans: feasibility and effects on body composition and abdominal adipose tissue. *J Gerontol A Biol Sci Med Sci* 2006;61(9):943-50.

24. Weiss EP, Racette SB, Villareal DT, Fontana L, Steger-May K, Schechtman KB, Klein S, Holloszy JO. Improvements in glucose tolerance and insulin action induced by increasing energy expenditure or decreasing energy intake: a randomized controlled trial. *American Journal of Clinical Nutrition* 2006 (in press).

25. Heilbronn LK, de Jonge L, Frisard MI, DeLany JP, Larson-Meyer DE, Rood J, Nguyen T, Martin CK, Volaufova J, Most MM, Greenway FL, Smith SR, Deutsch WA, Williamson DA, Ravussin E, Pennington CALERIE Team. Effect of 6-month calorie restriction on biomarkers of longevity, metabolic adaptation, and oxidative stress in overweight individuals: a randomized controlled trial. *JAMA* 2006;295(13):1539-48.

26. Fontana L. Excessive adiposity, calorie restriction and aging. *JAMA* 2006;295(13):1577-8.

27. Meyer TE, Kovács SJ, Ehsani AA, Klein S, Holloszy JO, Fontana L. Long-term Caloric Restriction Ameliorates the Decline in Diastolic Function in Humans. *Journal of American Collage Cardiology* 2006;47(2):398-402.

28. Fontana L, Klein S, Holloszy JO, Premachandra BN. Effect of Long-term Calorie Restriction with Adequate Protein and Micronutrients on Thyroid Hormones. *Journal of Clinical Endocrinology & Metabolism* 2006;91:3232-5.

Session 3. Poster

EFFECTS OF NATIVE AND MODIFIED HDL ON PERIPHERAL BLOOD MONONUCLEAR CELLS AND ENDOTHELIAL CELLS

Benedetta Mattioli (a), Giuseppe Danilo Norata (b,c), Maria Giovanna Quaranta (a),
Luciana Giordani (a), Alberico Luigi Catapano (b,c), Marina Viora (a)
(a) Department of Therapeutic Research and Medicines Evaluation, Istituto Superiore di Sanità, Rome, Italy
(b) Dipartimento di Scienze Farmacologiche, Università di Milano, Italy
(c) Centro per lo Studio dell'Aterosclerosi, SISA, Ospedale Bassini, Milano, Italy

Introduction

Several *in vivo* and *in vitro* studies have investigated the role of high density lipoproteins (HDL) in modulating cholesterol metabolism and preventing cardiovascular diseases. It has been shown that HDL protect the artery wall against the development of atherosclerosis and this atheroprotective effect has been attributed in part to the ability of the major protein of HDL, apolipoprotein (apo) A-I, to mobilize cholesterol from arterial macrophages (1). However, HDL is also the major carrier of lipid hydroperoxide in plasma. Therefore, several other mechanisms, including the ability of HDL to inhibit LDL oxidation, may also be atheroprotective. Pathways that oxidize HDL and thereby impair its function might thus contribute to the development of atherosclerosis (2). It is known that damaged lipoproteins are implicated in vascular injury, but little is known on the role of oxidized HDL (oxHDL) in atherogenesis. A body of evidence suggests that behind the role in reverse cholesterol transport, oxHDL similarly to oxLDL, exert several effects on vascular wall cells (3-5). We previously demonstrated that oxLDL also act as modulators of immune system homeostasis down-regulating proliferative response, NK-cell mediated cytotoxic activity, cytokine production and induction of a specific antibody response (6-9). Few data are available at the present on the effects of native HDL (nHDL) and oxHDL on immune function. Here, we investigate whether native and oxidized HDL modulate the proliferative response of normal human peripheral blood mononuclear cells (PBMC) and the differentiation of human DC. Moreover, we investigated whether perturbation in HDL metabolism affects vascular wall gene expression.

Materials and methods

Treatments

HDL subfraction 3 (d 1.125-1.21 g/mL) was obtained from freshly isolated human plasma by preparative ultracentrifugation and dialyzed in PBS containing 0.01% EDTA. HDL_3 (1 mg protein/ml) was oxidized with 20 μM $CuSO_4$ for 24 hours at 37°C. The oxidation was blocked by the addition of 40 μM butylated hydroxytoluene (BHT). The levels of oxidation were evaluated by TBARS determination. In all experiments performed, HDL and oxHDL were used at concentration of 0.12 mg/ml and added at the beginning of the culture period and left throughout.

Cell cultures

Human PBMC were isolated by Ficoll-Hypaque gradient separation of buffy coats obtained from healthy volunteer blood donors by the Transfusion Center of Università degli Studi "La Sapienza" Rome. DC were generated from monocytes purified from PBMC by positive selection using magnetic cell separation columns and CD14 Microbeads (Miltenyi Biotec). Highly enriched monocytes (>95%CD14+) were cultured with 250 ng/ml GM-CSF and 500U/ml IL-4 for 5 days. Untreated immature DC (iDC) were used as controls. Mature DC (mDC) were obtained by a 24h incubation with 200 ng/ml lipopolysaccharide (LPS).

Human umbilical vein endothelial cells (HUVECs) were isolated as described (10) and cultured under standard conditions in medium M-199 containing 20% FCS (fetal calf serum), heparin (15 U/ml) and ECGF (endothelial cell growth factor, 20 μg/ml) (Roche, Italy). The cells were used within the 4th passage. Cells were plated in 6-well plates and used after 48 hours as subconfluent cultures. In all experiments, cells were preincubated with serum-free medium for 6 hours, and then native or Ox-HDL3 were added for different times. Cells were incubated in the presence or absence of compounds with appropriate chemicals or vehicle additions (DMSO, 0.1% vol/vol).

Flow cytometry

Cell staining was performed using mouse monoclonal antibodies FITC- or PE-conjugate. The following mAbs were used: CD14 (IgG1, PE), CD1a (IgG1, FITC), HLA-DR (IgG2a, FITC), HLA-ABC (IgG1, FITC), CD80 (IgG1, FITC), CD86 (IgG1, FITC); CD83 (IgG2b, PE), (all from Pharmingen). Samples were analyzed using a FACScan flow cytometer and CellQuest software (Becton Dickinson).

Proliferative response

PBMC were resuspended at $1x10^6$/ml and stimulated with 10 mg/ml PHA. After 3 days, the cultures were pulsed for 18 h with 0.5 mCi/well of [^{3}H]. Cells were then harvested and TdR incorporation was measured by liquid scintillation spectroscopy.

Real Time quantitative RT-PCR

Total RNA was extracted and underwent reverse transcription as described (11). Three μL of cDNA were amplified by real-time quantitative PCR with 1X Syber green universal PCR mastermix (Biorad). The primers used, the amplicon size and the melting temperature have been published elsewhere (11). Each sample was analyzed in duplicate using the IQTM-Cycler (Biorad). The PCR amplification was related to a standard curve ranging from 10-11 M to 10-14 M.

Immunoblotting

Cox-1 and Cox-2 expression was investigated as described (12). Briefly, cells were plated in 6-well plates and treated with Ox-HDL3 or native HDL3 for 5 to 40 minutes, then lysed using a Tris-glycine buffer (0.25 M Tris, 0.173 M glycine) containing 3% SDS and 1 mM PMSF. Aliquots of the samples (15 μg) were loaded on a 12% SDS-PAGE and analysed by Western Blot using anti-Cox-1 and anti-Cox-2 antibodies. Immunocomplexes were detected by an

enhanced chemiluminescence method (ECL, Amersham, Italy), followed by autoradiography and quantified by the Image program (NIH 1.52).

Transfection assay

Transfection experiments were performed in CHO cells, a cell line widely used for studies involving the effects of HDL *in vitro* (11). CHO cells were transiently transfected with Cox-2 (nucleotide –327/+59), the NF-kB mutated site (KBM) or the CRE mutated site (CRM) luciferase reporter vectors using a calcium phosphate precipitation method as described (11). Luciferase activity was determined and normalized the β-gal activity of the cotransfected pRSV-galactosidase construct.

Results

oxHDL induce changes in DC phenotype

To investigate whether nHDL or oxHDL induce phenotypic differentiation of human DC, iDC and mDC were cultured with nHDL or oxHDL for 24 h and then analysed for the following surface molecule expression: CD1a and HLA class I and II molecules (HLA-ABC and HLA-DR) involved in the presentation of lipidic and antigenic peptides respectively, the costimulatory/signaling molecules CD86 and CD80, and the maturation antigen CD83. Despite some variability between donors, there was no consistent modulation of any marker in response to nHDL both in iDC and mDC (data not shown). On the other hand oxHDL induce a down-regulation of the expression of HLA-ABC and HLA-DR and CD83 in mDC (Figure 1) while have no effects on iDC (data not shown).

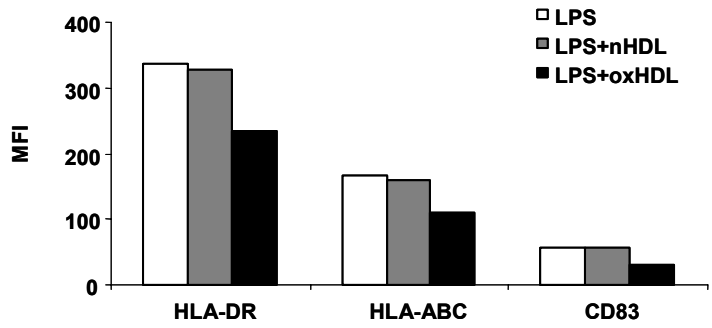

Figure 1. Effects of *in vitro* nHDL and oxHDL exposure on mDC phenotype

nHDL or oxHDL do not interfere PBMC proliferative response

We examined the effects of nHDL or oxHDL, added at the beginning of the culture and left throughout the culture period, on PHA-induced proliferation of normal human PBMC, and we

found that both nHDL and oxHDL do no interfere with the proliferative response (data not shown).

oxHDL induce Cox-2 expression in endothelial cells

Modified HDL have been suggested to modulate endothelial expression of pro-inflammatory genes. Since oxHDL has been found in atheromatous plaques and receptors for modified HDL are present on endothelial cells, we investigated the effect of oxHDL on the expression of Cox-1 or Cox-2. OxHDL, increase Cox2 mRNA and protein expression in endothelial cells while no effect on Cox-1 expression is observed (Figure 2).

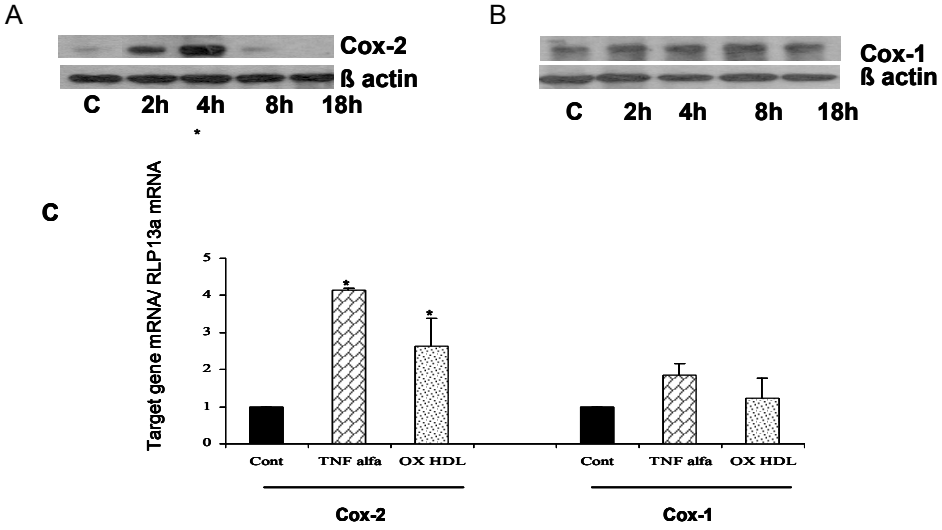

Figure 2. Effects of oxHDL on the expression of Cox-1 or Cox-2

To investigate the role of ERK1/2 and p38 MAPK and PI3K/Akt pathways in Cox-2 expression induced by oxHDL, cells were preincubated with the MEK1 inhibitor U0126, the p38 MAPK inhibitor SB 203580 and the PI3K inhibitor LY 294002 for 1 hour; oxHDL (30 μg/mL) were then added for 2 and 4 hours to evaluate Cox-2 mRNA and protein expression (Figure 3a-3b). U0126 was unable to block oxHDL induced Cox-2 expression. SB 203580 partially inhibited oxHDL-induced Cox-2 expression while LY 294002 completely abolished oxHDL induced Cox-2 mRNA expression and partially inhibited protein expression. No effect of SB 203580 and LY 294002 was observed on Cox-1 protein expression. Next we examined the effects of oxHDL on the Cox-2 promoter activity (Figure 4). The human Cox-2 promoter region (-327/+59) contains the NF-kB, the NF-IL6 and the CRE sites. Transient transfection assay showed that oxHDL induced promoter activity by 199 ±27%. PMA, used as positive control, induced promoter activity by 218 ±35% while LPS induced promoter activity by 160 ±29%. Upon incubation with oxHDL, the promoter activity of the construct carrying the mutation at the NF-kB site was 140 ±48%, that of the construct carrying the mutation at the NF-IL6 site was 71 ±26%. Upon incubation with PMA the promoter activity of the construct carrying the mutation at the NF-kB site was 155 ±14%, that of the construct carrying the

mutation at the NF-IL6 site was 93 ±13%; finally upon incubation with LPS the promoter activity of the construct carrying the mutation at the NF-kB site was 156 ±24%, that of the construct carrying the mutation at the NF-IL6 site was 83 ±32% (Figure 4), thus suggesting a major role of the NF-IL6 site on the effect observed.

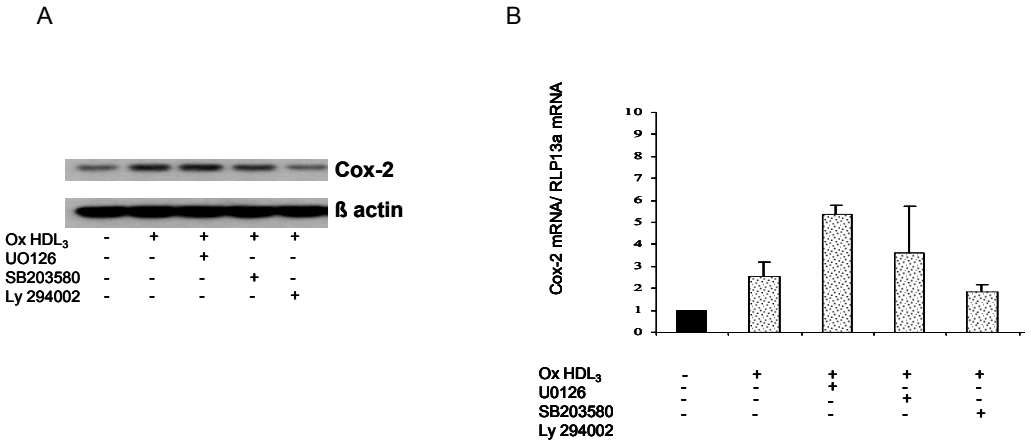

Figure3. PI3K is involved in the oxHDL-dependent Cox-2 induction

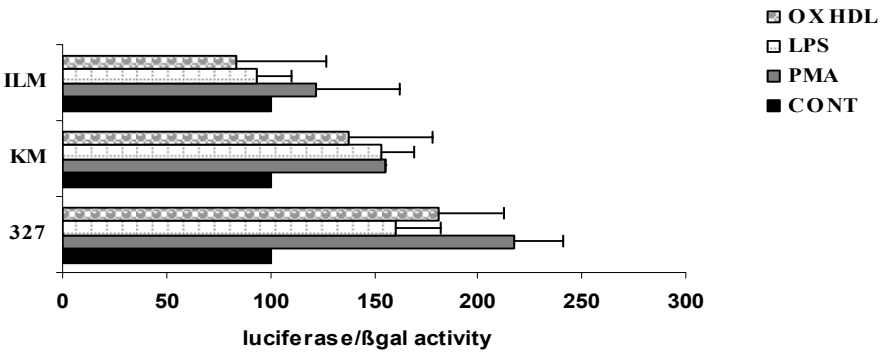

Figure 4. The response elements NF-IL6 is involved in oxHDL-mediated Cox-2 expression

Conclusions

It has been established that the innate and adaptive immune response are involved in pathogenesis of atherosclerosis and both proatherogenic and atheroprotective effects of immune activation can be demonstrated. In this study we investigate the effects of nHDL and oxHDL on immune functions PBMC, DC and endothelial cells. Our findings suggest that nHDL and

oxHDL do not affect PBMC proliferative response while oxHDL induce changes in DC phenotype. Furthermore, the induction by oxHDL of Cox-2 expression in endothelial cells through a PI3K/NF-IL6 dependent pathway, suggests an involvement of these lipoproteins in vascular wall inflammation.

This work was supported by a grant from ISS-NIH collaboration program to MV.

References

1. Bergt C, Pennathur S, Fu X, Byun J, O'Brien K, McDonald TO, Singh P, Anantharamaiah GM, Chait A, Brunzell J, Geary RL, Oram JF, Heinecke JW. The myeloperoxidase product hypochlorous acid oxidizes HDL in the human artery wall and impairs ABCA1-dependent cholesterol transport. *Proc Natl Acad Sci U S A* 2004;101(35):13032-7.
2. Navab M, Anantharamaiah GM, Fogelman AM. The role of high-density lipoprotein in inflammation. *Trends Cardiovasc Med* 2005;15(4):158-61.
3. Norata GD, Pirillo A, Catapano AL. Modified HDL: biological and physiopathological consequences. *Nutr Metab Cardiovasc Dis* 2006;16(5):371-86.
4. Callegari E, Norata GD, Inoue H, Catapano AL. Oxidized-HDL3 modulates the expression of Cox-2 in human endothelial cells. *Int J Mol Med* 2006;18(1):209-13.
5. Norata GD, Banfi C, Pirillo A, Tremoli E, Hamsten A, Catapano AL, Eriksson P. Oxidised-HDL3 induces the expression of PAI-1 in human endothelial cells. Role of p38MAPK activation and mRNA stabilization. *Br J Haematol* 2004;127(1):97-104.
6. Viora M, Straface E, Di Genova G, Fattorossi A, Rivabene R, Camponeschi B, Masella R, Malorni W. Oxidized low density lipoproteins impair peripheral blood mononuclear cell proliferation and cytokine production. *Biochem Biophys Res Commun* 1997;232(2):359-63.
7. Malorni W, Straface E, Di Genova G, Fattorossi A, Rivabene R, Camponeschi B, Masella R, Viora M. Oxidized low-density lipoproteins affect natural killer cell activity by impairing cytoskeleton function and altering the cytokine network. *Exp Cell Res* 1997;236(2):436-45.
8. Viora M, Quaranta MG, Straface E, Vari R, Masella R, Malorni W. Redox imbalance and immune functions: opposite effects of oxidized low-density lipoproteins and N-acetylcysteine. *Immunology* 2001;104(4):431-8.
9. Giordani L, Mattioli B, Quaranta MG, Giacomini E, Libri I, Vari R, Masella R, Viora M. Mildly oxidized low-density lipoprotein inhibits the in vitro induction of the specific antibody response to Candida albicans. *Free Radic Biol Med* 2005;39(7):960-9.
10. Norata GD, Callegari E, Marchesi M, Chiesa G, Eriksson P, Catapano AL. High-density lipoproteins induce transforming growth factor-beta2 expression in endothelial cells. *Circulation* 2005;111:2805-11.
11. Norata GD, Callegari E, Inoue H, Catapano AL. HDL3 induces cyclooxygenase-2 expression and prostacyclin release in human endothelial cells via a p38 MAPK/CRE-dependent pathway: effects on COX-2/PGI-synthase coupling. *Arterioscler Thromb Vasc Biol* 2004;24:871-7.
12. Norata GD, Pirillo A, Pellegatta F, Inoue H, Catapano AL. Native LDL and oxidized LDL modulate cyclooxygenase-2 expression in HUVECs through a p38-MAPK, NF-kappaB, CRE dependent pathway and affect PGE2 synthesis. *Int J Mol Med* 2004;14:353-9.

Session 3. Poster

PROTECTIVE EFFECTS, ABSORPTION AND BIOAVAILABILITY OF BIOPHENOLS CONTAINED IN MEDITERRANEAN DIET COMPONENTS ASSOCIATED WITH A DECREASED RISK OF CARDIOVASCULAR DISEASES

Roberta Masella, Claudio Giovannini, Beatrice Scazzocchio, Carmela Filesi, Massimo D'Archivio, Carmela Santangelo, Rosaria Varì, Roberta Di Benedetto
National Centre for Food Quality and Risk Assessment. Istituto Superiore di Sanità, Rome, Italy

Introduction

Several epidemiological studies have demonstrated that the incidence of coronary heart disease and cancer is lower in the Mediterranean area than in other Western countries. This finding has been attributed to the Mediterranean diet, based on foods containing high amounts of vitamins and phenolic compounds with antioxidant activity. Reactive oxygen species (ROS) from both exogenous and endogenous sources may be, indeed, involved in the aetiology of several human chronic-degenerative diseases, such as coronary artery disease, diabetes, obesity and cancer. Several *in vitro* studies have demonstrated the efficacy of phenolic compounds in counteracting oxidative stress, by acting as scavenger of free radicals, chain breaker of peroxidative reactions and chelator of metal ions. Human and animal studies have suggested that olive oil consumption may increase the resistance to oxidation of circulating LDL, and that some olive oil simple biophenols, such as hydroxytyrosol and tyrosol, are absorbed and excreted with urine (1). In addition biophenols could exert indirect protective actions, such as: i) stimulating endogenous antioxidative defences (glutathione and its related enzymes) (2); ii) inhibiting the synthesis of inflammatory cytokines and the activity of enzymes involved in inflammation; and iii) inhibiting platelet aggregation (3).

Despite the wide body of evidence linking the *in vitro* properties of olive oil biophenols with positive health outcomes, there are limited data on their effective mechanisms of action *in vivo*, and their biological fate after consumption, i.e. their intestinal absorption, bioavailability and metabolism.

Aim of the study

We have previously demonstrated that extra virgin olive oil biophenols such as oloeuropeine and protocatechuic acid: i) inhibited cell-mediated oxidation of LDL, involved in the pathogenesis of atherosclerosis, ii) increased antioxidant cell defences by acting on gene expression of glutathione-related enzymes and that iii) these effects were related to their capability to penetrate inside cells (2).

The aim of this study was to compare the protective effects exerted by two other EVOO compounds, i.e. tyrosol and hydroxytyrosol, similar in chemical structure but greatly different in antioxidant power (Figure 1).

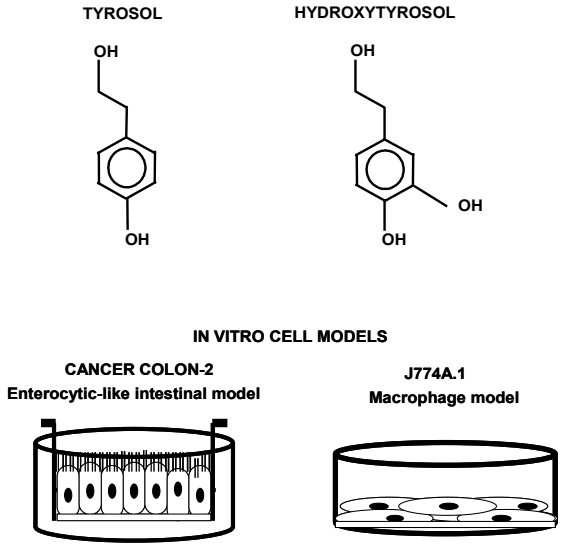

Figure 1. Chemical structure of the EVOO poliphenols and the *in vitro* cell models

In particular, we studied their bioavailability and efficacy in preventing the development of cell-poor, lipid-rich cores of advanced atherosclerotic plaques. To this purpose the degree of antioxidant activity, the mechanisms of action and the cellular uptake and fate, were studied in macrophage J774 A.1 cells throughout cell-mediated oxidation of LDL.

Moreover we studied intestinal absorption and systemic secretion of the two phenolic compounds in intestinal Caco-2 cells, which, *in vitro*, spontaneously undergo full differentiation with enterocyte-like features. Thus, they are suitable to evaluate effects, absorption and metabolism of nutrients on intestinal epithelial cells. Because intestinal mucosa consists of cells that differ in stages of differentiation, Caco-2 cells were used both undifferentiated and differentiated.

Methods

J774 A.1 Cell culture. J774 A.1 cells ($5x10^5$) were seeded in a 25 cm^2 flask and grown in RPMI 1640 medium containing 0.2 mM/L glutamine, 10 U/ml antibiotics and 10% FCS at 37°C, 5% CO_2.

LDL isolation. LDL was isolated from pooled fresh plasma of healthy volunteers by density gradient ultracentrifugation in vertical rotor (Beckman Vti 50) and then dialysed with a centrifugal filter device with a molecular weight cut-off of 5,000 at 4°C as previously described (2).

LDL oxidation by J774 A.1 macrophage-like cell line. $5x10^5$ cells per mL of phenol red-free DMEM, containing 0.2 mM/L glutamine, 10U/ml antibiotics, 2% Ultroser G and LDL (0.2 mg protein), was added to each well in a six-well culture plate and incubated at 37°C in the presence of 2 μmol/L $CuSO_4$ for 6, 12 and 24 hr. The oxidation was stopped by the addition of 1mmol/L EDTA and 20 μM/L BHT. TBARS and relative electrophoretic mobility analyses were performed to evaluate the occurrence of LDL oxidation (data not shown). To evaluate the antioxidant activity of biophenols, tyrosol or hydroxytyrosol at different concentrations (1.5-500μM/L) were added to the cells together with LDL, and left in the medium during all the experimental period.

Determination of total intracellular GSH levels. The intracellular GSH content was evaluated by using 5-chloromethyl-2',7'-dichloro-dihydrofluoresceindiacetate (CM-H_2DCFDA) as previously described (2). Cells exposed to L-buthionine-[S,R]-sulfoximine 7.5 μM/L, a GSH depleting drug, for 16 hours were considered as negative controls. Propidium-iodide (PI)-positive cells were excluded from our analysis.

Glutathione reductase and glutathione peroxidase activities. The enzymatic activities of glutathione reductase (GRed) and glutathione peroxidase (GPx) were measured by colorimetric assays (GR-340, GPx-340, Oxis International).

Extraction of total RNA and semiquantitation by Reverse Transcriptase-Polymerase Chain Reaction (RT-PCR). Total RNA was extracted by the TRIZOL isolation method. The isolated RNA was used for reverse transcription polymerase chain reaction (RT-PCR) analysis. PCR was performed using the following couples of primers: 5'-GGA CAG CCC TAC GGA GGA AC-3' and 5'-GGC TTG GAA TGT CAC CTG GA-3' for amplification of γglutamylcysteine synthetase (γGCS); 5'-ATG TGG AAC ACA GCA GTG CA-3' and 5'-GTG CAC TTG GAA CTG ATG AG-3' for glutathione reductase (GRed); 5'-CCT CAA GTA CGT CCG ACC TG-3' and 5'-TAG GAG TTG CCA GAC TGC TG-3' for glutathione peroxidase (GPx); 5'-GGA AAG ACT GTT CCA AAA ACA GTG-3' and 5'-GTC TTG GTG CTC TCC ACC TTC CG-3' for amplification of cyclophilin B as housekeeping gene. The samples were incubated in an automated heat-block according to the following parameters: 94°C for 1 min, 58°C for 1 min and 72°C for 2 min (using 31 cycles) for GRed and GPx amplification; 94°C for 30 sec, 65°C for 30 sec and 72°C for 1 min for γGCS (using 35 cycles). The PCR products were electrophoresed on a 1.5% agarose gel containing ethidium bromide. The densitometric analysis was performed by a molecular imager FX.

Measurement of intracellular reactive oxygen species (ROS). Cells were incubated in 490 μl of Hanks' balanced salt solution (HBSS, pH 7.4) with 5 μl of dihydroetidium (DHE) or dihydrorhodamine 123 (DHR123) in polypropylene test tubes for 15 min at 37°C. To exclude PI-positive cells from the analysis of H_2O_2 production, we performed a double staining procedure with DHR123/PI, whereas, to estimate the percentage of dead cells in samples stained with DHE (which emits in FL2 channel like PI) we incubated parallel tubes with PI for 15 min at 37°C.

Caco-2 cell differentiation. Cells, grown in DMEM with 25mM glucose, supplemented with 1% (vol/vol) nonessential aminoacids, 0.58 mg/ml L-glutamine, 5 U/ml penicillin and 5 μg/ml streptomycin, and 10% (vol/vol) fetal bovine serum, and cultured at 37°C in a humidified atmosphere of 5% CO_2 in air, were seeded at $6x10^4$ in 25 mm diameter inserts composed of a cyclopore polyester membrane (pore size 0.45 μm). These chambers were inserted into 6 well-plates. In this type of arrangement, the growing environment was divided in two compartments: the apical (AP) and the basolateral (BL) compartment, separated by a polyester membrane. This culture system simulates an *in vivo* situation, with the upper surface corresponding to the luminal enterocyte surface and lower surface, to the

compartment that is in contact with extracellular matrix and vasa. The polyester membrane is permeable to the medium components and metabolites. However, when the cells reach confluency, they start to differentiate, producing a tight impermeable monolayer which prevents passive diffusion of compounds from the apical to the basolateral compartment (Figure 1). The cells were kept on filters for up to 23 days.

Biophenol uptake and release evaluation. 3 μM hydroxytyrosol and 0.5 mM tyrosol were added to the cells to evaluate the J774 A.1 uptake; while 0.25 mM hydroxytyrosol and 0,25 mM tyrosol were used for Caco-2 cell uptake and release evaluation. After rinsing the cells twice with PBS, the absorbed polyphenols were extracted with 2 ml of methanol for 30 minutes. The extracts, evaporated under N_2, reconstituted in 200μl of mobile phase, and centrifuged at 18,000 g for 5 min, were analyzed by HPLC as previously described (4). In differentiated Caco-2 cells 0.5 ml of the medium from basolateral compartment was mixed for 30 sec with 0.1ml methanol and 0.1ml of 3% acetic acid, centrifuged and injected as described before.

Statistical analysis. The results are expressed as mean ± SEM (standard error of the means) of at least three experiments performed in duplicate. The two groups were compared by Student's t-test. Analysis of variance ANOVA plus Student-Newman-Keuls multiple comparison test were used when more than two groups were compared. Differences were considered significant when $P < 0.05$.

Results and discussion

Effects on macrophage cells

During J774 A.1-mediated oxidation of LDL, redox cell imbalance resulted in ROS overproduction and impairment of cellular antioxidant defences. Both the biophenols are able to preserve GSH content, activities and mRNA expressions of GPx and GRed, and to prevent the reactive expression of γGCS (Figure 2).

Hydroxytyrosol prevented the increase of radicals associated with the oxidative process at every time point tested, while tyrosol counteracted the rise of H_2O_2 and O_2^- only later (Figure 3).

The antioxidative properties of tyrosol, although at a concentration 10^3 higher than hydroxytyrosol, were quite unexpected considering the weak antioxidant power of its chemical structure that did not allow an efficient scavenging of radicals. Interestingly, tyrosol fully prevented ROS overproduction at earlier time (hour 6), like hydroxytyrosol did, when added to the cells for 2 hours and removed before LDL treatment (Figure 4).

These findings were probably related to cell-polyphenol interactions. Experiments aimed to elucidate the different behaviour of the two biophenols were performed. Hydroxytyrosol was as much rapidly found in the cells (1.12±0.05 ng/mg cell protein at min 5) as it declined (70% less at hour 2) until it disappeared at hour 18. Tyrosol was also early detectable, but showed a time-dependent intracellular storage, doubling its concentration from minute 5 to hour 18 (0.68±0.09 and 1.72±0.13 ng/mg cell protein at min 5 and hour 18, respectively) (Figure 5).

These results suggest that the effectiveness of tyrosol in this biological system is tightly related to its capability to penetrate the cells.

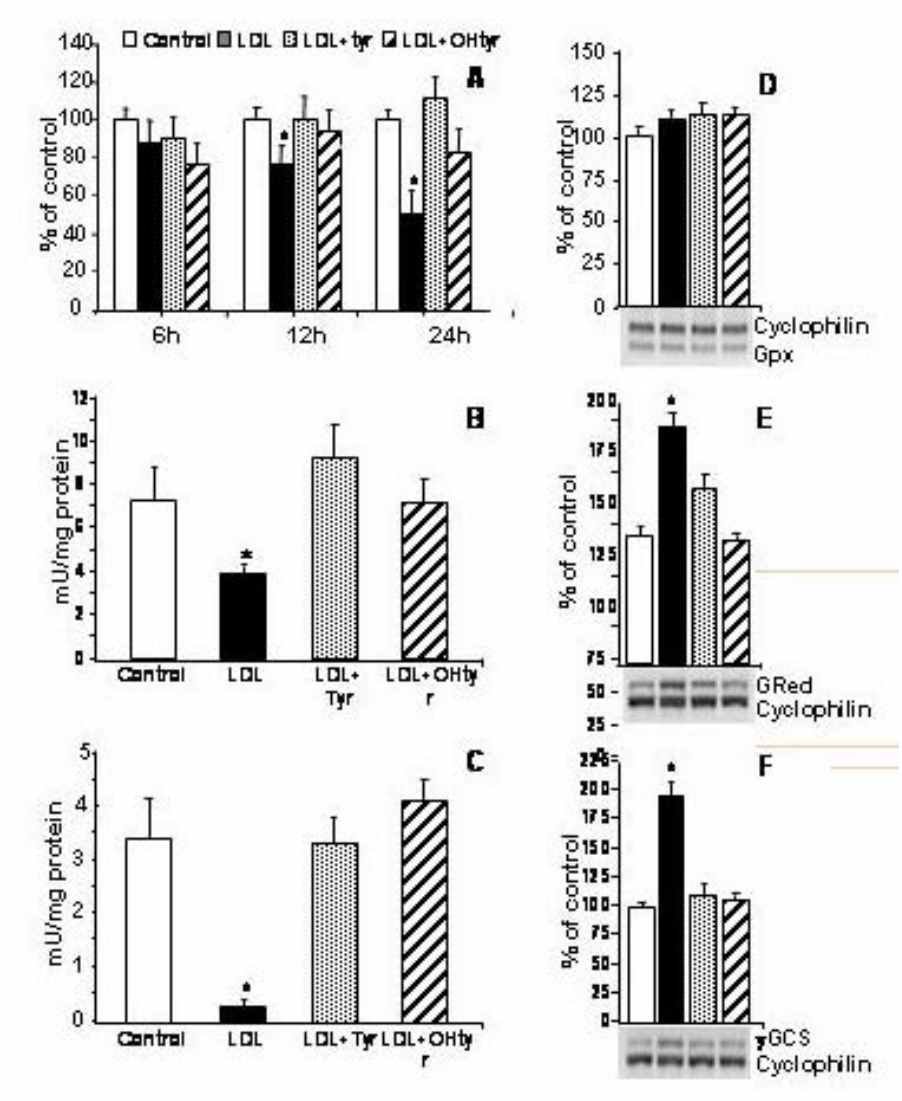

A: Cytofluorimetric analyses of intracellular reduced glutathione after 6,12, and 24 hr incubation of LDL alone and in the presence of 0.5mmol/L tyrosol or 3 µmol/L hydroxytyrosol. Values represent the mean ± SEM (n=4) of the fluorescence intensity histograms obtained in treated cells and compared with those of untreated cells (control) considered as 100%. **B**: GRed and **C**: GPx activities in J774 A.1 cells after 24h incubation with LDL alone and in the presence of tyrosol or hydroxytyrosol. Values, expressed as mU/mg of protein, represent the mean ± SEM of 3 independent experiments performed in duplicate. *P<0.05 vs control, LDL+Tyr, LDL+OHtyr. Semiquantitative RT-PCR evaluation of mRNA for: GPx (**D**), GRed (**E**) and γGCS (**F**) genes in untreated cells (control) and in cells incubated for 24h with LDL alone and with tyrosol or hydroxytyrosol. Values, reported as optical density, are the mean ± SEM of three independent experiments.*P<0.001 vs control, LDL+Tyr, LDL+OHtyr. Representative blots of the experiments are shown. Cyclophillin was used as housekeeping gene.

Figure 2. Effects of biophenols on GSH content and GSH-related enzyme activities and gene expressions in J774 A.1 cells incubated with LDL

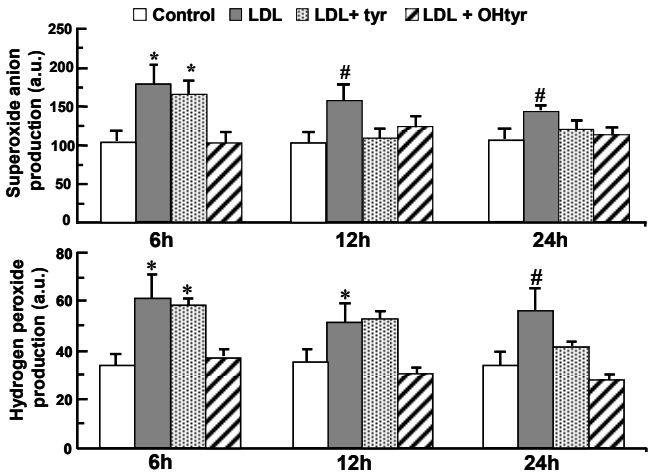

Cytofluorimetric analyses of superoxide anion (A) and hydrogen peroxides (B) production after 6,12 and 24 hr incubation of LDL alone (LDL) and with 0.5mmol/L tyrosol (LDL+Tyr) or 3 µmol/L hydroxytyrosol (LDL+OHtyr). Values reported represent the mean ± SEM of the median values of fluorescence intensity, expressed as arbitrary units (a.u.) of four independent experiments performed in duplicate. *P<0.001 vs control, LDL+OHtyr, # P<0.01 vs control, LDL+Tyr, LDL+OHtyr.

Figure 3. ROS production in J774 A.1 cells during cell-mediated oxidation of LDL.

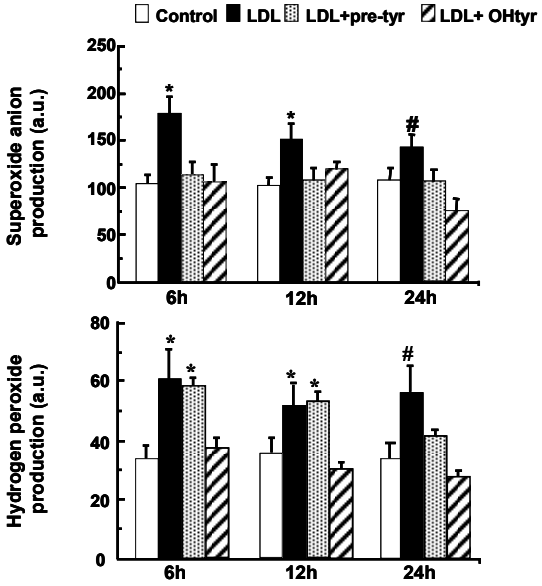

Cytofluorimetric analyses of superoxide anion (A) and hydrogen peroxides (B) production after 6,12 and 24 hr incubation of LDL alone (LDL) and 0.5 mmol/L tyrosol (LDL+pre-Tyr) or 3 µmol/L hydroxytyrosol (LDL+pre-OHtyr) added to the cells for 2 hours and then removed from the culture medium before LDL addition. Values reported represent the mean ± SEM of the median values of fluorescence intensity, expressed as arbitrary units (a.u.) of four independent experiments performed in duplicate. * P<0.001, # P< 0,01 vs control, LDL + pre-Tyr, LDL + pre-OHtyr.

Figure 4. ROS production in J774 A.1 cells preloaded with biophenols

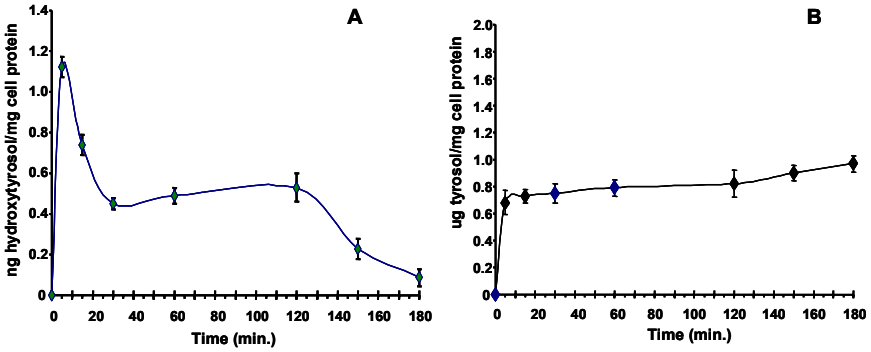

Time-dependent (0-18hr) intracellular content of hydroxytyrosol (A) and tyrosol (B) evaluated by HPLC in J774.A1 cells exposed to 3 µmol/L hydroxytyrosol or 0.5 mmol/L tyrosol. Values represent the mean ± SEM of three independent experiments, expressed as ng (hydroxytyrolsol) or γg (tyrosol) / mg cell protein.

Figure 5. Intracellular determination of biophenol content.

Intestinal cell absorbtion

Differences in cell absorption were also found in intestinal cells. Hydroxytyrosol rapidly penetrate in undifferentiated and differentiated Caco-2 cells as rapidly disappeared after 2 h; on the contrary, tyrosol accumulated inside the cells with the time (Table 1).

Table 1. Biophenol absorption and secretion in undifferentiated and differentiated intestinal cells

UNDIFFERENTIATED CACO-2						
	Biophenol cell uptake (ng/mg prot)					
	15’	30’	2h	18h	36h	48h
Hydroxytyrosol	1.45+0.3	1.51+0.1	1.41+0.4	n.d.	n.d.	n.d.
Tyrosol	244+9	330+0	267+2	73+3	72+3	102+6
DIFFERENTIATED CACO-2						
	Biophenol cell uptake (ng/mg prot)					
	15’	30’	2h	18h	36h	48h
Hydroxytyrosol	1.80+0.2	1.22+0.1	1.60+0.2	n.d.	n.d.	n.d.
Tyrosol	98+26	26+0.7	106+3.4	76+3.6	37+4.8	78+11
	Biophenol cell release (ng/mg prot)					
	15’	30’	2h	18h	36h	48h
Hydroxytyrosol	11.5+1	13.5+2	91+1	10.1+2	n.d.	n.d.
Tyrosol	9.2+1.2	3.8+0.2	15.2+0.4	8.4+0.2	4.3+1	13.3+3

Differentiated Caco-2 cells allowed us to compare cell secretion in basolateral compartment in order to understand the systemic release. Hydroxytyrosol was immediately released indicating a fast passage through the cells, while tyrosol was essentially accumulated inside the cells with a low release in the medium throughout 48h observation (Table 1). These data showed that both the polyphenols easy penetrated into the intestinal cells and were released unmodified.

Conclusions

In conclusion our data showed the effectiveness of hydroxytyrosol in counteracting the oxidative modification of LDL in a biological system, thus confirming its highly antioxidant properties. On the other hand, in spite of its weak antioxidant activity, tyrosol was effecting in preserving cellular antioxidant defences, probably by intracellular accumulation. These data suggest that it may act in several ways. Moreover tyrosol could be mainly involved in the intestinal defence against oxidative insult exerted by diet pro-oxidants, while hydroxytyrosol may be more effective in protecting different body districts. These findings give further evidence in favour of extra virgin olive oil consumption to counteract oxidative stress-based pathologies.

References

1. Marrugat J, *et al*. *Eur J Nutr* 2004;43:140-7.
2. Masella R, *et al*. *J Nutr* 2004;134:785-91.
3. Masella R, *et al. J Nutr Biochem* 2005;16(10):577-86.
4. Di Benedetto R, *et al. Nutr Metab Cardiovasc Dis* 2006 (in press).

Session 3. Poster

PERIPHERAL BLOOD DETERMINANTS OF REDOX CHANGES IN HUMAN RESPIRATORY DISEASES: BIOCHEMICAL AND PATHOPHYSIOLOGICAL EVALUATION

Donatella Pietraforte (a), Lucrezia Gambardella (b), Barbara Ascione (b), Alessio Metere (a), Giuseppe Scorza (a), Gianni Schmidt (c), Enrico Li Bianchi (c), Thomas L Leto (d), Walter Malorni (b), Maurizio Minetti (a)

(a) Department of Cell Biology and Neurosciences, Istituto Superiore di Sanità, Rome, Italy

(b) Department of Therapeutic Research and Medicines Evaluation, Istituto Superiore di Sanità, Rome, Italy

(c) C.U.B.E. Department of Cardiovascular and Respiratory Sciences, University of Rome "La Sapienza" Forlanini Hospital, Rome, Italy

(d) The Molecular Defenses Section, Laboratory of Host Defenses, National Institutes of Health, NIAID, Bethesda, MD, USA.

Introduction

Chronic Obstructive Pulmonary Disease (COPD) is one of the major cause of hospitalization in developed countries and there is evidence that it will become soon the third cause of mortality throughout the world. Inflammation of the airways seems to play an important pathogenetic role in COPD, although the inflammatory mechanism is not well understood as treatment with corticosteroids, which are potent anti-inflammatory agents, does not induce substantial beneficial effects (1). Given the relative ineffectiveness of corticosteroids, and the risk of adverse effects, both new therapeutic strategies and new biomarkers of disease progression are required. COPD, is characterized by a decreased expression of antioxidant enzymes, an increased production of cytokines and an increased or uncontrolled production of toxic free radicals (2-4). There are evidence that under all inflammatory conditions, including COPD, there is an increased production of superoxide ($O_2^{\bullet-}$) and nitric oxide ($^{\bullet}NO$) radicals. Inflammatory cells produce large amount of superoxide through a family of enzymes known as NAD(P)H-oxidases, collectively termed Nox (5-7), whereas the vasodilator nitric oxide is synthesized by specific $^{\bullet}NO$ synthases (NOS). In tissues efficient scavengers of these free radicals are present (superoxide dismutase for superoxide and hemoproteins for nitric oxide) but if $O_2^{\bullet-}$ and $^{\bullet}NO$ interacts they can rapidly combine to form a potent cytotoxic species, peroxynitrite ($ONOO^-$/ONOOH). The principal aim of the project was to identify "real-time biomarkers" of oxidative changes in COPD peripheral blood and to reproduce these oxidative changes *in vitro* by treating normal cells with known radicals or reactive oxygen/nitrogen species. These biomarkers may be of potential prognostic value, while the knowledge of damaging species may suggest new therapies and be transferred in the clinical practice.

Results

Identification of oxidative changes in peripheral COPD erythrocytes and reproduction of the oxidative changes

We evaluate (a) whether the oxidative imbalance can lead to specific alterations of red blood cells (RBCs) from stable COPD patients; (b) whether treatment with N-acetyl-cysteine (NAC), in widespread clinical use as mucolytic agent, can counteract these effects; and (c) whether an *in vitro* model represented by the exposure of RBC to ROS/RNS could mimic the *in vivo* situation. The results obtained clearly indicated that the RBC integrity and function are similarly altered in COPD patients and in ROS/RNS *in vitro*-treated samples. In fact, our results indicate that RBC form COPD patients or control RBC treated with ROS/RNS underwent modifications of morphological and functional parameters such as cytoskeleton rearrangement, ultrastructural alterations and decreased expression of glycophorin A. Moreover, NAC administration was capable of counteracting RBC oxidative modifications both *in vivo*, as detected by clinical and laboratory evaluations, and *in vitro.* Peroxynitrite, in particular, reproduced at least in part the alterations found in COPD RBCs (see for example Figure 1). Overall these results point to RBC oxidative modifications as valuable bioindicators in the clinical management of COPD and indicate that *in vitro* RBC exposure to ROS/RNS as a useful tool in experimental studies aimed at the comprehension of the pathogenic mechanisms of the redox-associated diseases.

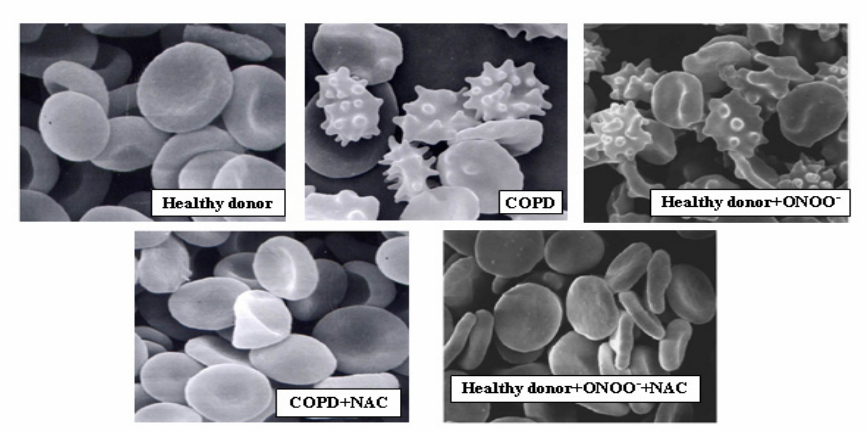

Figure 1. Morphological features of untreated- or $ONOO^-$-treated RBC from healthy donor and COPD patient and counteracting effects of NAC administration (1,8 mg/day) *in vivo*

Modifications induced by peroxynitrite on human red blood cells

We evaluated subcellular effects induced by peroxynitrite on RBC from healthy donors. Peroxynitrite induced 1) oxidation of oxyhemoglobin to methemoglobin, 2) cytoskeleton rearrangement, 3) ultrastructural alterations, and 4) altered expression of band-3 and decreased expression of glycophorin A. With respect to control cells, this occurred in a significantly higher percentage of human RBCs (~40%). The presence of NAC inhibited these modifications. Furthermore, besides these senescence-associated changes, other important modifications,

absent in control RBC and usually associated with apoptotic cell death, were detected in a small but significant subset of peroxynitrite-exposed RBCs (~7%). Active protease cathepsin E and μ-calpain increased (Figure 2, left panel); activation of caspase 2 and caspase 3 was detected (Figure 2, right panel); and phosphatidylserine externalization, an early marker of apoptosis, was observed. Conversely, inhibition of cathepsin E, μ-calpain, as well as caspase 2 and 3 by specific inhibitors (Figure 2) resulted in a significant impairment of erythrocyte "apoptosis." Altogether, these results indicate that peroxynitrite, a milestone of redox-mediated damage in human pathology, can hijack human RBCs toward senescence and apoptosis by a mechanism involving both cysteinyl and aspartyl proteases.

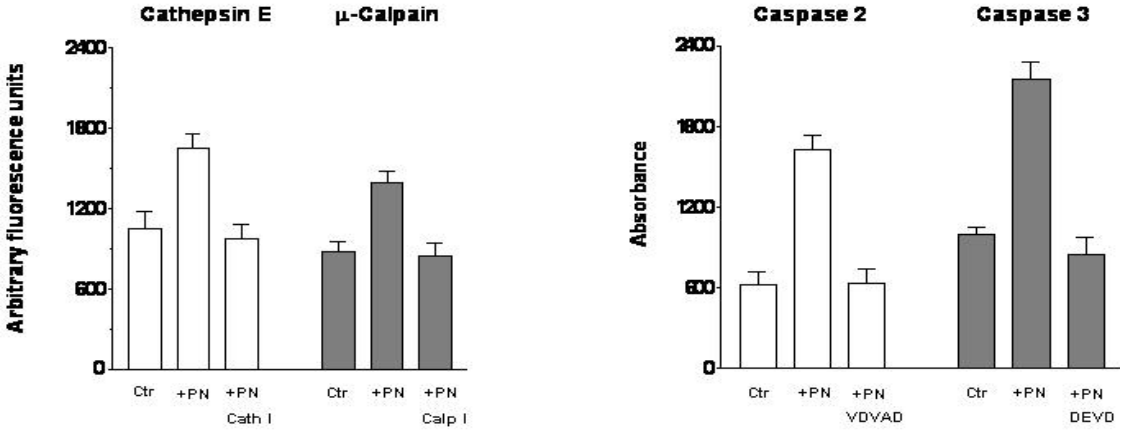

Figure 2. Increase of RBC protease activity induced by peroxynitrite (PN) and effects of the pretreatment with specific protease inhibitors. Cath I: cathepsin E inhibitor; Calp I: μ-calpain inhibitor; VDVAD: caspase 2 inhibitor; DEVD: caspase 3 inhibitor

Two different pathways are involved in peroxynitrite-induced senescence and apoptosis of human erythrocytes

CO_2, which is present in tissues at millimolar concentrations (1-2 mM), changes the biochemistry of peroxynitrite basically in two ways: (i) the oxidant species becomes the $CO_3^{\bullet}$ / $^{\bullet}NO_2$ radical pair, and (ii) peroxynitrite diffusion distance is significantly reduced. For extracellular peroxynitrite and at low cell density this last effect is particularly dramatic because these radicals are short-lived and decay mostly in the extracellular space or at the cell surface/membrane. On the other end, the fraction of peroxynitrite that escapes the CO_2 reaction can cross the RBC membrane and oxidizes intracellular targets with hemoglobin being the preferential target. In consideration of the complex oxidation mechanism of peroxynitrite we used a low cell density with/without CO_2 to distinguish between extra- and intra-cellular modifications induced by peroxynitrite.

Our results show that in the presence of CO_2 (i.e. under conditions of almost complete extracellular peroxynitrite decay) peroxynitrite induced the oxidation of surface thiols, the formation of 3-nitrotyrosine and DMPO adducts and the down-regulation of glycophorins A and C (a biomarker of senescence). Reactivation of glycolysis reversed only the oxidation of surface

thiols (Table 1). Without CO_2 peroxynitrite induced, in addition, the hemoglobin and glutathione oxidation, lactate accumulation, ATP decrease, band 3 clustering, phosphatidyl serine externalization, and caspases 8 and 3 activation (biomarkers of apoptosis). All these last biomarkers were reversed by reactivation of glycolysis (Table 1).

Table 1. Comparison between the effect of CO2 and glucose post-incubation on peroxynitrite-induced RBC modifications

Modification	Effect of CO_2	Reversibilità by D-Glucose
Methemoglobin formation	protective	Yes
ROS formation	protective	Yes
Band 3 clustering	protective	Yes
Annexin V binding	protective	Yes
Caspase 8 activation	protective	Yes
Caspase 3 activation	protective	Yes
Glycophorin A down-regulation	no-protection	No
Glycophorin C down-regulation	no-protection	No
ATP decrease	protective	Yes
GSH oxidation	protective	Yes
Surface Thiol oxidation	no-protection	Yes
Membrane 3-nitrotyrosine	no-protection	No
DMPO-RBC adducts	no-protection	No

The glycophorin A/band 3 and glycophorin C/protein 4.1 macrocomplexes were among the main sites modified by peroxynitrite-derived radicals. We hypothesize that cell senescence could generally be derived by irreversible radical-mediated oxidation of membrane targets, while the appearance of apoptotic biomarkers could be bolstered by oxidation of intracellular targets. Hence, these results suggest that, depending upon extracellular homolysis or diffusion to the intracellular space, peroxynitrite prompts the erythrocyte towards either senescence or apoptosis through different oxidation mechanisms. Interestingly, no proof of apoptotic biomarkers was found in RBCs from COPD patients suggesting that these cells may be removed from circulation.

Discussion

Far from being only a carrier of hemoglobin, the RBC is also one of the major components of blood antioxidant capacity and one of the cells more resistant to oxidative stress. Its very efficient intracellular reducing machinery coupled with its walking across the whole organism makes the erythrocyte an effective "sink" of reactive oxygen/nitrogen species. Probably not only the blood *per se* but, more important, the whole organism can benefit for the scavenging ability of RBCs. On the other end, the scavenging of reactive species leads, among other effects, to the formation of RBCs with redox alterations. Thus, the erythrocyte may be considered a potential "reporter" cell of the redox status of the whole organism. We observed in COPD patients some alteration in the oxidative status suggestive of a damage caused by oxygen/nitrogen reactive species. By treatment of normal RBCs with peroxynitrite, a reactive species likely formed under inflammatory conditions including COPD, we succeeded in reproducing at least some of the alterations of COPD RBCs. In addition, a detailed analysis of peroxynitrite-dependent RBC modifications revealed a complex oxidation mechanism. About

50% of peroxynitrite generated outside the RBC reacts with CO_2 forming two oxidant radicals ($CO_3^{\bullet}$ and $^{\bullet}NO_2$) which modified the cell surface and induced some biomarkers indicative of cell senescence or aging. The remainder 50% of peroxynitrite penetrates the RBC inducing hemoglobin oxidation, activation of glycolysis and the appearance of some biomarkers of apoptosis. Although the RBC does not possess a complete apoptotic machinery, the appearance of apoptotic markers has been detected in pathologic, aged or chemically–treated RBCs (8,9). Our data add a further complexity to the unusual apoptotic process of this anucleated cell: senescence and apoptosis are induced by two different oxidation pathways. Future experiments will be performed to investigate whether the modifications observed in RBCs of COPD patients are due to intra/extracellular oxidations and whether Nox knockout mice could be a useful model to study the etiology of COPD disease.

Interestingly, treatment with NAC, a potent antioxidant and sulfhydryl supplier, not only inhibited the oxidative changes induced by peroxynitrite but significantly reverted RBC oxidative modifications and ameliorated the clinical prognosis in COPD patients.

Altogether our work supports the idea that the RBC features, although intensively studied in the course of the last 50 years, still hide biologic information of great relevance to the comprehension of the Pathogenetic mechanisms of human diseases as well as to the improvement of therapeutic strategies relevant to the maintenance of the total oxidant/antioxidant balance of the whole organism.

References

1. Pauwels R. Inhaled glucocorticosteroids and chronic obstructive pulmonary disease: How full is the glass? *Am J Respir Crit Care Med* 2002;165:1579-80.
2. Barcelo B, Pons J, Fuster A, Sauleda J, Noguera A, Ferrer JM, Agusti AG. Intracellular cytokine profile of T lymphocytes in patients with chronic obstructive pulmonary disease. *Clin Exp Immunol* 2006;145:474-9.
3. Tomaki M, Sugiura H, Koarai A, Komaki Y, Akita T, Matsumoto T, Nakanishi A, Ogawa H, Hattori T, Ichinose M. Decreased expression of antioxidant enzymes and increased expression of chemokines in COPD lung. *Pulm Pharmacol Ther* 2006; in press.
4. Ricciardolo FL, Nijkamp FP, Folkerts G. Nitric oxide synthase (NOS) as therapeutic target for asthma and chronic obstructive pulmonary disease. *Curr Drug Targets* 2006;7:721-35.
5. Geiszt M, Leto TL. The Nox family of NADPH oxidase: Host defense and beyond. *J Biol Chem* 2004;279:51715-8.
6. Ueyama T, Geiszt M, Leto TL. Involvement of Rac1 in activation of multicomponent Nox1- and Nox3-based NADPH oxidases. *Mol Cell Biol* 2006;26:2160-74.
7. Geiszt M, Lekstrom K, Witta J, Baffi J, Leto TL. Dual oxidases represent novel hydrogen peroxide sources supporting mucosal surface host defense. *FASEB J* 2003;17:1502-4.
8. Lang KS, Roll B, Myssina S, Schittenhelm M, Scheel-Walter H-S, Kanz L, Fritz J, Lang F, Huber SM, Wieder T. Enhanced Erythrocyte Apoptosis in Sickle Cell Anemia, Thalassemia and Glucose-6-Phosphate Dehydrogenase Deficiency. *Cell Physiol Biochem* 2002;12:365-72.
9. Bosman GJCGM, Willekens FLA, Werre JM. Erythrocyte Aging: A More than Superficial Resemblance to Apoptosis? *Cell Physiol Biochem* 2005;16:1-8.
10. Matarrese P, Straface E, Pietraforte D, Gambardella L, Vona R, Maccaglia A, Minetti M, Malorni W. Peroxynitrite induces senescence and apoptosis of red blood cells through the activation of aspartyl and cysteinyl proteases. *FASEB J* 2005;19:416-8.

11. Vona R, Gambardella L, Straface E, Matarrese P, Minetti M, Malorni W, Pietraforte D. *Il perossinitrito come induttore di senescenza e apoptosi nell'eritrocita*. Roma: Istituto Superiore di Sanità; 2005 (Rapporti ISTISAN 05/40), p. 80-99.

12. Lucantoni G, Pietraforte D, Matarrese P, Gambardella L, Metere A, Paone G, Li Bianchi E, Straface E. The red blood cell as a bio-sensor for monitoring oxidative imbalance in chronic obstructive pulmonary disease (COPD): an ex vivo and in vitro study. *Antiox Redox Signal* 2006;8:1171-82.

13. Minetti M, Malorni W. The red blood cell as a target and source of pro-oxidant species. *Antiox Redox Signal* 2006;8:1165-9.

14. Pietraforte D, Matarrese P, Straface E, Gambardella L, Metere A, Scorza G, Leto TL, Malorni W, Minetti M. Two different pathways are involved in peroxynitrite-induced senescence and apoptosis of human erythrocytes. *Free Radic Biol Med* (submitted, first revision).

Session 4
INFECTIOUS DISEASES

Session 4. Plenary lecture

THE REGULATION OF MUCOSAL INFLAMMATION THROUGH NOD2 SIGNALING

Ivan J Fuss, Tomohiro Watanabe, Warren Strober
Mucosal Immunity Section, Laboratory of Host Defenses, NIAID, National Institutes of Health, Bethesda, MD, USA

Over the past few years, intense research has been devoted to the study of the innate immune system and how it can be activated by microbial components of the intestinal flora (1). This system of host recognition and response is not limited to microbial receptors such as toll-like receptors (TLR), but also includes the recently discovered family NACH T (2). These include the nucleotide-binding oligomerization domain (NOD) proteins, NACHT-LRR pyrin-domains containing proteins (NALPS). These molecules function in the recognition of microbial components and the subsequent activation of the innate immune system (2,3).

The NOD protein NOD2 (which is encoded by CARD15) recognize peptidoglycan (PGN), a component of bacterial cell walls, and is mainly expressed by two cell types that are exposed to this component under physiological conditions: antigen-presenting cells (APCs) and epithelial cells. So, the study of NOD2 might allow us to improve our understanding of how mucosal cells respond to commensal organisms in the normal gastrointestinal tract. However, a more compelling interest in the function of these proteins arises from the recent discovery that NOD2 has a role in the pathogenesis of human gastrointestinal disease. CARD15 is a susceptibility gene for Crohn's disease (4,5). In this summary, it will focus on the signaling function NOD2, with the aim of clarifying how such signaling contributes to inflammation and host defense. In doing so, we attempt to construct a foundation for understanding how mutations in CARD15 might lead to Crohn's disease.

As mentioned above, NOD2 is a member of the phylogenetically conserved NLR protein family (2,3,6,7), which encompasses proteins that were previously identified as members of the CATERPILLER (CARD, transcription enhancer, R (purine-binding, pyrin, lots of LRRs), NOD, NOD-LRR, and NALP groups of proteins. In general, members of this family share a tripartite domain structure that consists of the following: a carboxy c-terminal LRR domain, which is involved in ligand recognition; a central NOD (also known as a NACHT domain), which facilitates self-oligomerization and has ATPase activity, and an amino (N)-terminal domain that is composed of protein-protein interaction cassettes, such as CARDS or pyrin domains.

Expression of NOD2

In contrast to TLRs which are associated with the plasma membrane, or, in some cases, with lysosomal and/or endosomal vesicles, NOD2 is expressed mainly in the cytosol (3). So, whereas TLRs function as cell-surface receptors, NOD2 does not have this property. However, there is recent evidence that in some instances in epithelial cells, NOD2 contains molecular sequences that allows association with the cell surface plasma membrane (8). This pattern of intracellular expression implies that the ligands for these molecules are not native microbial components per se but, instead, products that are derived from microbial components. Indeed, NOD2 has been

shown to recognize peptides that are derived from the degradation of PGN, which is a component of bacterial cell walls (9,10).

Thus, NOD2 is mainly expressed by two cell types that are exposed to and/or deal with microorganisms that express PGN: APCs and epithelial cells. In both humans and mice, APCs such as macrophages and dendritic cells (DCs) express NOD2, whereas other hematopoietic cells (such as T cells and B cells) do not express these proteins (3,11). However, in other cell types, whereas most intestinal epithelial cells express NOD2 at the mRNA level., expression at the protein level is low or undetectable (12,13) at least using the antibodies that are available at present. In addition, among primary epithelial-cell populations, NOD2 expression seems to be limited to Paneth cells, which are located at the base of the intestinal crypt (14). This concept will be returned to shortly.

The expression of NOD2 can be modulated by proinflammatory cytokines. In the case of NOD2, baseline expression of protein by epithelial cells is low, and TNF induces upregulation of expression, which can be further augmented by IFN-γ (15). NF-κB binding sites in the CARD15 promoter are involved in this response to TNF, implying that, when NOD2 activates NF-κB following activation by it's ligand, NOD2 can upregulate itself.

Signaling pathways involved in NOD2 activation

Bacteria-derived ligands recognized by NOD2. Whereas initial studies identified lipopolysaccharide (LPS) as a NOD2 ligand (5), it is now well established that the NOD2 ligand is the PGN-derived peptide, muramyl dipeptide (MDP) (9,10). Because PGN from both Gram-positive and Gram-negative bacteria contains MDP, NOD2 functions as a general sensor of most bacteria. This specificity for MDP has been confirmed by studies which demonstrate that APC's derived from NOD2 deficient mice are unresponsive to MDP (16).

The NOD-protein ligands need to reach the LRR domains of the respective NOD protein for activation of this protein to be initiated. However, information on how this is accomplished is limited at present. One possibility that relates to phagocytic cells such as macrophages or DCs is that these cells generate the peptide ligands by ingesting whole bacteria and then digesting them in phagolysosomes (17,18).

After small peptides derived from PGN have been released into the cytosol, they are thought to interact with NOD2 through the LRR domains of these molecules. The postulated interactions is then proposed to initiate the activation of NOD2 through the induction of a complex conformational change of the NOD2 molecule (19). The NOD2 protein can then undergo self-oligomerization. In one study, Inohara *et al.* proposed that this oligomerization allows binding to a downstream effector molecule through a CARD-CARD interaction, in this case a serine/threoine kinase named RICK, which subsequently can activate/modulate NF-κB (19,20).

One of the main outcomes of NOD2 activation by it's respective ligands is the activation of NF-κB. Whereas such activation is evident in MDP-stimulated epithelial cells that had been transfected with constructs encoding wild-type NOD2, it was reduced in cells that were transfected with constructs encoding a mutated NOD2 that had alterations in the LRR domain such as those found in Crohn's disease patients (9). This paradoxical finding will be discussed below.

Interrelated roles of NOD2 and TCR signaling

Studies of NOD2 activity in APCs are complicated by the fact that intact PGN is postulated to signal through TLR2, and after uptake of PGN and release into the cytosol, a component of PGN (MDP) can signal through NOD2. So, in theory, it is possible that different molecular forms of the same microbial component can modify each other's function. In a recent study in which interactions between TLRs and NOD2 were examined, such cross-regulation does seem to occur. In particular, it was found that NOD2-deficient splenic macrophages that were stimulated *in vitro* with a wide range of TLR ligands produced markedly more IL-12 than NOD2-sufficient macrophages, but this occurred only when they were stimulated with PGN and not with other TLR ligands (21). By contrast, NOD2-deficient APCs produced normal amounts of TNF and IL-10 when they were stimulated with PGN, indicating that NOD2 does not affect all functions of TLR2. These *in vitro* results were corroborated by *in vivo* studies in which it was shown that NOD2-deficient mice mounted far higher serum IL-12 responses to systemic challenge with PGN than did their wild-type counterparts. A final point is that stimulation of splenocyte populations from NOD2-deficient mice with PGN led to greatly increased IFN-γ-production by T cells, indicating that the increased IL-12 production by the splenocytes of these mice has the expected effect on downstream cytokine production.

A reasonable interpretation of these results is that PGN-mediated activation of TLR2 signaling is negatively regulated by MDP-mediated activation of NOD2 signaling and that, in the absence of NOD2, the negative regulation is released. To test this hypothesis, APCs from NOD2-sufficient and NOD2-deficient mice were stimulated with PGN and increasing concentrations of exogenous MDP. It was observed that this co-stimulation was associated with a dose-dependent inhibition of PGN-induced IL-12 production, but this occurred only in NOD2-sufficient APCs and not in NOD2-deficient APCs.

One clue to how NOD2 might negatively regulate PGN-induced IL-12 production is provided by its effect on nuclear translocation of the NF-κB subunit REL. Although the activation and nuclear translocation of the NF-κB subunits p50 (also known as NF-κB1) and p65 (also known as REL-A) is increased in the absence of NOD2, the activation and nuclear translocation of REL is increased to a far greater extent (21). This specific ability of NOD2 deficiency to increase REL activation correlates with previous findings that both the p35 and the p40 subunits of IL-12 are particularly dependent on the activation of this NF-κB subunit.

It should be noted that the observation that MDP downregulates PGN-mediated signaling through TLR2 has not been correlated by other investigators, including those who have reported studies of mice with *Card15* abnormalities (22,23). For example, in a study of macrophages from a different NOD2-deficient mouse, responses to various TLR ligands were generally equivalent in wild-type and NOD2-deficient mice, and the addition of MDP to TLR2 stimulated cultures resulted in an increase in IL-6 production in wild-type mice but not in NOD2-deficient mice. In addition, these NOD2-deficient mice had a reduced total IgG and IgG1 response to antigen plus MDP, indicating that they have reduced cytokine production by T helper (T_H) cells (22). Moreover, in a study of macrophages from mice carrying a knocked-in gene encoding a NOD2 molecule comparable to that containing the frameshift mutation that is observed in human Crohn's disease, no differences between wild-type and mutated mice were seen after stimulation with various TLR ligands or TLR2 ligand (PGN) plus MDP, except in the case of stimulation with MDP alone, in which IL-1β production was increased. In addition, in this study, IL-12 responses were not increased in mutated mice either in the presence or absence of inflammation (23).

It is important to remember, however, that the observation that co-stimulation of macrophages with PGN and MDP in the study by Watanabe *et al.* leading to decreased IL-12 (especially IL-12 p70) responses was carried out using wild-type mice; thus, this mechanism appears to play a modulatory suppressive role under innate physiologic conditions (21).

Crohn's disease and the importance of NOD2

During the past few years, several genetic studies of large cohorts of patients with Crohn's disease showed that homozygous mutations in CARD15 (which encodes NOD2) accounts for 10-15% of patients with this disease (4,5). These mutations result in frame shift abnormalities. These are all localized to the LRR domain of NOD2 and therefore interfere with its ability to recognize the MDP ligand. So, cells that carry such mutant forms of NOD2 have a reduced capacity to induce NF-κB activation on stimulation with MDP (9).

Our current understanding of how these mutations give rise to susceptibility to Crohn's disease is best discussed in the context of general immunological abnormalities that underlie Crohn's disease in all patients. Briefly, Crohn's disease is a consequence of a disturbance in the normal immunological unresponsiveness of the mucosal immune system to components of the mucosal microflora. The hyper-responsiveness to these components that ensues gives rise to the T_H1-cell-mediated inflammation that underlies the disease. Therefore, building upon the previous concepts presented, three main views of how CARD15 mutations are associated with Crohn's disease are being considered. The first is based on the possibility (21) that NOD2 normally functions as a negative regulator of IL-12 production mediated by PGN through TLR2 (discussed earlier), and in the absence of this regulation, PGN elicits an excessive NF-κB-dependent IL-12 response by APCs that drives the inflammation of Crohn's disease (Figure 1).

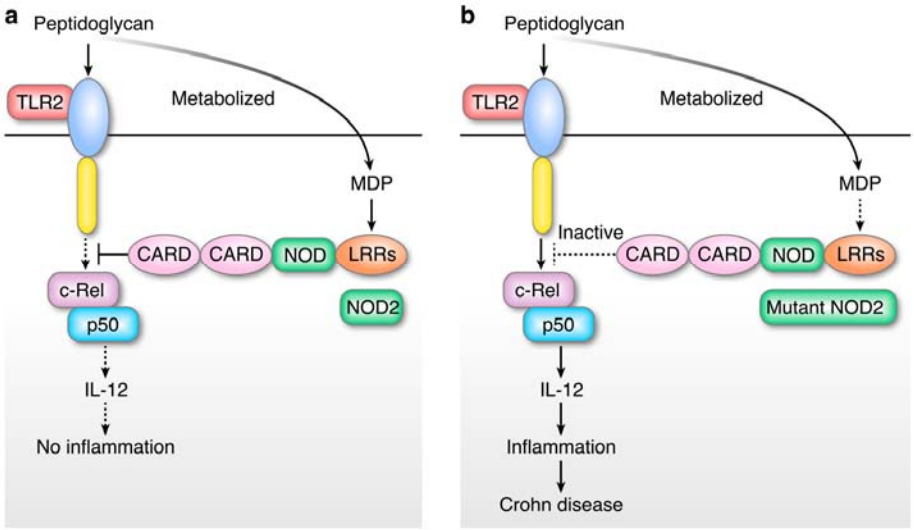

PGN can bind and activate TLR2 which in turn can cause the activation of NFκBcomponents such as c-Rel. This leads to the increased production of IL-12. MDP can bind the NOD2 molecule which can downmodulate this pathway. In Crohn's disease patients the mutations in NOD2 lead to the inability to activate this downmodulatory pathway.

Figure 1. Mechanism of Mucosal Inflammation Secondary to NOD2 Deficiency.

In normal individuals, bacterial penetration "sets the stage" for an innate immune response by PGN; this immune response would be downmodulated secondary to NOD2 modulation, and would therefore be contained by mucosal regulatory T cells. By contrast, in individuals with a CARD15 mutation, the innate immune response to PGN is much stronger, and the resultant IL12 and/or IL-23 production is sufficient to create a milieu that could support T_H1-cell-induced colitis. Therefore, mutated NOD2 leads to the inability to downmodulate an innate immune response (IL-12) that is mediated by a PGN driven TLR 2 response. This then facilitates a strong adaptive Th1 T cell response with ensuing inflammation.

The second model for the role of CARD15 mutations in Crohn's disease alluded to above is based on the role of NOD2 in mucosal host defenses. In this view, the abnormality is located in IECs in that epithelial cells expressing mutated NOD2 have defective activation of NF-κB on stimulation with MDP (9), as well as a reduced capacity to restrict proliferation of *Salmonella enterica* serovar Typhimurium in monolayer cultures (12). This type of abnormality could be a consequence, in part, of impaired NOD2-dependent α-defensin production by Paneth cells and could therefore lead to colonization of the intestine with bacteria that cause Crohn's disease (13,14,24). This possibility is supported by recent evidence showing the role of α-defensins in host defense in the intestine: human α-defensin-5 has been shown to have antimicrobial activity against *E. coli*, *L. monocytogenes*, *S. typhimurium* and *Candida albicans in vitro* (25), and human α-defensin-5 transgenic mice are resistant to oral challenge with *S. typhimurium* (26). In addition, although almost all patients with Crohn's disease have reduced expression of two α-defensins in the ileal mucosa, human α-defensin-5 and human α-defensin-6, this reduction is more pronounced in patients with Crohn's disease who have CARD15 mutations (27). In addition, it has been reported that Paneth cells in NOD2-deficient mice have defective production of mRNA encoding α-defensins.

The final explanation for the association between CARD15 mutations and Crohn's disease is learned from the analysis of knock-in mice expressing NOD2 that contains the frameshift mutation associated with Crohn's disease (23). It was found that, on stimulation with MDP, macrophages from these mice had increased IL-1β production (23). These data, together with the finding that the knock-in mice were more susceptible to DSS-induced colitis, indicated that the frameshift mutation that is associated with Crohn's disease is a gain-of-function mutation that results in disease associated with increased IL-1β production. However, this model does not explain *in vitro* data showing that epithelial cells transfected with CARD15 that contain Crohn's-disaese-associated mutations have defective NF-κB activation in response to stimulation with MDP (9,10) and, more importantly, it also cannot explain why peripheral-blood mononuclear cells isolated from patients with Crohn's disease that have a frameshift mutation in CARD15 show a marked defect in IL-1β production (28). Finally, these knock-in mice did not have any abnormality in the production of T_H1 cytokines, which is a pronounced feature in Crohn's disease.

Thus, the recent discovery of NOD2 abnormalities opens up a new and challenging area of innate microbial recognition studies and how these interactions affect the immune system. The above studies indicate the variety of different pathway abnormalities that may occur in the presence of NOD2 deficiency which may ultimately give rise to inflammatory bowel disease illness, such as Crohn's disease.

References

1. Akira S, Takeda K. Toll-like receptor signaling. *Nature Rev Immunol* 2004;4:499-511.
2. Martinon F, Tschopp J. NRLs join TLRs as innate sensors of pathogens. *Trends Immunol* 2005;13:323-35.

3. Inohara N, Nunez G. NODS: intracellular proteins involved in inflammationa dn apoptosis. *Nature Rev Immunol* 2003;3:371-82.
4. Hugot J, *et al.* Association of NOD2 leucine-rich repeat variants with susceptibility to Crohn's disease. *Nature* 2001;411:599-603.
5. Ogura Y, *et al.* A frameshift mutation in NOD2 associated with susceptibility to Crohn's disease. *Nature* 2001;411:603-6.
6. Ting J, Davis B. CATERPILLAR, a novel gene family important in immunity cell death, and diseases. *Ann Rev Immunol* 2005;23:387-414.
7. Chamaillard M, Girardin S, Viala J, Philpott D. Nods, Nalps and Naip: intracellular regulators of bacteria-induced inflammation. *Cell Microbiol* 2003;5:581-92.
8. Barnisch N, Aguirre J, Reinecker H, Xavier R, Podolsky D. Membrane recruitment of NOD2 in intestinal epithelial cells is essential for nuclear factor-κB activation in muramyl dipeptide recognition. *J Cell Biol* 2005;170:21-6.
9. Inohara N, *et al.* Host recognition of bacterial muramyl dipeptide mediated through NOD2. Implications for Crohn's disease. *J Biol Chem* 2003;278:5509-12.
10. Girardin S, *et al.* NOD2 is a general sensor of peptidoglycan through muramyl dipeptide (MDP) detection. *J Biol Chem* 2003;278:8869-72.
11. Gutierrez O, *et al.* Induction of NOD2 in myelomonocytic and intestinal and epithelial cells via nuclear factor-κB activation. *J Biol Chem* 2002;277:41701-5.
12. Hisamatsu T, *et al.* CARD15/NOD2 functions as an antibacterial factor in human intestinal epithelial cells. *Gastroenterology* 2003;124:993-1000.
13. Lala S, *et al.* Crohn's disease and the NOD2 gene: a role for Paneth cells. *Gastroenterology* 2003;125:47-57.
14. Ogura Y, *et al.* Expression of NOD2 in Paneth cells: a possible link to Crohn's ileitis. *Gut* 2003;52:1591-7.
15. Rosenstiel P, *et al.* TNF-α and IFN-γ regulate the expression of the NOD2 (CARD15) gene in human intestinal epithelial cells. *Gastroenterology* 2003;124:1001-9.
16. Pauleau A, Murray P. Role of NOD2 in the response of macrophages to Toll-like receptor agonists. *Mol Cell Biol* 2003;23:7531-9.
17. Gupta D, Theisen N, von Figura K, Hasilik A. Comparison of biosynthesis and subcellular distribution of lysozyme and lysosomal enzymes in U937 monocytes. *Biochim Biophys Acta* 1985;847:217-222.
18. Araki Y, Nakatani T, Makino R, Hayashi H, Ito E. Isolation of glucosaminyl-β(1-4) muramic acid and phosphoric acid ester of this disaccharide from acid hydrolysates of peptidoglycan of Bacillus cereus AHU 1356 cell walls. *Biochem Biophys Res Commun* 1971;42:684-590.
19. Tanabe T, *et al.* Regulatory regions and critical residues of NOD2 involved in muramyl dipeptide recognition. *EMBO J* 2004;23:1587-97.
20. Inohara N, *et al.* An induced proximity model for NF-κB activation in the NOD1/RICK and RIP signaling pathways. *J Biol Chem* 2000;275:27823-31.
21. Watanabe T, Kitani A, Murray P, Strober W. NOD2 is a negative regulator of Toll-like receptor 2-mediated T helper type 1 responses. *Nature Immunol* 2004;5:800-8.
22. Kobayashi K, *et al.* NOD2-depdent regulation of innate and adaptive immunity in the intestinal tract. *Science* 2005;307:731-4.
23. Maeda S, *et al.* NOD2 mutation in Crohn's disease potentiates NF-κB activation and IL-1β processing. *Science* 2005;307:734-8.

24. Ayabe T, *et al.* Secretion of microbicidal α-defensins by intestinal Paneth cells in response to bacteria. *Nature Immunol* 2000;1:113-8.

25. Porter E, van Dam E, Valore E, Ganz T. Broad-spectrum antimicrobial activity of human intestinal defensin 5. *Infect Immunol* 1997;65:2396-401.

26. Salzman N, Ghosh D, Huttner K, Paterson Y, Bevins C. Protectin against enteric salmonellosis in transgenic mice expressing a human intestinal defensin. *Nature* 2003;422:522-6.

27. Wekhamp J, *et al.* NOD2 (CARD15) mutations in Crohn's disease are associated with diminished mucosal α-defensin expression. *Gut* 2004;53:1658-64.

28. Li J, *et al.* Regulation of IL-8 and IL-1β expression in Crohn's disease associated NOD2/CARD15 mutations. *Hum Mol Genet* 2004;13:1715-25.

Session 4A. Immunity and infectious diseases

HUMAN HERPESVIRUS 8 AND KAPOSI'S SARCOMA: A MODEL FOR VIRAL ONCOGENESIS (EPIDEMIOLOGICAL AND MOLECULAR ASPECTS)

Giovanni Rezza (a), James Goedert (b)
(a) Department of Infectious, Parasitic and Immune-Mediated Diseases, Istituto Superiore di Sanità, Rome, Italy
(b) Viral Epidemiology Branch, National Cancer Institute, National Institutes of Health, Bethesda, MD, USA

The human herpesvirus-8 (HHV-8) (Figure 1), an oncogenic virus related to Epstein Barr virus (EBV), is considered to be the most important determinant of Kaposi's sarcoma (KS), a relatively rare human skin tumour. A large amount of information has been gathered in recent years on the epidemiology of HHV-8 and KS and on pathogenetic mechanisms; thus, HHV-8/KS may be used as a model for studying the relationship between infection and human cancer. In the current presentation, the attention is focused on epidemiological and molecular studies conducted by our group over the last decade.

We started to work on HHV-8 just after its first identification in 1994. Our early studies were conducted in several countries and were addressed to estimate HHV-8 antibody prevalence in different settings and to identify determinants of HHV8 transmission. Our work contributed to understanding the global distribution of HHV8. As shown in the map below, HHV8 prevalence is high in central, east and south Africa; intermediate in Egypt, Greece and southern Italy; and lower in the rest of Europe and the U.S.

Among AIDS patients, homosexual men were known to be at higher risk of KS compared to other exposures categories. This lead to the hypothesis that the cause of KS was a sexually transmitted agent (i.e., HHV-8). However, in developing countries, where the incidence of KS is higher compared to industrialized countries, modalities of transmission of HHV-8 were still undefined. We conducted a study in Cameroon that showed high prevalence of HHV-8 antibodies in the early phases of life. These studies also showed that HHV8 prevalence tends to increase with increasing age. These findings suggest that HHV-8 infection may spread through saliva contact during the early phase of life, but then the infection continues slowly to spread in the adulthood, probably through sexual contact. Interestingly, our study also showed an association between HHV-8 positivity and history of STDs (1).

Similar findings were found in Egypt (2), a country with lower KS incidence. HHV-8 seroprevalence was surprisingly high among the children, suggesting non-sexual routes of transmission. Furthermore, the inconsistency of the ecological association between HHV-8 and KS (i.e., high KS incidence and HHV-8 seroprevalence was found in Cameroon but not in Egypt, where we found high HHV-8 seroprevalence in presence of relatively low KS incidence rates) suggests that other cofactors may affect the risk of KS among HHV-8 positive individuals.

As a consequence of the high prevalence of HHV8 antibodies found in Alexandria, a study was conducted to evaluate signs and symptoms associated to primary HHV8 infection among Egyptian children. Of 80 febrile children, 50 were initially HHV8 seronegative: HHV8 DNA sequences were detected in the saliva of 6 of them, and 5 of these children had a maculopapualr rash; 3 of the 6 children had a convalescent sample available which showed seroconversion against HHV8. These findings suggested that primary HHV-8 infection may cause symptomatic acute disease (3).

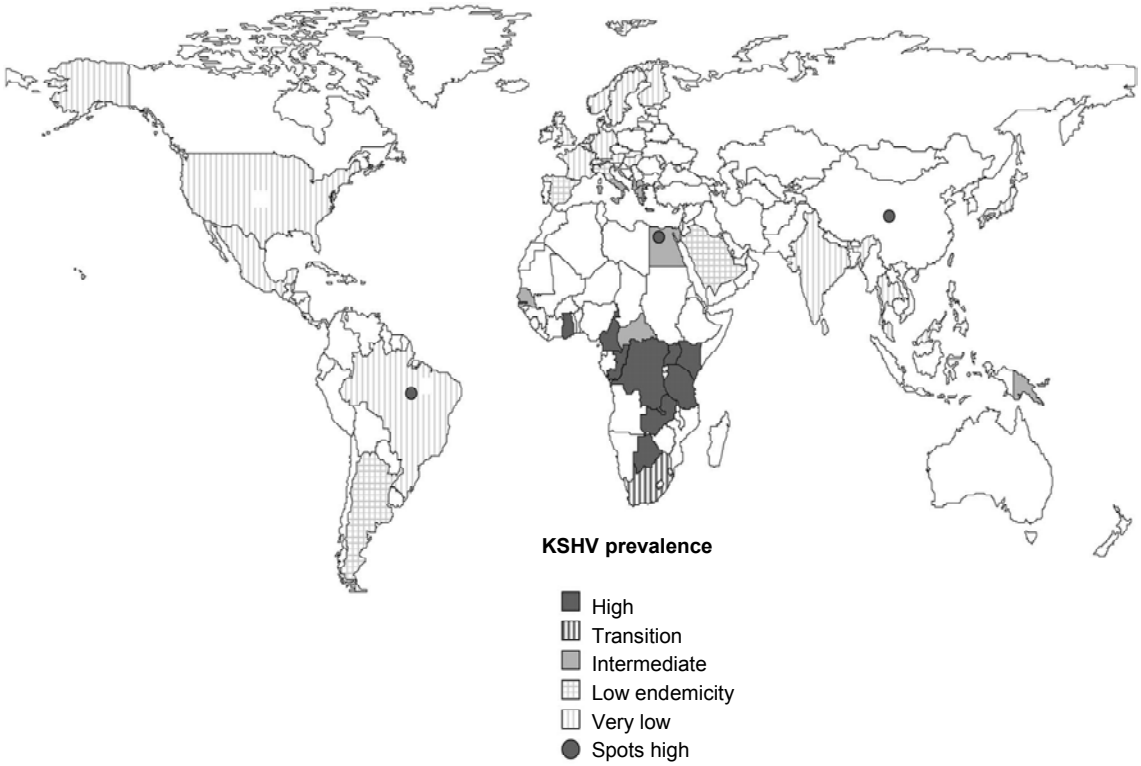

Figure 1. Prevalence and transmission of HHV-8 infection

Several relevant questions on the natural history of HHV-8 infection remained to be answered:
- what proportion of HHV-8 infected individuals develops KS;
- what the cofactors for progression to KS are.

First, we studied a cohort of HIV seroconverters and found that about 30% of HIV/HHV8 coinfected individuals developed KS by 10 years after HIV seroconversion. Among HHV-8 positive persons, higher HHV8 titer was found to be a strong predictor of KS development (4).

Secondly, there was little information on the risk of developing classical KS among HHV-8-positive HIV-uninfected people. A study that we conducted in 3 Mediterranean islands showed that about 1 every 3000 HHV8 infected men develop KS but the risk more than 2-fold lower among women (5). The study was repeated in Sassari and Latina, finding very similar results (6).

A summary of the results is reported in Table 1.

Table 1. Yearly incidence rates of KS among HHV-8 seropositive men and women

	Men	Women	W/W
Malta	1:3,574	1:4,866	1.4
Sicily	1:3,290	1:8,000	2.4
Sardinia	1:3,108	1:10,970	3.5
Sassari	1:2,846	1:6,827	2.4
Cagliari	1:5,483	1:12,489	2.3
Latina	1:2,200	1:4,110	1.9

Sources: Vitale, Int J Cancer 2001 (5); Serraino, Infection 2006 (6)

Since, without AIDS, only a small proportion of HHV-8 seropositive individuals develops KS, it was considered of great importance to identify cofactors for KS development; to this end, a collaborative project between ISS and NIH was initiated. The case-control study, designed by NIH, was conducted in 3 Italian Regions. For each confirmed case of classical (i.e., non-AIDS) KS, up to two age- and sex-matched controls were recruited. To identify a sufficient number of controls, up to 20 individuals attending the same general practitioner of each case were screened. The results showed a lower risk of KS, compared to HHV8 infection without KS, associated with tobacco smoking and an increased risk of KS with infrequent bathing, topical corticosteroid use, and asthma (7).

Based on the lower risk of classical KS among cigarette smokers, we postulated that nicotine might modulate peri-vascular inflammation, thus controlling the migration and expansion of HHV8 infected cells. By analogy, we considered the possibility that nicotine might affect regression of established KS lesions, which is known to occasionally occur. To test this hypothesis, we conducted a Phase I/II clinical trial in Milan in which 24 patients with classical KS were treated for 15 weeks. In each patient, one lesion was treated continuously with a commercially available nicotine patch (Nicoderm-CQ), a second lesion was treated continuously with an identical placebo patch, and a third lesion was left untreated. No major toxicities or differences between lesions was noted, but digital photographs are still being analyzed for the final analysis.

Since a large number of specimens were stored both in Italy and in the States, further analyses were performed, leading to a series of publications. The main results concerned the identification of correlates of HHV8 DNA detection (8), and associations of KS development with polymorphisms in host genes controlling cytokines, interleukins and their receptors (9,10,11). This work is expected to continue, with an expanded focus on the many genes related to innate and adaptive immunity.

In terms of future developments, a series of research priorities has been identified:

- stored samples from the case-control study conducted in Italy are available. These samples should now be used further to corroborate previous and identify new host and virus determinants of KS and other tumours associated with HHV-8 infection;
- an international network has been set for further studies that might provide insight into cofactors for HHV8 infection and for KS following HHV8 infection, for other tumours that might result from HHV8 infection, and for novel investigations of cancer or other diseases related to both HHV8 and the related virus EBV. In particular, the distributions of cofactors may explain heterogeneity and apparent discrepancies in HHV-8 prevalence and KS incidence. Examples include Cameroon, where both HHV-8 prevalence and KS incidence are high, and Egypt, where HHV-8 prevalence is higher but KS incidence is low. Possible co-factors include differences in exposures to parasites, soils, vegetation, and in host and viral genetics;
- the network may be expanded to other sites, particularly in Uganda, where ISS and NIH funded activities could investigate the relationship not only of KS with HHV8 but also of Burkitt lymphoma (BL) with EBV and various environmental exposures.

To this end, further studies are needed. The already existing and experienced ISS/NIH collaborative effort may represent the necessary framework to guarantee the success of future initiatives.

References

1. Rezza G, Tchangmena OB, Andreoni M, *et al.* Prevalence and risk factors for human herpesvirus 8 infection in northern Cameroon. *Sex Transm Dis* 2000;27(3):159-64.

2. Andreoni M, El-Sawaf G, Rezza G, *et al.* High seroprevalence of antibodies to human herpesvirus-8 in Egyptian children: evidence of nonsexual transmission. *J Natl Cancer Inst* 1999;91(5):465-9.
3. Andreoni M, Sarmati L, Nicastri E, *et al.* Primary human herpesvirus 8 infection in immunocompetent children. *JAMA* 2002;287(10):1295-300.
4. Rezza G, Andreoni M, Dorrucci M, *et al.* Human herpesvirus 8 seropositivity and risk of Kaposi's sarcoma and other acquired immunodeficiency syndrome-related diseases. *J Natl Cancer Inst* 1999;91(17):1468-74.
5. Vitale F, Briffa DV, Whitby D, *et al.* Kaposi's sarcoma herpes virus and Kaposi's sarcoma in the elderly populations of 3 Mediterranean islands. *Int J Cancer* 2001;91(4):588-91.
6. Serraino D, Cerimele D, Piselli P, *et al.* Infection with human herpesvirus type 8 and Kaposi's sarcoma in Sardinia. *Infection* 2006;34(1):39-42.
7. Goedert JJ, Vitale F, Lauria C, Serraino D, *et al.* Classical Kaposi's Sarcoma Working Group. Risk factors for classical Kaposi's sarcoma. *Journal of National Cancer Institute* 2002;94(22):1712-8.
8. Brown EE, Whitby D, Vitale F, *et al.* Correlates of Human Herpesvirus-8 DNA detection among adults in Italy without Kaposi sarcoma. *Int J Epidemiol* 2005;34(5):1110-1117. Epub 2005 Jul 25.
9. Brown EE, Fallin MD, Goedert JJ, *et al.* Kaposi Sarcoma Genetics Working Group. A common genetic variant in FCGR3A-V158F and risk of Kaposi sarcoma herpesvirus infection and classic Kaposi sarcoma. *Cancer Epidemiol Biomarkers Prev* 2005;14(3):633-7.
10. Brown B, Chanock S, Whitby D, *et al.* Associations of Classic Kaposi Sarcoma with Common Variants in Genes that Modulate Host Immunity. *Cancer Epidemiology, Biomarkers & Prevention* 2006;15(5):926-34.
11. Brown EE, Fallin MD, Goedert JJ, *et al.* Kaposi Sarcoma Genetics Working Group. Host immunogenetics and control of human herpesvirus-8 infection. *J Infect Dis* 2006;193(8):1054-62. Epub 2006 Mar 6.

Session 4A. Immunity and infectious diseases

NEW MECHANISMS OF MYCOBACTERIUM TUBERCULOSIS IMMUNE EVASION: IMPACT ON DISEASE OUTCOME AND STRATEGIES OF IMMUNE INTERVENTION

Eliana Marina Coccia (a), Maria Cristina Gagliardi (a), Maria Elena Remoli (a), Valérie Gafa (a), Elena Giacomini (a), Marta Scandurra (a), Marta Severa (a), Roberto Lande (a), Sabrina Mariotti (a), Valeria Sargentini (a), Raffaela Teloni (a), Lanfranco Fattorini (a), Elisabetta Iona (a), Manuela Pardini (a), Richard Pine (b), Roberto Nisini (a)

(a) Department of Infectious, Parasitic and Immuno-Mediated Diseases, Istituto Superiore di Sanità, Rome, Italy

(b) Public Health Research Institute, Newark, NJ, USA

Tuberculosis (TB) is a chronic bacterial infection that still causes more deaths worldwide than any other infectious disease. It is responsible for 3 million deaths for years and one-third of humanity is infected by *M. tuberculosis*. Key reasons for this are the unavailability of an efficacious vaccine for adult disease; the rise of multidrug-resistant strains, and the dreadful association of TB with human immunodeficiency virus infection (1,2). Moreover, TB is a disease in which traditional prophylactic approaches have been largely unsuccessful.

On the first encountering *M. tuberculosis*, the majority of individuals mounts an effective immune response leading to the control of the infection (3). Consequently, most of these individuals experience a mild disease (primary TB), often without clinical relevance (4). T cells specific for *M. tuberculosis* antigens are, in fact, expanded and limit *M. tuberculosis* growth either directly by killing intracellular *M. tuberculosis* or indirectly by secreting cytokines such as IFN-γ and TNF-α which promote killing by macrophages (2). However, the immune response that causes such a clinical cure does not clear the bacilli from infected individuals and after primary TB, *M. tuberculosis* persists causing a latent infection (5).

The notorious success of *M. tuberculosis* as a highly adapted human pathogen rests on its ability to evade the immune response and, in turn, to persist in an immunocompetent host. The persistence of *M. tuberculosis* in macrophages contrasts with the observed induction of a vigorous specific immune response, which is, however, rarely effective in eradicating the infection and suggests the ability of *M. tuberculosis* to induce some form of immune-regulation. In immunocompetent adults TB typically occurs as a reactivation of pre-existing *foci* (6). This suggests the existence of a dynamic balance between the host immune system and *M. tuberculosis*. In most cases, the host response is sufficient to forestall activation of the disease for a lifetime. However, occasionally the immune response fails in some way and the infection reactivates to cause active disease. The immune factors contributing to the establishment of latent infection and the immunological components that are required to maintain such an infection and prevent reactivation are still unknown (7). Regarding the adaptive response of mycobacteria to host's antimicrobial defenses, it is unclear how the bacilli survive in the face of a strong immune response, whereas it is now clear that they profoundly change several metabolic activities leading to a non replicating status (dormancy) (8).

Despite wide debate (3), a full understanding of the mechanisms used by *M. tuberculosis* to escape sterilizing immunity is still lacking, but it could be crucial for the identification of novel

strategies for immuno/chemotherapy of tuberculosis. The search for new therapeutic interventions is required to overcome the low compliance to complex chemo-antibiotic regimens and to avoid multi-drug resistance. Aim of this project is to produce new knowledge and insight that bear a potential for new therapeutic or prophylactic interventions focusing on the mechanism used by *M. tuberculosis* to evade the immune response.

It is known that *M. tuberculosis* is able to switch to a dormant status of latency and to evade two major antimicrobial mechanisms of macrophages: killing mechanisms, such as those mediated by nitric oxide, and the interference with antigen processing and presentation, thus rendering the infected cells invisible to the immune response (Figure 1).

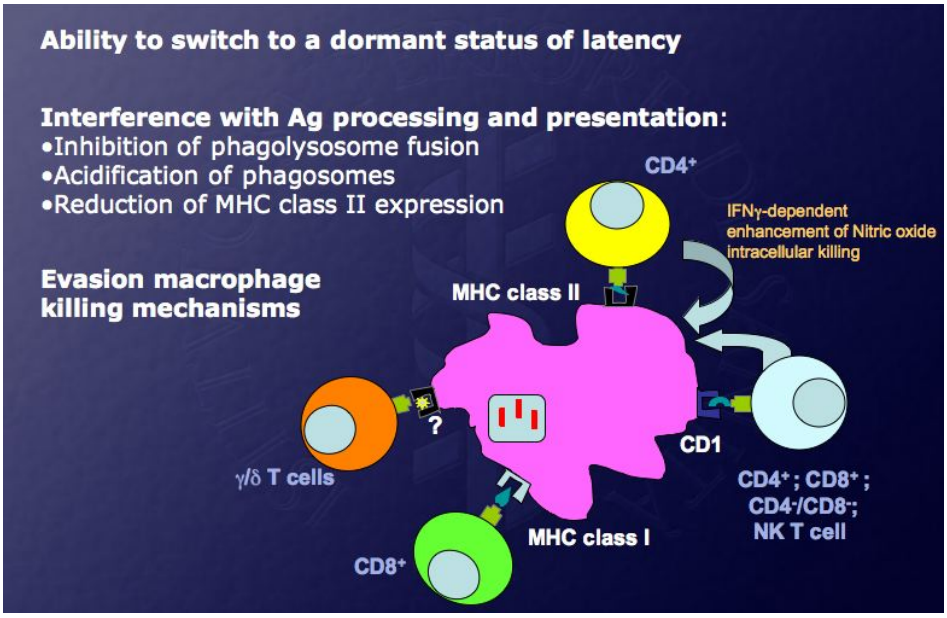

Figure 1. Immune evasion by *M. tuberculosis*.
Mechanisms utilized by *M. tuberculosis* to evade the killing activities of infected macrophage are shown

Besides these mechanisms operating in *M. tuberculosis*-infected macrophages, we have recently suggested that a possible mechanism for *M. tuberculosis* immune evasion may rely on its ability to hijack monocyte differentiation into dendritic cells (DC) (9). Thus, affecting the generation of functionally active DC, *M. tuberculosis* could block the afferent limb of the specific immune response, preventing the development of a functional T cell response.

Generally, monocytes may differentiate *in vitro* into DC in the presence of two cytokine cocktails: IFN-α and GM-CSF or IL-4 and GM-CSF. In both situations DC express a characteristic surface phenotype as shown in Figure 2A.

We demonstrated that in the presence of IFN-α and GM-CSF *M. tuberculosis*-infected monocytes do not differentiate into DC, but they develop into macrophage-like cells which retain CD14 without acquiring CD1a, partially express CD86, and do not up-regulate CD80 and HLA-DR (Figure 2B) (10). Conversely in the presence of IL-4 and GM-CSF infected monocytes differentiate into mature $CD83^+$ DC characterized by a selective failure in the expression of CD1 molecules and no up-regulation of CD80 and HLA-DR molecules (Figure 2B) (9).

A)

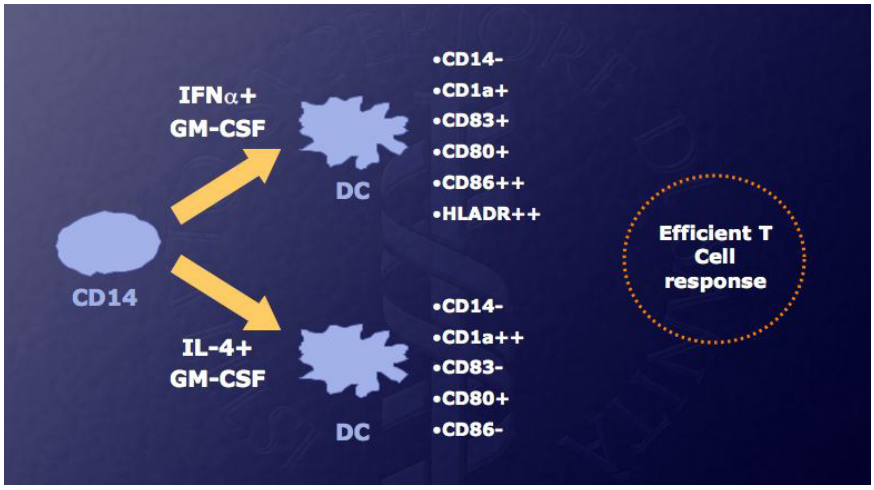

B)

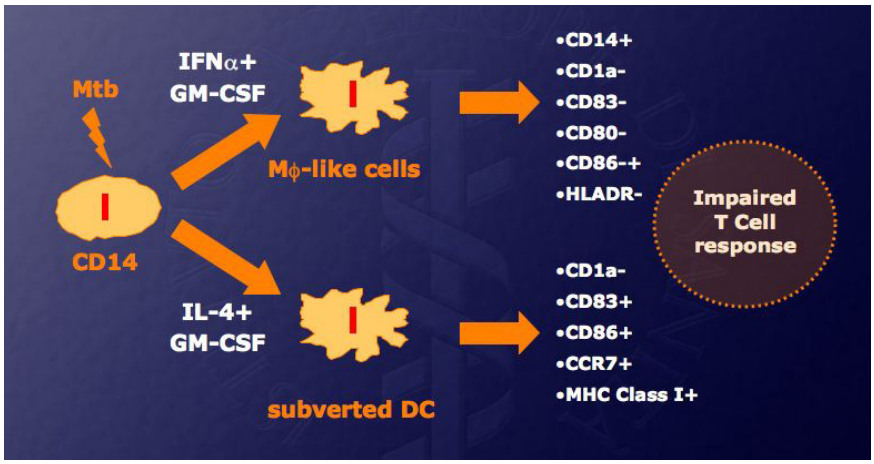

Figure 2. New mechanism of M. tuberculosis immune evasion: interference with monocyte differentiation to DC. A) Differentiation of human monocytes into DC stimulated by IFN-α and GM-CSF or IL-4 and GM-CSF. B) Impaired differentiation of M. tuberculosis infected- monocyte into DC and impact on T cell response

Both cell populations are not able to induce a protective T cell response. Indeed, T lymphocytes stimulated by macrophage-like cells or subverted DC showed a reduced ability to proliferate and to produce IFN-γ. Thus, the expansion of T lymphocytes lacking effector function would reduce the T cell help provided to infected alveolar macrophages for killing the intracellular pathogen. Moreover, *M. tuberculosis*-infected macrophage-like cells, by their low expression of stimulatory and co-stimulatory molecules, could turn into immunoprivileged host-cells for pathogen replication. We suggested that this model might reproduce *in vivo* situations in which monocytes are recruited into sites of chronic inflammatory environment, such as the granuloma in TB, and are subjected to DC differentiation. In fact, granulomas are dynamic

entities undergoing remodeling during a lifelong *M. tuberculosis* infection and *in vivo* models have shown that mycobacteria may traffic into infected tissues transported by monocytes.

Based on this premise the main objective of our project was to investigate the mechanisms underlying the subversion of monocyte differentiation to DC. Among the cytokines that promote the differentiation of monocytes into DC, type I IFN has been shown to act as an inducer of DC differentiation (11-13). Since type I IFN can be produced in response to different infectious agents and inflammatory stimuli, such as *M. tuberculosis* infection (14-16), we studied the ability of type I IFN to induce the differentiation of *M. tuberculosis* -infected monocytes into DC. We have found that, whilst *M. tuberculosis* induces the expression of type I IFN in macrophages and DC (17,18), it inhibits the IFN-α-induced monocyte differentiation into DC (10). Thus, we investigated the mechanisms induced by *M. tuberculosis* which are involved in the regulation and modulation of the responsiveness of the infected cells to type I IFN.

Type I IFN influences cellular function largely by regulating gene expression, as the culmination of a signal transduction cascade (19). High affinity binding of IFN to the type I IFN receptor, mediated by dimerization of IFNAR1 and IFNAR2 subunits, is followed by tyrosine phosphorylation of associated protein tyrosine kinases, Janus kinase 1 (JAK1) and TYK2, another kinase in the JAK family. JAKs in turn activate the latent cytoplasmic transcription factors Signal Transducer and Activator of Transcription (STAT)-1 and STAT-2 by catalyzing tyrosine phosphorylation. Phosphorylated STAT-1 can form a homodimer, which can act alone or together with IFN Regulatory Factor 9 (IRF-9). Activated STAT-1 and activated STAT-2 can also form a heterodimer, which associates with IRF-9 to constitute IFN-stimulated Gene Factor 3 (ISGF-3). After translocation to the nucleus, STAT-1 homodimers bind to STAT binding element (SBE) while ISGF-3 and the $(STAT\text{-}1)_2$/IRF-9 complex bind the IFNα/β-stimulated-response-element (ISRE). Many genes have one regulatory element or the other, although some have both. Interestingly, several primary response genes are themselves transcription factors that are required for induction of secondary effectors of the cellular response to IFN and to other cytokines. Among these, IRF-1 and IRF-7 are transcriptionally regulated by SBE and ISRE sites present within their respective promoters. Thus, the response to IFN as well as its production can be amplified and potentiated through the enhanced expression of IRF factors. Moreover, the JAK/STAT pathway is subjected to relatively rapid downregulation through different negative feedback mechanisms: receptor-mediated endocytosis, expression of dominant negative isoforms of STAT proteins, expression of CIS/SOCS/SSI family members that bind the cytokine receptors or the JAK kinases, and the activation of tyrosine phosphatases (20). In addition, a new family of negative regulators of signal transducer, the PIAS (Protein Inhibiting Activated STAT) proteins, has been identified recently. PIAS seems to bind directly to STAT and to inhibit DNA binding (21). Thus, a variety of mechanisms can modulate a cell's response to cytokine and, in turn, control many biological functions.

In collaboration with Dr. R. Pine we have previously shown that type I IFN signalling was affected in human macrophages infected by *M. tuberculosis* infection (18,22). In addition, Dr R. Pine has recently showed that *M. tuberculosis* inhibits type I IFN signal through the activation of a phosphatase (binding to IFNAR1) that dephosphorylates JAk/STAT leading to a reduced IFN-dependent gene transcription (23).

These results prompt us to investigate whether a similar mechanism could be operative also in *M. tuberculosis* infected monocytes. To this aim, STAT-1 and -2 activation as well as the induction of some IFN stimulated genes were analyzed in monocytes non-infected or infected by *M. tuberculosis* following the treatment with IFN-α and GM-CSF. Surprisingly, we observed that STAT phosphorylation was not affected in *M. tuberculosis* infected monocyte both at earlier and later time points of IFN treatment (Figure 3A). Accordingly, the expression of IRF-7 evaluated by real time PCR was induced following 24 hr of type I IFN treatment both in non

infected and in *M. tuberculosis*-infected monocytes (Figure 3B). Similarly, the expression of B7H1, another IFN inducible gene, was up-regulated on the cell membrane of control and *M. tuberculosis*-infected monocytes following IFN treatment (Figure 3B). These results clearly indicated that *M. tuberculosis*-infected monocytes were fully responsive to the differentiating effects of type I IFN.

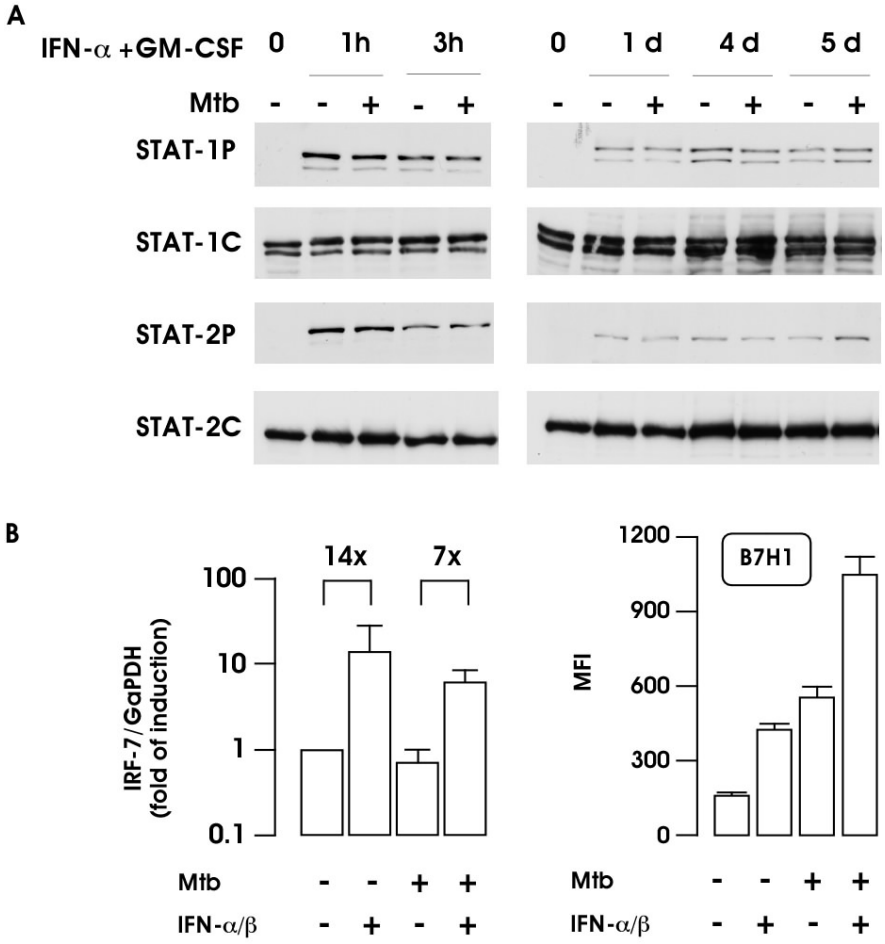

A) Monocytes were treated with IFN-α (1000 U/ml) and GM-CSF (200 U/ml). Where indicated, cells were infected with *M. tuberculosis* (MOI 1:1) for the indicated times. Whole cell lysates (30 µg) were analyzed by immunoblot with the indicated antibodies to evaluate STAT phosphorylation (P) and protein content (C).
B) Monocytes were left untreated or infected *M. tuberculosis* (MOI 1:1) in presence or absence of IFN-α/β Total RNA was extracted after 4 h and analyzed for IRF-7 mRNA expression by real-time RT-PCR. The relative fold induction values are indicated within each subset. The surface level of B7H1 was analyzed 24 h following the indicated treatments by flow cytometry. A total of 5000 cells were tested per sample. The analysis was repeated four additional times, using DC from a total of five different blood donors.

Figure 3. Analysis of type I IFN response in *M. tuberculosis*-infected monocytes

We also investigated which *M. tuberculosis* component could be responsible for DC subversion. For this purpose we treated monocytes with different *M. tuberculosis* structural components and then induced their differentiation into DC (Gagliardi MC *et al.*, submitted

manuscript). We first observed that the pool of secreted proteins (CFP) of *M. tuberculosis* did not interfere with monocyte differentiation into DC (Figure 4).

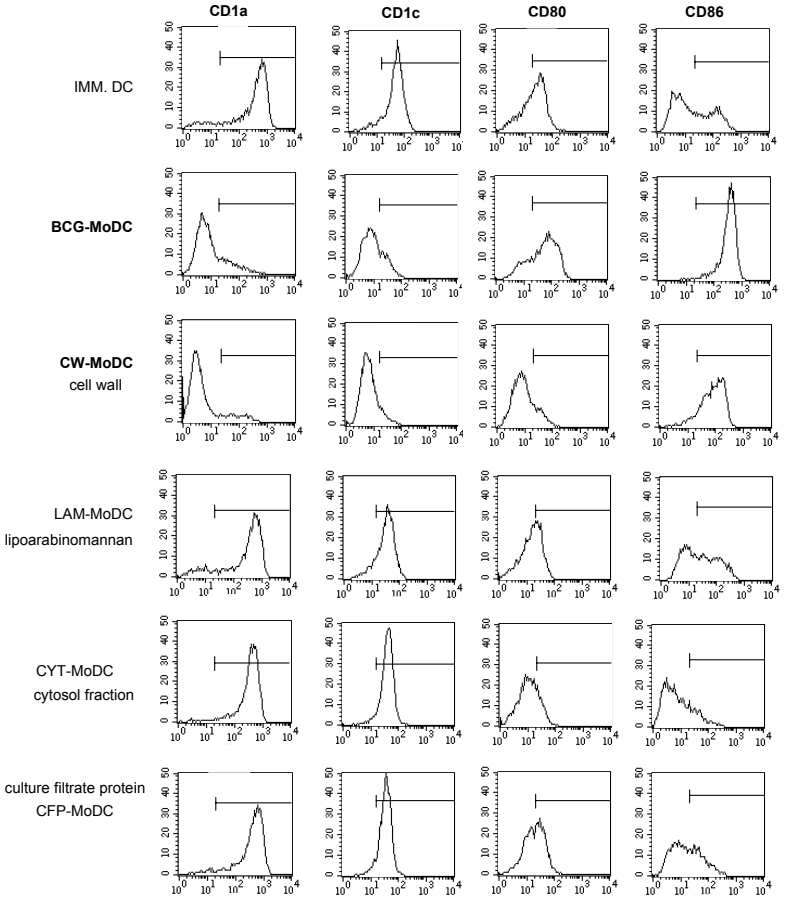

Figure 4. Flow cytometric analysis of surface phenotype of DC derived from monocytes treated with isolated mycobacterial components or infected with *M. tuberculosis*.
Cell surface expression of the indicated molecules was determined by flow cytometry on DC derived from non-infected monocytes (Mo-DC), *M. tuberculosis*-infected monocytes (Mtb-MoDC) and from monocytes treated with *M. tuberculosis* cell wall (CW-MoDC), lipoarabinomannan (LAM-MoDC), isolated cytosolic fraction of *M. tuberculosis* (CYT-MoDC) and protein fitrate from Mtb culture broth (CFP-MoDC). A total of 5000 cells were tested per sample. Markers were set to exclude 95% of events recorded with the appropriate isotype control antibody. Data are from one experiment representative of five independent experiments

This result is in line with our previous observation that heat-killed *M. tuberculosis* induce the same subversive effect of live *M. tuberculosis*, thus suggesting that structural component(s) and not products of the bacterial metabolism were involved in this phenomenon. We then showed that the cytosol fraction (CYT) of *M. tuberculosis* did not have any effect as well. This data is in line with the hypothesis that a component of *M. tuberculosis* exposed on its external surface would be more easily responsible for interacting with monocytes. Thus, we tested lipoarabinomannan (LAM), a non-proteinous compound of mycobacterial cell wall (CW) that

has been indicated as a major DC interacting molecules capable of interfering with DC differentiation, but we could demonstrate its inability to subvert monocyte differentiation. Finally, we tested CW and observed that this structure mimics the effects of the whole bacterium, drastically inhibiting CD1a, CD1c, CD80 surface expression (Figure 4) and antigen presenting capacity (data not shown).

In conclusion our results indicate that:

- *M. tuberculosis* does not inhibit type I IFN signalling in primary monocytes therefore experiments are in progress to identify other intracellular pathways that could account for the subversion of DC differentiation induced by *M. tuberculosis*. Among the possible pathways, we will focus our attention on the MAPK signalling since it has been described that its activation in certain circumstances causes the inhibition of monocyte differentiation to DC. According to recent evidence that this suppression can be rescued by interfering with the activation of p38 MAPK (24), it is interesting to speculate that the inhibitory effect of *M. tuberculosis* may be reversed by blocking p38 MAPK.
- CW contains a bacterial component different from ManLam primarily responsible for the interference with monocyte differentiation to DC. We will proceed in the isolation of other component of the CW in order to identify a defined M. tuberculosis structural component responsible for the subversion. The identification of such a component will allow us to better investigate the signalling, and the monocyte receptor involved in the subversion of DC differentiation.

References

1. Flynn JL, Chan J. Immunology of tuberculosis. *Annu Rev Immunol* 2001;19:93-129.
2. Kaufmann SH. How can immunology contribute to the control of tuberculosis? *Nat Rev Immunol* 2001;1(1):20-30.
3. Schluger NW, Rom WN. The host immune response to tuberculosis. *Am J Respir Crit Care Med* 1998;157(3 Pt 1):679-91.
4. Lauzardo M, Ashkin D. Phthisiology at the dawn of the new century. *Chest* 2000;117(5):1455-1473.
5. Manabe YC, Bishai WR. Latent Mycobacterium tuberculosis-persistence, patience, and winning by waiting. *Nat Med* 2000;6(12):1327-9.
6. Boom WH, Canaday DH, Fulton SA, Gehring AJ, Rojas RE, Torres M. Human immunity to M. tuberculosis: T cell subsets and antigen processing. *Tuberculosis* (Edinb) 2003;83(1-3):98-106.
7. Tufariello JM, Chan J, Flynn JL. Latent tuberculosis: mechanisms of host and bacillus that contribute to persistent infection. *Lancet Infect Dis* 2003;3(9):578-90.
8. Cardona PJ, Ruiz-Manzano J. On the nature of Mycobacterium tuberculosis-latent bacilli. *Eur Respir J* 2004;24(6):1044-51.
9. Mariotti S, Teloni R, Iona E, Fattorini L, Giannoni F, Romagnoli G, *et al.* Mycobacterium tuberculosis subverts the differentiation of human monocytes into dendritic cells. *Eur J Immunol* 2002;32(11):3050-8.
10. Mariotti S, Teloni R, Iona E, Fattorini L, Romagnoli G, Gagliardi MC, *et al.* Mycobacterium tuberculosis diverts alpha interferon-induced monocyte differentiation from dendritic cells into immunoprivileged macrophage-like host cells. *Infect Immun* 2004;72(8):4385-92.
11. Blanco P, Palucka AK, Gill M, Pascual V, Banchereau J. Induction of dendritic cell differentiation by IFN-alpha in systemic lupus erythematosus. *Science* 2001;294(5546):1540-3.

12. Le Bon A, Schiavoni G, D'Agostino G, Gresser I, Belardelli F, Tough DF. Type i interferons potently enhance humoral immunity and can promote isotype switching by stimulating dendritic cells in vivo. *Immunity* 2001;14(4):461-70.

13. Santini SM, Di Pucchio T, Lapenta C, Parlato S, Logozzi M, Belardelli F. The natural alliance between type I interferon and dendritic cells and its role in linking innate and adaptive immunity. *J Interferon Cytokine Res* 2002;22(11):1071-80.

14. Coccia EM, Severa M, Giacomini E, Monneron D, Remoli ME, Julkunen I, *et al.* Viral infection and Toll-like receptor agonists induce a differential expression of type I and lambda interferons in human plasmacytoid and monocyte-derived dendritic cells. *Eur J Immunol* 2004;34(3):796-805.

15. Bogdan C. The function of type I interferons in antimicrobial immunity. *Curr Opin Immunol* 2000;12(4):419-24.

16. Decker T, Muller M, Stockinger S. The yin and yang of type I interferon activity in bacterial infection. *Nat Rev Immunol* 2005;5(9):675-87.

17. Remoli ME, Giacomini E, Lutfalla G, Dondi E, Orefici G, Battistini A, *et al.* Selective expression of type I IFN genes in human dendritic cells infected with Mycobacterium tuberculosis. *J Immunol* 2002;169(1):366-74.

18. Prabhakar S, Qiao Y, Hoshino Y, Weiden M, Canova A, Giacomini E, *et al.* Inhibition of response to alpha interferon by Mycobacterium tuberculosis. *Infect Immun* 2003;71(5):2487-97.

19. Darnell JE Jr, Kerr IM, Stark GR. Jak-STAT pathways and transcriptional activation in response to IFNs and other extracellular signaling proteins. *Science* 1994;264(5164):1415-21.

20. Coccia EM, Uze G, Pellegrini S. Negative regulation of type I interferon signaling: facts and mechanisms. *Cell Mol Biol* (Noisy-le-grand) 2006;52(1):77-87.

21. Liu B, Liao J, Rao X, Kushner SA, Chung CD, Chang DD, *et al.* Inhibition of Stat1-mediated gene activation by PIAS1. *Proc Natl Acad Sci U S A* 1998;95(18):10626-31.

22. Qiao Y, Prabhakar S, Coccia EM, Weiden M, Canova A, Giacomini E, *et al.* Host defense responses to infection by Mycobacterium tuberculosis. Induction of IRF-1 and a serine protease inhibitor. *J Biol Chem* 2002;277(25):22377-85.

23. Prabhakar S, Qiao Y, Canova A, Tse DB, Pine R. IFN-alpha beta secreted during infection is necessary but not sufficient for negative feedback regulation of IFN-alpha beta signaling by Mycobacterium tuberculosis. *J Immunol* 2005;174(2):1003-12.

24. Xie J, Qian J, Wang S, Freeman ME 3rd, Epstein J, Yi Q. Novel and detrimental effects of lipopolysaccharide on in vitro generation of immature dendritic cells: involvement of mitogen-activated protein kinase p38. *J Immunol* 2003;171(9):4792-800.

Session 4A. Immunity and infectious diseases

A MULTIPLE-APPROACH-BASED STUDY ON THE MECHANISMS OF PROTECTION AGAINST PERTUSSIS

Paola Mastrantonio, Paola Stefanelli, Giorgio Fedele, Fabiana Spensieri, Cecilia Fazio, Antonio Cassone, Clara M Ausiello
Department of Infectious, Parasitic and Immuno-Mediated Diseases, Istituto Superiore di Sanità, Rome, Italy

Bordetella pertussis is the causative agent of whooping cough. The disease continues to be a major cause of childhood morbidity and mortality, even in developed countries with good primary vaccination coverage. An estimated 50 million cases and 300 000 deaths occur every year worldwide (1).

Whooping cough has been traditionally considered a disease of childhood. However, in many countries this disease is being increasingly recognized as an important cause of respiratory disease in older children, adolescents and adults. These groups usually serve as reservoir and transmit bacteria to more vulnerable populations, including newborns and infants to whom pertussis may be a severe and life-threatening illness. The disease can also be very severe for adolescents and adults (2).

Whooping cough has remained an endemic disease with incidence peaks occurring every 3 to 5 years in fully vaccinated human populations. Furthermore, this disease is on the rise in many countries despite high vaccination coverage. The resurgence of pertussis may be explained by waning vaccine-induced immunity, changes in vaccine effectiveness and immune-driven selection of new bacterial variants. Concerning the last point, a shift in the *B. pertussis* population has been observed and is associated with polymorphism in the virulence factors pertussis toxin (Ptx), pertactin (Prn) and fimbriae (Fim) (3). These three virulence factors are also constituents of acellular component vaccines which have started to replace the conventional whole-cell vaccines in Europe and America (2,4).

Immunity conferred by anti pertussis vaccines is still subject of debate since the kinetics and meaning of antibodies elicited by the vaccines, as well as the role of cell mediated immunity have yet to be fully understood. In particular, the correlates of protection have not been identified. Our recent data obtained from the cohort of the Italian Efficacy Trial on Acellular Pertussis Vaccines (NIH-NIAID/ISS 1992-2000 funded), showed a rapid decline of antibody response after the vaccination and suggest a critical involvement of cell-mediated immunity, particularly for the polarization of a protective type 1 cytokine response (5-8). Persistence of clinical protection is fundamental in deciding the number of doses required to keep pertussis disease in check especially in 5-6- year old children where incidence is at its peak. The cohort of the Italian Efficacy Trial completed primary immunization 3 years before the rest of the target population and before the recent advent of combined vaccine preparations. Therefore, it is still an important source of samples (sera and strains), data, and information for future studies which could provide further, valuable insight on the mechanisms of vaccine-induced protection against pertussis.

Project description

The complexity of the mechanisms underlying immune protection against pertussis is reflected in the absence of well-established correlates or surrogates of protection. Indeed, equally protective primary vaccinations such as those achieved by whole cell (wP) or acellular (aP) vaccines may induce different Th cytokine profiles (6). This situation not only hampers our understanding of the immunologic basis of anti-*B. pertussis* defense, but requires lengthy and expensive clinical trials for assessing the efficacy of new vaccine preparations. In this context, the availability of serological markers of T cell responses would be of great help. In addition the issue of easily measurable serological markers of a protective T cell immune response in children receiving vaccination warrants attention for its potential value for further vaccination policies. Thus, chemokines, cytokines and soluble receptors associated with induction of memory T helper responses are primary candidates for the critical roles of these responses in protection. Among these factors, IFN-gamma and IL-4 would theoretically represent the best tool for tracking Th1/Th2 responses *in vivo* (9). However, since these cytokines are short-range molecules which are rapidly bound by their receptors and/or inactivated by proteases, their levels in the plasma are not reliable to assess the Th1/Th2 balance *in vivo*.

In this line, sCD30 and lymphocyte activation gene-3 (CD223) molecules are considered of particular relevance for their apparent association with Th2 and Th1 polarized response patterns (10,11) which are differently stimulated by the different pertussis vaccines and will be one of the focus of immunological studies in this project.

Moreover, considering the pivotal role of dendritic cells (DC) in regulation of immune response we intend to evaluate the ability of human DC to phagocytose *B. pertussis*, the ability of bacteria to survive intracellularly and finally whether infected DC may differently regulate specific adaptive or natural immunity. To clarify these aspects additional issues will be addressed:

- the interaction of *B. pertussis* and its virulence factors with DC to evaluate the role of the virulence factors in main functions of antigen presenting cells (APCs) and immune adjuvancity;
- the direct action of pertussis toxin (Ptx) on human DC to dissect its adjuvant properties previously demonstrated (12). Both active and inactivated forms (genetically and chemically) of toxins will be studied in order to mimic the immune response to infection and that to vaccination.

The expression of the known virulence factors of *B. pertussis*, Ptx, filamentous haemagglutinin (Fha), Prn, Fim, adenylate-cyclase (AC-Hly), and *Bordetella* resistance to killing (BrkA), is regulated by a two-component signalling system termed *bvg* that responds to environmental stimuli (13). Recently, polymorphism in Ptx, Prn and Fim has been found. These bacterial proteins which come into contact with the immune system (i.e. proteins located in the outer membrane) will be investigated in this study to assess the role of such variability in the protection from the disease.

Furthermore, it is known that Prn antibody titers are correlated with protection (14). In animal models it has been shown that variation in Prn can affect vaccine efficacy (15). Epidemiological studies also suggest a role for Prn variation in immune escape. Recent evidences indicate that Prn binds specifically to macrophages, possibly affecting macrophage function (16). Since a large number of sera belonging to the Italian collection is available, the follow-up of the study will include different categories of subjects. Specifically, sera from infected children and from vaccinees with acellular vaccines will be included in the bactericidal assay to evaluate if the protection conferred to bacteria by the effect of BrkA may be neutralized

by sera with high titers of IgG against Prn, since BrkA and Prn share a great sequence homology.

In particular, the study could answer the following questions:

- do Prn variants affect the functions of anti-Prn antibodies such as opsonisation and complement activation in both *B. pertussis* and *B. parapertussis* infections?
- are Prn antibodies able to block also the BrkA function?
- can Prn act indirectly through interaction with BrkA?

Since the genome sequences of *B. pertussis* and *B. parapertussis* have been completed recently, it is known that *B. pertussis* genome contains 3,816 genes, of which 358 (9.4%) are pseudogenes. The corresponding figures are 4,404 and 220 (5.0%) for *B. parapertussis*. The 2 species are closely related, and share most of their genes. In order to systematically detect single gene differences between these pathogens, a DNA microarray approach has been already developed (17).

In our study the microarray technology is used to outline the most significant genetic differences between:

- *B. pertussis* strains isolated from cases in vaccinated and unvaccinated individuals
- *B. parapertussis* strains isolated from severe pertussis-like cases and *B. parapertussis* strains isolated from cases with mild symptoms
- *B. pertussis* antigenic variants are detected with this inexpensive technology and the genome variability overtime of *B. pertussis* strains can be assessed after many years since the introduction of the acellular vaccines in the infant population.

Results

Validation of sCD223 and sCD30 as markers of different regulatory T cell population able to induce Th2- or Th1- oriented immune-response

We examined the levels of sCD223 and sCD30 proteins in children recipients of acellular pertussis (aP) and diphtheria-tetanus (DT) vaccines and in children receiving DT vaccine only, as control. The correlation of the two proteins with specific antibody and T cell responses was assessed. The main findings are:

- There is a clear-cut inverse relationship between sCD30 and sCD223 in children, both before and after vaccination, strongly suggesting that the two markers are the expression of different and counter-regulated T-cell responses.
- The level of sCD30 decreased significantly from pre- to post-vaccination measurement in children receiving the DT vaccine but not in those receiving the DT plus aP vaccine, suggesting that the presence of pertussis antigens in the vaccine was inductive of sCD30.
- The increased sCD30 level in the aP-DT vaccine recipients was bound to induction of CMI and anti-IgG PT responses. In particular, the children who did not acquire a measurable CMI response to pertussis antigens at the post- vaccination assay showed a decrease of sCD30 level, exactly as the children who received the DT vaccine only.

Overall, the highest sCD30 and the lowest sCD223 values, indicative of a preferential Th2 pattern, were detected in CMI-responsive children receiving the aP-DT vaccine. These data were well in accordance with the ability of this pertussis vaccine to induce pertussis antigen-specific proliferation and preferentially a Th2 or a Th2/Th0 cytokine pattern in primary vaccination, strongly suggesting that modulation of sCD30 and sCD223 markers could indeed be associated with vaccine immunogenicity (18).

sCD30 marker as predictive of protection or suscettibility to pertussis

The sCD30 levels in the pre- and post-vaccination sera of children who suffered from pertussis during the active post-vaccination surveillance period were compared with those measured in serum samples from children protected from pertussis during an equal period of active surveillance. Preliminary results indicated that, among the protected children, the greatest and only statistically significant difference between pre- and post-vaccination levels of sCD30 was attributable to the aP-DT vaccine recipients. Thus, in these children, the enhancement of sCD30 serum concentration appears to correlate with protection. Since this was not verified in recipients of other type of anti-pertussis vaccine, a conclusion about the general performance of the marker cannot be drawn before larger studies are performed. The levels of the sCD223 were measured in only few sera of children and results obtained so far are not conclusive.

B. pertussis effects on DC induced regulation of adaptive and natural immunity

We demonstrated that *Bordetella* shows a low susceptibility to be internalized by - and to survive in - human monocyte-derived dendritic cells (MDDC). Upon contact with the bacteria, immature MDDC were induced to undergo phenotypic maturation, and acquired the antigen presenting cells functions (19). Despite high levels of Interleukin-(IL-)10 and the barely detectable levels of IL-12 induced by *B. pertussis*, the bacterium induced maturation of MDDC and T helper 1 (Th1) polarized effectors cells. Gene expression analysis of the IL-12 cytokine family clearly demonstrated that *B. pertussis* induced high levels of p40 and p19 subunits of IL-23, yet failed to induce the expression of p35 subunit of IL-12 (19).

Then, we assessed the impact of cyclic (c)AMP intoxication due to the action of adenylate cyclase toxin (ACT), on DC driven immune response, by infecting MDDC with an ACT deficient *B. pertussis* mutant (ACT$^-$18HS19) or its parental strain (WT18323). Only ACT$^-$ 18HS19 infected MDDC induced production of IL-12p70. Gene expression analysis of the IL-12 cytokine family subunits revealed that both strains induced high levels of p40 (protein chain commune to IL-12p70 and IL-23) as well as p19, subunit of IL-23. Conversely only ACT$^-$ 18HS19 infection induced consistent transcription of IL-12p35, subunit of IL-12 p70. Addition of the cAMP analogous d-butyril-cAMP (d-cAMP) abolished IL-12p70 production and IL-12p35 expression in ACT$^-$18HS19 infected MDDC. ACT$^-$18HS19 infection induced the expression of the transcription factors IRF-1 and IRF-8 and of IFN-β, involved in IL-12p35 regulation and the expression of these genes was inhibited by d-cAMP addition and in WT18323 infected MDDC. The concomitant expression of IL-12p70 and IL-23 allowed ACT–18HS19 to trigger a more pronounced T helper 1 (Th1) polarization as compared to WT18323. Thus, ACT-dependent cAMP induction leads to the inhibition of pathways ultimately leading to IL-12p35 production, thus representing a mechanism for *B. pertussis* to escape the host immune response (20).

Overall our findings show that *B. pertussis*, even if only briefly surviving in MDDC, promotes the synthesis of IL-23, and a Th1 oriented immune response is thus allowed, relevant in the induction of an adequate CMI response and typical of protection induced by natural infection or vaccination with whole cell vaccines.

Role of the virulence factors in main functions of APCs and immune adjuvancity

We characterized the adjuvant properties of genetically modified Ptx (12) and demonstrated that Ptx treated DC are able to induce high levels of IL-12p70 and a Th1 driven polarization. The interaction of Ptx with Toll-like receptors (TLR)2- and TLR4 and the intracellular signaling pathways triggered in DC are under investigation.

In collaboration with Alison Weiss's group at the Cincinnati University School of Medicine we studied the ability of *B. pertussis* cell wall lipooligosaccharide (LOS) to modulate DC functions and demonstrated that LOS activatesTLR2- and TLR4-transfected HEK 293 cells and induces partially mature, low level IL-10 producing MDDC, able to skew T helper cells polarization towards a Th2 phenotype. In addition LOS protects MDDC from undergoing apoptosis, influencing their longevity and prolonging their functions on innate and adaptive responses. In conclusion, LOS may contribute to the pathogenicity of the microorganism by perturbing the fine balance of inflammatory and regulatory cytokines. Moreover, due to the ability of LOS treated MDDC to license Th2 effectors, it may be included in the formulation of acellular pertussis vaccines to potentiate protective capacity and as adjuvant (Fedele *et al.*, manuscript submitted).

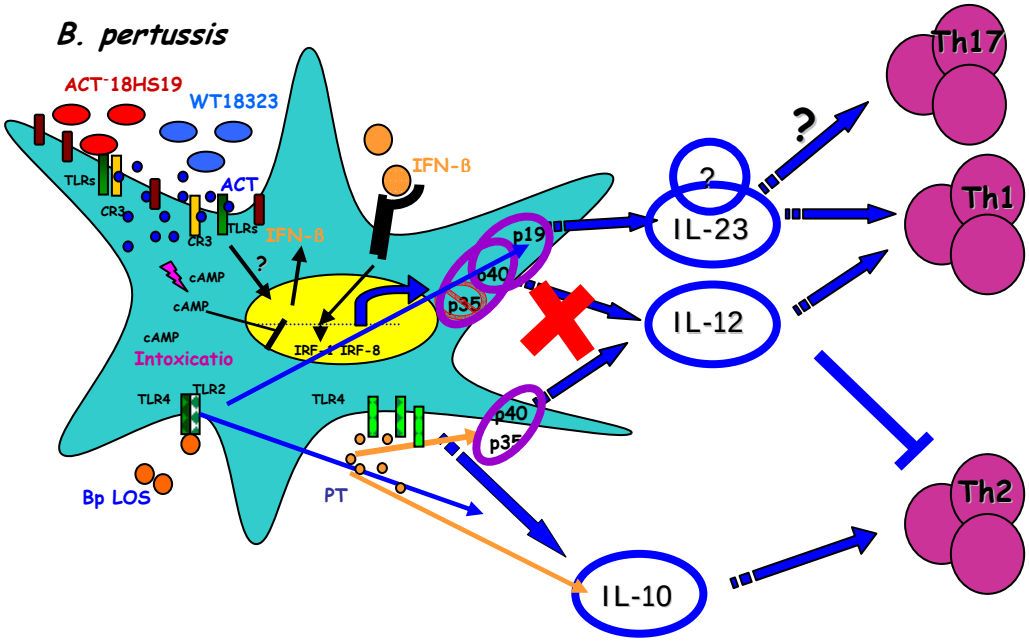

Figure 1. Supra-physiological levels of cAMP induced by ACT inhibit IRFs transcription (IRF-1 and 8) and IL-12p70 production; preferential expression of IL-23 is a useful tool for *Bp* to escape host immune response and potentiate its survival. *B. pertussis* PT induces high IL-12 production and Th1 driven polarization. *B. pertussis* LOS protects MDDC from apoptosis, induces low levels of IL-10 and drives a Th2 response

Differential *in vitro* expression of brkA gene in *Bordetella pertussis* and *Bordetella parapertussis* clinical isolates

BrKA protein is involved in the protection of *Bordetella* against serum bactericidal activity by circumventing the action of the complement system. We first checked if the protein is equally expressed in different *Bordetella* isolates responsible for whooping cough episodes and set up a real-time reverse-transcriptase (RT)-PCR assay to measure the relative amount of brkA transcript in 40 *Bordetella* clinical isolates (37 *B. pertussis* and 3 *B. parapertussis*) collected from infants with whooping cough. The results identified different levels of brkA gene expression among *Bordetella*, suggesting a specific gene regulation in each strain. To verify how the expression of the gene may influence the serum killing sensitivity of the isolates, three representative strains and 27 postvaccination or convalescent immunocompetent sera for pertussis, were used in a serum bactericidal assay. Among strains representative of a high amount of transcript, 98.4±1.8% and 87±4.9% survived against postvaccination or convalescent sera, respectively. On the contrary, strains with a low amount of brkA transcript were highly susceptible to the same sera with a survival of 44±12% and 28±6.7%, respectively. *B. parapertussis* survival was high using sera immunocompetent for pertussis, whereas, more than 90% of colonies was killed by convalescent sera collected from patients with *B. parapertussis* infection.

In conclusion, the real-time RT-PCR was very efficient in quantifying the relative amount of *in vitro* transcript of the brkA gene among several Bordetella isolates, suggesting that the brkA expression is strain-dependent and its amount may play a role in determining the serum resistant or susceptible phenotype. The lack of cross-reaction between *B. pertussis* and *B. parapertussis* outlines the inability of pertussis immunocompetent sera to efficiently kill *B. parapertussis* via complement deposition (21).

Construction of a microarray with all gene sequences (ORF) of *B. pertussis* and *B. parapertussis* to outline the most significant genetic differences between the two species

An expanded *Bordetella* microarray was constructed in collaboration with David Relman's group at the Stanford University School of Medicine. 5670 PCR products representing 97.4% of the *B. pertussis* Tohama I ORFs, 97.9% of the *B. parapertussis* 12822 ORFs were printed in duplicate on poly-L-lysine-coated glass slides. By this approach it was possible not only to map the entire genome from different isolates but also to detect genome rearrangements due to the presence of many insertion elements. The latter define chromosomal deletions and inversions depending on the location of the repeated sequences. The analysis of data provide a detailed picture of the *Bordetella* DNA characterized by little loss or gain, but with capacity to generate variation by rearranging its chromosome and altering gene expression. In particular, we found a high level of conservation of gene content among 137 *B. pertussis* strains with different geographical, temporal, and epidemiological associations, using comparative genomic hybridization. The limited number of regions of difference were frequently located adjacent to the insertion element IS481, which is present at high copy number in the *B. pertussis* chromosome. This repeated sequence appears to provide targets for homologous recombination, resulting in deletion of intervening sequences.

Using subtractive hybridization, we searched for previously-undetected genes in diverse clinical isolates, but did not detect any new genes, indicating that gene acquisition is rare in *B.*

pertussis. In contrast, we found evidence of altered gene order in the several strains that were examined, and again found an association of IS481 with sites of rearrangement.

Finally, we compared whole-genome expression profiles of different strains, and found significant changes in transcript abundance, even in the same strain after as few as 12 laboratory passages. This combination of approaches provides a detailed picture of a pathogenic species with little gene loss or gain, but with the capacity to generate variation by rearranging its chromosome and altering gene expression. These findings have broad implications for host adaptation by microbial pathogens (22).

Acknowledgments

This work was supported by grants from ISS-NIH (USA) scientific cooperation agreement (# 5303). The editorial assistance of Tony Sofia is gratefully acknowledged.

References

1. Mattoo S, Cherry JD. Molecular pathogenesis, epidemiology, and clinical manifestations of respiratory infections due to Bordetella pertussis and other Bordetella subspecies. *Clinical Microbiology Review* 2005;18(2):326-82.
2. Yeh SH. Pertussis persistent pathogen, imperfect vaccines. *Expert review of vaccines* 2003;2(1):113-27.
3. Godfroid F. Are vaccination programs and isolate polymorphism linked to pertussis re-emergence? *Expert Review Vaccines* 2005;4(5):757-78.
4. Heiniger U, Cherry JD. Pertussis immunisation in adolescents and adults--Bordetella pertussis epidemiology should guide vaccination recommendations. *Expert opinion on biological therapy* 2006;6(7):685-97.
5. Cassone A, Ausiello CM, Urbani F, Lande R, Giuliano M, La Sala A, Piscitelli A, Salmaso S. Cell-mediated and antibody responses to Bordetella pertussis antigens in children vaccinated with acellular or whole-cell pertussis vaccines. The Progetto Pertosse-CMI Working Group. *Arch Pediatr Adolesc Med* 1997;151(3):283-9.
6. Ausiello CM, Urbani F, Lande R, La Sala A, Cassone A. Vaccine- and antigen-dependent type 1 and type 2 cytokine induction after primary vaccination of infants with whole-cell or acellular pertussis vaccines. *Infection and Immunity* 1997;65(6):2168-74.
7. Ausiello CM, Lande R, Urbani F, La Sala A, Stefanelli P, Salmaso S, Mastrantonio P, Cassone A. Cell-mediated immune responses in four-year-old children after primary immunization with acellular pertussis vaccines. *Infection and Immunity* 1999;67(8):4064-71.
8. Ausiello CM, Lande R, Urbani F, Di Carlo B, Stefanelli P, Salmaso S, Mastrantonio P, Cassone A. Cell-mediated immunity and antibody responses to Bordetella pertussis antigens in children with a history of pertussis infection and in recipients of an acellular pertussis vaccine. *Journal of Infectious Diseases* 2000;181(6):1989-95.
9. Romagnani S. The Th1/Th2 paradigm. *Immunology Today* 1997;18(6):263-6.
10. Del Prete G, De Carli M, Almerigogna F, Daniel CK, D'Elios MM, Zancuoghi G, Vinante F, Pizzolo G, Romagnani S. Preferential expression of CD30 by human CD4+ T cells producing Th2-type cytokines. *FASEB Journal* 1995;9(1):81-6.
11. Annunziato F, Manetti R, Tomasevic I, Guidizi MG, Biagiotti R, Gianno V, Germano P, Mavilia C, Maggi E, Romagnani S. Expression and release of LAG-3-encoded protein by human CD4+ T cells are associated with IFN-gamma production. *FASEB Journal* 1996;10(7):769-76.

12. Ausiello CM, Fedele G, Urbani F, Lande R, Di Carlo B, Cassone A. Native and genetically inactivated pertussis toxins induce human dendritic cell maturation and synergize with lipopolysaccharide in promoting T helper type 1 responses. *Journal of Infectious Diseases* 2002;186(3):351-60.

13. Kinner SM, Marques RR, Carbonetti NH. Differential reulation of Bvg-activated virulence factors plays a role in Bordetella pertussis pathogenicity. *Infection and Immunity* 2001;69:1983-93.

14. Desauziers E, Danve B, Decker MD, Veitch K. Role of pertactin in pertussis vaccines: the jury is still out. *Journal of Infectious Diseases* 2004;189:1332-3.

15. Mooi FR, van Oirschot H, Heuvelman K, van der Heide HG, Gaastra W, Willems RJ. Polymorphism in the Bordetella pertussis virulence factors P.69/pertactin and pertussis toxin in The Netherlands: temporal trends and evidence for vaccine-driven evolution. *Infection and Immunity* 1998;66:670-5.

16. Stefanelli P, Ippoliti R, Fazio C, Mastrantonio P. Role of immune sera in the in-vitro phagocytosis of Bordetella pertussis strains. *Microbial Pathogenesis* 2002;32:135-41.

17. Brinig MM, Cummings CA, Sanden GN, Stefanelli P, Lawrence A, Relman DA. Significant gene order and expression differences despite limited gene content variation in Bordetella pertussis. *Journal of Bacteriology* 2006;188:2375-82.

18. Ausiello CM, Palazzo R, Spensieri F, Urbani F, Massari M, Triebel F, Benagiano M, D'Elios MM, Del Prete G, Cassone A. Soluble CD30 and lymphocyte activation gene-3 (CD223), as potential serological markers of T helper-type cytokine response induced by acellular pertussis vaccine. *International Journal of Immunopathology and Pharmacology* 2006;19(1):97-104.

19. Fedele G, Stefanelli P, Spensieri F, Fazio C, Mastrantonio P, Ausiello CM. Bordetella pertussis-Infected Human Monocyte-Derived Dendritic Cells Undergo Maturation and Induce Th1 Polarization and Interleukin-23 Expression. *Infection and Immunity* 2005;73:1590-7.

20. Spensieri F, Fedele G, Fazio C, Nasso M, Stefanelli P, Mastrantonio P, Ausiello CM. Bordetella pertussis inhibits IL-12p70 in human monocyte-derived dendritic cell blocking IL-12p35 through adenylate cyclase toxin-dependent cAMP induction. *Infection and Immunity* 2006;74(5):2831-8.

21. Stefanelli P, Sanguinetti M, Fazio C, Posteraro B, Fadda G, Mastrantonio P. Differential in vitro expression of brkA gene in Bordetella pertussis and Bordetella parapertussis clinical isolates. *Journal of Clinical Microbiology* 2006;44(9):3397-400.

22. Brinig MM, Cummings CA, Sanden GN, Stefanelli P, Lawrence A, Relman DA. Significant gene order and expression differences despite limited gene content variation in Bordetella pertussis. *Journal of Bacteriology* 2006;188:2375-82.

Session 4A. Immunity and infectious diseases

STUDY AND VALIDATION OF UNDEREXPLORED MOLECULAR PROCESSES IN PLASMODIUM AS POTENTIAL DRUG TARGETS FOR NEW INTERVENTION STRATEGIES

Marta Ponzi (a), Xin-zhuan Su (b), Pietro Alano (a), Elisabetta Pizzi (a), Fabiana Superti (c), Lucia Bertuccini (c), Andrew P Waters (d), Chris J Janse (d)

(a) Department of Infectious, Parasitic and Immuno-Mediated Diseases, Istituto Superiore di Sanità, Rome, Italy

(b) Laboratory of Malaria and Vector Research, National Institute of Allergy and Infectious Diseases, National Institutes of Health, Bethesda, MD, USA

(c) Department of Technology and Health, Istituto Superiore di Sanità, Rome, Italy

(d) Parasitology, Center of Infectious Diseases Leiden University Medical Center

Malaria, along with AIDS and Tuberculosis, are considered now days a global emergency (1). Malaria is mainly confined to tropical and subtropical areas of Africa, Asia and Latin America but most cases occur in tropical Africa. According to WHO, it is responsible for 273 million clinical cases and 1.12 million deaths annually, particularly among young children and pregnant women.

Despite massive efforts to eradicate the disease more than 40% of the global population is estimated to be at risk due to the insurgence and spreading of parasites resistant to effective drugs, the appearance of mosquitoes resistant to insecticides, the lack of a licensed malaria vaccine and the complexity of parasite life cycle.

The unicellular parasite *Plasmodium falciparum* is the main cause of severe human malaria and lethal cases. Transmission occurs via the bite of an infected mosquito of the genus *Anopheles*. The injected parasites undergo an asynptomatic multiplication in the liver cells of a human host and successively develop and replicate within the red blood cells. During the erythrocyte cycle, a fraction of parasites differentiate into gamete precursors (male and female gametocytes), the sole forms able to infect mosquitoes and hence responsible for transmission and spreading of drug resistant parasites.

These facts emphasize the need to find new treatments and new ways of preventing malaria and that more should be learnt on basic biology of the parasite to identify vulnerable aspects.

The availability of the genome sequences of the three components of the malaria life cycle, *P. falciparum* (2), *Anopheles gambiae* (3) and humans (4), represented a milestone in malaria research with the great opportunity to find genes and/or metabolic pathways unique to, or substantially different in, *Plasmodium* as potential drug targets or vaccine candidates.

Status of the ISS/NIH project

The collaborative project ISS/NIH aimed at identifying and characterising, with the tools of the functional genomics, new molecules/metabolic pathways specific for sexual stages with the ultimate goal to provide a wealth of information and potential targets useful to design new

intervention strategies to control transmission, and overcoming the spread of drug-resistant *P. falciparum*.

In a first phase of the project the group at the ISS pursued the following objectives:

- The identification of new gametocyte-specific genes expressed/upregulated during the early phases of sexual development of *P. falciparum* through microarray experiments.
- The identification and characterisation of genes specifically/differently expressed in male and female gametocytes and the generation of reagents to analyse the progression of sexual development (transgenic lines, specific antibodies) in the rodent model *P. berghei*.
- The development/improving of bioinformatic tools for data mining and comparative analysis of *Plasmodium* genome, transcriptome and proteome.
- The functional analysis of a novel parasite protein (MVD 1/PfPEG3) conserved within *Plasmodium* genus.

Results

The molecular mechanisms responsible for sexual commitment during erythrocyte cycle of malaria parasite are completely unknown and the early events of gametocytogenesis poorly understood. Early proteins are most likely important for the progression of sexual cell differentiation, and hence good transmission blocking candidates. Only two genes (*pfs16* and *pfg27*) expressed at the onset of gametocytogenesis, which takes place in 9-10 days, have been characterised so far in *P. falciparum*. In order to identify *P. falciparum* molecules specifically expressed few hours after induction of sexual cell differentiation, when gametocytes are still indistinguishable from asexual parasites, microarray experiments were conducted on parasite populations characterised for their ability to produce gametocytes.

The transcription profile of a gametocyte-producer line was compared with that of an isogenic clone unable to undergo sexual differentiation.

These experiments were conducted with oligo-microarrays representative for 4500 of 5400 predicted open reading frames. A cluster of 117 genes, the expression of which significantly correlated with that of the two known markers of the early gametocytogenesis, was identified (Figure 1).

The study of gametocytogenesis in rodent models affords the opportunity to extend functional analysis of specific genes/metabolic pathways to the mosquito cycle. Male and female gametocytes complete their differentiation in gametes once taken up by mosquito and several gene products expressed during gametocyte development within the host erythrocytes exhert their function later in mosquito host. This is the case of SET; a conserved nuclear protein involved in chromatin dynamics and expressed throughout parasite cycle in vertebrate and mosquito hosts. Protein abundance in asexual/sexual stages is regulated at the transcription level by the activation of two distinct, developmentally regulated promoters. SET is particularly abundant in male gametocytes and this is consistent with the fact that male gamete maturation involves three rounds of replication and mitosis that occur in few minutes in the mosquito midgut to generate eight flagellated gametes, while no replication event occurs in female gametocytes.

Transgenic lines harbouring SET fused to the green fluorescent protein (GFP) under the control of asexual or sexual promoter along with immune sera raised against parasite proteins specific for male and/or female gametocytes generated at the ISS, constitute reagents useful to trace the entire sexual cycle.

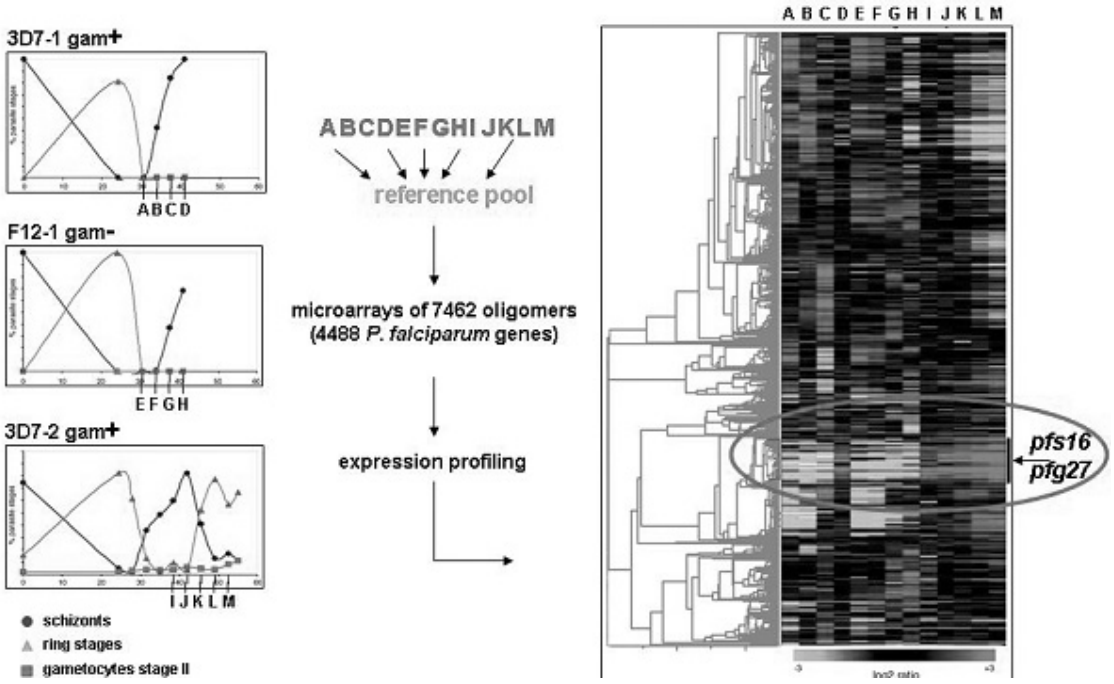

Figure 1. Genome-wide identification of genes upregulated in early sexual development. Transcriptome analysis on different RNA samples from *P. falciparum* 3D7 able (gam+) and unable (gam-) to undergo sexual differentiation (Silvestrini *et al.*, 2005). The expression profiles specific for the early gametocyte genes *pfg27* and *pfs16* plus 141 additional correlated array elements, representative of 117 genes, are boxed in figure

One of the most intriguing features of *Plasmodium falciparum* genome is the high AT content, which determines an unusual amminoacidic composition of the encoded proteins and the absence of recognisable regulatory motifs within the intergenic regions. A procedure based on statistical methods has been developed to define specific features, which discriminate between coding and non-coding regions. In addition, algorithms for sequence alignment have been improved by generating a group of new matrices specifically designed to analyse and compare *Plasmodium* proteins with a biased amminoacidic composition.

Among the early gametocyte-specific molecules identified through comparative microarray analysis are proteins located at the surface of the parasitophorous vacuole. This compartment generated by the parasite early after erythrocyte invasion is maintained in both asexual and sexual cells. It constitutes a host/parasite interface and participates to protein sorting and trafficking during the development of asexual stage; its functional role and protein composition in sexual stages has been poorly investigated.

A novel protein (PfPEG3/MDV-1) targeted at the membrane of this compartment at the onset of gametocytogenesis (Figure 2), and conserved in the rodent parasites has been identified with different approaches by the group of Dr. Alano at the ISS (5) and by the group of Dr. Su at the NIAD (6).

This suggests that remodelling of the vacuolar membrane by the insertion of specific proteins is an early event in sexually committed parasites. Notably, a *P. falciparum* line knocked out for the encoding gene, generated at the NIAD, indicated that the absence of PfPEG3/MDV-1 strongly affects the ability to produce fully developed gametocytes.

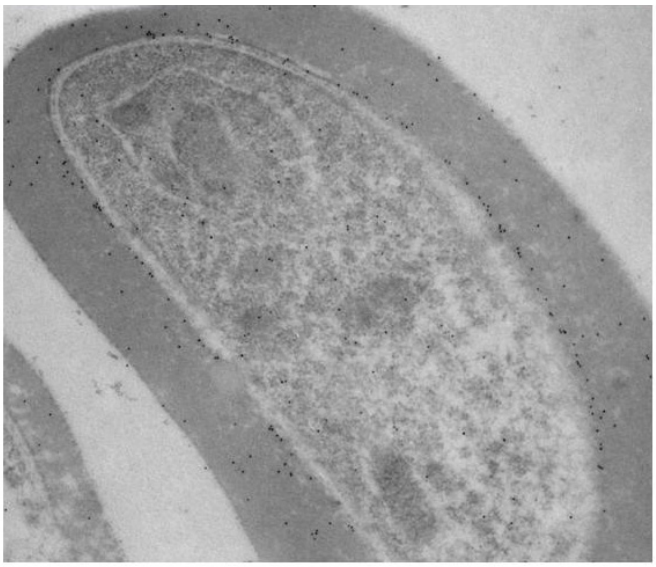

Figure 2. Immunoelectron microscopy localization of PfPEG3/PfMDV-1.
A *P. falciparum* gametocyte section, reacted with anti-PfPEG3/MDV-1 antibodies, showing protein localization on the membrane of the parasitophorous vacuole
(kindly provided by Lucia Bertuccini, Dept.TESA)

Conclusions and future outlook

Important achievements have been made in characterising parasite-specific processes and/or cellular compartments by comparative analyses between different *Plasmodium* species. PfPEG3/MDV-1 is conserved within the *genus* and this will give us the opportunity to extend functional analysis to the rodent *in vivo* model including mosquito stages.

References

1. Breman JG, Egan A, Keusch GT. The intolerable burden of malaria: a new look at the numbers. *Am J Trop Med Hyg* 2001;64(1-2 Suppl):iv-vii.
2. Gardner MJ *et al.* Genome sequence of the human malaria parasite Plasmodium falciparum. *Nature* 2002;419:498-511.
3. Holt RA *et al.* The genome sequence of the malaria mosquito Anopheles gambiae. *Science* 2002;298:129-49.
4. International Human Genome Sequencing Consortium. Finishing the euchromatic sequence of the human genome. *Nature* 2004;431:931-45.
5. Silvestrini F, Bozdech Z, Lanfrancotti A, Di Giulio E, Bultrini E, Picci L, Derisi JL, Pizzi E, Alano P. Genome-wide identification of genes upregulated at the onset of gametocytogenesis in Plasmodium falciparum. *Mol Biochem Parasitol* 2005;143:100-10.

6. Furuya T, Mu J, Hayton K, Liu A, Duan J, Nkrumah L, Joy DA, Fidock DA, Fujioka H, Vaidya AB, Wellems TE, Su XZ. Disruption of a Plasmodium falciparum gene linked to male sexual development causes early arrest in gametocytogenesis. *Proc Natl Acad Sci U S A* 2005;102:16813-8.
7. Di Girolamo F, Raggi C, Bultrini E, Lanfrancotti A, Silvestrini F, Sargiacomo M, Birago C, Pizzi E, Alano P, Ponzi M. Functional genomics, new tools in malaria research. *Ann Ist Super Sanità* 2005;41:469-77.
8. Pace T, Olivieri A, Sanchez M, Albanesi V, Picci L, Siden-Kiamos I, Janse CJ, Waters AP, Pizzi E, Ponzi M. Set regulation in asexual and sexual Plasmodium parasites reveals a novel mechanism of stage-specific expression. *Mol Microbiol* 2006;60:870-82.
9. Bultrini E, Pizzi E. A new parameter to study compositional properties of non-coding regions in eukaryotic genomes. *Gene* 2006; in press.

Session 4A. Immunity and infectious diseases

THE TREATMENT OF HIV-AIDS. INTEGRASE AS A NEW TARGET OF ANTIRETROVIRAL THERAPY

Lucia Palmisano (a), Clementina Maria Galluzzo (a), Mauro Andreotti (a), Roberta Costi (b), Maurizio Cianfriglia (a), Maria Luisa Dupuis (a), Alessandra Roux (b), Roberta Amici(a), Maria Grazia Mancini (a), Anna Teresa Palamara (c), Yves Pommier (d), Roberto Di Santo (b)

(a) Department of Therapeutic Research and Medicines Evaluation, Istituto Superiore di Sanità, Rome, Italy

(b) Istituto Pasteur-Fondazione Cenci Bolognetti, Dipartimento di Studi Farmaceutici, Università di Roma "La Sapienza", Rome, Italy

(c) Istituto di Microbiologia, Università di Roma "La Sapienza", Rome, Italy

(d) Laboratory of Molecular Pharmacology, National Cancer Institute, National Institutes of Health, Bethesda, MD, USA

Introduction

Twenty-five years have passed since the first cases of AIDS were recognized, and 23 years from the discovery of HIV as its causative agent. Following the advent of Highly Active Antiretroviral Therapy (HAART) (1) dramatic changes occurred in the natural history of the disease. Indeed, the projected individual survival after an AIDS diagnosis increased from 1.6 years in the absence of treatment to 14.9 years by 2003, and the trend has been continuous in geographical areas with widespread access to antiretroviral agents. In fact, recent estimates indicate that HAART has saved at least 3 millions years of life in the only Unites States (2). At the same time, factors potentially limiting the effectiveness of antiretroviral agent are represented by the spread of resistance (3) and the toxicity of HAART, especially coronary heart disease and metabolic abnormalities. From these considerations it clearly appears that the list of available antiretrovirals, despite impressive (21 agents approved by FDA), does not satisfy the needs of HIV patients, especially those who acquired the infection several years ago and have now to face up to a multiresistant virus and/or to the serious metabolic consequences of a chronic therapy. With the exception of entry inhibitors, that block the fusion of HIV to host cell, all the antiretroviral regimens currently in use target two viral enzymes: reverse transcriptase (RT, a DNA polymerase that transcribes single strand HIV RNA into double-stranded DNA) and protease (PR, which cleaves viral polyproteins into the individual proteins of the mature virus). Integrase (IN) is the third HIV enzyme, carrying out the integration of viral DNA into the host chromosome; its role is essential because provirus formation is required to ensure the efficient transcription of viral genes and the persistence of viral genomic information within the host cell. In fact, IN has been an appealing target for antiretroviral therapy for about 15 years, also because it is unique to retroviruses and has no cellular counterpart in humans.

Mechanism of action of HIV Integrase

IN is a 288 aminoacids molecule, encoded at the 3'-end of the viral *pol* gene, that catalyzes two key steps required for the integration of viral DNA into the host chromosome. The first step, a reaction known as 3' processing, takes place in the cytoplasm of the infected cell: IN recognises and cleaves two nucleotides from the 3' terminal of the retro-transcribed viral DNA and then translocates to cell nucleus as a component of the pre-integration complex (PIC), which contains also other cellular and viral proteins facilitating the whole process of viral integration. In the second step, the so called DNA strand transfer (ST), host DNA is cleaved and a pair of the processed viral DNA ends is covalently and irreversibly linked to it. The integrated HIV is usually referred to as proviral DNA (Figure 1).

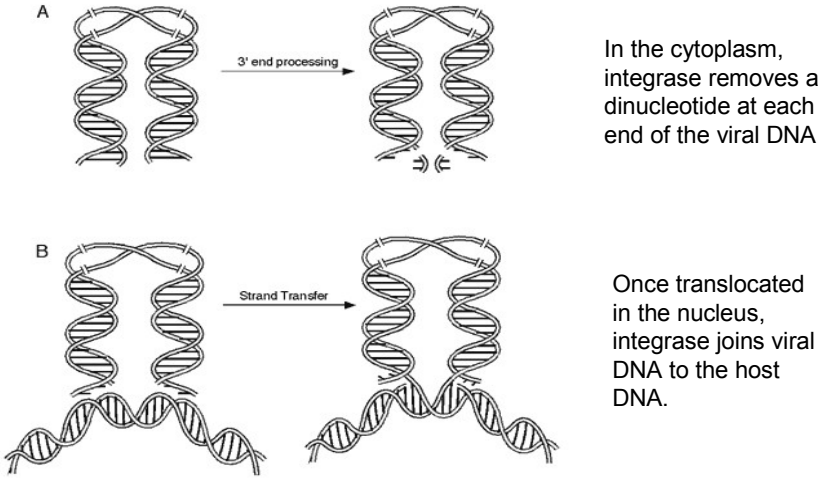

Figure 1. Schematic mechanism of action of HIV-1 Integrase

Development of IN inhibitors

Despite the great interest that integrase inhibitors (II) have raised among scientists and clinicians involved in HIV disease, their clinical development has been long and full of pitfalls and disappointments: since the discovery of the first molecule with this property in 1993 (4), many natural and synthetic substances have been shown to block IN in enzymatic assays. However, most of these compounds did not meet the minimum requirements needed to define them lead molecules, and did not undergo further development.

A great contribution to the research on II has come from two companies, Merck and Shionogi, who discovered aryl diketo acid (DKA) derivatives, characterized by an ability to preferentially inhibit ST versus 3'-P reactions (5,6). These early compounds are typified by 5-CITEP produced by Shionogi and the pyrrole derivative L-731,988 synthesized by Merck. Both these products represented a breakthrough and a milestone in the pharmacology of HIV infection, driving most of the subsequent research in the field. Thanks to extensive structure-activity relationship (SAR) studies, further compounds were designed, such as the naphthyridine

derivatives (7). One of these compounds, the L-870,812, provided the first evidence of *in vivo* antiretroviral activity of II in rhesus macaques infected with the simian-human immunodeficiency virus (SHIV) (8). A congener of L-870,812, the L-870,810, provided the first clinical proof of concept for this new pharmacological class, but was placed on hold because of toxicity in dogs (9). Eventually a Merck back-up compound of the same family, currently known as MK-0518, quickly moved into clinical development, showing potent anti HIV activity in treatment-naïve and treatment-experienced HIV+ subjects (10,11). Phase III clinical trials with this agent are ongoing. Another II developed by Gilead, the GS-9137, yielded promising results in phase II clinical trials (12). These two agents are the most probable candidates to an FDA/EMEA regulatory approval in the medium term.

Quinolones derivatives as inhibitors of HIV-1 integrase

4(1*H*)-Quinolinone-3-carboxylic acid derivatives (briefly quinolones) are potent antibacterials widely used in chemotherapy. Their potency and well known safety profile make them suitable to be utilized as special scaffolds for developing II. A further advantage is that a number of substituents can be easily introduced in all positions of these molecules.

On the basis of these considerations, starting from two prototypes (RDS 1624 and RDS 1625, ethylic ester and free acid, respectively), a panel of compounds were designed and screened for their activity in assays utilising recombinant IN. Design and synthesis took place at "La Sapienza" University in Rome, whereas the anti-IN assays were performed at NIH (Bethesda, US). The IC50 values on 3'-P and ST were calculated. In addition, bifunctional DKAs (BDKAs) based on the 4-(4(1*H*)-quinolinon-3-yl)-2,4-dioxobutanoic acid skeleton and characterized by the presence of two diketo acid chains in 3 and 6 position of the quinolinone skeleton of the inhibitor, were designed and synthesized. The most potent compound belonging to this series was RDS 1997 characterized by the presence of 2 diketo acid chains in 3 and 6 position and a 4-F-benzyl group in position 1. These compounds inhibited both ST and 3'-P steps at similar concentrations . According to molecular modeling (MM) studies, the first diketo acid branch in 3-position of the quinolinone ring binds the DNA acceptor site (human DNA), while the second diketo acid function is directed towards the DNA donor site (viral DNA) (Figure 2). This may explain the low selectivity showed by these compounds in inhibiting ST and 3'-P steps of integration process, resulting in a potential enhancement of anti-IN activity (13).

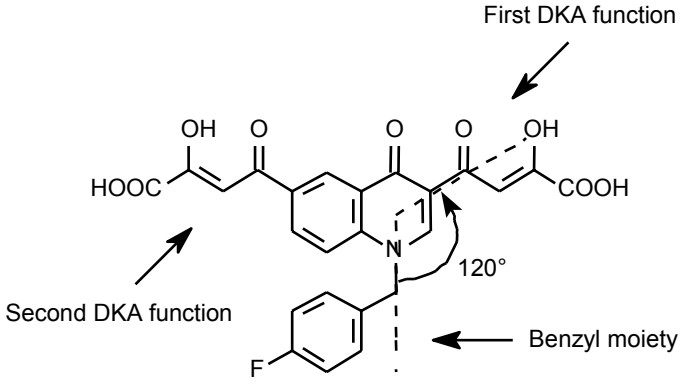

Figure 2. An example of bifunctional DKA: RDS 1997

Compounds that were active on at least one of the two steps of the integration reaction were subsequently tested in cell based assays, employing H9 cells and/or PBMC from healthy donors infected by HIV-1. These studies were performed at ISS, Dept of Drug Research and Evaluation, and provided the EC50 values. In the same cell system cell vitality was evaluated by the Trypan Blue method and the CC50 (drug concentration producing cytotoxicity in 50% of cells) values were calculated. A summary of results obtained in the different assays for the most interesting compounds is provided in Table 1.

Table 1. Activity of the most representative quinolone derived II

Compound code	IC50 3'-P (μM) Mn++	IC50 ST (μM) Mn++	EC50 (μM)	CC50 (μM)
RDS 1974	>333	32	>50	>50
RDS 1975	18	<0.45	>50	>50
RDS 1980	333	120	>50	>50
RDS 1981	>333	<0.45	>50	>50
RDS 1989	125	0.28	2.2	>>50
RDS 1990	1.2	0.016	9.3	>>50
RDS 1992	>1000	0.70	20.5	>>50
RDS 1993	4.0	0.034	7.2	>>50
RDS 1997	0.20	0.012	2.4	>>50
RDS 1999	>1000	3.5	>50	>50
RDS 2000	70	0.40	>50	>50
RDS 1983	>12.3	0.25	5.9	>50
RDS 1984	0.7	0.019	9.6	>50
RDS 1986	>12.3	4.9	>50	>50
RDS 1987	4.6	0.015	>50	>>50
RDS 2080	>333	80	>50	45.8
RDS 2081	>4.1	0.43	>50	37.8
RDS 2173	>333	1.4	>50	>>50
RDS 2174	>37	0.45	>50	>>50
RDS 2160	>333	16	>50	>50
RDS 2161	>4.1	0.14	>50	>50
RDS 2163	>333	.1.4	>50	>50
RDS 2164	>4.1	0.038	>50	30.6
RDS 2021	25	1.9	>50	>50
RDS 2022	1.9	0.042	>50	>50
RDS 2077	>37	0.49	>50	>50
RDS 2078	2.9	0.047	>50	>50
RDS 2107	>333	4	>50	>50
RDS 2108	>4.1	0.025	>50	>50
RDS 2111	>333	4	>50	>50
RDS 2112	>4.1	0.014	>50	>50
RDS 2034	>37	>37	>50	>50
RDS 2035	28	0.51	>50	>50
RDS 2085	>633	14	>50	>50
RDS 2017	>37	>37	>50	>50
RDS 2012	22	0.54	1.8	>>50
RDS 2011	>37	>37	>50	>50
RDS 2018	27	0.64	19.5	>50
RDS 1625	2.20	0.0313	1.2	27
RDS 1624	>100	0.326	34.8	>50
RDS 1787	28.7	0.124	46.1	>>50
RDS 1996	40	0.34	24.8	2.8
RDS 1792	1792	0.0210	>50	>50

IC50 indicates the concentration required for a 50% inhibition of recombinant IN. EC50 indicates the concentration required for a 50% inhibition of viral replication in H9 infected cells. CC50 indicates the concentration required to induce cytotoxicity in 50% of cells.

As a general consideration, the activity in the enzymatic assay (that is conducted in a cell-free environment) is in the nanomolar range, whereas in cell based assays it is in the micromolar range. In addition, in some case discordant results were found in the two assays, Factors such as cell penetration and metabolism may play a role in determining these discrepancies.

An interesting finding is that some of these compounds retain their ability to inhibit recombinant IN when tested in the presence of Mg++ instead of Mn++. This provides an indirect evidence of *in vivo* activity since Mg++ is involved in the *in vivo* activity of IN.

SAR studies produced additional insights on the relationship between chemical structure and anti-IN activity that can be summarized as follows: for a compound to be active, a benzyl in position 1 is required; acids are constantly more active than corresponding esters; a fluorine atom on benzyl is associated with greatest activity; the optimal position for substitution on the benzyl ring is 2 (or 3); the presence of two fluorine atoms in position 2,6 provides potent activity.

HIV integrase inhibitors as substrate of multidrug transporter P-glycoprotein (P-gp)

P-gp is a membrane pump responsible for the efflux of unrelated substances and toxic agents. Several compounds have been recognized as substrates of this molecule; this property is shared by some anti-retroviral agents, especially in the class of protease inhibitors, and may influence their pharmacokinetics and bioavailability.

We therefore evaluated 9 IN for their capability to modulate P-gp activity in CEM-VBL cell line, that express P-gp on their surface. These studies were performed at ISS, Dept of Drug Research and Evaluation, and showed that : 1) IN inhibitors interfere with P-gp activity, since they block Pg-mediated doxorubicin efflux from CEM-VBL100 cells which express high levels of P-gp; 2) they recognise P-gp in an activated conformation since they increase the expression of the Moab UIC2 which has a high affinity for P-gp when it is in the process of transporting substrates. These properties were not correlated with antiviral activity (14).These preliminary results, that will be further expanded with additional experiments, may have important clinical implications for the biovailability of II, since P-gp is widely expressed in human body and is also present at the blood-brain barrier, thereby affecting drug penetration in Central Nervous System.

Conclusions

Integrase inhibitors represent one of the most promising new class of anti-HIV agents, with two compounds in a relatively advanced stage of clinical development. In fact for one of them, the MK-0518, a request of approval is likely to be submitted to FDA by 2007. In the context of our project, novel quinolinyl-diketo-butanoic acid derivatives were designed and synthesized that were active on recombinant IN. The majority of these compounds, which utilise a quinolone scaffold, were also active in cell based assays, where they induced a significant block in HIV-1 replication. An evolution of the original compounds led to the design and synthesis of bifunctional diketoacids; these molecules deserve special interest for their capacity of inhibiting both steps of integration, the 3'-P and the ST, thereby inhibiting IN activity at both donor (viral) and acceptor (human) DNA.

Finally, our results on P-gp provide interesting information on the functional properties of II, which may have clinical implications for their availability and also open new perspectives for their potential use in other fields, such as anti-cancer chemotherapy, where they might be as explored as modulators of anticancer agents.

References

1. Fischl MA, Richman DD, Grieco MH *et al.* The efficacy of azidothymidine (AZT) in the treatment of patients with AIDS and AIDS-related complex. A double-blind, placebo-controlled trial. *N Eng J Med* 1987;317:185-91.
2. Walensky RP, Paltiel AD, Losina E. The survival benefits of AIDS treatment in the United States. *J Infect Dis* 2006;194(1):11-9.
3. Vella S, Palmisano L. The global status of resistance to antiretroviral drugs. *Clin Infect Dis* 2005;41(Suppl 4):S239-46.
4. Fesen MR, Kohn KW, Lefeurtre F, Pommier Y. Inhibitors of human immunodeficiency virus integrase. *Proc Nat Acad Sci USA* 1993;90:2399-403.
5. Goldgur Y, Craigie R, Cohen GH, *et al.* Structure of the HIV-1 integrase catalytic domain complexed with an inhibitor: a platform for antiviral drug design. *Proc Natl Acad Sci USA* 1999;96:13040-3.
6. Hazuda D, Felock P, Wilmer M, *et al.* Inhibitors of strand transfer that prevent integration and inhibit HIV replication in cells. *Science* 2000;287:646-50.
7. Hazuda D, Anthony NJ, Gomez RP, *et al.* A naphthyridine carboxamide provides evidence for discordant resistance between mechanistically identical inhibitors of HIV-1 integrase. *Proc Nat. Acad Sci USA* 2004;101:11233-8.
8. Hazuda DJ, Young SD, Guare JP, *et al.* Integrase inhibitors and cellular immunity suppress retroviral replication in rhesus macaques. *Science* 2004;305:528-32.
9. Little S, Drusano C, Schooley R, *et al.* Antiretroviral effect of L-000870810, a novel HIV-1 integrase inhibitor, in HIV-1-infected patients. *Proceedings of the 12th Conference on Retroviruses and Opportunistic Infection,* Boston MA, February 22-25 Abstr 161, (2005).
10. Morales-Ramirez JO, Teppler H, Kovacs C, *et al.* Antiretroviral effect of MK-0518, a novel HIV-1 integrase inhibitor, in ART-naïve HIV-1 infected patients. *Proceedings of the 10th European AIDS Conference,* Dublin, November 17-20 2005. Abstract LBPS1/6.
11. Grinsztejn B, Nguyen BY, Katlama C, *et al.* Potent antiretroviral effect of MK-0518, a novel HIV-1 integrase inihibitor, in patients with triple-class resistant virus. *Proceedings of the 13th Conference on Retroviruses and Opportunistic Infection;* Denver CO, February 5-8 2006. Abstract LB160.
12. DeJesus E, Berger D, Markowitz M, *et al.* The HIV integrase inhibitor GS-9137 (JTK-303) exhibits potent antiviral activity in treatment-naive and experienced patients. *Proceedings of the 13th Conference on Retroviruses and Opportunistic Infections;* February 5-8, 2006. Denver, Colorado abstract 160LB.
13. Di Santo R, Costi R, Roux A, *et al.* Novel Bifunctional Quinolonyl Diketo Acid Derivatives as HIV-1 Integrase Inibitors: Design, Synthesis, Biological Activities and Mechanism of Actions. *J Med Chem* 2006;49:1939-45.
14. Dupuis ML, Cianfriglia M, Costi R, *et al.* HIV-1 Integrase Inibitors Are Potent Sustrates for the MDR1 Multidrug Transporter. *Proceedings of the 13th Conference on Retroviruses and Opportunistic Infections*. Denver Co abstract 565 (2006).

Session 4B. Vaccines

MOLECULAR AND ANTIGENIC EVOLUTION OF ROTAVIRUS STRAINS OF HUMAN AND ANIMAL ORIGIN

Franco Maria Ruggeri (a), Patrizia Battista (a), Marina Monini (a), Federica Cappuccini (a), Emiliana Falcone (a), Antonio Lavazza (c), Olga Tcheremenskaya (a), Gianluca Marucci (b), Lucia Fiore (b)

(a) Department of Food Safety and Veterinary Public Health, Istituto Superiore di Sanità, Rome, Italy

(b) Department of Infectious, Parasitic and Immuno-Mediated Diseases, Istituto Superiore di Sanità, Rome, Italy

(c) Istituto Zooprofilattico Sperimentale della Lombardia e dell'Emilia-Romagna, Brescia, Italy

Introduction

Rotaviruses are classified into groups A-E sharing a double-stranded RNA genome made of 11 segments and a triple-layered unenveloped protein capsid. Group A is associated with most part of human infections and is also widespread among wild and domestic animal species. Within group A, subgroups I, II, I+II and nonI, nonII, and at least 14 G- and 20 P-types can be distinguished based on the reactivity of antibodies to epitopes on viral proteins VP6, VP7 and VP4, respectively. Like other RNA viruses, rotaviruses display a great degree of diversity reflected by both the presence of many combinations of G and P types and the occurrence of intratypic variation. The evolutionary potential of rotaviruses is linked to three distinct mechanisms: (i) antigenic drift, due to the accumulation of mutations during replication; (ii) antigenic shift, due to reassortment of genomic segments in the course of dual infections; (iii) rearrangement, based on the concatamerization or truncation of RNA.

Rotavirus is a major cause of severe acute gastroenteritis among children, with a death toll of over 800,000 individuals per year particularly in developing countries and more than two episodes per child before age 5 in industrialized areas (1,2). In developed countries, the burden of disease may exceed 125 million cases annually, of which 18 million are severe cases requiring hospitalization or medical care. Group A rotaviruses are distributed worldwide, and disease occurs typically in winter peaks in temperate climate zones of the world. Rotaviruses are also widespread in most animal species, representing a leading cause of neonatal death in bovines.

The incidence and distribution of group A rotavirus sero/genotypes may vary between geographical areas during a same epidemic season as well as from a season to another. Strains belonging to G1 through G4 and P[4] and P[8] are the most common viruses causing disease in humans worldwide. Whereas G1P[8], G2P[4], G3P[8] and G4P[8] are predominant in North America, Europe and Australia, other G/P combinations appear to be largely spread in South America, Asia and Africa (3,4). Further, an increasing number of reports concern the occurrence of previously unusual rotavirus types in man such as the G9 strains (5).

The burden of rotavirus disease justifies the efforts in developing effective human vaccines for both reducing mortality in developing countries and abating morbidity worldwide. A first generation tetravalent vaccine (G1-4) has been used in the USA in 1998-9, but was withdrawn due to possible association with risk of intussusception. At least two further vaccines (mono-

and penta-valent) will be licensed in either US or Europe during 2006-2007. These are both based on the assumption of a broad cross-reactive immunity elicited by vaccination against the most important human rotavirus serotypes, although the impact of mass vaccination onto the spectrum of rotaviruses presently circulating is unpredictable.

Because of the evidence collected for a possible serotype-specific nature of the immunity elicited by rotavirus infection, it is highly desirable to implement an extended surveillance of natural rotavirus infections before and after vaccination. Recent knowledge on the changing molecular epidemiology of rotaviruses with the emergence of new sero/genotypes is a challenge to vaccine development, and urges studies on circulating strains of human and animal origin to identify novel molecular and antigenic variants. In addition to the most common sero/genotypes in man, G1 through G4, P[8], P[4], and P[6], serotyping should encompass the globally emerging human G9 strains, and virus antigen specificities prevalent among animals, i.e. G5, G6, G8, G10 and P[1], P[5-7], P[11], some of which are involved in zoonotic transmission.

Description of the Project

The project is aimed to gather information onto the circulation of rotavirus strains in Italy and neighboring countries and compare the observed geno/serotypes with those described in US and other areas. Particular attention is dedicated to the recognition of unusual genotype combinations that may be spread into humans originating from animal species, through zoonotic transmission and evolution. To pursue these objectives, the project is taking advantage of the collaboration with Drs. Albert Z. Kapikian and Yasutaka Hoshino at the NIAID, NIH of Bethesda, who developed molecular techniques for virus genotyping and have established a broad collection of rotavirus strains with different genotype and sequences. Strains of rotavirus of potential zoonotic origin found at the ISS are finely characterized at the level of nucleotide sequence of genes 4 and 9 at ISS, being subsequently examined at the NIH to establish the origin of the 9 other segments of their genomic dsRNA. After screening and initial typing of unusual strains is achieved in Italy, comparison of sequence data and phylogenetic studies will be completed at the NIH using the worldwide rotavirus database there established. Strict collaborations are in place with Prof.s Vito Martella and Canio Buonavoglia of the Faculty of Veterinary Medicine of the University of Bari (6), and with Dr. Antonio Lavazza at the Istituto Zooprofilattico Sperimentale of Brescia, where detection and characterization of rotavirus strains from domestic animals has been performed. The project is also involving collaborators of public health institutes or virological laboratories of the WHO polio lab network in five countries of the Balkan and eastern-central European regions, in order to supply rotavirus strains from diarrhoic children including areas characterized by a rural setting and closer contact with farm animals.

Materials and methods

Human rotavirus surveillance

A hospital-based surveillance was established in the Czech Republic (National Institute of Public Health, Prague), Slovenia (Institute of Public Health, Ljubljana), Croatia (National Institute of Public Health, Zagreb), Albania (Institute of Public Health, Tirana), and Bulgaria (National Enterovirus Laboratory, NCIPD, Sofia). Patients up to 5 years of age, admitted to

hospitals with acute diarrhea, were enrolled into the study. Stools were taken at admission for search of conventional enteropathogens, and questionnaires collecting household and patient's information, clinical data and laboratory findings were administered. Group A rotavirus diagnosis was carried out on stools by either an immunoenzymatic or latex-agglutination assay, and positive specimens were frozen between –20°C and –70°C before being shiped to the ISS in Rome for molecular characterization.

Animal rotavirus surveillance

Stool samples from animal farms (mostly bovine) and stools or intestinal contents from animals with or without specific gastroenteritis records from slaughter houses were collected in order to represent a consistent number of farms in Northern Italy. Laboratory diagnosis was conducted by immunoenzymatic methods for group A rotavirus.

Sero-genotyping

Rotavirus genotyping was conducted at the ISS using water dilutions of clarified stools or caecal fluids. Rotavirus RNA was extracted by guanidine/silica based column purification (Qiagen; QIAmp Viral RNA Mini Kit), and was subjected to RT/PCR amplification of full-length genomic segments encoding for VP4 and VP7 using the SuperScript One-Step RT-PCR kit (Invitrogen), according to previously reported methods (7). For G-typing, the amplified DNA was then analyzed in a second round of multiplex-PCR (40 cycles: 94°C for 1 min; 42°C for 1 min, 72°C for 75 sec) with combinations of genotype-specific primers (VP7-R1 + G1, G2, G3, G4, G8, G9, G10), and results were read by agarose gel fractionation and ethidium staining. For P-typing, the procedure was essentially the same except that annealing was performed at 45°C (primers used were: Con3 + P[4], P[6], P[8], P[9], P[10], P[11]). Genotyping was defined according to the size of amplified DNA fragments upon agarose gel electrophoretic separation and ethidium bromide staining.

Sequencing

Representative rotavirus strains genotyped by RT/PCR were subjected to sequencing of genomic segments encoding for VP4, VP7 and NSP4 in order to identify minor variation in the nucleotide sequence between similar strains and for conclusive assignment to a genotype.

Monoclonal antibody characterization

For fine antigenic characterization of rotavirus strains of particular interest, established monoclonal antibodies (MAbs) were used in neutralization tests of infectious viruses as well as in ELISA and Western blot assays against purified virions. In addition, MAbs hybrydoma cell cultures were generated and cloned in order to produce novel MAbs panels to bovine rotaviruses, according to previously reported methods (8).

Results

Approximately 1,200 rotavirus-positive stools were collected between 2005 and 2006 from children with diarrhea less than 5 year-old in Slovenia, Croatia, Czech Republic, Bulgaria, and Albania. Fecal specimens were screened with diagnostic kits for rotavirus antigen detection. Stools positive for group A rotavirus were sent for strain characterization to the ISS, Rome.

Epidemiological and patients' data were collected using *ad hoc* questionnaires, and entered into a database for linkage to the genotyping data.

G- and P-types of rotavirus strains were analyzed by RT/PCR after viral RNA extraction, first-round reverse transcription-PCR and second-round nested-PCR, with specific G- and P-type primers.

VP7 genotype G1 was the most frequently found in Croatia, Slovenia and Czech Republic (40 to 60% of all strains), whereas in Albania and Bulgaria we observed a predominance of G4 rotaviruses (between 40 and 60%). The G2 genotype occurred to a similar extent (approximately 10%) in all countries with the exception of Croatia where it reached as high as 30% of the total. The G3 type was found only in Croatia, Slovenia and Czech Republic with rates close to 5%. G8 genotype was observed in 11% of cases in Croatia. The globally emerging G9 genotype was found in several countries (from 3 to 7%), and showed an unexpectedly high frequency in Bulgaria in 2006 (35%). G10 strains were identified rarely.

Among VP4 genotypes, P8 occurred most frequently (up to 90%), followed by P4 (from 10 to 50%). P6, P9 and P11 were all identified in a minor proportion of cases.

The relative distribution of G and P type combinations showed differences between regions. Overall, the most common binary types were G1P[8], G2P[4], G4P[4], G4P[8], and G9P[8]. Strains with unusual G and P combinations were however found. Further characterization of these strains is undergoing by sequence analysis, in order to evaluate the origin and genomic evolution of these viruses within and between countries (Table 1).

Table 1. Human rotavirus isolates from Croatia, Slovenia, Albania, Bulgaria and Czech Republic during 2005-2006 genotyped in ISS, Rome (percent values in parenthesis)

	Croatia	Slovenia	Czech Rep	Albania	Bulgaria
Total	457	248	84	158	70
Common genotypes[1]	187 (40.9)	98 (39.5)	145 (78.8)	49 (31.0)	55 (78.6)
Uncommon genotypes[2]	72 (15.8)	8 (5.4)	9 (4.9)	67 (42.4)	2 (2.9)
Others[3]	32	0	0	0	0
Mixed inf. total	31 (6.8)	53 (21.4)	3 (1.6)	20 (12.7)	4 (5.7)
Mixed inf. Subtotal[4]	13 (2.8)	0	0	2 (1.3)	2 (2.9)
GntPnt	68	41	8	15	2
No G	74 (16.2)	46 (18.5)	10 (5.4)	16 (10.1)	2 (2.9)
No P	133 (29.1)	84 (33.9)	24 (13.0)	21 (13.3)	8 (11.4)

1 Common genotypes: G1P[8], G2P[4], G3P[8], G4P[8], G9P[8]
2 Uncommon genotypes (possible reassortants between common genotypes): G1P[4], G2P[8], G3P[4], G4P[4], G9P[4].
3 Others: G8P[8], G10P[6], etc
4 Mixed infections subtotal, favouring reassortment, e.g. G1G2P[8], G1G2P[8]P[4], etc

Besides human rotavirus strains, the study also encompassed approximately 280 stool and intestinal samples obtained particularly from bovines with signs of diarrhea belonging to farms of Northern Italy. Samples were examined during the daily diagnostic and necroscopic practice at the Istituto Zooprofilattico Sperimentale (IZS) della Lombardia e dell'Emilia-Romagna, and resulted positive for rotavirus by a group A commercial ELISA test. Genotyping was performed

using both RT/PCR primers specifically designed for conventional animal rotavirus and primers suitable for recognition of human G- and P- specificities. Differently than human rotavirus strains, complete genotype assignment of bovine isolates could be achieved only in approximately 70% of cases. The only G- and P- type could be defined in 10% each of the remaining strains, whereas in the other 10% of samples neither G- nor P-typing was possible. The occurrence of as high as 20% of partially untypable rotaviruses suggest that G/P specificities other than the ones conventionally accounted for by the PCR typing system adopted universally are present to a significant extent among Italian farmed bovines. A comparison was done between the rotavirus genotypes detected in 2002-2004 with the viral types identified from the same area during a previous study conducted in our laboratory (9). Rotavirus strains collected in 2004 belonged mostly to appeared to G6P[5] (45%) e G6P[11] (24%) combinations, followed by G8P[11] and G10P[11], accounting for 12 and 8% of cases, respectively. These types were uniformly spread in all the farms surveyed during that period. During the 1994-8 study, genotypes G6P[5] and G6P[11] were also widely spread, accounting approximately 30% and 60%, respectively. Strains belonging to G8P[11] and G10P[11] were also present in that period but to a lesser extent.

Table 2. G- and P- type combinations among bovine rotaviruses during different years of surveillance

Genotype	Period of investigation		
	1994-1998*	2002-2003	2004
G6[P5]	38.3%	4.5%	9%
G8[P11]	3.4%	-	3.8%
G10[P11]	31.5%	13.6%	5.1%
G6[P11]	15.4%	52.3%	29.5%
Others	11.4%	29.6%	52.6%

*Adapted from Ref. 9

In contrast, during 2002 and 2003 the G and P types detected appeared remarkably different than in the other periods surveyed, with the emergence of G6P[11] as the most predominant type of rotavirus circulating (approximately 85% of all cases) followed by G10P[11] in a proportion close to 13%. In 2002-3, no rotavirus was found to belong to the combination G6P[5], which was otherwise largely present throughout the study. Interestingly, bovine strains with genotype G10P[11] have been previously found in humans in India, and have been hypothesized to follow a zoonotic transmission (10). These strains will be further analyzed in detail by genomic sequencing of several genes in order to establish possible affinity with sequences reported in similar strains from humans. This specific analysis will be completed in USA.

An unusual rotavirus strain isolated from a buffalo at the University of Bari and belonging to type G3P[3] was studied by a wide panel of MAbs elicited against the Rhesus rotavirus strain RRV G3P[1], sharing the same VP4 protein gene. The buffalo strain (BuRV) reacted quite well with virtually all of the VP4-specific MAbs assayed, by ELISA and neutralization test, whereas no reaction could be seen with any of the MAbs directed at the VP7 outer capsid protein that is encoded for by gene 9 (G-type). This finding indicates that, despite a different capsid protein VP7, the spike protein VP4 (P antigen) of the buffalo virus apparently presents an unaltered antigenic reactivity compared to the simian RRV. Highly concentrated preparations of BuRV virions were used to immunize mice and produce MAbs. Several hybrydoma cells were stabilized in culture and approximately 20 distinct MAbs produced were tested against both

BuRV and RRV in a series of immunological tests. Both MAbs reacting or not with BuRV by Western blot were unable to recognize RRV by any assay, including neutralization, indicating that the BuRV is not able to elicit antibodies to the conformational epitopes present on VP4 and shown to be shared by both BuRV and RRV. Similar results were obtained using mouse hyperimmune sera. Furthermore, we were unable to isolate any neutralizing monoclonal antibody active on the same BuRV used as an immunogen, suggesting that the VP4 of BuRV is not correctly presented to the mouse immune system in order to trigger a protective immune response.

Table 3. Reactivity of BuRV buffalo rotavirus with anti-BuRV mouse sera and anti-RRV MAbs

Antibody	Protein	ELISA	IPA	NT
1A9	VP4(8)[a]	0.227[b]	++[c]	++
23	VP4(8)	1.107	++	++
7A12	VP4(8)	0.676	++	++
2G4	VP4(5)	1.006	+/-	+/-
2A10	VP4(8)	1.371	+	++
3G6	VP4(8)	2.202	++	++
2B12	VP4(8)	1.951	++	++
4B7	VP4(8)	1.349	++	++
5E2	VP4(8)	2.342	++	++
4B6	VP4(8)	1.558	nt	++
IE4	VP4(8)	2.198	++	++
M14	VP4(8)	1.681	++	++
159	VP7	0.168	--	--
Pre-L	-	0.517		--
Pre-R	-	0.06		--
Post-R	BuRV	2.054	+	+/-
Post-L	BuRV	1.364	+	+/-

a Rotavirus protein recognized
b OD492 reading
c Intensity scale from – through ++.

Conclusions

The establishment of a surveillance program based on the molecular characterization of rotavirus strains infected children in a wide geographic area of the Balkans and Central-eastern Europe has allowed to verify that several different genotypes may circulate in a same period in a given population. Also, major difference in the predominant genotypes of rotavirus can be seen between countries and seasons. Quite interesting, in at least one country viruses belonging to the emerging G9 type appeared to have spread enormously in recent times, and it should be mentioned that G9 is possibly originated by an ancestral rotavirus swine strain. Although most of rotaviruses detected in this study belonged to the widely diffused G1-G4, and P8 genotypes, in addition to G9 strains also unusual types or combinations were observed. Some of these G- and P- combinations may reasonably indicate a zoonotic transmission of the virus from farm animals (mostly bovines or swine) to humans, a fact that is standing with the close contact of people with animals in some of the surveyed areas. The proximity of some of the investigated countries to Italy remarks the risk for possible entry of unusual rotavirus types along the immigration flows.

Data from the characterization of bovine rotavirus strains circulating in different farms of Italy indicate that, as in humans, also in farmed animals particular rotavirus genotypes prove able to spread very efficiently and to become predominant over other and previously established viral types sometimes from a year to another. That is likely related to the elicitation of an efficient immune response in bovines at the herd level, usually sufficient to halt further spread of endemic or epidemic viruses. Although we mostly found that rotavirus G- and P- genotype combinations were similar to those reported elsewhere in bovines, in some cases we have isolated viral types which may be suited for an animal-to-human transmission. These strains will be next investigated thoroughly at the nucleotide sequence level in different genes besides those encoding G and P specificities.

The comparison of immunogenicity and antigenicity of the buffalo BuRV and simian RRV rotavirus strains sharing a same VP4 specificity but a distinct G-type may suggest that VP7 may be critical for the stability and/or correct presentation of the VP4 spike protein to the immune system. This finding is of particular interest since some modern human vaccines to rotavirus are produced by reassorting the genomic segments of human and animal viruses on a same vaccine strain, particularly genes encoding VP4 and VP7. Polyvalent vaccines active on multiple rotavirus serotypes might thus include some unstable reassorted viruses, which might eventually prove unable to elicit protective antibody to a major antigen involved in protection.

These aspects will also be further investigated during the continuation of the collaborative project activity.

References

1. Gauci C, *et al.* Challenges in identifying the methodology to estimate the prevalence of infectious intestinal disease in Malta. *Epidemiol Infect* 2006;134(2):393-9.
2. Glass RI, *et al.* The epidemiology of rotavirus diarrhea in the United States: surveillance and estimates of disease burden. *J Infect Dis* 1996;174 Suppl 1:S5-11.
3. Arguelles MH, *et al.* VP7 and VP4 genotyping of human group A rotavirus in Buenos Aires, Argentina. *J Clin Microbiol* 2000;38(1):252-9.
4. Fischer TK, *et al.* Genotype profiles of rotavirus strains from children in a suburban community in Guinea-Bissau, Western Africa. *J Clin Microbiol* 2000;38(1):264-7.
5. Ramachandran M, *et al.* Molecular characterization of serotype G9 rotavirus strains from a global collection. *Virology* 2000;278(2):436-44.
6. Martella V, *et al.* Sequence analysis of the VP7 and VP4 genes identifies a novel VP7 gene allele of porcine rotaviruses, sharing a common evolutionary origin with human G2 rotaviruses. *Virology* 2005;337(1):111-23.
7. Iturriza Gomara M, *et al.* Molecular characterization of VP6 genes of human rotavirus isolates: correlation of genogroups with subgroups and evidence of independent segregation. *J Virol* 2002;76(13):6596-601.
8. Giammarioli A.M, *et al.* Production and characterization of murine IgA monoclonal antibodies to the surface antigens of rhesus rotavirus. *Virology* 1996;225(1):97-110.
9. Falcone E, *et al.* Determination of bovine rotavirus G and P serotypes in Italy by PCR. *J Clin Microbiol* 1999;37(12):3879-82.
10. Iturriza Gomara M, *et al.* Characterization of G10P[11] rotaviruses causing acute gastroenteritis in neonates and infants in Vellore, India. *J Clin Microbiol* 2004;42(6):2541-7.

Session 4B. Vaccines

ITALY-USA (ISS-NIH) JOINT PROGRAM FOR THE DEVELOPMENT OF A VACCINE AGAINST HIV/AIDS

Barbara Ensoli (a), Marjorie Robert Guroff (b)
(a) National AIDS Centre, Istituto Superiore di Sanità, Rome, Italy
(b) Basic Research Laboratory, National Cancer Institute, National Institutes of Health, Bethesda, MD, USA

Within the Italy-USA Joint Program, various vaccine candidates of combined immunization based on priming with adenoviral vectors encoding HIV-1 Env and Tat and SIV Gag, followed by boosting with the corresponding proteins adjuvanted by either Alum or ISCOM, have been tested and compared both in cynomolgus and rhesus macaques. With regard to Tat, also the vaccination with the single protein has been evaluated in both macaque species. Depending on the vaccine formulation the vaccine has been administered either systemically (subcute, intradermal, intramuscular) or mucosally (intranasal, intratracheal).

Results

Within this collaboration prelimary studies on murine models have been conducted to evaluate the safety and immunogenicity of vaccination with a replication competent adenoviral vector encoding HIV-1 Tat (wild type or Cys22 mutated) administered alone or in association with a similar vector encoding SIV Gag. Results from these studies have proven the safety of all vaccine formulations. Concerning the immunogenicity, no differences have been found between Tat wild-type and Cys22 mutant proteins with regard to the induction of antibodies and cellular responses. Of note, the administration of either type of the Tat together with Gag has induced a significant increase of cellular response, as indicated by Elispot responses and lymphoproliferation assays. As far as the humoral response is concerned, there have not been significant differences towards the group vaccinated with Gag only.

Based on this study (Zhao *et al.*, Virology, 2005) two protocols have been started in monkeys to test and compare the safety, immunogenicity and efficacy of the vaccination with either Tat alone or associated to other antigens in rhesus (*Macaca mulatta*) and cynomolgus (*Macaca fascicularis*) macaques.

In the first study 30 rhesus female macaques, divided in 6 groups (included two control groups), have been immunized to evaluate the safety, immunogenicity and efficacy of a vaccine based on either Tat-wild type alone (group A, immunized with recombinant Tat protein; group B, immunized with a replication competent adenoviral vector encoding Tat) or on Tat associated with either HIV-1 Env (group C), or with HIV-1 Env and SIV Gag and Nef (group D). Groups E and F include controls for the protein and the vectors, respectively. The immunization protocol included several vaccine administrations over 36 weeks, a resting period of 14 weeks to avoid interference by non-specific effects due to vaccine administration, followed by an intravenous challenge with 20 MID_{50} of SHIV89.6P grown in rhesus macaques.

In the second study, 20 cynomolgus female macaques have been divided in 4 groups (included two control groups) to test and compare the safety, immunogenicity and efficacy of a

vaccine based on HIV-1 Tat delivered either as a protein (group A, 8 macaques) or by a replication competent adenoviral vector (group B, 8 macaques). Groups C and D, of 3 macaques each, represented the respective control groups. As in the previous study, the immunization protocol included several vaccine administrations over 36 weeks, a resting period of 14 weeks to avoid interference by non-specific effects due to vaccine administration, followed by an intravenous challenge with 15 MID_{50} of SHIV89.6P_{cy243} grown in cynomolgus macaques.

Conclusions

Even though the studies are not concluded yet because efficacy evaluation is still ongoing, all the vaccine formulations have proven to be safe and immunogenic in both studies, as showed by the induction of both cellular and humoral responses. Of note, humoral responses were detected both systemically (i.e., in the serum) and mucosally (broncho-alveolar lavages and vaginal washes), an important finding in light of the role of mucosal immunity in HIV-1 transmission.

Ongoing and future studies

These include the evaluation of the efficacy of the vaccine formulations as well as the identification of the correlates of protection. Finally, the vaccine candidate that has provided the best protection will be evaluated again in the two macaque models in a new study in which the challenge will be mucosal (vaginal) to determine whether the vaccine is effective at protecting against the most prevalent route of transmission in human.

Session 4C. Immunity and metabolic diseases

GENERATION OF REGULATORY T-LYMPHOCYTES FOR THE CONTROL OF INFLAMMATORY BOWEL DISEASES

Simona Vecchione (a), Antonello Amendola (a), Alessia Butera (a), Anna Maria Pronio (b), Ivan Fuss (c), Warren Strober (c), Monica Boirivant (a)

(a) Department of Infectious, Parasitic and Immuno-Mediated Diseases, Istituto Superiore di Sanità, Rome, Italy

(b) Department of General Surgery "Paride Stefanini" University "La Sapienza", Rome, Italy

(c) Mucosal Immunity Section, National Institute of Allergy and Infectious Diseases, National Institutes of Health, Bethesda, MD, USA

Introduction

Immune-homeostasis at mucosal level results from controlled response to intestinal luminal antigens. Thus, antigens tend to induce a state of non-responsiveness via a complex process involving both the deletion of antigen-reactive cells and the generation of one or more types of regulatory (suppressor) T cells (1). Such non-responsiveness appears to be a means of limiting responses to mucosal antigens, particularly those arising from the microflora, so that they do not induce harmful inflammatory responses.

In Crohn's Disease (CD), genetic and environmental factors interact to produce an immunopathogenic process that results in chronic, relapsing intestinal inflammation (2). Recent insights into the nature of this disease, derived mainly from studies of experimental models of colonic inflammation, strongly suggest that it can result from a loss of immune tolerance to antigens in the bacterial microflora. This, in turn, can occur as a consequence of an absolute or relative defect in the function of regulatory T cells or to an excessive immune response to these antigens that cannot be controlled by normal regulatory T cell function (3).

Generation of regulatory T-lymphocytes might therefore represent a valuable therapeutic approach for the control of inflammatory bowel diseases.

We planned a project to investigate the possibility to expand regulatory T lymphocytes at the mucosal level.

Study design

The project was organized in 3 sequential steps:

- Analysis of the % of regulatory T lymphocytes in the mononuclear cells isolated from intestinal specimens of patients with Crohn's Disease.
- Investigation on the possibility to expand regulatory T lymphocytes by a) feeding TNP-haptenated colonic proteins (a complex mixture of proteins obtained by homogenization of colonic specimens and then subjecting the mixture to TNP-haptenization by TNBS) b) administration of probiotics in the murine model of TNBS-colitis.

– Analysis of the prevalence of regulatory T lymphocytes in the mononuclear cells isolated from intestinal specimens of patients with ileal pouch-anal anastomosis after total proctocolectomy for ulcerative colitis. The patients were treated with the same probiotics used in the study in the animal model of colitis.

For the analysis of the prevalence of regulatory T lymphocytes, we isolated lamina propria mononuclear cells (LPMC) from involved and uninvolved intestinal tissues of patients with Crohn's Disease experiencing surgical resection for intestinal obstruction or no response to medical therapy (study 1) or from biopsies collected during colonoscopy in patients with ileo-anal anastomosis, enrolled in a clinical trial on the efficacy of probiotic administration in the prevention of pouchitis (study 3). Tissue samples obtained from uninvolved region of patients undergoing resection for colon cancer were used as control. LPMC were isolated by sequence DTT-EDTA-Collagenase and purified on density gradient. Percent of regulatory cells was evaluated by FACS analysis after staining of cells for different markers.

For the study in the animal model of colitis, we utilized the TNBS-colitis, a Th-1 mediated colitis induced by intrarectal administration of the haptenating agent TNBS characterized by a transmural inflammation (considered on histologic ground as a model of Crohn's disease). In this model we administered by oral route: a) TNP-haptenated colonic protein (TNP-HCP) for two weeks before the induction of colitis. b) probiotics. Since in the studies on protection of colitis by administration of TNP-HCP, we observed that the regulatory cells generated during the feeding were able to prevent colitis (4), but not to treat (reverse) established TNBS-colitis (I. Fuss, personal observation), we treated the mice with oral administration of probiotics [VSL#3 (VSL Pharmaceutical Inc.), a probiotic compound containing $3x10^{11}$/g of viable lyophilized bacteria including bifidobacteria (*B. longum*, *B. infantis*, and *B. breve*), lactobacilli (*L. acidophilus*, *L. casei*, *L. delbrueckii subsp. L. bulgaricus*, and *L. plantarum*), and *Streptococcus salivarius subsp. Thermophilus*] for three weeks in the interval between two induction of colitis, a condition that mimics a treatment during clinical remission of the disease in humans. Colitis course was monitored by daily recording of body weight. At different time points mice were sacrificed and the colons collected for histologic analysis, assessment of the % of LPMC with regulatory phenotype (FACS analysis) and production of cytokines (ELISA).

Results

Regulatory T cells in Chron's Disease

We analyzed at mucosal level the % of two different populations of regulatory T cells: CD4+CD25+ T cells and CD4+LAP+ cells. In the CD4+CD25+ T cell population, regulatory CD4+CD25+ T cells in humans can be identified as the subpopulation with high density of the IL-2-receptor a-chain (5). CD4+LAP+ cells represent a population of T cells recently described in the mouse, that express on its surface TGF-β in inactive form and that has been demonstrated to protect from experimental colitis (6). As shown in Figure 1 LPMC isolated from involved tissue of Crohn's disease patients show a significant increase of the % of CD4+CD25high+ cells when compared to LPMC isolated from control tissue.

The data confirm recent published data (7) and suggest that expansion of CD4+CD25+ T reg during the active phase of disease is unable to counteract inflammation. More interesting, % of CD4+LAP+ T cells is significantly lower in the the involved tissue of CD patients when compared to uninvolved tissue and control tissue. Studies in experimental colitis have demonstrated an essential role of TGF-b in the protection from colitis that involves also the protection mediated by CD4+CD25+ cells(8).

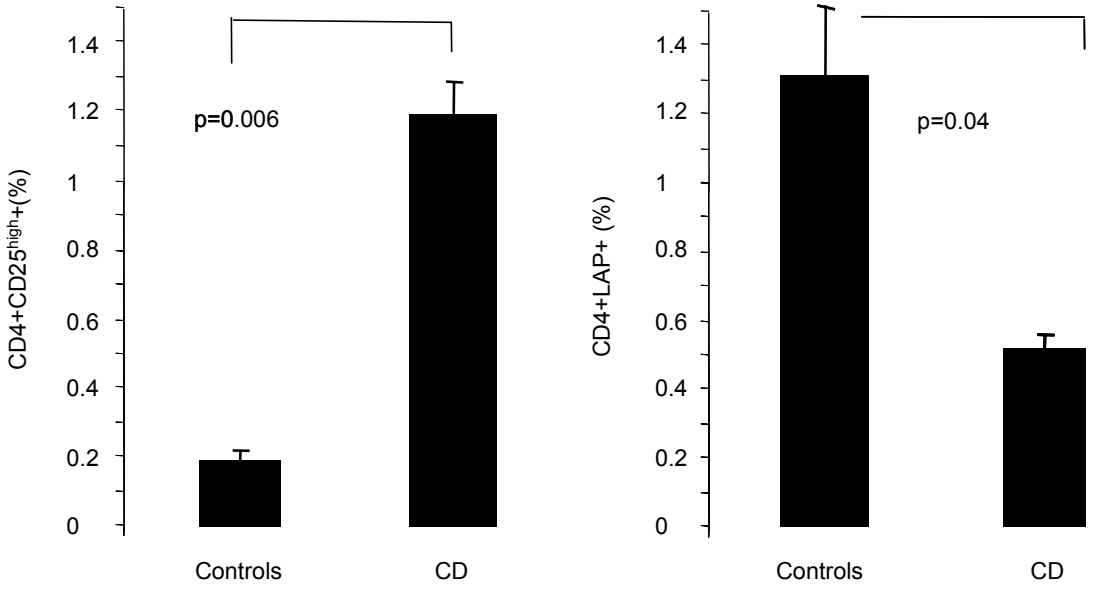

Figure 1. % of regulatory T lymphocytes in lamina propria of patients with Crohn's Disease

Therefore, the significant reduction of TGF-b production by T cells observed in CD (9), as well as the present observation involving the reduction of CD4+LAP+ cells, might account for the apparently insufficient increase of CD4+CD25high+ cells in involved intestine.

Generation of regulatory T-lymphocytes for the control of experimental colitis

As demonstrated in previous studies, TNBS-colitis can be influenced by the provision of regulatory T cells. Feeding of TNP-haptenated colonic proteins (TNP-HPC: a mixture of proteins obtained by homogenization of colonic specimens and then subjected to TNP-haptenization by TNBS) has the effect of inducing regulatory T cells in the same manner as does the feeding of soluble protein in the induction of oral tolerance. As result of such feeding, T cells producing TGF-β appear in the lamina propria that suppress TNBS-colitis in the same mouse or in a recipient mouse to which the cells are transferred (10). We investigated the ability of regulatory cells induced by this treatment to suppress a colitis induced by a different haptenating agent (oxazolone colitis (11)). We found that feeding TNP-HCP protected mice from the development of oxazolone-colitis, albeit to a lesser extent than it protected mice from TNBS colitis. In addition, we showed that protection was associated with the appearance of mononuclear cells producing regulatory cytokines.These data strongly imply that the cells induced by feeding one type of haptenated protein are capable of cross-reacting with antigens present in colitis produced by a second type of haptenated protein. This cross-protection certainly arises from the fact that the regulatory cells are antigen nonspecific in their suppressor function. However, this observation also suggests that during the feeding some regulatory cells specific for luminal antigens are generated and that these cells are activated during the induction of colitis. The most likely possibility regarding specificity is that the fed HCP lead to the induction of cells that react both with the inducing antigen that has been fed to the mice and

with cross-reacting proteins in the mucosal Microflora, so that the latter can be activating antigens in the absence of the antigen that has been fed (12).

We then modulated the local microenviromnent with the use of probiotics to evaluate the ability of such treatment to influence the course of TNBS colitis by expansion of regulatory cells. We observed that probiotic administration (VSL#3) over a three weeks period to mice that have recovered from an initial induction of TNBS-colitis greatly reduces the severity of a subsequent second induction of TNBS-colitis. This protection was due to mononuclear cells in the lamina propria of the treated mice since it could be transferred to naive mice by adoptive transfer of these cells. Further studies showed that probiotic treatment was associated with the appearance of CD4+CD25+ T cells and regulatory T cells bearing cell-surface TGF-b (CD4+ LAP+ cells), two populations with minimal overlap (Figure 2 A and B).

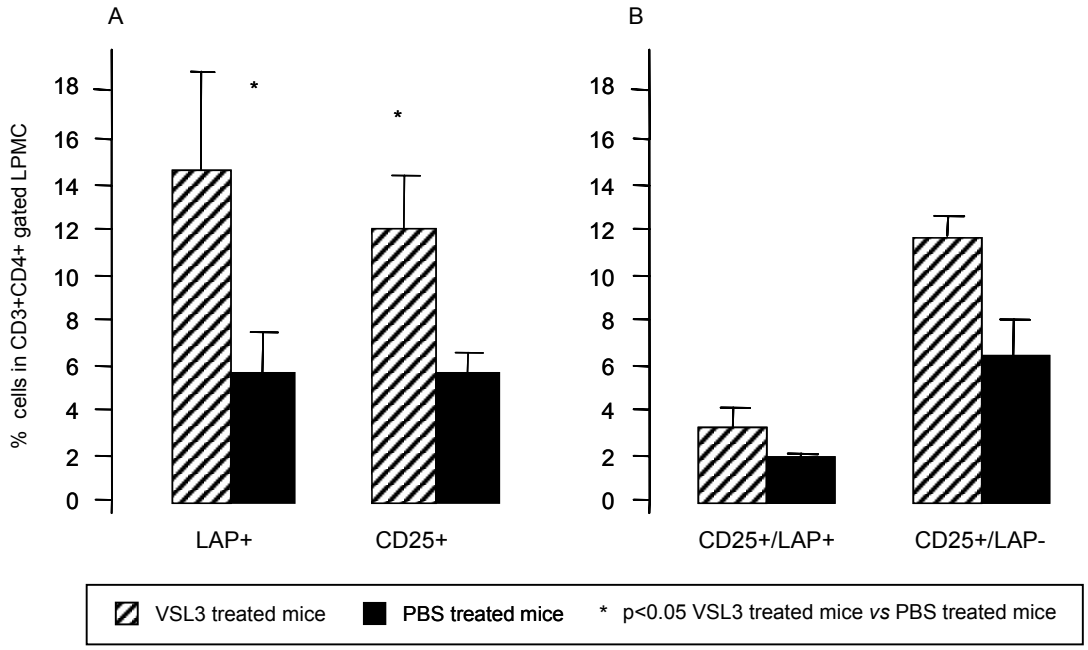

Figure 2. A:% of regulatory cells at day 3 after second induction of recurrent TNBS colitis in mice treated or not with VSL3 during the three weeks interval between the two induction of colitis. B: % of CD4+CD25+ LAP+ and CD4+CD25+ LAP- T cells at day 3 after second induction of recurrent TNBS colitis in mice

CD4+ LAP+ cells proved to be the protective cells since lamina propria cell populations from probiotic-treated mice depleted of these cells failed to transfer protection and transferred protection was blocked by adminstration of anti-TGF-b antibodies. The development of these cells was dependent on IL-10, as shown by the fact that the administration of probiotics was accompanied by the production of this cytokine and treatment of mice with anti-IL-10R blocked the appearance of TGF-b-bearing regulatory cells (13). These studies provide evidence that probiotic effects are indeed linked to the ability to induce the development of IL-10-dependent, TGF-b-bearing regulatory cells. The role (if any) of CD4+CD25+ T cells in the protection is not clear since the presence of CD4+CD25+ T cells in the absence of TGF-b-bearing regulatory cells does not protect from colitis.

Generation of regulatory T-lymphocytes in humans

Preliminary analysis of the data derived from the isolation of LPMC from biopsies of patients treated or not with VSL3 suggests that administration of VSL3 is able to increase the % of regulatory T lymphocytes at the mucosal level.

Conclusions

The results obtained in the above described studies demonstrate that it is possible to modulate intestinal inflammation by regulatory T cells. These cells may be preferentially expanded during the remission phase of the disease. Probiotics administration may represent, for their safety, a valuable terapeutic option for a long term treatment aimed to induce regulatory T cells.

Acknowledgments

We thank Prof. C. De Simone (University of L'Aquila) for providing VSL3. We thank Nazzareno Di Carlo (Immune-Mediated Diseases Section, Department of Infectious, Parasitic, and Immune-Mediated Diseases, Istituto Superiore di Sanità) for animal care and technical assistance.

References

1. Strober W, Fuss I, Boirivant M, Kitani A. Insights into the mechanism of oral tolerance derived from the study of models of mucosal inflammation. *Ann N Y Acad Sci* 2004;1029:115-31.
2. Podolsky DK. Inflammatory Bowel Disease. *N Engl J Med* 2002;347:417-29.
3. Duchmann R, Kaiser I, Hermann E, Mayet W, Ewe K, Meyer zum Buschenfelde KH. Tolerance exists towards resident intestinal flora but is broken in active inflammatory bowel disease (IBD). *Clin Exp Immunol* 1995;102:448-55.
4. Fuss IJ, Boirivant M, Lacy B, W Stroberl. The interrelated roles of TGF-ß and IL-10 in the regulation of experimental colitis. *J Immunol* 2002;168(2):900-8.
5. Baecher-Allan C, Brown JA, Freeman GJ, Hafler DA. CD4+CD25 high regulatory cells in human peripheral blood. *J Immunol* 2001;167:1245-53.
6. Oida T, Zhang X, Goto M, Hachimura S, Totsuka M, Kaminogawa S, Weiner HL. CD4+CD25- T cells that express Latency-Associated Peptide on the surface suppress CD4+CD45Rbhigh-induced colitis by a TGF-b-dependent mechanism. *J Immunol* 2003;170:2516-22.
7. Maul J, Loddenkemper C, Mundt P, Berg E, Giese T, Stallmach A, Zeitz M, Duchmann R. Peripheral and Intestinal Regulatory CD4+CD25high T Cells in Inflammatory Bowel Disease. *Gastroenterology* 2005;128:1868-78.
8. Nakamura K, Kitani A, Strober W. Cell contact-dependent immunosuppression by CD4+CD25+ regulatory T cells is mediated by cell surface-bound transforming growth factor beta. *J Exp Med* 2001;194:629-44.
9. Del Zotto B, Mumolo G, Pronio AM, Montesani C, Tersigni R, Boirivant M. TGF-beta1 production in inflammatory bowel disease: differing production patterns in Crohn's disease and ulcerative colitis. *Clin Exp Immunol* 2003;134:120-6.
10. Neurath MF, Fuss I, Kelsall BL, Strober W. Experimental granulomatous colitis in mice is abrogated by induction of TGF- beta–mediated oral tolerance. *J Exp Med* 1996;183:2605-16.

11. Boirivant M, Fuss IJ, Chu A, Strober W. Oxazolone colitis: a murine model of T helper cell type 2 colitis treatable with antibodies to interleukin 4. *J Exp Med* 1998;188:1929-39.

12. Boirivant M, Strober W, Fuss IJ. Regulatory cells induced by feeding TNP-Haptenated Colonic Protein cross-protect mice from colitis induced by an unrelated hapten. *Inflamm Bowel Dis* 2005;11:48-55.

13. Di Giacinto C, Marinaro M, Sanchez M, Strober W, Boirivant M. Probiotics Ameliorate Recurrent Th1-Mediated Murine Colitis by Inducing IL-10 and IL-10-Dependent TGF-{beta}-Bearing Regulatory Cells. *J Immunol* 2005;174(6):3237-46.

Session 4C. Immunity and metabolic diseases

GROUP A STREPTOCOCCAL INFECTIONS AND NEUROBEHAVIOURAL DISORDERS IN CHILDREN

Graziella Orefici (a), Francesco Cardona (b), Lucilla Baldassarri (a), Roberta Creti (a), Monica Imperi (a), Marco Pataracchia (a), Susan Swedo (c)

(a) Department of Infectious, Parasitic, and Immuno-Mediated Diseases, Istituto Superiore di Sanità, Rome, Italy

(b) Departments of Child Neuropsychiatry, University "La Sapienza", Rome, Italy

(c) Pediatrics and Developmental Neuropsychiatry Branch, National Institue of Menthal Health, Bethesda (MD) USA

Streptococcus pyogenes (group A streptococcus – GAS) is an important species of gram-positive bacterial pathogens. GAS colonizes the human throat or skin and is responsible for a number of suppurative infections (pharyngitis, tonsillitis, scarlet fever, impetigo, necrotizing fasciitis) and nonsuppurative sequelae, including acute rheumatic fever (RF), Sydenham's Chorea (SC), acute glomerulonephritis and reactive arthritis.

The post-streptococcal nature of the nonsuppurative sequelae has been a topic of great debate throughout the last century. Lacking a biological marker, the pathogenic relationship between streptococcal infections and RF was definitely achieved on the basis of epidemiological studies and the efficacy of penicillin prophylaxis(1).

Infections by Group A streptococci (GAS) were first associated with neuropsychiatric symptoms at the end of the 19th century (2), with the suggestion of an association with the Sydenham Chorea (SC) but only in the 1992 revision of Jone's criteria SC was included among the major criteria for the diagnosis of Rheumatic Fever (RF)(3).

The hypothesis that in some children affected by tic disorders (including Tourette Syndrome) the sudden onset or recrudescence of neuropsychiatric symptoms could be secondary to a streptococcal infection was put forward several years ago by the NIH group. This diagnostic subgroup was designated by the acronym PANDAS (Pediatric Autoimmune Neuropsychiatric Disorders Associated with Streptococcal Infections) (4-5). The authors hypothesized that PANDAS are caused by an abnormal immune response to streptococcal antigens targeting basal ganglia and interrupting their function. The medical model for such subset of patients was that of Sydenham's Chorea (SC), and then of Rheumatic Fever (RF).

Diagnostic criteria for PANDAS defined in 1998 (6), were: 1) presence of OCD and/or tics; 2) prepubertal onset of symptoms; 3) Episodic course of symptom severity; 4) temporal relationship between symptom exacerbations and streptococcal infections (confirmed by positive cultures and/or elevated antistreptococcal titers); 5) association with neurological abnormalities (e.g. choreiform movements).

PANDAS's concept has been subject to much criticism. It was firstly emphasized that since both tic disorders and streptococcal infections are common in childhood, this makes difficult to demonstrate a firm link between these conditions.

In any case in PANDAS, the role of the immune system in the etiology has been suggested but not confirmed and while anti-brain antibodies were found in PANDAS vs. uncomplicated streptococcal infections by several investigators (7-9), others have failed in inducing behavioural changes in animal models after antibodies infusion (10).

In a previous study we reported that children affected by tic disorders seem to constitute a peculiar population, in which the rate of streptococcal infections, or, in any case, that of exposure to streptococcal antigens (as measured by ASO titer) is higher than in normal population (11).

The present study is being carried out in collaboration with Dr. Swedo of the National Institute of Mental Health of Bethesda. Dr. Swedo's group, that have a long and well documented experience in the field, provided the guidelines and criteria for inclusion of subjects in the study and reviewed the clinical data already available.

Our group specific aims were: (i) to evaluate the role of streptococcal infections in tic disorders; (ii) to study the microbiological characteristics of GAS strains isolated; (iii) to verify the possibility of cross reactions between brain epitopes and streptococcal antigens.

Study design. Children under 15 years of age affected by tics seen at the Department of Neuropsychiatry of the University of Rome since 2003, underwent clinical and laboratory examinations that took into account a series of parameters listed in Table 1. After the first visit children were seen again at established intervals or in case of any recrudescence of symptoms. The same parameters were used for both first and follow-up visits.

The parameters considered for clinical evaluation of patients are:

- History of tics
- Neurological and Tic evaluation (Yale Global Tic Severity Scale, YGTSS)
- Complete blood cell counts and routine laboratory tests
- Immunoglobulin determination
- ASLO titer
- ESR
- Pharyngeal swab
- Cardiological assessment

Exposure to streptococcal antigens was evaluated through direct culture of pharyngeal swabs and/or determination of the ASLO titre. Threshold for ASLO titres was fixed at 407 UI (i.e. mean of the controls + 2SD in the previous study (11).

Strains isolated from pharyngeal swabs were typed by molecular and serological methods (*emm* type, T type, genes for antibiotic resistance *erm* and *mef*, erythrogenic toxins *spe*A and *spe*C) according to previously published methods (12). Moreover, the ability to form biofilm and efficiency to enter epithelial cells were evaluated. Microbiological characteristics were compared to those of a collection of GAS isolated from invasive infections.

Patients sera were utilized in western blot experiments against extract of human brain and/or extracts of whole GAS cells, to evaluate the presence of crossreacting epitopes.

In the period 2003-2006, 196 patients have entered the study. None of the children was symptomatic or reported recent pharyngitis or other streptococcal infections episodes, but many of them showed to have had contacts with GAS: ASLO titres were higher than 400 IU in 42% of the patients vs. 7% of the controls. Mean ASLO titer in GAS positive patients was 499 IU, 367 IU in GAS negative tic patients but was 155 IU among controls.

From these patients 550 pharyngeal swabs were obtained during the first and the follow-up visits, 13% being GAS culture positive at least once and 4% being culture positive in two or more occasions. Among the latter, half subjects carried strains of the same *emm* type. A large range of *emm* types was detected but no types specifically associated to tic disorder were found (12). It was observed that when compared to strains from invasive infections the erythrogenic toxin *spe*C gene appeared to be significantly more frequent in the tic group. Resistance to macrolides was also very frequent almost 40% of isolates carrying either the *mef*A or the *erm*B genes. Tics isolates appear to be more prone to survive within epithelial cells compared to isolates from invasive infections, moreover biofilm formation was interestingly associated to

antibiotic susceptibility rather than to the source of isolation since susceptible strains were better biofilm producers than macrolide resistant (13). This might be of relevance in maintaining infection foci difficult to eradicate and constant source of streptococcal antigens.

Forty-eight tic patients, with elevated ASLO titres and/or positive GAS culture, and eighteen control patients (i.e. children with tics but without evidences of exposure to streptococcal antigens) received echocardiographic examinations for cardiological abnormalities (14). In 58% of the patients abnormalities of different degrees were observed: minimal or mild mitral regurgitations in 54% and 2% mitral valve prolapse in comparison with 22% of controls.

Evaluation of the presence of antibodies to human brain extracts in patients' sera, modimensional electrophoresis and western blot, evidenced the presence of specific bands (at least three bands of about 50, 60, and more than 100 KDa) in the group of tic/high ASLO titres/and-or positive culture vs. tic/low ASLO titres or Sydenham's Chorea groups. Similar bands appeared to be recognized by the patients' sera in streptococcal extracts. Very preliminary experiments by bi-dimensional electrophoresis/western blot confirmed the presence of group-specific protein spots, which will be characterized by Maldi-tof analysis.

A number of data collected up to now points towards an autoimmune basis of tics in patients that have been exposed to streptococcal antigens. This hypothesis have to verified by further studies.

Since the preliminary identification of proteins targeted by the immune system because of mimicry with streptococcal antigens we have started a further collaboration with the group of Dr. Cunningham from the University of Oklahoma, a group which has already studied the immunologic base of other post-streptococcal syndromes, such as Sydenham Chorea (15).

In summary, presently we can say that the virulence traits of GAS isolated from patients with tics appear to be related more to the *emm* type rather than to the source of isolation. The finding on biofilm formation may explain the persistence of susceptible GAS strains despite appropriate antibiotic therapy, thus providing a source of streptococcal antigens constantly stimulating the immune system and worsening tic symptoms. Future studies will be directed to identify whether antibodies stimulating neuronal cells CaMII proteinkinase and release of dopamine may be present in sera of tic patients.

References

1. Stollerman GH, Rusoff JH. Prophylaxis against group A streptococcal infections in rheumatic fever patients: use of new repository penicillin preparation. *JAMA* 1952;150:1571-5.
2. Osler W. *On Chorea and Choreiform Affections.* Philadelphia: P. Blakiston, Sons & Co.; 1894.
3. Special Writing Group of the Committee on Rheumatic Fever, Endocarditis, and Kawasaki Disease of the Council on Cardiovascular Disease. Guidelines for the diagnosis of rheumatic fever. Jones Criteria, 1992 update. *JAMA* 1992;268:2069-73.
4. Allen AJ, Leonard HL, Swedo SE. Case study: a new infection-triggered autoimmune subtype of pediatric OCD and Tourette's Syndrome. *J Am Acad Child Adolesc Psychiatry* 1995;34:307-11.
5. Swedo SE, Leonard HL, Kiessling LS. Speculations on antineuronal antibody-mediated neuropsychiatric disorders in childhood. *Pediatrics* 1994;93:323-6.
6. Swedo SE, Leonard HL, Garvey M, *et al.* Pediatric Autoimmune Neuropsychiatric Disorders associated with streptococcal infections: clinical descriptions of the first 50 cases. *Am J Psychiatry* 1998;155:264-71.
7. Kiessling LS, Marcotte AC, Culpepper L. Antineuronal antibodies: tics and obsessive-compulsive symptoms. *J Dev Behav Pediatr* 1994;15:421-5.

8. Singer HS, Giuliano JD, Hansen BH, Hallet JJ, Laurino JP, Benson M, Kiessling LS. Antibodies against human putamen in children with Tourette syndrome. *Neurology* 1998;50:1618-24.
9. Morshed SA, Parveen S, Leckman JF, Mercadante MT, Bittencourt K, Miguel EC, Eman A, Yazgan Y, Fujii T, Paul S, Peterson BS, Zhang H, King RA, Sgahill L, Lombroso PJ. Antibodies against neural nuclear cytoskeletal, and streptococcal epitopes in children adults with Tourette's syndrome, Sydenham Chorea, and autoimmune disorders. *Biol Psychiatry* 2001;50:566-77.
10. Loiselle CR, Le O, Moran TH, Singer HS. Striatal microinfusion of Tourette Sindrome and PANDAS sera: failure to induce behavioral changes. *Mov Disord* 200;19:390-6.
11. Cardona F, Orefici G. Group A streptococcal infections and tic disorders in an Italian pediatric population. *J Pediatr* 2001;138:71-5.
12. Creti R, Gherardi G, Imperi M, von Hunolstein C, Baldassarri L, Pataracchia M, Alfarone G, Cardona F, Orefici G. Association of group A streptococcal emm types with virulence traits and macrolide-resistance genes is independent of the source of isolation. *J Med Microbiol* 2005;54:913-7.
13. Baldassarri L, Creti R, Recchia S, Imperi M, Facinelli B, Giovanetti E, Pataracchia M, Alfarone G, Orefici G. Therapeutic failures of antibiotics used to treat macrolide-susceptible Streptococcus pyogenes infections may be due to biofilm formation. *J Clin Microbiol* 2006;44:2721-7.
14. Cardona F, Romano A, Cundari G, Ventriglia F, Versacci P, Orefici G. Color Doppler echocardiography in children with group A streptococcal infection related tic disorders. *Ind J Med Res* 2004;119:186-90.
15. Kirvan CA, Swedo SE, Heuser JS, Cunningham MW. Mimicry and autoantibody-mediated neuronal cell signaling in Sydenham chorea. *Nature Med* 2003;9:914-20.

Session 4C. Immunity and metabolic diseases

THE ROLE OF CD4+CD25+ T REGULATORY CELLS IN INFECTIONS BY FACULTATIVE INTRACELLULAR BACTERIA

Paolo Pasquali (a), Andrea Battistoni (b), Angela Thornton (c), Ethan M Shevach (c)
(a) Department of Food Safety and Veterinary Public Health, Istituto Superiore di Sanità, Rome, Italy
(b) Department of Biology, University of Rome Tor Vergata. Via della Ricerca Scientifica, Rome, Italy
(c) Laboratory of Immunology, National Institute of Allergy and Infectious Diseases, National Institute of Health (NIH), Bethesda, MD, USA

The interaction between facultative intracellular bacteria and vertebrate host is a complex and delicate balance whose outcome can lead different clinical features, from asymptomatic carriage until death (1). On one hand, bacteria have evolved a series of mechanisms and virulence factors to colonize propitious biological niches and to multiply within. Vertebrate host, on the other hand, have developed defence mechanisms for counteracting pathogen survival. In this struggle between the former and the latter the immune system is the main responsible for the control of the infection, being devoted to mount a prompt and effective response to foreign invaders.

Facultative intracellular pathogens have adapted to survive intracellularly and successful elimination of them requires the destruction of infected cells by cytotoxic mechanisms, which in many cases are exaggerated, causing the pathology of the infection (2). Thus, immune mechanisms represent a double-edged sword with one side against the invaders and the other potentially causing damage to host cells and tissues. In order to limit the immune response or counterbalance the harmful activity, the immune system has developed a wide array of mechanisms. Of those, the existence of suppressor T cells was theorized since the early 1970, but the failure to clone this subpopulation of T cells reduced the scientific interest upon these enigmatic cells (3). In the mid 1990s Sakaguchi and associates (4) shed new interest in the concept of T-cell-mediated suppression by showing that a minor population of CD4+ T cells, which co-expresses the interleukin-2 receptor (CD25) is crucial for the control of T cells *in vivo*. The clinical relevance of these cells is still largely unknown, but its detrimental effect has been found in the induction of tumour immunity and in autoimmune diseases (5). CD4+CD25+ T regulatory cells prevent the activation and proliferation of potentially autoreactive T cells (6), but these cells have been shown to contribute to the maintenance of chronic infection by *Leishmania major* (7), and to contribute to immune suppression during malaria infection (8), suggesting that CD4+CD25+ T regulatory cells may also play a pivotal role in infections and could contribute to the immune-based pathogenesis. On the other hand, we can postulate that these cells have a protective role in other infectious systems as they are able to protect against pulmonary hyperinflammation driven by *Pneumocystis carinii* (9). An host-protecting role has been also played by IL-10 producing CD4+CD25+ T regulatory cells in Schistosoma infection, supporting a complicated and articulated role of these cells in infectious diseases (10). These findings have led to a great interest in the investigation of the role of CD4+CD25+ T regulatory cells in the infection due to facultative intracellular cellular pathogens in order to give insights on the pathogenesis of, and to develop new strategies to prevent or treat these infections.

The main purpose of this project is to evaluate the role of CD4+CD25+ T regulatory cells in the interaction between facultative intracellular bacteria and host and if any, its relevance in the pathogenesis of the infections. Two different models were used: brucellosis and salmonellosis in mouse. The former is characterized by a chronic infection with spontaneous resolution in several weeks, the latter induces septicemia that leads to death in few days. The characterization of the role of CD4+CD25+ T cells in either salmonellosis and brucellosis models was assessed by means of the evaluation of the infection in mice in which CD4+CD25+ T cells were functionally inactivated and the evaluation of the effect of CD4+CD25+ T cells in an experimental model of infection using immunodeficient SCID mouse reconstituted by CD4+CD25-T cells.

To inactivate *in vivo* CD4+CD25+T cells *in vivo* we set up a system using antibodies able to bind and eliminate target cells, according to published protocols. Clone PC61 (ATCC) was purchased and cultivated *in vitro*. This clone is able to produce rat IgG2 antibodies which are able to bind to the CD25 cell receptor and functionally inactivate and probably deplete target cells for a period of 1-3 weeks according to the experimental setting (11). For the evaluation of the role of CD4+CD25+ T cells during salmonellosis, 5 female BALB/c mice were intraperitoneally injected with 500 ng of PC61 and 5 mice remained as untreated controls. Five days LATE, mice were intraperitoneally infected with 100 LD_{50} of *Salmonella enterica serovar Typhimurium* (*S. Typhimurium*) znuA$^-$ ($5x10^6$ CFU) and mortality was assessed daily. For the evaluation of the role of CD4+CD25+ T cells during brucellosis, 8 female Balb/c mice were intraperitoneally injected with 500 ng of PC61 and 5 mice remained as untreated controls. Five days after, mice were intraperitoneally infected with $5x10^4$ CFU *Brucella abortus* 2308 and killed 20 days after to assess bacterial colonization in spleen as a mean to evaluate the infection.

As depicted in Figure 1 we found that CD4+CD25+ T cells are able to downregulate the immune system in controlling infection due to *Brucella*, since mice with a functional deficit of CD4+CD25+T cells were able to control more effectively infection when compared to untreated mice (Figure 1a). On the contrary, in mice infected with *Salmonella*, mortality was not different between PC61 treated and untreated mice (Figure 1b).

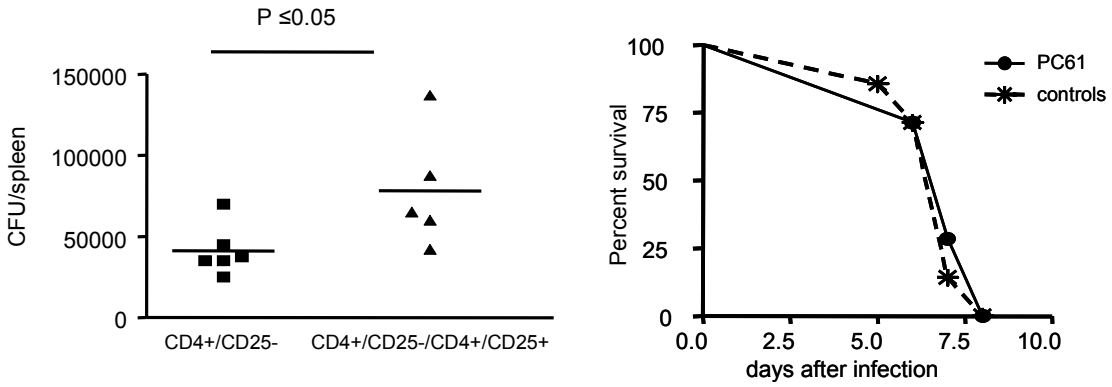

Figure 1. Effect of functional inactivation of CD4+CD25+ T cells on the course of the infections. Persistence of bacteria (A) and mortality rate (B) in treated and untreated BALB/c mice infected with *B. abortus* 2308 and S.Typhimurium znuA-, respectively

To better address the significance of CD4+CD25+ T cells in the course of *Brucella* infection we used a model of infection using immunodeficient SCID mice. CD4+CD25-and CD4+CD25+

T cells were isolated from normal BALB/c mice. SCID mice were randomly grouped in animals reconstituted with CD4+CD25-T cell or CD4+CD25-and CD4+CD25+ T cells. Mice were challenged with $5x10^4$ CFU *B. abortus* 2308 5 days after reconstitution, and killed 20 days after challenge. Bacteria were counted in spleens as a mean to evaluate the infection. We found that animals reconstituted by CD4+CD25- and CD4+CD25+ T cells showed an higher number of bacteria in spleen compared with those reconstituted only by CD4+CD25- T cells (Figure 2).

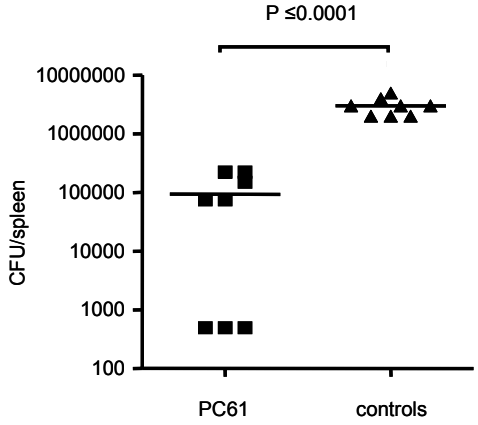

Figure 2. Persistence of *B. abortus* 2308 in spleen of SCIDcid mice reconstituted with either CD4+CD25-T cells or CD4+ T cells and CD4+CD25+ T cells, successively infected with *B. abortus* 2308

These preliminary findings shed light on the discrete role of CD4+CD25+ T cells in different models of infection. In acute salmonellosis, the immune system is promptly activated and the protective response to face pathogen is mainly due to the innate response. In this contest, it seems that CD4+CD25+ T cells are not able to play any role. On the contrary, in brucellosis CD4+CD25+ T cells are able to modulate the immune response, particularly of CD4+CD25- T cells and hence play a strong negative influence for the outcome of the infection. In order to understand the pathogenetic mechanisms of chronic infections, it is pivotal to understand if this mechanism is a secondary effect or the by-product of CD4+CD25+T cells function which controls the immune response in order to avoid an exaggerated response or, finally, it is induced someway by the pathogens themselves in order to take advantage over hosts.

References

1. Schaible UE, Collins HL, Kaufmann SH. Confrontation between intracellular bacteria and the immune system. *Advances in Immunology* 1999;71:267-377.
2. Netea MG, van der Meer JW, van Deuren M, Kullberg BJ. Proinflammatory cytokines and sepsis syndrome: not enough, or too much of a good thing? *Trends in Immunology* 2003;24:254-8.
3. Gershon RK, Kondo K. Infectious immunological tolerance. *Immunology* 1971;21:903-14.
4. Sakaguchi S, Sakaguchi N, Asano M, Itoh M, Toda M. Immunologic self-tolerance maintained by activated T cells expressing IL-2 receptor alpha-chains (CD25). Breakdown of a single mechanism of self-tolerance causes various autoimmune diseases. *Journal of Immunology* 1995;155:1151-64.

5. Shevach EM. CD4+ CD25+ suppressor T cells: more questions than answers. *Nature Reviews of Immunology* 2002;2:389-400.
6. Shevach EM, McHugh RS, Piccirillo CA, Thornthon AM. Control of T-cell activation by CD4+ CD25+ suppressor T cells. *Immunological Review* 2001;182:58-67.
7. Belkaid Y, Piccirillo CA, Mendez S, Shevach EM, Sacks DL. CD4+CD25+ regulatory T cells control Leishmania major persistence and immunity. *Nature* 2002;420:502-7.
8. Hisaeda H, Maekawa Y, Iwakawa D, Okada H, Himeno K, Kishihara K, Tsukumo S, Yasutomo K. Escape of malaria parasites from host immunity requires CD4+CD25+ regulatory T cells. *Nature Medicine* 2004;10:29-30.
9. Hori S, Carvalho TL, Demengot J. CD25+CD4+ regulatory T cells suppress CD4+ T cell mediated pulmonary hyperinflammation driven by Pneumocystis carinii in immunodeficient mice. *European Journal of Immunology* 2002;32:1282-91.
10. Hesse M, Piccirillo CA, Belkaid Y, Prufer J, Mentink-Kane M, Leusink M, Cheever AW, Shevach EM, Wynn TA. The pathogenesis of schistosomiasis is controlled by cooperating IL-10 producing innate effector and regulatory T cells. *Journal of Immunology* 2004,172:3157-66.
11. Kohm A, McMahon JS, Podojil JR, Begolka WS, DeGutes M, Kasprowicz DJ, Ziegler SF, Miller SD. Cutting Edge: Anti-CD25 Monoclonal Antibody Injection Results in the Functional Inactivation, Not Depletion, of CD4+CD25+ T Regulatory Cells. *Journal of Immunology* 2006;176:3301-5.

Session 4. Poster

HIV ENVELOPE GLYCOPROTEIN GP 120 INTERACTION WITH CD4/LCK/EZR CYTOSKELETON COMPLEX DOES OCCUR IN LIPID RAFTS

Isabella Parolini (a), Francesca Luciani (b), Katia Fecchi (c), Carlo Ramoni (d), Robert Blumenthal (e), Stefano Fais (c), Massimo Sargiacomo (c)

(a) Department of Haematology, Oncology and Molecular Medicine, Istituto Superiore di Sanità, Rome, Italy

(b) Department of Infectious, Parasitic and Immuno-Mediated Diseases, Istituto Superiore di Sanità, Rome, Italy

(c) Department of Therapeutic Research and Medicines Evaluation, Istituto Superiore di Sanità, Rome, Italy

(d) Department of Cell Biology and Neurosciences, Istituto Superiore di Sanità, Rome, Italy

(e) Dept Center for Cancer Research NCI-Frederick, National Institutes of Health, Bethesda, MD, USA

Introduction

The existence of lipid rafts also called Low Density Triton Insoluble (LDTI) in intact cells has been established. At 4°C LDTI form a liquid-ordered state where acyl chains are tightly packed, and highly ordered. Their easily isolation with Triton X-100 (TX-100), due to the unique lipid composition (enriched in cholesterol and sphingolipid) made it possible to decipher a rafts specific protein pattern including glycosylphosphatidyl -inositol (GPI)-anchored proteins, acylated intracellular protein tyrosine kinases and membrane receptors.

Several studies indicated a role for lipid rafts at various stages of HIV-1 replication cycle, such as virion packaging (1), assembly (2), budding from infected cells (3) and entry in the host cell. Regarding the latter, it seems likely that rafts represent privileged plasma membrane sites for virus binding to host cells, by concentrating CD4 (4) and coreceptors, CXCR4 (5,6) and CCR5 (7) in these domains. In addition the integrity of lipid rafts is an important requirement for virus entry, since destabilizing rafts by either extraction of cholesterol or inhibition of glycosphingolipid synthesis inhibit virus entry.

However little is known about the mechanisms employed by HIV to elicit host cell cytoskeleton rearrangements productive to viral entry.The raft resident src protein, Lck, is found in its acylated form to interact with CD4 and to play an important role in anchoring CD4 with raft microdomains present on microvilli (8).

Ligation of Gp120 with CD4 stimulates receptor phosphorylation on serine residues leading to CD4 separation from the non covalently interacting tyrosine kinase p56 Lck and subsequent receptor endocytosis. A very recent study conducted by extensive mutagenesis of the CD4 receptor showed that a raft-localizing marker, consisting of a short sequence of positively charged amino acid residues, RHRRR, was present in the membrane-proximal cytoplasmic domain of the receptor. Substitution of the entire RHRRR sequence with alanine residues completely abolished raft localization of the CD4 mutant. Accordingly CD4 represents an interesting exception among rafts protein in that, its palmitoylation or association with Lck does not affect raft partitioning but it exclusively relies on RHRRR (9).

Similar cluster of positively charged amino acids in the juxta-membrane cytoplasmic domain of CD44, CD43, and ICAM-2 binds ERM (ezrin/radixin/moesin) proteins (10). ERM proteins are a family of proteins involved in the linking of transmembrane proteins to the actin cytoskeleton (11) through ERM phosphorylation state which induces an open conformation state exposing ERM binding sites to actin and membrane proteins. Ezrin (EZR) has been shown to colocalize with lipid rafts and CD4 was found to colocalize with actin and EZR in microvilli and membrane ruffles (12). Thus LDTI-resident CD4 may represent a potential site for the interaction with ERM proteins that may anchor the receptor to cortical actin filaments that form a tight, regulated association with the plasma membrane (membrane-skeleton).

In this view we exploited CD4/EZR/Lck molecules association and their activation state in plasma membrane compartments of viral activated T cells as responsible of first signals occurring in cytoskeleton rearrangement after viral encountering.

Methods

Western blot and immunoprecipitation

For immunoprecipitation experiments, cells were lysed in the presence of a cocktail of protease inhibitors, in a buffer containing Tris 10 mM pH 8.0, NaCl 150 mM, EDTA 1 mM, orthovanadate 1 mM, plus, as detergents, Triton X-100 1% and N-octyl-β-D-glucopyranoside 60 mM. Supernatants were loaded on a 7.5% SDS-PAGE and subjected to WB analysis. To test Ab specificity, irrelevant anti-IgG Abs were also immunoprecipitated. The antibodies used were: anti-EZR monoclonal (Sigma, St.Louis, Mo), anti-CD4 monoclonal (Novocastra lab. Newcastle upon Tyne, UK), anti-Lck polyclonal (Santa Cruz Biotechnology Inc., Santa Cruz, CA), anti.phosphotyrosine (4G10) (Transduction Laboratories, Lexington, UK).

Isolation of LDTI microdomains

Cells were lysed at 4°C in 25 mM morpholineethanesulfonic acid (MES) Ph 6.5, 0.15 M NaCl, 1% (v/v) TX-100 buffer supplemented with protease inhibitors. The lysate was then homogenized and adjusted to 40% sucrose. A 5-30% linear sucrose gradient was formed above the homogenate. The centrifugation was carried out at 45,000 rpm for 16 h, then 12 fraction collected for further western blotting or immunoprecipitation analysis.

Results

CD4/cytoskeleton/EZR complex formation in Gp120 activated T cells

Analysis of CD4 with lipid rafts marker PKH 26 after 1% TX-100 solubilization showed that not all CD4 molecules were localized within lipid rafts (Figure 1a, panel 1), thus revealing a possible CD4-cytoskeleton linkage. In this regard untreated cells labelled with CD4 and actin antibodies showed a low colocalization (panel b, white colour) that was greatly enhanced by Gp 120 (panel 3).

Moreover Gp120 induced CD4 clustering coincided with complete actin colocalization. Since it has been proposed EZR as a membrane-cytoskeleton organizer that can mediate the rearrangement and the function of F-actin, we first verified if CD4/EZR interaction could occur

in basal condition. Co-immunoprecipitation experiments indicated a weak CD4/EZR association strictly confined in rafts domains (Figure 1b). CD4/EZR association was previously found to occur in cell microvilli that are considered a subpopulation of rafts.

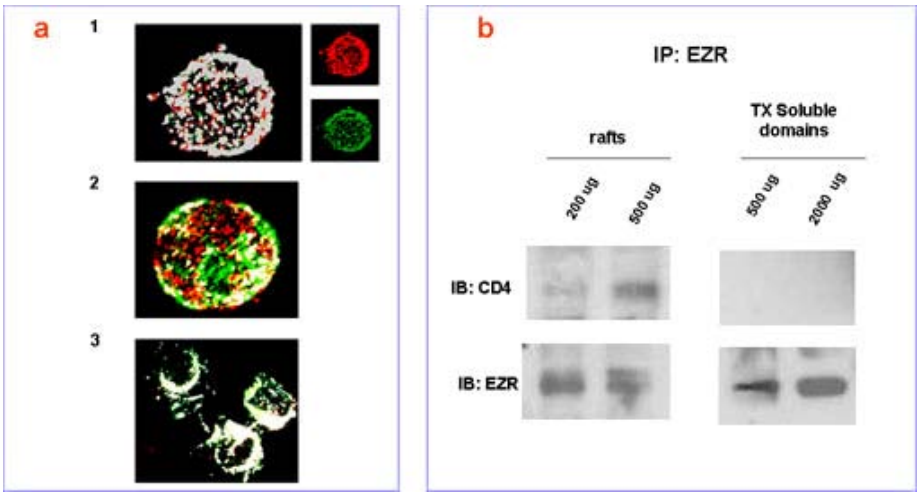

Figure 1. a) HUT cells were first labelled with anti CD4 antibody followed by alexa Fluor 594-conjugated secondary antibody (green). Cells were then fixed, treated with 0.5 % TX-100, labelled with lipid probe PKH26 red fluorescent cell linker, and examined by confocal microscopy (panel 1). Inserts show single labelling. White colour indicate CD4 and lipid colocalization area. Hut cells were left untreated (panel 2) or Gp 120 (3 min 37 °C, 10 µg/ml) treated (panel 3), then labelled with anti CD4 antibody followed by alexa Fluor 594-conjugated secondary antibody, fixed, permeabilized and stained with Alexa Fluor 488-conjugated phalloidin (green). It is clearly visible a strong Gp 120 induced CD4 clustering coinciding with complete actin colocalization (white colour). b) Hut cells were lysed with 1% TX-100 and rafts and TX-soluble membrane increasing amount (200 and 500 µg and 500 and 2000 µg, respectively) analyzed for EZR/CD4 complex. EZR was immunoprecipitated and blotted with CD4. Results indicate a weak CD4/EZR association strictly confined in rafts domains

Gp 120-induced opposite effects on CD4/Lck and EZR/Lck complex association

The src kinase-Lck has been extensively described as CD4 partner in several T cell activation process. In our previous study examining the role of specific protein kinase inhibitors in HIV mediated fusion process, we found the src kinase inhibitor PP2 as the strongest modulator of HIV fusion (13). Thus we focused on Lck as protein mediating signalling between virus encountering in LDTI-lipid rafts and cytoskeleton rearrangements. It has been proposed yet a Lck/EZR association in T cell with no direct evidences. In a first series of immunoprecipitation experiments performed on total T cell line, HUT, or in primary CD4+ PBL cells, we could clearly detect an EZR/Lck association in basal conditions (Figure 2a).

Moreover Gp120 short activation induced a 1.4 fold reduction of EZR/Lck complex (Figure 2b). Parallel immunoprecipitations experiments of CD4/Lck complex on the contrary showed a 1.3 fold increase of CD4/Lck complex after Gp120 stimulus (Figure 2b).

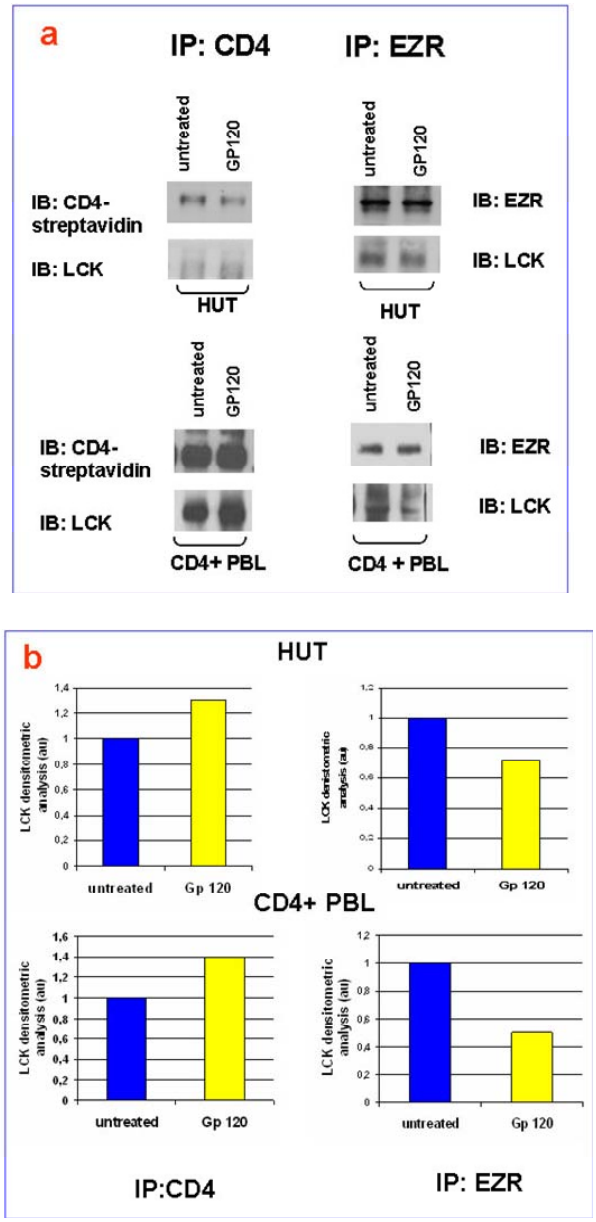

Figure 2. a) parallel CD4 and EZR immunoprecipitations from 1 mg HUT or CD4+PBL lysates untreated or Gp120 (3 min, 37 °C) activated were blotted with Lck.
b) Densitometric quantitation of western blotting CD4 and EZR associated-Lck.
Values are representative of three experiments

Gp120-induced disruption of CD4/Lck complex in lipid rafts

To elucidate a biological significance of Lck opposite behaviour under Gp120 stimulus we focused our experiments on CD4/Lck/EZR complex analysis in rafts.

CD4 and Lck are mainly localized in rafts domains and EZR too was described to be expressed in rafts. Thus we first analyzed if Gp120 could affect EZR, CD4 and Lck rafts

localization. Western blotting results (Figure 3a) followed by densitometric quantitation (Figure 3b) of pooled rafts fractions (3-6) indicated that EZR and Lck expressions were basically not affected, whereas CD4 expression was slightly decreased by Gp 120 treatment.

Next we examined if CD4/Lck association in lipid rafts could be modified by Gp120.

CD4 rafts immunoprecipitation of Gp120 treated cells indicated about 30% CD4 reduced expression (Figure 4a). Moreover CD4-associated Lck analysis on the 70% residual raft resident CD4 showed a decrease in Lck/CD4 complex when compared to resting CD4+ PBL (Figure 4b).

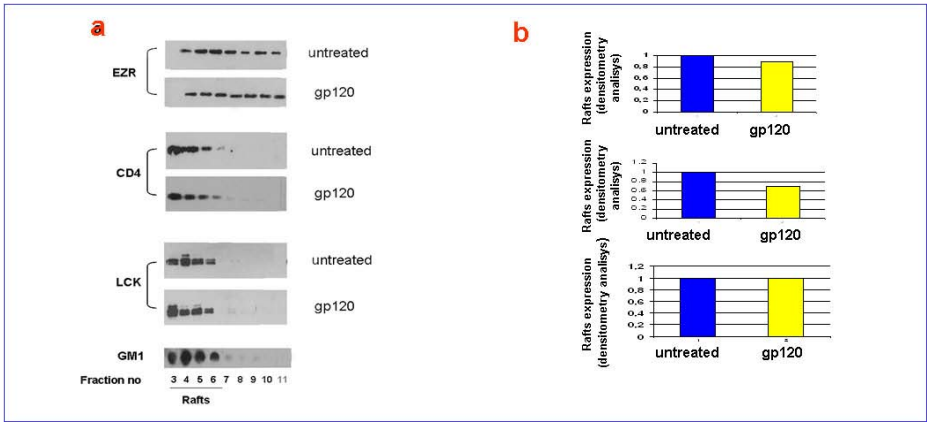

Figure 3. CD4+ PBL were left untreated or Gp120 stimulated (3 min, 37 °C) then lysed with 1% Tx-100 and subjected to sucrose gradient analysis to isolate rafts. a) EZR, CD4, Lck Western blotting analysis of 10 µg protein of each fraction. GM1 ganglioside was used as rafts marker. b) Rafts fraction (3-6) of EZR, CD4 and Lck probed filters were analyzed by densitometry quantitation and expressed as mean value for each condition. Values are representative of three experiments

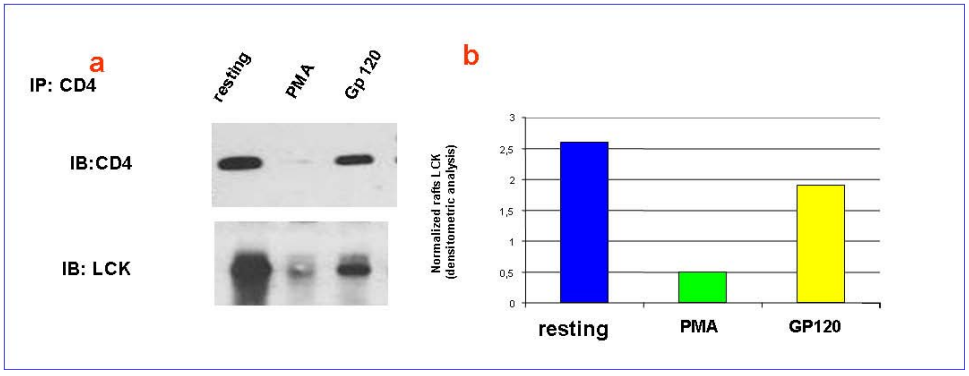

Figure 4. a) CD4+ PBL were left untreated or Gp120 and PMA (100 ng/ml) treated then lysed with 1% TX-100 and subjected to sucrose gradient. 8 µg of rafts from each condition were CD4 immunoprecipitated then blotted for Lck expression. b) Densitometric analysis of CD4 associated Lck expression obtained by normalization with relative CD4 expression of each condition and expressed in arbitrary units indicated that about 30% of rafts resident CD4-associated Lck is delocalised by Gp 120 short stimulus from rafts to other cell compartments (see Figure 2). PMA condition was used as positive control of CD4/Lck complex disruption

Gp 120 induced P- Tyr EZR in rafts is mediated by EZR associated Lck

In order to assess if the diminished CD4/Lck complex in rafts could be reflected in a variation in Lck/EZR complex in rafts we first analyzed EZR functional state in Gp120 activated rafts and if EZR could be substrate of Lck.

It is known that Gp120 induces a rapid EZR phosphorylation on tyrosine residues that is responsible of EZR binding to plasmamembrane. Thus we analysed the cell compartment localization of P-Tyr EZR following Gp 120 stimulus by EZR immunoprecipitation from lipid rafts and more general membrane compartments TX-100 soluble. Results clearly indicate that Gp 120 P-Tyr EZR is confined in rafts either in PBL or in Hut cells (Figure 5b).

Finally, to assess functional relationship between EZR/Lck , we performed *in vitro* kinase assay of immunoprecipitated EZR/Lck complex followed by WB analysis of activated EZR. Result indicate a major P-Tyr band corresponding to 78 Kda EZR, that is completely abolished in presence of Lck specific inhibitor, PP1 (Figure 5a).

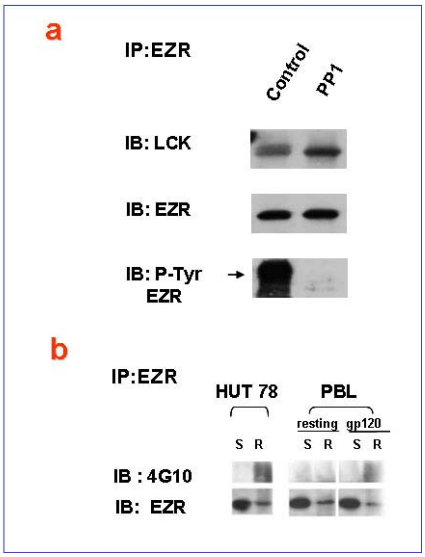

Figure 5. HuT and PBL resting and Gp120 activated were lysed with TX-100 and same protein amount of TX soluble (s) and rafts domains (r) analyzed for EZR immunoprecipitation followed by phosphotyrosine blotting (4G10) (b). Note that all Ptyr-EZR is confined in rafts.
a) *in vitro* kinase activity of immunoprecipitated EZR/Lck complex followed by western blotting analysis. Result indicate a major P-Tyr band corresponding to 78 Kda EZR , that is completely abolished in presence of src kinase specific inhibitor, PP1 (10 µM, 30 min 37 °C)

Discussion

In the complex network of signals triggered from HIV encountering at host cell plasma membrane, most of which are still unknown, a role has been assigned to Pyk2 and MAPK/ERK activation as responsible of a profound remodelling effect on raft components and cytoskeleton molecular association (13). In this scenario we focused our study on CD4/EZR/Lck functional

association as one of the first possible molecular mechanism leading to host cytoskeleton rearrangement productive to viral entry.

Our results show how lymphocytes cells undergoing HIV-1 Gp120 CD4 ligation trig dissociation of CD4/Lck complex within the rafts. This event is in accordance with the observation made by others, in which CD4/Lck complex dissociation decreased positive charge of CD4 cytoplasmic domain and CD4 binding to ERM proteins, promoting the CD4-HIV-1 aggregates to microvilli to enter in a fusion-competent environment.

On the other side CD4/Lck complex dissociation may enable free raft resident tyrosine kinase Lck to specifically phosphorylate EZR, as documented by immunoprecipitation of Lck/EZR complex and *in vitro* phosphorylation assay. In addition we describe as a novelty that all the detectable P- Tyr-EZR is completely confined in rafts. Furthermore we were able to detect a CD4/EZR complex restrict to raft. This association was previously only hypothetically predicted being responsible of the CD4 raft localization through charged amino acid residues RHRRR.

Dynamical molecular features of CD4/Lck and EZR/Lck association following Gp120 activation in total cell lysate and rafts were also carried out. Mutually exclusive results characterized this investigation: CD4/Lck complex diminished while the Lck/P-Tyr-EZR increased after addition of Gp120 in rafts, whereas the same complexes scrutinised on total cell extract gave opposite results. This apparent discrepancy can be reconciled by the fact that Gp120 acts in recruiting an overabundance of complexes sidestepping membrane compartment competent for the viral entry, while rafts do represent the only recognizable cellular site where the active molecules make their functional encounter productive (HIV processing and fusion).

References

1. Rousso I, Mixon MB, Chen BK, Kim PS. Palmitoylation of the HIV-1 envelope glycoprotein is critical for viral infectivity. *Proc Natl Acad Sci U S A* 2000;97(25):13523-5.
2. Lindwasser OW, Resh MD. Multimerization of human immunodeficiency virus type 1 Gag promotes its localization to barges, raft-like membrane microdomains. *J Virol* 2001;75:7913-7924.
3. Nguyen DH, Hildreth JE. Evidence for budding of human immunodeficiency virus type 1 selectively from glycolipid-enriched membrane lipid rafts. *J Virol* 2000;74(7):3264-72.
4. Parolini I, Sargiacomo M, Lisanti MP, Peschle C. Signal transduction and glycophosphatidylinositol-linked proteins (lyn, lck, CD4, CD45, G proteins, and CD55) selectively localize in Triton-insoluble plasma membrane domains of human leukemic cell lines and normal granulocytes. *Blood* 1996;87(9):3783-94.
5. Manes S, del Real G, Lacalle RA, Lucas P, Gomez-Mouton C, Sanchez-Palomino S, Delgado R, Alcami J, Martinez-AC. Membrane raft microdomains mediate lateral assemblies required for HIV-1 infection. *EMBO Rep*. 2000;1(2):190-6.
6. Viard M, Parolini I, Sargiacomo M, Fecchi K, Ramoni C, Ablan S, Ruscetti FW, Ming Wang J, Blumenthal R. Role of cholesterol in human immunodeficiency virus type 1 envelope protein-mediated fusion with host cells. *J Virol* 2002;76:11584-95.
7. Nieto M, Frade JM, Sancho D, Mellado M, Martinez AC, Sanchez-Madrid F. Polarization of chemokine receptors to the leading edge during lymphocyte chemotaxis. *J Exp Med* 1997;186(1):153-8.
8. Parolini I, Topa S, Sorice M, Pace A, Ceddia P, Montesoro E, Pavan A, Lisanti MP, Peschle C, Sargiacomo M. Phorbol ester-induced disruption of the CD4-Lck complex occurs within a detergent-resistant microdomain of the plasma membrane. Involvement of the translocation of activated protein kinase C isoforms. *J Biol Chem* 1999;274(20):14176-87.

9. Popik W, Alce TM. CD4 receptor localized to non-raft membrane microdomains supports HIV-1 entry. Identification of a novel raft localization marker in CD4. *J Biol Chem* 2004;279(1):704-12.
10. Yonemura S, Hirao M, Doi Y, Takahashi N, Kondo T, Tsukita S. Ezrin/radixin/moesin (ERM) proteins bind to a positively charged amino acid cluster in the juxta-membrane cytoplasmic domain of CD44, CD43, and ICAM-2. *J Cell Biol* 1998;140(4):885-95.
11. Fais S, Luciani F, Logozzi M, Parlato S, Lozupone F. Linkage between cell membrane proteins and actin-based cytoskeleton: the cytoskeletal-driven cellular functions. *Histol Histopathol* 2000;15(2):539-49. Review.
12. Steffens CM, Hope TJ. Localization of CD4 and CCR5 in living cells. *J Virol* 2003;77(8):4985-91.
13. Viard M, Parolini I, Rawat S, Fecchi K, Sargiacomo M, Puri A, Blumenthal R. The role of glycosphingolipids in HIV signaling, entry and pathogenesis. *Glycoconj J* 2004;20:213-22.

Session 4. Poster

ANIMAL HU-SCID MODEL OF VAGINAL TRANSMISSION OF HIV-1 FOR THE PRECLINICAL EVALUATION OF MICROBICIDES. DEVELOPMENT OF PEPTIDOMIMETICS AND MINI-ANTIBODIES AS A NEW CLASS OF MICROBICIDES OF BIOTECHNOLOGICAL ORIGIN

Simonetta Di Fabio, Maurizio Cianfriglia, Michela Flego, Alessandro Ascione, Mara Gellini, Silvia Zamboni, Andrea Binelli, Francesca Carlini, Elena Germinario, Stefano Vella
Department of Therapeutic Research and Medicines Evaulation Istituto Superiore di Sanità, Rome, Italy

Inhibition of vaginal transmission of HIV-1 in Hu-SCID mice by plant lectins the *Galanthus nivalis* (GNA) and *Hippeastrum* hybrid (HHA) in a gel formulation

Plant lectins [i.e., *Galanthus nivalis* agglutinin (GNA) and *Hippeastrum* hybrid agglutinin (HHA)] were recently demonstrated to represent potential candidate anti-HIV microbicides; they lack mitogenic activity, do not lead to human blood cell agglutination, and show marked stability at relatively low pH and high temperatures for prolonged time periods. Preincubation of cell-free HIV particles or persistently HIV-infected cells with these plant lectins resulted in a further potentiation of their antiviral efficiency by at least 10- to 20-fold. The plant lectins clearly interact with the entry of HIV into its target cell.

A preclinical evaluation of the potential effectiveness of GNA and HHA also as a topical microbicide to prevent vaginal HIV-1 transmission in a humanized severe combined immunodeficient (hu-SCID) mouse model has been recently investigated. Reconstituted mice received an intravaginal application of a *Galanthus nivalis* (GNA) and *Hippeastrum* hybrid (HHA) - containing gel 20 min prior to a non-invasive vaginal challenge with cell-associated HIV. The possible cytotoxic effect of GNA and HHA - containing-gel on lymphocytes was assessed and their *in vivo* migration was followed using fluorescently labelled human lymphocytes. Systemic infection was monitored by p24 antigen detection in culture supernatant from cocultured intraperitoneal cells using antigen capture enzyme-linked immunosorbent assay test and by the presence of integrated proviral HIV-1 DNA in DNA extracted from spleen cells. *In vivo* migration of labelled lymphocytes was examined by analysis of cells isolated from regional lymphonodes.

Preliminary results suggest that systemic infection was successfully inhibited by the presence of GNA and HHA containing gel at vaginal level. However, since the presence of contradictory results observed in the presence of the highest GNA and HHA concentrations (very likely due to the toxicity of the compounds) this observation has to be confirmed and more critically evaluated in additional studies.

Development of peptidomimetics and single chain fragment variable (scfv) human mini-antibodies for the identification of new microbicides of biotechnological origin

Identification of synthetic peptides mimicking LFA1 ligand by phage display technology

The molecular events that mediate HIV-1-induced cytopathology have not yet been clarified, although some experimental data suggest that the CD4 receptor is necessary, but not sufficient, for viral infection. In this regard the involvement of the LFA-1 molecule in both cell fusion and cell-mediated virus spread in infected $CD4^+$ T lymphocytes has been demonstrated. Moreover, the treatment with mAb against LFA-1 and its counter-receptor ICAM inhibits the formation of $CD4^+$ cell syncytia *in vitro*, demonstrating that the interaction between ICAM and their ligand LFA-1 is a major event in the generation of multinucleated giant cells. Because of the importance of these molecules, we used mAb MHM23 to the subunit of LFA-1 (CD18 determinant) with the aim of identifying the region involved in syncytia formation via cell fusion. In fact the MHM23 antibody inhibits this phenomenon and reduces HIV-1 cell-mediated virus spread in infected human $CD4^+$ cells. Various methods are currently used for the analysis of membrane protein topology, including biochemical, genetic and immunological approaches.

Using phage-display technology, we have applied a strategy based upon the epitope mapping of specific mAb directed against a defined protein domain. Random peptide phage libraries can be used to affinity select phage clones that specifically interact with mAb and mimic the natural epitope. Through the structural and functional definition of these selected phage clones, or "mimotopes", it is possible to characterize the protein against which the mAb was generated, even if in some cases the interpretation of sequence data may be complex. The reliability of this technology for the study of protein structure and function prompted us to use this method to analyze the subunit of the LFA-1 determinant (CD18), which plays a central role in HIV-1 infection. In this study we used random phage libraries containing linear (pVIII-9aa) or cysteine-constrained (pVIII-9aa.Cys) nonapeptides fused to the N-terminal portion of phage coat protein VIII. Several MHM23-specific phage clones were affinity isolated and their ability to mimic the CD18 antigen was verified by testing whether they blocked mAb MHM23 reactivity on LFA-1-expressing cells. By sequencing and comparing the phage clone inserts with the gene encoding for the CD18 determinant, the epitope recognized by mAb MHM23 was identified. Two synthetic peptides and various affinity-selected phage clones have demonstrated ability in inhibiting the syncytia formation during HIV-1 infection in *in vitro* assay. This finding could be important in elucidating the role of pre-defined functional LFA-1 domains involved in the cellular events associated with viral-induced cytopathology.

To investigate whether the MHM23-selected phage clones, and specific peptides were able to mimic the LFA-1 region involved in HIV-1-induced giant cell formation, we analyzed the syncytia induced by virus infection in LFA-1- and ICAM-1-positive C8166 cells (data not shown) pre-incubated for 30 min. with the various competitors. Then, cells were infected with 0.1 TCID 50/cell of virus in the simultaneous presence of the substances, and incubated for 2 h.

After incubation, cells were washed to remove non adsorbed virus, and medium containing phage clones and peptides was added to the cells, which were then incubated for 48-72 h. As preliminary experiments performed with decreasing concentrations of peptides had indicated that doses higher than 5 μg/ml significantly interfere with syncytia formation, we decided to

carry out experiments with the lower efficacious concentration of peptide to avoid toxic effect on cells. Similarly, a suitable concentration of phage particles (1012 TU/ml) to be used in this assay was identified.

Table 1. Syncytia formation of C8166 HIV-1-infected cells

Treatment	Characteristics	Number of syncytia/well ± SD (72 h) [a]
Medium		43 ± 7.5
Antibodies [b]		
UPC-10	Irrelevant	43 ± 7.8
MHM23	CD18-specific	1 ± 1.5
Phages [c]		
pC88	Clone from pVIII-9aa library	32 ± 9.5
3.41	Clone from pVIII-9aa.Cys library	13 ± 2
Synthetic peptides [d]		
CIP1	CD18 domain (200 - 207 aa)	3 ± 3.4
CIP2	3.41 phage-displayed peptide	13 ± 4
47	Irrelevant	40 ± 12

a) Average values of total number of syncytia/well from four independent experiments. b) 20 µg/ml. c) 1012 TU/ml. d) 10 µg/ml.

As shown in Table 1, the treatment of cells with the 3.41 phage clone resulted in a significant reduction of syncytia formation (13 syncytia/well) in respect with the controls untreated (medium: 43 syncytia/well) and pC88 phage (32 syncytia/well)-treated cells. Similar results were obtained with the specific 4.196 and unrelated R1.A2 phage clones, both coming from the pVIII-9aa.Cys constrained phage library (data not shown). Of interest, the presence of the CIP1 peptide (PPFAFRHV) (10 µg / ml), corresponding to the CD18 residues 200-207, during the HIV infection of cells, determined a dramatic reduction in the number of syncytia (3 syncytia / well) compared to the respective peptide control 13-mer peptide 47 (40 syncytia/well). A protective efficacy, but to a lesser extent, could be observed by treating the cells with the CIP2 peptide (PPWYSKTDL) (10 µg/ml) corresponding to the 3.41 phage clone insert (13 syncytia/well). The control peptides SCR1 (FVRPHFPA) and SCR2 (WSYPTLPKD), scrambled versions of CIP1 and CIP2 peptides, respectively, as the 13-mer 47 peptide, did not block syncytia formation in analogous experiments (data not shown). As expected, in the presence of mAb MHM23 (20 µg/ml), we observed a strong reduction of the number of syncytia (1 syncytia/well) compared to the respective isotype control antibody UPC-10 (20 µg/ml; 43 syncytia/well).

Selection of human mini-antibodies in scFv format to the HIV-1 Env o-gp140ΔV2 mutated protein

A major problem in the development of effective therapeutic agents against viruses, including therapeutic antibodies, is the viruses' heterogeneity and mutability. A related problem is the low binding affinity of crossreactive antibodies able to neutralize a variety of primary isolates. Combinations of mAbs or mAbs with other drugs, and/or the identification of potent new mAbs and their derivatives that target highly conserved viral structures, which are critical for virus entry into cells, are some of the possible solutions to these problems, and will continue to be a major focus of antiviral research. HIV envelope glycoprotein (Env) is the target for

inducing neutralizing antibodies. Env is present on the virus surface as a trimer, and, upon binding to CD4, a cascade of events leads to structural rearrangement exposing the co-receptor binding site and entry into the $CD4^+$ host target cells. A recently designed and developed monomeric and trimeric Env constructs with and without deletion of the variable loop 2 (DeltaV2) from SF162, a subtype B primary isolate has been used for human mini-antibody targeting selection. Infact, it has been suggested that the V2 region of gp120 represent the major obstacle for directing to the HIV protein neutralizing antibodies targeting.

The development of novel technologies has now allowed the identification and manufacturing of antigen-specific recombinant human mini-antibodies, so-called scFvs. The human synthetic single-chain fragment variable (scFv) ETH-2 phage antibody library was used for the isolation of scFvs against the recombinant protein of o-gp140ΔV2 using a bio panning-based strategy. The selected scFvs were characterized under genetics-molecular aspects and HIV protein detection in ELISA. These *in vitro* selected human scFvs possess neutralizing activity in *in vitro* HIV infection (Figure 1) and may be used with other different human monoclonal antibodies to gp120 and/or in combination with specific anti HIV-1 drugs for the immunochemotherapy of HIV infection.

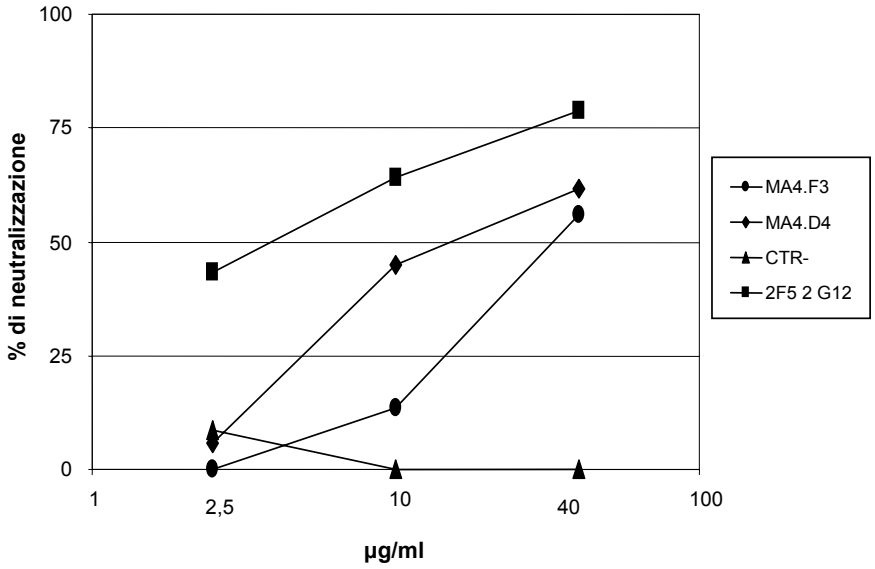

Figure 1. Neutralizating activity of the human scFvs MA4.F3 and MA4.D4 in TZM-bl cells infected with the HIV-1 viral strain SF162. The neutralizing activity of the human scFvs has been verified with the TZM-bl cell line, which express CD4 and CCR5 receptors together with the luciferase reporter gene under control of the HIV-1 promotor. The viral strain SF162 has been incubated in presence of different concentrations of the scFvs MA4.F3 and MA4.D4. As controls the Mabs 2F5 and 2G12 (neutralizing Mabs) and the scFv anti glucose oxidase (irrelevant) were used. An activation of the luciferase gene TAT–mediated is present in the case of HIV-1 infection while a consistent reduction of such an activation measured with a lowered luminescence intensity may be observed following the exposure of the infected cells to neutralizing antibodies. In the y axis the % of neutralizing activity of the antibodies is reported in relationship with the luminescence intensity observed in HIV-1 untreated TZM-bl cells

These new human mini-antibodies to HIV-1 gp120 me*et al.*l criteria for a potential antiviral compound: they are human, hence poorly or not at all immunogenic, and it binds selectively the viral strain SF162 by inhibiting its cell to cell transmission. Furthermore, its small molecular size should provide for efficient tissue penetration, yet give rapid plasma clearance.

Session 4. Poster

NOVEL STRATEGIES TOWARD DEVELOPING A PROPHYLACTIC AND THERAPEUTIC VACCINE AGAINST HEPATITIS C VIRUS

Alfonso Mele (a), Enea Spada (a), Riccardo Cortese (b), Antonella Folgori (b), Alfredo Nicosia (b), Robert Purcell (c)

(a) National Centre for Epidemiology, Surveillance and Health Promotion, Istituto Superiore di Sanità, Rome, Italy

(b) Istituto di Ricerche di Biologia Molecolare P. Angeletti, Pomezia, Rome, Italy

(c) National Institute of Allergy and Infectious Diseases, National Institutes of Health, Bethesda, MD, USA

The project: rational and aims

Since the current therapy of chronic hepatitis C virus (HCV) infection is still unsatisfactory due to low response rates and significant side effects and, on the other hand, and the usual asymptomatic course of acute hepatitis C lowers the favourable impact of an early treatment of the infection in this phase, the development of novel therapeutic strategies as well as a prophylactic vaccine represent an un-met overriding medical need. The troubles found in developing a traditional anti-HCV vaccine, mainly due to the high genetic variability of the virus, make the use of non conventional strategies necessary. The experimentation of potential candidate vaccines developed till now has gone no further on the preclinical phase and for the most part their efficacy have not been tested, because of the difficulties in getting chimpanzees. Performing a comprehensive study of the natural history of HCV infection represents the optimal approach to acquire crucial information toward devising a novel vaccination strategy against HCV. Therefore, the principal aims of the this project are: i) Prospective study of host and viral factors in acutely infected HCV individuals; ii) Analysis of cell mediated immunity (CMI) in acutely infected HCV individuals to define immune correlates of infection resolution or progression to chronicity; iii) Generation and test of a novel genetic vaccine against HCV by vaccination and challenge of chimpanzees; iv) Feasibility study of an efficacy vaccination trial against HCV.

Obtained and expected results

The foreseen activities in the project allowed us to fully reach the prearranged objectives. We here report on the project advancement with reference to its specific aims.

Prospective study of host and viral factors in acutely infected HCV individuals.

Eighty with acute HCV infection, followed for at least 12 months in absence of therapy or for 6 months in case of treatment due to the development of a chronic infection, have been till

now recruited. A preliminary analysis (Spada *et al.* Gut, 2004) performed on 35 out of these 80 individuals with acute HCV infection who were followed for a median period of 13 months, and on 56 patients with chronic HCV infection showed:

- a chronicity rate of about 30%;
- a positive significant association between a favourable self-limiting course of infection and female gender and high bilirubin levels at the disease onset;
- the frequent detection during the acute phase of the infection of a measurable T cell response that is usually absent during the chronic phase;
- that the viral clearance in acutely infected individuals was very efficaciously predicted by the detection of a negative HCV RNA test and a broad CMI within the first month after the disease onset.

The latter data could be used as criteria in selecting candidates for antiviral treatment.

Analysis of CMI in acutely infected HCV individuals to define immune correlates of infection resolution or progression to chronicity

The findings of the preliminary study above reported, still further support the hypothesis that an efficacious HCV vaccine has to elicit a strong, broad and sustained T cell response. To obtain further insight into the immune mechanisms underlying the spontaneous resolution or establishment of chronic infection we designed a prospective immunological study of HCV specific CMI in a cohort of 31 acutely infected individuals enrolled at the onset of the infection and followed for a median period of one year (Folgori *et al.* Gut, 2006). CMI was analysed by performing at multiple time points interferon (IFN) γ ELIspot, IFN γ intracellular staining and FACS analysis, bromouridine proliferation assay and tetramer's analysis. The results if this study indicated that while a measurable CMI with effector function was detected in the majority of subjects, after approximately 6 months less than 10% of chronically infected individuals displayed significant CMI compared with 70% of subjects who cleared the virus. Furthermore, the study showed that the progressive disappearance of HCV specific T cells from the peripheral blood of chronic patients was due to an impaired ability to proliferate that could be rescued *in vitro* by concomitant exposure to interleukin 2 and the antigen. These data provided evidence of strong and broad (multispecific) T cell responses with a sustained ability to proliferate in response to antigen stimulation as a reliable pharmacodynamic measures of a protective CMI during acute infection, and suggested that early impairment of proliferation might contribute to loss of T cell response and HCV persistence. However, this study also demonstrated that an important proportion of individuals who developed chronic infection showed T helper and cytotoxic T cell responses during the first weeks from the onset of symptoms. Indeed, the accumulation of mutations in T helper and/or cytotoxic immunodominant epitopes capable of altering the recognition of T cell lymphocytes might represent a possible mechanism of immune response escape and chronic infection occurrence. To verify whether viral escape could account for the failure of cell-mediated immunity during the natural course of HCV infection, we also performed an in depth analysis of the relation between CMI and viral evolution in a patient with chronically evolving infection (Giulietta *et al.* European Journal of Immunology, 2005). In this study, by evaluating *ex vivo* T cellular immune responses against genotype-specific peptides spanning a large proportion of HCV polyprotein immunodominat helper and cytotoxic T cell (CTL) epitopes in the NS3 protein targeted during the early phase of the infection were identified. It was also found that the presence of cytotoxic T cells directed against a new highly immunodominant $CD8^+$ T cell epitope was associated with the elimination of the quasispecies harbouring the original amino acid sequence within this epitope, and with its replacement at a single residue within the CTL epitope that strongly affected recognition by primary $CD8^+$ T

cells. In contrast no escape phenomena from recognition by helper T cells were detected. These results support the view that acute-phase $CD8^+$ T cell response exert a biologically relevant pressure on HCV replication and that viruses escaping could have a significant survival advantage. The analysis of cellular and humoral immune responses against the hyper variable region 1 (HVR1) of the E2 protein and the effects of the variability of this region on B and T cells recognition is in progress.

Generation and test of a novel genetic vaccine against HCV by vaccination challenge of chimpanzees

Since the viral clearance during self-limiting acute HCV infection is characterized by a strong multispesific and sustained $CD4^+$ and $CD8^+$ T-cell responses, we chose a vaccination strategy based on the use of a genetic vaccine, which is capable to elicit a potent T cell immune response more efficiently than a classic protein-based vaccine.

We therefore generated plasmid DNA and Adenoviral vectors encoding for the entire Non Structural region of HCV (NS). These vectors were tested for immunogenicity in a number of pre-clinical studies in mice and Rhesus monkeys and in all cases the candidate vaccines were able to induce cell-mediated responses. We tested the efficacy of this vaccine candidate by performing a vaccination and challenge study in chimpanzees prior to consider its suitability for further testing in humans (Folgori *et al.* Nature Medicine 2006). A segment of DNA coding for NS region, was used as genetic vaccine and delivered as replication-defective adenoviral vector and by electroporated plasmid DNA, in a combined modality regimen. The vaccine was administered to 5 chimpanzees while 5 age - and sex - matched chimpanzees, used as control, received adenoviral vectors and plasmid DNA coding for HIV-1 gag antigen. The induction of antiviral CMI was measured by using IFNγ ICS, BrdU proliferation and cytotoxicity assays. All ten chimpanzees were infected at week 49 with a heterologus inoculum (strain H77, 1a), differing from the vaccine by more than 13% at the amino acid level. The vaccine induced a fully functional CD4+ and CD8+ T cell responses in all immunized chimps. After challenge with H77 stain, all control chimps experienced an episode of acute hepatitis that on the contrary was not observed in any of vaccines. Suppression of acute viremia in 4 of 5 chimps occurred as result of massive expansion of peripheral and intrahepayic HCV-specific CD8+ cells that cross-reacted with vaccine and virus epitopes. T cell response in controls was delayed and 3 of them resolved the infection (normal rate of resolution 50%). The findings of this study showed that it is possible to elicit effective immunity against heterologous HCV by stimulating only the cellular arm of the immune system, and suggested a path for new immunotherapy against highly variable pathogens.

Feasibility study of an efficacy vaccination trial against HCV

Because of the low incidence of HCV infection in the general population, to evaluate the efficacy of a hepatitis C vaccine it would be necessary to test it in a high risk population group. In Italy the most suitable population group to perform a vaccination trial is represented by intravenous drug users, among which high but variable incidence rate of infection have been reported in earlier studies. By assuming, in the present years an annual incidence rate of about 20% and assuming a vaccine efficacy off 90%, it would be necessary the enrolment of a small group of individuals (nearly 70 individuals for each of two treatment group) to demonstrate the vaccine efficacy in a preliminary randomized double-blind placebo controlled trial. Population homogeneity, small size sample and few exclusion criteria represent the principal advantages of

such a trial. The most important disadvantages include poor compliance by using a complex vaccination protocol and high costs for each enrolled individual. To evaluate the feasibility of such a clinical trial we have planned to perform an incidence study of HCV infection among a large sample of IDUs attending the Italian Drug Dependency Units scattered all over the country. Counselling for hepatitis virus infections and administering of hepatitis B vaccine and/or hepatitis A vaccine will also be important activities of this study.

References

1. Spada E, Mele A, Berton A, Ruggeri L, Ferrigno L, Garbuglia AR, Perrone MP, Girelli G, Del Porto P, Piccolella E, Mondelli MU, Amoroso P, Cortese R, Nicosia A, Vitelli A, Folgori A. On behalf of the Acute Hepatitis C Italian Study Group. Multi-specific T-cell response and negative HCV RNA tests during acute HCV infection are early prognostic factors of spontaneous clearance. *Gut* 2004;53:1673-81.
2. Guglietta S, Garbuglia AR, Pacciani V, Scottà C, Perrone MP, Laurenti L, Spada E, Mele A, Capobianchi MR, Folgori A, Vitelli A, Ruggeri L, Nicosia A, Piccolella E, Del Porto P. Positive selection of cytotoxic T lymphocyte escape variants during acute hepatitis C virus infection. *European Journal of Immunology* 2005;35:2627-37.
3. Folgori A, Spada E, Pezzanera M, Ruggeri L, Mele A, Garbuglia AR, Perrone M, Del Porto P, Piccolella E, Cortese R, Nicosia A, Vitelli A. Early impairment of HCV-specific T-cell proliferation during acute to infection leads to failure of viral clearance. *Gut* 2006;55:112-9.
4. Folgori A, Capone S, Ruggeri L, Meola A, Sporeno E, Ercole BB, Pezzanera M, Tafi R, Arcuri M, Fattori E, Lahm A, Luzzago A, Vitelli A, Colloca S, Cortese R, Nicosia A. A T-cell HCV vaccine eliciting effective immunity against heterologous virus challenge in chimpanzees. *Nat Med* 2006;12:190-7.

Stampato in proprio dal Settore Attività Editoriali

Roma, dicembre 2006 (n. 4) 15° Suppl.